Statistical structure and inference methods for discrete high-frequency observations of SPDEs in one and multiple space dimensions

Dissertation

zur Erlangung des akademischen Grades
Dr. rer. nat.
im Fach Mathematik

eingereicht an der
Fakultät für Mathematik und Informatik
der Julius-Maximilians-Universität Würzburg

vorgelegt von
Patrick Bossert, M.Sc.

Würzburg, 15.12.2023
Betreut durch Prof. Dr. Markus Bibinger

Acknowledgements

I express my sincere appreciation to my Ph.D. advisor, Markus Bibinger, for his guidance and support throughout my doctoral research. His valuable suggestions and input have played a crucial role in enhancing the quality of my work and deepening my understanding of the research field. I am grateful to Professor Mathias Trabs and Professor Masayuki Uchida for agreeing to be the second and third assessors of this thesis, respectively.

Special thanks go to my mother, Christina, and all my dear friends, especially Daniel, Yasmin, and Maik, for their enduring support and encouraging words during the writing of this thesis and its challenging phases. I would like to specifically emphasize Daniel for his continuous and invaluable support, motivating me through numerous conversations, and helping me to enhance the quality of my work with his excellent English skills. I want to thank Tina for her consistent support during the final stages of this demanding endeavour. Finally, I wish to express my gratitude to Janosch and Vincent for reviewing parts of this thesis and providing constructive comments and helpful corrections.

Präsident der Julius-Maximilians-Universität Würzburg
Prof. Dr. Paul Pauli

Dekan der Fakultät für Mathematik und Informatik
Prof. Dr. Marc Erich Latoschik

Gutachter:
1. Prof. Dr. Markus Bibinger
2. Prof. Dr. Mathias Trabs
3. Prof. Dr. Masayuki Uchida

Eingereicht am: 19.12.2023
Tag der Disputation: 15.04.2024

Contents

Introduction

Stochastic partial differential equations (SPDEs) form a powerful framework for modelling and analysing systems that evolve in both time and space under the influence of random fluctuations. They provide a mathematical description of processes that exhibit randomness, often arising in various fields such as physics, finance, biology, and engineering. SPDEs extend the classical theory of partial differential equations (PDEs) by incorporating stochastic terms, which account for the uncertainties present in the system. Unlike deterministic PDEs, where the evolution of a system is fully determined by its initial conditions and governing equations, SPDEs introduce randomness into the equations, capturing the inherent variability and noise in the underlying phenomena. While PDEs have been extensively researched over the past decades, research on SPDEs is comparatively still in its infancy.

To introduce stochastic partial differential equations, we begin by considering a separable Hilbert space denoted as H. The mathematical expression for an SPDE takes on a general form:

$$\mathrm{d}X_t + (\theta A + B)X_t \,\mathrm{d}t = (MX_t + \sigma)\,\mathrm{d}W_t^Q,$$

where $X_0 = \xi \in H$ denotes the initial condition, A, B and M are operators, W^Q represents a Q-cylindrical Brownian motion, and θ, σ are parameters. The operator A is linear, positive definite, and self-adjoint in H, while B is a linear or nonlinear operator in H. Additionally, A and M are commonly differential or pseudo-differential operators. For further readings on operators and other fundamental concepts of functional analysis, we recommend consulting the work of Rudin (1987).

Similar to PDEs, various classes of SPDEs emerge based on the choice of the operators, each exhibiting distinct properties and characteristics. Some notable classes of SPDEs include:

(1) Linear SPDEs: This class encompasses SPDEs, where the differential operator is linear, i.e., $B = 0$. Linear SPDEs are often solvable analytically or numerically and have well-defined properties such as existence, uniqueness, and regularity of solutions. They serve as a fundamental building block for further SPDE models.

(2) Nonlinear SPDEs: Nonlinear SPDEs feature nonlinear terms in either the differential operator or the drift term, characterized by $B \neq 0$, with B being a nonlinear operator. These equations are commonly employed when modelling systems with nonlinearity or interactions between different components. Solving nonlinear SPDEs often presents substantial challenges concerning the existence and uniqueness of solutions. As a result, their analysis frequently relies on numerical methods or approximation techniques to explore their behaviour and properties.

(3) SPDEs with additive noise: This class of SPDEs involves a stochastic noise term that is additive, meaning it is directly added to the deterministic part of the equation, i.e., $M = 0$. The noise introduces randomness and captures the effects of unpredictable factors in the system. SPDEs with

additive noise are widely used in various fields to model phenomena with inherent uncertainties and fluctuations.

(4) SPDEs with multiplicative noise: In this class of SPDEs, the noise term is multiplicative, meaning it interacts with the solution or the coefficients of the equation, i.e., $M \neq 0$. Multiplicative noise can arise in various applications, such as models of financial markets, fluid dynamics, or biological systems. SPDEs with multiplicative noise present additional challenges in terms of well-posedness, stability, and numerical approximation.

Each class has its own mathematical properties, challenges, and applications. The study of SPDEs involves a combination of analytical techniques, numerical methods, and probabilistic tools to understand the behaviour of these complex systems and make predictions about their dynamics.

The relevance of statistical techniques for SPDEs is evident by the works of Hambly and Søjmark (2019), Fuglstad and Castruccio (2020), Altmeyer and Reiß (2021), and Altmeyer et al. (2022), which provide calibration options for SPDEs in one space dimension. Although there has been significant research on linear stochastic partial differential equations with additive noise, there are still open questions that remain unresolved. Two particular areas that warrant further investigation are the statistical inference on the model parameters and the extension of the SPDE model to higher dimensions. In terms of statistical inference, understanding how to accurately estimate the parameters of linear SPDEs with additive noise is a critical challenge. This includes determining the identifiability of the parameters, devising efficient estimation methods, and assessing the associated statistical properties, such as consistency and asymptotic normality. Addressing these questions is essential for reliable parameter estimation and for making informed inferences about the underlying system motivating ongoing research efforts to advance our understanding of linear SPDEs with additive noise. A first step was taken by the authors Bibinger and Trabs (2020) and Hildebrandt and Trabs (2021), where they analysed the identifiability of the parameters of a one-dimensional SPDE model and developed respective estimators. Thus, we aim to link to their work and discuss remaining problems.

While research on linear SPDEs in one space dimension has garnered considerable interest in recent decades, extending the model to multi-dimensional spaces is still in its early stages. This extension introduces complexities in terms of the theoretical analysis, computational methods, and interpretation of the results. Investigating the behaviour of linear SPDEs in higher dimensions can provide valuable insights into the dynamics of multi-dimensional systems and pave the way for their application in diverse fields. Addressing statistical inference and exploring the behaviour of these models in higher dimensions will contribute to the development of more robust estimation techniques, improved model selection criteria, and a deeper comprehension of complex systems across various scientific disciplines. The initial strides in this emerging field were taken by Tonaki et al. (2023), where they delved into a linear SPDE model within a two-dimensional spatial framework. Their work not only introduced pioneering estimation techniques for model parameters but also shed light on the asymptotic properties underpinning these estimators.

In this thesis, our focus is on studying a linear SPDE with additive noise, both in one and multiple space dimensions. We aim to derive statistical inference methods by observing data on a bounded discrete space-time grid.

However, it is essential to acknowledge that SPDEs extend beyond the scope of linear models with additive noise. For further readings on nonlinear SPDEs, we recommend referring to the work of Cialenco and Glatt-Holtz (2011). Similarly, for insights into SPDEs with multiplicative noise, we suggest the works

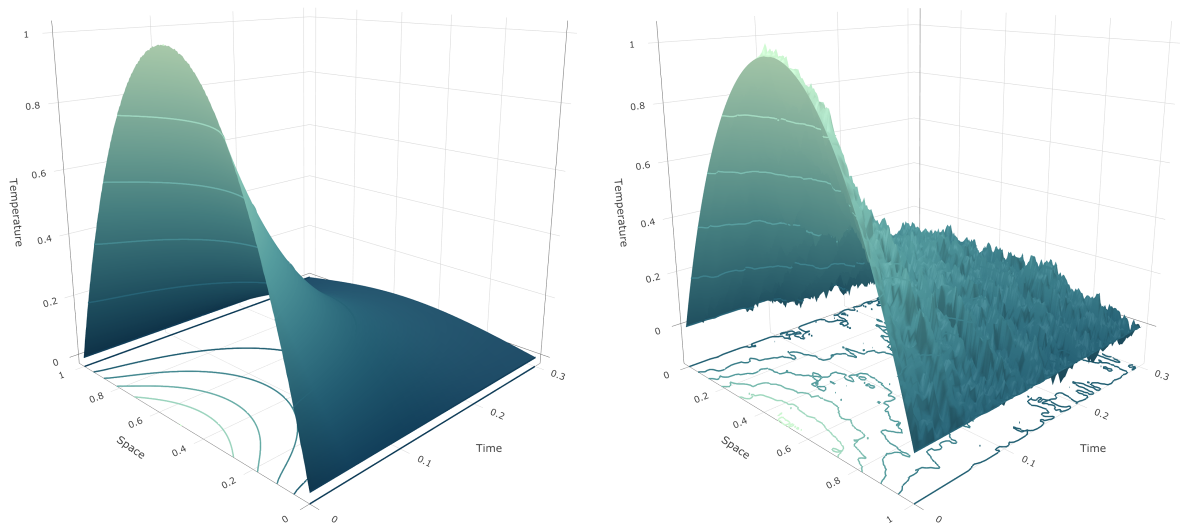

Figure 1.: The figure shows a comparison between the deterministic heat equation (left) and its stochastic counterpart (right). The initial condition $\xi(y)$ for both cases is set to $\xi(y) = 4x(1-x)$, and the volatility parameter is chosen to be $\sigma = 1/4$.

of Chong (2020b) and Cialenco and Huang (2020). Additionally, for readings on semilinear SPDEs, we refer to the works of Altmeyer et al. (2023) or Hildebrandt and Trabs (2023), which provide valuable contributions in this area. For a comprehensive overview of statistical inference for SPDEs, along with an introduction to the different classes of SPDEs and their statistical approaches, the work of Cialenco (2018) serves as a valuable resource.

One of the most famous examples for linear SPDEs with additive noise is given by the stochastic heat equation. The stochastic heat equation is a fundamental SPDE that models the diffusion of heat in a medium with stochastic input. It combines the deterministic heat equation, which describes the evolution of temperature over time, with a stochastic term that captures the random fluctuations or noise affecting the system, transforming the PDE into a SPDE. Mathematically, the one-dimensional stochastic heat equation can be represented as

$$\mathrm{d}X_t(y) = \frac{\partial^2}{\partial y^2} X_t(y)\,\mathrm{d}t + \sigma\,\mathrm{d}W_t(y),$$

where the spatial domain of y is one-dimensional. Here, $X_t(y)$ represents the temperature at time t and spatial position y, and W_t denotes the spatiotemporal white noise process. Referring back to the general SPDE introduced earlier, we find that the operator A corresponds to the second partial derivative with respect to y, i.e., $A = \partial^2/(\partial y^2)$, while both B and M are equal to zero. The stochastic heat equation has been widely studied in the field of mathematical physics and stochastic analysis, cf. Khoshnevisan (2016) or Cialenco and Kim (2022). It serves as a fundamental model for understanding diffusion processes in various contexts, such as heat transfer, finance, and population dynamics. In finance, it finds application in option pricing models and risk management, where random fluctuations in market prices are taken into account. In physics, it is used to model heat diffusion in materials with random variations, such as in heterogeneous media. As an example, consider the spatial domain as the one-dimensional unit interval, i.e., $y \in [0,1]$. In this context, the deterministic heat equation

$$\mathrm{d}X_t(y) = \frac{\partial^2}{\partial y^2} X_t(y)\,\mathrm{d}t$$

can be interpreted as a physical description of the cooling process of a rod initially heated by a heat source. The equation describes how the temperature of the rod changes over time and space due to heat diffusion. To further analyse the model, we impose a Dirichlet boundary condition, specifying that the temperature at both ends of the rod is fixed at zero, i.e., $X_t(0) = X_t(1) = 0$, for all time points $t \geqslant 0$. This boundary condition reflects the fact that the rod's temperature dissipates at its boundaries, resulting in a cooling process. To solve the deterministic heat equation, we use a Fourier decomposition, where we define the functions

$$e_k(y) := \sqrt{2}\sin(\pi k y),$$

which form an orthonormal basis of the Hilbert space $H = L^2([0,1])$ with the associated inner product

$$\langle f, g \rangle := \int_0^1 f(y)g(y)\,\mathrm{d}y,$$

for all $f, g \in H$ and $k \in \mathbb{N}$. Considering $X_t(y) \in H$ to be a solution of the deterministic heat equation, we can write

$$X_t(y) = \sum_{k=1}^{\infty} x_k(t)e_k(y), \qquad \text{where} \qquad x_k(t) := \langle X_t, e_k \rangle = \int_0^1 X_t(y)e_k(y)\,\mathrm{d}y.$$

By examining the first derivative in time, we can obtain an explicit representation of the Fourier modes x_k. This representation is given by

$$\frac{\partial}{\partial t} x_k(t) = \int_0^1 \frac{\partial}{\partial t} X_t(y)e_k(y)\,\mathrm{d}y = \int_0^1 \left(\frac{\partial^2}{\partial y^2} X_t(y)\right) e_k(y)\,\mathrm{d}y.$$

Using integration by parts and the Dirichlet boundary condition further yields

$$\begin{aligned}\frac{\partial}{\partial t} x_k(t) &= -\int_0^1 \left(\frac{\partial}{\partial y} X_t(y)\right)\left(\frac{\partial}{\partial y} e_k(y)\right)\mathrm{d}y = \int_0^1 X_t(y)\left(\frac{\partial^2}{\partial y^2} e_k(y)\right)\mathrm{d}y \\ &= \int_0^1 X_t(y)\big(-k^2\pi^2\sqrt{2}\sin(\pi k y)\big)\,\mathrm{d}y = -\pi^2 k^2 x_k(t).\end{aligned}$$

Therefore, variation of constants yields the following solution for the Fourier modes:

$$x_k(t) = x_k(0)e^{-\pi^2 k^2 t} = \langle \xi, e_k \rangle e^{-\pi^2 k^2 t}.$$

Consequently, X can be represented as

$$X_t(y) = \sum_{k=1}^{\infty} e^{-\pi^2 k^2 t} \langle \xi, e_k \rangle e_k(y).$$

By introducing stochasticity into the heat equation, we can capture random fluctuations and uncertainties in the cooling process, which is illustrated in Figure 1. This is particularly relevant in ecological modelling, where population growth and migration are subject to various sources of randomness and environmental variability. However, adding stochasticity to the heat equation requires more care than the presented example for the deterministic heat equation. We will therefore revisit this procedure for a linear SPDE model in one space dimension in the first chapter of this thesis and in Chapter 4 for a linear SPDE model in multiple space dimensions.

Structure of the thesis

The focus of this thesis is on analysing a linear stochastic partial differential equation with a bounded domain. The first part of the thesis (Part I) commences with an examination of a one-dimensional SPDE. In this context, we are directing our attention towards a specific category of linear SPDEs, specifically, a linear parabolic SPDE with one space dimension and an additive noise. Drawing on the work of Bibinger and Trabs (2020), which focused on estimating the volatility of the random field X generated by a linear parabolic SPDE in one spatial dimension, along with introducing estimators for the natural parameters of the model, we first address the question of finding an estimator for the curvature parameter in this model. Additionally, we analyse the task of improving the existing estimators for the natural parameters of the one-dimensional SPDE model.

Chapter 1 serves as an introduction to the mentioned SPDE, providing a recap of its basic properties and presenting initial results from Bibinger and Trabs (2020) and Hildebrandt and Trabs (2021). We also conduct a heuristic discussion on the model parameters, emphasizing the curvature effect that some parameters have on the random field X.

In Chapter 2, our focus shifts to the development of statistical inference for the curvature in the random field. We consider a high-frequency observation scheme and derive two estimators based on a maximum likelihood approach. One estimator relies on prior knowledge of the remaining model parameters, while the other is independent of any such knowledge. We establish consistency and asymptotic normality for both estimators. Additionally, we discuss numerical simulation methods for one-dimensional SPDEs and provide simulation results for the estimators.

Moving forward, Chapter 3 tackles the problem of estimating both the so called normalized volatility parameter and the curvature of the random field, which we refer to as the natural parameters of the model. We draw parallels between existing statistics for estimating the volatility parameter and those for a linear model. A key aspect of this procedure is the transformation of the realized volatility, a concept well-known in various statistical models such as Itô processes, using the natural logarithm. We develop estimators for the normalized volatility and curvature of X and demonstrate consistency and asymptotic normality. We also establish a connection between the resulting curvature estimator from the linear model approach and the estimator from Chapter 2. Hence, we introduce a novel method for estimating the natural parameters of the model, significantly improving upon the M-estimator presented by Bibinger and Trabs (2020), which is also discussed in Chapter 3. Simulation results for the estimator resulting from the log-linear model approach are provided to conclude this chapter.

Overall, Part I delves into the statistical analysis of a linear parabolic SPDE in one spatial dimension. It covers estimation of the normalized volatility, estimation of the curvature, and joint estimation of both parameters. The development and analysis of estimators, along with simulation results, contribute to our understanding of the underlying model and provide practical insights into statistical inference for SPDEs. Especially the connection between the log-linear model and our SPDE model offers a new link between the two, enabling the application of efficient statistical methods to our SPDE model, which are well-established in the linear model. Furthermore, the R-package `ParabolicSPDEs`[1] offers a valuable tool for simulating and estimating the model parameters. This package provides convenient functionalities to simulate data from the parabolic SPDE model and estimate the associated parameters using various estimation techniques. For a concise overview of the key findings and contributions in Chapters 2 and 3, refer to the publication by Bibinger and Bossert (2023). This paper provides an efficient summary of the main results, methodologies, and insights presented in these chapters, offering a comprehensive understanding of the statistical inference and estimation procedures for the considered one-dimensional SPDE model.

In the second part of this thesis (Part II), we extend the existing research on linear, second-order SPDEs to multiple spatial dimensions. A preliminary step was taken by Tonaki et al. (2023) when they extended the SPDE model to two spatial dimensions. Building upon their work, we further explore the d-dimensional space, thereby enabling the application of statistical methods to multi-dimensional systems. Moving forward, we analyse the task of providing estimators for the model's parameters and subsequently proving asymptotic results. Specifically, we conduct the estimation of the volatility parameter, as well as the natural parameters of the d-dimensional SPDE model. To the best of our knowledge, this extension to higher spatial dimensions has not been previously studied.

To begin, Chapter 4 establishes the theoretical framework required for analysing SPDEs in multiple space dimensions. This chapter addresses the absence of previous research on higher spatial dimensions and covers the necessary mathematical foundations for statistical inference. Similar to Part I, we employ the spectral decomposition technique, which allows us, under certain conditions, to decompose a solution using discrete Fourier analysis. However, in higher spatial dimensions, accurately approximating the resulting series from the Fourier transform necessitates advanced techniques, particularly in the context of Riemann approximations. Once the theoretical framework is in place, we adopt the approach of estimating model parameters using realized volatility. Initially, we investigate the identifiability of the model parameters and construct a method of moments estimator for the volatility parameter in the multi-dimensional SPDE. Notably, a significant difference between one-dimensional and multi-dimensional settings is the introduction of a new parameter, which we refer to as the damping parameter. The emergence of this parameter naturally occurs when transitioning from one space dimension to multiple dimensions. Its inclusion is essential to guarantee that the solution process is square-integrable, i.e., $\mathbb{E}[\|X_t\|_\vartheta^2] < \infty$. The damping parameter influences the roughness of the temporal marginal processes of the solution field and therefore fundamentally affects the underlying model structure. We conclude this chapter by discussing two simulation methods for simulating the presented linear, second-order SPDE model in multiple spatial dimensions. Of particular interest is the extension of a simulation method introduced by Hildebrandt (2020) for one spatial dimension to higher dimensions. This extension demonstrates the applicability and effectiveness of the method in handling complex multi-dimensional SPDE models. Furthermore, to facilitate simulations, parameter estimations, and result visualizations, we provide a useful tool, the R-package `SecondOrderSPDEMulti`[2]. This package offers convenient

[1]see: https://github.com/pabolang/ParabolicSPDEs.
[2]see: https://github.com/pabolang/SecondOrderSPDEMulti.

functionalities for simulating, estimating, and plotting multi-dimensional SPDEs, making the analysis of such models more accessible and efficient.

In Chapter 5, our attention shifts towards the volatility estimator, and we delve into proving both its consistency and a central limit theorem (CLT). To achieve this, we conduct an analysis that involves the careful examination and appropriate bounding of temporal dependencies for quadratic increments in higher spatial dimensions. To validate our theoretical findings and assess the performance of the volatility estimator, we provide simulation results at the end of this chapter. These simulations underscore the theoretical findings and provide valuable insights into its behaviour under various scenarios.

As we establish consistency and a central limit theorem for the volatility estimator in Chapter 5, we simultaneously lay the foundation for extending the realized volatilities, used for estimating the volatility of the random field, to a log-linear model. Building on the approach introduced in Chapter 3, Chapter 6 takes a step further and addresses the estimation of the natural parameters of the multi-dimensional SPDE model. This involves a systematic and rigorous examination of the model's natural parameters, allowing us to gain deeper insights into their behaviour and impact on the overall model structure. To be more precise, our findings will demonstrate that the realized volatilities exhibit asymptotic equivalence to a log-linear model, which allows us to transfer statistical inference methods, well-known in the theory of linear models.

Moreover, in Chapter 6, we introduce an estimator for the damping parameter, drawing inspiration from a commonly used technique for estimating the Hurst parameter in fractional Brownian motions. This estimator provides key information on the roughness of the temporal marginal processes and plays a crucial role in understanding the behaviour of the SPDE model in multiple spatial dimensions. To support our theoretical findings, we present simulation results for all the estimators introduced in Chapter 6.

In conclusion, Part II of this thesis delves into the theoretical and practical aspects of analysing SPDEs in multiple spatial dimensions. The research conducted in Part II significantly contributes to our understanding of SPDEs in higher dimensions, providing essential theoretical foundations, parameter estimation techniques, and simulation methods. With practical applications in various fields, the findings from Part II offer valuable insights and open new avenues for future research in the field of SPDE analysis. The research undertaken in the second part of this thesis is also accessible in the recent preprint Bossert (2023). This paper serves as a concise and efficient summary of the substantial results within Part II.

The thesis concludes with Chapter 7, which summarizes the new findings of Part I and Part II and situates them within the existing research landscape. Additionally, an outlook section discusses open questions and offers some intuitive approaches for future exploration.

In Part III of the thesis, we present the thesis appendices. Within these appendices, we provide a comprehensive overview of the notational conventions used in this thesis in Appendix A. Additionally, Appendix B offers additional plots related to the simulation studies discussed in Part II. A reference for the R-codes used for simulations and plotting of the theoretical results within this thesis can be found on the webpage `R-codes-Bossert-Ph.D.-thesis`[3].

[3] see: `https://github.com/pabolang/R-codes-Bossert-Ph.D.-thesis`.

Part I.

One-Dimensional Stochastic Partial Differential Equation

1. Essentials of one-dimensional SPDEs

In this chapter, we delve into the analysis of linear parabolic stochastic partial differential equations with additive noise. Given their inherent complexity, understanding and studying SPDEs often necessitate a combination of probabilistic techniques and functional analysis. Therefore, we begin by introducing the spectral approach, a valuable tool for tackling SPDEs, and lay the theoretical groundwork for the first part of this thesis. Linear SPDEs in one spatial dimension have been extensively studied in the past few decades, and their insights prove to be crucial for deriving new understanding in this first part of the thesis. Hence, we recall essential results from this research, particularly those presented by Bibinger and Trabs (2020) and Hildebrandt and Trabs (2021), as they play a fundamental role in the upcoming analysis and provide a strong foundation for the subsequent exploration of more complex SPDE models.

1.1. Introduction of the model and statistical assumptions

For the first part of this thesis we consider the following linear parabolic stochastic partial differential equation:

$$\left[\begin{array}{ll} \mathrm{d}X_t(y) = \Big(\vartheta_2 \frac{\partial^2}{\partial y^2} X_t(y) + \vartheta_1 \frac{\partial}{\partial y} X_t(y) + \vartheta_0 X_t(y)\Big)\,\mathrm{d}t + \sigma\,\mathrm{d}B_t(y), & (t,y) \in \mathbb{R}^+ \times [y_{min}, y_{max}] \\ X_0(y) = \xi(y), & y \in [y_{min}, y_{max}] \\ X_t(y_{min}) = X_t(y_{max}) = 0, & t \geqslant 0 \end{array}\right] \tag{1}$$

in one spatial dimension with deterministic parameters $\vartheta_0, \vartheta_1 \in \mathbb{R}$ and $\vartheta_2, \sigma > 0$. We consider without loss of generality $(t, y) \in \mathbb{R}^+ \times [0, 1]$, where we set the spatial domain to be the unit interval. Nevertheless, a generalization of the spatial domain to an arbitrary bounded domain can be concluded easily. Since we need an entirely different theory for unbounded spatial domains, we will focus on bounded domains throughout. For reference for a SPDE model with unbounded spatial domain consider Bibinger and Trabs (2019) or Chong (2020a). The stochastic influence in this model is given by a cylindrical Brownian motion $B = (B_t(y))$ in a Sobolev space on $[y_{\min}, y_{\max}] = [0, 1]$. Furthermore, we consider a Dirichlet boundary condition and we want the initial condition ξ to be independent from the cylindrical Brownian motion B. For a brief discussion on other choices of boundary conditions, refer to Bibinger and Trabs (2020).

1.1.1. Probabilistic structure

Two main approaches have been established for statistical inference for SPDE models. An approach commonly known as discrete sampling utilizes discrete observations in both time and space, leading to the development of statistical inference methods. The core concept of this method bears resemblance to the approach used for estimating the volatility coefficient in finite-dimensional diffusions, employing quadratic variation arguments or in general power variations. For references on this approach, we refer the reader to Cialenco and Huang (2020), Pospíšil and Tribe (2007), Kaino and Uchida (2021b) and Bibinger and Trabs (2019). The spectral approach is a powerful and widely used method for analysing SPDEs. This approach stands out as an effective technique for studying SPDEs due to its ability to decompose solution processes using discrete Fourier analysis. By decomposing the solution processes of SPDEs using Fourier analysis, we gain insights into the underlying dynamics and behaviour of the systems. One of the key advantages of the spectral approach is its ability to handle both linear and nonlinear SPDEs. To explore the spectral approach for nonlinear equations, refer to the work by Cialenco and Glatt-Holtz (2011). This flexibility makes it applicable to a wide range of real-world problems. Moreover, the spectral approach has shown great success in capturing the spatial and temporal characteristics of uncertainties in a computationally efficient manner, cf. Section 2.5. In addition to its practical applicability, the spectral approach has undergone significant advancements in recent years, leading to a deeper understanding of SPDEs. Researchers have developed refined techniques, improved convergence properties, and extended the approach to handle more complex scenarios. The origins of this approach can be traced back to the works of Huebner et al. (1993) and Huebner and Rozovskii (1995), as referenced in the literature.

In this part of the first chapter, we will explore the spectral approach for SPDEs in detail. We will delve into the mathematical foundations of Fourier analysis, its application to SPDEs, and the insights it provides into the behaviour and properties of these systems. For details on discrete Fourier analysis see, for instance, Stein and Shakarchi (2011). Additionally, we will conduct an examination of the most recent advancements in the field, focusing on the research conducted by Bibinger and Trabs (2020). This work has contributed significantly to the understanding and application of the spectral approach for SPDEs, shedding light on novel techniques and insights that have emerged in recent times. By analysing and discussing the findings of this research, we aim to stay at the forefront of the field's progress and identify potential avenues for further exploration and development in Chapters 2 and 3.

For understanding the core concept of the spectral approach we consider a Hilbert space

$$H_\vartheta := \{f : [0,1] \to \mathbb{R} : \|f\|_\vartheta < \infty, f(0) = f(1) = 0\},$$

with an inner product $\langle \cdot, \cdot \rangle_H$ defined by

$$\langle f, g \rangle_\vartheta := \int_0^1 \exp[\vartheta_1 y/\vartheta_2] f(y) g(y) \, \mathrm{d}y \quad \text{and} \quad \|f\|_\vartheta := \langle f, f \rangle_\vartheta = \int_0^1 \exp[\vartheta_1 y/\vartheta_2] f^2(y) \, \mathrm{d}y.$$

The spectral approach operates under the key assumption that the SPDE model given by equation (1) is diagonalizable. The diagonalizability property of the model pertains to the underlying differential operator A_ϑ defined as

$$A_\vartheta := \vartheta_0 + \vartheta_1 \frac{\partial}{\partial y} + \vartheta_2 \frac{\partial^2}{\partial y^2},$$

where the SPDE model can be written as

$$\mathrm{d}X_t = A_\vartheta X_t \, \mathrm{d}t + \sigma \, \mathrm{d}B_t.$$

The eigenfunctions $(e_k)_{k\in\mathbb{N}}$ of A_ϑ and the corresponding eigenvalues $(-\lambda_k)_{k\in\mathbb{N}}$ are given by

$$e_k(y) = \sqrt{2}\sin(\pi k y)\exp[-\vartheta_1 y/(2\vartheta_2)] \qquad \text{and} \qquad \lambda_k := -\vartheta_0 + \vartheta_1^2/(4\vartheta_2) + \vartheta_2\pi^2 k^2, \tag{2}$$

where $y \in [0,1]$ and $k \in \mathbb{N}$. The functions $(e_k)_{k\in\mathbb{N}}$ represent a system of eigenfunctions that form a complete orthonormal system in H_ϑ. Indeed, through standard calculations it can be proved that $(e_k)_{k\in\mathbb{N}}$ are the eigenvectors belonging to A_ϑ and that $(e_k)_{k\in\mathbb{N}}$ define an orthonormal basis. To derive such a solution, the Sturm-Liouville problem can be referenced, as demonstrated by Hartman (1982, p. 337 ff.). At this juncture, it is important to highlight a few key points. First, the inner product $\langle\cdot,\cdot\rangle_\vartheta$ includes a rescaling factor obtained from the exponential function which also hinges on the parameters ϑ_1/ϑ_2. It is also possible to think of different choices of the inner product, cf. Bibinger and Trabs (2020, Remark 2.3.) or under more restrictive assumptions to the observations scheme see Section 2.5.1. Furthermore, we obtained the differential operator A_ϑ to be diagonalizable. When working with SPDEs involving a differential operator as the corresponding operator to the model, it becomes necessary to consider bounded domains when implementing the spectral approach. We choose the Hilbert space H_ϑ as the state space for the solutions in the SPDE model from equation (1) and suppose that the initial condition $\xi \in H_\vartheta$. In addition, the differential operator is self-adjoint on H_ϑ, which can be shown by standard calculations. The spectral approach enables us to decompose a solution process of equation (1). To achieve this, we need to define our understanding of a solution for the underlying SPDE model given by equation (1). In the study of stochastic processes, one important concept is that of mild solutions. These solutions provide a powerful framework for understanding the dynamics of various stochastic systems, ranging from ordinary differential equations to partial differential equations driven by stochastic processes. Mild solutions offer a flexible and tractable approach to analyse the behaviour of stochastic processes over time. Unlike strong solutions, which require strong continuity and differentiability properties, mild solutions provide a more relaxed notion of solutions that can handle a wider range of equations and noise structures. A mild solution is based on the variations of constants and delivers a solution process X_t, which is separated into the initial condition and a time developing process driven by a cylindrical Brownian motion B. In detail, a process $(X_t)_{t\geqslant 0}$ is said to be a mild solution of equation (1) if it satisfies

$$X_t = e^{tA_\vartheta}\xi + \int_0^t e^{(t-s)A_\vartheta}\sigma\,\mathrm{d}B_s, \tag{3}$$

for all $t \geqslant 0$ almost surely. For details on existence and uniqueness of mild solutions, cf. Da Prato and Zabczyk (2014, Thm. 7.7. ff.). The cylindrical Brownian motion B can be expressed via

$$\langle B_t, f\rangle_H = \sum_{k=1}^{\infty}\langle f, e_k\rangle_H W_t^k \tag{4}$$

using the orthonormal system $(e_k)_{k\in\mathbb{N}}$ of the Hilbert space H from equation (2), where $f \in H$ and with independent Brownian motions $(W_t^k)_{t\geqslant 0}$, for all $k \geqslant 1$. For details on cylindrical Brownian motions, see, for instance, Gawarecki and Mandrekar (2010). Combining the mild solution from equation (3) with discrete Fourier transformation as used in the spectral approach, the random field X_t can be represented as the infinite factor model

$$X_t(y) = \sum_{k=1}^{\infty} x_k(t)e_k(y), \qquad \text{with} \qquad x_k(t) = e^{-\lambda_k t}\langle \xi, e_k\rangle_\vartheta + \sigma \int_0^t e^{-\lambda_k(t-s)}\,\mathrm{d}W_s^k, \tag{5}$$

where the coordinate processes are $x_k := \langle X_t, e_k\rangle_\vartheta$, for any $k \in \mathbb{N}$. In addition, the coordinate processes x_k satisfy the Ornstein-Uhlenbeck dynamic, which is

$$\mathrm{d}x_k(t) = -\lambda_k x_k(t)\,\mathrm{d}t + \sigma_t\,\mathrm{d}W_t^k,$$

with $x_k(0) = \langle \xi, e_k\rangle_\vartheta$, for all $k \in \mathbb{N}$. Furthermore, we can assume $(t, y) \mapsto X_t(y)$ to be continuous, since there exists a stochastic convolution $\int_0^\cdot e^{(\cdot-s)A_\vartheta}\sigma_s\,\mathrm{d}B_s$, which is continuous in time and space, cf. Da Prato and Zabczyk (2014, Thm. 5.22.).

1.1.2. Statistical assumptions

Statistical assumptions play a crucial role in SPDE modelling, providing a framework to capture and analyse the uncertainties inherent in these complex systems. Additionally, statistical assumptions are often made regarding the spatial and temporal correlations within the SPDE model. Controlling these correlations are crucial for statistical inference. Our primary focus lies in parameter estimation using a discrete observation scheme of a solution process denoted as $X = X_t(y), (t_i, y_j) \in [0, T] \times [0, 1]$, with $i = 1, \ldots, n$ and $j = 1, \ldots, m$, where $T > 0$ is a predetermined constant. Specifically, our analysis will operate within a high-frequency framework, where we consider $T = 1$ and equidistant temporal points $t_i = i\Delta_n = i/n$. As we expand upon the research conducted by Bibinger and Trabs (2020), we incorporate the assumptions they have outlined in this section. The high-frequency observation scheme is recorded in the following assumption.

Assumption 1.1.1 (Observation scheme)
Suppose we observe a mild solution X of the SPDE model from equation (1) on a discrete grid $(t_i, y_j) \in [0, 1]^2$, with equidistant temporal observations $t_i = i\Delta_n$, for $i = 1, \ldots, n$ and $\delta \leqslant y_1 < \ldots < y_m \leqslant 1-\delta$, where $n, m \in \mathbb{N}$ and $\delta \in (0, 1/2)$. We consider one of the following two asymptotic regimes, respectively:

(I) $\Delta_n \to 0$, as $n \to \infty$, while $n\Delta_n = 1$ and $m < \infty$ is fixed,

(II) $\Delta_n \to 0$ and $m = m_n \to \infty$, as $n \to \infty$, while $n\Delta_n = 1$ and $m = \mathcal{O}(n^\rho)$ for some $\rho \in (0, 1/2)$.

Furthermore, we consider $m \cdot \min_{j=2,\ldots,m} |y_j - y_{j-1}|$ is bounded from below, uniformly in n for both regimes.

Note that Assumption 1.1.1 especially implies $m_n^2\Delta_n \to 0$ and $m_n \log(m_n)\Delta_n^{1/2} \to 0$, as $n \to \infty$. Considering the presence of a Dirichlet boundary condition in the SPDE model from equation (1), it is expected that the solution process X will converge towards zero near the spatial domain's edge. This deterministic influence becomes increasingly pronounced in proximity to the spatial boundary. Consequently, meaningful estimators for the parameters $\vartheta = (\vartheta_0, \vartheta_1, \vartheta_2)^\top$ and σ can only be obtained at a relative distance $\delta > 0$ away from the boundary. To visually demonstrate this effect, Figure 1.1 illustrates the

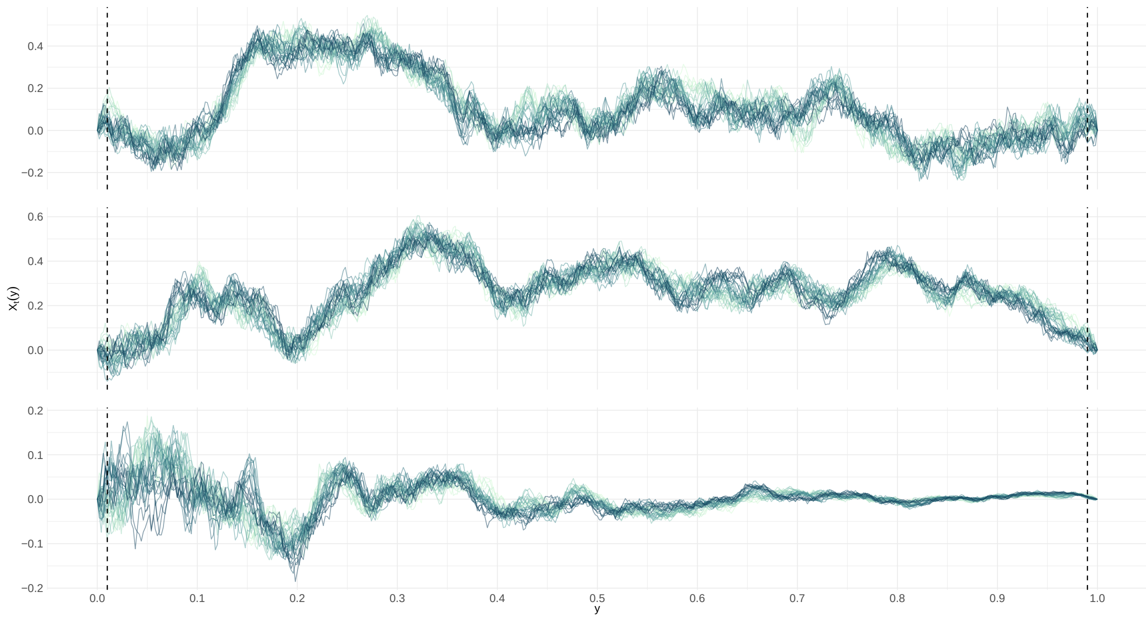

Figure 1.1.: Spatial sample paths of the SPDE model from equation (1) for 60 fixed time points and a possible choice of $\delta \in (0,1)$ indicated by the dashed lines. We simulated the SPDE model with $M = 500$ spatial points and $N = 250.000$ temporal points and with an initial condition $\xi \equiv 0$. The three panels represent three different choices of the parameters $\vartheta_0, \vartheta_1, \vartheta_2, \sigma$. In the top panel we employed $\vartheta_0 = 0, \vartheta_1 = 0, \vartheta_2 = 1, \sigma = 1$, middle: $\vartheta_0 = 0, \vartheta_1 = 1/2, \vartheta_2 = 1, \sigma = 1$, bottom: $\vartheta_0 = 0, \vartheta_1 = 6, \vartheta_2 = 1, \sigma = 1$.

impact of the boundary condition on 60 sample paths of $X_{t_i}(y)$, where $t_i = (i - 1 + 10^4)\Delta_n \in [0,1]$ and $i = 1, \ldots, 60$. The corresponding SPDE model was generated using different combinations of the parameters $\vartheta_0, \vartheta_1, \vartheta_2, \sigma$. In each panel, the dashed line represents an exemplary choice of δ and showcases the deterministic influence of the Dirichlet condition within the range $[0, \delta)$ and $(\delta, 1]$.

The upcoming chapter will reveal the crucial role of the chosen parameter δ in affecting the asymptotic variances in the central limit theorems. Consequently, the selection of δ significantly impacts the quality of the estimation process. When δ is approximately zero, we observe larger errors in the estimations. This occurs because the asymptotically negligible error terms grow larger due to the deterministic influence, requiring a larger number of observations to minimize their impact effectively. Conversely, if δ is approximately equal to $1/2$, we lose a substantial portion of the spatial grid points. Since the high-frequency Assumption 1.1.1 necessitates a finer temporal resolution n compared to the spatial resolution $m = \mathcal{O}(n^\rho)$, we consequently require a significantly larger number of temporal grid points to capture an adequate amount of spatial information. In either case, we require the boundary parameter δ to remain constant and independent of any potential indices.

Furthermore, we introduce the following mild regularity condition for the initial condition ξ.

Assumption 1.1.2 (Regularity)
For the SPDE in equation (1) we assume that

(i) either $\mathbb{E}[\langle \xi, e_k \rangle_\vartheta] = 0$ for all $k \geqslant 1$ and $\sup_k \lambda_k \mathbb{E}[\langle \xi, e_k \rangle_\vartheta^2] < \infty$ holds true or $\mathbb{E}[\|A_\vartheta^{1/2} \xi\|_\vartheta^2] < \infty$,

(ii) $(\langle \xi, e_k \rangle_\vartheta)_{k \geqslant 1}$ are independent.

This assumption holds particularly true when the random variable ξ follows the stationary distribution of the SPDE model from equation (1). Stationarity assumptions are frequently employed in SPDE modelling. Stationarity assumes that the statistical properties of the system remain invariant across space or time, simplifying the analysis and estimation procedures. In this case, the inner products $\langle \xi, e_k \rangle_\vartheta$ are independently distributed as $\mathcal{N}(0, \sigma^2/(2\lambda_k))$. When considering a stationary initial condition, the random field becomes Gaussian. This is due to the independence of $(\langle \xi, e_k \rangle_\vartheta)_{k \geqslant 1}$, and as a result, the random field can be fully characterized by its covariance structure. Assuming independence of the sequence $(\langle \xi, e_k \rangle_\vartheta)_{k \geqslant 1}$ also provides a convenient condition for analysing the variance-covariance structure of our upcoming estimators. To conclude, we note that $\mathbb{E}[\|A_\vartheta^{1/2} \xi\|_\vartheta^2] < \infty$ implies $\sup_{k \in \mathbb{N}} \lambda_k \mathbb{E}[\langle \xi, e_k \rangle_\vartheta^2] = \sup_{k \in \mathbb{N}} \mathbb{E}[\langle A_\vartheta^{1/2} \xi, e_k \rangle_\vartheta^2] < \infty$.

1.2. Basic properties and essential theorems

We initiate this section by exploring the influence of the parameters $(\vartheta_0, \vartheta_1, \vartheta_2, \sigma)$ on sample paths, accompanied by graphical examples. However, we provide an argumentative insight into the effects of these parameters on a solution process X. In the preceding section, we established the theoretical framework by introducing an orthonormal system and subsequently a Fourier decomposition of a solution process for the SPDE model given in equation (1). Within this factor model, a clear separation exists between the temporal coordinates represented by the stochastic coordinate processes $(x_k(t))_{k \in \mathbb{N}}$ and the spatial coordinates determined by the deterministic eigenfunctions $(e_k(y))_{k \in \mathbb{N}}$. Therefore, we can leverage this framework to examine the influence of the parameters $(\vartheta_0, \vartheta_1, \vartheta_2, \sigma)$ on a solution process X. To enhance our argumentative insight, we present the following covariance structure:

$$\mathbb{C}\mathrm{ov}\big(\tilde{X}_s(y_1), \tilde{X}_t(y_2)\big) = \sigma^2 \sum_{k \in \mathbb{N}} \frac{e^{-\lambda_k |t-s|}}{2\lambda_k} e_k(y_1) e_k(y_2), \tag{6}$$

where $\tilde{X}$ denotes a mild solution with stationary initial condition and $y_1, y_2 \in [0,1]$, $s, t \geqslant 0$. This covariance structure can be observed by the following calculations:

$$\mathbb{C}\mathrm{ov}\big(\tilde{X}_s(y_1), \tilde{X}_t(y_2)\big) = \sum_{k \in \mathbb{N}^d} e_k(y_1) e_k(y_2) \mathbb{E}[\tilde{x}_k(s) \tilde{x}_k(t)]$$

and

$$\mathbb{E}[\tilde{x}_k(s) \tilde{x}_k(t)] = \sigma^2 \frac{e^{-\lambda_k (s+t)}}{2\lambda_k} + \sigma^2 e^{-\lambda_k (s+t)} \mathbb{E}\Big[\Big(\int_0^{\min(s,t)} e^{\lambda_k s} \, \mathrm{d}W_s^k \Big)^2\Big]$$

$$= \sigma^2 \frac{e^{-\lambda_k(s+t)}}{2\lambda_k} + \sigma^2 e^{-\lambda_k(s+t)} \left(\frac{e^{2\lambda_k \min(s,t)} - 1}{2\lambda_k} \right),$$

where we used equation (5), Assumption 1.1.2 and Itô isometry.

The parameter ϑ_0 solely affects the eigenvalues within the coordinate processes. By considering the structure of the coordinate processes and the eigenvalues, we observe that ϑ_0 seems to have a visually minimal impact on the solution X, as it is not connected to the index $k \in \mathbb{N}$. In addition, the covariance structure given in display (6) confirms this conjecture. Furthermore, classical theory in statistics for stochastic processes indicates that a drift parameter, such as ϑ_0, cannot be consistently estimated within a fixed time horizon. Similar conclusions hold true for the linear SPDE model in equation (1) as also demonstrated in Hildebrandt and Trabs (2021, Prop. 2.3.). Consequently, the parameter ϑ_0 is not identifiable within a fixed time horizon, leading us to set $\vartheta_0 = 0$ in our simulations. For further insights into the estimation of the parameter ϑ_0, Kaino and Uchida (2021b) provides a valuable resource. However, note that in the general form of an SPDE, the drift term is typically considered as a function of the state variables and time. This drift term introduces a deterministic component that governs the evolution of the stochastic process, in contrast to the random fluctuations represented by the noise term. For comprehensive readings on the definition of SPDE models with such understanding of the drift term and estimation methods for this context, Cialenco and Huang (2020) and Cialenco et al. (2020) offer valuable references. These works delve into the mathematical foundations and practical implications of drift modelling in SPDEs, shedding light on the complexities involved in estimating the drift parameters in these dynamic systems.

In contrast, the parameter ϑ_1 exhibits a noticeable impact on the solution process. When $\vartheta_1 \neq 0$, we observe an effect on both the noise level of the temporal process and the spatial process. Particularly, the influence on the spatial process is visually discernible. In this case, $\vartheta_1 \neq 0$ leads to varying levels of fluctuations within the spatial dimension, resulting in lower fluctuations in one half of the spatial domain $[0, 1]$ compared to the other half. For the influence of $\vartheta_1 \neq 0$ on the noise level of the temporal process, the author Hildebrandt (2021) pointed out, that by assuming a stationary initial condition, the solution process $\tilde{X}_t(y)$ approximately looks like $e^{-y\vartheta_1/(2\vartheta_2)} X'_t(y)$, where X'_t solves the equation $\mathrm{d}X'_t = \vartheta_2 \partial^2/(\partial y^2) X'_t \,\mathrm{d}t + \sigma \,\mathrm{d}B_t$. Consequently, when $\vartheta_1 = 0$, the solution field does not exhibit any curvature. In this scenario, the orthonormal system simplifies to a sine basis, and the inner product becomes unweighted. Figure 1.2 presents a visual representation in the top panel, offering an impression of the observed data. Note that a negative choice of ϑ_1 significantly scales up the solution process. This impact becomes evident when examining the exponential term $e^{-\vartheta_1/\vartheta_2 y}$ present in the eigenfunctions (e_k), where $\vartheta_2 > 0$ is always a positive parameter.

The parameters (ϑ_2, σ) significantly impact the noise level of the random field. Specifically, the parameter σ directly governs the overall noise level of the solution field, which is evident from the covariance structure in display (6). This becomes even more apparent when considering that σ is directly linked to the additive noise in equation (1). Hence, we refer to the parameter σ as the volatility. Conversely, as the parameter ϑ_2 increases, it diminishes the impact of noise while simultaneously weakening the curvature effect driven by ϑ_1. To provide a visual understanding of different choices of (ϑ_2, σ), the middle and bottom panels of Figure 1.2 showcase various scenarios. Notably, in the last panel, we observe that the parameter ϑ_2 can counteract the curvature effect induced by the parameter ϑ_1.

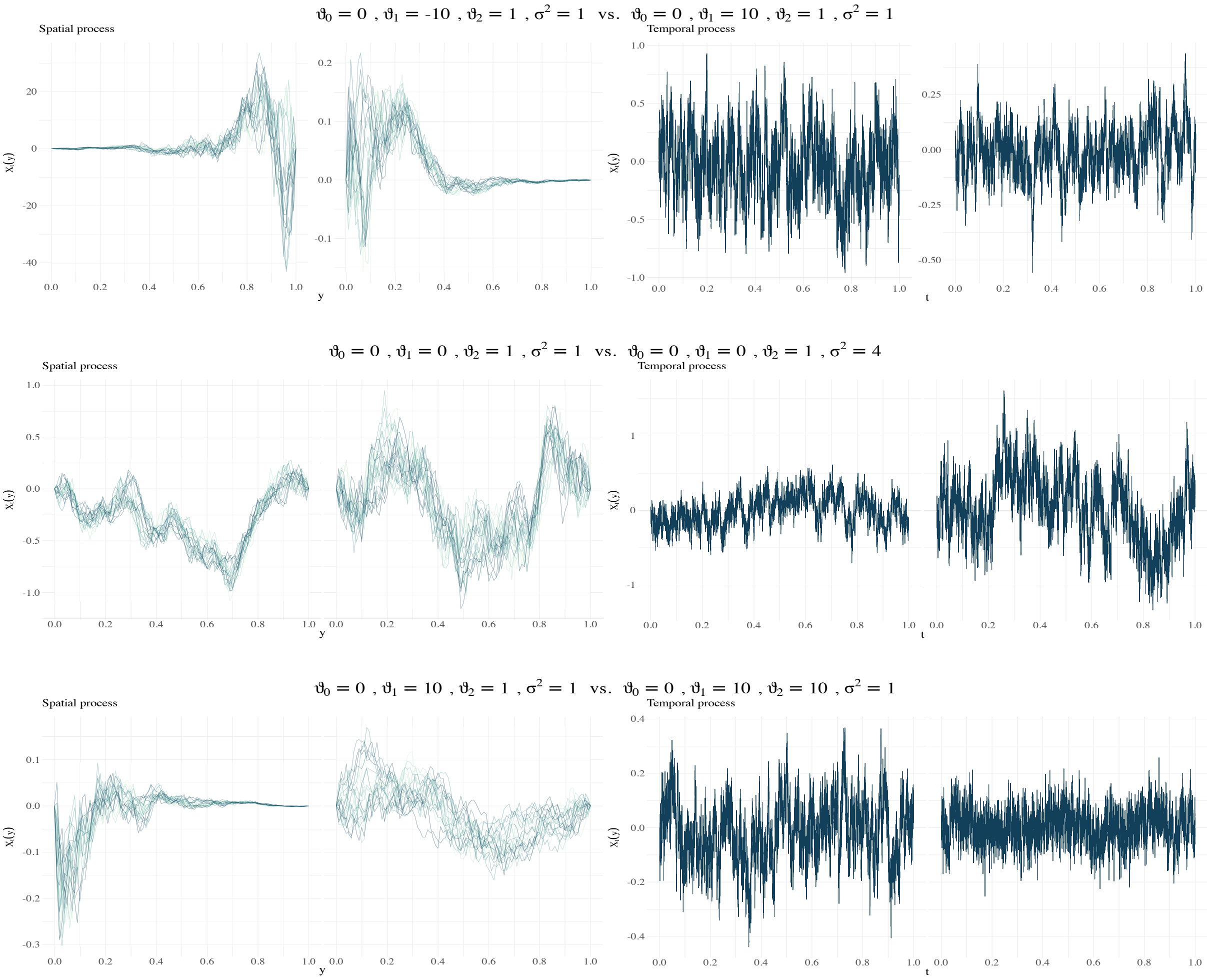

Figure 1.2.: The figure presented depicts sample paths of the SPDE model, as outlined in equation (1). The sample paths are generated using an equidistant grid in both time and space, where $N = 10^4$, $M = 100$, and $\xi \equiv 0$. Each row of the figure consists of four plots. The first two plots on the right showcase the spatial processes, $y \mapsto X_t(y)$, for $t = 0.1 + k/10^3$ where $k = 0, \ldots, 20$. The last two plots exhibit the temporal processes, $t \mapsto X_t(y)$, with $y = 1/10$. The specific parameter choices for each row are indicated in the title. In each row, the first spatial and temporal plots correspond to the first parameter choice mentioned in the title, while the remaining plots correspond to the second option. Note that only the top panel has a freely adjustable y-scale, whereas the other panels share a common y-scale.

The identifiability of parameters in a SPDE model is a crucial aspect in understanding and analysing the underlying dynamics of the system. Identifiability refers to the ability to uniquely estimate the values of model parameters based on observed data. In the context of SPDE models, it pertains to determining whether the parameters governing the stochastic processes can be accurately estimated or distinguished from each other using available information. Therefore, assume the parameters $(\vartheta_1, \vartheta_2, \sigma)$ to be unknown. In their study, Hildebrandt and Trabs (2021) demonstrated that consistent estimation is only possible for the quantity $\sigma_0^2/e^{-\kappa y_0}$ when utilizing high frequency observations within a finite time horizon and on a single spatial observation $y_0 \in [\delta, 1-\delta]$, which especially corresponds to Assumption 1.1.1. Here, the parameters κ and σ_0^2 are defined as follows:

$$\kappa := \frac{\vartheta_1}{\vartheta_2} \quad \text{and} \quad \sigma_0^2 := \frac{\sigma^2}{\sqrt{\vartheta_2}}.$$

This result highlights the specific parameter combination that can be consistently estimated in the presence of high-frequency observations. Henceforth, our focus will be directed towards estimating two crucial parameters: the curvature parameter $\kappa \in \mathbb{R}$ and the normalized volatility parameter $\sigma_0^2 > 0$. Note that the orthonormal system $(e_k)_{k\in\mathbb{N}}$ now exhibits a representation that is dependent on the parameter κ. In the forthcoming chapters, specifically Chapters 2 and 3, we will present estimators for both of these natural parameters, κ and σ_0^2. Let X be a mild solution of the SPDE model from equation (1) with an arbitrary initial condition and $\tilde{X}$ be a mild solution with an stationary choice of the initial condition. The identifiability of parameters in the SPDE model from equation (1) has been demonstrated by Hildebrandt and Trabs (2021) through the use of Gaussian arguments, building upon the earlier work of Ibragimov and Rozanov (2012, Chapter III). In their analysis, the researchers assumed that the initial condition follows a stationary distribution. This assumption was facilitated by the regularity assumptions on ξ, as outlined in Assumption 1.1.2. Consequently, any choice of ξ could be replaced with a stationary initial condition if the temporal observations n are sufficiently large, cf. Bibinger and Trabs (2020, Lemma 6.4.).

Furthermore, the authors Bibinger and Trabs (2020) showed that the identifiability of the two natural parameters is sharp, where they used a summation over quadratic increments, also known as realized volatility, in order to derive consistent estimators for σ^2 and a M-estimator based on realized volatility for estimating both natural parameters. The realized volatility is defined as the sum of squared increments over a specified time interval, given by

$$\mathrm{RV}_n(y) := \sum_{i=1}^{n} (\Delta_i X)^2(y) := \sum_{i=1}^{n} \left(X_{i\Delta_n}(y) - X_{(i-1)\Delta_n}(y)\right)^2,$$

where $y \in [\delta, 1-\delta]$. Furthermore, the rescaled realized volatility is denoted as $\mathrm{RV}_n/\sqrt{n}$, where the rescaling is only with respect to the factor $\sqrt{n}$. However, rescaling can also be understood as $\mathrm{RV}_n \cdot e^{y\kappa}/\sqrt{n}$. Consequently, the exponentially rescaled volatility is defined as

$$V_{p,\Delta_n}(y) := \frac{1}{p\sqrt{\Delta_n}} \sum_{i=1}^{p} (\Delta_i \tilde{X})^2(y) e^{y\kappa},$$

where $1 \leqslant p \leqslant n$. Note that the definition of V_{p,Δ_n} directly employs a mild solution with a stationary initial condition. The incorporation of realized volatility and its rescaled version plays a pivotal role in estimating and analysing the parameters of the SPDE model. Consequently, it is essential to establish fundamental properties of these statistics, as demonstrated by Bibinger and Trabs (2020). We begin by recalling the expected value of the rescaled realized volatility.

Proposition 1.2.1

On Assumptions 1.1.1 and 1.1.2, we have uniformly in $y \in [\delta, 1-\delta]$ that

$$\mathbb{E}\big[(\Delta_i X)^2(y)\big] = \Delta_n^{1/2} e^{-y\kappa} \frac{\sigma_0^2}{\sqrt{\pi}} + r_{n,i} + \mathcal{O}(\Delta_n^{3/2}),$$

for $i = 1, \ldots, n$, with terms $r_{n,i}$ that satisfy $\sup_{1,\ldots,n} |r_{n,i}| = \mathcal{O}(\Delta_n^{1/2})$, $\sum_{i=1}^n r_{n,i} = \mathcal{O}(\Delta_n^{1/2})$, and become negligible when summing all squared increments:

$$\mathbb{E}\left[\frac{\mathrm{RV}_n(y)}{\sqrt{n}}\right] = e^{-y\kappa} \frac{\sigma_0^2}{\sqrt{\pi}} + \mathcal{O}(\Delta_n). \tag{7}$$

The preceding proposition highlights an almost 1/4-Hölder regularity in time, where Hildebrandt and Trabs (2021, Prop. 3.3.) shows an almost 1/2-Hölder regularity in space. This reveals that the paths in time are considerably rougher compared to those in space as supported by the Kolmogorov continuity theorem presented in Stroock and Varadhan (1997). This disparity in regularity justifies the rescaling of the realized volatility by the quantity $\sqrt{\Delta_n}$. Additionally, by rescaling the realized volatility and under Assumption 1.1.1, consistent estimators can be constructed when $m_n = \mathcal{O}(n^\rho)$, with $\rho \in (0, 1/2)$. This assumption especially controls the dependencies inherited by the SPDE model. However, even if this condition is violated, consistent estimators with optimal rates can still be constructed using double increments in both time and space, as shown by Hildebrandt and Trabs (2021). Based on equation (7), Bibinger and Trabs (2020) developed a consistent estimator for the volatility parameter σ^2 using the method of moments, relying on the first moment of the rescaled realized volatility. The resulting estimator is given by

$$\hat{\sigma}_y^2 = \frac{\mathrm{RV}_n(y)}{\sqrt{n}} e^{y\kappa} \sqrt{\pi \vartheta_2},$$

and is derived under the assumption that $\vartheta = (\vartheta_0, \vartheta_1, \vartheta_2)$ is known. Note that this estimator is based on the rescaled realized volatility at a single spatial point, such as $m = 1$. Moreover, Bibinger and Trabs (2020) also constructed an estimator that incorporates multiple spatial points, leveraging the above estimator by taking the average across different spatial coordinates.

The asymptotic theory concerning realized volatility and associated statistics, derived from high-frequency observations of Itô diffusions that solve stochastic differential equations (SDEs), heavily relies on the martingale structure inherent to these processes. This martingale structure, along with various approximation steps, forms the foundation of the asymptotic analysis with general semimartingales, as exemplified in Jacod and Protter (2011), for instance.

One of the primary distinctions between these well-established martingale techniques and our asymptotic analysis of the SPDE model lies in the correlation structure of their discrete increments. In the context of SDE models, the discrete increments are uncorrelated. However, in the SPDE model, we observe negatively correlated discrete-time increments. As a consequence, the proofs of central limit theorems exhibit significant differences and bear more resemblance to asymptotic statistics for fractional diffusions.

According to Bibinger and Trabs (2020, Prop. 3.2.), in the SPDE model, the autocorrelation of the discrete increments decreases as the time gap between the increments increases. This indicates that while the increments may not be perfectly uncorrelated, their correlation diminishes as the gap widens. As the estimation of σ^2 relies on realized volatilities, the analysis of the variance-covariance structure of realized volatility becomes vital for asymptotic results. This crucial aspect is exploited by the following result, as presented in Bibinger and Trabs (2020, Prop. 6.5.).

Proposition 1.2.2
On Assumptions 1.1.1 and 1.1.2, the covariance of the exponentially rescaled realized volatility V_{p,Δ_n} for two spatial points $y_1, y_2 \in [\delta, 1-\delta]$ satisfies for any $\eta \in (0,1)$:

$$\begin{aligned}\mathbb{C}\mathrm{ov}\big(V_{p,\Delta_n}(y_1), V_{p,\Delta_n}(y_2)\big) &= \mathbb{1}_{\{y_1=y_2\}} p^{-1} \Gamma \sigma_0^4 \big(1 + \mathcal{O}(1 \wedge (p^{-1}\Delta_n^{\eta-1}))\big) \\ &\quad + \mathcal{O}\big(p^{-1}\Delta_n^{1/2}(\mathbb{1}_{\{y_1 \neq y_2\}}|y_1-y_2|^{-1} + \delta^{-1})\big),\end{aligned}$$

where $\Gamma \approx 0.75$ is a constant numerically given in equation (8). In particular, we have

$$\mathbb{V}\mathrm{ar}\big(V_{n,\Delta_n}\big) = \frac{\Gamma\sigma_0^4}{n}\big(1+\mathcal{O}(\sqrt{\Delta_n})\big).$$

Analogously, we can exploit the covariance structure of the rescaled realized volatility $\mathrm{RV}_n(y)/\sqrt{n}$ by a simple transformation. Concerning the constant Γ in the variance, we provide the analytical form which is determined by a series of covariances given by

$$\Gamma := \frac{1}{\pi}\sum_{r=0}^{\infty} I(r)^2 + \frac{2}{\pi}, \qquad \text{with} \qquad I(r) := 2\sqrt{r+1} - \sqrt{r+2} - \sqrt{r}. \tag{8}$$

By establishing the variance and covariance structure of the exponentially rescaled realized volatility, Bibinger and Trabs (2020) successfully demonstrated the applicability of a central limit theorem.

Proposition 1.2.3
On Assumptions 1.1.1 and 1.1.2, for any $y \in [\delta, 1-\delta]$ the estimator $\hat{\sigma}_y^2$ obeys, as $n \to \infty$, the central limit theorem

$$n^{1/2}\big(\hat{\sigma}_y^2 - \sigma^2\big) \xrightarrow{d} \mathcal{N}(0, \pi\Gamma\sigma^4).$$

The factor $\Gamma\pi \approx 2.357$ appearing in the asymptotic variance of Proposition 1.2.3 is notably close to the factor 2, which represents the Cramér-Rao lower bound for estimating σ^2 from independent and identically distributed (i.i.d.) standard normals. The difference $(\Gamma\pi - 2)$ precisely accounts for the contribution of the non-negligible covariances of squared increments in the SPDE model from equation (1).

Due to these temporal covariances, conventional methods are insufficient for proving the central limit theorems in the forthcoming chapters. Therefore, it is necessary to employ non-standard approaches. To address this, we conclude this section by introducing a central limit theorem for weakly dependent triangular arrays, as provided by Peligrad et al. (1997). This theorem serves as a valuable tool for establishing the central limit theorems in the subsequent chapters, accounting for the presence of temporal covariances in the model.

Proposition 1.2.4
Let $(Z_{k_n,i})_{1\leqslant i\leqslant k_n}$ be a centred triangular array, with a sequence $(k_n)_{n\in\mathbb{N}}$. Then, it holds

$$\sum_{i=1}^{k_n} Z_{k_n,i} \xrightarrow{d} \mathcal{N}(0, \upsilon^2),$$

with $\upsilon^2 = \lim_{n\to\infty} \mathbb{V}\mathrm{ar}(\sum_{i=1}^{k_n} Z_{k_n,i}) < \infty$ if the following conditions hold:

(I) $\mathbb{V}\mathrm{ar}\Big(\sum_{i=a}^{b} Z_{k_n,i}\Big) \leqslant C \sum_{i=a}^{b} \mathbb{V}\mathrm{ar}(Z_{k_n,i})$, for all $1 \leqslant a \leqslant b \leqslant k_n$,

(II) $\limsup_{n\to\infty} \sum_{i=1}^{k_n} \mathbb{E}[Z_{k_n,i}^2] < \infty$,

(III) $\sum_{i=1}^{k_n} \mathbb{E}\Big[Z_{k_n,i}^2 \mathbb{1}_{\{|Z_{k_n,i}|>\varepsilon\}}\Big] \overset{n\to\infty}{\longrightarrow} 0$, for all $\varepsilon > 0$,

(IV) $\mathbb{C}\mathrm{ov}\Big(e^{\mathrm{i}t\sum_{i=a}^{b} Z_{k_n,i}}, e^{\mathrm{i}t\sum_{i=b+u}^{c} Z_{k_n,i}}\Big) \leqslant \rho_t(u) \sum_{i=a}^{c} \mathbb{V}\mathrm{ar}(Z_{k_n,i})$, for all $1 \leqslant a \leqslant b < b+u \leqslant c \leqslant k_n$ and $t \in \mathbb{R}$,

where $C > 0$ is a universal constant and $\rho_t(u) \geqslant 0$ denotes a function satisfying $\sum_{j=1}^{\infty} \rho_t(2^j) < \infty$.

The first two conditions of the prior CLT are straightforward and require no further explanation. The third condition represents the Lindeberg condition, which is well-known and can be established by verifying a Lyapunov condition. The fourth condition is of particular importance as it governs the covariance structure within the triangular array. Consequently, special attention needs to be given to this condition.

Considering a scenario where we aim to prove a CLT of the form $\sqrt{r_n}(\hat{\theta} - \theta) \overset{d}{\to} \mathcal{N}(0, \upsilon^2)$, where $\hat{\theta} = \sum_{i=1}^{n} \hat{\theta}_i$ represents an estimator for an unknown parameter θ, and r_n denotes the convergence rate. If we want to apply the CLT from Proposition 1.2.4 introduced by Peligrad et al. (1997), then the appropriate choice for the corresponding triangular is given by $Z_{n,i} = \sqrt{r_n}(\hat{\theta}_i - \theta)$. In line with this scheme, we will discuss the selection of triangular arrays for our respective estimators at the beginning of Section 2.4. Nevertheless, alternative methods are available for deriving CLTs for SPDE models. One such approach is the Malliavin-Stein's method, employed by Cialenco and Kim (2022), to derive asymptotic results. This powerful probabilistic technique combines ideas from Malliavin calculus and Stein's method, enabling researchers to obtain quantitative rates of convergence in CLTs. For reference on Stein's method, see, for instance, Diaconis and Holmes (2004), which provides a comprehensive overview of the method. For an introduction to Malliavin calculus, refer to Viens et al. (2013), offering insights into its applications and theory.

2. Parametric estimation of the curvature parameter

The objective of this chapter is to develop a consistent estimator for the curvature parameter $\kappa \in \mathbb{R}$, with an optimal rate of convergence and a smaller asymptotic variance than that of the minimum contrast estimator known from Bibinger and Trabs (2020, Chapter 4). To achieve this, we propose a new estimator, denoted as $\hat{\kappa}$, based on realized volatilities of a mild solution and the knowledge of the normalized volatility parameter σ_0^2 of the SPDE model from equation (1). We establish consistency of $\hat{\kappa}$ and derive a central limit theorem for this new curvature estimator. Furthermore, in the case where σ_0^2 is unknown, we present a second estimator, denoted as $\hat{\varkappa}$, for κ.

To exploit the structure of both estimators, we begin the asymptotic analysis by considering the case where $m \in \mathbb{N}$ is fixed. In the latter part of this chapter, we extend our results to the more general scenario where the temporal and spatial observations n and m tend to infinity. Additionally, we provide statistical tests that allow us to assess whether κ is a valid component of the SPDE model from equation (1) model or not. Finally, we contextualize our new estimators within the existing literature, providing a comprehensive overview of their significance and contributions to the field.

2.1. Motivation

In this chapter, we delve into the development of a new estimator for the curvature parameter κ based on high-frequency observations. Recalling the SPDE model from equation (1) introduced in Chapter 1, the curvature parameter is represented by the quotient $\kappa = \vartheta_1/\vartheta_2 \in \mathbb{R}$. Despite some research using the spectral approach for SPDEs, an efficient estimator that is both consistent and exhibits a preferably small variance for κ remains elusive.

To bridge this gap, we progress towards constructing a novel estimator for the curvature parameter, leveraging the central limit theorem presented in Proposition 1.2.3. Under Assumptions 1.1.1 and 1.1.2, and with a sufficiently large number n of temporal observations, we arrive at the following approximation:

$$\frac{\mathrm{RV}_n(y)}{\sqrt{n}} e^{\kappa y} \sqrt{\pi \vartheta_2} \sqrt{n} \approx \sqrt{n}\sigma^2 + \mathcal{N}\big(0, \Gamma\pi\sigma^4\big). \tag{9}$$

This leads to the subsequent expression:

$$\frac{\mathrm{RV}_n(y)}{\sqrt{n}} \approx e^{-\kappa y} \frac{\sigma_0^2}{\sqrt{\pi}} + \mathcal{N}\left(0, \frac{\Gamma}{n}\sigma_0^4 e^{-2\kappa y}\right).$$

Furthermore, it becomes evident that

$$\frac{\mathrm{RV}_n(y)}{\sqrt{n}} \approx e^{-\kappa y}\sigma_0^2 \cdot \mathcal{N}\left(\frac{1}{\sqrt{\pi}}, \frac{\Gamma}{n}\right).$$

Given that we know the parameter σ_0^2, we can estimate the parameter κ using the following calculations:

$$\ln\left(\frac{\mathrm{RV}_n(y)}{\sqrt{n}}\right) \approx -\kappa y + \ln(\sigma_0^2) + \ln\left(\frac{1}{\sqrt{\pi}} + \sqrt{\frac{\Gamma}{n}}Z\right),$$

where $Z \sim \mathcal{N}(0,1)$. Let $y_1,\ldots,y_m \in [\delta, 1-\delta]$ denote spatial points for a suitable $\delta \in (0,1/2)$, and $Z_1,\ldots,Z_m$ i.i.d. standard normal random variables. By using the first-order Taylor expansion of the natural logarithm, we obtain that

$$\ln\left(\frac{\mathrm{RV}_n(y_j)}{\sqrt{n}}\right) \approx -\kappa y_j + \ln(\sigma_0^2) + \ln\left(\frac{1}{\sqrt{\pi}}\left(1 + \sqrt{\frac{\Gamma\pi}{n}}Z_j\right)\right) \approx -\kappa y_j + \ln(\sigma_0^2) + \ln\left(\pi^{-1/2}\right) + \sqrt{\frac{\Gamma\pi}{n}}Z_j, \tag{10}$$

for $j = 1,\ldots,m$. As the variance of $n^{-1/2}Z_j$ decreases with increasing $n \in \mathbb{N}$, using the first-order Taylor expansion appears sufficient. However, we will discuss this technical detail in Section 2.2. Reordering the latter expression yields

$$\kappa \approx \frac{-\ln\left(\frac{\mathrm{RV}_n(y_j)}{\sqrt{n}}\right) + \ln\left(\frac{\sigma_0^2}{\sqrt{\pi}}\right)}{y_j} + \frac{1}{y_j}\cdot\sqrt{\frac{\Gamma\pi}{n}}Z_j. \tag{11}$$

Thus, κ can be regarded as the unknown expected value of a normal distribution with a variance that depends on the respective spatial coordinates. In the upcoming example, we will briefly discuss the maximum likelihood estimation in a related statistical model.

Example 2.1.1
Consider a model with independent random variables $Y_i \sim \mathcal{N}(\mu, \varsigma_i^2)$, where μ is unknown, and $\varsigma_i^2 > 0$ is known for $i = 1,\ldots,m$. The maximum likelihood estimator (MLE) with the likelihood function

$$L_m(\mu; y) = \prod_{i=1}^m \frac{1}{\sqrt{2\pi\varsigma_i^2}}\exp\left[-\frac{(y_i-\mu)^2}{2\varsigma_i^2}\right]$$

is given by

$$\hat{\mu} = \frac{\sum_{i=1}^m Y_i\varsigma_i^{-2}}{\sum_{i=1}^m \varsigma_i^{-2}}. \tag{12}$$

If the random variables Y_i have a common scaling parameter in the variance, i.e., $Y_i \sim \mathcal{N}(\mu, a\varsigma^2)$, where $a > 0$, we still derive the same MLE since this parameter is part of the variance of every observation. Furthermore, we can analyse the expected value and variance of the MLE $\hat{\mu}$ in this model, where we have

$$\mathbb{E}[\hat{\mu}] = \mu \qquad \text{and} \qquad \mathbb{V}\mathrm{ar}(\hat{\mu}) = \left(\sum_{i=1}^m \varsigma_i^{-2}\right)^{-1}.$$

In the latter example, the term ς_i^{-2} can be viewed as Fisher information of observing Y_i. Hence, efficiency of the MLE in this model is implied by standard asymptotic statistics. Utilizing the weighted average estimator within the model $\mu = \kappa$ and $\varsigma_i^2 = y_i^{-2}$, and incorporating the approximation from display (11) for estimating κ, we obtain the following estimator:

$$\hat{\kappa} := \hat{\kappa}_{n,m} := \frac{\sum_{j=1}^{m}\Big(\frac{-\ln\big(\frac{\mathrm{RV}_n(y_j)}{\sqrt{n}}\big)+\ln\big(\frac{\sigma_0^2}{\sqrt{\pi}}\big)}{y_j}\Big)y_j^2}{\sum_{j=1}^{m} y_j^2} = \frac{-\sum_{j=1}^{m}\ln\Big(\frac{\mathrm{RV}_n(y_j)}{\sqrt{n}}\Big)y_j + \sum_{j=1}^{m}\ln\Big(\frac{\sigma_0^2}{\sqrt{\pi}}\Big)y_j}{\sum_{j=1}^{m} y_j^2}. \tag{13}$$

Hence, we have derived an oracle estimator for the curvature parameter, assuming that the normalized volatility σ_0^2 is known. Note that we have neglected the expression $\sqrt{\Gamma\pi/n}$ since it scales the variance uniformly.

The notation of this estimator indicates the use of a spatial resolution with $m \in \mathbb{N}$ coordinates, where each spatial point $y_j \in [\delta, 1-\delta]$ for some $\delta \in (0, 1/2)$. However, the relation between the spatial and temporal resolution is predetermined by Assumption 1.1.1. As the rescaled realized volatility is only asymptotically normally distributed, we can anticipate that $\hat{\kappa}$ is asymptotically unbiased. By referring to Example 2.1.1, we can expect an asymptotic variance (AVAR) of $\Gamma\pi\big(\sum_{j=1}^{m} y_j^2\big)^{-1}$ for the rescaled estimator $n^{1/2}\hat{\kappa}$, when m remains finite. We will discuss the asymptotic variance for the case where $m = m_n \to \infty$ in Section 2.4.

During the construction of this first estimator for κ, we capitalized on the natural logarithm of the rescaled realized volatility. Furthermore, Example 2.1.1 demonstrated that we can anticipate the asymptotic variance to be a known constant. In particular, the asymptotic variance is independent of the unknown parameter κ or any other model parameter. This is because we employ a variance-stabilizing transformation, which is achieved by using the natural logarithm. This fact is evident from the central limit theorem presented in Proposition 1.2.3. Defining $g_y(x) = \ln(xe^{-\kappa y}(\pi\vartheta_2)^{-1/2})$. By employing the delta method, we can show that

$$\sqrt{n}\big(g_y(\hat{\sigma}_y^2) - g_y(\sigma^2)\big) = \sqrt{n}\bigg(\ln\Big(\frac{\mathrm{RV}_n(y)}{\sqrt{n}}\Big) + \kappa y - \ln\Big(\frac{\sigma_0^2}{\sqrt{\pi}}\Big)\bigg) \xrightarrow{d} \mathcal{N}\Big(0, \Gamma\pi\sigma^4\big(g_y'(\sigma^2)\big)^2\Big) = \mathcal{N}(0, \Gamma\pi).$$

As a result, we can construct confidence intervals without any dependence on the model parameters.

By utilizing the same ideas as before, it is possible to construct an estimator for κ without any knowledge of the normalized volatility parameter σ_0^2. To achieve this, we revisit the approximation (10). By leveraging the basic properties of the logarithm, we eliminate the unknown parameter σ_0^2 by subtracting two logarithmized rescaled realized volatilities at different spatial points $y_j \neq y_k$. Performing this operation, we obtain

$$\ln\Big(\frac{\mathrm{RV}_n(y_j)}{\mathrm{RV}_n(y_k)}\Big) = \ln\Big(\frac{\mathrm{RV}_n(y_j)}{\sqrt{n}}\Big) - \ln\Big(\frac{\mathrm{RV}_n(y_k)}{\sqrt{n}}\Big) \approx -\kappa(y_j - y_k) + \sqrt{\frac{\Gamma\pi}{n}}(Z_j - Z_k).$$

Consequently, we have

$$\kappa \approx \frac{-\ln\Big(\frac{\mathrm{RV}_n(y_j)}{\mathrm{RV}_n(y_k)}\Big)}{y_j - y_k} + \frac{1}{y_j - y_k}\cdot\sqrt{\frac{\Gamma\pi}{n}}(Z_j - Z_k). \tag{14}$$

Consider a random vector $(Y_1, \ldots, Y_m) \sim \mathcal{N}(\mu, \Sigma)$, where $\mu = \{\mu_1\}^m \in \mathbb{R}^m$ is a vector with all elements equal to μ_1, and Σ is a covariance matrix. In this multivariate normal distribution, we can derive the same maximum likelihood estimator $\hat{\mu}_1$ for the parameter μ_1 as illustrated in Example 2.1.1.

Hence, using equation (14), we can construct an estimator for κ using every combination of different spatial points:

$$\hat{\varkappa} := \hat{\varkappa}_{n,m} := \frac{\sum_{j \neq l} \ln\left(\frac{\mathrm{RV}_n(y_j)}{\mathrm{RV}_n(y_l)}\right)(y_l - y_j)}{\sum_{j \neq l}(y_j - y_l)^2}, \tag{15}$$

where $\{j \neq l\}$ denotes the set $\{j, l = 1, \ldots m : j \neq l\}$. We can also expect the estimator $\hat{\varkappa}$ to be asymptotically unbiased. Albeit, the variance depends on the covariance structure Σ. Let $Y_{j,k}$ be the random variables corresponding to each combination of different spatial points from equation (14).

Assuming the random variables $Y_{j,k}$ to be independent for each combination of $j, k = 1, \ldots, m$, $j \neq k$, then the variance of $\hat{\varkappa}$ has the same structure as the variance of the maximum likelihood estimator in equation (12). However, let us assume $Y_{j,k} := Y_j - Y_k$, where (Y_i) are independent centred normal random variables with variances $\varsigma_i^2 > 0$, i.e., $Y_i \sim \mathcal{N}(0, \varsigma_i^2)$. Then, $(Y_{j,k})$ are not independent, as $\mathbb{C}\mathrm{ov}(Y_{j,k}, Y_{j,l}) = \varsigma_j^2 > 0$, where $j, k, l = 1, \ldots, m$, and all indices take different values. Nevertheless, we will calculate the variance of a similar form in Proposition 2.3.5.

As this estimator also uses the logarithm of the rescaled realized volatility, we can infer that the asymptotic variance is independent of the unknown parameters κ and σ_0^2 due to the variance-stabilizing transformation.

Our main goal will now be to prove consistency and demonstrate a central limit theorem for $\hat{\varkappa}_{n,m}$ with a special interest in its asymptotic variance. Therefore, we will continue by highlighting technical details for both estimators, $\hat{\kappa}_{n,m}$ and $\hat{\varkappa}_{n,m}$, respectively.

2.2. Methodology

As we have observed heuristically in the previous section, by utilizing the central limit theorem for the estimator $\hat{\sigma}_y^2$, we can create a new estimator for κ using the method of weighted average. Now, we will investigate a decomposition of the realized volatility with a specific focus on its remainder to lay the groundwork for the first part of the asymptotic analysis for both estimators. Therefore, we introduce the following lemma.

Lemma 2.2.1

Let $y_1 < \ldots < y_m \in [\delta, 1-\delta]$ be in accordance with Assumption 1.1.1, where $\delta \in (0, 1/2)$. Furthermore, let $\tilde{y}_1, \ldots, \tilde{y}_m \in [0,1]$ and $Y_1, \ldots, Y_m \in \mathcal{L}^2$ square-integrable random variables. Then, it holds:

(i) For $\alpha \in \mathbb{R}$ and $\beta > 0$ we have $\left(\sum_{j=1}^m \tilde{y}_j^\beta\right)^\alpha = \mathcal{O}(m^\alpha)$,

(ii) $\sum_{j \neq l} |y_j - y_l|^{-1} = \mathcal{O}\big(m^2 \log(m)\big)$,

(iii) $\sum_{j \neq l}(Y_j - Y_l)(y_l - y_j) = 2\sum_{j=1}^m Y_j\big(\sum_{l=1}^m (y_l - y_j)\big)$ and

$$\mathbb{V}\mathrm{ar}\bigg(\sum_{j \neq l}(Y_j - Y_l)(y_l - y_j)\bigg) = 4\sum_{j=1}^m \bigg(\sum_{l=1}^m (y_l - y_j)\bigg)^2 \mathbb{V}\mathrm{ar}(Y_j) + \mathcal{O}\bigg(m^2 \sum_{j_1 \neq j_2} \mathbb{C}\mathrm{ov}(Y_{j_1}, Y_{j_2})\bigg).$$

Proof. The first statement is evident since $0 \leqslant \tilde{y}_j^{\beta} \leqslant 1$ for every $\beta > 0$ and $\sum_{j=1}^{m} y_j = \mathcal{O}(m)$. For the second statement, we have $\min_{j=2,\dots,m} |y_j - y_{j-1}| \geqslant C_m$, where $C_m > 0$ and mC_m is a bounded constant for all $m \in \mathbb{N}$. Therefore, it holds

$$\sum_{j\neq l} \frac{1}{|y_j - y_l|} \leqslant m \sum_{j\neq l} \frac{1}{mC_m|j-l|} = \mathcal{O}\Big(m \sum_{j\neq l} \frac{1}{|y-l|}\Big) = \mathcal{O}\Big(m \sum_{j=1}^{m} \frac{1}{j}(m-j)\Big) = \mathcal{O}\big(m^2 \log(m)\big),$$

where we know by the Maclaurin-Cauchy test that $\sum_{j=1}^{m} 1/j = \mathcal{O}\big(\log(m)\big)$. For the last statement the variance identity is trivial by using statement (i) if we can show the identity $\sum_{j\neq l}(Y_j - Y_l)(y_l - y_j) = 2\sum_{j=1}^{m} Y_j\big(\sum_{l=1}^{m}(y_l - y_j)\big)$. Here, we obtain that

$$\begin{aligned}\sum_{j\neq l}(Y_j - Y_l)(y_l - y_j) &= 2\sum_{j<l}(Y_j - Y_l)(y_l - y_j)\\ &= 2\sum_{j=1}^{m} Y_j\Big(\sum_{l=j+1}^{m}(y_l - y_j) - \sum_{l=1}^{j-1}(y_j - y_l)\Big)\\ &= 2\sum_{j=1}^{m} Y_j\Big(\sum_{l=1}^{m}(y_l - y_j)\Big),\end{aligned}$$

where we have rearranged the random variables in such a way that the respective random variables have been combined. Note that we assign a value of zero to an empty sum. ◻

We start by employing the decomposition based on the CLT as stated in Proposition 1.2.3. Let $y_j \in [\delta, 1-\delta]$, with $j = 1,\dots,m$ and a suitable $\delta \in (0, 1/2)$. Then, for the rescaled realized volatility, we have

$$\frac{\mathrm{RV}_n(y_j)}{\sqrt{n}} = e^{-\kappa y_j}\frac{\sigma_0^2}{\sqrt{\pi}}\Big(1 + \sqrt{\frac{\Gamma\pi}{n}}Z_j + R_{n,y_j}\Big),$$

where $Z_j \sim \mathcal{N}(0,1)$, $j = 1,\dots,m$, denote standard normal random variables, and R_{n,y_j} represents the remainder. In particular, the random variables Z_j are independent and identically distributed, and they are also independent of the remainder R_{n,y_j}. This is because the rescaled realized volatilities are asymptotically Gaussian, and its autocovariances in different spatial points vanish asymptotically. The remainders R_{n,y_j} contain all asymptotic negligible terms concerning the expected value and variance-covariance structures of the rescaled realized volatilities. Therefore, we need to consider especially those terms that depend on the spatial coordinates. Using Bibinger and Trabs (2020, Prop. 3.1. and 6.5.), we can determine its asymptotic behaviour, which can be expressed as

$$R_{n,y} = \mathcal{O}_{\mathbb{P}}\big(\Delta_n + \Delta_n^{(1+\eta)/2} + \Delta_n^{3/4}/\sqrt{\delta}\big) = \mathcal{O}_{\mathbb{P}}\big(\Delta_n^{(1+\eta)/2} + \Delta_n^{3/4}/\sqrt{\delta}\big), \tag{16}$$

where $\eta \in (0,1)$ is an arbitrary constant. Note that we additionally used Bibinger and Trabs (2020, Prop. 6.4.). Hence, we can write $R_{n,y} = \mathcal{O}_{\mathbb{P}}(\sqrt{\Delta_n})$. When summing the remainder over different spatial points, we get that

$$R_{n,y}^{\Sigma} := \sum_{j=1}^{m} R_{n,y_j} = \mathcal{O}_{\mathbb{P}}\Bigg(m^{1/2}\Delta_n^{(1+\eta)/2} + \Delta_n^{3/4}\Big(\sum_{j\neq k}(|y_j - y_k|^{-1}) + m^2\delta^{-1}\Big)^{1/2}\Bigg).$$

Using Lemma 2.2.1, we find that

$$R^{\Sigma}_{n,y} = \sum_{j=1}^{m} R_{n,y_j} = \mathcal{O}_{\mathbb{P}}\Big(m^{1/2}\Delta_n^{(1+\eta)/2} + \Delta_n^{3/4} m\big(\log(m) + \delta^{-1}\big)^{1/2}\Big). \tag{17}$$

Therefore, we can particularly state $\sum_{j=1}^{m} R_{n,y_j} = \mathcal{O}_{\mathbb{P}}(\sqrt{m\Delta_n})$. Since our estimators for κ utilize the natural logarithm to obtain information on κ from the rescaling factor in the inner product, we need to analyse the logarithm of the rescaled realized volatility. As a first step, we have

$$\begin{aligned}\ln\left(\frac{\mathrm{RV}_n(y)}{\sqrt{n}}\right) &= -\kappa y + \ln\left(\frac{\sigma_0^2}{\sqrt{\pi}}\right) + \ln\left(1 + \sqrt{\frac{\Gamma\pi}{n}} Z + R_{n,y}\right) \\ &= -\kappa y + \ln\left(\frac{\sigma_0^2}{\sqrt{\pi}}\right) + \ln\left(1 + \sqrt{\frac{\Gamma\pi}{n}} Z\right) + \ln\left(1 + \frac{R_{n,y}}{1+\sqrt{\Delta_n\Gamma\pi}Z}\right),\end{aligned}$$

where $Z \sim \mathcal{N}(0,1)$. We can simplify further by using Taylor expansion:

$$\ln\left(\frac{\mathrm{RV}_n(y)}{\sqrt{n}}\right) = -\kappa y + \ln\left(\frac{\sigma_0^2}{\sqrt{\pi}}\right) + \sqrt{\frac{\Gamma\pi}{n}} Z + \mathcal{O}_{\mathbb{P}}(\Delta_n) + \ln\left(1 + \frac{R_{n,y}}{1+\sqrt{\Delta_n\Gamma\pi}Z}\right).$$

Since Z follows a standard normal distribution and $\sqrt{\Delta_n\Gamma\pi}Z$ has a standard deviation of $\mathcal{O}(\sqrt{\Delta_n})$, we can rewrite the last term using Taylor expansion, considering only the first-order term:

$$\begin{aligned}\ln\left(1 + \frac{R_{n,y}}{1+\sqrt{\Delta_n\Gamma\pi}Z}\right) &= \ln\left(1 + \left(R_{n,y} - \frac{R_{n,y}\sqrt{\Delta_n\Gamma\pi}Z}{1+\sqrt{\Delta_n\Gamma\pi}Z}\right)\right) \\ &= R_{n,y} - \big(1 + \mathcal{O}_{\mathbb{P}}(\sqrt{\Delta_n})\big) R_{n,y}\sqrt{\Delta_n\Gamma\pi}Z + \mathcal{O}_{\mathbb{P}}\left(\Delta_n^{1+\eta} + \frac{\Delta_n^{3/2}}{\delta}\right) \\ &= R_{n,y} + \mathcal{O}_{\mathbb{P}}\left(\Delta_n^{1+\eta/2} + \frac{\Delta_n^{5/4}}{\sqrt{\delta}}\right) + \mathcal{O}_{\mathbb{P}}\left(\Delta_n^{1+\eta} + \frac{\Delta_n^{3/2}}{\delta}\right),\end{aligned}$$

by utilizing equation (16). As we consider the asymptotic regime based on Assumption 1.1.1, the sum of different spatial points becomes asymptotically negligible. Therefore, we can safely ignore the latter term and arrive at the following conclusion:

$$\ln\left(1 + \frac{R_{n,y}}{1+\sqrt{\Delta_n\Gamma\pi}Z}\right) = R_{n,y} + \mathcal{O}_{\mathbb{P}}\left(\Delta_n^{1+\eta/2} + \frac{\Delta_n^{5/4}}{\sqrt{\delta}}\right).$$

As a result, we obtain that

$$\ln\left(\frac{\mathrm{RV}_n(y)}{\sqrt{n}}\right) = -\kappa y + \ln\left(\frac{\sigma_0^2}{\sqrt{\pi}}\right) + \sqrt{\Delta_n\Gamma\pi}Z + \mathcal{O}_{\mathbb{P}}(\Delta_n) + R_{n,y} + \mathcal{O}_{\mathbb{P}}\left(\Delta_n^{1+\eta/2} + \frac{\Delta_n^{5/4}}{\sqrt{\delta}}\right). \tag{18}$$

To simplify notation, we introduce two random variables to represent the higher-order error terms, where we rewrite the latter expression as follows:

$$\ln\left(\frac{\mathrm{RV}_n(y)}{\sqrt{n}}\right) = -\kappa y + \ln\left(\frac{\sigma_0^2}{\sqrt{\pi}}\right) + \sqrt{\Delta_n\Gamma\pi}Z + R_{n,y} + r^1_{n,y} + r^2_{n,y},$$

where $r^1_{n,y} = \mathcal{O}_{\mathbb{P}}\big(\Delta_n^{1+\eta/2} + \Delta_n^{5/4}/\sqrt{\delta}\big)$ is primarily influenced by the product $\sqrt{\Delta_n} Z_j R_{n,y}$, whereas $r^2_{n,y} = \mathcal{O}_{\mathbb{P}}(\Delta_n)$ is mainly driven by $\Delta_n Z_j^2$. Additionally, by utilizing Propositions 1.2.1 and 1.2.2, we can determine the first moment, variance, and covariance of the remainder $R_{n,y}$. We obtain

$$\mathbb{E}[R_{n,y}] = \mathcal{O}(\Delta_n), \quad \mathbb{C}\mathrm{ov}(R_{n,y_1}, R_{n,y_2}) = \mathcal{O}\big(\mathbb{1}_{\{y_1=y_2\}}\Delta_n^{\eta+1} + \Delta_n^{3/2}(\mathbb{1}_{\{y_1\neq y_2\}}|y_1-y_2|^{-1} + \delta^{-1})\big). \tag{19}$$

Lastly, we examine the sum of the log-rescaled realized volatility over different spatial points:

$$\sum_{j=1}^m \ln\left(\frac{\mathrm{RV}_n(y_j)}{\sqrt{n}}\right) = -\kappa\sum_{j=1}^m y_j + m\ln\left(\frac{\sigma_0^2}{\sqrt{\pi}}\right) + \sqrt{\Delta_n\Gamma\pi}\sum_{j=1}^m Z_j + R^{\Sigma}_{n,y} + \sum_{j=1}^m r^1_{n,y_j} + \sum_{j=1}^m r^2_{n,y_j}. \tag{20}$$

Using equation (17), we find that

$$\sum_{j=1}^m r^1_{n,y_j} = \mathcal{O}_{\mathbb{P}}\big(m^{1/2}\Delta_n^{1+\eta/2} + m\delta^{-1/2}\Delta_n^{5/4}\big),$$

since Z_j and R_{n,y_j} are independent. Additionally, we have

$$\sum_{j=1}^m r^2_{n,y_j} = \mathcal{O}_{\mathbb{P}}(\sqrt{m}\Delta_n).$$

As the sum of the spatial points of the higher-order error terms vanishes faster than the sum of the spatial points of $R_{n,y}$, we conclude

$$\ln\left(\frac{\mathrm{RV}_n(y)}{\sqrt{n}}\right) = -\kappa y + \ln\left(\frac{\sigma_0^2}{\sqrt{\pi}}\right) + \sqrt{\Delta_n\Gamma\pi}Z + R_{n,y}, \tag{21}$$

$$\sum_{j=1}^m \ln\left(\frac{\mathrm{RV}_n(y_j)}{\sqrt{n}}\right) = -\kappa\sum_{j=1}^m y_j + m\ln\left(\frac{\sigma_0^2}{\sqrt{\pi}}\right) + \sqrt{\Delta_n\Gamma\pi}\sum_{j=1}^m Z_j + R^{\Sigma}_{n,y}. \tag{22}$$

With this decomposition, we can now express the oracle estimator from equation (13) as follows:

$$\begin{aligned}\hat{\kappa}_{n,m} &= \frac{\kappa\sum_{j=1}^m y_j^2 - \sum_{j=1}^m \ln\left(\frac{\sigma_0^2}{\sqrt{\pi}}\right)y_j + \sqrt{\Delta_n\Gamma\pi}\sum_{j=1}^m Z_j y_j + \sum_{j=1}^m R_{n,y_j}y_j + \sum_{j=1}^m \ln\left(\frac{\sigma_0^2}{\sqrt{\pi}}\right)y_j}{\sum_{j=1}^m y_j^2} \\ &= \kappa + \left(\sum_{j=1}^m y_j^2\right)^{-1}\left(\sqrt{\Delta_n\Gamma\pi}\sum_{j=1}^m Z_j y_j + \sum_{j=1}^m R_{n,y_j}y_j\right). \end{aligned} \tag{23}$$

We conclude the methodology by presenting a similar decomposition for the non-oracle estimator $\hat{\varkappa}$. Using the same methods as in equation (20), we have

$$\begin{aligned}\sum_{j\neq l}\ln\left(\frac{\mathrm{RV}_n(y_j)}{\mathrm{RV}_n(y_l)}\right) &= \sum_{j\neq l}\left(\ln\left(\frac{\mathrm{RV}_n(y_j)}{\sqrt{n}}\right) - \ln\left(\frac{\mathrm{RV}_n(y_l)}{\sqrt{n}}\right)\right) \\ &= \kappa\sum_{j\neq l}(y_l - y_j) + \sqrt{\Delta_n\Gamma\pi}\sum_{j\neq l}(Z_j - Z_l) + \sum_{j\neq l}(R_{n,y_j} - R_{n,y_l}). \end{aligned} \tag{24}$$

Again, considering that the higher-order error terms $r^1_{n,y}$ and $r^2_{n,y}$ vanish faster than $R_{n,y}$, we can neglect these remainders. Now, we analyse the $\mathcal{O}_{\mathbb{P}}$ order of the double sum of the remainder. Using Lemma

2.2.1, we find that

$$\sum_{j\neq l}(R_{n,y_j}-R_{n,y_l})(y_l-y_j)=2\sum_{j=1}^{m}R_{n,y_j}\sum_{l=1}^{m}(y_l-y_j)=\mathcal{O}_{\mathbb{P}}\big(mR_{n,y}^{\Sigma}\big),$$

where we have used that $|y_l-y_j|\leqslant 1$ for $j\neq l$. Additionally, we have

$$\sum_{j\neq l}(R_{n,y_j}-R_{n,y_l})=\mathcal{O}_{\mathbb{P}}\big(mR_{n,y}^{\Sigma}\big)=\mathcal{O}_{\mathbb{P}}\Big(m^{3/2}\Delta_n^{(1+\eta)/2}+\Delta_n^{3/4}m^2\big(\log(m)+\delta^{-1}\big)^{1/2}\Big). \tag{25}$$

Using the representation from display (24) for the estimator $\hat{\varkappa}$ from equation (15), we arrive at the following expression:

$$\begin{aligned}\hat{\varkappa}_{n,m}&=\frac{\kappa\sum_{j\neq l}(y_l-y_j)^2+\sqrt{\Delta_n\Gamma\pi}\sum_{j\neq l}(Z_j-Z_l)(y_l-y_j)+\sum_{j\neq l}(R_{n,y_j}-R_{n,y_l})(y_l-y_j)}{\sum_{j\neq l}(y_j-y_l)^2}\\&=\kappa+\Big(\sum_{j\neq l}(y_j-y_l)^2\Big)^{-1}\Big(\sqrt{\Delta_n\Gamma\pi}\sum_{j\neq l}(Z_j-Z_l)(y_l-y_j)+\sum_{j\neq l}(R_{n,y_j}-R_{n,y_l})(y_l-y_j)\Big).\end{aligned} \tag{26}$$

2.3. Fixed spatial observations

In this section, we begin the investigation of properties for the estimators $\hat{\kappa}$ and $\hat{\varkappa}$, respectively. This analysis involves determining their expected values and covariance structures. To explore asymptotic properties, we initially focus on the case where only the number of temporal observations goes to infinity, hence, we assume $m\in\mathbb{N}$ to be fixed throughout this section. By utilizing the technical details presented in Section 2.2, we establish the first central limit theorems and lay the groundwork for investigating asymptotic results concerning both temporal and spatial observations.

2.3.1. Analysis of the curvature parameter with known normalized volatility

In this section, we analyse $\hat{\kappa}$ under the assumption that $\sigma_0^2=\sigma^2/\sqrt{\vartheta_2}$ is known, and the number of spatial observations $m\in\mathbb{N}$ is fixed, according to the asymptotic regime (I) on Assumption 1.1.1. To begin, we determine the expected value of the log-rescaled realized volatilities. Next, we derive its covariance structure, and finally, we establish a central limit theorem for the estimator $\hat{\kappa}$.

Proposition 2.3.1
On Assumptions 1.1.1 and 1.1.2, with $y\in[\delta,1-\delta]$ for a $\delta\in(0,1/2)$, we have

$$\mathbb{E}\bigg[\ln\bigg(\frac{\mathrm{RV}_n(y)}{\sqrt{n}}\bigg)\bigg]=-\kappa y+\ln\bigg(\frac{\sigma_0^2}{\sqrt{\pi}}\bigg)+\mathcal{O}(\Delta_n).$$

In particular, the expected value of the estimator $\hat{\kappa}_{n,m}$ from equation (13) satisfies:

$$\mathbb{E}\big[\hat{\kappa}_{n,m}\big]=\kappa+\mathcal{O}(\Delta_n).$$

Proof. Using the equations (21) and (19) yields the first statement. The second statement follows from equation (23) and again equation (19). □

We continue with the calculation of the variance of the estimator $\hat{\kappa}$ from equation (13).

Proposition 2.3.2
On Assumptions 1.1.1 and 1.1.2, we have

$$\mathbb{V}\mathrm{ar}\big(\hat{\kappa}_{n,m}\big) = \Big(\sum_{j=1}^{m} y_j^2\Big)^{-1} \Gamma\pi\Delta_n\Big(1 + \mathcal{O}\big(\sqrt{\Delta_n}\big)\Big),$$

where $\Gamma \approx 0.75$ is a constant analytically given in equation (8).

Proof. Using Lemma 2.2.1, equations (23) and (17), we have

$$\begin{aligned}\mathbb{V}\mathrm{ar}\big(\hat{\kappa}_{n,m}\big) &= \Big(\sum_{j=1}^{m} y_j^2\Big)^{-2}\Big(\Delta_n\Gamma\pi\sum_{j=1}^{m} y_j^2 + \mathbb{V}\mathrm{ar}\Big(\sum_{j=1}^{m} R_{n,y_j}y_j\Big)\Big)\\ &= \Big(\sum_{j=1}^{m} y_j^2\Big)^{-1}\Delta_n\Gamma\pi + \mathcal{O}\Big(\Big(\sum_{j=1}^{m} y_j^2\Big)^{-2}\Big(m\Delta_n^{\eta+1} + \Delta_n^{3/2}m^2\big(\log(m) + \delta^{-1}\big)\Big)\Big).\end{aligned}$$

Choosing $\eta = 1/2$ and having $m \in \mathbb{N}$ fixed completes the proof. □

The last proposition reinforces the conjecture that we can expect an asymptotic variance of $\big(\sum_{j=1}^m y_j^2\big)^{-1}\Gamma\pi$ with a convergence speed of $\sqrt{\Delta_n}$. Taking this proposition into account, we can rescale the sum to take the form of a Riemann sum, preparing for subsequent asymptotic results. Since the spatial points $\delta \leqslant y_1, \dots, y_m \leqslant 1-\delta$ lie within the range from δ to $1-\delta$, we rescale by the factor $(1-2\delta)/m$, resulting in:

$$\mathbb{V}\mathrm{ar}\big(\hat{\kappa}_{n,m}\big) = \frac{\Delta_n}{m}\cdot\frac{\Gamma\pi(1-2\delta)}{\frac{1-2\delta}{m}\sum_{j=1}^m y_j^2}\Big(1 + \mathcal{O}\big(\sqrt{\Delta_n}\big)\Big).$$

To prove a central limit theorem and establish consistency when m is fixed, we first consider the case where $m = 1$. In this situation, the estimator takes on the following form:

$$\hat{\kappa}_{n,1} = \frac{-\ln\Big(\frac{\mathrm{RV}_n(y_1)}{\sqrt{n}}\Big)y_1 + \ln\Big(\frac{\sigma_0^2}{\sqrt{\pi}}\Big)y_1}{y_1^2} = \frac{-\ln\Big(\frac{\mathrm{RV}_n(y_1)}{\sqrt{n}}\Big) + \ln\Big(\frac{\sigma_0^2}{\sqrt{\pi}}\Big)}{y_1} = \ln\Big(\frac{\sqrt{n}\sigma_0^2}{\sqrt{\pi}\mathrm{RV}_n(y_1)}\Big)\frac{1}{y_1}.$$

As illustrated in Proposition 1.2.3, the following central limit theorem holds:

$$\sqrt{n}\big(\hat{\sigma}_{y_1}^2 - \sigma^2\big) = \sqrt{n}\Big(\sqrt{\vartheta_2\pi}\frac{\mathrm{RV}_n(y_1)}{\sqrt{n}}e^{y_1\kappa} - \sigma^2\Big) \xrightarrow{d} \mathcal{N}(0, \Gamma\pi\sigma^4).$$

Applying the delta method with the function

$$f(x) = \ln\left(\left(\frac{x}{\sqrt{\vartheta_2 \pi}} e^{-y_1\kappa}\right)^{-1} \frac{\sigma_0^2}{\sqrt{\pi}}\right) y_1^{-1} = \ln\left(x^{-1} e^{y_1\kappa}\sigma^2\right) y_1^{-1}$$

and the derivative $f'(x) = -(y_1 x)^{-1}$, we obtain that

$$\sqrt{n}\big(f(\hat{\sigma}^2_{y_1}) - f(\sigma^2)\big) = \sqrt{n}\big(\hat{\kappa} - \kappa\big) \xrightarrow{d} f'(\sigma^2)\mathcal{N}(0, \Gamma\pi\sigma^4) = \mathcal{N}(0, y_1^{-2}\Gamma\pi),$$

which proves a central limit theorem in the simple case $m = 1$. Moreover, the assumption of an asymptotic variance from Example 2.1.1 has been confirmed in this case. Next, we consider the case where $m > 1$ but fixed.

Proposition 2.3.3

Under Assumptions 1.1.1 and 1.1.2, for $y_1, \ldots, y_m \in [\delta, 1-\delta]$ with $m \in \mathbb{N}$ fixed and $\delta \in (0, 1/2)$, we have the following central limit theorem:

$$\sqrt{n}\big(\hat{\kappa}_{n,m} - \kappa\big) \xrightarrow{d} \mathcal{N}\left(0\ ,\ \frac{\Gamma\pi(1-2\delta)}{m\big(\frac{1-2\delta}{m}\sum_{j=1}^m y_j^2\big)}\right),$$

as $n \to \infty$.

Proof. We define

$$g_j(x) := \frac{\ln\left(\left(\frac{x}{\sqrt{\vartheta_2\pi}} e^{-y_j\kappa}\right)^{-1} \frac{\sigma_0^2}{\sqrt{\pi}}\right) y_j}{\sum_{l=1}^m y_l^2} = \frac{\ln\left(x^{-1}e^{y_j\kappa}\sigma^2\right) y_j}{\sum_{l=1}^m y_l^2},$$

for $j = 1, \ldots, m$. Since g_j is differentiable with $g_j'(x) = -(x\sum_{l=1}^m y_l^2)^{-1} y_j$, we have by using Proposition 1.2.3 that

$$\begin{aligned}\sqrt{n}\big(g_j(\hat{\sigma}^2_{y_j}) - g_j(\sigma^2)\big) &= \sqrt{n}\left(\frac{-\ln\left(\frac{\mathrm{RV}_n(y_j)}{\sqrt{n}}\right)y_j + \ln\left(\frac{\sigma_0^2}{\sqrt{\pi}}\right)y_j}{\sum_{l=1}^m y_l^2} - \frac{y_j^2\kappa}{\sum_{j=l}^m y_l^2}\right) \\ &\xrightarrow{d} g_j'(\sigma^2)\mathcal{N}(0, \Gamma\pi\sigma^4) = \mathcal{N}\left(0, \Gamma\pi y_j^2\left(\sum_{l=1}^m y_l^2\right)^{-2}\right).\end{aligned}$$

According to Bibinger and Trabs (2020, Prop. 3.2.), the covariance of the random variables $\hat{\sigma}^2_{y_j}$ and $\hat{\sigma}^2_{y_l}$ vanishes asymptotically for $y_j \neq y_l$. The asymptotic Gaussian structure of these random variables implies that $U^{\sigma}_{j,n} := \sqrt{n}(\hat{\sigma}^2_{y_j} - \sigma^2)$ and $U^{\sigma}_{l,n}$ are asymptotically independent, for $j \neq l$. Consequently, for a continuous function g, the random variables

$$U^{g(\sigma)}_{j,n} := \sqrt{n}\big(g(\hat{\sigma}^2_{y_1}, \ldots, \hat{\sigma}^2_{y_m}) - g(\sigma^2, \ldots, \sigma^2)\big)_j,$$

and $U_{l,n}^{g(\sigma)}$ are also asymptotically independent. Defining the function $g:\mathbb{R}_+^m\to\mathbb{R}^m$ as

$$g(x_1,\dots,x_m)=\begin{pmatrix} g_1(x_1)\\ \vdots \\ g_m(x_m)\end{pmatrix},$$

we have the following multivariate convergence:

$$\sqrt{n}\big(g(\hat\sigma^2_{y_1},\dots,\hat\sigma^2_{y_m})-g(\sigma^2,\dots,\sigma^2)\big)\xrightarrow{d}\mathcal{N}(\mathbf{0},\Sigma),$$

where $\mathbf{0}=(0,\dots,0)^\top\in\mathbb{R}^m$ and

$$\Sigma=\begin{pmatrix} \Gamma\pi y_1^2\Big(\sum_{j=1}^m y_j^2\Big)^{-2} & 0 & \dots & 0\\ 0 & \Gamma\pi y_2^2\Big(\sum_{j=1}^m y_j^2\Big)^{-2} & \dots & 0\\ \vdots & \vdots & \ddots & \vdots\\ 0 & 0 & \dots & \Gamma\pi y_m^2\Big(\sum_{j=1}^m y_j^2\Big)^{-2}\end{pmatrix}\in\mathbb{R}^{m\times m}.$$

Using Cramér-Wold, we have

$$\begin{aligned}\alpha^\top\sqrt{n}\big(g(\hat\sigma^2_{y_1},\dots,\hat\sigma^2_{y_m})-g(\sigma^2,\dots,\sigma^2)\big)&=\sqrt{n}\left(\frac{-\sum_{j=1}^m\ln\Big(\frac{\mathrm{RV}_n(y_j}{\sqrt{n}}\Big)y_j+\sum_{j=1}^m\ln\Big(\frac{\sigma_0^2}{\sqrt{\pi}}\Big)y_j}{\sum_{j=1}^m y_j^2}-\kappa\right)\\ &\xrightarrow{d}\mathcal{N}\big(0,\alpha^\top\Sigma\alpha\big)=\mathcal{N}\left(0,\Big(\sum_{j=1}^m y_j^2\Big)^{-1}\Gamma\pi\right),\end{aligned}$$

where $\alpha=(1,\dots,1)^\top\in\mathbb{R}^m$. Rescaling the spatial sum completes the proof. □

A direct consequence of Proposition 2.3.3 is the consistency of the curvature estimator $\hat\kappa_{n,m}$ as confirmed by Slutsky's theorem, which concludes this section.

2.3.2. Analysis of the curvature estimator with unknown normalized volatility

In this section, we will focus on the non-oracle estimator $\hat\varkappa_{n,m}$ from equation (15) for the parameter κ, with the number of spatial observations $m\in\mathbb{N}$ fixed. Following a similar structure as seen in Section 2.3.1, we begin by examining the expected value of $\hat\varkappa_{n,m}$. Considering Proposition 2.3.1, we can readily deduce the following corollary.

Corollary 2.3.4
On Assumptions 1.1.1 and 1.1.2, with $y\in[\delta,1-\delta]$ for a $\delta>0$, we have

$$\mathbb{E}\left[\ln\left(\frac{\mathrm{RV}_n(y_j)}{\mathrm{RV}_n(y_k)}\right)\right]=\kappa(y_k-y_j)+\mathcal{O}(\Delta_n).$$

Furthermore, we have

$$\mathbb{E}\Big[\hat{\kappa}_{n,m}\Big] = \kappa + \mathcal{O}(m^2\Delta_n).$$

Proof. The proof is completed by utilizing Proposition 2.3.1 and the equations (24), (19), (25). □

The preceding corollary demonstrates that the non-oracle estimator $\hat{\varkappa}$ is asymptotically unbiased. The forthcoming examination of the variance structure of the estimator $\hat{\varkappa}$ is of special significance as a conjecture regarding the estimator's asymptotic variance remains unresolved.

Proposition 2.3.5
On Assumptions 1.1.1 and 1.1.2, we have

$$\begin{aligned}\mathbb{V}\mathrm{ar}(\hat{\varkappa}_{n,m}) &= \Delta_n \Gamma \pi \frac{4\sum_{j=1}^m \big(\sum_{l=1}^m (y_l - y_j)\big)^2}{\big(\sum_{j\neq l}(y_j-y_l)^2\big)^2}\big(1+\mathcal{O}(\sqrt{\Delta_n})\big) \\ &= \frac{\Delta_n\Gamma\pi}{m\Big(\frac{1}{1-2\delta}\big(\frac{1-2\delta}{m}\sum_{j=1}^m y_j^2\big) - \frac{1}{(1-2\delta)^2}\big(\frac{1-2\delta}{m}\sum_{j=1}^m y_j\big)^2\Big)}\big(1+\mathcal{O}(\sqrt{\Delta_n})\big).\end{aligned}$$

Proof. Using equation (26) we get

$$\mathbb{V}\mathrm{ar}(\hat{\varkappa}_{n,m}) = \\ \Big(\sum_{j\neq l}(y_j-y_l)^2\Big)^{-2}\Big(\Delta_n\Gamma\pi\mathbb{V}\mathrm{ar}\Big(\sum_{j\neq l}(Z_j-Z_l)(y_l-y_j)\Big) + \mathbb{V}\mathrm{ar}\Big(\sum_{j\neq l}(R_{n,y_j}-R_{n,y_l})(y_l-y_j)\Big)\Big).$$

First, we obtain by Lemma 2.2.1 that

$$\mathbb{V}\mathrm{ar}\Big(\sum_{j\neq l}(Z_j-Z_l)(y_l-y_j)\Big) = 4\sum_{j=1}^m\Big(\sum_{l=1}^m (y_l-y_j)\Big)^2.$$

Further calculations yields that

$$\mathbb{V}\mathrm{ar}\Big(\sum_{j\neq l}(Z_j-Z_l)(y_l-y_j)\Big) = 4\Big(m^2\sum_{j=1}^m y_j^2 - m\Big(\sum_{j=1}^m y_j\Big)^2\Big) = 4m\Big(m\sum_{j=1}^m y_j^2 - \Big(\sum_{j=1}^m y_j\Big)^2\Big)$$

and

$$\Big(\sum_{j\neq l}(y_j-y_l)^2\Big)^2 = \Big(2m\sum_{j=1}^m y_j^2 - 2\Big(\sum_{j=1}^m y_j\Big)^2\Big)^2 = 4\Big(m\sum_{j=1}^m y_j^2 - \Big(\sum_{j=1}^m y_j\Big)^2\Big)^2.$$

Therefore, we conclude

$$\mathbb{V}\mathrm{ar}(\hat{\varkappa}_{n,m}) = \Delta_n\Gamma\pi\frac{m}{m\sum_{j=1}^m y_j^2 - \big(\sum_{j=1}^m y_j\big)^2} + \Big(\sum_{j\neq l}(y_j-y_l)^2\Big)^{-2}\mathbb{V}\mathrm{ar}\Big(\sum_{j\neq l}(R_{n,y_j}-R_{n,y_l})(y_l-y_j)\Big).$$

It remains to analyse the remainder. By equation (25) we have

$$\mathbb{V}\mathrm{ar}\Big(\sum_{j\neq l}(R_{n,y_j}-R_{n,y_l})(y_l-y_j)\Big)=\mathcal{O}\Big(m^3\Delta_n^{\eta+1}+m^4\Delta_n^{3/2}\big(\log(m)+\delta^{-1}\big)\Big).$$

We complete the proof by rescaling the leading term and by using Lemma 2.2.1 for the remainder, where we have

$$\mathbb{V}\mathrm{ar}(\hat{\varkappa}_{n,m})=\frac{\Delta_n\Gamma\pi}{m\Big(\frac{1}{1-2\delta}\big(\frac{1-2\delta}{m}\sum_{j=1}^m y_j^2\big)-\frac{1}{(1-2\delta)^2}\big(\frac{1-2\delta}{m}\sum_{j=1}^m y_j\big)^2\Big)}+\mathcal{O}\Big(\Delta_n^{\eta+1}m^{-1}+\Delta_n^{3/2}\big(\log(m)+\delta^{-1}\big)\Big),$$

with an arbitrary $\eta\in(0,1)$. □

Note that we can can express the preceding variance in the following form:

$$\mathbb{V}\mathrm{ar}(\hat{\varkappa}_{n,m})=\frac{4\Gamma\pi\Delta_n}{\sum_{j\neq l}(y_j-y_l)^2}+\frac{4\Gamma\pi\Delta_n\sum_{j=1}^m\sum_{l_1\neq l_2}(y_{l_1}-y_j)(y_{l_2}-y_j)}{\Big(\sum_{j\neq l}(y_j-y_l)^2\Big)^2}\big(1+\mathcal{O}(\sqrt{\Delta_n})\big),$$

where we have used that $(\sum_{j=1}^m a_j)^2=\sum_{j=1}^m a_j^2+\sum_{j\neq l}a_ja_l$, for a sequence $(a_n)_{n\in\mathbb{N}}$. With this representation, we can observe that the asymptotic variance can be decomposed into two distinct parts. The first part arises from the variance of the log-quotient of the rescaled realized volatilities. The second part arises from the covariance of two combinations of the log-quotients, where one rescaled volatility is common to both log-quotients, while the other rescaled volatility is associated with two different spatial points. Specifically, we will employ this identity in the proof of the following Proposition 2.3.6.

Following a similar approach as in Proposition 2.3.3, we can establish the following central limit theorem and demonstrating consistency of the estimator.

Proposition 2.3.6
On Assumptions 1.1.1 and 1.1.2, we have for $y_1,\ldots,y_m\in[\delta,1-\delta]$, with $\delta\in(0,1/2)$ and $m\in\mathbb{N}$ fixed that

$$\sqrt{n}\big(\hat{\varkappa}_{n,m}-\kappa\big)\xrightarrow{d}\mathcal{N}\left(0\ ,\ \frac{\Gamma\pi}{m\big(\frac{1}{1-2\delta}\big(\frac{1-2\delta}{m}\sum_{j=1}^m y_j^2\big)-\frac{1}{(1-2\delta)^2}\big(\frac{1-2\delta}{m}\sum_{j=1}^m y_j\big)^2\big)}\right).$$

Proof. In accordance with the CLT as stated in Proposition 1.2.3, we have

$$\sqrt{n}\left(\begin{pmatrix}\hat{\sigma}_{y_j}^2\\ \hat{\sigma}_{y_l}^2\end{pmatrix}-\begin{pmatrix}\sigma^2\\ \sigma^2\end{pmatrix}\right)\xrightarrow{d}\mathcal{N}\left(\begin{pmatrix}0\\0\end{pmatrix},\begin{pmatrix}\pi\Gamma\sigma^4 & 0\\ 0 & \pi\Gamma\sigma^4\end{pmatrix}\right),$$

by considering that $\hat{\sigma}_{y_j}^2$ and $\hat{\sigma}_{y_l}^2$ are asymptotically independent if $y_j\neq y_l$ and $y_j,y_l\in[\delta,1-\delta]$. Using the delta method with the function $g_{j,l}:\mathbb{R}_+^2\to\mathbb{R}$ defined as

$$g_{j,l}(x_1,x_2):=\frac{\ln\big(\frac{x_1}{x_2}e^{-\kappa(y_j-y_l)}\big)(y_l-y_j)}{\sum_{j\neq l}^m(y_j-y_l)^2}=\frac{\ln\big(\frac{x_1}{x_2}\big)(y_l-y_j)+\kappa(y_j-y_l)^2}{\sum_{j\neq l}^m(y_j-y_l)^2},$$

we have

$$\sqrt{n}\big(g_{j,l}(\hat\sigma^2_{y_j},\hat\sigma^2_{y_l}) - g_{j,l}(\sigma^2,\sigma^2)\big) = \sqrt{n}\left(\frac{\ln\big(\frac{\mathrm{RV}_n(y_j)}{\mathrm{RV}_n(y_l)}\big)(y_l-y_j)}{\sum_{j\neq l}(y_j-y_l)^2} - \frac{\kappa(y_j-y_l)^2}{\sum_{j\neq l}(y_j-y_l)^2}\right)$$
$$\xrightarrow{d} \mathcal{N}\left(0, \nabla g_{j,l}(\sigma^2,\sigma^2)^\top \begin{pmatrix}\pi\Gamma\sigma^4 & 0\\ 0 & \pi\Gamma\sigma^4\end{pmatrix} \nabla g_{j,l}(\sigma^2,\sigma^2)\right)$$
$$= \mathcal{N}\left(0\,,\,2\frac{(y_j-y_l)^2\Gamma\pi}{\big(\sum_{j\neq l}(y_j-y_l)^2\big)^2}\right),$$

where

$$\nabla g_{j,l}(x_1,x_2) = \begin{pmatrix}\frac{(y_l-y_j)}{x_1\sum_{j\neq l}^m (y_j-y_l)^2}\\ -\frac{(y_l-y_j)}{x_2\sum_{j\neq l}^m (y_j-y_l)^2}\end{pmatrix}.$$

Note that

$$\sqrt{n}\big(g_{l,j}(\hat\sigma^2_{y_l},\hat\sigma^2_{y_j}) - g_{l,j}(\sigma^2,\sigma^2)\big) \xrightarrow{d} \mathcal{N}\left(0\,,\,2\frac{(y_j-y_l)^2\Gamma\pi}{\big(\sum_{j\neq l}(y_j-y_l)^2\big)^2}\right).$$

Consider the function $g:\mathbb{R}^m\to\mathbb{R}^{m(m-1)}$, with

$$g(x_1,\dots,x_m) = \Big(g_{1,2}(x_1,x_2),\dots,g_{1,m}(x_1,x_m),g_{2,1}(x_2,x_1),g_{2,3}(x_2,x_3),\dots,g_{2,m}(x_2,x_m),\dots,g_{m-1,m}(x_{m-1},x_m)\Big)^\top.$$

Since the normal distribution is stable under linear transformations, we obtain that

$$\sqrt{n}\big(g(\hat\sigma^2_{y_1},\dots,\hat\sigma^2_{y_m}) - g(\sigma^2,\dots,\sigma^2)\big) \xrightarrow{d} \mathcal{N}(0,\Sigma),$$

where Σ denotes the corresponding covariance matrix. In order to examine its structure, we will analyse the covariance structure between the different combinations of indices of the function $g_{j,l}$. Let l_1,l_2,j be three distinct indices. Then, we observe the following covariance relationships:

$$\begin{aligned}
&\mathbb{C}\mathrm{ov}\big(g_{j,l_1}(\hat\sigma^2_{y_j},\hat\sigma^2_{y_{l_1}}),g_{j,l_2}(\hat\sigma^2_{y_j},\hat\sigma^2_{y_{l_2}})\big)\\
&= \Big(\sum_{j\neq l}(y_j-y_l)^2\Big)^{-2}(y_{l_1}-y_j)(y_{l_2}-y_j)\mathbb{C}\mathrm{ov}\Big(\ln\Big(\frac{\mathrm{RV}_n(y_j)}{\sqrt{n}}\Big)-\ln\Big(\frac{\mathrm{RV}_n(y_{l_1})}{\sqrt{n}}\Big),\ln\Big(\frac{\mathrm{RV}_n(y_j)}{\sqrt{n}}\Big)-\ln\Big(\frac{\mathrm{RV}_n(y_{l_2})}{\sqrt{n}}\Big)\Big)\\
&= \Big(\sum_{j\neq l}(y_j-y_l)^2\Big)^{-2}(y_{l_1}-y_j)(y_{l_2}-y_j)\Big(\mathbb{V}\mathrm{ar}\Big(\ln\Big(\frac{\mathrm{RV}_n(y_j)}{\sqrt{n}}\Big)\Big)+\mathcal{O}(\Delta_n^{3/2})\Big)\\
&= \mathbb{C}\mathrm{ov}\big(g_{l_1,j}(\hat\sigma^2_{y_{l_1}},\hat\sigma^2_{y_j}),g_{l_2,j}(\hat\sigma^2_{y_{l_2}},\hat\sigma^2_{y_j})\big).
\end{aligned}$$

Analogously, we have

$$\begin{aligned}
&\mathbb{C}\mathrm{ov}\big(g_{j,l_1}(\hat\sigma^2_{y_j},\hat\sigma^2_{y_{l_1}}),g_{l_2,j}(\hat\sigma^2_{y_{l_2}},\hat\sigma^2_{y_j})\big)\\
&= -\Big(\sum_{j\neq l}(y_j-y_l)^2\Big)^{-2}(y_{l_1}-y_j)(y_j-y_{l_2})\Big(\mathbb{V}\mathrm{ar}\Big(\ln\Big(\frac{\mathrm{RV}_n(y_j)}{\sqrt{n}}\Big)\Big)+\mathcal{O}(\Delta_n^{3/2})\Big)
\end{aligned}$$

$$= \Big(\sum_{j\neq l}(y_j-y_l)^2\Big)^{-2}(y_{l_1}-y_j)(y_{l_2}-y_j)\bigg(\mathbb{V}\mathrm{ar}\bigg(\ln\Big(\frac{\mathrm{RV}_n(y_j)}{\sqrt{n}}\Big)\bigg)+\mathcal{O}(\Delta_n^{3/2})\bigg)$$
$$= \mathbb{C}\mathrm{ov}\big(g_{l_1,j}(\hat\sigma^2_{y_{l_1}},\hat\sigma^2_{y_j}),g_{j,l_2}(\hat\sigma^2_{y_j},\hat\sigma^2_{y_{l_2}})\big).$$

Additionally, equation (25) demonstrates that the covariances in the latter calculations vanish when summing over every combination of different spatial points. Thus, by utilizing equation (18), we obtain the following expression:

$$\lim_{n\to\infty} n\,\mathbb{C}\mathrm{ov}\big(g_{j_1,l_1}(\hat\sigma^2_{y_{j_1}},\hat\sigma^2_{y_{l_1}}),g_{j_2,l_2}(\hat\sigma^2_{y_{j_2}},\hat\sigma^2_{y_{l_2}})\big)=\begin{cases}2\frac{(y_j-y_l)^2\Gamma\pi}{\big(\sum_{j\neq l}(y_j-y_l)^2\big)^2} & ,\text{if } j_1=j_2 \text{ and } l_1=l_2\\ \frac{(y_{l_1}-y_{j_1})(y_{l_2}-y_{j_1})\Gamma\pi}{\big(\sum_{j\neq l}(y_j-y_l)^2\big)^2} & ,\text{if } j_1=j_2 \text{ and } l_1\neq l_2\\ \frac{(y_{l_1}-y_{j_1})(y_{j_2}-y_{j_1})\Gamma\pi}{\big(\sum_{j\neq l}(y_j-y_l)^2\big)^2} & ,\text{if } j_1=l_2 \text{ and } l_1\neq j_2\\ \frac{(y_{j_1}-y_{l_1})(y_{l_2}-y_{l_1})\Gamma\pi}{\big(\sum_{j\neq l}(y_j-y_l)^2\big)^2} & ,\text{if } l_1=j_2 \text{ and } j_1\neq l_2\\ \frac{(y_{j_1}-y_{l_1})(y_{j_2}-y_{l_1})\Gamma\pi}{\big(\sum_{j\neq l}(y_j-y_l)^2\big)^2} & ,\text{if } l_1=l_2 \text{ and } j_1\neq j_2\\ 0 & ,\text{ else}\end{cases}.$$

Therefore, the covariance matrix Σ is fully described. By employing Cramér-Wold, where $\alpha=(1,\dots,1)\in\mathbb{R}^{m(m-1)}$, we obtain

$$\sqrt{n}\Big(\alpha^\top g(\hat\sigma^2_{y_1},\dots,\hat\sigma^2_{y_m})-\alpha^\top g(\sigma^2,\sigma^2)\Big)=\sqrt{n}\left(\frac{\sum_{j\neq l}\ln\Big(\frac{\mathrm{RV}_n(y_j)}{\mathrm{RV}_n(y_l)}\Big)(y_l-y_j)}{\sum_{j\neq l}(y_j-y_l)^2}-\kappa\right)\xrightarrow{d}\mathcal{N}(0,\alpha^\top\Sigma\alpha),$$

where

$$\alpha^\top\Sigma\alpha = 2\cdot\sum_{j\neq l}\frac{2(y_j-y_l)^2\Gamma\pi}{\big(\sum_{j\neq l}(y_j-y_l)^2\big)^2}+\frac{4\Gamma\pi\sum_{j=1}^m\sum_{l_1\neq l_2}(y_{l_1}-y_j)(y_{l_2}-y_j)}{\Big(\sum_{j\neq l}(y_j-y_l)^2\Big)^2}$$
$$=4\Gamma\pi\frac{\sum_{j=1}^m\big(\sum_{l=1}^m(y_l-y_j)\big)^2}{\big(\sum_{j\neq l}(y_j-y_l)^2\big)^2}.$$

Using Proposition 2.3.5 completes the proof. □

2.4. Asymptotic analysis in time and space

In the previous section, we established central limit theorems for the estimators $\hat\kappa$ from equation (13) and $\hat\varkappa$ from equation (15) in the case where the number of spatial observations m is fixed. In this section, our aim is to prove a generalized CLT for both estimators, allowing for both the number of temporal and spatial observations to go to infinity, while respecting the asymptotic regime (II) presented in Assumption 1.1.1. Since Cramér-Wold cannot be directly applied in this context, we will establish the central limit theorems using the ρ-mixing CLT by Peligrad et al. (1997), as recalled in Proposition 1.2.4.

2.4.1. Methodology

In order to establish central limit theorems for the estimators $\hat{\kappa}_{n,m_n}$ and $\hat{\varkappa}_{n,m_n}$, where the temporal and spatial observation $n, m_n \to \infty$, we need to consider the corresponding triangular arrays for these estimators. The ρ-mixing central limit theorem by Peligrad et al. (1997) uses a covariance inequality to bound potential dependencies in time and space.

Although a possible choice for the triangular arrays for the estimators $\hat{\kappa}_{n,m_n}$ and $\hat{\varkappa}_{n,m_n}$ would be a structure depending on the spatial coordinates, i.e., $\Xi_{n,j}$, where $j = 1, \ldots, m$, we know from Proposition 1.2.2 that the covariance structure between two different spatial points vanishes asymptotically. However, the behaviour of the covariance structure in time is not clear yet, which is why we will define the triangular arrays with a dependence on the temporal dimension, i.e., $\Xi_{n,i}$, $i = 1, \ldots, n$.

The temporal dependency of these estimators is given by the logarithm of the rescaled realized volatility. In order to access the temporal sum given in the realized volatilities, we utilize a suitable decomposition. By applying the first-order Taylor expansion $\ln(a + x) = \ln(a) + a^{-1}x + \mathcal{O}(a^{-2}x^2)$, where a is a constant and x is a small number tending to zero, we obtain by using Proposition 1.2.1:

$$\begin{aligned}
\ln\left(\frac{\mathrm{RV}_n(y)}{\sqrt{n}}\right) &= \ln\left(\mathbb{E}\left[\frac{\mathrm{RV}_n(y)}{\sqrt{n}}\right] + \left(\frac{\mathrm{RV}_n(y)}{\sqrt{n}} - \mathbb{E}\left[\frac{\mathrm{RV}_n(y)}{\sqrt{n}}\right]\right)\right) \\
&= \ln\left(e^{-\kappa y}\frac{\sigma_0^2}{\sqrt{\pi}} + \mathcal{O}(\Delta_n)\right) + \frac{\sum_{i=1}^n \left((\Delta_i\tilde{X})^2(y) - \mathbb{E}[(\Delta_i\tilde{X})^2(y)]\right)}{\sqrt{n}\big(e^{-\kappa y}\frac{\sigma_0^2}{\sqrt{\pi}} + \mathcal{O}(\Delta_n)\big)} \\
&\quad + \mathcal{O}_{\mathbb{P}}\left(\left(\frac{\mathrm{RV}_n(y)}{\sqrt{n}} - \mathbb{E}\left[\frac{\mathrm{RV}_n(y)}{\sqrt{n}}\right]\right)^2\right) \\
&= -\kappa y + \ln\left(\frac{\sigma_0^2}{\sqrt{\pi}}\right) + \ln\big(1 + \mathcal{O}(\Delta_n)\big) + \frac{\sum_{i=1}^n \overline{(\Delta_i\tilde{X})^2(y)}}{\sqrt{n}\frac{\sigma_0^2}{\sqrt{\pi}}} e^{\kappa y}\big(1 + \mathcal{O}(\Delta_n)\big) \\
&\quad + \mathcal{O}_{\mathbb{P}}\left(\left(\overline{\frac{\mathrm{RV}_n(y)}{\sqrt{n}}}\right)^2\right) \\
&= -\kappa y + \ln\left(\frac{\sigma_0^2}{\sqrt{\pi}}\right) + \frac{\sqrt{\pi}\sum_{i=1}^n \overline{(\Delta_i\tilde{X})^2(y)}}{\sqrt{n}\sigma_0^2} e^{\kappa y} + \mathcal{O}(\Delta_n) + \mathcal{O}_{\mathbb{P}}\big(\Delta_n\big),
\end{aligned} \tag{27}$$

where $\overline{Y} := Y - \mathbb{E}[Y]$ denotes the compensated random variable for all integrable random variables and $y \in [\delta, 1 - \delta]$. Here, we use a stationary mild solution $\tilde{X}$ with a stationary initial condition, i.e., $\langle \xi, e_k \rangle_\vartheta \sim \mathcal{N}(0, \sigma^2/(2\lambda_k))$. As the difference between a mild solution X and a stationary mild solution $\tilde{X}$ tends stochastically to zero, it is sufficient to analyse $\tilde{X}$, cf. Bibinger and Trabs (2020, Lemma 6.4.). The Gaussian structure for the remainder in this decomposition allows us to observe a rate of at least Δ_n. Utilizing this decomposition we obtain

$$\hat{\kappa}_{n,m_n} = \frac{\sum_{j=1}^{m_n}\Big(-\ln\big(\frac{\mathrm{RV}_n(y_j)}{\sqrt{n}}\big) + \ln\big(\frac{\sigma_0^2}{\sqrt{\pi}}\big)\Big)y_j}{\sum_{i=1}^{m_n} y_i^2} = \kappa - \frac{\sum_{j=1}^{m_n} y_j \sum_{i=1}^n \overline{(\Delta_i\tilde{X})^2(y_j)}}{\sqrt{n}\frac{\sigma_0^2}{\sqrt{\pi}}\sum_{i=1}^{m_n} y_i^2} e^{\kappa y_j} + \mathcal{O}_{\mathbb{P}}(\Delta_n), \tag{28}$$

where we have used Lemma 2.2.1 to show that

$$\Delta_n \frac{\sum_{j=1}^{m_n} y_j}{\sum_{j=1}^{m_n} y_j^2} = \mathcal{O}(\Delta_n).$$

As discussed in the remark on Proposition 1.2.4, the first triangular array is given by

$$\Xi^{\sigma_0^2} := \Xi^{\sigma_0^2}_{k_n,i} := \xi^{\sigma_0^2}_{k_n,j} - \mathbb{E}[\xi^{\sigma_0^2}_{k_n,j}] \quad \text{and} \quad \xi^{\sigma_0^2}_{k_n,i} := -\frac{\sqrt{m_n \pi}}{\sigma_0^2 \sum_{i=1}^{m_n} y_i^2} \sum_{j=1}^{m_n} (\Delta_i \tilde{X})^2(y_j) e^{y_j \kappa} y_j, \tag{29}$$

where $k_n = n$. The decomposition in equation (28) also shows that it is sufficient to prove a CLT for the chosen triangular array in order to prove a CLT for the estimator $\hat{\kappa}_{n,m_n}$. Now, we focus on the triangular array for the non-oracle estimator $\hat{\varkappa}_{n,m_n}$. By using equation (27), we can express the estimator as

$$\begin{aligned} \hat{\varkappa}_{n,m_n} &= \frac{\sum_{j\neq k}\left(\ln\left(\frac{\mathrm{RV}_n(y_j)}{\sqrt{n}}\right) - \ln\left(\frac{\mathrm{RV}_n(y_l)}{\sqrt{n}}\right)\right)(y_l - y_j)}{\sum_{j\neq l}(y_j - y_l)^2} \\ &= \kappa + \frac{\sum_{j\neq l}\sum_{i=1}^{n}\left(\overline{(\Delta_i \tilde{X})^2(y_j)e^{\kappa y_j}} - \overline{(\Delta_i \tilde{X})^2(y_l)e^{\kappa y_l}}\right)(y_l - y_j)}{\sqrt{n}\frac{\sigma_0^2}{\sqrt{\pi}}\sum_{j\neq l}(y_j - y_l)^2} + \mathcal{O}_{\mathbb{P}}(\Delta_n), \end{aligned} \tag{30}$$

where it also holds by Lemma 2.2.1 that

$$\Delta_n \frac{\sum_{j\neq l}(y_l - y_j)}{\sum_{j\neq l}(y_j - y_l)^2} = \mathcal{O}(\Delta_n),$$

since $|y_j - y_l| \leqslant 1$ for all $j \neq l$. Therefore, we define the triangular array for the estimator $\hat{\varkappa}_{n,m_n}$ by

$$\Xi := \Xi_{k_n,i} := \xi_{k_n,i} - \mathbb{E}[\xi_{k_n,i}]\ ,\ \xi_{k_n,i} := \frac{\sqrt{m_n \pi}}{\sigma_0^2 \sum_{j\neq l}(y_j - y_l)^2} \sum_{j\neq l}\left((\Delta_i \tilde{X})^2(y_j)e^{\kappa y_j} - (\Delta_i \tilde{X})^2(y_l)e^{\kappa y_l}\right)(y_l - y_j), \tag{31}$$

where $k_n = n$ and $m_n = \mathcal{O}(n^\rho)$, for $\rho \in (0, 1/2)$. Once more, the decomposition in equation (30) demonstrates that proving a CLT for the chosen triangular array is sufficient to establish a CLT for the estimator $\hat{\varkappa}_{n,m_n}$.

The triangular arrays $\Xi^{\sigma_0^2}$ and Ξ are naturally dependent on the statistics $(\Delta_i \tilde{X})^2(y)$, for $y \in [\delta, 1-\delta]$ and $1 \leqslant i \leqslant n$, linked to some deterministic functions. In Bibinger and Trabs (2020, Corollary 6.7.) it has been already proven that triangular arrays based on quadratic increments satisfy the general mixing type Condition (IV) as well as Conditions (I) to (III) from Proposition 1.2.4. We will now proceed to generalize these results by Bibinger and Trabs (2020). We define the sets $\mathcal{F}_\alpha$ and $\mathcal{G}_\alpha$ as follows:

$$\mathcal{F}_\alpha = \{f_\vartheta : \mathbb{N} \to \mathbb{R} \mid \exists C_\vartheta > 0 : f_\vartheta^2(m) \leqslant C_\vartheta m^{-(\alpha+1)}\} \tag{32}$$

and

$$\mathcal{G}_\alpha = \{g_\vartheta : \mathbb{N} \to \mathbb{R} \mid \exists C_\vartheta > 0 : |g_\vartheta(m)| \leqslant C_\vartheta m^{\alpha/2} \text{ uniformly in } m \in \mathbb{N}\},$$

for a $\alpha \geqslant 0$. Note that we allow the functions $f_\vartheta \in \mathcal{F}_\alpha$ and $g_\vartheta \in \mathcal{G}_\alpha$ to be dependent on some parameter ϑ. With these definitions, we proceed to define the class of generalized triangular arrays $\mathcal{H}_\alpha$ as follows:

$$\mathcal{H}_\alpha = \left\{(Z_{n,i})_{1\leqslant i\leqslant n, n\in\mathbb{N}} : Z_{n,i} = \zeta_{n,i} - \mathbb{E}[\zeta_{n,i}] \text{ and } \zeta_{n,i} = f_\vartheta(m)\sum_{j=1}^{m}(\Delta_i \tilde{X})^2(y_j)g_\vartheta(j),\ \text{ where } f_\vartheta \in \mathcal{F}_\alpha, g_\vartheta \in \mathcal{G}_\alpha\right\},$$

where $\alpha \geqslant 0$. As a result of the definitions in $\mathcal{F}_\alpha$ and $\mathcal{G}_\alpha$, we obtain the following properties:

$$f_\vartheta^2(m)\frac{1}{m}\sum_{j=1}^{m} g_\vartheta^2(j) = \mathcal{O}(m^{-1}) \quad \text{and} \quad f_\vartheta^2(m)\frac{1}{m^2}\sum_{j,l=1}^{m} g_\vartheta(j)g_\vartheta(l) = \mathcal{O}(m^{-1}), \tag{33}$$

for a fixed parameter ϑ and $f_\vartheta \in \mathcal{F}_\alpha$, $g_\vartheta \in \mathcal{G}_\alpha$. We will now proceed to prove that the triangular arrays $Z_{n,i} \in \mathcal{H}_\alpha$ satisfy the conditions for the central limit theorem in Proposition 1.2.4, starting with the mixing-type Condition (IV).

Proposition 2.4.1
Grant Assumptions 1.1.1 and 1.1.2 and suppose a triangular array $Z_{n,i} \in \mathcal{H}_\alpha$. If it holds that

$$f_\vartheta^2(m)\sum_{j=1}^{m_n}\sum_{i=b+u}^{c} \mathbb{E}\big[(\Delta_i\tilde{X})^4(y_j)\big]g_\vartheta^2(j) \geqslant \tilde{C}\Delta_n p_u,$$

for all $1 \leqslant b < b+u \leqslant c \leqslant n$, where $p_u := c-b-u+1$, $u \geqslant 2$ and $\tilde{C} := \tilde{C}_\vartheta > 0$, then the general mixing type Condition (IV) of Proposition 1.2.4 holds, i.e.:

$$\Big|\mathbb{C}\mathrm{ov}\big(e^{\mathrm{i}t\sum_{i=a}^{b} Z_{n,i}}, e^{\mathrm{i}t\sum_{i=b+u}^{c} Z_{n,i}}\big)\Big| \leqslant \frac{Ct^2}{u^{3/4}}\mathbb{V}\mathrm{ar}\Bigg(\sum_{i=a}^{b} Z_{n,i}\Bigg)^{1/2}\mathbb{V}\mathrm{ar}\Bigg(\sum_{i=b+u}^{c} Z_{n,i}\Bigg)^{1/2},$$

for all $1 \leqslant a \leqslant b < b+u \leqslant c \leqslant n$.

Proof. Let $1 \leqslant a \leqslant b < b+u \leqslant c \leqslant n$. We define

$$Q_a^b := \sum_{i=a}^{b}\zeta_{n,i} \quad \text{and} \quad Q_{b+u}^c := \sum_{i=b+u}^{c}\zeta_{n,i}.$$

Suppose there exists a decomposition of $Q_{b+u}^c = A_1 + A_2$, with A_2 independent of Q_a^b. According to Bibinger and Trabs (2020, Prop. 6.6.), we have

$$\Big|\mathbb{C}\mathrm{ov}\big(e^{\mathrm{i}t\bar{Q}_a^b}, e^{\mathrm{i}t\bar{Q}_{b+u}^c}\big)\Big| \leqslant 2t^2\mathbb{E}\big[(\bar{Q}_a^b)^2\big]^{1/2}\mathbb{E}\big[\bar{A}_1^2\big]^{1/2},$$

where $\bar{X} = X - \mathbb{E}[X]$ denotes the compensation of the random variable X. Since we build upon the proof strategy as presented in Bibinger and Trabs (2020, Prop. 6.6.), we review the fundamental elements of their proof. For this purpose, we define

$$\begin{aligned}
\tilde{Q}_{b+u}^c &:= \sum_{i=b+u}^{c}(\Delta_i\tilde{X})^2(y) \\
&= \sum_{i=b+u}^{c}\Bigg(\sum_{k=1}^{\infty} D_1^{k,i}e_k(y) + D_2^{k,i}e_k(y)\Bigg)^2 \\
&= \sum_{i=b+u}^{c}\Bigg(\sum_{k=1}^{\infty} D_1^{k,i}e_k(y)\Bigg)^2 + 2\sum_{i=b+u}^{c}\Bigg(\sum_{k=1}^{\infty} D_1^{k,i}e_k(y)\Bigg)\Bigg(\sum_{k=1}^{\infty} D_2^{k,i}e_k(y)\Bigg) + \sum_{i=b+u}^{c}\Bigg(\sum_{k=1}^{\infty} D_2^{k,i}e_k(y)\Bigg)^2,
\end{aligned}$$

and

$$\tilde{A}_1(y) := \sum_{i=b+u}^{c} \left(\sum_{k=1}^{\infty} D_1^{k,i} e_k(y) \right)^2 + 2 \sum_{i=b+u}^{c} \left(\sum_{k=1}^{\infty} D_1^{k,i} e_k(y) \right) \left(\sum_{k=1}^{\infty} D_2^{k,i} e_k(y) \right),$$
$$\tilde{A}_2(y) := \sum_{i=b+u}^{c} \left(\sum_{k=1}^{\infty} D_2^{k,i} e_k(y) \right)^2,$$

as well as

$$D_1^{k,i} := \int_{-\infty}^{r\Delta_n} \sigma e^{-\lambda_k \big((i-1)\Delta_n - s\big)} \big(e^{-\lambda_k \Delta_n} - 1\big) \,\mathrm{d}W_s^k, \tag{34}$$
$$D_2^{k,i} := \int_{r\Delta_n}^{(i-1)\Delta_n} \sigma e^{-\lambda_k \big((i-1)\Delta_n - s\big)} \big(e^{-\lambda_k \Delta_n} - 1\big) \,\mathrm{d}W_s^k + \int_{(i-1)\Delta_n}^{i\Delta_n} e^{-\lambda_k (i\Delta_n - s)} \sigma \,\mathrm{d}W_s^k, \tag{35}$$

where $r < i$. Since $D_1^{k,i}$ and $D_2^{k,i}$ are independent, we have $\tilde{A}_2$ independent of $\tilde{Q}_a^b$. Hence, we have

$$Q_{b+u}^c = \sum_{i=b+u}^{c} \zeta_{n,i} = f_\vartheta(m) \sum_{j=1}^{m} \sum_{i=b+u}^{c} (\Delta_i \tilde{X})^2(y_j) g_\vartheta(j)$$
$$= f_\vartheta(m) \sum_{j=1}^{m} \big(\tilde{A}_1(y_j) + \tilde{A}_2(y_j)\big) g_\vartheta(j),$$

and we continue analysing

$$A_1 := f_\vartheta(m) \sum_{j=1}^{m} \tilde{A}_1(y_j) g_\vartheta(j).$$

Using results by Bibinger and Trabs (2020, Corollary 6.7.), we find that

$$\sum_{j=1}^{m} \mathbb{V}\mathrm{ar}\big(\tilde{A}_1(y_j)\big) \leqslant \frac{C\sigma^4 (c-b-u+1)\Delta_n m}{(u-1)^{3/2}},$$

where $u \geqslant 2$, $y_j \in [\delta, 1-\delta]$ and $C > 0$. Additionally, we have the following covariance structure for $\tilde{A}_1(y)$:

$$\sum_{j \neq l} \mathbb{C}\mathrm{ov}\big(\tilde{A}_1(y_j), \tilde{A}_1(y_l)\big) = \mathcal{O}\left(\frac{\Delta_n^{3/2}(c-b-u+1)}{(u-1)^{3/2}} m^2 \log(m) \right),$$

where again $u \geqslant 2$ and $y_j, y_l \in [\delta, 1-\delta]$ with $y_j \neq y_l$. Therefore, we conclude for $p_u := c - b - u + 1$ that

$$\mathbb{V}\mathrm{ar}(A_1) = f_\vartheta^2(m) \left(\sum_{j=1}^{m} g_\vartheta^2(j) \mathbb{V}\mathrm{ar}\big(\tilde{A}_1(y_j)\big) + \sum_{j \neq l} g_\vartheta(j) g_\vartheta(l) \mathbb{C}\mathrm{ov}\big(\tilde{A}_1(y_j), \tilde{A}_1(y_l)\big) \right)$$
$$\leqslant C_1 m^{-(\alpha+1)} m^\alpha \left(\sum_{j=1}^{m} \mathbb{V}\mathrm{ar}\big(\tilde{A}_1(y_j)\big) + \sum_{j \neq l} \mathbb{C}\mathrm{ov}\big(\tilde{A}_1(y_j), \tilde{A}_1(y_l)\big) \right)$$

$$\leqslant \frac{C_2 p_u \Delta_n}{(u-1)^{3/2}} + \mathcal{O}\Big(\frac{\Delta_n^{3/2} p_u}{(u-1)^{3/2}} m_n \log(m_n)\Big),$$

where $C_1, C_2 > 0$ are suitable constants. Since it holds that

$$\mathbb{V}\mathrm{ar}(Q^c_{b+u}) \geqslant C_3 \mathbb{E}\big[(Q^c_{b+u})^2\big] \geqslant C_4 f_\vartheta^2(m) \sum_{j=1}^{m_n} \sum_{i=b+u}^{c} \mathbb{E}\big[(\Delta_i \tilde{X})^4(y_j)\big] g_\vartheta^2(j) \geqslant C_5 p_u \Delta_n,$$

where $C_3, C_4, C_5 > 0$ are suitable constants, we conclude for $u \geqslant 2$. It remains to bound A_1 in the case where $u = 1$. Here, we have by analysing the proof of Bibinger and Trabs (2020, Prop. 6.6.) that

$$\sum_{j=1}^{m} \mathbb{V}\mathrm{ar}\big(\tilde{A}_1(y_j)\big) \leqslant C\sigma^4 p_1 \Delta_n m,$$

where $C > 0$. Therefore, we have with $C_6 > 0$ that

$$\mathbb{V}\mathrm{ar}(A_1) \leqslant C_6 p_1 \Delta_n + \mathcal{O}\big(\Delta_n p_1 m \log(m)\big),$$

which completes the proof. □

Now that we have established the general mixing type condition on the generalized triangular arrays, we are in a position to prove the following central limit theorem.

Proposition 2.4.2
Grant Assumptions 1.1.1 and 1.1.2 and suppose a triangular array $Z_{n,i} \in \mathcal{H}_\alpha$. Then, it holds that

$$\sum_{i=1}^{n} Z_{n,i} \xrightarrow{d} \mathcal{N}(0, \nu^2),$$

as $n \to \infty$ and $\nu^2 = \lim_{n\to\infty} \mathbb{V}\mathrm{ar}(\sum_{i=1}^n Z_{n,i}) < \infty$, if it holds that

$$f_\vartheta^2(m) \sum_{j=1}^{m_n} \sum_{i=b+u}^{c} \mathbb{E}\big[(\Delta_i \tilde{X})^4(y_j)\big] g_\vartheta^2(j) \geqslant \tilde{C} \Delta_n p_u, \tag{36}$$

for all $1 \leqslant b < b+u \leqslant c \leqslant n$, where $p_u := c - b - u + 1$, $u \geqslant 2$ and a constant $\tilde{C} := \tilde{C}_\vartheta > 0$.

Proof. The Conditions (I), (II), and (III) remain to be verified, as indicated by Propositions 1.2.4 and 2.4.1.

(I) It is known that the centred random variables $\Delta_i \tilde{X}(y)$ follow a normal distribution. Proposition 1.2.1 yields that $\mathbb{E}[(\Delta_i \tilde{X})^2(y)] = \mathbb{V}\mathrm{ar}\big((\Delta_i \tilde{X})(y)\big) \propto \Delta_n^{1/2}$ uniformly in i. Additionally, we can infer from Proposition 1.2.2 that

$$\mathbb{V}\mathrm{ar}(Z_{n,i}) = f_\vartheta^2(m)\Big(\sum_{j=1}^{m_n} g_\vartheta^2(j) \mathbb{V}\mathrm{ar}(\sqrt{\Delta_n} V_{1,\Delta_n}(y_j) e^{-\kappa y_j})$$

$$
\begin{aligned}
&+\sum_{j\neq l} g_\vartheta(j)g_\vartheta(l)\mathbb{C}\mathrm{ov}(\sqrt{\Delta}_n V_{1,\Delta_n}(y_j)e^{-\kappa y_j},\sqrt{\Delta}_n V_{1,\Delta_n}(y_l)e^{-\kappa y_l})\Big)\\
&\leqslant C_1 m^{-1}\Delta_n\Big(\Gamma\sigma_0^4 m\big(1+\mathcal{O}(1\wedge\Delta_n^{\eta-1})\big)+\mathcal{O}\big(\Delta_n^{1/2}m_n^2\log(m_n)\big)\Big)\\
&=\mathcal{O}(\Delta_n)+\mathcal{O}\big(\Delta_n^{3/2}m_n\log(m_n)\big)=\mathcal{O}(\Delta_n).
\end{aligned}
$$

Therefore, we can find a constant $c>0$, such that $\sum_{i=a}^b \mathbb{V}\mathrm{ar}(\Xi_{m,i}^{\sigma_0^2})\geqslant c(b-a+1)\Delta_n$. Furthermore, in a similar manner, we also have

$$
\begin{aligned}
&\mathbb{V}\mathrm{ar}\Big(\sum_{i=a}^b Z_{n,i}\Big)\\
&=f_\vartheta^2(m)\Big((b-a+1)\Delta_n\Gamma\sigma_0^4\sum_{j=1}^{m_n}g_\vartheta^2(j)\Big(1+\mathcal{O}\Big(1\wedge\frac{\Delta_n^{\eta-1}}{b-a+1}\Big)\Big)+\mathcal{O}\big((b-a+1)\Delta_n^{3/2}m_n^{\alpha+2}\log(m_n)\big)\Big)\\
&=(b-a+1)\mathcal{O}(\Delta_n).
\end{aligned}
$$

Thus, the first condition has been established.

(II) As demonstrated in the proof of the first condition, it is evident that

$$\sum_{i=1}^n \mathbb{V}\mathrm{ar}(Z_{n,i})=\mathcal{O}(n\Delta_n)<\infty,$$

and therefore the second condition is verified.

(III) In order to establish the Lindeberg condition, we demonstrate a Lyapunov condition. Hence, we need to show the existence of a $\tilde{\delta}>0$ such that

$$\lim_{n\to\infty}\sum_{i=1}^n \mathbb{E}\big[|\Xi_{n,i}^{\sigma_0^2}|^{2+\tilde{\delta}}\big]=0.$$

Let $\tilde{\delta}=2$. As mentioned in Condition (I), the centred random variables $\Delta_i\tilde{X}(y)$ are normally distributed with $\mathbb{E}[(\Delta_i\tilde{X})^2(y)]\propto\Delta_n^{1/2}$ uniformly in i. Consequently, we can deduce that $\mathbb{E}[(\Delta_i\tilde{X})^8]=\Delta_n^2$. By applying the Cauchy-Schwarz inequality, we obtain the following result:

$$
\begin{aligned}
\sum_{i=1}^n \mathbb{E}\big[Z_{n,i}^4\big]&\leqslant\sum_{i=1}^n\mathbb{E}\big[\zeta_{n,i}^4\big]\\
&=\sum_{i=1}^n f_\vartheta^4(m_n)\sum_{j_1,\dots,j_4=1}^{m_n} g_\vartheta(y_{j_1})\cdot\ldots\cdot g_\vartheta(y_{j_4})\mathbb{E}\big[(\Delta_i\tilde{X})(y_{j_1})^2\cdot\ldots\cdot(\Delta_i\tilde{X})^2(y_{j_4})\big]\\
&\leqslant C\sum_{i=1}^n m_n^{-2(1+\alpha)}m_n^{2\alpha}\sum_{j_1,\dots,j_4=1}^{m_n}\mathbb{E}\big[(\Delta_i\tilde{X})^2(y_{j_1})\cdot\ldots\cdot(\Delta_i\tilde{X})^2(y_{j_4})\big]\\
&\leqslant C\sum_{i=1}^n m_n^{-2}\sum_{j_1,\dots,j_4=1}^{m_n}\mathbb{E}\big[(\Delta_i\tilde{X})^8(y_{j_1})\big]^{1/4}\cdot\ldots\cdot\mathbb{E}\big[(\Delta_i\tilde{X})^8(y_{j_4})\big]^{1/4}\\
&\leqslant C\sum_{i=1}^n m_n^2\max_{y\in\{y_1,\dots,y_{m_n}\}}\mathbb{E}\big[(\Delta_i\tilde{X})^8(y)\big]\\
&=\mathcal{O}\big(\Delta_n m_n^2\big)=\mathcal{o}(1),
\end{aligned}
$$

which completes the proof. □

The preceding proposition demonstrated that we can consistently apply the central limit theorem to triangular arrays utilizing quadratic increments, given that the associated deterministic functions satisfy a specific order as described in equations (33) and (48). This observation will prove to be exceedingly valuable in the subsequent two sections, where we will establish central limit theorems for both the oracle estimator $\hat{\kappa}$ and its robustification $\hat{\varkappa}$.

2.4.2. CLT for the curvature estimator with known normalized volatility

In this section, we establish a central limit theorem for the estimator $\hat{\kappa}$, where the parameter $m = m_n$ satisfies $m_n = \mathcal{O}(n^\rho)$, with $\rho \in (0, 1/2)$. We will employ the central limit theorem from Proposition 2.4.2 to achieve this. According to Proposition 2.4.2, it is necessary to demonstrate that $\Xi^{\sigma_0^2} \in \mathcal{H}_0$, as well as proving the condition given in equation (48).

Proposition 2.4.3
Grant Assumptions 1.1.1 and 1.1.2, with $y_1 = \delta$, $y_{m_n} = 1-\delta$ and $m_n \min_{j=2,\dots,m_n} |y_j - y_{j-1}|$ is bounded from above and below, then we have

$$\sqrt{nm_n}\big(\hat{\kappa}_{n,m_n} - \kappa\big) \xrightarrow{d} \mathcal{N}\left(0, \frac{3\Gamma\pi}{(1-\delta)^2+\delta}\right),$$

as $n \to \infty$ and $m_n = \mathcal{O}(n^\rho)$, where $\rho \in (0, 1/2)$.

Proof. To compute the asymptotic variance, we obtain by using Lemma 2.2.1:

$$\begin{aligned}
\lim_{n\to\infty} \mathbb{V}\mathrm{ar}\left(\sum_{i=1}^{n} \Xi_{n,i}^{\sigma_0^2}\right) &= \lim_{n\to\infty} \mathbb{V}\mathrm{ar}\left(\sum_{i=1}^{n} \xi_{n,i}^{\sigma_0^2}\right) = \lim_{n\to\infty} \frac{m_n\pi}{\sigma_0^4\big(\sum_{i=1}^{m_n} y_i^2\big)^2} \mathbb{V}\mathrm{ar}\left(\sum_{i=1}^{n}\sum_{j=1}^{m_n} (\Delta_i \tilde{X})^2(y_j) e^{y_j\kappa} y_j\right) \\
&= \lim_{n\to\infty} \frac{nm_n\pi}{\sigma_0^4\big(\sum_{i=1}^{m_n} y_i^2\big)^2} \mathbb{V}\mathrm{ar}\left(\frac{1}{\sqrt{n}}\sum_{j=1}^{m_n}\sum_{i=1}^{n} (\Delta_i \tilde{X})^2(y_j) e^{y_j\kappa} y_j\right) \\
&= \lim_{n\to\infty} \frac{nm_n\pi}{\sigma_0^4\big(\sum_{i=1}^{m_n} y_i^2\big)^2} \left(\sum_{j=1}^{m_n} y_j^2 \mathbb{V}\mathrm{ar}\big(V_{n,\Delta_n}(y_j)\big) + \sum_{j\neq l}^{m_n} y_j y_l \mathbb{C}\mathrm{ov}\big(V_{n,\Delta_n}(y_j), V_{n,\Delta_n}(y_l)\big)\right) \\
&= \lim_{n\to\infty} \frac{nm_n\pi}{\sigma_0^4\big(\sum_{i=1}^{m_n} y_i^2\big)^2} \left(\frac{\Gamma\sigma_0^4 \sum_{j=1}^{m_n} y_j^2}{n}\big(1 + \mathcal{O}(1 \wedge \Delta_n^\eta)\big)\right. \\
&\qquad \left. + \mathcal{O}\left(\Delta_n^{3/2}\left(\sum_{j\neq l}^{m_n}\left(\frac{y_j y_l}{|y_j - y_l|}\right) + m_n^2\delta^{-1}\right)\right)\right) \\
&= \lim_{n\to\infty} \frac{\Gamma\pi(1-2\delta)}{\frac{1-2\delta}{m_n}\sum_{i=1}^{m_n} y_i^2}\big(1 + \mathcal{O}(\Delta_n^\eta)\big) + \mathcal{O}\left(\Delta_n^{1/2}\left(\sum_{j\neq l}^{m_n}\left(\frac{y_j y_l}{m_n|y_j - y_l|}\right) + \frac{m_n}{\delta}\right)\right) \\
&= \lim_{n\to\infty} \frac{\Gamma\pi(1-2\delta)}{\frac{1-2\delta}{m_n}\sum_{i=1}^{m_n} y_i^2}\big(1 + \mathcal{O}(\Delta_n^\eta)\big) + \mathcal{O}\left(\Delta_n^{1/2}\left(m_n \log(m_n) + \frac{m_n}{\delta}\right)\right) \\
&= \frac{\Gamma\pi(1-2\delta)}{\int_\delta^{1-\delta} y^2\,\mathrm{d}y} = \frac{3\Gamma\pi}{(1-\delta)^2+\delta}.
\end{aligned}$$

Notably, the assumptions that $y_1 = \delta$, $y_{m_n} = 1-\delta$, and the upper bound on $m_n \min_{j=2,\dots,m_n} |y_j - y_{j-1}|$ were solely necessary to ensure the convergence of the Riemann sum to an integral over the interval $[\delta, 1-\delta]$. Now, our focus is on demonstrating that $\Xi_{n,i}^{\sigma_0^2} \in \mathcal{H}_0$ and proving equation (48). Here, we have

$$\begin{aligned}\xi_{n,i}^{\sigma_0^2} &= -\frac{\sqrt{m_n \pi}}{\sigma_0^2 \sum_{i=1}^{m_n} y_i^2} \sum_{j=1}^{m_n} (\Delta_i \tilde{X})^2(y_j) e^{y_j \kappa} y_j \\ &= f_\vartheta(m_n) \sum_{j=1}^{m_n} (\Delta_i \tilde{X})^2(y_j) g_\vartheta(j),\end{aligned}$$

where

$$f_\vartheta(m_n) := -\frac{\sqrt{m_n \pi}}{\sigma_0^2 \sum_{i=1}^{m_n} y_i^2} \quad \text{and} \quad g_\vartheta(j) := e^{y_j \kappa} y_j.$$

By Lemma 2.2.1 we have $f_\vartheta^2(m_n) = \mathcal{O}(m_n^{-1})$ and $|g_\vartheta(j)| = \mathcal{O}(1)$ uniformly in j and therefore $\Xi_{n,i}^{\sigma_0^2} \in \mathcal{H}_0$. By Proposition 1.2.1 we have

$$\begin{aligned}\frac{m_n \pi}{\sigma_0^4 \big(\sum_{i=1}^{m_n} y_i^2\big)^2} \sum_{j=1}^{m_n} \sum_{i=b+u}^{c} \mathbb{E}\big[(\Delta_i \tilde{X})^4(y_j)\big] e^{2y_j\kappa} y_j^2 &\geqslant C'' \frac{m_n \pi}{\sigma_0^4 \big(\sum_{i=1}^{m_n} y_i^2\big)^2} p_u \Delta_n \frac{\sigma_0^4}{\pi} \sum_{j=1}^{m_n} y_j^2 e^{2y_j\kappa} e^{-2y_j\kappa} \\ &= C'' \frac{\Delta_n m_n p_u}{\sum_{i=1}^{m_n} y_i^2} \geqslant C'' p_u \Delta_n,\end{aligned}$$

where $p_2 := c - b - u + 1$. The proof is completed by invoking Proposition 2.4.2. □

The asymptotic variance of the estimator $\hat{\kappa}_{n,m_n}$, thanks to its variance-stabilizing transformation, is independent of the unknown parameter κ. Consequently, we conclude this section with the following normalized central limit theorem, which directly follows by applying an elementary transformation.

Corollary 2.4.4
Grant Assumptions 1.1.1 and 1.1.2, then we have

$$\sqrt{n m_n} \left(\frac{\Gamma \pi}{\frac{1}{m_n} \sum_{j=1}^{m_n} y_j^2} \right)^{-1/2} \big(\hat{\kappa}_{n,m_n} - \kappa\big) \xrightarrow{d} \mathcal{N}\big(0,1\big),$$

as $n \to \infty$ and $m_n = \mathcal{O}(n^\rho)$, where $\rho \in (0, 1/2)$. Moreover, with $y_1 = \delta$, $y_{m_n} = 1 - \delta$ and $m_n \min_{j=2,\dots,m_n} |y_j - y_{j-1}|$ bounded from above and below, we have

$$\sqrt{n m_n} \left(\frac{3 \Gamma \pi}{(1-\delta)^2 + \delta} \right)^{-1/2} \big(\hat{\kappa}_{n,m_n} - \kappa\big) \xrightarrow{d} \mathcal{N}\big(0,1\big),$$

as $n \to \infty$.

2.4.3. CLT for the curvature estimator with unknown normalized volatility

In this section, we will establish a central limit theorem for the estimator $\hat{\varkappa}$, where the parameter $m = m_n$ satisfies $m_n = \mathcal{O}(n^\rho)$, with $\rho \in (0, 1/2)$. Analogously to Section 2.4.2, this will be achieved by utilizing the presented central limit theorem from Proposition 2.4.2.

To proceed, we make use of the triangular array defined as

$$\Xi_{n,i} = \xi_{n,i} - \mathbb{E}[\xi_{n,i}], \xi_{n,i} = \frac{\sqrt{m_n \pi}}{\sigma_0^2 \sum_{j \neq l}(y_j - y_l)^2} \sum_{j \neq l} \big((\Delta_i \tilde{X})^2(y_j) e^{\kappa y_j} - (\Delta_i \tilde{X})^2(y_l) e^{\kappa y_l}\big)(y_l - y_j),$$

as introduced in Section 2.4.1.

Proposition 2.4.5
Grant Assumptions 1.1.1 and 1.1.2, with $y_1 = \delta$, $y_{m_n} = 1 - \delta$ and $m_n \min_{j=2,\dots,m_n} |y_j - y_{j-1}|$ is bounded from above and below, then we have

$$\sqrt{n m_n}\big(\hat{\varkappa}_{n,m_n} - \kappa\big) \xrightarrow{d} \mathcal{N}\bigg(0, \frac{12\Gamma\pi}{(1-2\delta)^2}\bigg),$$

as $n \to \infty$ and $m_n = \mathcal{O}(n^\rho)$, where $\rho \in (0, 1/2)$.

Proof. To initiate this proof, we start by calculating the asymptotic variance. Utilizing Lemma 2.2.1, we obtain

$$\begin{aligned}
\lim_{n\to\infty} \mathbb{V}\text{ar}\bigg(\sum_{i=1}^n \Xi_{n,i}\bigg) &= \lim_{n\to\infty} \mathbb{V}\text{ar}\bigg(\sum_{i=1}^n \xi_{n,i}\bigg) \\
&= \lim_{n\to\infty} \frac{n m_n \pi}{\sigma_0^4 \big(\sum_{j\neq l}(y_j - y_l)^2\big)^2} \mathbb{V}\text{ar}\bigg(\sum_{j \neq l} \big(V_{n,\Delta_n}(y_j) - V_{n,\Delta_n}(y_l)\big)(y_l - y_j)\bigg) \\
&= \lim_{n\to\infty} \frac{4 n m_n \pi}{\sigma_0^4 \big(\sum_{j\neq l}(y_j - y_l)^2\big)^2} \mathbb{V}\text{ar}\bigg(\sum_{j=1}^{m_n} V_{n,\Delta_n}\bigg(\sum_{l=1}^{m_n}(y_l - y_j)\bigg)\bigg) \\
&= \lim_{n\to\infty} \frac{4 n m_n \pi}{\sigma_0^4 \big(\sum_{j\neq l}(y_j - y_l)^2\big)^2} \mathbb{V}\text{ar}\bigg(\sum_{j=1}^{m_n} V_{n,\Delta_n}(y_j) G_j\bigg),
\end{aligned}$$

where $G_j := \sum_{l=1}^{m_n}(y_l - y_j)$. Additionally, considering $G_j = \mathcal{O}(m)$ and using an analogous procedure as in Proposition 2.3.5, we find

$$\begin{aligned}
&\lim_{n\to\infty} \mathbb{V}\text{ar}\bigg(\sum_{i=1}^n \Xi_{n,i}\bigg) \\
&= \lim_{n\to\infty} \frac{4 n m_n \pi}{\sigma_0^4 \big(\sum_{j\neq l}(y_j - y_l)^2\big)^2} \bigg(\sum_{j=1}^{m_n} G_j^2 \mathbb{V}\text{ar}\big(V_{n,\Delta_n}(y_j)\big) + \sum_{j_1 \neq j_2} \mathbb{C}\text{ov}\big(V_{n,\Delta_n}(y_{j_1}) G_{j_1}, V_{n,\Delta_n}(y_{j_2}) G_{j_2}\big)\bigg) \\
&= \lim_{n\to\infty} \frac{4 n m_n \pi}{\sigma_0^4 \big(\sum_{j\neq l}(y_j - y_l)^2\big)^2} \bigg(\sum_{j=1}^{m_n} G_j^2 \frac{\Gamma \sigma_0^4}{n}\big(1 + \mathcal{O}(1 \wedge \Delta_n^\eta)\big) + \sum_{j_1 \neq j_2} G_{j_1} G_{j_2} \mathbb{C}\text{ov}\big(V_{n,\Delta_n}(y_{j_1}), V_{n,\Delta_n}(y_{j_2})\big)\bigg) \\
&= \lim_{n\to\infty} \frac{4 m_n \pi \Gamma \sum_{j=1}^{m_n} G_j^2}{\big(\sum_{j\neq l}(y_j - y_l)^2\big)^2}\big(1 + \mathcal{O}(\Delta_n^\eta)\big) + \mathcal{O}\bigg(\frac{4 n m_n \pi \Delta_n^{3/2}}{\sigma_0^4 \big(\sum_{j\neq l}(y_j - y_l)^2\big)^2}\bigg(\sum_{j_1 \neq j_2}\bigg(\frac{G_{j_1} G_{j_2}}{|y_{j_1} - y_{j_2}|}\bigg) + m_n^4 \delta^{-1}\bigg)\bigg)
\end{aligned}$$

$$= \lim_{n\to\infty} \frac{4m_n\pi\Gamma\sum_{j=1}^{m_n} G_j^2}{\big(\sum_{j\neq l}(y_j-y_l)^2\big)^2}\big(1+\mathcal{O}(\Delta_n^\eta)\big) + \mathcal{O}\bigg(\Delta_n^{1/2}\sum_{j_1\neq j_2}\Big(\frac{1}{m_n|y_{j_1}-y_{j_2}|}\Big) + \Delta_n^{1/2}m_n\delta^{-1}\bigg)$$
$$= m_n\Gamma\pi\frac{4\sum_{j=1}^{m_n}\big(\sum_{l=1}^{m_n}(y_l-y_j)\big)^2}{\big(\sum_{j\neq l}(y_j-y_l)^2\big)^2}\big(1+\mathcal{O}(\Delta_n^\eta)\big) + \mathcal{O}\big(\Delta_n^{1/2}m_n\log(m_n)+\Delta_n^{1/2}m_n\delta^{-1}\big)$$
$$= \frac{\Gamma\pi}{\Big(\frac{1}{1-2\delta}\big(\frac{1-2\delta}{m_n}\sum_{j=1}^{m_n}y_j^2\big) - \frac{1}{(1-2\delta)^2}\big(\frac{1-2\delta}{m_n}\sum_{j=1}^{m_n}y_j\big)^2\Big)}\big(1+\mathcal{O}(\Delta_n^\eta)\big) + \mathcal{O}\big(\Delta_n^{1/2}m_n\log(m_n)+\Delta_n^{1/2}m_n\delta^{-1}\big).$$

Finally, through elementary calculations, we obtain

$$\lim_{n\to\infty}\mathbb{V}\mathrm{ar}\bigg(\sum_{i=1}^n \Xi_{n,i}\bigg) = \frac{\Gamma\pi(1-2\delta)}{\int_\delta^{1-\delta}y^2\,\mathrm{d}y - \frac{1}{1-2\delta}\big(\int_\delta^{1-\delta}y\,\mathrm{d}y\big)^2} = \frac{12\Gamma\pi}{(1-2\delta)^2}.$$

It remains to show $\Xi_{n,i}\in\mathcal{H}_2$ and that the proof of the condition given in equation (48) holds. By rearranging the triangular array Ξ as defined in equation (31), we obtain that

$$\xi_{n,i} = \frac{\sqrt{m_n\pi}}{\sigma_0^2\sum_{j\neq l}(y_j-y_l)^2}\sum_{j\neq l}\big((\Delta_i\tilde{X})^2(y_j)e^{\kappa y_j} - (\Delta_i\tilde{X})^2(y_l)e^{\kappa y_l}\big)(y_l-y_j)$$
$$= \frac{2\sqrt{m_n\pi}}{\sigma_0^2\sum_{j\neq l}(y_j-y_l)^2}\sum_{j=1}^{m_n}(\Delta_i\tilde{X})^2(y_j)e^{\kappa y_j}\sum_{l=1}^{m_n}(y_l-y_j),$$

where we have used Lemma 2.2.1. Hence, we have

$$f_\vartheta(m_n) := \frac{2\sqrt{m_n\pi}}{\sigma_0^2\sum_{j\neq l}(y_j-y_l)^2} \quad\text{and}\quad g_\vartheta(j) = e^{\kappa y_j}\sum_{l=1}^{m_n}(y_l-y_j).$$

Once more, we can employ Lemma 2.2.1 to deduce that $f_\vartheta^2(m_n)=\mathcal{O}(m_n^{-3})$ and $|g_\vartheta(j)|\leqslant Cm_n$ uniformly in j. Consequently, $\Xi_{n,i}\in\mathcal{H}_2$. Using Proposition 1.2.1, we derive the following expression:

$$\frac{4m_n\pi}{\sigma_0^4\big(\sum_{j\neq l}(y_j-y_l)^2\big)^2}\sum_{j=1}^{m_n}\sum_{i=b+u}^{c}\mathbb{E}\big[(\Delta_i\tilde{X})^4(y_j)\big]e^{2\kappa y_j}\bigg(\sum_{l=1}^{m_n}(y_l-y_j)\bigg)^2$$
$$\geqslant C_1\frac{\Delta_n\sigma_0^4 m_n\pi p_u}{\pi\sigma_0^4\big(\sum_{j\neq l}(y_j-y_l)^2\big)^2}\sum_{j=1}^{m_n}\bigg(\sum_{l=1}^{m_n}(y_l-y_j)\bigg)^2$$
$$\geqslant C_2 p_u\Delta_n,$$

where $C_1, C_2>0$ are suitable constants and $p_u := c-b-u+1$. This concludes the proof. □

Since the asymptotic variance is independent of any unknown parameter, we conclude this section by establishing a normalized version of the previous central limit theorem using an elementary transformation.

Corollary 2.4.6

Grant Assumptions 1.1.1 and 1.1.2, then we have

$$\sqrt{nm_n}\left(\frac{\Gamma\pi(1-2\delta)}{\frac{1-2\delta}{m_n}\sum_{j=1}^{m_n}y_j^2-\frac{1}{1-2\delta}\left(\frac{1-2\delta}{m_n}\sum_{j=1}^{m_n}y_j\right)^2}\right)^{-1/2}\big(\hat{\varkappa}_{n,m_n}-\kappa\big)\xrightarrow{d}\mathcal{N}\big(0,1\big),$$

as $n\to\infty$ and $m_n=\mathcal{O}(n^\rho)$, where $\rho\in(0,1/2)$. Moreover, by setting $y_1=\delta$, $y_{m_n}=1-\delta$ and having $m_n\min_{j=2,\dots,m_n}|y_j-y_{j-1}|$ being bounded from above and below, we obtain

$$\sqrt{nm_n}\left(\frac{12\Gamma\pi}{(1-2\delta)^2}\right)^{-1/2}\big(\hat{\varkappa}_{n,m_n}-\kappa\big)\xrightarrow{d}\mathcal{N}\big(0,1\big),$$

as $n\to\infty$.

2.4.4. Curvature tests

In Sections 2.4.2 and 2.4.3, we have established the central limit theorems for the estimators $\hat{\kappa}$ and $\hat{\varkappa}$, respectively. The variance-stabilizing properties of these estimators render their asymptotic variances independent of any unknown parameter. As a consequence, we can construct confidence intervals to test for the unknown parameter $\kappa=\vartheta_1/\vartheta_2\in\mathbb{R}$ in the context of the SPDE model given by equation (1).

In particular, if we want to determine whether ϑ_1 is a part of the model, we can perform a test that examines whether $\kappa=0$ or $\kappa\neq 0$. To that end, we consider the following two-sided hypothesis test:

$$H_0:\kappa=\kappa_0\qquad\text{versus}\qquad H_1:\kappa\neq\kappa_0,$$

for a $\kappa_0\in\mathbb{R}$. Under the Assumptions 1.1.1 and 1.1.2, we proceed by defining the following two statistics:

$$\Lambda_{n,m}^{\sigma_0^2}:=\sqrt{nm}\left(\frac{\Gamma\pi}{\frac{1}{m}\sum_{j=1}^{m_n}y_j^2}\right)^{-1/2}\big(\hat{\kappa}_{n,m_n}-\kappa_0\big),$$

$$\Lambda_{n,m}:=\sqrt{nm}\left(\frac{\Gamma\pi(1-2\delta)}{\frac{1-2\delta}{m}\sum_{j=1}^{m}y_j^2-\frac{1}{1-2\delta}\left(\frac{1-2\delta}{m}\sum_{j=1}^{m}y_j\right)^2)}\right)^{-1/2}\big(\hat{\varkappa}_{n,m}-\kappa_0\big).$$

Using Corollaries 2.4.4 and 2.4.6, we establish the convergence of $\Lambda_{n,m}^{\sigma^2}\xrightarrow{d}\mathcal{N}(0,1)$ and $\Lambda_{n,m}\xrightarrow{d}\mathcal{N}(0,1)$. Leveraging these results, we construct the following asymptotic tests:

$$\varphi_{n,m}^{\sigma^2}:=\mathbb{1}_{\{|\Lambda_{n,m}^{\sigma_0^2}|>q_{1-\alpha/2}\}},$$

$$\varphi_{n,m}:=\mathbb{1}_{\{|\Lambda_{n,m}|>q_{1-\alpha/2}\}}.$$

Here, q_α represents the α quantile of the standard normal distribution. By Corollaries 2.4.4 and 2.4.6, both tests have an asymptotic Type I error probability of $\alpha\in(0,1)$. Correctly choosing between test $\varphi^{\sigma_0^2}$ and test φ depends on whether the normalized volatility σ_0^2 is known or unknown. Specifically, since test $\varphi^{\sigma_0^2}$ involves the statistic $\Lambda^{\sigma_0^2}$ which incorporates the estimator $\hat{\kappa}$, it is appropriate to use this test when the normalized volatility σ_0^2 is known. On the other hand, test φ should be utilized when the normalized volatility σ_0^2 is unknown.

One-sided asymptotic tests can be formulated in a manner akin to the conventional construction of the z-test used to assess the mean of a normal distribution. An implementation of these tests can be found in the R-function kappa_test within the package ParabolicSPDEs[4].

We close this section by constructing asymptotic confidence intervals for the unknown parameter κ, with an asymptotic confidence level of $1-\alpha$. Here, we obtain:

(1) If σ_0^2 is known:

$$I_{n,m}^{\sigma_0^2} := \left[\hat{\kappa}_{n,m} - q_{1-\alpha/2}\Big(\frac{\Gamma\pi}{n\sum_{j=1}^{m_n} y_j^2}\Big)^{1/2}, \hat{\kappa}_{n,m} + q_{1-\alpha/2}\Big(\frac{\Gamma\pi}{n\sum_{j=1}^{m_n} y_j^2}\Big)^{1/2}\right].$$

(2) If σ_0^2 is unknown:

$$I_{n,m} := \big[\hat{\varkappa}_{n,m} - q_{1-\alpha/2}\gamma_{n,m}, \hat{\varkappa}_{n,m} + q_{1-\alpha/2}\gamma_{n,m}\big],$$

where

$$\gamma_{n,m} = \left(\frac{\Gamma\pi(1-2\delta)}{n(1-2\delta)\sum_{j=1}^{m} y_j^2 - \frac{nm}{1-2\delta}\big(\frac{1-2\delta}{m}\sum_{j=1}^{m} y_j\big)^2\big)}\right)^{1/2}.$$

2.4.5. Comparison of the variances

In this section, our objective is to compare the performance of the estimators $\hat{\kappa}$ and $\hat{\varkappa}$, which estimate the parameter κ, with the estimator $\hat{\eta}^{\mathrm{BT}}$ presented in Bibinger and Trabs (2020), which estimates the parameter $\eta = (\sigma_0^2, \kappa)^\top \in (0,\infty) \times \mathbb{R}$. To facilitate the comparison, we define the coordinate projections $\eta_1 := \sigma_0^2$ and $\eta_2 := \kappa$.

The M-estimation of Bibinger and Trabs (2020) is based on the parametric regression model

$$\frac{\mathrm{RV}_n(y_j)}{\sqrt{n}} = \frac{\sigma_0^2}{\sqrt{\pi}} e^{-\kappa y_j} + \delta_{n,j}, \tag{37}$$

with non-standard estimation errors $(\delta_{n,j})$ satisfying

$$\mathbb{E}[\delta_{n,j}] = \mathcal{O}(\Delta_n),$$

and

$$\mathbb{C}\mathrm{ov}(\delta_{n,j}, \delta_{n,k}) = \mathbb{1}_{\{j=k\}}\Delta_n\Gamma\sigma_0^4 e^{-2\kappa y_j} + \mathcal{O}\Big(\Delta_n^{3/2}\big(\delta^{-1} + |y_j - y_k|^{-1}\big)\Big),$$

where $V_{n,\Delta_n}(y_j) = Z_j e^{-\kappa y_j}$. The M-estimator $\hat{\eta}^{\mathrm{BT}}$ is implicitly obtained by minimizing the sum of squares, given by

$$\hat{\eta}^{\mathrm{BT}} := \hat{\eta}^{\mathrm{BT}}_{n,m} := \big((\hat{\sigma}_0^{\mathrm{BT}})^2, \hat{\varkappa}^{\mathrm{BT}}\big) := \big((\hat{\sigma}_0^{\mathrm{BT}})^2_{n,m}, \hat{\varkappa}^{\mathrm{BT}}_{n,m}\big) := \arg\min_{s,k} \sum_{j=1}^{m} \Big(Z_{n,j} - f_{s,k}(y_j)\Big)^2, \tag{38}$$

[4] see: https://github.com/pabolang/ParabolicSPDEs.

where $Z_{n,j}$ is defined as

$$Z_{n,j} := \frac{1}{n\sqrt{\Delta_n}} \sum_{i=1}^{n} (\Delta_i X)^2(y_j) = f_{\sigma_0^2,\kappa}(y_j) + \delta_{n,j},$$

and $f_{s,k}(y) := se^{-ky}/\sqrt{\pi}$. Our aim is to compare the asymptotic variances derived from the central limit theorems presented in Propositions 2.4.3 and 2.4.5 with the asymptotic variance of the estimator $\hat{\eta}^{\mathrm{BT}}$ from Bibinger and Trabs (2020, Prop. 4.2.). However, before proceeding with the comparison, some preliminary work is required. We start by recalling the central limit theorem presented by Bibinger and Trabs (2020).

Proposition 2.4.7

Grant Assumptions 1.1.1 and 1.1.2, with $y_1 = \delta$ and $y_{m_n} = 1-\delta$ and $m_n \min_{j=2,\dots,m_n} |y_j - y_{j-1}|$ is uniformly bounded from above and from below. Let $\eta \in \Xi$ for some compact set $\Xi \subset (0,\infty) \times [0,\infty)$. The the estimator $\hat{\eta}^{\mathrm{BT}}$ satisfies for a sequence $m_n \to \infty$, as $n \to \infty$, the central limit theorem

$$\sqrt{nm_n}\big((\hat{\eta}^{\mathrm{BT}}_{n,m})^\top - \eta^\top\big) \xrightarrow{d} \mathcal{N}(0, \Sigma^{\mathrm{BT}}),$$

where $\Sigma^{\mathrm{BT}} := \Sigma^{\mathrm{BT}}(\eta,\delta) = \sigma_0^4 \Gamma \pi V(\eta,\delta)^{-1} U(\eta,\delta) V(\eta,\delta)^{-1}$ and the strictly positive definite matrices

$$U(\eta,\delta) := \begin{pmatrix} \int_\delta^{1-\delta} e^{-4\kappa y}\,\mathrm{d}y & -\sigma_0^2 \int_\delta^{1-\delta} y e^{-4\kappa y}\,\mathrm{d}y \\ -\sigma_0^2 \int_\delta^{1-\delta} y e^{-4\kappa y}\,\mathrm{d}y & \sigma_0^4 \int_\delta^{1-\delta} y^2 e^{-4\kappa y}\,\mathrm{d}y \end{pmatrix},$$

$$V(\eta,\delta) := \begin{pmatrix} \int_\delta^{1-\delta} e^{-2\kappa y}\,\mathrm{d}y & -\sigma_0^2 \int_\delta^{1-\delta} y e^{-2\kappa y}\,\mathrm{d}y \\ -\sigma_0^2 \int_\delta^{1-\delta} y e^{-2\kappa y}\,\mathrm{d}y & \sigma_0^4 \int_\delta^{1-\delta} y^2 e^{-2\kappa y}\,\mathrm{d}y \end{pmatrix}.$$

Firstly, it is reasonable to expect that the asymptotic variance of the estimator $\hat{\kappa}$ is uniformly smaller than the asymptotic variance of the estimator $\hat{\eta}_2^{\mathrm{BT}}$, as $\hat{\eta}^{\mathrm{BT}}$ estimates both parameters σ_0^2 and κ. Additionally, the asymptotic variance of $\hat{\eta}_2^{\mathrm{BT}}$ is likely dependent on the unknown parameter η, whereas Propositions 2.4.3 and 2.4.5 demonstrate that the asymptotic variances of the estimators $\hat{\kappa}$ and $\hat{\varkappa}$ are independent of these parameters.

Indeed, the difference between the estimators $\hat{\kappa}$ and $\hat{\varkappa}$ in terms of their asymptotic variances highlights a crucial distinction between them. Comparing the asymptotic variances of the estimators $\hat{\kappa}$ and $\hat{\varkappa}$, we observe that the asymptotic variance of $\hat{\kappa}$ significantly surpasses the asymptotic variance of the estimator $\hat{\varkappa}$, since

$$\frac{(1-\delta)^2+\delta}{3} = \frac{(1-2\delta)^2 + 3(\delta-\delta^2)}{3} = \frac{4(1-2\delta)^2}{12} + (\delta-\delta^2) > \frac{(1-2\delta)^2}{12},$$

for $\delta \in (0, 1/2)$. This result holds true for all δ values within the interval $(0, 1/2)$, which shows that the asymptotic variance of $\hat{\kappa}$ consistently outperforms the asymptotic variance of the estimator $\hat{\varkappa}$ across this entire range of δ values.

Now, our focus is to explore whether there are scenarios where the asymptotic variance of $\hat{\eta}_2^{\mathrm{BT}}$ is smaller than the asymptotic variance of the estimator $\hat{\varkappa}$. To achieve this, we require a representation of the asymptotic variance of $\hat{\eta}_2^{\mathrm{BT}}$, which does not have an integral representation. To proceed, we will present an explicit representation of the inverse matrix $V(\eta, \delta)^{-1}$. For ease of readability, we replace each entry with a simplified notation:

$$V(\eta, \delta) = \begin{pmatrix} a & b \\ b & d \end{pmatrix} \quad \text{and} \quad U(\eta, \delta) = \begin{pmatrix} A & B \\ B & D \end{pmatrix},$$

and have

$$V(\eta, \delta)^{-1} = \frac{1}{ad - b^2} \begin{pmatrix} d & -b \\ -b & a \end{pmatrix}.$$

Now, upon multiplying the matrices, we obtain the following expressions for the entries of the resulting matrix

$$V(\eta, \delta)^{-1} U(\eta, \delta) V(\eta, \delta)^{-1} = \frac{1}{(ad - b^2)^2} \begin{pmatrix} d^2 A - 2bdB + b^2 D & -bdA + b^2 B + adB - abD \\ -bdA + b^2 B + adB - abD & b^2 A - 2abB + a^2 D \end{pmatrix},$$

where $\Sigma_{2,2}^{\mathrm{BT}} = (b^2 A - 2abB + a^2 D)/(ad - b^2)^2$ represents the asymptotic variance of $\hat{\eta}_2^{\mathrm{BT}}$ and $\Sigma_{1,1}^{\mathrm{BT}} = (d^2 A - 2bdB + b^2 D)/(ad - b^2)^2$ represents the asymptotic variance of $\hat{\eta}_1^{\mathrm{BT}}$. Next, we proceed with the calculation of the elementary integrals:

$$\begin{aligned} \int e^{-cy} \, \mathrm{d}y &= \Big[-\frac{1}{c} e^{-cy} \Big], \\ \int y e^{-cy} \, \mathrm{d}y &= \Big[-\frac{cy + 1}{c^2} e^{-cy} \Big], \\ \int y^2 e^{-cy} \, \mathrm{d}y &= \Big[-\frac{cy(cy + 2) + 2}{c^3} e^{-cy} \Big], \end{aligned}$$

where $c \in \mathbb{R}$. In the case where $\kappa = 0$, we obtain the following:

$$V^{-1}\big((\sigma_0^2, 0), \delta\big) = \begin{pmatrix} \frac{4(1-\delta+\delta^2)}{(1-2\delta)^3} & \frac{6}{(1-2\delta)^3 \sigma^2} \\ \frac{6}{(1-2\delta)^3 \sigma^2} & \frac{12}{(1-2\delta)^3 \sigma^4} \end{pmatrix},$$

and therefore we have

$$\Sigma_{2,2}^{\mathrm{BT}}\big((\sigma_0^2, 0), \delta\big) = \begin{pmatrix} \frac{4\pi\Gamma(1-\delta+\delta^2)\sigma_0^4}{(1-2\delta)^3} & \frac{6\pi\Gamma\sigma_0^2}{(1-2\delta)^3} \\ \frac{6\pi\Gamma\sigma_0^2}{(1-2\delta)^3} & \frac{12\pi\Gamma}{(1-2\delta)^3} \end{pmatrix}.$$

Similarly, for $\kappa \neq 0$, i.e., $\eta_2 \neq 0$, we have

$$V(\eta,\delta)^{-1} = \begin{pmatrix} \frac{4\kappa e^{4\delta\kappa+2\kappa}\left(e^{-2(\delta-1)\kappa}(2\delta\kappa(\delta\kappa+1)+1)+e^{2\delta\kappa}(2(\delta-1)\kappa(-\delta\kappa+\kappa+1)-1)\right)}{-2e^{4\delta\kappa+2\kappa}(2(1-2\delta)^2\kappa^2+1)+e^{8\delta\kappa}+e^{4\kappa}} & \frac{4\kappa^2 e^{2(\delta+1)\kappa}\left(e^{4\delta\kappa}(2(\delta-1)\kappa-1)+e^{2\kappa}(2\delta\kappa+1)\right)}{\sigma_0^2(-2e^{4\delta\kappa+2\kappa}(2(1-2\delta)^2\kappa^2+1)+e^{8\delta\kappa}+e^{4\kappa})} \\ \frac{4\kappa^2 e^{2(\delta+1)\kappa}\left(e^{4\delta\kappa}(2(\delta-1)\kappa-1)+e^{2\kappa}(2\delta\kappa+1)\right)}{\sigma_0^2(-2e^{4\delta\kappa+2\kappa}(2(1-2\delta)^2\kappa^2+1)+e^{8\delta\kappa}+e^{4\kappa})} & \frac{16\kappa^3 e^{(4\delta+3)\kappa}\sinh(\kappa-2\delta\kappa)}{\sigma_0^4(-2e^{4\delta\kappa+2\kappa}(2(1-2\delta)^2\kappa^2+1)+e^{8\delta\kappa}+e^{4\kappa})} \end{pmatrix},$$

and therefore the asymptotic variance is given by

$$\Sigma_{2,2}^{\mathrm{BT}}(\eta,\delta) = \begin{pmatrix} a_{1,1} & a_{1,2} \\ a_{1,2} & a_{2,2} \end{pmatrix},$$

where

$$\begin{aligned} a_{1,1} = &-\frac{\pi\Gamma\kappa e^{8(\delta+1)\kappa}\sigma_0^4}{2\left(-2e^{4\delta\kappa+2\kappa}\left(2(1-2\delta)^2\kappa^2+1\right)+e^{8\delta\kappa}+e^{4\kappa}\right)^2} \\ &\times \Big(2e^{-2\kappa}\left(e^{-2(\delta-1)\kappa}(2\delta\kappa(\delta\kappa+1)+1)+e^{2\delta\kappa}(2(\delta-1)\kappa(-\delta\kappa+\kappa+1)-1)\right) \\ &\times \Big(e^{-6\delta\kappa}\left(2\delta\kappa+e^{4\delta\kappa-2\kappa}(2(\delta-1)\kappa-1)+1\right)\left(4\delta\kappa+e^{8\delta\kappa-4\kappa}(4(\delta-1)\kappa-1)+1\right) \\ &+4e^{-2\kappa}\left(e^{4(\delta-1)\kappa}-e^{-4\delta\kappa}\right)\left(e^{-2(\delta-1)\kappa}(2\delta\kappa(\delta\kappa+1)+1)+e^{2\delta\kappa}(2(\delta-1)\kappa(-\delta\kappa+\kappa+1)-1)\right)\Big) \\ &+e^{-2\delta\kappa}\left(2\delta\kappa+e^{4\delta\kappa-2\kappa}(2(\delta-1)\kappa-1)+1\right) \\ &\times \Big(2e^{-2(2\delta\kappa+\kappa)}\left(4\delta\kappa+e^{8\delta\kappa-4\kappa}(4(\delta-1)\kappa-1)+1\right) \\ &\times \left(e^{-2(\delta-1)\kappa}(2\delta\kappa(\delta\kappa+1)+1)+e^{2\delta\kappa}(2(\delta-1)\kappa(-\delta\kappa+\kappa+1)-1)\right) \\ &-e^{-2(\delta+2)\kappa}\left(2\delta\kappa+e^{4\delta\kappa-2\kappa}(2(\delta-1)\kappa-1)+1\right) \\ &\times \left(e^{-4(\delta-1)\kappa}(4\delta\kappa(2\delta\kappa+1)+1)+e^{4\delta\kappa}(4(\delta-1)\kappa(1-2(\delta-1)\kappa)-1)\right)\Big)\Big), \\ a_{1,2} = &\frac{2\pi\Gamma\kappa^2\sigma_0^2}{\left(-2e^{4\delta\kappa+2\kappa}\left(2(1-2\delta)^2\kappa^2+1\right)+e^{8\delta\kappa}+e^{4\kappa}\right)^2} \\ &\times \Big(-(2\delta-1)\kappa e^{8\delta\kappa+4\kappa}\left(8(1-2\delta)^2\kappa^2+4\kappa+9\right)+e^{16\delta\kappa}((\delta-1)\kappa-1) \\ &+e^{8\kappa}(\delta\kappa+1)+(\kappa+2)e^{4\delta\kappa+6\kappa}((4\delta-2)\kappa-1)+(\kappa+2)e^{2(6\delta\kappa+\kappa)}((4\delta-2)\kappa+1)\Big), \\ a_{2,2} = &\frac{2\pi\Gamma\kappa^3 e^{4(\delta-1)\kappa}\left(e^{2\kappa}-e^{4\delta\kappa}\right)^2\left(4(2\delta-1)\kappa e^{4\delta\kappa+2\kappa}-e^{8\delta\kappa}+e^{4\kappa}\right)}{\left(-2e^{6\delta\kappa}\left(2(1-2\delta)^2\kappa^2+1\right)+e^{2(\delta+1)\kappa}+e^{2(5\delta-1)\kappa}\right)^2}. \end{aligned}$$

This yields the asymptotic variance of the estimator $\hat{\eta}_2^{\mathrm{BT}}$, which is represented by the following expression:

$$\Sigma_{2,2}^{\mathrm{BT}} = \Gamma\pi \begin{cases} \frac{12\pi\Gamma}{(1-2\delta)^3} & \text{, for } \eta_2 = 0 \\ \frac{2\pi\Gamma\kappa^3 e^{4(\delta-1)\kappa}\left(e^{2\kappa}-e^{4\delta\kappa}\right)^2\left(4(2\delta-1)\kappa e^{4\delta\kappa+2\kappa}-e^{8\delta\kappa}+e^{4\kappa}\right)}{\left(-2e^{6\delta\kappa}(2(1-2\delta)^2\kappa^2+1)+e^{2(\delta+1)\kappa}+e^{2(5\delta-1)\kappa}\right)^2} & \text{, for } \eta_2 \neq 0 \end{cases}.$$

Additionally, it holds that $\lim_{\eta_2\to 0}\Sigma_{2,2}^{\mathrm{BT}}((\eta_1,\eta_2),\delta) = \Sigma_{2,2}^{\mathrm{BT}}((\eta_1,0),\delta)$, which ensures that the asymptotic variance remains continuous as $\eta_2 = \kappa \in \mathbb{R}$. The preceding analysis also demonstrates that the asymptotic variance of the M-estimator $\hat{\eta}_2^{\mathrm{BT}}$ for κ is dependent on the unknown parameter κ while being independent of σ_0^2.

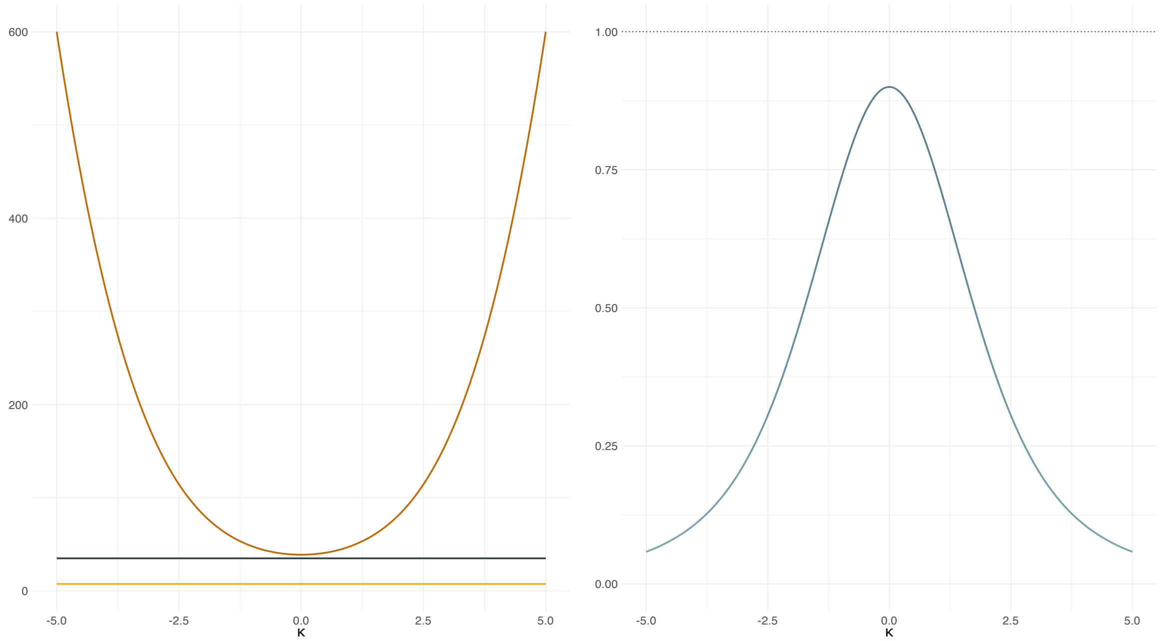

Figure 2.1.: We show the asymptotic variances of three estimators: $\hat{\eta}_2^{\mathrm{BT}}$ (brown), $\hat{\varkappa}$ (blue), and $\hat{\kappa}$ (yellow), where $\delta = 0.05$ and $\sigma_0^2 = 1$ are fixed. In the left panel, we showcase the asymptotic variance as a function of κ. The right panel displays the quotient of the asymptotic variances $\mathrm{AVAR}(\hat{\varkappa})/\mathrm{AVAR}(\hat{\eta}_2^{\mathrm{BT}})$.

Now, we further analyse the asymptotic variance to establish that it is always greater than or equal to $12\Gamma\pi/(1-2\delta)^2$, which corresponds to the asymptotic variance of $\hat{\varkappa}_{n,m_n}$.

When $\eta_2 = \kappa = 0$, the minimum asymptotic variance for both estimators $\hat{\eta}^{\mathrm{BT}}$ and $\hat{\varkappa}$ is given by

$$\lim_{\delta\to 0} \Sigma_{2,2}^{\mathrm{BT}}((\eta_1, 0), \delta) = 12\Gamma\pi = \lim_{\delta\to 0} \frac{12\Gamma\pi}{(1-2\delta)^2}.$$

Indeed, when $0 < \delta < 1/2$, the asymptotic variance of the estimator $\hat{\eta}^{\mathrm{BT}}$ is greater than the asymptotic variance of the non-oracle estimator $\hat{\varkappa}$, as $(1-2\delta)^3 < (1-2\delta)^2$.

Next, consider the case where $\kappa > 0$. We observe that $\Sigma_{2,2}^{\mathrm{BT}}(\eta, \delta)$ is monotonically increasing in δ while η remains arbitrary but fixed. Therefore, we can focus on analysing the case where $\delta = 0$. In this scenario, the asymptotic variance $\Sigma_{2,2}^{\mathrm{BT}}(\eta, 0)$ is independent of $\eta_1 = \sigma_0^2$ and monotonically increasing in $\eta_2 = \kappa$. We find a minimum at $\kappa = 0$ with an asymptotic variance of $12\Gamma\pi$, which coincides with the asymptotic variance of the estimator $\hat{\varkappa}_{n,m}$.

Since the asymptotic variance of $\hat{\varkappa}_{n,m}$ is constant in η_2, and the asymptotic variance of $\hat{\eta}_2^{\mathrm{BT}}$ is monotonically increasing in η_2, we can conclude that the asymptotic variance of $\hat{\varkappa}_{n,m}$ is uniformly smaller or equal to the asymptotic variance of $\hat{\eta}_2^{\mathrm{BT}}$ for all values of $\kappa > 0$. Analogous arguments hold for the case where $\kappa < 0$.

To conclude this section, we provide plots of the asymptotic variances for the estimators $\hat{\kappa}_{n,m}$, $\hat{\varkappa}_{n,m}$ and $\hat{\eta}_2^{\mathrm{BT}}$. As mentioned before, the asymptotic variance of each of these three estimators is independent of the parameter σ_0^2. Figure 2.1 illustrates the asymptotic variances for $\eta_2 = \kappa \in [-5, 5]$, $\delta = 0.05$, and a fixed normalized volatility $\sigma_0^2 = 1$. The left panel in Figure 2.1 displays the asymptotic variances of the three estimators as given in the central limit theorems in Proposition 2.4.3, Proposition 2.4.5, and Proposition 2.4.7. Here, we can observe that even for a moderate curvature, the asymptotic variance of the estimator $\hat{\eta}^{\mathrm{BT}}$ increases significantly, while the asymptotic variances of the other estimators remain constant. Since both estimators $\hat{\eta}^{\mathrm{BT}}$ and $\hat{\varkappa}$ do not require any information about the rescaled volatility, we provide a second plot in the right panel, which shows the quotient of the asymptotic variances of these estimators, where the the asymptotic variance of $\hat{\varkappa}$ is given in the numerator. By observing the right panel and considering the previous analysis, it is evident that the quotient is smaller than 1 for $\delta \in (0, 1/2)$. Additionally, it is monotonically increasing for $\eta_2 \in (-\infty, 0)$ and monotonically decreasing for $\eta_2 \in (0, \infty)$. As $\delta \to 0$, the maximum value of the quotient is 1.

2.5. Simulation

This section initiates with a discussion on simulating samples of a mild solution X_t from the SPDE model given in equation (1) generated on a discrete grid. Two methods for simulating data will be discussed: the truncation method and the replacement method, as introduced by Bibinger and Trabs (2020) and Hildebrandt (2020), respectively. As we apply these concepts to simulate a SDPE model in higher dimensions, which is discussed in Part II of this thesis, we will closely examine these methods.

Subsequently, we will present a simulation study for the estimators derived in this chapter. A comparison of the curvature estimators from this chapter, as well as the curvature estimator presented in Bibinger and Trabs (2020), will be conducted. This comparison aims to explore the relative performance and accuracy of these estimators by conducting a Monte Carlo simulation study.

2.5.1. Simulation methods

The objective of this section is to introduce simulation methods for generating a SPDE model outlined in equation (1). As discussed in Section 1.1.1, we can represent a mild solution $X_t(y) = \sum_{k\geqslant 1} x_k(t)e_k(y)$ of the SPDE model given in equation (1) as an infinite factor model, where the coordinate processes x_k satisfy the Ornstein-Uhlenbeck dynamic with decay rates λ_k, for $k \in \mathbb{N}$. By using the Fourier series for simulating a solution process X, we have the following options. Either we cut off the Fourier series at a suitable large cut-off rate $K \in \mathbb{N}$ which we call by the truncation method, or we take advantage of the so-called replacement method, cf. Hildebrandt (2020). For both methods, an exact simulation of the Ornstein-Uhlenbeck processes x_k is crucial for the quality of the simulation. Let $N \in \mathbb{N}$ and $M \in \mathbb{N}$ denote the number of temporal and spatial observations, respectively.

As seen in Section 1.1.1, the coordinate processes x_k for some solution X are given by $x_k(t) = e^{-t\lambda_k}\langle \xi, e_k\rangle_\vartheta + \int_0^t e^{-\lambda_k(t-s)}\sigma \,\mathrm{d}W_s^k$. Therefore, we can write the increments at times $t = 0, \Delta_N, \ldots, (N-1)\Delta_N$ as follows:

$$x_k(t+\Delta_N) = x_k(t)e^{-\lambda_k\Delta_N} + \sigma \int_t^{t+\Delta_N} e^{-\lambda_k(t+\Delta_N-s)}\,\mathrm{d}W_s^k.$$

Thus, we obtain the following recursive representation:

$$x_k(t+\Delta_N) = x_k(t)e^{-\lambda_k \Delta_N} + \sigma\sqrt{\frac{1-\exp\big[-2\lambda_k\Delta_N\big]}{2\lambda_k}}\mathcal{N}_t,$$

where $(\mathcal{N}_t)$ denote i.i.d. standard normal random variables for $t = 0, \Delta_N, \ldots, (N-1)\Delta_N$. The truncation method involves considering the first $K \in \mathbb{N}$ coordinate processes x_k to approximate the mild solution X. The effectiveness of this method is strongly influenced by the chosen cut-off rate $K \in \mathbb{N}$. Kaino and Uchida (2021b) observed through empirical study that insufficiently large values of K lead to considerable biases in the simulations. Selecting an appropriate cut-off rate also appears to be dependent on the number of spatial and temporal observations. Even for moderate sample sizes, a cut-off rate of $K = 10^5$ is recommended, but it comes with a significant computational cost. For instance, simulating a single realization of X on a grid with $M = 100$ spatial points and $N = 10^4$ temporal points, using a cut-off rate $K = 10^5$, takes approximately 6 hours when utilizing 64 cores. This computational challenge motivates the adoption of the replacement method. Building on the work of Davie and Gaines (2001), the replacement method takes a different approach by not merely truncating the Fourier series. Instead, it replaces the higher Fourier modes of the Fourier series with a suitable set of independent random variables. This alternative approach allows for an almost exact simulation of discrete samples of X, significantly reducing the computational costs.

We describe the replacement method procedure for the case when $\xi = 0$ and consider equidistant spatial points, such as $y_j = j/M$ for $j = 0, \ldots, M$. To simplify the Fourier representation of $X_t(y) = \sum_{k=1}^{\infty} x_k(t)e_k(y)$, we utilize the following weighted inner product:

$$\langle f, g\rangle_{\vartheta,M} := \frac{1}{M}\sum_{j=0}^{M} f(y_j)g(y_j)e^{\kappa y_j}, \tag{39}$$

for functions $f, g : [0,1] \to \mathbb{R}$. Using the orthonormal basis e_k as defined in equation (2), we perform the spectral approach. First, we find that the coefficient processes $(e_k)_{1\leqslant k\leqslant M-1}$ define an orthonormal basis with respect to the inner product $\langle\cdot,\cdot\rangle_{\vartheta,M}$. As described in Hildebrandt (2020), utilizing the properties $\bar{e}_M = 0$, $\bar{e}_{k+2lM} = \bar{e}_k$, and $\bar{e}_{2M-k+2lM} = -\bar{e}_k$ for $\bar{e}_k := \big(e_k(y_0), \ldots, \bar{e}_k(y_M)\big) \in \mathbb{R}^{M+1}$ yields the following Fourier representation:

$$X_t(y_j) = \sum_{m=1}^{M-1} U_m(t)e_m(y_j),$$

for $t \geqslant 0$ and $j = 0, \ldots, M$. Here, the coordinate processes U_m can be written as

$$U_m = \langle X_t, e_m\rangle_{\vartheta,M} = \sum_{l\in\mathcal{I}_m^+} x_l(t) - \sum_{l\in\mathcal{I}_m^-} x_l(t),$$

where x_l denotes the coordinate processes from equation (5) and the index sets are defined as

$$\mathcal{I}_m^+ = \{m + 2lM, l \in \mathbb{N}_0\}, \qquad \mathcal{I}_m^- = \{2M - m + 2lM, l \in \mathbb{N}_0\} \qquad \text{and} \qquad \mathcal{I}_m := \mathcal{I}_m^+ \cup \mathcal{I}_m^-. \tag{40}$$

Thus, we obtain a finite Fourier representation of X on a discrete grid. To complete our understanding of the replacement method, we need to address the simulation of the processes U_m. As discussed in Hildebrandt and Trabs (2021) and Hildebrandt (2020), when $\xi = 0$, the coordinate processes x_k are centred Gaussian with the covariance function

$$\mathbb{C}\mathrm{ov}\big((x_k(t_i), x_k(t_j)\big) = \frac{\sigma^2}{2\lambda_k} e^{-\lambda_k |i-j| \Delta_N} \big(1 - e^{-2\lambda_k \min(i,j)\Delta_N}\big),$$

where $1 \leqslant i, j \leqslant N$. If $\lambda_k \propto k^2$ is large compared to $1/\Delta_n = N$, the coordinate processes x_k effectively behave like i.i.d. centred Gaussian random variables with variances

$$\mathbb{V}\mathrm{ar}\big(x_k(t_i)\big) \approx \frac{\sigma^2}{2\lambda_k}.$$

We select a bound $L = L_{M,N} \in \mathbb{N}$, which represents multiples of M. Then, we can replace all x_k with sufficiently large $k \geqslant LM$ by a vector of i.i.d. centred normal random variables with variances $\sigma^2/(2\lambda_k)$. As the normal distribution is stable with respect to summation, it is sufficient to generate one set $\big(R_m^L(i)\big)_{1 \leqslant i \leqslant N}$ of random variables with $R_m^L(i) \sim \mathcal{N}(0, s_m^2)$, where

$$s_m^2 = \sum_{l \in \mathcal{I}_m, l \geqslant LM} \frac{\sigma^2}{2\lambda_l},$$

for $1 \leqslant m \leqslant M-1$. This leads to the following approximation for U_m:

$$U_m^L(0) = 0 \quad \text{and} \quad U_m^L(t_i) = \sum_{l \in \mathcal{I}_m, l < LM} x_l(t_i) + R_m^L(i),$$

for $1 \leqslant i \leqslant N$ and $1 \leqslant m \leqslant M-1$. According to Hildebrandt (2020, Lemma 3.1.), the infinite series s_m^2 has a closed form given by

$$s_m^2 = \frac{1}{M^2} b_m^\top \Sigma b_m - \sum_{l \in \mathcal{I}_m, l < LM} \frac{\sigma^2}{2\lambda_l}, \tag{41}$$

where $b_m := \sqrt{2}\big(\sin(\pi m y_0), \dots, \sin(\pi m y_M)\big)^\top \in \mathbb{R}^{M+1}$ and $\Sigma = (\Sigma_{j,l})_{j,l=0,\dots,M+1} = (\rho(y_j, y_l))_{j,l=0,\dots,M+1} \in \mathbb{R}^{(M+1)\times(M+1)}$, with the symmetric function $\rho : [0,1]^2 \to \mathbb{R}$, defined for $x \leqslant y$ as

$$\rho(x,y) = \frac{\sigma^2}{2\vartheta_2} \cdot \begin{cases} \frac{\sin(\Gamma_0(1-y))\sin(\Gamma_0 x)}{\Gamma_0 \sin(\Gamma_0)} & , \gamma < 0 \\ x(1-y) & , \gamma = 0 \\ \frac{\sinh(\Gamma_0(1-y))\sinh(\Gamma_0 x)}{\Gamma_0 \sinh(\Gamma_0)} & , \gamma > 0 \end{cases},$$

with

$$\gamma := \frac{\vartheta_1^2}{4\vartheta_2} - \frac{\vartheta_0}{\vartheta_2} \quad \text{and} \quad \Gamma_0 := \sqrt{|\gamma|}.$$

This method provides a finite spectral decomposition for a solution X, which significantly reduces the runtime. For example, in the same setting as before, where $M = 100$ and $N = 10^4$, one simulation takes just about 30 seconds when using 64 cores instead of 6 hours. The associated algorithm for this method

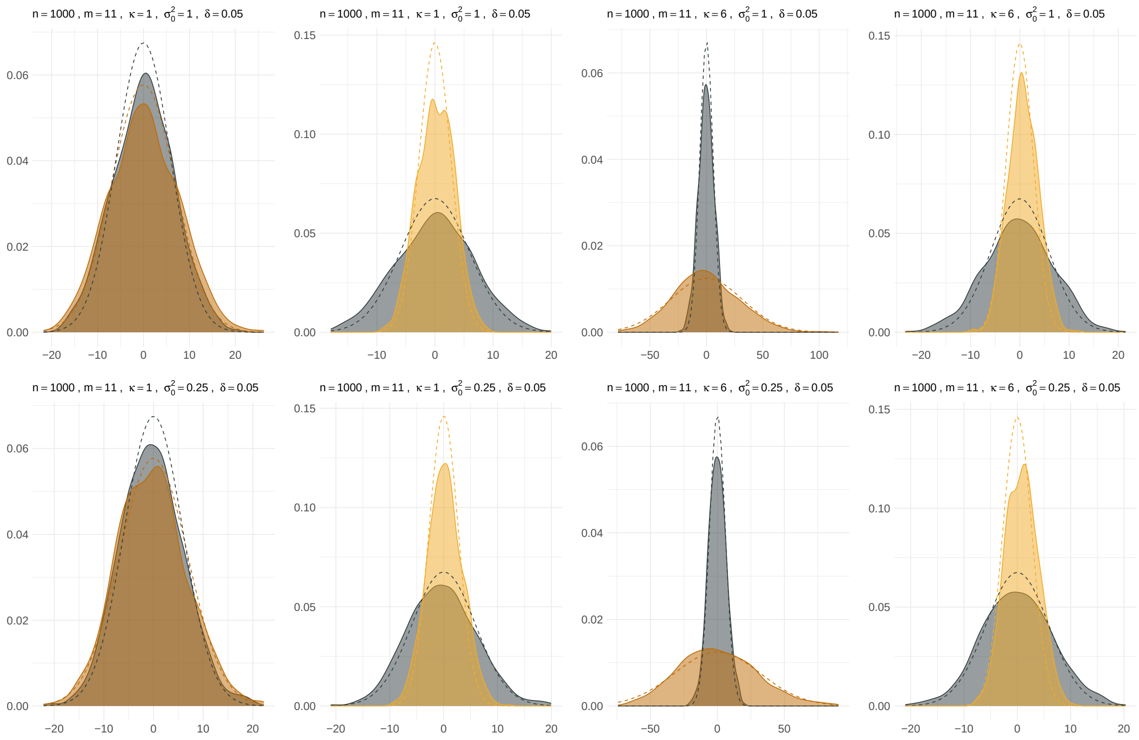

Figure 2.2.: Kernel-density plots for a equi-spaced grid with $M = 10$ and $N = 10^3$ using different constellations of the parameter $\eta = (\sigma_0^2, \kappa)$. Based on 1000 Monte Carlo repetitions each, orange denotes the kernel-density estimation of the results of the estimator $\hat{\eta}_2^{\mathrm{BT}}$. Similarly, the colors gray and yellow denote the results of the estimators $\hat{\varkappa}$ and $\hat{\kappa}$, respectively. In each case, the dotted lines represent the associated asymptotic distribution, respectively. A Gaussian kernel with Silverman's 'rule of thumb' was used for the kernel-density estimation.

is given in Hildebrandt (2020, Algorithm 3.2.), where the author also provided an algorithm for the case, where $\xi \neq 0$.

Finally, we present the total variation distance between the approximation X^L and the mild solution X of an SPDE from equation (1) to evaluate the power of the replacement method's approximation. Let $\mathcal{X} = (X_t(y_j))_{1\leqslant i\leqslant N, 1\leqslant j\leqslant M}$ and its approximation $\mathcal{X}^L$. Hildebrandt (2020, Prop. 3.3.) showed that there exist constants c and C, dependent only on (σ^2, ϑ), such that the total variation between $\mathcal{X}$ and $\mathcal{X}^L$ is bounded by

$$\mathrm{TV}(\mathcal{X}, \mathcal{X}^L) \leqslant C\sqrt{MN} e^{-cL^2M^2\Delta_N}.$$

Furthermore, suppose $\Delta_N^\alpha \to 0$ for some $\alpha > 0$. If there exists a $\beta > 1/2$ such that $M\Delta_N^\beta \to \infty$, then $\mathrm{TV}(\mathcal{X}, \mathcal{X}^1) \to 0$.

2.5.2. Simulation results for the curvature parameter

The purpose of this section is to visually compare the three different estimators: $\hat{\kappa}$, $\hat{\varkappa}$, and the curvature estimator $\hat{\eta}_2^{\mathrm{BT}}$ proposed by Bibinger and Trabs (2020) in equation (38). To achieve this, we conduct simulations for four distinct scenarios:

i) $\kappa = 1$ and $\sigma_0^2 = 1$, ii) $\kappa = 6$ and $\sigma_0^2 = 1$, iii) $\kappa = 1$ and $\sigma_0^2 = 1/4$, iv) $\kappa = 6$ and $\sigma_0^2 = 1/4$,

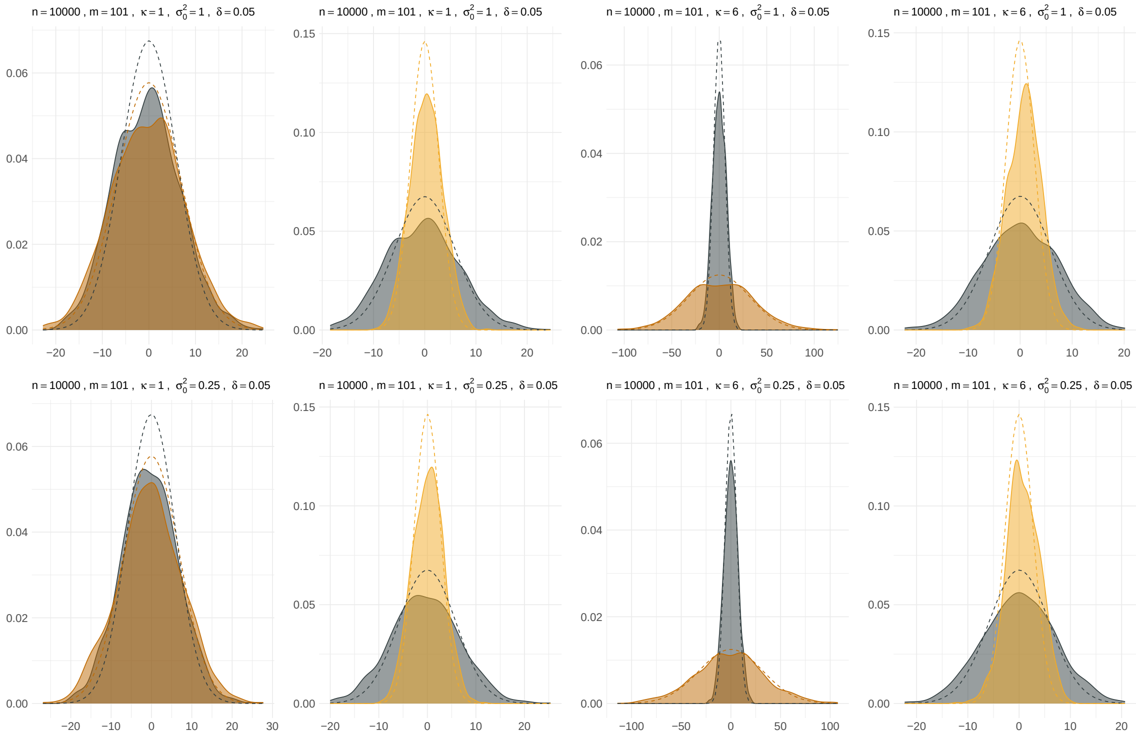

Figure 2.3.: Kernel-density plots for a equi-spaced grid with $M = 100$ and $N = 10^4$ using different constellations of the parameter $\eta = (\sigma_0^2, \kappa)$. Based on 1000 Monte Carlo repetitions each, orange denotes the kernel-density estimation of the results of the estimator $\hat{\eta}_2^{\mathrm{BT}}$. Similarly, the colors gray and yellow denote the results of the estimators $\hat{\varkappa}$ and $\hat{\kappa}$, respectively. In each case, the dotted lines represent the associated asymptotic distribution, respectively. A Gaussian kernel with Silverman's 'rule of thumb' was used for the kernel-density estimation.

where we performed 1000 Monte Carlo repetitions using the R programming language. The simulations are based on the replacement method with a replacement bound of $L = 20$ and a zero initial condition $\xi = 0$. We consider an equidistant grid in time and space, where two different spatial and temporal resolutions are used. The first grid has a spatial resolution of $M = 10$ and a temporal resolution of 10^3. Note that the spatial resolution of this grid is much smaller than $N^{1/2}$. Meanwhile, the second grid has a spatial resolution of $M = 100$ and a temporal resolution of $N = 10^4$, approximately satisfying the relation between Δ_n and m as stated in Assumption 1.1.1. As the estimator $\hat{\eta}_2^{\mathrm{BT}}$ is only given implicitly, we followed the instructions from Bibinger and Trabs (2020) on how to implement this estimator using the R function `nls`. Figure 2.2 and Figure 2.3 show kernel density estimations with a Gaussian kernel and Silverman's 'rule of thumb' for $\sqrt{nm}(\hat{\vartheta} - \kappa)$, where $\hat{\vartheta}$ represents the estimators $\hat{\kappa}$ in yellow, $\hat{\varkappa}$ in grey, and $\hat{\eta}_2^{\mathrm{BT}}$ in orange, respectively. The dotted lines represent the asymptotic variance as proved in the CLTs provided by the Propositions 2.4.3, 2.4.5, and 2.4.7, respectively. Figure 2.2 displays the simulation results on the first equi-spaced grid with $M = 10$ and $N = 10^3$, whereas Figure 2.3 presents the results on the second grid. For both grids, we can observe a good fit between the kernel density estimation and the asymptotic normal distribution. There is no significant difference in the quality of the fit between the two grids. As analysed in Section 2.4.5, for $\kappa \approx 0$, the estimator $\hat{\varkappa}$ and the estimator $\hat{\eta}_2$ by Bibinger and Trabs (2020) have about the same asymptotic variance. However, for larger (or smaller) κ, the performance of the estimator $\hat{\varkappa}$ significantly improves compared to the estimator $\hat{\eta}_2^{\mathrm{BT}}$. For instance, when $\kappa = 6$, a noticeable difference in the asymptotic variance can be observed.

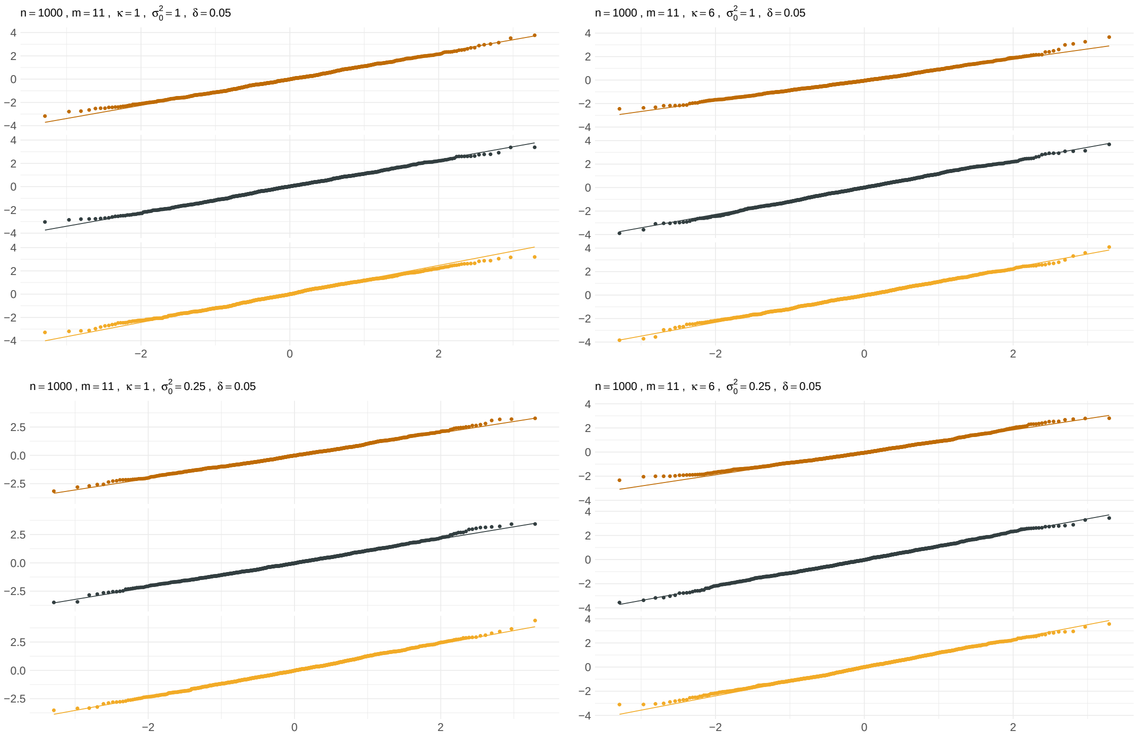

Figure 2.4.: QQ-normal plots for normalized estimation errors for κ from simulation with $N = 10^3, M = 10, \sigma_0^2 = 1, \kappa = 1$ in the left panels and $\kappa = 6$ in the right panels. Brown (top) shows the estimator from equation (38), grey is for the estimator in equation (15) and yellow (bottom) for the estimator in equation (13).

We conclude this section by providing QQ-plots. In these plots, we use the estimations of the respective curvature estimators $\hat{\vartheta}_{n,m}$ and rescale them according to the respective central limit theorem, i.e.,

$$\frac{\sqrt{nm}}{\sqrt{\mathrm{AVAR}(\hat{\vartheta}_{n,m})}}(\hat{\vartheta}_{n,m} - \kappa),$$

where $\mathrm{AVAR}(\hat{\vartheta}_{n,m_n}) := \lim_{n\to\infty} \mathbb{V}\mathrm{ar}(\sqrt{nm_n}\hat{\vartheta}_{n,m_n})$ denotes the asymptotic variance of the estimator $\hat{\vartheta}$. For the estimator from equation (38) we use an estimated asymptotic variance based on plug-in, while for our new estimators the asymptotic variances are known constants.

The QQ-plots shown in Figure 2.4 and Figure 2.5 offer a graphical comparison between the distributions of the estimators and the asymptotic normal distribution predicted by the CLT. Through this rescaling process, we can evaluate how closely the estimators align with the theoretical standard normal distribution when dealing with large sample sizes. Notably, all the presented curvature estimators demonstrate a strong fit, indicating a good agreement with the theoretical normal distribution.

2.6. Summary and Discussion

In this chapter, we have developed two new estimators for the curvature parameter κ in the context of linear parabolic SPDEs with additive noise. The first estimator $\hat{\kappa}$ assumes a known normalized volatility, while the second estimator $\hat{\varkappa}$ is a robustification and thus suitable for cases where the volatility σ_0^2

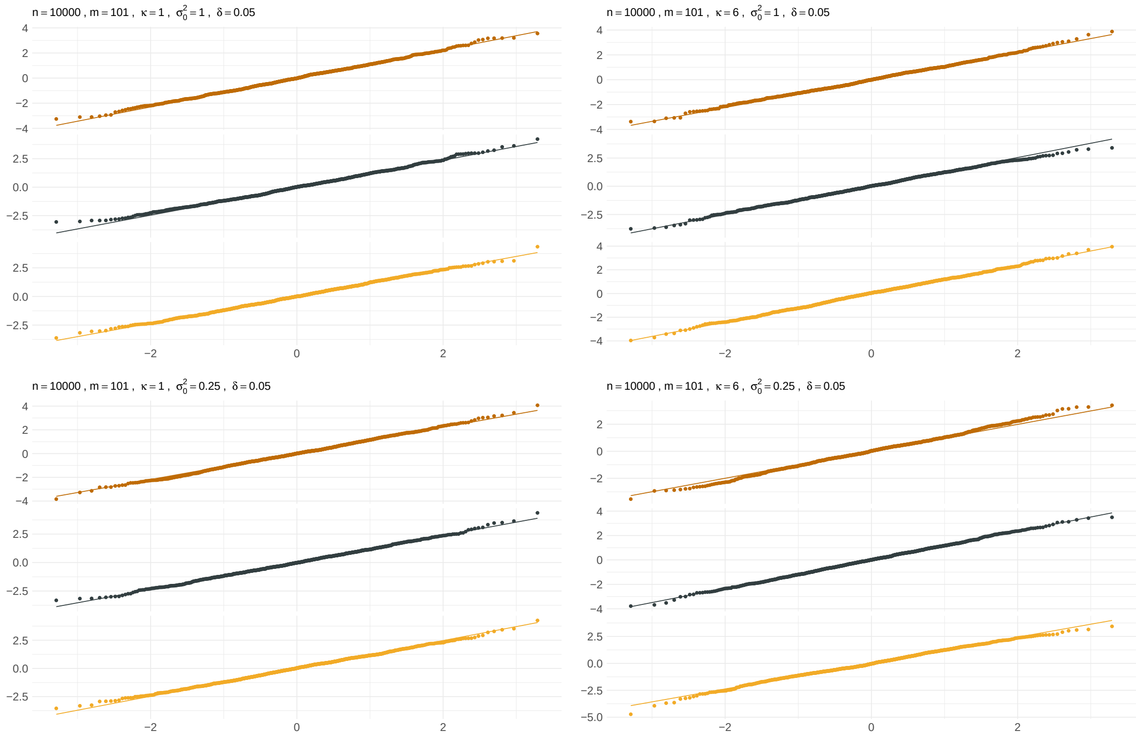

Figure 2.5.: QQ-normal plots for normalized estimation errors for κ from simulation with $N = 10^4, M = 100, \sigma_0^2 = 1, \kappa = 1$ in the left panels and $\kappa = 6$ in the right panels. Brown (top) shows the estimator from equation (38), grey is for the estimator in equation (15) and yellow (bottom) for the estimator in equation (13).

is unknown. We have proved central limit theorems for these estimators and compared them to the existing estimator $\hat{\eta}_2$ proposed by Bibinger and Trabs (2020). The key advantage of the new methods is the usage of a variance-stabilizing transformation of the statistic RV_n, resulting in feasible CLTs where the asymptotic variances are known constants and do not depend on any unknown parameters. On the other hand, the M-estimator $\hat{\eta}_2$ relies on the unknown curvature parameter κ. However, we have demonstrated that the non-oracle estimator $\hat{\varkappa}$ uniformly dominates and significantly improves upon the existing curvature estimator.

One important difference between the new estimators and $\hat{\eta}_2$ is in their formulations. Both of the new estimators are explicitly given, making them easier to implement and understand. In contrast, $\hat{\eta}_2$ is only provided implicitly. The fact that the M-estimator $\hat{\eta}_2$ has been widely adopted and utilized in various prominent papers reflects its importance in the field of parameter estimation for SPDEs. For instance:

(1) In the paper by Hildebrandt and Trabs (2021), the M-estimator was employed for rate-optimal estimation, catering to more general observation schemes. This indicates its versatility and usefulness in handling different types of data and scenarios.

(2) Kaino and Uchida (2021a) utilized the M-estimator for generalized estimation approaches, particularly focusing on small noise asymptotics. This suggests that the estimator's robustness and performance remain relevant and beneficial even in situations involving low-noise environments.

(3) The work by Kaino and Uchida (2021b) delved into long-span asymptotics, where the M-estimator was instrumental in capturing crucial features of the underlying SPDEs. This highlights its effec-

tiveness in dealing with large temporal spans and long-term data.

(4) Tonaki et al. (2023) employed the M-estimator for parameter estimation in two spatial dimensions. This indicates its suitability for higher-dimensional problems, which are often encountered in practical applications.

Considering the extensive use of the M-estimator in these influential papers, it emphasizes the significance and relevance of our new methods, namely $\hat{\kappa}$ and $\hat{\varkappa}$. The improvements and advantages of our estimators, which were demonstrated in this chapter, show great potential for enhancing the accuracy and efficiency of curvature parameter estimation in SPDEs. Therefore, we expect that substituting the curvature estimation, provided by the M-estimator, with our novel ML-estimators will prove effective in these extensions, yielding more efficient estimation techniques.

3. Asymptotic log-linear model for realized volatilities and least squares estimation

This chapter focusses on estimating the two-dimensional parameter $\eta = (\sigma_0^2, \kappa) \in (0, \infty) \times \mathbb{R}$. To achieve this, we utilize log-realized volatility statistics and establish a connection to the linear model. Our objective is to demonstrate a bivariate central limit theorem for this novel approach and subsequently compare it with the existing M-estimator developed by Bibinger and Trabs (2020). The comparison will encompass both analytical and Monte Carlo simulation assessments.

3.1. Motivation and Methodology

In Chapter 2.2, we derived equation (21) and demonstrated that the remainders $R_{n,y}$ become asymptotically negligible for the distribution of the estimators. Now, assuming the bivariate parameter $\eta = (\sigma_0^2, \kappa) \in (0, \infty) \times \mathbb{R}$ is unknown, we can use equation (21) and represent the log-realized volatilities as follows:

$$\ln\left(\frac{\mathrm{RV}_n(y_j)}{\sqrt{n}}\right) = -\kappa y_j + \ln\left(\frac{\sigma_0^2}{\sqrt{\pi}}\right) + \sqrt{\frac{\Gamma\pi}{n}} Z_j + R_{n,y_j}, \tag{42}$$

where $y_j \in [\delta, 1-\delta]$ and with independent $Z_j \sim \mathcal{N}(0,1)$, for $j = 1, \ldots, m$. By disregarding the remainders in the latter display, the equivalence to a simple ordinary linear regression model with normal errors becomes evident. In this analogy, the realized volatilities serve as response of the log-linear model with spatial explanatory variable, where our objective is to estimate both, the slope parameter $-\kappa$ and the intercept parameter $\varrho := \ln(\sigma_0^2/\sqrt{\pi})$. As we focus on estimating these two parameters, we introduce the two-dimensional parameter $\nu := (\varrho, \kappa)^\top \in \mathbb{R}^2$. In this process, we estimate the strictly monotone transformation $\varphi(\sigma_0^2) = \varrho \in \mathbb{R}$ of the normalized volatility σ_0^2, where $\varphi : \mathbb{R}_+ \to \mathbb{R}$ and $\varphi(x) := \ln(x/\sqrt{\pi})$. We review the parameter estimation for the simple ordinary linear regression model within a related statistical model.

Example 3.1.1
The simple ordinary linear regression model is given by

$$Y_j = \alpha y_j + \beta + \varepsilon_j,$$

where $j = 1 \ldots, m$, homoscedastic white noise errors ε_j, with $\mathbb{V}\mathrm{ar}(\varepsilon_j) = \varsigma^2$ and unknown parameters $(\alpha, \beta) \in \mathbb{R}^2$. Least squares estimation yields the following estimators:

$$\hat{\alpha}_m = \frac{\sum_{j=1}^m (Y_j - \bar{Y})(y_j - \bar{y})}{\sum_{j=1}^m (y_j - \bar{y})^2},$$

$$\hat{\beta}_m = \bar{Y} - \hat{\alpha}\bar{y},$$

where $\bar{Y}$ and $\bar{y}$ denote the sample averages and arithmetic mean, respectively, cf. Zimmerman (2020, Example 7.1-1). By plug-in and standard calculations we additionally derive the following representation:

$$\hat{\alpha}_m = \frac{\big(\sum_{j=1}^m Y_j\big)\big(\sum_{j=1}^m y_j\big) - m\sum_{j=1}^m Y_j y_j}{\big(\sum_{j=1}^m y_j\big)^2 - m\sum_{j=1}^m y_j^2},$$

$$\hat{\beta}_m = \frac{\big(\sum_{j=1}^m y_j\big)\big(\sum_{j=1}^m Y_j y_j\big) - \big(\sum_{j=1}^m Y_j\big)\big(\sum_{j=1}^m y_j^2\big)}{\big(\sum_{j=1}^m y_j\big)^2 - m\sum_{j=1}^m y_j^2}.$$

According to the well-known Gauss-Markov theorem, the estimators derived from the simple ordinary linear regression model are BLUE (best linear unbiased estimators), meaning they have the minimum variance among all linear and unbiased estimators. Now, for constructing estimators based on equation (42), we consider an asymptotic log-linear model with homoscedastic normal errors. Referring to Example 3.1.1 and associating $\alpha = -\kappa$ and $\beta = \varrho$, we derive the following estimators:

$$\hat{\hat{\varkappa}} := \hat{\hat{\varkappa}}_{n,m} := \frac{m\sum_{j=1}^m \ln\big(\frac{\mathrm{RV}_n(y_j)}{\sqrt{n}}\big)y_j - \Big(\sum_{j=1}^m \ln\big(\frac{\mathrm{RV}_n(y_j)}{\sqrt{n}}\big)\Big)\big(\sum_{j=1}^m y_j\big)}{\big(\sum_{j=1}^m y_j\big)^2 - m\sum_{j=1}^m y_j^2},$$

$$\hat{\varrho} := \hat{\varrho}_{n,m} := \frac{\big(\sum_{j=1}^m y_j\big)\Big(\sum_{j=1}^m \ln\big(\frac{\mathrm{RV}_n(y_j)}{\sqrt{n}}\big)y_j\Big) - \Big(\sum_{j=1}^m \ln\big(\frac{\mathrm{RV}_n(y_j)}{\sqrt{n}}\big)\Big)\big(\sum_{j=1}^m y_j^2\big)}{\big(\sum_{j=1}^m y_j\big)^2 - m\sum_{j=1}^m y_j^2}, \tag{43}$$

where $\hat{\varrho}$ is an estimator for the transformation $\varphi(\sigma_0^2)$ and $\hat{\hat{\varkappa}}$ estimates the parameter κ. Note that we have used the estimator $-\hat{\alpha}$ from Example 3.1.1 for estimating κ. Estimating the natural parameter $\sigma_0^2 > 0$ is given by the simple transformation of the estimator $\hat{\varrho}$, which is given by

$$\hat{\sigma}_0^2 := (\hat{\sigma}_0^2)_{n,m} := \exp\left[\frac{\big(\sum_{j=1}^m y_j\big)\Big(\sum_{j=1}^m \ln\big(\frac{\mathrm{RV}_n(y_j)}{\sqrt{n}}\big)y_j\Big) - \Big(\sum_{j=1}^m \ln\big(\frac{\mathrm{RV}_n(y_j)}{\sqrt{n}}\big)\Big)\big(\sum_{j=1}^m y_j^2\big)}{\big(\sum_{j=1}^m y_j\big)^2 - m\sum_{j=1}^m y_j^2}\right]\sqrt{\pi}.$$

It is well-established that maximum likelihood estimation for natural exponential families yields a unique ML-estimator and aligns with the estimators of the simple ordinary linear regression model with normal errors, as stated in Montgomery et al. (2021, Chapter 2.12). Moreover, least squares estimators in linear models with normal errors demonstrate asymptotic efficiency. Thus, we can deduce that the non-oracle estimator from equation (15) coincides with the estimator $\hat{\hat{\varkappa}}_{n,m}$. This identity can be easily established using Lemma 2.2.1 and standard calculations, resulting in the following identity:

$$\hat{\varkappa}_{n,m_n} = \frac{\sum_{j\neq l}\Big(\ln\big(\frac{\mathrm{RV}_n(y_j)}{\sqrt{n}}\big) - \ln\big(\frac{\mathrm{RV}_n(y_l)}{\sqrt{n}}\big)\Big)(y_l - y_j)}{\sum_{j\neq l}(y_j - y_l)^2}$$

$$= \frac{2\sum_{j=1}^{m_n} \ln\big(\frac{\mathrm{RV}_n(y_j)}{\sqrt{n}}\big)\sum_{l=1}^{m_n}(y_l - y_j)}{\sum_{j,l=1}^{m_n}\big(y_j^2 - 2y_j y_l + y_l^2\big)}$$

$$= \frac{2\Big(\sum_{j=1}^{m_n}\ln\big(\frac{\mathrm{RV}_n(y_j)}{\sqrt{n}}\big)\Big)\big(\sum_{l=1}^{m_n}y_l\big) - 2m_n\sum_{j=1}^{m_n}\ln\big(\frac{\mathrm{RV}_n(y_j)}{\sqrt{n}}\big)y_j}{2m_n\sum_{j=1}^{m_n}y_j^2 - 2\big(\sum_{j=1}^{m_n}y_j\big)^2} = \hat{\hat{\varkappa}}_{n,m}.$$

Hence, we note that the curvature estimator $\hat{\varkappa}$ as defined in equation (15) aligns with the curvature estimator $\hat{\hat{\varkappa}}$ derived from the ordinary least squares model. As a result, we will use the notation $\hat{\varkappa} := \hat{\varkappa}_{n,m}$ to denote the slope estimator $\hat{\hat{\varkappa}}$ in the log-linear model. To establish a central limit theorem for the two-dimensional estimators $\hat{\nu} := (\hat{\varrho}, \hat{\varkappa})^\top$ and $\hat{\eta} := (\hat{\sigma}_0^2, \hat{\varkappa})^\top$, we can determine the asymptotic variance-covariance matrix by analysing the variances and covariance of the estimators in the ordinary linear regression model from Example 3.1.1. It is well-known that these variances and covariance are given by

$$\begin{aligned}
\mathbb{V}\mathrm{ar}(\hat{\alpha}_m) &= \frac{\varsigma^2(1-2\delta)}{m\Big(\frac{1-2\delta}{m}\sum_{j=1}^m y_j^2 - \frac{1}{1-2\delta}\big(\frac{1-2\delta}{m}\sum_{j=1}^m y_j\big)^2\Big)},\\
\mathbb{V}\mathrm{ar}(\hat{\beta}_m) &= \frac{\varsigma^2\big(\frac{1-2\delta}{m}\sum_{j=1}^m y_j^2\big)}{m\Big(\big(\frac{1-2\delta}{m}\sum_{j=1}^m y_j^2\big) - \frac{1}{1-2\delta}\big(\frac{1-2\delta}{m}\sum_{j=1}^m y_j\big)^2\Big)},\\
\mathbb{C}\mathrm{ov}(\hat{\alpha}_m, \hat{\beta}_m) &= -\frac{\varsigma^2\big(\frac{1-2\delta}{m}\sum_{j=1}^m y_j\big)}{m\Big(\frac{1-2\delta}{m}\sum_{j=1}^m y_j^2 - \frac{1}{1-2\delta}\big(\frac{1-2\delta}{m}\sum_{j=1}^m y_j\big)^2\Big)}.
\end{aligned}$$

For a comprehensive overview of the linear model, we refer to Zimmerman (2020, Example 7.2-1). In fact, we will see, that the remainders R_{n,y_j} in equation (42) are negligible for the asymptotic distribution of the estimators $\hat{\varrho}$ and $\hat{\varkappa}$. Consequently, we derive an asymptotic variance-covariance matrix according to the variance-covariance structure given in Example 3.1.1, where $\varsigma^2 = \Gamma\pi$.

The estimator from equation (38) was shown to be rate-optimal and asymptotically normally distributed in Bibinger and Trabs (2020, Prop. 4.2.). However, considering the analogy to an ordinary linear regression model, it becomes clear that the estimation method by Bibinger and Trabs (2020) is inefficient, as ordinary least squares is applied to a model with heteroscedastic errors.

In the model from equation (37), the variances of $\delta_{n,j}$ depend on j via the factor $e^{-2\kappa y_j}$. This, moreover, induces that the asymptotic variance-covariance matrix of the estimator from equation (38) depends on the parameter (σ_0^2, κ). In line with the least squares estimator from Example 3.1.1, the asymptotic distribution of our estimator will not depend on the parameter (σ_0^2, κ).

In conclusion of this section, we lay the theoretical groundwork for the forthcoming multivariate central limit theorem. To begin the methodology part, we introduce a modification of the one-dimensional central limit theorem presented in Proposition 1.2.4. Utilizing the Cramér-Wold theorem, which asserts that multivariate convergence is equivalent to the univariate convergence of every linear combination, we can now present the following multivariate version of the central limit theorem, as proposed by Peligrad et al. (1997).

Corollary 3.1.2

Let $(Z_{k_n,i})_{1\leqslant i\leqslant k_n}$ a centred triangular array, with a sequence $(k_n)_{n\in\mathbb{N}}$, where $Z_{n,k_n} \in \mathbb{R}^d$ are random vectors. Then, it holds that

$$\sum_{i=1}^{k_n} Z_{n,i} \xrightarrow{d} \mathcal{N}(0, \Sigma),$$

as $n \to \infty$ and Σ denotes a variance-covariance matrix, which satisfies the equation

$$\lim_{n\to\infty} \mathbb{V}\mathrm{ar}\bigg(\sum_{i=1}^{k_n} \beta^\top Z_{n,i}\bigg) = \beta^\top \Sigma \beta < \infty,$$

for any $\beta \in \mathbb{R}^d$, if the following conditions hold for any $\beta \in \mathbb{R}^d$:

(I) $\mathbb{V}\mathrm{ar}\Big(\sum_{i=a}^{b} \beta^\top Z_{n,i}\Big) \leqslant C \sum_{i=a}^{b} \mathbb{V}\mathrm{ar}(\beta^\top Z_{n,i})$, for all $1 \leqslant a \leqslant b \leqslant k_n$,

(II) $\limsup_{n\to\infty} \sum_{i=1}^{k_n} \mathbb{E}[\beta^\top Z_{n,i}^2] < \infty$,

(III) $\sum_{i=1}^{k_n} \mathbb{E}\Big[\beta^\top Z_{k_n,i}^2 \mathbb{1}_{\{|\beta^\top Z_{k_n,i}|>\varepsilon\}}\Big] \overset{n\to\infty}{\longrightarrow} 0$, for all $\varepsilon > 0$,

(IV) $\mathbb{C}\mathrm{ov}\Big(e^{\mathrm{i}t\sum_{i=a}^{b} \beta^\top Z_{n,i}}, e^{\mathrm{i}t\sum_{i=b+u}^{c} \beta^\top Z_{n,i}}\Big) \leqslant \rho_t(u) \sum_{i=a}^{c} \mathbb{V}\mathrm{ar}(\beta^\top Z_{n,i})$, for all $1 \leqslant a \leqslant b \leqslant b+u \leqslant c \leqslant k_n$ and $t \in \mathbb{R}$,

where $C > 0$ is a universal constant and $\rho_t(u) \geqslant 0$ is a function with $\sum_{j=1}^{\infty} \rho_t(2^j) < \infty$. In addition, if $d = 2$ we can identify the asymptotic variance by

$$\lim_{n\to\infty} \mathbb{V}\mathrm{ar}\bigg(\sum_{i=1}^{k_n} \beta^\top Z_{n,i}\bigg) = \beta_1^2 \Sigma_{1,1} + 2\beta_1\beta_2\Sigma_{1,2} + \beta_2^2\Sigma_{2,2}, \quad \text{where} \quad \Sigma = \begin{pmatrix} \Sigma_{1,1} & \Sigma_{1,2} \\ \Sigma_{1,2} & \Sigma_{2,2} \end{pmatrix},$$

where $\beta \in \mathbb{R}^2$ is arbitrary.

In Section 2.4, we analysed the class $\mathcal{H}_\alpha$ of triangular arrays and established a central limit theorem for this class. By applying a Cramér-Wold argument in combination with Proposition 2.4.2, we can infer a central limit theorem for a class $\mathcal{H}_\alpha^d$ of generalized triangular arrays in higher dimensions. Specifically, we consider the set $\mathcal{F}_\alpha$ as defined in equation (32) and the set

$$\mathcal{G}_\alpha^d := \{g_\vartheta : \mathbb{N} \to \mathbb{R}^d \mid |\beta^\top g_\vartheta(m)| \leqslant C_\vartheta \|\beta\|_\infty m^{\alpha/2} \text{ uniformly in } m \in \mathbb{N}, C_\vartheta > 0\},$$

for a $\alpha \geqslant 0$, $d \in \mathbb{N}$ and the maximum norm $\|\cdot\|_\infty$. Then, we define the class of generalized multivariate triangular arrays by

$$\mathcal{H}_\alpha^d := \bigg\{(Z_{n,i})_{1\leqslant i\leqslant n, n\in\mathbb{N}} : Z_{n,i} = \zeta_{n,i} - \mathbb{E}[\zeta_{n,i}] \text{ and } \zeta_{n,i} = f_\vartheta(m) \sum_{j=1}^{m} (\Delta_i \tilde{X})^2(y_j) g_\vartheta(j), \\ \text{where } f_\vartheta \in \mathcal{F}_\alpha, g_\vartheta \in \mathcal{G}_\alpha^d\bigg\}, \tag{44}$$

where $\alpha \geqslant 0$. Suppose $\beta \in \mathbb{R}^d$, then we have

$$\beta^\top \zeta_{n,i} = f_\vartheta(m) \sum_{j=1}^{m} (\Delta_i \tilde{X})^2(y_j) \beta^\top g_\vartheta(j) \leqslant C_\vartheta \|\beta\|_\infty m^{\alpha/2} f_\vartheta(m) \sum_{j=1}^{m} (\Delta_i \tilde{X})^2(y_j),$$

for $\zeta_{n,i} \in \mathcal{H}_\alpha^d$. Different definitions are possible for the classes $\mathcal{F}_\alpha$ and $\mathcal{G}_\alpha$, encompassing triangular arrays in higher dimensions. In such cases, it becomes essential to impose the univariate condition on both classes' respective components in the multivariate setting. Our definition is grounded in the fact that the class $\mathcal{H}_\alpha^d$ incorporates triangular arrays with common scaling functions $f_\vartheta \in \mathcal{F}_\alpha$ and multivariate functions $g_\vartheta \in \mathcal{G}_\alpha^d$. These components represent the structure of the respective estimator $\hat{\nu} = (\hat{\varrho}, \hat{\varkappa})^\top$, which we establish in the following.

Following the procedure in Section 2.4.1, the remaining step is to define the triangular array for the two-dimensional estimator $\hat{\nu}$. By utilizing equation (27), we have

$$\begin{aligned}
\hat{\varrho}_{n,m_n} &= \frac{\big(\sum_{j=1}^{m_n} y_j\big)\Big(\sum_{j=1}^{m_n} \ln\big(\frac{\mathrm{RV}_n(y_j)}{\sqrt{n}}\big)y_j\Big) - \Big(\sum_{j=1}^{m_n} \ln\big(\frac{\mathrm{RV}_n(y_j)}{\sqrt{n}}\big)\Big)\big(\sum_{j=1}^{m_n} y_j^2\big)}{\big(\sum_{j=1}^{m_n} y_j\big)^2 - m_n \sum_{j=1}^{m_n} y_j^2} \\
&= \ln\left(\frac{\sigma_0^2}{\sqrt{\pi}}\right) + \frac{\frac{\sqrt{\pi}}{\sqrt{n}\sigma_0^2}\sum_{i=1}^{n}\sum_{j=1}^{m_n} \overline{(\Delta_i\tilde{X})^2(y_j)}e^{\kappa y_j}\Big(\big(\sum_{l=1}^{m_n} y_l\big)y_j - \big(\sum_{l=1}^{m_n} y_l^2\big)\Big)}{\big(\sum_{j=1}^{m_n} y_j\big)^2 - m_n \sum_{j=1}^{m_n} y_j^2} + \mathcal{O}_{\mathbb{P}}(\Delta_n),
\end{aligned}$$

and

$$\begin{aligned}
\hat{\varkappa}_{n,m_n} &= \frac{m_n \sum_{j=1}^{m_n} \ln\big(\frac{\mathrm{RV}_n(y_j)}{\sqrt{n}}\big)y_j - \Big(\sum_{j=1}^{m_n} \ln\big(\frac{\mathrm{RV}_n(y_j)}{\sqrt{n}}\big)\Big)\big(\sum_{j=1}^{m_n} y_j\big)}{\big(\sum_{j=1}^{m_n} y_j\big)^2 - m_n \sum_{j=1}^{m_n} y_j^2} \\
&= \kappa + \frac{\frac{\sqrt{\pi}}{\sqrt{n}\sigma_0^2}\sum_{i=1}^{n}\sum_{j=1}^{m_n} \overline{(\Delta_i\tilde{X})^2(y_j)}e^{\kappa y_j}\big(m_n y_j - \sum_{l=1}^{m_n} y_l\big)}{\big(\sum_{j=1}^{m_n} y_j\big)^2 - m_n \sum_{j=1}^{m} y_j^2} + \mathcal{O}_{\mathbb{P}}(\Delta_n).
\end{aligned}$$

Hence, we can redefine the triangular array by

$$\Xi_{n,i} := \xi_{n,i} - \mathbb{E}[\xi_{n,i}] \quad \text{and} \quad \xi_{n,i} := \begin{pmatrix} \xi_{n,i}^{(1)} \\ \xi_{n,i}^{(2)}, \end{pmatrix}, \tag{45}$$

where

$$\begin{aligned}
\xi_{n,i}^{(1)} &:= \frac{\sqrt{m_n\pi}}{\sigma_0^2\Big(\big(\sum_{j=1}^{m_n} y_j\big)^2 - m_n \sum_{j=1}^{m_n} y_j^2\Big)} \sum_{j=1}^{m_n} (\Delta_i\tilde{X})^2(y_j)e^{\kappa y_j}\left(\Big(\sum_{l=1}^{m_n} y_l\Big)y_j - \Big(\sum_{l=1}^{m_n} y_l^2\Big)\right), \\
\xi_{n,i}^{(2)} &:= \frac{\sqrt{m_n\pi}}{\sigma_0^2\Big(\big(\sum_{j=1}^{m_n} y_j\big)^2 - m_n \sum_{j=1}^{m_n} y_j^2\Big)} \sum_{j=1}^{m_n} (\Delta_i\tilde{X})^2(y_j)e^{\kappa y_j}\left(m_n y_j - \sum_{l=1}^{m_n} y_l\right),
\end{aligned}$$

and have

$$\xi_{n,i} := \frac{\sqrt{m_n\pi}}{\sigma_0^2\Big(\big(\sum_{j=1}^{m_n} y_j\big)^2 - m_n \sum_{j=1}^{m_n} y_j^2\Big)} \sum_{j=1}^{m_n} (\Delta_i\tilde{X})^2(y_j)e^{\kappa y_j} \begin{pmatrix} \big(\sum_{l=1}^{m_n} y_l\big)y_j - \sum_{l=1}^{m_n} y_l^2 \\ m_n y_j - \sum_{l=1}^{m_n} y_l \end{pmatrix}.$$

Let $\beta = (\beta_1, \beta_2) \in \mathbb{R}^2$, then we obtain

$$\beta^\top \xi_{n,i} = \frac{\sqrt{m_n\pi}}{\sigma_0^2\Big(\big(\sum_{j=1}^{m_n} y_j\big)^2 - m_n \sum_{j=1}^{m_n} y_j^2\Big)} \sum_{j=1}^{m_n} (\Delta_i\tilde{X})^2(y_j)e^{\kappa y_j}$$

$$\times \Bigg(\beta_1\Big(\Big(\sum_{l=1}^{m_n} y_l\Big)y_j - \sum_{l=1}^{m_n} y_l^2\Big) + \beta_2\Big(m_n y_j - \sum_{l=1}^{m_n} y_l\Big)\Bigg)$$
$$= f_\vartheta(m_n)\sum_{j=1}^{m_n}(\Delta_i\tilde{X})^2(y_j)e^{\kappa y_j}G_j^\beta,$$

where

$$f_\vartheta(m_n) := \frac{\sqrt{m_n\pi}}{\sigma_0^2\Big(\big(\sum_{j=1}^{m_n} y_j\big)^2 - m_n\sum_{j=1}^{m_n} y_j^2\Big)}, \tag{46}$$

$$G_j^\beta := G_j^{\beta_1} + G_j^{\beta_2} := \beta_1\Big(\Big(\sum_{l=1}^{m_n} y_l\Big)y_j - \sum_{l=1}^{m_n} y_l^2\Big) + \beta_2\Big(m_n y_j - \sum_{l=1}^{m_n} y_l\Big). \tag{47}$$

Based on Lemma 2.2.1, we observe that $f_\vartheta(m_n) = \mathcal{O}(m_n^{-3/2})$, $G_j^{\beta_1} = \mathcal{O}(m_n) = G_j^{\beta_2}$, and $g_\vartheta(j) := e^{\kappa y_j}G_j^\beta \leqslant C_\kappa\|\beta\|_\infty m_n$. Consequently, we can conclude that $\xi_{n,i} \in \mathcal{H}_2^2$, which enables us to establish a central limit theorem for the estimator $\hat{\nu}$ in the forthcoming section.

3.2. Central limit theorem in time and space

To establish a central limit theorem for the estimator $\hat{\nu}$, we begin with the following corollary, which directly follows from Proposition 2.4.2 and the Cramér-Wold device. Subsequently, by employing the multivariate delta method, we will deduce a central limit theorem for the estimator $\hat{\eta}$.

Corollary 3.2.1
Under the Assumptions 1.1.1 and 1.1.2, let us consider a triangular array $Z_{n,i} \in \mathcal{H}_\alpha^d$, where $\mathcal{H}_\alpha^d$ is defined in equation (44). Then, it holds that

$$\sum_{i=1}^{n} Z_{n,i} \xrightarrow{d} \mathcal{N}(0,\Sigma),$$

as $n \to \infty$, if it holds that

$$f_\vartheta^2(m)\sum_{j=1}^{m_n}\sum_{i=b+u}^{c}\mathbb{E}\big[(\Delta_i\tilde{X})^4(y_j)\big]\big(\beta^\top g_\vartheta(j)\big)^2 \geqslant \|\beta\|_\infty\tilde{C}\Delta_n p_u, \tag{48}$$

for all $1 \leqslant b < b+u \leqslant c \leqslant n$, where $p_u := c-b-u+1$, $u \geqslant 2$, a constant $\tilde{C} := \tilde{C}_\vartheta > 0$ and Σ is a variance-covariance matrix satisfying the equation

$$\lim_{n\to\infty}\mathbb{V}\mathrm{ar}\Big(\sum_{i=1}^{k_n}\beta^\top Z_{n,i}\Big) = \beta^\top\Sigma\beta < \infty,$$

for any $\beta \in \mathbb{R}^d$.

By utilizing the previous corollary, we can derive the following central limit theorem for the estimator $\hat{\nu}$.

Proposition 3.2.2
Grant Assumptions 1.1.1 and 1.1.2, with $y_1 = \delta$, $y_{m_n} = 1-\delta$ and $m_n \min_{2,\dots,m_n} |y_j - y_{j-1}|$ is bounded from above and below. Then, we have

$$\sqrt{nm_n}(\hat{\nu}-\nu) = \sqrt{nm_n}\left(\begin{pmatrix}\hat{\varrho}_{n,m_n}\\ \hat{\varkappa}_{n,m_n}\end{pmatrix} - \begin{pmatrix}\varrho\\ \kappa\end{pmatrix}\right) \xrightarrow{d} \mathcal{N}(0,\Sigma),$$

as $n\to\infty$ and $m_n = \mathcal{O}(n^\rho)$, where $\rho \in (0,1/2)$, and

$$\Sigma = \begin{pmatrix}\frac{4\Gamma\pi(1-\delta+\delta^2)}{(1-2\delta)^2} & \frac{6\Gamma\pi}{(1-2\delta)^2}\\ \frac{6\Gamma\pi}{(1-2\delta)^2} & \frac{12\Gamma\pi}{(1-2\delta)^2}\end{pmatrix}.$$

Proof. We initiate the proof by deriving the asymptotic variance. Let $\beta \in \mathbb{R}^2$ be arbitrary. Then, we obtain that

$$\begin{aligned}
\mathbb{V}\text{ar}\Big(\sum_{i=1}^n \beta^\top \Xi_{n,i}\Big) &= \mathbb{V}\text{ar}\Big(\sum_{i=1}^n \beta^\top \xi_{n,i}\Big) = f_\vartheta^2(m_n)\mathbb{V}\text{ar}\Big(\sqrt{n}\sum_{j=1}^{m_n}\sqrt{\Delta_n}\sum_{i=1}^n(\Delta_i\tilde{X})^2(y_j)e^{y_j\kappa}G_j^\beta\Big)\\
&= nf_\vartheta^2(m_n)\mathbb{V}\text{ar}\Big(\sum_{j=1}^{m_n} V_{n,\Delta_n}(y_j)G_j^\beta\Big)\\
&= nf_\vartheta^2(m_n)\Big(\sum_{j=1}^{m_n}(G_j^\beta)^2\mathbb{V}\text{ar}\big(V_{n,\Delta_n}(y_j)\big) + \sum_{j_1\neq j_2} G_{j_1}^\beta G_{j_2}^\beta \mathbb{C}\text{ov}\big(V_{n,\Delta_n}(y_{j_1}),V_{n,\Delta_n}(y_{j_2})\big)\Big)\\
&= nf_\vartheta^2(m_n)\Bigg(\frac{\Gamma\sigma_0^4}{n}\big(1+\mathcal{O}(1\wedge\Delta_n^{\tilde{\eta}})\big)\sum_{j=1}^{m_n}(G_j^\beta)^2\\
&\qquad + \mathcal{O}\bigg(\Delta_n^{3/2}\Big(\sum_{j_1\neq j_2}\Big(\frac{G_{j_1}^\beta G_{j_2}^\beta}{|y_{j_1}-y_{j_2}|}\Big) + m_n^2\delta^{-1}\Big)\bigg)\Bigg)\\
&= f_\vartheta^2(m_n)\Gamma\sigma_0^4\big(1+\mathcal{O}(\Delta_n^{\tilde{\eta}})\big)\sum_{j=1}^{m_n}(G_j^\beta)^2 + \mathcal{O}\bigg(\frac{\Delta_n^{1/2}}{m_n}\Big(\sum_{j_1\neq j_2}\Big(\frac{1}{|y_{j_1}-y_{j_2}|}\Big)+\delta^{-1}\Big)\bigg)\\
&= \frac{\Gamma\sigma_0^4 m_n\pi\sum_{j=1}^{m_n}(G_j^\beta)^2}{\sigma_0^4\Big(\big(\sum_{j=1}^{m_n}y_j\big)^2 - m_n\sum_{j=1}^{m_n}y_j^2\Big)^2}\big(1+\mathcal{O}(\Delta_n^{\tilde{\eta}})\big) + \mathcal{O}\big(\Delta_n^{1/2}m_n\log(m_n)\big)\\
&= \frac{m_n\Gamma\pi(1-2\delta)^2\sum_{j=1}^{m_n}(G_j^\beta)^2}{m_n^4\Big(\frac{1-2\delta}{m_n}\sum_{j=1}^{m_n}y_j^2 - (1-2\delta)^{-1}\big(\frac{1-2\delta}{m_n}\sum_{j=1}^{m_n}y_j\big)^2\Big)^2} + \scriptstyle{\mathcal{O}}(1),
\end{aligned}$$

where f_ϑ and G_j^β are defined in equations (46) and (47), respectively, and an arbitrary $\tilde{\eta} \in (0,1)$. Furthermore, we have

$$\begin{aligned}
\sum_{j=1}^{m_n}(G_j^\beta)^2 &= \sum_{j=1}^{m_n}\bigg(\beta_1\Big(\Big(\sum_{l=1}^{m_n}y_l\Big)y_j - \sum_{l=1}^{m_n}y_l^2\Big) + \beta_2\Big(m_ny_j - \sum_{l=1}^{m_n}y_l\Big)\bigg)^2\\
&= \beta_1^2\sum_{j=1}^{m_n}\Big(\Big(\sum_{l=1}^{m_n}y_l\Big)y_j - \sum_{l=1}^{m_n}y_l^2\Big)^2 + 2\beta_1\beta_2\sum_{j=1}^{m_n}\Big(\Big(\sum_{l=1}^{m_n}y_l\Big)y_j - \sum_{l=1}^{m_n}y_l^2\Big)\Big(m_ny_j - \sum_{l=1}^{m_n}y_l\Big)
\end{aligned}$$

$$
\begin{aligned}
&+\beta_2^2\sum_{j=1}^{m_n}\Big(m_n y_j-\sum_{l=1}^{m_n} y_l\Big)^2\\
&=\beta_1^2\bigg(m_n\Big(\sum_{j=1}^{m_n} y_j^2\Big)^2-\Big(\sum_{j=1}^{m_n} y_j^2\Big)\Big(\sum_{j=1}^{m_n} y_j\Big)^2\bigg)+2\beta_1\beta_2\bigg(m_n\Big(\sum_{j=1}^{m_n} y_j\Big)\Big(\sum_{j=1}^{m_n} y_j^2\Big)-\Big(\sum_{j=1}^{m_n} y_j\Big)^3\bigg)\\
&+\beta_2^2\bigg(m_n^2\sum_{j=1}^{m_n} y_j^2-m_n\Big(\sum_{j=1}^{m_n} y_j\Big)^2\bigg)\\
&=m_n^3\beta_1^2(1-2\delta)^{-2}\bigg(\Big(\frac{1-2\delta}{m_n}\sum_{j=1}^{m_n} y_j^2\Big)\Big(\frac{1-2\delta}{m_n}\sum_{j=1}^{m_n} y_j^2-(1-2\delta)^{-1}\Big(\frac{1-2\delta}{m_n}\sum_{j=1}^{m_n} y_j\Big)^2\Big)\bigg)\\
&+m_n^3 2\beta_1\beta_2(1-2\delta)^{-2}\bigg(\Big(\frac{1-2\delta}{m_n}\sum_{j=1}^{m_n} y_j\Big)\Big(\frac{1-2\delta}{m_n}\sum_{j=1}^{m_n} y_j^2-(1-2\delta)^{-1}\Big(\frac{1-2\delta}{m_n}\sum_{j=1}^{m_n} y_j\Big)^2\Big)\bigg)\\
&+m_n^3(1-2\delta)^{-1}\beta_2^2\bigg(\frac{1-2\delta}{m_n}\sum_{j=1}^{m_n} y_j^2-(1-2\delta)^{-1}\Big(\frac{1-2\delta}{m_n}\sum_{j=1}^{m_n} y_j\Big)^2\bigg).
\end{aligned}
$$

Therefore, we have

$$
\begin{aligned}
\lim_{n\to\infty}\mathbb{V}\mathrm{ar}\Big(\sum_{i=1}^{n}\alpha^\top\Xi_{n,i}\Big)&=\Gamma\pi\bigg(\beta_1^2\frac{\int_\delta^{1-\delta} y^2\,\mathrm{d}y}{\int_\delta^{1-\delta} y^2\,\mathrm{d}y-(1-2\delta)^{-1}\big(\int_\delta^{1-\delta} y\,\mathrm{d}y\big)^2}\\
&\quad+2\beta_1\beta_2\frac{\int_\delta^{1-\delta} y\,\mathrm{d}y}{\int_\delta^{1-\delta} y^2\,\mathrm{d}y-(1-2\delta)^{-1}\big(\int_\delta^{1-\delta} y\,\mathrm{d}y\big)^2}\\
&\quad+\beta_2^2\frac{(1-2\delta)}{\int_\delta^{1-\delta} y^2\,\mathrm{d}y-(1-2\delta)^{-1}\big(\int_\delta^{1-\delta} y\,\mathrm{d}y\big)^2}\bigg)\\
&=\beta_1^2\frac{4\Gamma\pi(1-\delta+\delta^2)}{(1-2\delta)^2}+2\beta_1\beta_2\frac{6\Gamma\pi}{(1-2\delta)^2}+\beta_2^2\frac{12\Gamma\pi}{(1-2\delta)^2}.
\end{aligned}
$$

Hence, the asymptotic variance is given by

$$
\Sigma=\begin{pmatrix}\frac{4\Gamma\pi(1-\delta+\delta^2)}{(1-2\delta)^2} & \frac{6\Gamma\pi}{(1-2\delta)^2}\\ \frac{6\Gamma\pi}{(1-2\delta)^2} & \frac{12\Gamma\pi}{(1-2\delta)^2}\end{pmatrix}.
$$

It remains to verify the condition given in equation (48) from Corollary 3.2.1. Having the following:

$$
f_\vartheta(m_n)=\frac{\sqrt{m_n\pi}}{\sigma_0^2\big((\sum_{j=1}^{m_n} y_j)^2-m_n\sum_{j=1}^{m_n} y_j^2\big)}\qquad\text{and}\qquad \beta^\top g_\vartheta(j)=e^{\kappa y_j}G_j^\beta,
$$

we derive that

$$
\begin{aligned}
f_\vartheta^2(m_n)\sum_{j=1}^{m_n}\sum_{i=b+u}^{c}\mathbb{E}\big[(\Delta_i\tilde X)^4(y_j)\big]e^{2y_j\kappa}(G_j^\beta)^2&\geqslant C_1\frac{f_\vartheta^2(m_n)\Delta_n\sigma_0^4p_u}{\pi}\sum_{j=1}^{m_n} e^{2y_j\kappa}(G_j^\beta)^2e^{-2y_j\kappa}\\
&\geqslant C_1\frac{\Delta_n p_u m_n}{\big((\sum_{j=1}^{m_n} y_j)^2-m_n\sum_{j=1}^{m_n} y_j^2\big)^2}\sum_{j=1}^{m_n}(G_j^\beta)^2\\
&\geqslant \|\beta\|_\infty C_2\Delta_n p_u,
\end{aligned}
$$

where $C_1, C_2>0$ are suitable constants. For the latter inequality we used Lemma 2.2.1 and obtained that

$$(G_j^\beta)^2 \propto \beta_1^2 m_n^2 y_j^2 + \beta_1\beta_2 m_n^2 y_j^2 + \beta_2^2 m_n^2 y_j^2,$$

which completes the proof. □

Finally, we examine the estimator $\hat{\eta}$ for the unknown parameter $\eta = (\sigma_0^2, \kappa) \in (0,\infty) \times \mathbb{R}$, where the estimator of the parameter σ_0^2 is given by

$$\hat{\sigma}_0^2 = \exp\left[\frac{\left(\sum_{j=1}^{m_n} y_j\right)\left(\sum_{j=1}^{m_n} \ln\left(\frac{\mathrm{RV}_n(y_j)}{\sqrt{n}}\right) y_j\right) - \left(\sum_{j=1}^{m_n} \ln\left(\frac{\mathrm{RV}_n(y_j)}{\sqrt{n}}\right)\right)\left(\sum_{j=1}^{m_n} y_j^2\right)}{\left(\sum_{j=1}^{m_n} y_j\right)^2 - m_n \sum_{j=1}^{m_n} y_j^2}\right]\sqrt{\pi}.$$

Utilizing the multivariate delta method yields the following corollary.

Corollary 3.2.3
Grant Assumptions 1.1.1 and 1.1.2, with $y_1 = \delta$, $y_m = 1-\delta$ and $m|y_j - y_{j-1}|$ is bounded from above and below, we have

$$\sqrt{n m_n}\left(\begin{pmatrix} (\hat{\sigma}_0^2)_{n,m_n} \\ \hat{\varkappa}_{n,m_n} \end{pmatrix} - \begin{pmatrix} \sigma_0^2 \\ \kappa \end{pmatrix}\right) \xrightarrow{d} \mathcal{N}(0, \tilde{\Sigma}),$$

as $n \to \infty$ and $m = m_n = \mathcal{O}(n^\rho)$, where $\rho \in (0, 1/2)$ and

$$\tilde{\Sigma} = \begin{pmatrix} \frac{4\sigma_0^4 \Gamma\pi(1-\delta+\delta^2)}{(1-2\delta)^2} & \frac{6\sigma_0^2\Gamma\pi}{(1-2\delta)^2} \\ \frac{6\sigma_0^2\Gamma\pi}{(1-2\delta)^2} & \frac{12\Gamma\pi}{(1-2\delta)^2} \end{pmatrix}.$$

Proof. Consider the function $h : \mathbb{R}^2 \to (0,\infty) \times \mathbb{R}$, defined as

$$h\left(\begin{pmatrix} x_1 \\ x_2 \end{pmatrix}\right) = \begin{pmatrix} \varphi^{-1}(x_1) \\ x_2 \end{pmatrix} = \begin{pmatrix} e^{x_1}\sqrt{\pi} \\ x_2 \end{pmatrix}.$$

Since each entry of h has a continuous partial derivative, the multivariate delta method yields

$$\sqrt{n m_n}\left(h\left(\begin{pmatrix} \hat{\varrho}_{n,m_n} \\ \hat{\varkappa}_{n,m_n} \end{pmatrix}\right) - h\left(\begin{pmatrix} \varphi(\sigma_0^2) \\ \kappa \end{pmatrix}\right)\right) \xrightarrow{d} \mathcal{N}\left(0, J_h(\eta)\Sigma J_h(\eta)^\top\right),$$

where J_h denotes the Jacobian matrix of h given by

$$J_h(\eta) = \begin{pmatrix} \sigma_0^2 & 0 \\ 0 & 1 \end{pmatrix}.$$

The proof is completed by having the variance-covariance matrix Σ from Proposition 3.2.2. □

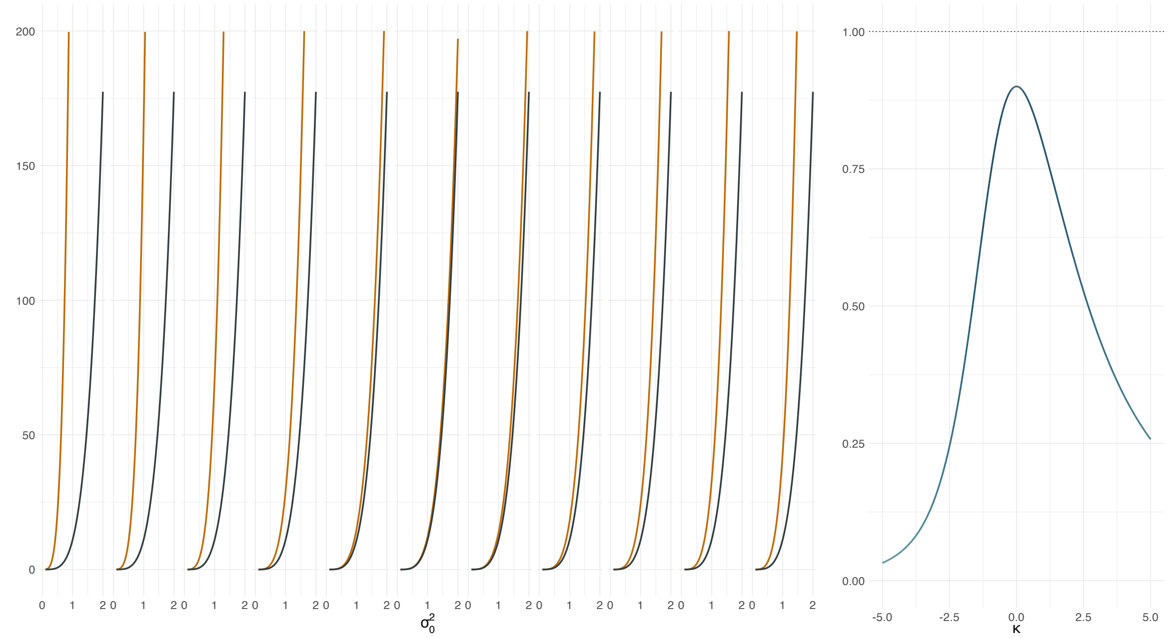

Figure 3.1.: The asymptotic variance of the estimator $\hat\sigma_0^2$ (blue) is compared to the estimator $\hat\eta_1^{\mathrm{BT}}$ (brown) from equation (38). From left to right, we observe the asymptotic variances for different values of $\kappa \in \{-5, -4, \ldots, 4, 5\}$. The rightmost panel displays the ratio $\mathrm{AVAR}(\hat\sigma_0^2)/\mathrm{AVAR}(\hat\eta_1^{\mathrm{BT}})$ of the asymptotic variances of both estimators for $\kappa \in [-5, 5]$.

In Section 2.4.4, we discussed confidence intervals for the curvature parameter κ. Proposition 3.2.2 enables the derivation of asymptotic confidence intervals, with a confidence level of $1-\alpha$, for the normalized volatility σ_0^2. These intervals are given by

$$I_{n,m} := \left[\exp\left[\hat\varrho_{n,m} - q_{1-\alpha/2}\gamma/\sqrt{nm}\right]\sqrt{\pi},\ \exp\left[\hat\varrho_{n,m} + q_{1-\alpha/2}\gamma/\sqrt{nm}\right]\sqrt{\pi}\right],$$

where q_α represents the α-quantile of the standard normal distribution. Here, $\hat\varrho_{n,m}$ is the estimator from equation (43) for the parameter $\varrho = \ln(\sigma_0^2/\sqrt{\pi})$, and γ is defined as

$$\gamma := \left(\frac{4\Gamma\pi(1-\delta+\delta^2)}{(1-2\delta)^2}\right)^{1/2}.$$

3.3. Simulation

In this section, we begin by providing a graphical comparison of the asymptotic variances of the estimators $\hat\eta^{\mathrm{BT}}$ from equation (38) as constructed by Bibinger and Trabs (2020) and the new estimator $\hat\eta$ for estimating $\eta = (\sigma_0^2, \kappa)$. For the analysis of the asymptotic variance and simulations of the non-oracle estimator $\hat\varkappa$, we refer to the Sections 2.4.3 and 2.5, respectively. Here, our focus is on comparing the asymptotic variances of the estimator $\hat\sigma_0^2$ and $\hat\eta_1^{\mathrm{BT}}$ for the parameter σ_0^2, as well as conducting a comparison of both estimators via Monte Carlo simulations.

The panels on the left in Figure 3.1 show the asymptotic variances of both estimators for fixed $\kappa \in \{-5, -4, \ldots, 4, 5\}$ and $\sigma \in (0, 2]$. The blue line represents the asymptotic variance of the estimator $\hat\sigma_0^2$, while the brown line denotes the asymptotic variance of the estimator $\hat\eta_1^{\mathrm{BT}}$ by Bibinger and Trabs (2020).

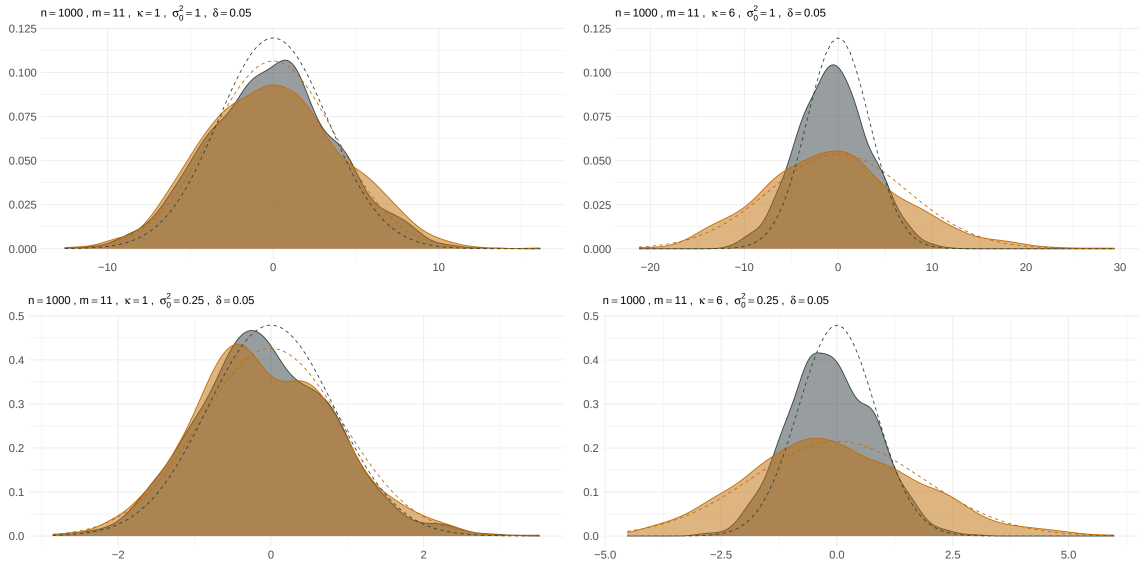

Figure 3.2.: Comparison of empirical distributions of normalized estimation errors for σ_0^2 from simulation with $N = 10^3$, $M = 10$, $\sigma_0^2 = 1$, and $\kappa = 1$ in the left panel, and $\kappa = 6$ in the right panel. Blue represents $\hat{\sigma}_0^2$, and brown represents the estimator $\hat{\eta}_1^{\mathrm{BT}}$ by Bibinger and Trabs (2020). The asymptotic distributions are denoted by the dotted lines, respectively.

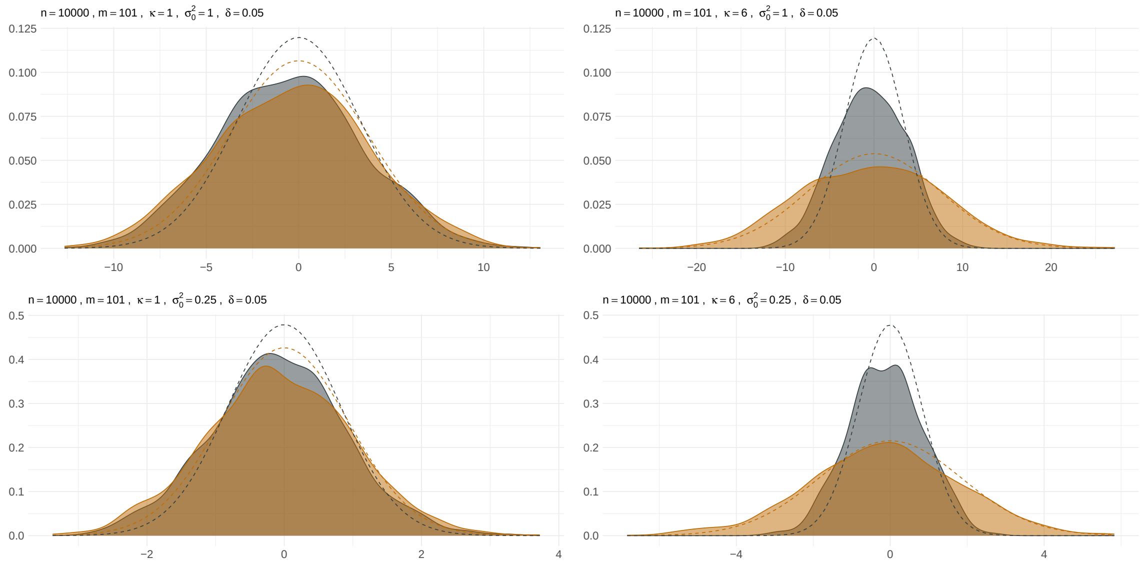

Figure 3.3.: Comparison of empirical distributions of normalized estimation errors for σ_0^2 from simulation with $N = 10^4$, $M = 100$, $\sigma_0^2 = 1$, and $\kappa = 1$ in the left panel, and $\kappa = 6$ in the right panel. Blue represents $\hat{\sigma}_0^2$, and brown represents the estimator $\hat{\eta}_1^{\mathrm{BT}}$ by Bibinger and Trabs (2020). The asymptotic distributions are denoted by the dotted lines, respectively.

As the asymptotic variance for our estimator $\hat{\sigma}_0^2$ is independent of the unknown parameter κ, we observe the same behaviour in the first eleven plots. The rightmost panel in Figure 3.1 displays the quotient for both estimators for $\kappa \in [-5, 5]$. As this quotient is independent of the parameter σ_0^2, we show the ratio between both asymptotic variances dependent on $\kappa \in [-5, 5]$ with fixed $\delta = 0.05$. We observe that the quotient curve is not symmetrical around zero, indicating that the new estimator $\hat{\sigma}_0^2$ performs even better than the estimator $\hat{\eta}_1^{\mathrm{BT}}$ when $\kappa < 0$. As discussed in Section 1.1, we observe much stronger activity of

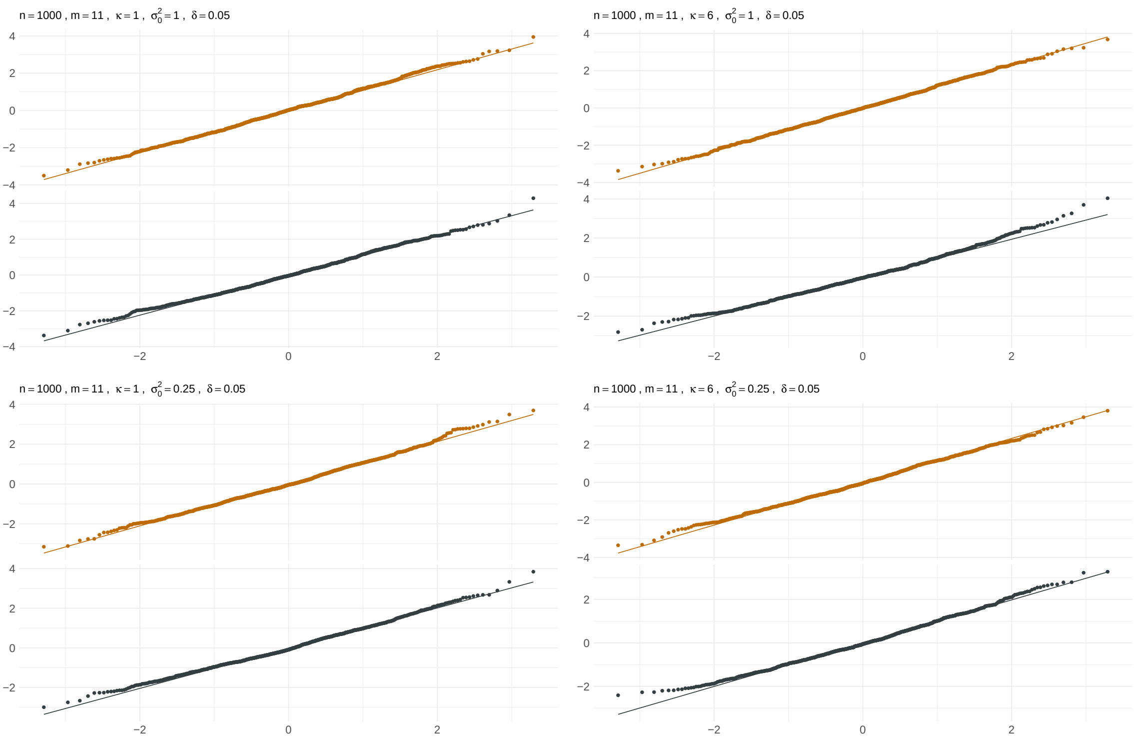

Figure 3.4.: QQ-normal plots for normalized estimation errors for σ_0^2 from simulation with $N = 10^3$, $M = 10$, $\sigma_0^2 = 1$, and $\kappa = 1$ in the left panel, and $\kappa = 6$ in the right panel. Brown is for the new estimator $\hat{\sigma}_0^2$, and grey is for the estimator defined in equation (38).

the random field when the curvature κ is negative compared to its positive equivalent. These structural differences also affect the quality of the estimation, i.e., the asymptotic variance, leading to the curvature observed in the rightmost panel. Even when the curvature is $\kappa = 0$, our new estimator $\hat{\sigma}_0^2$ outperforms the M-estimator $\hat{\eta}_1^{\mathrm{BT}}$.

Figures 3.2 and 3.3 compare the empirical distributions of normalized estimation errors for σ_0^2 for both estimators. The empirical distributions are based on 1000 Monte Carlo iterations. While the empirical distributions for $\kappa = 1$ are almost similar, we witness a significant difference for a stronger curvature $\kappa = 6$. In fact, our new estimator $\hat{\sigma}_0^2$ outperforms the existing one from Bibinger and Trabs (2020). Both figures display the limit distributions denoted by the dotted lines, respectively. For the generation of empirical distributions, we use a kernel density estimation with a Gaussian kernel and Silverman's 'rule of thumb' for the bandwidth. The QQ-normal plots in Figure 3.4 and Figure 3.5 compare standardized estimation errors to the standard normal. The fit of the asymptotic normal distributions is reasonably well for all estimators.

In Section 2.6, we discussed the extensive use of the M-estimator in influential works including Hildebrandt and Trabs (2021), Kaino and Uchida (2021a) and Tonaki et al. (2023). Combining the results from the Chapters 2 and 3 reveals that our novel estimator $\hat{\eta}$ outperforms the existing estimator $\hat{\eta}^{\mathrm{BT}}$ presented by Bibinger and Trabs (2020). Hence, we do not only expect that substituting the M-estimator with the ML-estimators $\hat{\kappa}$ and $\hat{\varkappa}$ from Chapter 2 for the curvature parameter κ will yield for more efficient

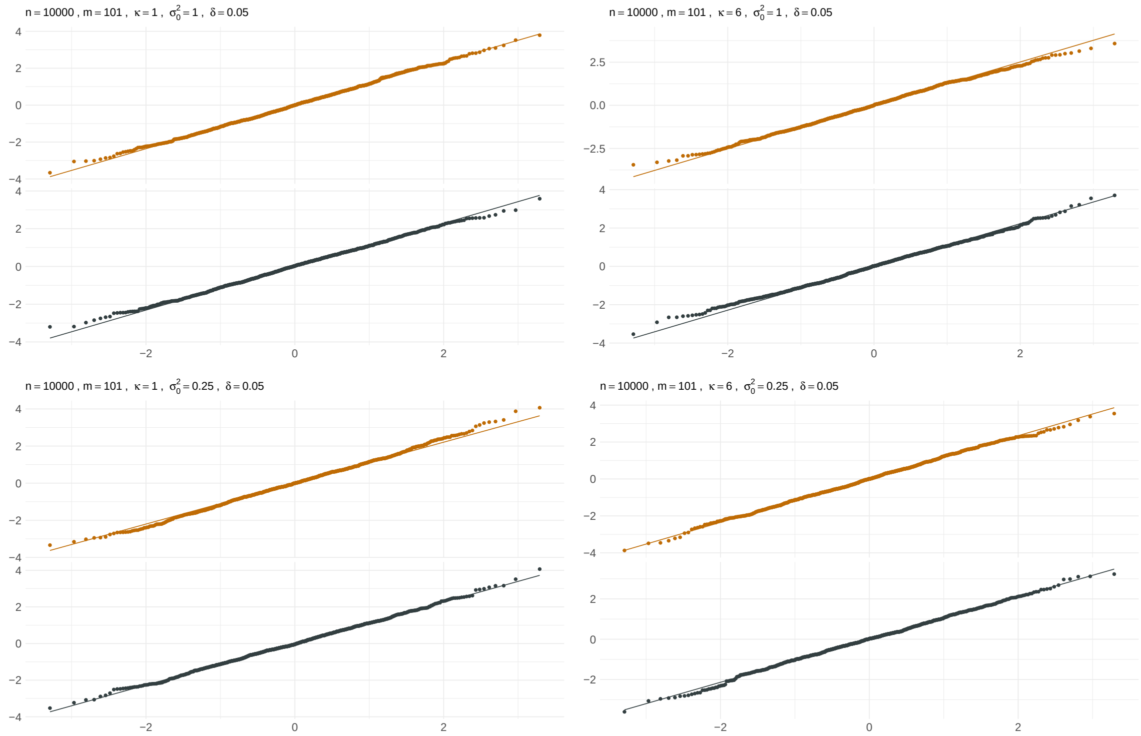

Figure 3.5.: QQ-normal plots for normalized estimation errors for σ_0^2 from simulation with $N = 10^4$, $M = 100$, $\sigma_0^2 = 1$, and $\kappa = 1$ in the left panel, and $\kappa = 6$ in the right panel. Brown is for the new estimator $\hat{\sigma}_0^2$, and grey is for the estimator defined in equation (38).

parameter estimation but also anticipate improved efficiency when substituting the M-estimator with the novel least squares estimator $\hat{\eta}$.

Part II.

Multi-Dimensional Stochastic Partial Differential Equation

4. Essentials of multi-dimensional SPDEs

Multi-dimensional SPDEs extend the foundational concepts of one-dimensional SPDEs to handle situations in which multiple spatial dimensions are at play. These equations have broad utility across various scientific disciplines, allowing for the examination of the interplay between deterministic dynamics and stochastic variations in a wide range of systems, including those in the fields of physics, geophysics, biology, finance, and environmental science. Multi-dimensional SPDE models offer a much larger variability for modelling natural phenomena. Therefore, it is intuitive that applications of these SPDEs is of great relevance, especially for two- and three-dimensional spaces. See, for instance, Mena and Pfurtscheller (2019) for an application in connection with the climate phenomenon El Niño and references therein for applications to sea temperature, Pereira et al. (2020) for an application in Geostatistics, and dealing with seismic data and Fioravanti et al. (2023) for an application in climate science. For an overview with many references to specific applications in various fields we refer to Lindgren et al. (2022).

While some research has been conducted on statistical inference for stochastic partial differential equations in one spatial dimension, the aim of this second part is to generalize the SPDE model to multiple space dimensions. Although the authors Tonaki et al. (2023) have provided valuable insights into a SPDE model in two spatial dimensions, this is the first work, which generalizes the theory to a d-dimensional framework, where $d \geqslant 2$.

Emanating from the fact that research on multi-dimensional SPDEs is still in its early stages, we begin this second part of the thesis by laying the foundations for the multi-dimensional model. Thus, we introduce stochastic partial differential equations in $d \geqslant 2$ spatial dimensions and briefly discuss the parameters of the model. A crucial difference between a SPDE model in one spatial dimension and multi-dimensional SPDE models is that the random field in higher dimensions is not square integrable when using a white noise structure as employed in the one-dimensional case. Consequently, introducing a new parameter to the higher-dimensional model becomes necessary. This new parameter, which we refer to as the damping parameter, ensures that we attain essential properties of the solution process, such as the random field being square integrable. The structural change in the stochastic force, due to the damping parameter, has a crucial impact on the model. In fact, we will observe that the damping parameter influences key elements, such as the expected value of the quadratic temporal increments and the autocovariance of temporal increments. We will also discuss the identifiability of the parameters in the multi-dimensional SPDE model, particularly in relation to the damping parameter.

Moving forward, we will develop a representation of a solution process for the corresponding multi-dimensional SPDE. Similar to the first part of this thesis, we choose the spectral approach for this purpose. However, we need to extend the mathematical background of this approach from one to multiple spatial dimensions. By obtaining a Fourier representation of a solution process, we provide technical tools to analyse such solutions and begin to derive initial insights into some properties of multi-dimensional SPDEs. These insights include investigating the structure of a d-dimensional random field in terms of dependencies between distinct spatial points and the variance-covariance structure of realized volatilities.

Statistical inference can be developed using these key insights. In concluding this introductory chapter, we will focus on simulation methods for d-dimensional SPDEs, building upon the one-dimensional approaches of cut-off and replacement method. Since higher dimensions naturally lead to more complex calculations, we will defer specific proofs to the last Section 4.4 in this chapter to enhance readability.

4.1. SPDE model in multiple space dimension

We consider the following linear, second-order stochastic partial differential equation in $d \in \mathbb{N}$ space dimensions with additive noise:

$$\begin{bmatrix} \mathrm{d}X_t(\mathbf{y}) = A_\vartheta X_t(\mathbf{y})\,\mathrm{d}t + \sigma\,\mathrm{d}B_t(\mathbf{y}), & (t,\mathbf{y}) \in [0,1] \times [0,1]^d \\ X_0(\mathbf{y}) = \xi(\mathbf{y}), & \mathbf{y} \in [0,1]^d \\ X_t(\mathbf{y}) = 0, & (t,\mathbf{y}) \in [0,1] \times \partial\,[0,1]^d \end{bmatrix}, \tag{49}$$

where $\mathbf{y} = (y_1,\ldots,y_d) \in [0,1]^d$. The operator A_ϑ from the SPDE model outlined in equation (49) is given by

$$A_\vartheta = \eta \sum_{l=1}^d \frac{\partial^2}{\partial y_l^2} + \sum_{l=1}^d \nu_l \frac{\partial}{\partial y_l} + \vartheta_0, \tag{50}$$

with fixed parameters $\vartheta = (\vartheta_0,\nu_1,\ldots,\nu_d,\eta)$, where $\vartheta_0,\nu_1,\ldots,\nu_d \in \mathbb{R}$ and $\eta,\sigma > 0$. The temporal domain is set as $t \in [0,1]$, which can be extended to $t \in [0,T]$ for $T > 0$ throughout the second part of this thesis. Likewise, the spatial domain is defined as the d-dimensional unit hypercube. Furthermore, B denotes a cylindrical Q-Brownian motion on $[0,1]^d$ as defined in equation (54), and the initial condition $\xi : [0,1]^d \to \mathbb{R}$ is independent from B. We impose a Dirichlet boundary condition to the model. As in the one-dimensional case, we define the natural parameters in this model as the normalized volatility $\sigma_0^2 := \sigma^2/\eta^{d/2} > 0$ and the curvature parameter $\kappa = (\kappa_1,\ldots,\kappa_d) \in \mathbb{R}^d$, where $\kappa_l := \nu_l/\eta \in \mathbb{R}$, $l = 1,\ldots,d$. Note, that the identifiability of the model parameters is discussed in the remark after Proposition 4.2.7.

Different to the situation with unbounded spatial support, the differential operator A_ϑ from equation (50) admits a discrete spectrum, hence enabling the use of the spectral approach. The spectral approach's corresponding Hilbert space is defined by

$$H_\vartheta := \{f : [0,1]^d \to \mathbb{R}, \|f\|_\vartheta < \infty \text{ and } f(\mathbf{y}) = 0, \text{ for } \mathbf{y} \in \partial\,[0,1]^d\}, \tag{51}$$

where $\partial[0,1]^d$ represents the boundary of the set $[0,1]^d$. The norm $\|\cdot\|_\vartheta$ is defined via the corresponding inner product $\|f\|_\vartheta := \langle f,f\rangle_\vartheta$ given by

$$\langle f,g\rangle_\vartheta := \int_0^1 \cdots \int_0^1 f(y_1,\ldots,y_d)g(y_1,\ldots,y_d) \exp\left[\sum_{l=1}^d \kappa_l y_l\right] \mathrm{d}y_1 \cdots \mathrm{d}y_d,$$

where $f,g \in H_\vartheta$. The domain of the operator A_ϑ is given by

$$\mathcal{D}(A_\vartheta) = \{f \in H_\vartheta : \|f\|_\vartheta, \|\partial/(\partial y_l)f\|_\vartheta, \|\partial^2/(\partial y_l^2)f\|_\vartheta < \infty, \text{ for all } l = 1,\ldots,d\}.$$

Before introducing the spectral decomposition of the SPDE model in equation (49), we clarify some notations for working in $d \geqslant 2$ space dimensions. We use the following abbreviated notation:

$$\int_{[0,1]^d} f(\mathbf{y})\,\mathrm{d}\mathbf{y} := \int_0^1 \cdots \int_0^1 f(y_1,\ldots,y_d)\,\mathrm{d}y_1\cdots\mathrm{d}y_d,$$

for a function with $\|f\|_\vartheta < \infty$. Note that the Fubini theorem yields the possibility to change the order of integration. Likewise, we use the notation

$$\sum_{\mathbf{k}\in\mathbb{N}^d} a_{\mathbf{k}} = \sum_{k_1=1}^{\infty}\cdots\sum_{k_d=1}^{\infty} a_{(k_1,\ldots,k_d)},$$

where $a_{\mathbf{k}} : \mathbb{N}^d \to \mathbb{R}$ denotes a sequence, for which the series converges absolutely. Bold letter indices and variables are used throughout this second part of the thesis to denote multivariate indices and variables. Furthermore, we introduce the following notations. Let $\mathbf{x} \in \mathbb{R}^d$, then

$$\|\mathbf{x}\|_0 := \min_{\substack{i=1,\ldots,d\\ x_i\neq 0}}\{|x_1|,\ldots,|x_d|\}, \qquad \|\mathbf{x}\|_1 := \sum_{l=1}^{d} x_l, \qquad \|\mathbf{x}\|_2 := \left(\sum_{l=1}^{d} x_l^2\right)^{1/2}, \qquad \|\mathbf{x}\|_\infty := \max_{l=1,\ldots,d}|x_l|,$$

where we set $\min\varnothing = 0$. Note that the introduced notations $\|\cdot\|_2, \|\cdot\|_\infty$ define a norm on $\mathbb{R}^d$. However, the notations $\|\cdot\|_0$ and $\|\cdot\|_1$ do not define a norm, as they do not even map to the non-negative real numbers. Nevertheless, we use a norm notation to indicate an operation across all the spatial dimensions. Moreover, for a measurable function $f : \mathbb{R}^d \to \mathbb{R}$ we define the $\mathcal{L}^p$-norm by

$$\|f\|_{\mathcal{L}^p(D)} := \left(\int_D |f(\mathbf{x})|^p\,\mathrm{d}\mathbf{x}\right)^{1/p},$$

where $D \subseteq \mathbb{R}^d$. Finally, we define the point-wise product by

$$\begin{aligned}\bullet : \mathbb{R}^d \times \mathbb{R}^d &\to \mathbb{R}^d\\ \mathbf{x}\bullet\mathbf{y} &\mapsto (x_1y_1,\ldots,x_dy_d)^\top.\end{aligned}$$

We say for $\mathbf{k},\mathbf{j} \in \mathbb{N}^d$ that they are not alike, i.e., $\mathbf{k} \neq \mathbf{j}$, if there exists at least one index $l_0 \in \{1,\ldots,d\}$ with $k_{l_0} \neq j_{l_0}$. A concise overview of these and other notations can be found in the Appendix A.

Now that we have clarified these notations, we proceed with the spectral decomposition of the operator A_ϑ on the Hilbert space H_ϑ. The eigenfunctions $(e_{\mathbf{k}})_{\mathbf{k}\in\mathbb{N}^d}$ and eigenvalues $(-\lambda_{\mathbf{k}})_{\mathbf{k}\in\mathbb{N}^d}$ of the differential operator A_ϑ are given by

$$e_{\mathbf{k}}(\mathbf{y}) := e_{\mathbf{k}}(y_1,\ldots,y_d) := 2^{d/2}\prod_{l=1}^{d}\sin(\pi k_l y_l)e^{-\kappa_l y_l/2}, \tag{52}$$

$$\lambda_{\mathbf{k}} := -\vartheta_0 + \sum_{l=1}^{d}\left(\frac{\nu_l^2}{4\eta} + \pi^2 k_l^2 \eta\right), \tag{53}$$

where $\mathbf{k} = (k_1, \ldots, k_d)^\top \in \mathbb{N}^d$. When comparing the representation of the eigenfunctions and eigenvalues in d-space dimensions to those in one space dimension as defined in display (2), we observe that we have extended the eigenfunctions and eigenvalues in one dimension to each spatial dimension. Furthermore, we demonstrate in Lemma 4.4.1 that the orthonormal property of the one-dimensional eigenfunctions extends seamlessly to multiple space dimensions, effectively defining an orthonormal system $(e_{\mathbf{k}})_{\mathbf{k}\in\mathbb{N}^d}$. This observation allows us to decompose each axis independently using the one-dimensional eigenfunctions, which involve rescaling, sine functions, and exponential terms with dependencies on the respective parameters κ_l. As a result, we obtain a powerful multivariate spectral decomposition by considering a product model over each dimension.

Furthermore, a crucial property of the operator A_ϑ is its self-adjoint nature on the Hilbert space H_ϑ, where we prove this property in Lemma 4.4.1. The self-adjoint nature of the operator is significant as it ensures that the eigenfunctions form a complete and orthogonal basis in H_ϑ, enabling us to effectively represent solutions to the SPDE model in equation (49) using this spectral decomposition.

Given that we have developed the spectral framework, we address the Q-Wiener process $W_t(\mathbf{y})$ in a Sobolev space on the bounded domain $[0,1]^d$. For comprehensive details on the Q-Wiener process, refer to works such as Da Prato and Zabczyk (2014), Lord et al. (2014) or Lototsky et al. (2017). An essential distinction when transitioning from one to higher space dimensions is that the solution process $X_t^Q(\mathbf{y})$ is not square integrable when considering a white noise, i.e., $\mathbb{E}[\|X_t^Q\|_\vartheta^2] = \infty$, where $Q = \mathrm{id}$ denotes the identity operator. The authors Tonaki et al. (2023) have demonstrated that this phenomenon arises even in two space dimensions. To ensure that X_t^Q is square integrable, it becomes necessary to employ a coloured cylindrical Wiener process instead of a white noise. This entails introducing an additional parameter to the model, which "dampens" the Wiener process. By considering a coloured noise and introducing different damping mechanisms, Tonaki et al. (2023) successfully developed statistical inference based on high-frequency observations using a spectral approach in two space dimensions.

To specify the damping mechanism in our model, we adopt one natural approach by defining $(B_t)_{t\geqslant 0}$ by its spectral decomposition, given by

$$\langle B_t, f\rangle_\vartheta := \sum_{\mathbf{k}\in\mathbb{N}^d} \lambda_{\mathbf{k}}^{-\alpha/2} \langle f, e_{\mathbf{k}}\rangle_\vartheta W_t^{\mathbf{k}}, \tag{54}$$

for $f \in H_\vartheta, t \geqslant 0$ and with independent real-valued Brownian motions $(W_t^{\mathbf{k}})_{t\geqslant 0}$, for all $\mathbf{k} \in \mathbb{N}^d$. To ensure that the latter definition is well-defined, we assume that $\lambda_{(1,\ldots,1)} > 0$. In the previous definition, the cylindrical Brownian motion B undergoes a structural change through the introduction of the term $\lambda_{\mathbf{k}}^{-\alpha/2}$ in its spectral decomposition. This alteration naturally brings about a complete shift in the probabilistic structure of the random field. The parameter α holds particular significance as it essentially governs the damping mechanism. Comparing this characterization of the Q-cylindrical Brownian motion to its one-dimensional counterpart in equation (4), we note that the noise's colouring is determined by the term $\lambda_{\mathbf{k}}^{-\alpha/2}$. When $\alpha = 0$, we observe a white noise structure.

Currently, the required domain for the new parameter α remains uncertain. To ensure that the expected value $\mathbb{E}[\|X_t^I\|_\vartheta^2]$ is finite and enable statistical inference in our model, the domain must be carefully chosen. Nonetheless, it is reasonable to impose $\alpha \geqslant 0$ initially.

In the forthcoming analysis, we will discover that an even more stringent restriction on this parameter is essential to guarantee that the Q-Brownian motion is well-defined, which corresponds to the square integrable property of the random field. Moreover, an even stronger limitation is required for the development of statistical inference.

Prior to exploring this restriction, we begin with analysing the well-definedness of B and offer a characterization for the operator Q in our model. For this purpose, we denote the domain of the operator $A_\vartheta^{-1/2}$ as $\mathcal{D}(A_\vartheta^{-1/2})$. Then, $H_\vartheta \subset \mathcal{D}(A_\vartheta^{-1/2})$ and $(\tilde{e}_{\mathbf{k}})_{\mathbf{k}\in\mathbb{N}^d}$ define an orthonormal system on $\mathcal{D}(A_\vartheta^{-1/2})$, where $\tilde{e}_{\mathbf{k}} := e_{\mathbf{k}}/\|A_\vartheta^{-1/2}e_{\mathbf{k}}\|_\vartheta$ for all $\mathbf{k}\in\mathbb{N}^d$. The covariance operator Q on $\mathcal{D}(A_\vartheta^{-1/2})$ is then given by

$$Qe_{\mathbf{k}} = \lambda_{\mathbf{k}}^{-\alpha}\|A_\vartheta^{-1/2}e_{\mathbf{k}}\|_\vartheta^2 e_{\mathbf{k}},$$

and the corresponding eigenvalues of Q are given by $\lambda_{\mathbf{k}}^{-\alpha}\|A_\vartheta^{-1/2}e_{\mathbf{k}}\|_\vartheta^2$. Assume the parameter α is such that

$$\sum_{\mathbf{k}\in\mathbb{N}^d}\|A_\vartheta^{-(1+\alpha)/2}e_{\mathbf{k}}\|_\vartheta^2 = \sum_{\mathbf{k}\in\mathbb{N}^d}\frac{1}{\lambda_{\mathbf{k}}^{1+\alpha}} < \infty, \qquad \mathbf{k}\in\mathbb{N}^d, \tag{55}$$

then the Q-Wiener process (B_t) is well-defined in $\mathcal{D}(A_\vartheta^{-1/2})$ and the definition of the Q-Wiener process, as given in equation (54), follows by

$$\langle B_t, f\rangle_\vartheta = \sum_{\mathbf{k}\in\mathbb{N}^d}\lambda_{\mathbf{k}}^{-\alpha/2}\|A_\vartheta^{-1/2}e_{\mathbf{k}}\|_\vartheta\left\langle f, \frac{e_{\mathbf{k}}}{\|A_\vartheta^{-1/2}e_{\mathbf{k}}\|_\vartheta}\right\rangle_\vartheta W_t^{\mathbf{k}}.$$

For a comprehensive overview of Wiener processes on Hilbert spaces, we refer to Da Prato and Zabczyk (2014, Chapter 4). For readings on a different approaches for the choice of Q in two space dimensions we refer to Tonaki et al. (2023).

To ensure the well-definedness of B, it is crucial to examine potential choices for α such that the series in equation (55) converges. Since the negative eigenvalues $(\lambda_{\mathbf{k}})_{\mathbf{k}\in\mathbb{N}^d}$ are proportional to

$$\lambda_{\mathbf{k}} = -\vartheta_0 + \sum_{l=1}^d\left(\frac{\nu_l^2}{4\eta}\right) + \pi^2\eta\sum_{l=1}^d k_l^2 \propto \sum_{l=1}^d k_l^2 = \|\mathbf{k}\|_2^2,$$

we can find constants $C_1, C_2 > 0$ such that $C_1\sum_{l=1}^d k_l^2 \leqslant \lambda_k \leqslant C_2\sum_{l=1}^d k_l^2$ for all $\mathbf{k}\geqslant\mathbf{k}_0$, where $\mathbf{k}_0\in\mathbb{N}^d$. In this context, the inequality for the multi-index $\mathbf{k}$ is defined component-wise. By the integral test for convergence we have

$$\begin{aligned}&\sum_{\mathbf{k}\in\mathbb{N}^d}\lambda_{\mathbf{k}}^{-(1+\alpha)} \leqslant C_1\sum_{k_1=1}^\infty\cdots\sum_{k_d=1}^\infty\frac{1}{(k_1^2+\ldots+k_d^2)^{1+\alpha}} < \infty\\ &\Leftrightarrow \int_1^\infty\cdots\int_1^\infty\frac{1}{(x_1^2+\ldots+x_d^2)^{1+\alpha}}\,\mathrm{d}x_1\cdots\mathrm{d}x_d < \infty.\end{aligned} \tag{56}$$

To evaluate this expression, we employ spherical coordinates in d-dimensions. As this technique will be highly beneficial in the subsequent analysis, we recall this method. Consider a function $f\in\mathcal{L}^1(\mathbb{R})$ and the integral $\int_{\mathbb{R}^d} f(|\mathbf{x}|^2)\,\mathrm{d}\mathbf{x}$. The transformation to d-dimensional spherical coordinates is accomplished through the substitution

$$\begin{aligned} &x_1 = r\cos(\varphi_1), \quad x_2 = r\sin(\varphi_1)\cos(\varphi_2), \quad x_3 = r\sin(\varphi_1)\sin(\varphi_2)\cos(\varphi_3), \quad \ldots, \\ &x_{d-1} = r\sin(\varphi_1)\cdot\ldots\cdot\sin(\varphi_{d-2})\cos(\varphi_{d-1}), \quad x_d = r\sin(\varphi_1)\cdot\ldots\cdot\sin(\varphi_{d-1}), \end{aligned} \tag{57}$$

where $r \in [0,\infty), \varphi_1 \in [0,\pi], \ldots, \varphi_{d-2} \in [0,\pi]$ and $\varphi_{d-1} \in [0, 2\pi)$. Note that integrating over the entire d-dimensional space requires only one angle to be in the range of $[0, 2\pi)$. Suppose we want to evaluate $\int_{\mathbb{R}^d_+} f(|\mathbf{x}|^2)\,\mathrm{d}\mathbf{x}$, then every angle $\varphi_l \in [0, \pi/2)$ is in the first quarter of the periodicity of sine and cosine, where $l = 1, \ldots, (d-1)$. The associated Jacobian matrix of the d-dimensional spherical transformation is denoted by J_d, and its determinant is given by

$$|J_d| = \prod_{l=1}^{d-2} r^{d-1}\sin^{d-1-l}(\varphi_l).$$

Let $\mathbf{x} \in \mathbb{R}^d$. Performing this substitution yields

$$\|\mathbf{x}\|_2^2 = r^2\big(\cos^2(\varphi_1) + \sin^2(\varphi_1)\cos^2(\varphi_2) + \ldots + \sin^2(\varphi_1)\cdots\cos^2(\varphi_{d-1}) + \sin^2(\varphi_1)\cdots\sin^2(\varphi_{d-1})\big) = r^2,$$

where we have used the identity $\cos^2(x) = 1 - \sin^2(x)$. For further readings on spherical coordinates, refer to Flanders (1963). Applying this transformation to the integral over the function $f \in \mathcal{L}^1(\mathbb{R})$, we obtain the convenient representation

$$\begin{aligned} \int_{\mathbb{R}^d} f(\|\mathbf{x}\|_2^2)\,\mathrm{d}x &= \int_0^\infty r^{d-1} f(r^2)\,\mathrm{d}r \int_0^\pi \sin^{d-2}(\varphi_1)\,\mathrm{d}\varphi_1 \cdots \int_0^\pi \sin(\varphi_{d-2})\,\mathrm{d}\varphi_{d-2} \int_0^{2\pi} \mathrm{d}\varphi_{d-1} \\ &= 2\pi \int_0^\infty r^{d-1} f(r^2)\,\mathrm{d}r \int_0^\pi \sin^{d-2}(\varphi_1)\,\mathrm{d}\varphi_1 \cdots \int_0^\pi \sin(\varphi_{d-2})\,\mathrm{d}\varphi_{d-2}. \end{aligned}$$

Continuing the analysis of the integral from equation (56), we have

$$\begin{aligned} &\int_1^\infty \cdots \int_1^\infty \frac{1}{(x_1^2 + \ldots + x_d^2)^{1+\alpha}}\,\mathrm{d}x_1\cdots\mathrm{d}x_d \leqslant \int_1^\infty \int_0^{\pi/2} \cdots \int_0^{\pi/2} \int_0^{\pi/2} \frac{1}{r^{2(1+\alpha)}} |J_d|\,\mathrm{d}\varphi_{d-1}\cdots\mathrm{d}\varphi_1\,\mathrm{d}r \\ &= \int_1^\infty \frac{r^{d-1}}{r^{2(1+\alpha)}}\,\mathrm{d}r \int_0^{\pi/2} \sin^{d-2}(\varphi_1)\,\mathrm{d}\varphi_1 \cdots \int_0^{\pi/2} \sin(\varphi_{d-2})\,\mathrm{d}\varphi_{d-2} \int_0^{\pi/2} \mathrm{d}\varphi_{d-1} \\ &\leqslant \left(\frac{\pi}{2}\right)^{d-1} \left[\frac{1}{d-2(1+\alpha)} r^{d-2(1+\alpha)}\right]_1^\infty < \infty \Leftrightarrow \alpha > \frac{d}{2} - 1. \end{aligned}$$

Hence we find, that the Q-Wiener process as defined in equation (54) is well-defined, if $\alpha > d/2 - 1$. As we delve into the analysis of multi-dimensional SPDE model, i.e., $d \geqslant 2$, it becomes evident that $\alpha > 0$. This observation confirms that a white noise is not suitable for any higher dimensional SPDE model except the one-dimensional case.
Now that the theoretical framework for the random field is established, we can introduce a spectral decomposition that forms the basis for the analysis of our multi-dimensional SPDE model. Therefore, we consider a mild solution X_t of the SPDE from equation (49), which satisfies the integral representation

$$X_t = e^{tA_\vartheta}\xi + \sigma\int_0^t e^{(t-s)A_\vartheta}\,\mathrm{d}B_s,$$

for every $t \in [0,1]$ almost surely. Then, the spectral decomposition of the random field X_t is given by

$$X_t(\mathbf{y}) = \sum_{\mathbf{k}\in\mathbb{N}^d} x_{\mathbf{k}}(t) e_{\mathbf{k}}(\mathbf{y}), \qquad \text{where} \qquad x_{\mathbf{k}}(t) := \langle X_t, e_{\mathbf{k}}\rangle_\vartheta. \tag{58}$$

The coordinate processes $(x_{\mathbf{k}})_{\mathbf{k}\in\mathbb{N}^d}$ follow the Ornstein-Uhlenbeck dynamics, governed by the equation

$$\mathrm{d}x_{\mathbf{k}}(t) = -\lambda_{\mathbf{k}} x_{\mathbf{k}}(t)\,\mathrm{d}t + \sigma\lambda_{\mathbf{k}}^{-\alpha/2}\,\mathrm{d}W_t^{\mathbf{k}},$$

where $(W_t^{\mathbf{k}})_{t\geqslant 0}$ are independent real-valued Brownian motions for all $\mathbf{k}\in\mathbb{N}^d$. The Ornstein-Uhlenbeck dynamics can be obtained by using that the operator A_ϑ is self-adjoint and the eigenvalue equation. More precisely, we have

$$\begin{aligned}
x_{\mathbf{k}}(t) = \langle X_t, e_{\mathbf{k}}\rangle_\vartheta &= \left\langle e^{tA_\vartheta}\xi + \sigma\int_0^t e^{(t-s)A_\vartheta}\,\mathrm{d}B_s, e_{\mathbf{k}}\right\rangle_\vartheta \\
&= \left\langle e^{tA_\vartheta}\xi, e_{\mathbf{k}}\right\rangle_\vartheta + \left\langle \sigma\int_0^t e^{(t-s)A_\vartheta}\,\mathrm{d}B_s, e_{\mathbf{k}}\right\rangle_\vartheta \\
&= e^{-\lambda_{\mathbf{k}}t}\langle \xi, e_{\mathbf{k}}\rangle_\vartheta + \left\langle \sigma\sum_{\mathbf{j}\in\mathbb{N}^d}\Big(\lambda_{\mathbf{j}}^{-\alpha/2}\int_0^t e^{(t-s)A_\vartheta}\,\mathrm{d}W_s^{\mathbf{j}}\Big)e_{\mathbf{j}}, e_{\mathbf{k}}\right\rangle_\vartheta \\
&= e^{-\lambda_{\mathbf{k}}t}\langle \xi, e_{\mathbf{k}}\rangle_\vartheta + \sigma\lambda_{\mathbf{k}}^{-\alpha/2}\int_0^t e^{-\lambda_{\mathbf{k}}(t-s)}\,\mathrm{d}W_s^{\mathbf{k}},
\end{aligned} \tag{59}$$

where we used that $\langle e^{tA_\vartheta}f, e_{\mathbf{k}}\rangle_\vartheta = e^{-\lambda_{\mathbf{k}}t}\langle f, e_{\mathbf{k}}\rangle_\vartheta$, for a $f\in H_\vartheta$. To conclude the probabilistic framework, we show, that the random field, governed by the cylindrical Brownian motion, is square integrable for each $t\geqslant 0$. Therefore, suppose $t>0$ as the case where $t=0$ is trivial. By employing the spectral decomposition of a mild solution X_t, we observe that

$$\begin{aligned}
\mathbb{E}[\|X_t\|_\vartheta^2] &= \mathbb{E}\Big[\Big\|\sum_{\mathbf{k}\in\mathbb{N}^d} x_{\mathbf{k}}(t)e_{\mathbf{k}}\Big\|_\vartheta^2\Big] = \sum_{\mathbf{k}\in\mathbb{N}^d}\sum_{\mathbf{j}\in\mathbb{N}^d}\mathbb{E}\big[\|x_{\mathbf{k}}(t)e_{\mathbf{k}}x_{\mathbf{j}}(t)e_{\mathbf{j}}\|_\vartheta\big] \\
&= \sum_{\mathbf{k}\in\mathbb{N}^d}\|e_{\mathbf{k}}\|_\vartheta^2\mathbb{E}\big[x_{\mathbf{k}}(t)^2\big] \\
&\leqslant C\sum_{\mathbf{k}\in\mathbb{N}^d}\left(e^{-2\lambda_{\mathbf{k}}t}\mathbb{E}\big[\langle\xi,e_{\mathbf{k}}\rangle_\vartheta^2\big] + \sigma^2\lambda_{\mathbf{k}}^{-\alpha}\mathbb{E}\Big[\Big(\int_0^t e^{-\lambda_{\mathbf{k}}(t-s)}\,\mathrm{d}W_s^{\mathbf{k}}\Big)^2\Big]\right) \\
&= C\sum_{\mathbf{k}\in\mathbb{N}^d}\left(e^{-2\lambda_{\mathbf{k}}t}\mathbb{E}\big[\langle\xi,e_{\mathbf{k}}\rangle_\vartheta^2\big] + \sigma^2\lambda_{\mathbf{k}}^{-\alpha}\int_0^t e^{-2\lambda_{\mathbf{k}}(t-s)}\,\mathrm{d}s\right) \\
&= C\sum_{\mathbf{k}\in\mathbb{N}^d}\left(e^{-2\lambda_{\mathbf{k}}t}\mathbb{E}\big[\langle\xi,e_{\mathbf{k}}\rangle_\vartheta^2\big] + \sigma^2\lambda_{\mathbf{k}}^{-\alpha}\frac{e^{-2\lambda_{\mathbf{k}}t}\big(e^{2\lambda_{\mathbf{k}}t}-1\big)}{2\lambda_{\mathbf{k}}}\right) \\
&= C\sum_{\mathbf{k}\in\mathbb{N}^d}\left(e^{-2\lambda_{\mathbf{k}}t}\mathbb{E}\big[\langle\xi,e_{\mathbf{k}}\rangle_\vartheta^2\big] + \sigma^2\frac{1-e^{-2\lambda_{\mathbf{k}}t}}{2\lambda_{\mathbf{k}}^{1+\alpha}}\right) \\
&\leqslant C'\sum_{\mathbf{k}\in\mathbb{N}^d}\left(\frac{e^{-2\lambda_{\mathbf{k}}t}}{\lambda_{\mathbf{k}}^{1+\alpha}} + \sigma^2\frac{1-e^{-2\lambda_{\mathbf{k}}t}}{2\lambda_{\mathbf{k}}^{1+\alpha}}\right) \\
&\leqslant C''\sum_{\mathbf{k}\in\mathbb{N}^d}\frac{1}{\lambda_{\mathbf{k}}^{1+\alpha}},
\end{aligned}$$

where we utilized Itô isometry for suitable constants $C, C', C'' > 0$. We also used that $\sup_{\mathbf{k}\in\mathbb{N}^d} \lambda_{\mathbf{k}}^{1+\alpha}\mathbb{E}[\langle \xi, e_{\mathbf{k}}\rangle_\vartheta^2] < \infty$, which is a part of Assumption 4.1.2, which is introduced at the end of this section. Thus, we have for a suitable constant $C > 0$ that

$$\mathbb{E}[\|X_t\|_\vartheta^2] \leqslant C \sum_{k\in\mathbb{N}^d} \frac{1}{\lambda_k^{1+\alpha}} < \infty,$$

if $\alpha > d/2 - 1$. As already mentioned and evidenced by the preceding calculation, the property of the random field of being square-integrable is directly related to the well-definedness of B_t from equation (54), serving as a singular constraint that ensures both properties. Since the constraint for damping parameter α is related to the dimension of the SPDE model from equation (49), we introduce the notation

$$\alpha = \frac{d}{2} - 1 + \alpha',$$

where $\alpha' > 0$. As we assume the dimension d of the SPDE model from equation (49) to be known, the parameter α' enables us to analyse the "pure" damping rate.

Having established the probabilistic structure of our multi-dimensional SPDE model, we shift our focus to the statistical assumptions. Similar to the one-dimensional case, we aim to develop statistical inference using a high-frequency observation scheme. Assumption 1.1.1 illustrated that even in one space dimension, it is essential to restrict the observations to bound the correlations of the SPDE model given in equation (1). Intuitively, we will require similar restrictions to develop consistent estimators. The following assumption outlines the high-frequency observation scheme.

Assumption 4.1.1 (Observation scheme)
Suppose we observe a mild solution X of the SPDE model from equation (49) on a discrete grid $(t_i, \mathbf{y}_j) \in [0,1]\times[0,1]^d$, with equidistant observations in time $t_i = i\Delta_n$ for $i = 1,\ldots,n$ and $\mathbf{y}_1,\ldots,\mathbf{y}_m \in [\delta, 1-\delta]^d$, where $n, m \in \mathbb{N}$ and $\delta \in (0, 1/2)$. We consider one of the following two asymptotic regimes, respectively:

(I) $\Delta_n \to 0$, as $n \to \infty$, while $n\Delta_n = 1$ and $m < \infty$ is fixed,

(II) $\Delta_n \to 0$ and $m = m_n \to \infty$, as $n \to \infty$, while $n\Delta_n = 1$ and $m = \mathcal{O}(n^\rho)$ for some $\rho \in \big(0, (1-\alpha')/(d+2)\big)$,

where $\alpha = d/2 - 1 + \alpha'$ and $\alpha' \in (0,1)$. Furthermore, we consider that

$$m_n \cdot \min_{\substack{j_1,j_2=1,\ldots,m_n\\ j_1\neq j_2}} \|\mathbf{y}_{j_1} - \mathbf{y}_{j_2}\|_0$$

is bounded from below, uniformly in n for both regimes.

For the spatial coordinates $y_l^{(j)}$, we use the subscript $l = 1,\ldots,d$ for the respective dimension component of $\mathbf{y}_j$, and the superscript $(j) = 1,\ldots,m$ for the respective j-th observation. As seen in this Assumption, we have further restricted the damping parameter to $\alpha \in (d/2 - 1, d/2)$. This limitation is necessary to enable statistical inference.

Similar to Assumption 1.1.1, we require fewer spatial observations than temporal ones. The damping parameter also influences the relationship between the observation resolutions in temporal and spatial dimensions. As the dimension increases, the spatial resolution decreases. Note that we specifically have $\rho < 1/2$. Additionally, Assumption 1.1.1 states that

$$m \cdot \min_{j=2,\ldots,m} |y_j - y_{j-1}| \tag{60}$$

is bounded from below, for $y_1 < \ldots < y_m \in [\delta, 1-\delta]$. Since this assumption primarily controls the covariances of the realized volatilities in distinct one-dimensional spatial coordinates, it is crucial to adapt equation (60) to multiple space dimensions.

A significant difference between SPDEs in one and multiple space dimensions is that the spatial coordinates $\mathbf{y}_1, \ldots, \mathbf{y}_d$ in multiple space dimensions lack a directly feasible order as we have in the one-dimensional case with $y_1 < \ldots < y_m$. Suppose we have two distinct spatial points $\mathbf{y}_1, \mathbf{y}_2 \in [\delta, 1-\delta]^d$. Then, there must exist only one index $l \in 1, \ldots, d$, such that $y_l^{(1)} \neq y_l^{(2)}$, whereas the remaining coordinates can be equal. Assuming the first $(d-1)$ coordinates of spatial observations $\mathbf{y}_1, \ldots, \mathbf{y}_d$ to be fixed at $1/2$, such that we can only observe the d-th coordinates $y_d^{(j)}$ for $j = 1, \ldots, m$. Then, the observation scheme reduces to one space dimension, which motivates the need for a similar structure of observations in multiple space dimensions as we used in one space dimension, i.e., equation (60). The last example also motivates the mapping $\|\cdot\|_0$. This mapping ignores those coordinates that remain the same and measures only the smallest change on the axis on which $\mathbf{y}_{j_1} - \mathbf{y}_{j_2}$ moves, where $j_1 \neq j_2$. Note that we also measure the smallest distance between every combination of spatial points $\mathbf{y}_1, \ldots, \mathbf{y}_d$ due to the lack of order in $\mathbb{R}^d$. Since we also impose a Dirichlet boundary condition on the SPDE model from equation (49) in multiple space dimensions, we transfer the boundary condition $\mathbf{y}_1, \ldots, \mathbf{y}_d \in [\delta, 1-\delta]^d$ for the spatial observations to Assumption 4.1.1.

We also introduce a regularity assumption to our model.

Assumption 4.1.2 (Regularity)
For the SPDE model from equation (49) we assume that

(i) either $\mathbb{E}[\langle \xi, e_{\mathbf{k}} \rangle_\vartheta] = 0$ for all $\mathbf{k} \in \mathbb{N}^d$ and $\sup_{\mathbf{k}\in\mathbb{N}^d} \lambda_{\mathbf{k}}^{1+\alpha} \mathbb{E}[\langle \xi, e_{\mathbf{k}} \rangle_\vartheta^2] < \infty$ holds true or $\mathbb{E}[\|A_\vartheta^{(1+\alpha)/2} \xi\|_\vartheta^2] < \infty$, for $\alpha \in (d/2-1, d/2)$,

(ii) $(\langle \xi, e_{\mathbf{k}} \rangle_\vartheta)_{\mathbf{k}\in\mathbb{N}^d}$ are independent.

We observe that the coloured noise introduces more stringent regularity conditions on our model compared to the white noise used in one space dimension, cf. Assumption 1.1.2. This added complexity calls for more careful analysis and considerations when dealing with the multi-dimensional framework.

We conclude this section by examining how the parameters impact the solution process of our model. Building upon our initial discussion in Section 1.2 regarding the one-dimensional case, our focus now shifts to understanding the impact of parameters such as η, $\nu_1, \ldots, \nu_d, \sigma$, and α on both the spatial and temporal marginal processes of the random field. To facilitate this exploration, we employ Figure 4.1 to visually represent the effects of these parameters. In this visualization, we simulated a three-dimensional SPDE model on a temporal grid with $N = 10^4$ time points and $M = 10$ spatial points, where the respective parameter combinations are provided in the plot titles. For readings on the simulation methods, we refer to Section 4.3.

Analogously to the calculations leading to equation (6) in Section 1.2, we obtain the following covariance structure:

$$\mathbb{C}\mathrm{ov}\big(\tilde{X}_s(\mathbf{y}_1), \tilde{X}_t(\mathbf{y}_2)\big) = \sigma^2 \sum_{\mathbf{k}\in\mathbb{N}^d} \frac{e^{-\lambda_{\mathbf{k}}|t-s|}}{2\lambda_{\mathbf{k}}^{1+\alpha}} e_{\mathbf{k}}(\mathbf{y}_1) e_{\mathbf{k}}(\mathbf{y}_2), \tag{61}$$

where $\tilde{X}_t(\mathbf{y})$ denotes a mild solution of the multi-dimensional SPDE model with a stationary initial condition, i.e., $\langle \xi, e_{\mathbf{k}} \rangle_\vartheta \sim \mathcal{N}(0, \sigma^2/(2\lambda_{\mathbf{k}}^{1+\alpha}))$. We will use this covariance structure in order to enhance the following argumentative insights.

First, similar to the one-dimensional case, the parameter ϑ_0 has no noticeable visual impact on the random field, which is evident by utilizing equation (61) and analogous argumentation as in the one-dimensional case. On the other hand, the parameter ν plays a crucial role in controlling the curvature effect within the spatial domain. Each component ν_i of ν, where $i = 1, \dots, d$, corresponds to i-th spatial axis on which a potential curvature on the solution field is applied. For instance, in the first row of Figure 4.1, we observe sample paths of the spatial marginal processes with $\nu = (10, -10, 0)$. Here, we notice a contrasting curvature effect on the first two spatial axes, while the third spatial axis exhibits no observable curvature. As in the one-dimensional SPDE model, where the analogous parameter is denoted as ϑ_1, the curvature effect can be mitigated by the parameter η, which can be observed in the second row of Figure 4.1. When η is relatively large compared to ν_i, the curvature in the spatial field becomes less pronounced. In fact, the influence of these parameters on a solution field $X_t(\mathbf{y})$ from the multi-dimensional SPDE model in equation (49) can be explained in a manner analogous to the one-dimensional SPDE model. Since we decomposed $X_t(\mathbf{y})$ using an orthonormal basis, which is derived from the respective one-dimensional orthonormal basis of each axis, the behaviour of the one-dimensional equivalent parameters transfers directly, i.e., ν_i corresponds to ϑ_1 and η to ϑ_2. Therefore, we refer to the one-dimensional discussion on these model parameters.

Furthermore, as in the one-dimensional SPDE model, the parameter σ^2 governs the overall volatility of the solution field, as evident by equation (61). This effect is visually demonstrated in the third and fourth row of Figure 4.1. In the one-dimensional case, we referred to this parameter as σ_0^2 and recognized that the volatility level is also influenced by the parameter η. With the same reasoning as for the parameter ν and η, this effect can be elucidated by examining the one-dimensional case. Notably, the first and second row of Figure 4.1 also showcase the impact of η on the volatility level. Note that the sample paths of the temporal processes displayed in the first and second row do not share a common y-scale. Consequently, we conclude that the parameter ν controls the relative curvature of the solution field, while σ influences the relative volatility, with the observable curvature and volatility additionally depending on the parameter η. We will delve deeper into the relationships between these parameter combinations in Proposition 4.2.7, where we examine the identifiability of the model parameters, effectively identifying

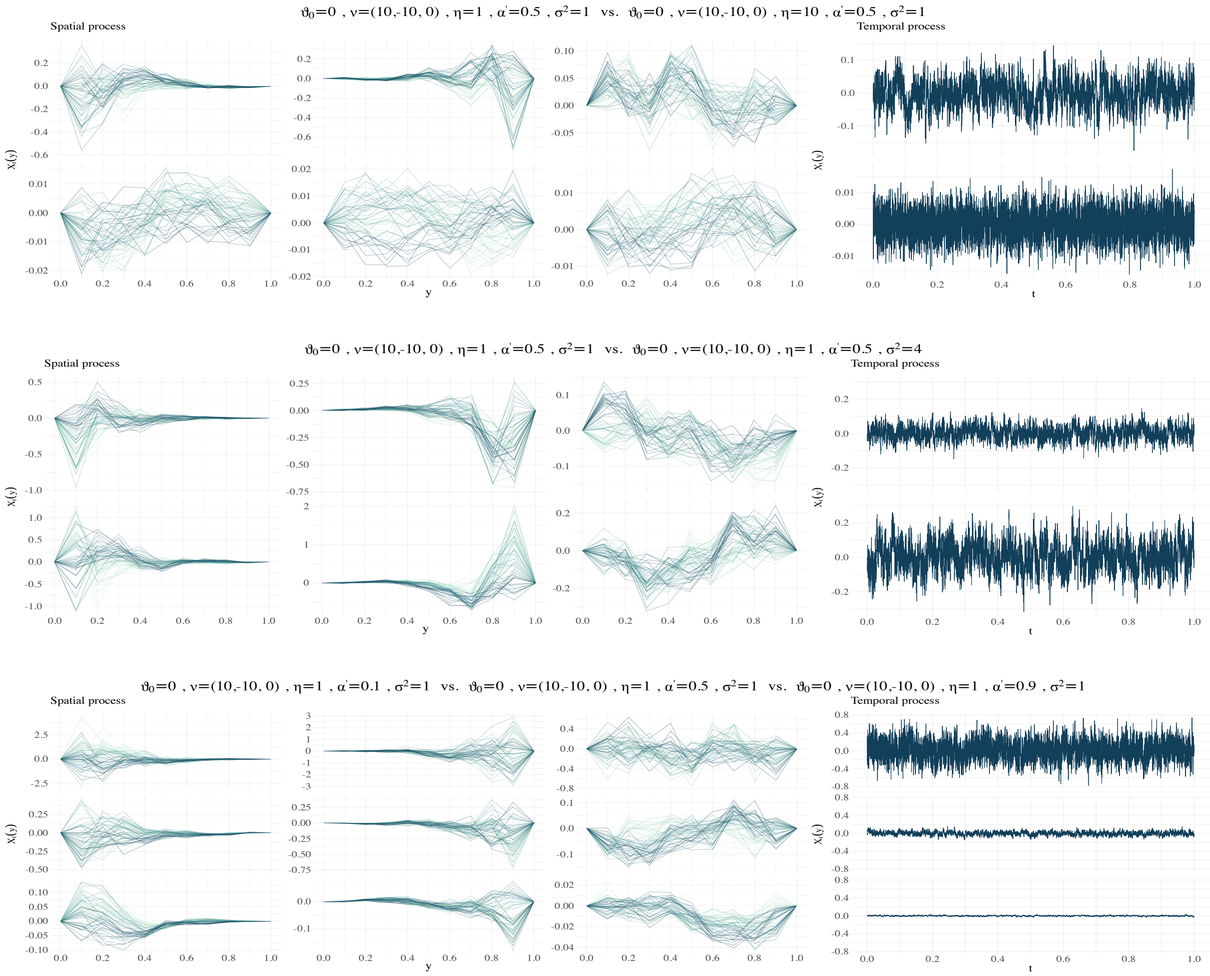

Figure 4.1.: The provided figure displays sample paths of a three-dimensional SPDE model described by equation (49). The sample paths are generated using an equidistant grid in both time and space, where $N = 10^4$, $M = 10$, and $\xi \equiv 0$. Each row in the figure consists of four plots. In each row, the first three plots from the left illustrate the spatial processes, $\mathbf{y} \mapsto X_t(\varphi(\mathbf{y}))$, for time points $t = 0.1 + k/10^3$, where $k = 0, \dots, 50$. The first column displays the spatial processes for the first spatial axis, while keeping the other axes fixed, i.e., $\varphi(\mathbf{y}) = (y_1, 1/2, 1/2)$. The second column shows the spatial processes for the second spatial axis, with $\varphi(\mathbf{y}) = (1/2, y_2, 1/2)$, and the third column illustrates the spatial processes for the third spatial axis, with $\varphi(\mathbf{y}) = (1/2, 1/2, y_3)$. The last column presents the temporal processes, $t \mapsto X_t(\mathbf{y})$, with $\mathbf{y} = (1/10, 1/10, 1/10)^\top$ fixed. The titles indicate the different parameter scenarios under comparison, with the first scenario depicted in the first row, and subsequent scenarios shown in the subsequent rows. Note that only the second and third panels of the temporal processes share a common y-scale, whereas the other panels have a freely adjustable y-scale.

the natural parameters of the model.

Concluding our heuristic exploration of multi-dimensional parameters, we analyse the behaviour of the random field for various values of α, which we describe in terms of the corresponding parameter $\alpha' \in (0, 1)$. In equation (58), we decomposed $X_t(\mathbf{y})$ using a Fourier series. Here, the orthonormal and deterministic basis $(e_\mathbf{k})_{\mathbf{k}\in\mathbb{N}^d}$ are not influenced by the so-called damping parameter α and the pure damping parameter α', whereas the coordinate processes $(x_\mathbf{k})_{\mathbf{k}\in\mathbb{N}^d}$ depend on α'. Specifically, α' governs the influence of the eigenvalues $(\lambda_\mathbf{k})_{\mathbf{k}\in\mathbb{N}^d}$, signifying a fundamental impact of this damping parameter on the multi-dimensional SPDE model. Furthermore, the damping effect of α is also identifiable when considering the covariance structure in equation (61). As our upcoming analysis will reveal, α' plays a role similar to the Hurst parameter for fractional Brownian motions, affecting the roughness of the temporal paths, as evident in the last three rows of Figure 4.1. When the pure damping parameter α' is relatively small, the sample paths of the temporal marginal processes accelerate noticeably, whereas a relatively large α' slows down the sample paths of the temporal marginal processes. Since the parameter α' has no direct impact on the orthonormal basis $(e_{\mathbf{k}})_{\mathbf{k}\in\mathbb{N}}$, we do not observe a qualitative impact on the sample paths of the spatial marginal processes, which is also explainable by the covariance structure given in equation (61).

4.2. Analysis of the quadratic increments

In the preceding section, we laid the groundwork for our SPDE model in multiple space dimensions. In this section, our objective is to conduct an initial analysis of the random field. Drawing from the work of Bibinger and Trabs (2020) in the one-dimensional case, we will employ quadratic increments and the method of moments to construct consistent estimators. To achieve this, we will delve into the examination of the first moment of quadratic temporal increments and also investigate the covariance of temporal increments.

To accomplish these tasks, we need to address some technical intricacies, including a Riemann approximation for sums on $\mathbb{N}^d$. Once we have successfully elaborated on the first moment for quadratic increments and its extension to realized volatilities, we can leverage this information to construct a primary estimator within this model.

Suppose we have a mild solution X_t, then we can adopt the spectral approach and decompose an increment of X_t as follows:

$$(\Delta_i X)(\mathbf{y}) := X_{i\Delta_n}(\mathbf{y}) - X_{(i-1)\Delta_n}(\mathbf{y}) = \sum_{\mathbf{k}\in\mathbb{N}^d} \Delta_i x_{\mathbf{k}} e_{\mathbf{k}}(\mathbf{y}), \quad \text{where} \quad \Delta_i x_{\mathbf{k}} := x_{\mathbf{k}}(i\Delta_n) - x_{\mathbf{k}}\big((i-1)\Delta_n\big).$$

Therefore, analysing the temporal increments of the coordinate processes is crucial for understanding the structure of the increments $\Delta_i X_t$. As we have observed in equation (59), the coordinate processes satisfy the Ornstein-Uhlenbeck dynamics, and we can employ its representation to decompose the increments of $x_{\mathbf{k}}$, for $\mathbf{k} \in \mathbb{N}^d$, as follows:

$$\begin{aligned}\Delta_i x_{\mathbf{k}} &= \langle \xi, e_{\mathbf{k}}\rangle_\vartheta \big(e^{-\lambda_{\mathbf{k}} i\Delta_n} - e^{-\lambda_{\mathbf{k}}(i-1)\Delta_n}\big) + \sigma\lambda_{\mathbf{k}}^{-\alpha/2} \int_0^{(i-1)\Delta_n} e^{-\lambda_{\mathbf{k}}(i\Delta_n - s)} - e^{-\lambda_{\mathbf{k}}((i-1)\Delta_n - s)} \, \mathrm{d}W_s^{\mathbf{k}} \\ &\quad + \sigma\lambda_{\mathbf{k}}^{-\alpha/2} \int_{(i-1)\Delta_n}^{i\Delta_n} e^{-\lambda_{\mathbf{k}}(i\Delta_n - s)} \, \mathrm{d}W_s^{\mathbf{k}} \\ &= A_{i,\mathbf{k}} + B_{i,\mathbf{k}} + C_{i,\mathbf{k}}, \end{aligned} \tag{62}$$

where

$$A_{i,\mathbf{k}} := \langle \xi, e_{\mathbf{k}}\rangle_\vartheta \big(e^{-\lambda_{\mathbf{k}} i\Delta_n} - e^{-\lambda_{\mathbf{k}}(i-1)\Delta_n}\big), \tag{63}$$

$$B_{i,\mathbf{k}} := \sigma\lambda_{\mathbf{k}}^{-\alpha/2} \int_0^{(i-1)\Delta_n} e^{-\lambda_{\mathbf{k}}((i-1)\Delta_n - s)} \big(e^{-\lambda_{\mathbf{k}}\Delta_n} - 1\big) \, \mathrm{d}W_s^{\mathbf{k}}, \tag{64}$$

$$C_{i,\mathbf{k}} := \sigma \lambda_{\mathbf{k}}^{-\alpha/2} \int_{(i-1)\Delta_n}^{i\Delta_n} e^{-\lambda_{\mathbf{k}}(i\Delta_n - s)} \, \mathrm{d}W_s^{\mathbf{k}}. \tag{65}$$

The latter decomposition involves the temporal origin represented by $A_{i,\mathbf{k}}$, the evolution of the temporal increments represented by $B_{i,\mathbf{k}}$, and the youngest past, which contains the most recent temporal increment, represented by $C_{i,\mathbf{k}}$. Given that this decomposition (almost) aligns with the one-dimensional case, as demonstrated by Bibinger and Trabs (2020), we can anticipate the term $A_{i,\mathbf{k}}$ to be negligible. Consequently, the terms $B_{i,\mathbf{k}}$ and $C_{i,\mathbf{k}}$ will significantly impact the calculation of the first moment of the realized volatility.

Given the alterations in the noise structure for the multi-dimensional SPDE model, it is expected that these changes will influence the decomposition of the temporal increments. Specifically, the temporal evolution parts $B_{i,\mathbf{k}}$ and $C_{i,\mathbf{k}}$ now incorporate the damping mechanism $\lambda_{\mathbf{k}}^{-\alpha/2}$, whereas the term $A_{i,\mathbf{k}}$ remains relatively similar to the one-dimensional case.

To introduce the technical part of this section, we begin with the following lemma, which serves as a fundamental tool for the entire forthcoming analysis.

Lemma 4.2.1

Let $f : [0, \infty) \to \mathbb{R}$ be twice continuously differentiable with $\|x^{d-1} f(x^2)\|_{\mathcal{L}^1([0,\infty))}$, $\|x^d f'(x^2)\|_{\mathcal{L}^1([1,\infty))}$, and $\|x^{d+1} f''(x^2)\|_{\mathcal{L}^1([1,\infty))} \leqslant C$, for some $C > 0$, then it holds:

(i)
$$\Delta_n^{d/2} \sum_{\mathbf{k}\in\mathbb{N}^d} f(\lambda_{\mathbf{k}}\Delta_n) = \frac{1}{2^d(\pi\eta)^{d/2}\Gamma(d/2)} \int_0^\infty x^{d/2-1} f(x)\,\mathrm{d}x - \sum_{\substack{\|\gamma\|_1=1 \\ \gamma\in\{0,1\}^d}}^{d-1} \int_{B_\gamma} f(\pi^2\eta\,\|\mathbf{z}\|_2^2)\,\mathrm{d}\mathbf{z}$$
$$+\mathcal{O}\bigg(\int_0^{\sqrt{\Delta_n}} r^{d-1}|f(r^2)|\,\mathrm{d}r \vee \Delta_n \int_{\sqrt{\Delta_n}}^1 r^{d-1}|f'(r^2)|\,\mathrm{d}r \vee \Delta_n \int_{\sqrt{\Delta_n}}^1 r^{d+1}|f''(r^2)|\,\mathrm{d}r \bigg),$$
where B_γ defined in equation (82).

(ii) For $\{j_1, \ldots, j_l\} \subset \{1, \ldots, d\}$, $\gamma_{j,l} \in \{0,1\}^d$, where $(\gamma_{j,l})_i = \mathbb{1}_{i\in\{j_1,\ldots,j_l\}}$, with $i = 1, \ldots, d$ and $l = 1, \ldots, (d-1)$, we have
$$\Delta_n^{d/2} \sum_{\mathbf{k}\in\mathbb{N}^d} f(\lambda_{\mathbf{k}}\Delta_n) \cos(2\pi k_{j_1} y_{j_1}) \cdot \ldots \cdot \cos(2\pi k_{j_l} y_{j_l}) = (-1)^l \int_{B_{\gamma_{j,l}}} f(\pi^2\eta\,\|\mathbf{z}\|_2^2)\,\mathrm{d}\mathbf{z}$$
$$+ \mathcal{O}\bigg(\max_{k=0,\ldots,l} \frac{\Delta_n^{k/2+1}}{\delta^{l+1}} \int_{\sqrt{\Delta_n}}^1 r^{d-k+1}|f''(r^2)|\,\mathrm{d}r \vee \max_{k=0,\ldots,l} \frac{\Delta_n^{k/2+1}}{\delta^{l+1}} \int_{\sqrt{\Delta_n}}^1 r^{d-k-1}|f'(r^2)|\,\mathrm{d}r \bigg)$$
$$+ \mathcal{O}\bigg(\frac{\Delta_n^{(l+1)/2}}{\delta^l} \int_{\sqrt{\Delta_n}}^1 r^{d-l}|f'(r^2)|\,\mathrm{d}r \bigg).$$

(iii) For $\{j_1, \ldots, j_l\} = \{1, \ldots, d\}$, i.e., $l = d$, we have
$$\Delta_n^{d/2} \sum_{\mathbf{k}\in\mathbb{N}^d} f(\lambda_{\mathbf{k}}\Delta_n) \cos(2\pi k_1 y_1) \cdot \ldots \cdot \cos(2\pi k_d y_d) = \mathcal{O}\big(\Delta_n^{d/2}|f(\Delta_n)|\big) + \mathcal{O}\bigg(\frac{\Delta_n^{d/2}}{\delta^d} \int_{\sqrt{\Delta_n}}^1 r|f'(r^2)|\,\mathrm{d}r \bigg)$$
$$+ \mathcal{O}\bigg(\max_{k=0,\ldots,d-1} \frac{\Delta_n^{k/2+1}}{\delta^{d+1}} \int_{\sqrt{\Delta_n}}^1 r^{d-k+1}|f''(r^2)|\,\mathrm{d}r \vee \max_{k=0,\ldots,d-1} \frac{\Delta_n^{k/2+1}}{\delta^{d+1}} \int_{\sqrt{\Delta_n}}^1 r^{d-k-1}|f'(r^2)|\,\mathrm{d}r \bigg).$$

In particular, it holds for a $\tilde{\gamma} \in \{0,1\}^d$, with $\|\tilde{\gamma}\|_1 = l$ and $1 \leqslant l \leqslant d-1$, that

$$\int_{B_{\tilde{\gamma}}} f(\pi^2 \eta \, \|\mathbf{z}\|_2^2) \, \mathrm{d}\mathbf{z} = \mathcal{O}\bigg(\Delta_n^{l/2} \int_{\sqrt{\Delta_n}}^1 r^{d-1-l} |f(r^2)| \, \mathrm{d}r \bigg),$$

and

$$\sum_{\substack{\|\gamma\|_1=1 \\ \gamma \in \{0,1\}^d}}^{d} \int_{B_\gamma} f(\pi^2 \eta \, \|\mathbf{z}\|_2^2) \, \mathrm{d}\mathbf{z} = \mathcal{O}\bigg(\max_{l=1,\dots,d-1} \Delta_n^{l/2} \int_{\sqrt{\Delta_n}}^1 r^{d-1-l} |f(r^2)| \, \mathrm{d}r \vee \int_0^{\sqrt{\Delta_n}} r^{d-1} |f(r^2)| \, \mathrm{d}r \bigg).$$

The proof of the preceding lemma relies on standard Riemann approximation techniques. In addition to these standard ideas, it is crucial to handle the remainder terms of the approximation carefully. In order to analyse these remainders, we utilize a transformation into spherical coordinates, which offers the advantage of tracing the order of the remainder terms back to the behaviour of the function being approximated in a vicinity near zero. This procedure enables the use of the concept of regularly varying functions. For readings on this topic we refer to Bingham et al. (1989) for a comprehensive discussion.

Statement (i) of the previous lemma provides the desired Riemann approximation of a series over $\mathbb{N}^d$, which corresponds to the inherited structure resulting from the spectral decomposition. The first remainder term in statement (i) is of particular interest. By considering the leading term in statement (ii), we approximate a function f that satisfies the conditions of Lemma 4.2.1 in conjunction with cosine functions.

The leading term of the Riemann approximation from (ii) can compensate for the remainder term from (i). Depending on whether the number of cosine terms is even or odd, we observe an alternating sign in the leading term from (ii). This behaviour results in the complete compensation of the first error term from (i) when Lemma 4.2.1 is explicitly applied.

Comparing this lemma with the corresponding lemma from Bibinger and Trabs (2020, Lemma 6.2.) and Tonaki et al. (2023, Lemma 5.1.), statement (ii) provides new insights regarding the compensation of remainder terms in the main approximation from (i) in higher dimensions. In addition, this behaviour is absent in one and two dimensions, respectively. The detailed proof of this lemma can be found in Section 4.4, see Proof of Lemma 4.2.1 on page 119, owing to its complexity and scope.

We now specify the application of regularly varying functions in our case. Our objective is to determine the order of the error terms. In particular, we are not interested in finding exact constants. The previous Lemma 4.2.1 demonstrates that, for this purpose, only the behaviour of the function and its first and second derivatives in a vicinity near zero is relevant. Accordingly, we introduce the following class of functions:

$$\begin{aligned} \mathcal{Q}_\beta := \Big\{ f : [0,\infty) \to \mathbb{R} | \; f \text{ is twice differentiable, } \|x^{d-1} f(x^2)\|_{\mathcal{L}^1([0,\infty))}, \; \|x^d f^{(1)}(x^2)\|_{\mathcal{L}^1([1,\infty))}, \\ \|x^{d+1} f^{(2)}(x^2)\|_{\mathcal{L}^1([1,\infty))} \text{ and } \limsup_{x \to 0} |f^{(j)}(x^2)/x^{-\beta_j}| \leqslant C < \infty, \text{ for } j = 0,1,2 \Big\}, \end{aligned} \tag{66}$$

where $f^{(j)}$ denotes the j-th derivative and $\beta = (\beta_0, \beta_1, \beta_2) \in (0,\infty)^3$. The first conditions ensure that a function $f \in \mathcal{Q}_\beta$ satisfies the requirements of Lemma 4.2.1. The concept of regularly varying functions, as also utilized in extreme value theory, is thus incorporated in the last part of the latter definition. By employing this class of functions, we can formulate the following corollary.

Corollary 4.2.2
Let $f \in \mathcal{Q}_\beta$ for $\beta = (\beta_0, \beta_1, \beta_2) \in (0, \infty)$, then it holds that

(i)
$$\Delta_n^{d/2} \sum_{\mathbf{k}\in\mathbb{N}^d} f(\lambda_{\mathbf{k}}\Delta_n) = \frac{1}{2^d(\pi\eta)^{d/2}\Gamma(d/2)} \int_0^\infty x^{d/2-1} f(x)\,\mathrm{d}x - \sum_{\substack{\|\gamma\|_1=1\\ \gamma\in\{0,1\}^d}}^{d-1} \int_{B_\gamma} f(\pi^2\eta\,\|\mathbf{z}\|_2^2)\,\mathrm{d}\mathbf{z}$$
$$+\mathcal{O}\big(\Delta_n \vee \Delta_n^{(d-\beta_0)/2} \vee \Delta_n^{(d+2-\beta_1)/2} \vee \Delta_n^{(d+4-\beta_2)/2}\big),$$

where B_γ is defined in equation (82).

(ii) For $\{j_1,\ldots,j_l\} \subset \{1,\ldots,d\}$, $\gamma_{j,l} \in \{0,1\}^d$, where $(\gamma_{j,l})_i = \mathbb{1}_{i\in\{j_1,\ldots,j_l\}}$, with $i = 1,\ldots,d$ and $l = 1,\ldots,(d-1)$, we have

$$\Delta_n^{d/2} \sum_{\mathbf{k}\in\mathbb{N}^d} f(\lambda_{\mathbf{k}}\Delta_n)\cos(2\pi k_{j_1}y_{j_1})\cdot\ldots\cdot\cos(2\pi k_{j_l}y_{j_l}) = (-1)^l \int_{B_{\gamma_{j,l}}} f(\pi^2\eta\,\|\mathbf{z}\|_2^2)\,\mathrm{d}\mathbf{z}$$
$$+\,\mathcal{O}\big(\delta^{-(l+1)}\Delta_n \vee \delta^{-l}\Delta_n^{(l+1)/2} \vee \delta^{-(l+1)}\Delta_n^{(d+2-\beta_1)/2} \vee \delta^{-(l+1)}\Delta_n^{(d+4-\beta_2)/2}\big).$$

(iii) For $\{j_1,\ldots,j_l\} = \{1,\ldots,d\}$, i.e., $l = d$, we have

$$\Delta_n^{d/2} \sum_{\mathbf{k}\in\mathbb{N}^d} f(\lambda_{\mathbf{k}}\Delta_n)\cos(2\pi k_1 y_1)\cdot\ldots\cdot\cos(2\pi k_d y_d)$$
$$= \mathcal{O}\big(\delta^{-(d+1)}\Delta_n \vee \Delta_n^{(d-\beta_0)/2} \vee \delta^{-(d+1)}\Delta_n^{(d+2-\beta_1)/2} \vee \delta^{-(d+1)}\Delta_n^{(d+4-\beta_2)/2}\big).$$

In particular, it holds for a $\tilde{\gamma} \in \{0,1\}^d$, with $\|\tilde{\gamma}\|_1 = l$ and $1 \leqslant l \leqslant d-1$, that

$$\int_{B_{\tilde{\gamma}}} f(\pi^2\eta\,\|\mathbf{z}\|_2^2)\,\mathrm{d}\mathbf{z} = \mathcal{O}\big(\Delta_n^{l/2} \vee \Delta_n^{(d-\beta_0)/2}\big)$$

and

$$\sum_{\substack{\|\gamma\|_1=1\\ \gamma\in\{0,1\}^d}}^{d} \int_{B_\gamma} f(\pi^2\eta\,\|\mathbf{z}\|_2^2)\,\mathrm{d}\mathbf{z} = \mathcal{O}\big(\Delta_n^{1/2} \vee \Delta_n^{(d-\beta_0)/2}\big).$$

Suppose we have a function $f \in \mathcal{Q}_\beta$, where the parameter $\beta = (\beta_0, \beta_1, \beta_2)$ is known. In this case, thanks to the aforementioned corollary, the Riemann approximation and the corresponding remainders can be readily obtained. For the proof of this corollary, see Proof of Corollary 4.2.2 on page 138. However, as an approximation is only of use if the approximation error diminishes, the parameter β should be upper-bounded by $\beta \in (0,d) \times (0,d+2) \times (0,d+4)$. To express this boundary on the parameter β in terms of the damping parameter α, we find that

$$\beta = (\beta_0, \beta_1, \beta_2) \in \big(0, 2(\alpha+1-\alpha')\big) \times \big(0, 2(\alpha+2-\alpha')\big) \times \big(0, 2(\alpha+3-\alpha')\big),$$

where we used the identity $\alpha = d/2 - 1 + \alpha'$, with $\alpha' \in (0,1)$. Consequently, the corollary is applicable in a reasonable manner if the parameter β satisfies the condition $\beta \in (0, 2\alpha] \times (0, 2(\alpha+1)] \times (0, 2(\alpha+2)]$.

The following two functions:

$$f_\alpha(x) := \frac{1-e^{-x}}{x^{1+\alpha}} \qquad \text{and} \qquad g_{\alpha,\tau}(x) = \frac{(1-e^{-x})^2}{2x^{1+\alpha}} e^{-\tau x}, \tag{67}$$

for $\alpha, \tau > 0$, play a crucial role in the forthcoming analysis, particularly in calculating the expected value of the realized volatility. When comparing these functions to their one-dimensional counterpart, as discussed in Bibinger and Trabs (2020, p. 18), we observe a dependency on the parameter α due to the coloured noise in the multi-dimensional model. In order to apply Corollary 4.2.2 on these functions, we need to verify them belonging to the class $\mathcal{Q}_\beta$ and determine the corresponding parameter β. The following lemma serves this purpose.

Lemma 4.2.3
It holds: $f_\alpha \in \mathcal{Q}_{\beta_1}$ and $g_{\alpha,\tau} \in \mathcal{Q}_{\beta_2}$, where

$$\beta_1 = \big(2\alpha, 2(1+\alpha), 2(2+\alpha)\big) \qquad \text{and} \qquad \beta_2 = \big(2\alpha, 2(1+\alpha), 2(1+\alpha)\big).$$

The proof of this lemma, being of technical nature, can be found in the last section of this chapter, see Proof of Lemma 4.2.3 on page 138.

The preceding lemma demonstrates that we can apply the Riemann approximation from Corollary 4.2.2 to the functions f_α and $g_{\alpha,\tau}$ from equation (67). Moreover, we observe that the error terms of the first and second derivatives of g vanish at a faster rate in the Riemann approximation compared to the function f. This is primarily due to the fact that the function $(1-e^{-x})$ converges to zero as $x \to 0$, whereas the function e^{-x} does not. We will make use of this fact in the subsequent proofs.

The following lemma concludes the technical part of this section by applying the discussed Riemann approximation on the functions f_α and $g_{\alpha,\tau}$.

Lemma 4.2.4
On Assumptions 4.1.1 and 4.1.2 it holds that

$$\Delta_n^{d/2} \sum_{\mathbf{k}\in\mathbb{N}^d} f_\alpha(\lambda_{\mathbf{k}}\Delta_n) = \frac{\Gamma(1-\alpha')}{2^d(\pi\eta)^{d/2}\alpha'\Gamma(d/2)} - \sum_{\substack{\|\gamma\|_1=1\\ \gamma\in\{0,1\}^d}}^{d-1} \int_{B_\gamma} f_\alpha(\pi^2\eta\,\|\mathbf{z}\|_2^2)\,\mathrm{d}\mathbf{z} + \mathcal{O}\big(\Delta_n^{1-\alpha'}\big),$$

where Γ denotes the Gamma function. Furthermore, it holds that

$$\Delta_n^{d/2} \sum_{\mathbf{k}\in\mathbb{N}^d} g_{\alpha,\tau}(\lambda_{\mathbf{k}}\Delta_n) = \frac{1}{2}\left(-\tau^{\alpha'} + 2(\tau+1)^{\alpha'} - (\tau+2)^{\alpha'}\right)\frac{\Gamma(1-\alpha')}{2^d(\pi\eta)^{d/2}\alpha'\Gamma(d/2)}$$
$$- \sum_{\substack{\|\gamma\|_1=1\\ \gamma\in\{0,1\}^d}}^{d-1} \int_{B_\gamma} g_{\alpha,\tau}(\pi^2\eta\,\|\mathbf{z}\|_2^2)\,\mathrm{d}\mathbf{z} + \mathcal{O}\big(\Delta_n^{1-\alpha'}\big).$$

In addition, we have

$$\frac{\Gamma(1-\alpha')}{2^d(\pi\eta)^{d/2}\alpha'\Gamma(d/2)} = \begin{cases} \frac{\Gamma(1-\alpha')}{(d-1)!2^d(\pi\eta)^{d/2}\alpha'} & \text{, if } d \text{ is even} \\ \frac{\Gamma(1-\alpha')}{2^{(d+1)/2}(d-2)!!\sqrt{\pi}(\pi\eta)^{d/2}\alpha'} & \text{, if } d \text{ is odd} \end{cases}.$$

The presence of the Gamma function appears natural due to the constraint $\alpha > 0$ for $d \geqslant 2$. For the proof of this lemma, refer Proof of Lemma 4.2.4 on page 140.

Now that we have addressed the technical details, we proceed with the analysis of the squared increments and, consequently, the realized volatility. As the upcoming proofs offer a deeper insight into the structure of SPDEs in d space dimensions, we will not relegate them to the last section. The following lemma initiates the analysis of the expected value of the temporal quadratic increments of X_t based on the spectral decomposition from display (62).

Lemma 4.2.5
On Assumptions 4.1.1 and 4.1.2, we have

$$\mathbb{E}[(\Delta_i X)^2(\mathbf{y})] = \sigma^2 2^d e^{-\|\kappa\bullet\mathbf{y}\|_1} \sum_{\mathbf{k}\in\mathbb{N}^d} \mathcal{D}_{i,\mathbf{k}} \sin^2(\pi k_1 y_1)\cdot\ldots\cdot\sin^2(\pi k_d y_d) + r_{n,i},$$

where $r_{n,i}$ is a sequence satisfying $\sum_{i=1}^n r_{n,i} = \mathcal{O}(\Delta_n^{\alpha'})$ and

$$\mathcal{D}_{i,\mathbf{k}} = \Delta_n^{d/2+\alpha'}\left(\frac{1-e^{-\lambda_\mathbf{k}\Delta_n}}{(\lambda_\mathbf{k}\Delta_n)^{1+\alpha}} - \frac{(1-e^{-\lambda_\mathbf{k}\Delta_n})^2}{2(\lambda_\mathbf{k}\Delta_n)^{1+\alpha}}e^{-2\lambda_\mathbf{k}(i-1)\Delta_n}\right), \tag{68}$$

with $\alpha' = 1+\alpha-d/2 \in (0,1)$.

Proof. First, $A_{i,\mathbf{k}}, B_{i,\mathbf{k}}$, and $C_{i,\mathbf{k}}$ are independent of each other, where $i = 1,\ldots,n$ and $\mathbf{k}\in\mathbb{N}^d$. Exploiting the fact that $(W^\mathbf{k})_{\mathbf{k}\in\mathbb{N}^d}$ are independent Brownian motions, the Itôintegrals $B_{i,\mathbf{k}}$ and $C_{i,\mathbf{k}}$ are also independent and centred. Thus, we have

$$\begin{aligned}\mathbb{E}[(\Delta_i X)^2(\mathbf{y})] &= \sum_{\mathbf{k}_1\in\mathbb{N}^d}\sum_{\mathbf{k}_2\in\mathbb{N}^d}\mathbb{E}[e_{\mathbf{k}_1}(\mathbf{y})e_{\mathbf{k}_2}(\mathbf{y})\Delta_i x_{\mathbf{k}_1}\Delta_i x_{\mathbf{k}_2}] = \sum_{\mathbf{k}_1\in\mathbb{N}^d}\sum_{\mathbf{k}_2\in\mathbb{N}^d} e_{\mathbf{k}_1}(\mathbf{y})e_{\mathbf{k}_2}(\mathbf{y})\mathbb{E}[\Delta_i x_{\mathbf{k}_1}\Delta_i x_{\mathbf{k}_2}]\\ &= \sum_{\mathbf{k}_1\in\mathbb{N}^d}\sum_{\mathbf{k}_2\in\mathbb{N}^d} e_{\mathbf{k}_1}(\mathbf{y})e_{\mathbf{k}_2}(\mathbf{y})\big(\mathbb{E}[A_{i,\mathbf{k}_1}A_{i,\mathbf{k}_2}] + \mathbb{E}[B_{i,\mathbf{k}_1}B_{i,\mathbf{k}_2}] + \mathbb{E}[C_{i,\mathbf{k}_1}C_{i,\mathbf{k}_2}]\big)\\ &= \sum_{\mathbf{k}\in\mathbb{N}^d} e_\mathbf{k}^2(\mathbf{y})\big(\mathbb{E}[B_{i,\mathbf{k}}^2] + \mathbb{E}[C_{i,\mathbf{k}}^2]\big) + r_{n,i},\end{aligned}$$

where $r_{n,i} := \sum_{\mathbf{k}_1,\mathbf{k}_2\in\mathbb{N}^d} e_{\mathbf{k}_1}(\mathbf{y})e_{\mathbf{k}_2}(\mathbf{y})\mathbb{E}[A_{i,\mathbf{k}_1}A_{i,\mathbf{k}_2}]$. Itô isometry yields the following:

$$\begin{aligned}\mathbb{E}[B_{i,\mathbf{k}}^2] &= \mathbb{E}\left[\left(\sigma\lambda_\mathbf{k}^{-\alpha/2}\int_0^{(i-1)\Delta_n} e^{-\lambda_\mathbf{k}\left((i-1)\Delta_n - s\right)}\left(e^{-\lambda_\mathbf{k}\Delta_n}-1\right)\mathrm{d}W_s^\mathbf{k}\right)^2\right]\\ &= \int_0^{(i-1)\Delta_n}\sigma^2\lambda_\mathbf{k}^{-\alpha}\mathbb{E}\Big[e^{-2\lambda_\mathbf{k}\left((i-1)\Delta_n-s\right)}\left(e^{-\lambda_\mathbf{k}\Delta_n}-1\right)^2\Big]\,\mathrm{d}s\end{aligned}$$

$$
\begin{aligned}
&= \sigma^2\lambda_{\mathbf{k}}^{-\alpha}\big(e^{-\lambda_{\mathbf{k}}\Delta_n}-1\big)^2\Big[\frac{1}{2\lambda_{\mathbf{k}}}e^{-2\lambda_{\mathbf{k}}\big((i-1)\Delta_n-s\big)}\Big]_0^{(i-1)\Delta_n}\\
&= \sigma^2\big(1-e^{-\lambda_{\mathbf{k}}\Delta_n}\big)^2\frac{1-e^{-2\lambda_{\mathbf{k}}(i-1)\Delta_n}}{2\lambda_{\mathbf{k}}^{1+\alpha}},
\end{aligned}
$$

$$
\mathbb{E}[C_{i,\mathbf{k}}^2] = \sigma^2\lambda_{\mathbf{k}}^{-\alpha}\int_{(i-1)\Delta_n}^{i\Delta_n} e^{-2\lambda_{\mathbf{k}}(i\Delta_n-s)}\,\mathrm{d}s = \sigma^2\lambda_{\mathbf{k}}^{-\alpha}\Big[\frac{1}{2\lambda_{\mathbf{k}}}e^{-2\lambda_{\mathbf{k}}(i\Delta_n-s)}\Big]_{(i-1)\Delta_n}^{i\Delta_n} = \sigma^2\frac{1-e^{-2\lambda_{\mathbf{k}}\Delta_n}}{2\lambda_{\mathbf{k}}^{1+\alpha}}.
$$

Additionally, we possess the following expression for the remainder $r_{n,i}$:

$$
\begin{aligned}
\mathbb{E}[A_{i,\mathbf{k}_1}A_{i,\mathbf{k}_2}] &= \big(e^{-\lambda_{\mathbf{k}_1}i\Delta_n}-e^{-\lambda_{\mathbf{k}_1}(i-1)\Delta_n}\big)\big(e^{-\lambda_{\mathbf{k}_2}i\Delta_n}-e^{-\lambda_{\mathbf{k}_2}(i-1)\Delta_n}\big)\mathbb{E}\big[\langle\xi,e_{\mathbf{k}_1}\rangle_\vartheta\langle\xi,e_{\mathbf{k}_2}\rangle_\vartheta\big]\\
&= \big(e^{-\lambda_{\mathbf{k}_1}(i-1)\Delta_n-\lambda_{\mathbf{k}_1}\Delta_n}-e^{-\lambda_{\mathbf{k}_1}(i-1)\Delta_n}\big)\big(e^{-\lambda_{\mathbf{k}_2}(i-1)\Delta_n-\lambda_{\mathbf{k}_2}\Delta_n}-e^{-\lambda_{\mathbf{k}_2}(i-1)\Delta_n}\big)\\
&\quad\times\mathbb{E}\big[\langle\xi,e_{\mathbf{k}_1}\rangle_\vartheta\langle\xi,e_{\mathbf{k}_2}\rangle_\vartheta\big]\\
&= \big(1-e^{-\lambda_{\mathbf{k}_1}\Delta_n}\big)\big(1-e^{-\lambda_{\mathbf{k}_2}\Delta_n}\big)e^{-(\lambda_{\mathbf{k}_1}+\lambda_{\mathbf{k}_2})(i-1)\Delta_n}\mathbb{E}\big[\langle\xi,e_{\mathbf{k}_1}\rangle_\vartheta\langle\xi,e_{\mathbf{k}_2}\rangle_\vartheta\big].
\end{aligned}
$$

Hence, we obtain the representation

$$
\begin{aligned}
\mathbb{E}[(\Delta_iX)^2(\mathbf{y})] &= \sigma^2\sum_{\mathbf{k}\in\mathbb{N}^d}e_{\mathbf{k}}^2(\mathbf{y})\bigg(\big(1-e^{-\lambda_{\mathbf{k}}\Delta_n}\big)^2\frac{1-e^{-2\lambda_{\mathbf{k}}(i-1)\Delta_n}}{2\lambda_{\mathbf{k}}^{1+\alpha}}+\frac{1-e^{-2\lambda_{\mathbf{k}}\Delta_n}}{2\lambda_{\mathbf{k}}^{1+\alpha}}\bigg)+r_{n,i}\\
&= \sigma^2 2^d e^{-\sum_{l=1}^d\kappa_l y_l}\sum_{\mathbf{k}\in\mathbb{N}^d}\bigg(\big(1-e^{-\lambda_{\mathbf{k}}\Delta_n}\big)^2\frac{1-e^{-2\lambda_{\mathbf{k}}(i-1)\Delta_n}}{2\lambda_{\mathbf{k}}^{1+\alpha}}+\frac{1-e^{-2\lambda_{\mathbf{k}}\Delta_n}}{2\lambda_{\mathbf{k}}^{1+\alpha}}\bigg)\\
&\quad\times\sin^2(\pi k_1y_1)\cdot\ldots\cdot\sin^2(\pi k_dy_d)+r_{n,i}.
\end{aligned}
$$

In addition, we define

$$
\begin{aligned}
\mathcal{D}_{i,\mathbf{k}} &:= \Delta_n^{1+\alpha}\bigg(\big(1-e^{-\lambda_{\mathbf{k}}\Delta_n}\big)^2\frac{1-e^{-2\lambda_{\mathbf{k}}(i-1)\Delta_n}}{2(\lambda_{\mathbf{k}}\Delta_n)^{1+\alpha}}+\frac{1-e^{-2\lambda_{\mathbf{k}}\Delta_n}}{2(\lambda_{\mathbf{k}}\Delta_n)^{1+\alpha}}\bigg)\\
&= \Delta_n^{1+\alpha}\bigg(\frac{1-e^{-2\lambda_{\mathbf{k}}\Delta_n}+(1-e^{-\lambda_{\mathbf{k}}\Delta_n})^2}{2(\lambda_{\mathbf{k}}\Delta_n)^{1+\alpha}}-\frac{(1-e^{-\lambda_{\mathbf{k}}\Delta_n})^2}{2(\lambda_{\mathbf{k}}\Delta_n)^{1+\alpha}}e^{-2\lambda_{\mathbf{k}}(i-1)\Delta_n}\bigg)\\
&= \Delta_n^{d/2+\alpha'}\bigg(\frac{1-e^{-\lambda_{\mathbf{k}}\Delta_n}}{(\lambda_{\mathbf{k}}\Delta_n)^{1+\alpha}}-\frac{(1-e^{-\lambda_{\mathbf{k}}\Delta_n})^2}{2(\lambda_{\mathbf{k}}\Delta_n)^{1+\alpha}}e^{-2\lambda_{\mathbf{k}}(i-1)\Delta_n}\bigg),
\end{aligned}
$$

where $\alpha'\in(0,1)$. Then, we have

$$
\mathbb{E}[(\Delta_iX)^2(\mathbf{y})] = \sigma^2 2^d e^{-\|\kappa\cdot y\|_1}\sum_{\mathbf{k}\in\mathbb{N}^d}\mathcal{D}_{i,\mathbf{k}}\sin^2(\pi k_1y_1)\cdot\ldots\cdot\sin^2(\pi k_dy_d)+r_{n,i}.
$$

The analysis of the remainder $r_{n,i}$ remains to be conducted. Here, we have

$$
r_{n,i} = \sum_{\mathbf{k}_1,\mathbf{k}_2\in\mathbb{N}^d}e_{\mathbf{k}_1}(\mathbf{y})e_{\mathbf{k}_2}(\mathbf{y})\big(1-e^{-\lambda_{\mathbf{k}_1}\Delta_n}\big)\big(1-e^{-\lambda_{\mathbf{k}_2}\Delta_n}\big)e^{-(\lambda_{\mathbf{k}_1}+\lambda_{\mathbf{k}_2})(i-1)\Delta_n}\mathbb{E}\big[\langle\xi,e_{\mathbf{k}_1}\rangle_\vartheta\langle\xi,e_{\mathbf{k}_2}\rangle_\vartheta\big].
$$

To demonstrate that $\sum_{i=1}^n r_{n,i}=\mathcal{O}(\Delta_n^{\alpha'})$, we use Assumption 4.1.2. Under the conditions $\mathbb{E}[\langle\xi,e_{\mathbf{k}}\rangle_\vartheta]=0$ and $\sup_{\mathbf{k}\in\mathbb{N}^d}\lambda_{\mathbf{k}}^{1+\alpha}\mathbb{E}[\langle\xi,e_{\mathbf{k}}\rangle_\vartheta^2]<\infty$, we can find a constant $C>0$ such that $\mathbb{E}[\langle\xi,e_{\mathbf{k}}\rangle_\vartheta^2]\leqslant C/\lambda_{\mathbf{k}}^{1+\alpha}$ for all

$\mathbf{k} \in \mathbb{N}^d$. Consequently, given that $\big(\langle \xi, e_{\mathbf{k}} \rangle_\vartheta\big)_{\mathbf{k}\in\mathbb{N}^d}$ are independent, we have

$$r_{n,i} = \sum_{\mathbf{k}\in\mathbb{N}^d} \big(1-e^{-\lambda_{\mathbf{k}}\Delta_n}\big)^2 e^{-2\lambda_{\mathbf{k}}(i-1)\Delta_n} e_{\mathbf{k}}^2(\mathbf{y}) \mathbb{E}[\langle \xi, e_{\mathbf{k}}\rangle_\vartheta^2] \leqslant C \sum_{\mathbf{k}\in\mathbb{N}^d} \frac{\big(1-e^{-\lambda_{\mathbf{k}}\Delta_n}\big)^2}{\lambda_{\mathbf{k}}^{1+\alpha}} e^{-2\lambda_{\mathbf{k}}(i-1)\Delta_n} e_{\mathbf{k}}^2(\mathbf{y}).$$

Assuming the second alternative in Assumption 4.1.2, where $\mathbb{E}\big[\|A_\vartheta^{(1+\alpha)/2}\xi\|_\vartheta^2\big] < \infty$, we can proceed with the following steps. Exploiting the self-adjointness of A_ϑ on H_ϑ and employing the Cauchy-Schwarz inequality, we obtain

$$\begin{aligned} r_{n,i} &= \mathbb{E}\Big[\Big(\sum_{\mathbf{k}\in\mathbb{N}^d} \big(1-e^{-\lambda_{\mathbf{k}}\Delta_n}\big) e^{-\lambda_{\mathbf{k}}(i-1)\Delta_n} \langle \xi, e_{\mathbf{k}}\rangle_\vartheta e_{\mathbf{k}}(\mathbf{y})\Big)^2\Big] \\ &= \mathbb{E}\Big[\Big(\sum_{\mathbf{k}\in\mathbb{N}^d} \frac{1-e^{-\lambda_{\mathbf{k}}\Delta_n}}{\lambda_{\mathbf{k}}^{(1+\alpha)/2}} e^{-\lambda_{\mathbf{k}}(i-1)\Delta_n} \langle A_\vartheta^{(1+\alpha)/2}\xi, e_{\mathbf{k}}\rangle_\vartheta e_{\mathbf{k}}(\mathbf{y})\Big)^2\Big] \\ &\leqslant \sum_{\mathbf{k}\in\mathbb{N}^d} \frac{\big(1-e^{-\lambda_{\mathbf{k}}\Delta_n}\big)^2}{\lambda_{\mathbf{k}}^{1+\alpha}} e^{-2\lambda_{\mathbf{k}}(i-1)\Delta_n} e_{\mathbf{k}}^2(\mathbf{y}) \mathbb{E}\Big[\sum_{\mathbf{k}\in\mathbb{N}}^{\infty} \langle A_\vartheta^{(1+\alpha)/2}\xi, e_{\mathbf{k}}\rangle_\vartheta^2\Big]. \end{aligned}$$

Applying Parseval's identity yields

$$r_{n,i} \leqslant \mathbb{E}\Big[\|A_\vartheta^{(1+\alpha)/2}\xi\|_\vartheta^2\Big] \sum_{\mathbf{k}\in\mathbb{N}^d} \frac{\big(1-e^{-\lambda_{\mathbf{k}}\Delta_n}\big)^2}{\lambda_{\mathbf{k}}^{1+\alpha}} e^{-2\lambda_{\mathbf{k}}(i-1)\Delta_n} e_{\mathbf{k}}^2(\mathbf{y}).$$

Since we can uniformly bound the eigenfunctions $(e_{\mathbf{k}})_{\mathbf{k}\in\mathbb{N}^d}$, it is sufficient to bound the following expression:

$$\begin{aligned} \sum_{i=1}^{n} r_{n,i} &\leqslant C \sum_{\mathbf{k}\in\mathbb{N}^d} \frac{\big(1-e^{-\lambda_{\mathbf{k}}\Delta_n}\big)^2}{\lambda_{\mathbf{k}}^{1+\alpha}} \sum_{i=1}^{n} e^{-2\lambda_{\mathbf{k}}(i-1)\Delta_n} \\ &= C \sum_{\mathbf{k}\in\mathbb{N}^d} \frac{\big(1-e^{-\lambda_{\mathbf{k}}\Delta_n}\big)^2}{\lambda_{\mathbf{k}}^{1+\alpha}\big(1-e^{-2\lambda_{\mathbf{k}}\Delta_n}\big)} \big(1-e^{-2\lambda_{\mathbf{k}}n\Delta_n}\big) \\ &\leqslant C \sum_{\mathbf{k}\in\mathbb{N}^d} \frac{\big(1-e^{-\lambda_{\mathbf{k}}\Delta_n}\big)^2}{\lambda_{\mathbf{k}}^{1+\alpha}\big(1-e^{-2\lambda_{\mathbf{k}}\Delta_n}\big)} \\ &\leqslant C \sum_{\mathbf{k}\in\mathbb{N}^d} \frac{1-e^{-\lambda_{\mathbf{k}}\Delta_n}}{\lambda_{\mathbf{k}}^{1+\alpha}} \\ &= C \Delta_n^{d/2+\alpha'} \sum_{\mathbf{k}\in\mathbb{N}^d} \frac{1-e^{-\lambda_{\mathbf{k}}\Delta_n}}{(\lambda_{\mathbf{k}}\Delta_n)^{1+\alpha}}, \end{aligned}$$

for both cases in Assumption 4.1.2, where we have used the partial sum formula of the geometric series and a suitable constant $C > 0$. Utilizing Lemma 4.2.4, we obtain

$$\Delta_n^{d/2} \sum_{\mathbf{k}\in\mathbb{N}^d} \frac{1-e^{-\lambda_{\mathbf{k}}\Delta_n}}{(\lambda_{\mathbf{k}}\Delta_n)^{1+\alpha}} = \Delta_n^{d/2} \sum_{\mathbf{k}\in\mathbb{N}^d} f_\alpha(\lambda_{\mathbf{k}}\Delta_n) = C + \mathcal{O}(1),$$

with a suitable constant $C>0$. Hence, we have

$$\sum_{i=1}^{n} r_{n,i} = \mathcal{O}(\Delta_n^{\alpha'}),$$

which completes the proof. □

The preceding proof reveals that the part of the decomposition from the temporal increments of X_t, which contains the initial condition $A_{i,\mathbf{k}}$, is negligible. The order here, once again, depends on the damping parameter α. By employing a trigonometric identity, we are now able to identify the expected value of quadratic temporal increments, which is recorded in the following proposition.

Proposition 4.2.6
On Assumptions 4.1.1 and 4.1.2, we have uniformly in $\mathbf{y}\in[\delta,1-\delta]^d$ that

$$\mathbb{E}[(\Delta_i X)^2(\mathbf{y})] = \Delta_n^{\alpha'}\sigma^2 e^{-\|\kappa\boldsymbol{\cdot}\mathbf{y}\|_1}\frac{\Gamma(1-\alpha')}{2^d(\pi\eta)^{d/2}\alpha'\Gamma(d/2)} + r_{n,i} + \mathcal{O}(\Delta_n),$$

where $\alpha'\in(0,1)$ and a sequence $r_{n,i}$ satisfying $\sup_{1\leqslant i\leqslant n}|r_{n,i}| = \mathcal{O}(\Delta_n^{\alpha'})$ and $\sum_{i=1}^n r_{n,i} = \mathcal{O}(\Delta_n^{\alpha'})$. Furthermore, rescaling yields that

$$\mathbb{E}\left[\frac{1}{n\Delta_n^{\alpha'}}\sum_{i=1}^{n}(\Delta_i X)^2(\mathbf{y})\right] = \sigma^2 e^{-\|\kappa\boldsymbol{\cdot}\mathbf{y}\|_1}\frac{\Gamma(1-\alpha')}{2^d(\pi\eta)^{d/2}\alpha'\Gamma(d/2)} + \mathcal{O}(\Delta_n^{1-\alpha'}).$$

Proof. We begin by recalling Lemma 4.2.5:

$$\mathbb{E}[(\Delta_i X)^2(\mathbf{y})] = \sigma^2 e^{-\|\kappa\boldsymbol{\cdot}\mathbf{y}\|_1}\mathcal{T}_i + r_{n,i},$$

where

$$\begin{aligned}
\mathcal{T}_i :=& 2^d \sum_{\mathbf{k}\in\mathbb{N}^d}\sin^2(\pi k_1 y_1)\cdot\ldots\cdot\sin^2(\pi k_d y_d)\mathcal{D}_{i,\mathbf{k}}\\
=& \, 2^d \sum_{\mathbf{k}\in\mathbb{N}^d}\frac{1-\cos(2\pi k_1 y_1)}{2}\cdot\ldots\cdot\frac{1-\cos(2\pi k_d y_d)}{2}\mathcal{D}_{i,\mathbf{k}}\\
=& \sum_{\mathbf{k}\in\mathbb{N}^d}\mathcal{D}_{i,\mathbf{k}} + \sum_{l=1}^{d}\sum_{1\leqslant j_1<\ldots<j_l\leqslant d}(-1)^l\sum_{\mathbf{k}\in\mathbb{N}^d}\mathcal{D}_{i,\mathbf{k}}\cos(2\pi k_{j_1}y_{j_1})\cdot\ldots\cdot\cos(2\pi k_{j_l}y_{j_l})\\
=& \sum_{\mathbf{k}\in\mathbb{N}^d}\mathcal{D}_{i,\mathbf{k}} + \sum_{l=1}^{d-1}\sum_{1\leqslant j_1<\ldots<j_l\leqslant d}(-1)^l\sum_{\mathbf{k}\in\mathbb{N}^d}\mathcal{D}_{i,\mathbf{k}}\cos(2\pi k_{j_1}y_{j_1})\cdot\ldots\cdot\cos(2\pi k_{j_l}y_{j_l})\\
&+(-1)^d\sum_{\mathbf{k}\in\mathbb{N}^d}\mathcal{D}_{i,\mathbf{k}}\cos(2\pi k_1 y_1)\cdots\cos(2\pi k_d y_d),
\end{aligned}$$

for $\mathcal{D}_{i,\mathbf{k}}$ defined in display (68). Furthermore, we define

$$h_{\alpha,\tau}(x) := \left(\frac{1-e^{-x}}{x^{1+\alpha}} - \frac{(1-e^{-x})^2}{2x^{1+\alpha}}e^{-x\tau}\right).$$

Note that $h_{\alpha,\tau}(x) = f_\alpha(x) - g_{\alpha,\tau}(x)$, where f_α and $g_{\alpha,\tau}$ are defined in equation (67). By Lemma 4.2.3 we have $h_{\alpha,\tau} \in \mathcal{Q}_\beta$, where $\beta = \big(2\alpha, 2(1+\alpha), 2(2+\alpha)\big)$. Hence, we obtain

$$\begin{aligned}\Delta_n^{-\alpha'} \sum_{\mathbf{k}\in\mathbb{N}^d} \mathcal{D}_{i,\mathbf{k}} &= \Delta_n^{d/2} \sum_{\mathbf{k}\in\mathbb{N}^d} h_{\alpha,2(i-1)}(\lambda_{\mathbf{k}}\Delta_n)\\ &= \frac{1}{2^d(\pi\eta)^{d/2}\Gamma(d/2)} \int_0^\infty x^{d/2-1} h_{\alpha,2(i-1)}(x)\,\mathrm{d}x - \sum_{\substack{\|\gamma\|_1=1\\ \gamma\in\{0,1\}^d}}^{d-1} \int_{B_\gamma} h_{\alpha,2(i-1)}(\pi^2\eta\,\|\mathbf{z}\|_2^2)\,\mathrm{d}\mathbf{z} + \mathcal{O}\big(\Delta_n^{1-\alpha'}\big),\end{aligned}$$

and

$$\begin{aligned}&\Delta_n^{d/2} \sum_{l=1}^{d-1} \sum_{1\leqslant j_1<\ldots<j_l\leqslant d} (-1)^l \sum_{\mathbf{k}\in\mathbb{N}^d} h_{\alpha,2(i-1)}(\lambda_{\mathbf{k}}\Delta_n)\cos(2\pi k_{j_1}y_{j_1})\cdot\ldots\cdot\cos(2\pi k_{j_l}y_{j_l})\\ &= \sum_{\substack{\|\gamma\|_1=1\\ \gamma\in\{0,1\}^d}}^{d-1} \int_{B_{\tilde{\gamma}_l}} h_{\alpha,2(i-1)}(\pi^2\eta\|\mathbf{z}\|_2^2)\,\mathrm{d}\mathbf{z} + \mathcal{O}(\Delta_n^{1-\alpha'}).\end{aligned}$$

Thus, by using Corollary 4.2.2 we have

$$\begin{aligned}&\sum_{\mathbf{k}\in\mathbb{N}^d} \mathcal{D}_{i,\mathbf{k}} + \sum_{l=1}^{d-1} \sum_{1\leqslant j_1<\ldots<j_l\leqslant d} (-1)^l \sum_{\mathbf{k}\in\mathbb{N}^d} \mathcal{D}_{i,\mathbf{k}} \cos(2\pi k_{j_1}y_{j_1})\cdot\ldots\cdot\cos(2\pi k_{j_l}y_{j_l})\\ &\quad + (-1)^d \sum_{\mathbf{k}\in\mathbb{N}^d} \mathcal{D}_{i,\mathbf{k}}\cos(2\pi k_1 y_1)\cdots\cos(2\pi k_d y_d)\\ &= \frac{\Delta_n^{\alpha'}}{2^d(\pi\eta)^{d/2}\Gamma(d/2)} \int_0^\infty x^{d/2-1} h_{\alpha,i-1}(x)\,\mathrm{d}x\\ &\quad + (-1)^d \sum_{\mathbf{k}\in\mathbb{N}^d} \mathcal{D}_{i,\mathbf{k}}\cos(2\pi k_1 y_1)\cdots\cos(2\pi k_d y_d) + \mathcal{O}(\Delta_n)\\ &= \frac{\Delta_n^{\alpha'}}{2^d(\pi\eta)^{d/2}\Gamma(d/2)} \int_0^\infty x^{d/2-1} h_{\alpha,2(i-1)}(x)\,\mathrm{d}x + \mathcal{O}(\Delta_n).\end{aligned}$$

Utilizing Lemma 4.2.4 yields

$$\begin{aligned}&\frac{1}{2^d(\pi\eta)^{d/2}\Gamma(d/2)}\left(\int_0^\infty f_{\alpha'}(x)\,\mathrm{d}x - \int_0^\infty g_{\alpha',2(i-1)}(x)\,\mathrm{d}x\right)\\ &= \frac{\Gamma(1-\alpha')}{2^d(\pi\eta)^{d/2}\alpha'\Gamma(d/2)}\left(1 + \frac{1}{2}\big(2(i-1)\big)^{\alpha'} - \big(1+2(i-1)\big)^{\alpha'} + \frac{1}{2}\big(2+2(i-1)\big)^{\alpha'}\right).\end{aligned}$$

Therefore, we have with Lemma 4.2.5 that

$$\begin{aligned}\mathbb{E}[(\Delta_i X)^2(\mathbf{y})] &= \sigma^2 e^{-\|\kappa\mathbf{y}\|_1} \frac{\Delta_n^{\alpha'}\Gamma(1-\alpha')}{2^d(\pi\eta)^{d/2}\alpha'\Gamma(d/2)}\left(1 + \frac{1}{2}\big(2(i-1)\big)^{\alpha'} - \big(1+2(i-1)\big)^{\alpha'} + \frac{1}{2}\big(2+2(i-1)\big)^{\alpha'}\right)\\ &\quad + r_{n,i} + \mathcal{O}(\Delta_n)\\ &= \Delta_n^{\alpha'} \frac{\sigma^2 e^{-\|\kappa\mathbf{y}\|_1}\Gamma(1-\alpha')}{2^d(\pi\eta)^{d/2}\alpha'\Gamma(d/2)} + \tilde{r}_{n,i} + \mathcal{O}(\Delta_n),\end{aligned}$$

where $\tilde{r}_{n,i}$ includes $r_{n,i}$ and the i dependent term from the last display. For this i-dependent term we analyse the following expression:

$$\frac{1}{2}\big(-\tau^{\alpha'}+2(\tau+1)^{\alpha'}-(\tau+2)^{\alpha'}\big)=\frac{\tau^{\alpha'}}{2}\big(-1+2(1+1/\tau)^{\alpha'}-(1+2/\tau)^{\alpha'}\big).$$

As our objective is to ascertain the order of the preceding expression, we define

$$t(x):=\frac{x^{\alpha'}}{2}\big(-1+2(1+1/x)^{\alpha'}-(1+2/x)^{\alpha'}\big),$$

and have with $y=1/x$ for the inner term that

$$q(y):=-1+2(1+y)^{\alpha'}-(1+2y)^{\alpha'}.$$

Using Taylor expansion at $y_0\to 0$ we obtain

$$q(y)=\lim_{y_0\to 0}q(y_0)+q'(y_0)(y-y_0)+\frac{1}{2}q''(y_0)(y-y_0)^2+\mathcal{O}(y^3)=2(1-\alpha')\alpha' y^2+\mathcal{O}(y^3),$$

where $q(y_0),q'(y_0)\overset{y_0\to 0}{\longrightarrow}0$, and therefore we conclude that

$$t(x)=x^{\alpha'}\left(\frac{(1-\alpha')\alpha}{x^2}+\mathcal{O}\big(x^{-3}\big)\right)=\frac{2(1-\alpha')\alpha}{x^{2-\alpha'}}+\mathcal{O}\big(x^{\alpha'-3}\big)=\mathcal{O}\big(x^{\alpha'-2}\big). \tag{69}$$

Since $2-\alpha'>1$, we have, with substituting $x=2(i-1)$, that

$$\sum_{i=1}^{n}t\big(2(i-1)\big)=\mathcal{O}\left(\sum_{i=0}^{\infty}\frac{1}{i^{2-\alpha'}}\right)=\mathcal{O}(1). \tag{70}$$

Hence, we have by Lemma 4.2.5 that $\sum_{i=1}^{n}\tilde{r}_{n,i}=\mathcal{O}(\Delta_n^{\alpha'})$, which completes the proof. □

Regarding the preceding proposition, we can express the expectation value of the rescaled realized volatility as follows:

$$\mathbb{E}\left[\frac{1}{n\Delta_n^{\alpha'}}\sum_{i=1}^{n}(\Delta_i X)^2(\mathbf{y})\right]=\sigma_0^2 e^{-\|\kappa\boldsymbol{\cdot}\mathbf{y}\|_1}\frac{\Gamma(1-\alpha')}{\alpha'}\cdot\frac{1}{2^d\pi^{d/2}\Gamma(d/2)}+\mathcal{O}(\Delta_n^{1-\alpha'}).$$

Comparing this result to SPDEs in one space dimension, as stated in Proposition 1.2.1, where

$$\mathbb{E}\left[\frac{\mathrm{RV}_n(y)}{\sqrt{n}}\right]=\sigma_0^2 e^{-y\kappa}\frac{1}{\sqrt{\pi}}+\mathcal{O}(\Delta_n),$$

reveals some crucial differences concerning the structure of the random fields. In higher space dimensions, we observe the appearance of the normalized volatility σ_0^2 and the curvature term $e^{-y\kappa}$, which are transposed from one space dimension. Furthermore, in higher dimensions, we obtain extra constants, among others, depending on α'. However, the most significant distinction when working in higher dimensions is that the parameter α', resulting from the coloured noise in this model, influences the leading term on one side and reduces the convergence speed of the error term on the other side. Note that the space dimension d of the model primarily influences the constants within the leading term of the expected value, whereas the order of the error term is exclusively determined by the parameter α'. This is because the spatial dimension d solely serves as a multiplicative constant within the error term. Consequently, constructing an estimator based on the method of moments will yield better results for small α'. Furthermore, setting $d = 2$ yields the same result as shown by Tonaki et al. (2023). Additionally, the latter proposition reveals that the remainders $r_{n,i}$ becomes negligible when summing over the squared increments. As these remainders include the initial condition, we observe that the impact of the initial condition becomes irrelevant when using the realized volatility statistic.

Assuming the parameters $\kappa \in \mathbb{R}^d$, $\eta > 0$, and $\alpha' \in (0,1)$ to be known, an estimator based on the first moment method of the rescaled realized volatility for the volatility parameter σ^2 is therefore given by

$$\hat{\sigma}^2_{\mathbf{y}} := \frac{2^d(\pi\eta)^{d/2}\alpha'\Gamma(d/2)}{n\Delta_n^{\alpha'}\Gamma(1-\alpha')}\sum_{i=1}^{n}(\Delta_i X)^2(\mathbf{y})e^{\|\kappa\cdot\mathbf{y}\|_1}. \tag{71}$$

Since the estimator $\hat{\sigma}^2_{\mathbf{y}}$ estimates the volatility parameter σ^2 based on a single spatial point, we also introduce the following estimator:

$$\hat{\sigma}^2 := \hat{\sigma}^2_{n,m} := \frac{1}{m}\sum_{j=1}^{m}\hat{\sigma}^2_{\mathbf{y}_j} = \frac{2^d(\pi\eta)^{d/2}\alpha'\Gamma(d/2)}{nm\Delta_n^{\alpha'}\Gamma(1-\alpha')}\sum_{j=1}^{m}\sum_{i=1}^{n}(\Delta_i X)^2(\mathbf{y}_j)e^{\|\kappa\cdot\mathbf{y}_j\|_1}, \tag{72}$$

for spatial points $\mathbf{y}_1,\dots,\mathbf{y}_m \in [\delta, 1-\delta]^d$. We will investigate the asymptotic properties of these estimators in the upcoming Chapter 5.

An important distinction between coloured and white noise is that coloured noise often leads to correlated discrete increments, whereas we often find uncorrelated increments in white noise models. As demonstrated in Bibinger and Trabs (2020), discrete temporal increments of a SPDE model in one spatial dimension are already negatively correlated, despite the use of white noise. This circumstance implies that we do not need to develop a fundamentally different theory, for instance, for proofs of central limit theorems.

Nevertheless, by varying the structure of the cylindrical Brownian motion, we can expect a change in the autocovariance structure, which now depends on α'. The following proposition investigates the autocovariance structure of temporal increments for our multi-dimensional SPDE model.

Proposition 4.2.7

On Assumptions 4.1.1 and 4.1.2, it holds for the covariance of the increments $(\Delta_i X)(\mathbf{y}), 1 \leqslant i \leqslant n$ uniformly in $\mathbf{y} \in [\delta, 1-\delta]^d$, for all $\delta \in (0, 1/2)$, that

$$\begin{aligned}&\mathbb{C}\mathrm{ov}(\Delta_i X(\mathbf{y}), \Delta_j X(\mathbf{y})) = \\ &\quad -\sigma^2 e^{-\|\kappa\cdot\mathbf{y}\|_1}\Delta_n^{\alpha'}\frac{\Gamma(1-\alpha')}{2^{d+1}(\pi\eta)^{d/2}\alpha'\Gamma(d/2)}\Big(2|i-j|^{\alpha'} - \big(|i-j|-1\big)^{\alpha'} - \big(|i-j|+1\big)^{\alpha'}\Big) + r_{i,j} + \mathcal{O}(\Delta_n),\end{aligned}$$

where $|i-j| \geqslant 1$ and the remainders $(r_{i,j})_{i,j=1,\dots,n}$ are negligible, i.e., $\sum_{i,j=1}^{n} r_{i,j} = \mathcal{O}(1)$.

Proof. We begin with the following expression:

$$\begin{aligned}\mathbb{C}\mathrm{ov}(\Delta_i X(\mathbf{y}),\Delta_j X(\mathbf{y})) &= \sum_{\mathbf{k}_1,\mathbf{k}_2\in\mathbb{N}^d}\mathbb{C}\mathrm{ov}(\Delta_i x_{\mathbf{k}_1},\Delta_j x_{\mathbf{k}_2})e_{\mathbf{k}_1}(\mathbf{y})e_{\mathbf{k}_2}(\mathbf{y})\\ &= \sum_{\mathbf{k}\in\mathbb{N}^d}\mathbb{C}\mathrm{ov}(A_{i,\mathbf{k}}+B_{i,\mathbf{k}}+C_{i,\mathbf{k}},A_{j,\mathbf{k}}+B_{j,\mathbf{k}}+C_{j,\mathbf{k}})e_{\mathbf{k}}^2(\mathbf{y}).\end{aligned}$$

Since $\big(\langle\xi,e_{\mathbf{k}}\rangle_\vartheta\big)_{\mathbf{k}\in\mathbb{N}^d}$ are independent by Assumption 4.1.2, we can use the independence of $A_{i,\mathbf{k}}$ and $B_{i,\mathbf{k}}$ and analyse the covariance of the remaining terms. Here, we have, by the Itôisometry and $i<j$:

$$\begin{aligned}\Sigma_{i,j}^{B,\mathbf{k}} &:= \mathbb{C}\mathrm{ov}(B_{i,\mathbf{k}},B_{j,\mathbf{k}})\\ &= \sigma^2\lambda_{\mathbf{k}}^{-\alpha}\big(e^{-\lambda_{\mathbf{k}}\Delta_n}-1\big)^2 e^{-\lambda_{\mathbf{k}}(i-1)\Delta_n}e^{-\lambda_{\mathbf{k}}(j-1)\Delta_n}\mathbb{C}\mathrm{ov}\Bigg(\int_0^{(i-1)\Delta_n} e^{\lambda_{\mathbf{k}}s}\,\mathrm{d}W_s^{\mathbf{k}},\int_0^{(j-1)\Delta_n} e^{\lambda_{\mathbf{k}}s}\,\mathrm{d}W_s^{\mathbf{k}}\Bigg)\\ &= \sigma^2\lambda_{\mathbf{k}}^{-\alpha}\big(1-e^{-\lambda_{\mathbf{k}}\Delta_n}\big)^2 e^{-\lambda_{\mathbf{k}}(i+j-2)\Delta_n}\mathbb{C}\mathrm{ov}\Bigg(\int_0^{(i-1)\Delta_n} e^{\lambda_{\mathbf{k}}s}\,\mathrm{d}W_s^{\mathbf{k}},\int_0^{(i-1)\Delta_n} e^{\lambda_{k}s}\,\mathrm{d}W_s^{\mathbf{k}}\Bigg)\\ &= \sigma^2\lambda_{\mathbf{k}}^{-\alpha}\big(1-e^{-\lambda_{\mathbf{k}}\Delta_n}\big)^2 e^{-\lambda_{\mathbf{k}}(i+j-2)\Delta_n}\int_0^{(i-1)\Delta_n} e^{2\lambda_{\mathbf{k}}s}\,\mathrm{d}s\\ &= \sigma^2\big(e^{-\lambda_{\mathbf{k}}\Delta_n(j-i)}-e^{-\lambda_{\mathbf{k}}(i+j-2)\Delta_n}\big)\frac{\big(1-e^{-\lambda_{\mathbf{k}}\Delta_n}\big)^2}{2\lambda_{\mathbf{k}}^{1+\alpha}}.\end{aligned}$$

Therefore, it follows for $1\leqslant i,j\leqslant n$ that

$$\Sigma_{i,j}^{B,\mathbf{k}} = \sigma^2\big(e^{-\lambda_{\mathbf{k}}\Delta_n|i-j|}-e^{-\lambda_{\mathbf{k}}(i+j-2)\Delta_n}\big)\frac{\big(1-e^{-\lambda_{\mathbf{k}}\Delta_n}\big)^2}{2\lambda_{\mathbf{k}}^{1+\alpha}}. \tag{73}$$

Next, we have $\Sigma_{i,j}^{C,\mathbf{k}}=\mathbb{C}\mathrm{ov}(C_{i,\mathbf{k}},C_{j,\mathbf{k}})=0$, for $i\neq j$, and we derive the following:

$$\begin{aligned}\Sigma_{i,j}^{C,\mathbf{k}} = \mathbb{1}_{\{j=i\}}\mathbb{C}\mathrm{ov}(C_{i,\mathbf{k}},C_{i,\mathbf{k}}) &= \mathbb{1}_{\{j=i\}}\sigma^2\lambda_{\mathbf{k}}^{-\alpha}e^{-2\lambda_{\mathbf{k}}i\Delta_n}\mathbb{E}\Bigg[\bigg(\int_{(i-1)\Delta_n}^{i\Delta_n} e^{\lambda_{\mathbf{k}}s}\,\mathrm{d}W_s^{\mathbf{k}}\bigg)^2\Bigg]\\ &= \mathbb{1}_{\{j=i\}}\sigma^2\frac{1-e^{-2\lambda_{\mathbf{k}}\Delta_n}}{2\lambda_{\mathbf{k}}^{1+\alpha}}.\end{aligned} \tag{74}$$

It remains to analyse the covariance of $B_{i,\mathbf{k}}$ and $C_{j,\mathbf{k}}$. Since $\Sigma_{i,j}^{BC,\mathbf{k}}:=\mathbb{C}\mathrm{ov}(B_{i,\mathbf{k}},C_{j,\mathbf{k}})=0$, for $i\leqslant j$, we analyse the following:

$$\begin{aligned}\Sigma_{i,j}^{BC,\mathbf{k}} &= \mathbb{1}_{\{i>j\}}\mathbb{C}\mathrm{ov}(B_{i,\mathbf{k}},C_{j,\mathbf{k}})\\ &= \mathbb{1}_{\{i>j\}}\mathbb{C}\mathrm{ov}\Bigg(\int_0^{(j-1)\Delta_n} H_{i,\mathbf{k}}^B(s)\,\mathrm{d}W_s^{\mathbf{k}}+\int_{(j-1)\Delta_n}^{j\Delta_n} H_{i,\mathbf{k}}^B(s)\,\mathrm{d}W_s^{\mathbf{k}}\\ &\quad+\int_{j\Delta_n}^{(i-1)\Delta_n} H_{i,\mathbf{k}}^B(s)\,\mathrm{d}W_s^{\mathbf{k}},\int_{(j-1)\Delta_n}^{j\Delta_n} H_{j,\mathbf{k}}^C(s)\,\mathrm{d}W_s^{\mathbf{k}}\Bigg)\end{aligned}$$

$$
\begin{aligned}
&= \mathbb{1}_{\{i>j\}}\sigma^2\lambda_{\mathbf{k}}^{-\alpha}\big(e^{-\lambda_{\mathbf{k}}\Delta_n}-1\big)e^{-\lambda_{\mathbf{k}}(i-1)\Delta_n}e^{-\lambda_{\mathbf{k}}j\Delta_n}\mathbb{C}\mathrm{ov}\left(\int_{(j-1)\Delta_n}^{j\Delta_n} e^{\lambda_{\mathbf{k}}s}\,\mathrm{d}W_s^{\mathbf{k}},\int_{(j-1)\Delta_n}^{j\Delta_n} e^{\lambda_{\mathbf{k}}s}\,\mathrm{d}W_s^{\mathbf{k}}\right)\\
&= \mathbb{1}_{\{i>j\}}\sigma^2\lambda_{\mathbf{k}}^{-\alpha}\big(e^{-\lambda_{\mathbf{k}}\Delta_n}-1\big)e^{-\lambda_{\mathbf{k}}(i+j-1)\Delta_n}\int_{(j-1)\Delta_n}^{j\Delta_n} e^{2\lambda_{\mathbf{k}}s}\,\mathrm{d}s\\
&= \mathbb{1}_{\{i>j\}}\sigma^2\lambda_{\mathbf{k}}^{-\alpha}\big(e^{-\lambda_{\mathbf{k}}\Delta_n}-1\big)e^{-\lambda_{\mathbf{k}}(i+j-1)\Delta_n}\frac{e^{2\lambda_{\mathbf{k}}j\Delta_n}-e^{2\lambda_{\mathbf{k}}(j-1)\Delta_n}}{2\lambda_{\mathbf{k}}}\\
&= \mathbb{1}_{\{i>j\}}\sigma^2 e^{-\lambda_{\mathbf{k}}\Delta_n(i-j)}\big(e^{\lambda_{\mathbf{k}}\Delta_n}-e^{-\lambda_{\mathbf{k}}\Delta_n}\big)\frac{e^{-\lambda_{\mathbf{k}}\Delta_n}-1}{2\lambda_{\mathbf{k}}^{1+\alpha}},
\end{aligned}
\tag{75}
$$

where $H_{i,\mathbf{k}}^B$ and $H_{j,\mathbf{k}}^C$ denote the corresponding integrands of $B_{i,\mathbf{k}}$ from equation (64) and $C_{i,\mathbf{k}}$ from equation (65), respectively. Similarly, we have

$$
\Sigma_{j,i}^{BC,\mathbf{k}} := \Sigma_{i,j}^{CB,\mathbf{k}} := \mathbb{C}\mathrm{ov}(C_{i,\mathbf{k}},B_{j,\mathbf{k}}) = \mathbb{1}_{\{i<j\}}\sigma^2 e^{-\lambda_{\mathbf{k}}\Delta_n(j-i)}\big(e^{\lambda_{\mathbf{k}}\Delta_n}-e^{-\lambda_{\mathbf{k}}\Delta_n}\big)\frac{e^{-\lambda_{\mathbf{k}}\Delta_n}-1}{2\lambda_{\mathbf{k}}^{1+\alpha}}.
$$

For $i<j$ we obtain

$$
\begin{aligned}
\mathbb{C}\mathrm{ov}(\Delta_i X(\mathbf{y}),\Delta_j X(\mathbf{y})) &= \sum_{\mathbf{k}\in\mathbb{N}^d}\mathbb{C}\mathrm{ov}(A_{i,\mathbf{k}}+B_{i,\mathbf{k}}+C_{i,\mathbf{k}},A_{j,\mathbf{k}}+B_{j,\mathbf{k}}+C_{j,\mathbf{k}})e_{\mathbf{k}}^2(\mathbf{y})\\
&= \sum_{\mathbf{k}\in\mathbb{N}^d}\big(\Sigma_{i,j}^{B,\mathbf{k}}+\Sigma_{i,j}^{CB,\mathbf{k}}\big)e_{\mathbf{k}}^2(\mathbf{y})+r_{i,j},
\end{aligned}
$$

where

$$
\begin{aligned}
r_{i,j} &:= \sum_{\mathbf{k}\in\mathbb{N}^d}\mathbb{C}\mathrm{ov}(A_{i,\mathbf{k}},A_{j,\mathbf{k}})e_{\mathbf{k}}^2(\mathbf{y})\\
&= \sum_{\mathbf{k}\in\mathbb{N}^d}\big(e^{-\lambda_{\mathbf{k}}i\Delta_n}-e^{-\lambda_{\mathbf{k}}(i-1)\Delta_n}\big)\big(e^{-\lambda_{\mathbf{k}}j\Delta_n}-e^{-\lambda_{\mathbf{k}}(j-1)\Delta_n}\big)\mathbb{V}\mathrm{ar}\big(\langle\xi,e_{\mathbf{k}}\rangle_\vartheta\big)e_{\mathbf{k}}^2(\mathbf{y})\\
&= \sum_{\mathbf{k}\in\mathbb{N}^d}\big(e^{-\lambda_{\mathbf{k}}\Delta_n(i+j)}-2e^{-\lambda_{\mathbf{k}}\Delta_n(i+j-1)}+e^{-\lambda_{\mathbf{k}}\Delta_n(i+j-2)}\big)\mathbb{V}\mathrm{ar}\big(\langle\xi,e_{\mathbf{k}}\rangle_\vartheta\big)e_{\mathbf{k}}^2(\mathbf{y})\\
&= \sum_{\mathbf{k}\in\mathbb{N}^d}e^{-\lambda_{\mathbf{k}}\Delta_n(i+j-2)}\big(e^{-2\lambda_{\mathbf{k}}\Delta_n}-2e^{-\lambda_{\mathbf{k}}\Delta_n}+1\big)\mathbb{V}\mathrm{ar}\big(\langle\xi,e_{\mathbf{k}}\rangle_\vartheta\big)e_{\mathbf{k}}^2(\mathbf{y})\\
&= \sum_{\mathbf{k}\in\mathbb{N}^d}e^{-\lambda_{\mathbf{k}}\Delta_n(i+j-2)}\big(e^{-\lambda_{\mathbf{k}}\Delta_n}-1\big)^2\mathbb{V}\mathrm{ar}\big(\langle\xi,e_{\mathbf{k}}\rangle_\vartheta\big)e_{\mathbf{k}}^2(\mathbf{y}).
\end{aligned}
$$

We use that the operator A_ϑ is self-adjoint on H_ϑ, such that $-\lambda_{\mathbf{k}}^{(1+\alpha)/2}\langle\xi,e_{\mathbf{k}}\rangle = \langle A_\vartheta^{(1+\alpha)/2}\xi,e_{\mathbf{k}}\rangle$ and derive the following inequality for the remainder:

$$
\begin{aligned}
r_{i,j} &\leqslant \sum_{\mathbf{k}\in\mathbb{N}^d}e^{-\lambda_{\mathbf{k}}\Delta_n(i+j-2)}\frac{\big(e^{-\lambda_{\mathbf{k}}\Delta_n}-1\big)^2}{\lambda_{\mathbf{k}}^{1+\alpha}}\mathbb{E}\Big[\big(\lambda_{\mathbf{k}}^{(1+\alpha)/2}\langle\xi,e_{\mathbf{k}}\rangle_\vartheta\big)^2\Big]e_{\mathbf{k}}^2(\mathbf{y})\\
&\leqslant C\sup_{\mathbf{k}\in\mathbb{N}}\mathbb{E}\Big[\langle A_\vartheta^{(1+\alpha)/2}\xi,e_{\mathbf{k}}\rangle_\vartheta^2\Big]\sum_{\mathbf{k}\in\mathbb{N}^d}e^{-\lambda_{\mathbf{k}}\Delta_n(i+j-2)}\frac{\big(1-e^{-\lambda_{\mathbf{k}}\Delta_n}\big)^2}{\lambda_{\mathbf{k}}^{1+\alpha}}.
\end{aligned}
\tag{76}
$$

Furthermore, for $i<j$ we have

$$\begin{aligned}
\mathbb{C}\text{ov}(\Delta_i X(\mathbf{y}),\Delta_j X(\mathbf{y})) &= \sum_{\mathbf{k}\in\mathbb{N}^d}\big(\Sigma_{i,j}^{B,\mathbf{k}}+\Sigma_{i,j}^{CB,\mathbf{k}}\big)e_{\mathbf{k}}^2(\mathbf{y})+r_{i,j}\\
&= \sigma^2\sum_{\mathbf{k}\in\mathbb{N}^d}\Bigg(\big(e^{-\lambda_{\mathbf{k}}\Delta_n(j-i)}-e^{-\lambda_{\mathbf{k}}(i+j-2)\Delta_n}\big)\frac{\big(1-e^{-\lambda_{\mathbf{k}}\Delta_n}\big)^2}{2\lambda_{\mathbf{k}}^{1+\alpha}}\\
&\quad+e^{-\lambda_{\mathbf{k}}\Delta_n(j-i)}\big(e^{\lambda_{\mathbf{k}}\Delta_n}-e^{-\lambda_{\mathbf{k}}\Delta_n}\big)\frac{e^{-\lambda_{\mathbf{k}}\Delta_n}-1}{2\lambda_{\mathbf{k}}^{1+\alpha}}\Bigg)e_{\mathbf{k}}^2(\mathbf{y})+r_{i,j}\\
&= \sigma^2\sum_{\mathbf{k}\in\mathbb{N}^d}e_{\mathbf{k}}^2(\mathbf{y})e^{-\lambda_{\mathbf{k}}\Delta_n(j-i)}\frac{\big(1-e^{-\lambda_{\mathbf{k}}\Delta_n}\big)^2+\big(e^{\lambda_{\mathbf{k}}\Delta_n}-e^{-\lambda_{\mathbf{k}}\Delta_n}\big)\big(e^{-\lambda_{\mathbf{k}}\Delta_n}-1\big)}{2\lambda_{\mathbf{k}}^{1+\alpha}}\\
&\quad-\sigma^2\sum_{\mathbf{k}\in\mathbb{N}^d}e_{\mathbf{k}}^2(\mathbf{y})e^{-\lambda_{\mathbf{k}}(i+j-2)\Delta_n}\frac{\big(1-e^{-\lambda_{\mathbf{k}}\Delta_n}\big)^2}{2\lambda_{\mathbf{k}}^{1+\alpha}}+r_{i,j}.
\end{aligned}$$

We define the second remainder as

$$s_{i,j}:=-\sigma^2\sum_{\mathbf{k}\in\mathbb{N}^d}e_{\mathbf{k}}^2(\mathbf{y})e^{-\lambda_{\mathbf{k}}(i+j-2)\Delta_n}\frac{\big(1-e^{-\lambda_{\mathbf{k}}\Delta_n}\big)^2}{2\lambda_{\mathbf{k}}^{1+\alpha}}.$$

Using the identity $\sin^2(x)=(1-\cos(2x))/2$, we arrive at

$$\begin{aligned}
&\mathbb{C}\text{ov}(\Delta_i X(\mathbf{y}),\Delta_j X(\mathbf{y}))\\
&= \sigma^2\sum_{\mathbf{k}\in\mathbb{N}^d}e_{\mathbf{k}}^2(\mathbf{y})e^{-\lambda_{\mathbf{k}}\Delta_n(j-i)}\frac{\big(1-e^{-\lambda_{\mathbf{k}}\Delta_n}\big)^2+1-e^{\lambda_{\mathbf{k}}\Delta_n}-e^{-2\lambda_{\mathbf{k}}\Delta_n}+e^{-\lambda_{\mathbf{k}}\Delta_n}}{2\lambda_{\mathbf{k}}^{1+\alpha}}+s_{i,j}+r_{i,j}\\
&= \sigma^2\sum_{\mathbf{k}\in\mathbb{N}^d}e_{\mathbf{k}}^2(\mathbf{y})e^{-\lambda_{\mathbf{k}}\Delta_n(j-i)}\frac{2-e^{-\lambda_{\mathbf{k}}\Delta_n}-e^{\lambda_{\mathbf{k}}\Delta_n}}{2\lambda_{\mathbf{k}}^{1+\alpha}}+s_{i,j}+r_{i,j}\\
&= \sigma^2\sum_{\mathbf{k}\in\mathbb{N}^d}e_{\mathbf{k}}^2(\mathbf{y})e^{-\lambda_{\mathbf{k}}\Delta_n(j-i-1)}\frac{2e^{-\lambda_{\mathbf{k}}\Delta_n}-e^{-2\lambda_{\mathbf{k}}\Delta_n}-1}{2\lambda_{\mathbf{k}}^{1+\alpha}}+s_{i,j}+r_{i,j}\\
&= -\sigma^2\Delta_n^{1+\alpha}\sum_{\mathbf{k}\in\mathbb{N}^d}e_{\mathbf{k}}^2(\mathbf{y})e^{-\lambda_{\mathbf{k}}\Delta_n(j-i-1)}\frac{e^{-2\lambda_{\mathbf{k}}\Delta_n}-2e^{-\lambda_{\mathbf{k}}\Delta_n}+1}{2(\lambda_{\mathbf{k}}\Delta_n)^{1+\alpha}}+s_{i,j}+r_{i,j}\\
&= -\sigma^2\Delta_n^{1+\alpha}\sum_{\mathbf{k}\in\mathbb{N}^d}^{\infty}e_{\mathbf{k}}^2(\mathbf{y})e^{-\lambda_{\mathbf{k}}\Delta_n(j-i-1)}\frac{\big(1-e^{-\lambda_{\mathbf{k}}\Delta_n}\big)^2}{2(\lambda_{\mathbf{k}}\Delta_n)^{1+\alpha}}+s_{i,j}+r_{i,j}\\
&= -\sigma^2e^{-\|\kappa\bullet\mathbf{y}\|_1}\Delta_n^{1+\alpha}\sum_{\mathbf{k}\in\mathbb{N}^d}e^{-\lambda_{\mathbf{k}}\Delta_n(j-i-1)}\frac{\big(1-e^{-\lambda_{\mathbf{k}}\Delta_n}\big)^2}{2(\lambda_{\mathbf{k}}\Delta_n)^{1+\alpha}}\prod_{l=1}^d\big(1-\cos(2\pi k_l y_l)\big)+s_{i,j}+r_{i,j}.
\end{aligned}$$

By defining the following expression:

$$\mathcal{S}_{i,\mathbf{k}}:=e^{-\lambda_{\mathbf{k}}\Delta_n(j-i-1)}\frac{\big(1-e^{-\lambda_{\mathbf{k}}\Delta_n}\big)^2}{2(\lambda_{\mathbf{k}}\Delta_n)^{1+\alpha}}=g_{\alpha,(j-i-1)}(\lambda_{\mathbf{k}}\Delta_n),$$

we obtain that

$$-\sigma^2e^{-\|\kappa\bullet\mathbf{y}\|_1}\Delta_n^{1+\alpha}\sum_{\mathbf{k}\in\mathbb{N}^d}e^{-\lambda_{\mathbf{k}}\Delta_n(j-i-1)}\frac{\big(1-e^{-\lambda_{\mathbf{k}}\Delta_n}\big)^2}{2(\lambda_{\mathbf{k}}\Delta_n)^{1+\alpha}}\prod_{l=1}^d\big(1-\cos(2\pi k_l y_l)\big)$$

$$= -\sigma^2 e^{-\|\kappa\cdot\mathbf{y}\|_1}\Delta_n^{1+\alpha}\sum_{\mathbf{k}\in\mathbb{N}^d}\Big(\mathcal{S}_{i,\mathbf{k}}+\mathcal{S}_{i,\mathbf{k}}\sum_{l=1}^{d}(-1)^l\sum_{1\leqslant j_1<\ldots<j_l\leqslant n}\cos(2\pi k_{j_1}y_{j_1})\cdots\cos(2\pi k_{j_l}y_{j_l})\Big).$$

Since we know by Lemma 4.2.3 that $g_{\alpha,\tau}\in\mathcal{Q}_\beta$, with $\beta=\big(2\alpha,2(1+\alpha),2(1+\alpha)\big)$, we have with Lemma 4.2.4 and Corollary 4.2.2 that

$$\Delta_n^{d/2}\sum_{\mathbf{k}\in\mathbb{N}^d}g_{\alpha,\tau}(\lambda_\mathbf{k}\Delta_n)=\frac{\Gamma(1-\alpha')}{2^d(\pi\eta)^{d/2}\alpha'\Gamma(d/2)}\Big(-\frac{1}{2}\tau^{\alpha'}+\big(1+\tau\big)^{\alpha'}-\frac{1}{2}\big(2+\tau\big)^{\alpha'}\Big)$$
$$-\sum_{\substack{\|\gamma\|_1=1\\ \gamma\in\{0,1\}^d}}^{d-1}\int_{B_\gamma}g_{\alpha,\tau}(\pi^2\eta\|\mathbf{z}\|_2^2)\,\mathrm{d}\mathbf{z}+\mathcal{O}(\Delta_n^{1-\alpha'}),$$

and

$$\Delta_n^{d/2}\sum_{l=1}^{d}(-1)^l\sum_{1\leqslant j_1<\ldots<j_l\leqslant n}\sum_{\mathbf{k}\in\mathbb{N}^d}g_{\alpha,\tau}(\lambda_\mathbf{k}\Delta_n)\cos(2\pi k_{j_1}y_{j_1})\cdots\cos(2\pi k_{j_l}y_{j_l})$$
$$=\sum_{\substack{\|\gamma\|_1=1\\ \gamma\in\{0,1\}^d}}^{d-1}\int_{B_\gamma}g_{\alpha,\tau}(\pi^2\eta\|\mathbf{z}\|_2^2)\,\mathrm{d}\mathbf{z}+\mathcal{O}(\Delta_n^{1-\alpha'}).$$

In line with Proposition 4.2.6 and with $\tau=(j-i-1)$, we have

$$\mathbb{C}\mathrm{ov}(\Delta_iX(\mathbf{y}),\Delta_jX(\mathbf{y}))$$
$$=-\sigma^2e^{-\|\kappa\cdot\mathbf{y}\|_1}\Delta_n^{\alpha'}\frac{\Gamma(1-\alpha')}{2^d(\pi\eta)^{d/2}\alpha'\Gamma(d/2)}\Big(-\frac{1}{2}\big(j-i-1\big)^{\alpha'}+\big(j-i\big)^{\alpha'}-\frac{1}{2}\big(j-i+1\big)^{\alpha'}\Big)$$
$$+s_{i,j}+r_{i,j}+\mathcal{O}(\Delta_n).$$

It remains to show that $\sum_{i,j=1}^n(s_{i,j}+r_{i,j})=\mathcal{O}(1)$. Therefore, we use display (76) and obtain

$$\sum_{i,j=1}^n(s_{i,j}+r_{i,j})\leqslant\sum_{i,j=1}^n\Bigg(\sigma^2C\sum_{\mathbf{k}\in\mathbb{N}^d}e^{-\lambda_\mathbf{k}(i+j-2)\Delta_n}\frac{\big(1-e^{-\lambda_\mathbf{k}\Delta_n}\big)^2}{2\lambda_\mathbf{k}^{1+\alpha}}$$
$$+C\sup_{\mathbf{k}\in\mathbb{N}}\mathbb{E}\Big[\langle A_\vartheta^{(1+\alpha)/2}\xi,e_\mathbf{k}\rangle_\vartheta^2\Big]\sum_{\mathbf{k}\in\mathbb{N}^d}e^{-\lambda_\mathbf{k}\Delta_n(i+j-2)}\frac{\big(1-e^{-\lambda_\mathbf{k}\Delta_n}\big)^2}{\lambda_\mathbf{k}^{1+\alpha}}\Bigg)$$
$$\leqslant C\Big(\sigma^2+\sup_{\mathbf{k}\in\mathbb{N}}\mathbb{E}\Big[\langle A_\vartheta^{(1+\alpha)/2}\xi,e_\mathbf{k}\rangle_\vartheta^2\Big]\Big)\sum_{i,j=1}^n\sum_{\mathbf{k}\in\mathbb{N}^d}e^{-\lambda_\mathbf{k}\Delta_n(i+j-2)}\frac{\big(1-e^{-\lambda_\mathbf{k}\Delta_n}\big)^2}{\lambda_\mathbf{k}^{1+\alpha}}$$
$$=C\Big(\sigma^2+\sup_{\mathbf{k}\in\mathbb{N}}\mathbb{E}\Big[\langle A_\vartheta^{(1+\alpha)/2}\xi,e_\mathbf{k}\rangle_\vartheta^2\Big]\Big)\sum_{\mathbf{k}\in\mathbb{N}^d}\frac{\big(1-e^{-\lambda_\mathbf{k}\Delta_n}\big)^2}{\lambda_\mathbf{k}^{1+\alpha}}\Big(\sum_{i=1}^ne^{-\lambda_\mathbf{k}(i-1)\Delta_n}\Big)^2$$
$$=C\Big(\sigma^2+\sup_{\mathbf{k}\in\mathbb{N}}\mathbb{E}\Big[\langle A_\vartheta^{(1+\alpha)/2}\xi,e_\mathbf{k}\rangle_\vartheta^2\Big]\Big)\sum_{\mathbf{k}\in\mathbb{N}^d}\frac{\big(1-e^{-\lambda_\mathbf{k}\Delta_n}\big)^2}{\lambda_\mathbf{k}^{1+\alpha}}\Big(\frac{1-e^{-\lambda_\mathbf{k}n\Delta_n}}{1-e^{-\lambda_\mathbf{k}\Delta_n}}\Big)^2$$
$$\leqslant C\Big(\sigma^2+\sup_{\mathbf{k}\in\mathbb{N}}\mathbb{E}\Big[\langle A_\vartheta^{(1+\alpha)/2}\xi,e_\mathbf{k}\rangle_\vartheta^2\Big]\Big)\sum_{\mathbf{k}\in\mathbb{N}^d}\frac{1}{\lambda_\mathbf{k}^{1+\alpha}}=\mathcal{O}(1).$$

Analogous computations for $i>j$ complete the proof. □

The previous proposition confirms that coloured noise alters the autocovariance structure. By comparing Proposition 4.2.7 with the one-dimensional case, we observe that in multiple space dimensions, the remainders vanish at a rate of Δ_n, instead of $\Delta_n^{3/2}$ as observed in one space dimension, cf. Bibinger and Trabs (2020, Prop. 3.2.). Furthermore, the autocovariance of the coloured noise process depends solely on the spatial coordinate $\mathbf{y} \in [\delta, 1-\delta]^d$ through the exponential term, which implies that the autocorrelation is independent of the spatial coordinate. Consequently, the autocorrelation structure is determined by the temporal distance or lag between increments rather than the specific temporal locations themselves. Assume that n is sufficiently large, the autocorrelation of temporal increments can be approximated as follows:

$$\rho_{(\Delta_i X),\alpha'}(|i-j|) \approx -|i-j|^{\alpha'} + \frac{1}{2}\big(|i-j|-1\big)^{\alpha'} + \frac{1}{2}\big(|i-j|+1\big)^{\alpha'},$$

for $i \neq j$. Using analogous steps as in equation (69), we obtain the following:

$$\rho_{(\Delta_i X),\alpha'}(|i-j|) = \mathcal{O}(|i-j|^{\alpha'-2}).$$

As $\alpha' \in (0,1)$, the autocorrelation diminishes as the lag $|i-j|$ between observations increases. Furthermore, from the first derivative, we observe that the autocorrelation is monotonically decreasing. Thus, the most substantial negative correlation is found at $|i-j| = 1$, where the autocorrelation takes the value $\rho_{(\Delta_i X),\alpha'}(1) = 2^{\alpha'-1} - 1$. In the one-dimensional case with a white noise structure, corresponding to $\alpha' = 1/2$, the authors Bibinger and Trabs (2020) demonstrated a similar behaviour. They found the most significant (negative) autocorrelation occurred at consecutive increments, with a value of $(\sqrt{2}-2)/2$. Hence, this behaviour extends to multiple spatial dimensions.

Figure 4.2 showcases the autocorrelation of the temporal increments for a two-dimensional SPDE model for a single sample dataset (left) and the sample mean computed across 20 generated datasets (right). Notably, we observe a strong negative correlation between consecutive increments, corresponding to a lag of one. Given that the pure damping parameter in the generated data is specified as $\alpha' = 1/2$, we obtain a negative correlation of $\rho_{(\Delta_i X),\alpha'}(1) = 2^{-1/2} - 1 \approx -3/10$.

Assuming that the initial condition is a stationary normal distribution with $\langle \xi, e_{\mathbf{k}} \rangle_\vartheta \sim \mathcal{N}(0, \sigma^2/(2\lambda_{\mathbf{k}}^{1+\alpha}))$, the random field X_t becomes a Gaussian random field. Proposition 4.2.7 provides valuable information regarding the identifiability of parameters using temporal increments statistics such as realized volatility. In a manner similar to one space dimension, it appears feasible to consistently estimate the normalized volatility $\sigma_0^2 = \sigma^2/\eta^{d/2}$ and the curvature parameter κ. In Chapter 6 we will demonstrate, that the restrictions on the identifiability are sharp, which means that we can consistently estimate these natural parameters.

However, when it comes to the damping parameter, which becomes significant in higher spatial dimensions, starting from two spatial dimensions in the model, Proposition 4.2.7 offers insights into its identification. We observe that the pure damping parameter α' appears in almost every component of the leading term of the autocovariance. Except for $\Delta_n^{\alpha'}$, it is not evident how to extract information on α' from the other terms. Therefore, the main approach for estimating α' is to exploit the term $\Delta_n^{\alpha'}$.

Moreover, by referring to Da Prato and Zabczyk (2014, Thm. 5.22), we can see that α' governs the regularity in time, which is reflected in the presence of $\Delta_n^{\alpha'}$. Additionally, employing the Kolmogorov-

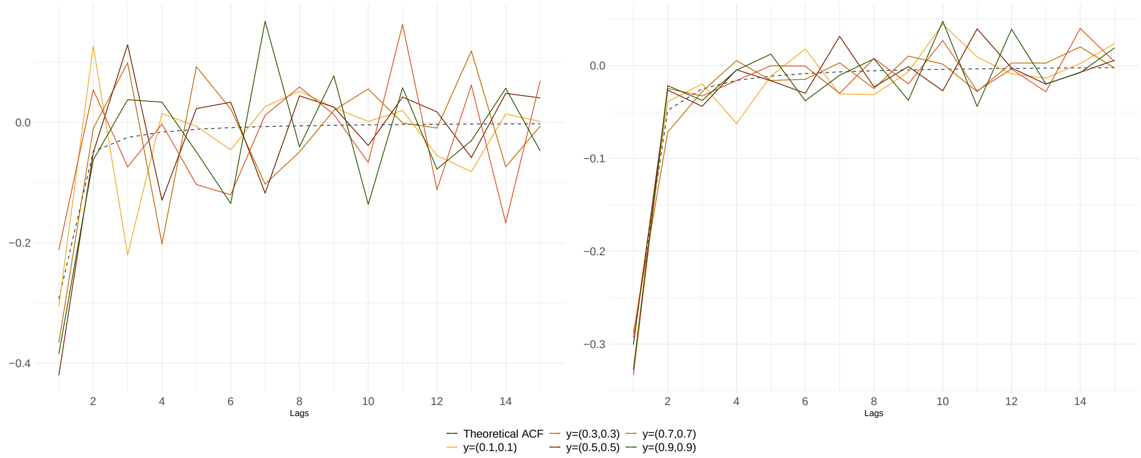

Figure 4.2.: We show the theoretical and empirical autocorrelation of the temporal increments for a two-dimensional SPDE model with the parameters $\theta_0 = 0$, $\nu = (6, 0)$, $\eta = \sigma = 1$, and $\alpha' = 1/2$. The samples were generated on an equidistant grid in both time and space, with $N = 10^4$ and $M = 10$. In both panels, the coloured lines depict the empirical autocorrelation, ranging from lags one to 15 in five spatial coordinates, while the theoretical autocorrelation is represented by the dotted grey line. The left panel illustrates the autocorrelation of a single sample data, whereas the right panel displays the sample mean of the autocorrelations derived from 20 sample datasets.

Chentsov theorem (Kolmogorov continuity theorem) and Proposition 4.2.6, we find that the temporal marginal processes of X_t are Hölder-continuous of almost order $\alpha'/2$. This property allows us to control the roughness of the temporal marginal processes and, consequently, identify the pure damping parameter α' and hence, α.

Rougher paths of the temporal marginal processes are generally advantageous for parameter estimation, implying that α' is likely to influence the asymptotic variance of the upcoming estimators. Hence, understanding and accounting for the value of α' becomes crucial in obtaining reliable parameter estimates.

4.3. Simulation methods for multi-dimensional SPDEs

In Section 2.5, we discussed the simulation of one-dimensional SPDEs and introduced the truncation method and the replacement method, as described by Bibinger and Trabs (2020) and Hildebrandt (2020), respectively. In this section, we aim to extend these methods to the context of multi-dimensional SPDEs given in equation (49).

We begin by discussing the truncation method for multi-dimensional SPDEs. Similar to the one-dimensional case, the truncation method allows us to simulate an SPDE model in arbitrary spatial coordinates, with any deterministic or normally distributed initial condition ξ. However, it comes with significant drawbacks, particularly in terms of runtime and the potential for introducing extra bias, depending on the cut-off frequency K. These issues become even more pronounced when dealing with multiple space dimensions. Despite these limitations, we explore this method due to its capability of selecting spatial coordinates freely. The concept of the truncation method involves truncating the Fourier series from equation (58) at a sufficiently large cut-off frequency $\mathbf{K} = (K_1, \ldots, K_d) \in \mathbb{N}^d$, simulating only the first K_l Fourier modes, respectively, where $l = 1, \ldots, d$. Hence, it becomes necessary to simulate the Fourier modes $x_{\mathbf{k}}$, for $\mathbf{k} \in \mathbb{N}$, with $\mathbf{k} \leqslant \mathbf{K}$. As mentioned in equation (59), we can represent the Fourier modes using the following representation:

$$x_{\mathbf{k}}(t) = e^{-\lambda_{\mathbf{k}} t} \langle \xi, e_{\mathbf{k}} \rangle_{\vartheta} + \sigma \lambda_{\mathbf{k}}^{-\alpha/2} \int_0^t e^{-\lambda_{\mathbf{k}}(t-s)} \, \mathrm{d}W_s^{\mathbf{k}},$$

where $\mathbf{k} \in \mathbb{N}$. Assuming that $\langle \xi, e_{\mathbf{k}} \rangle_{\vartheta} \sim \mathcal{N}(\mu_\xi, \sigma_\xi^2)$ is normally distributed, we have

$$\mathbb{E}[x_{\mathbf{k}}(t)] = e^{-\lambda_{\mathbf{k}} t} \mu_\xi,$$

where $t > 0$, and for $0 < t_1 \leqslant t_2$ we obtain

$$\mathbb{C}\mathrm{ov}\big(x_{\mathbf{k}}(t_1), x_{\mathbf{k}}(t_2)\big) = \mathbb{E}[x_{\mathbf{k}}(t_1) x_{\mathbf{k}}(t_2)] - e^{-\lambda_{\mathbf{k}}(t_1+t_2)} \mu_\xi^2,$$

where

$$\mathbb{E}[x_{\mathbf{k}}(t_1) x_{\mathbf{k}}(t_2)] = e^{-\lambda_{\mathbf{k}}(t_1+t_2)} \mathbb{E}[\langle \xi, e_{\mathbf{k}} \rangle_{\vartheta}^2] + \sigma^2 \lambda_{\mathbf{k}}^{-\alpha} \mathbb{E}\bigg[\int_0^{t_1} e^{-\lambda_{\mathbf{k}}(t_1-s)} \, \mathrm{d}W_s^{\mathbf{k}} \int_0^{t_2} e^{-\lambda_{\mathbf{k}}(t_2-s)} \, \mathrm{d}W_s^{\mathbf{k}} \bigg].$$

Hence, the covariance structure for the coordinate processes $x_{\mathbf{k}}$ are given by

$$\begin{aligned}
\mathbb{C}\mathrm{ov}\big(x_{\mathbf{k}}(t_1), x_{\mathbf{k}}(t_2)\big) &= e^{-\lambda_{\mathbf{k}}(t_1+t_2)} \sigma_\xi^2 + \sigma^2 \lambda_{\mathbf{k}}^{-\alpha} \mathbb{E}\bigg[\int_0^{t_1} e^{-\lambda_{\mathbf{k}}(t_1-s)} \, \mathrm{d}W_s^{\mathbf{k}} \int_0^{t_2} e^{-\lambda_{\mathbf{k}}(t_2-s)} \, \mathrm{d}W_s^{\mathbf{k}} \bigg] \\
&= e^{-\lambda_{\mathbf{k}}(t_1+t_2)} \sigma_\xi^2 + \sigma^2 \lambda_{\mathbf{k}}^{-\alpha} e^{-\lambda_{\mathbf{k}}(t_1+t_2)} \mathbb{E}\bigg[\Big(\int_0^{t_1} e^{\lambda_{\mathbf{k}} s} \, \mathrm{d}W_s^{\mathbf{k}} \Big)^2 \bigg] \\
&\quad + \sigma^2 \lambda_{\mathbf{k}}^{-\alpha} \mathbb{E}\bigg[\int_0^{t_1} e^{-\lambda_{\mathbf{k}}(t_1-s)} \, \mathrm{d}W_s^{\mathbf{k}} \int_{t_1}^{t_2} e^{-\lambda_{\mathbf{k}}(t_1-s)} \, \mathrm{d}W_s^{\mathbf{k}} \bigg] \\
&= e^{-\lambda_{\mathbf{k}}(t_1+t_2)} \sigma_\xi^2 + \sigma^2 \lambda_{\mathbf{k}}^{-\alpha} e^{-\lambda_{\mathbf{k}}(t_1+t_2)} \int_0^{t_1} e^{2\lambda_{\mathbf{k}} s} \, \mathrm{d}s \\
&= e^{-\lambda_{\mathbf{k}}(t_1+t_2)} \sigma_\xi^2 + \frac{\sigma^2}{2\lambda_{\mathbf{k}}^{1+\alpha}} \Big(e^{-\lambda_{\mathbf{k}}(t_2-t_1)} - e^{-\lambda_{\mathbf{k}}(t_2+t_1)} \Big),
\end{aligned}$$

where we have used the independence of ξ and $W_s^{\mathbf{k}}$, for all $\mathbf{k} \in \mathbb{N}^d$. For arbitrary $t_1, t_2 > 0$ we conclude

$$\mathbb{C}\mathrm{ov}\big(x_{\mathbf{k}}(t_1), x_{\mathbf{k}}(t_2)\big) = e^{-\lambda_{\mathbf{k}}(t_1+t_2)} \sigma_\xi^2 + \frac{\sigma^2}{2\lambda_{\mathbf{k}}^{1+\alpha}} \Big(e^{-\lambda_{\mathbf{k}}|t_2-t_1|} - e^{-\lambda_{\mathbf{k}}(t_2+t_1)} \Big), \tag{77}$$

and

$$\mathbb{V}\mathrm{ar}\big(x_{\mathbf{k}}(t)\big) = e^{-2\lambda_{\mathbf{k}} t} \sigma_\xi^2 + \frac{\sigma^2}{2\lambda_{\mathbf{k}}^{1+\alpha}} \Big(1 - e^{-2\lambda_{\mathbf{k}} t} \Big). \tag{78}$$

Thus, the coordinate processes are distributed as follows:

$$x_{\mathbf{k}}(t) \sim \mathcal{N}\bigg(e^{-\lambda_{\mathbf{k}} t} \mu_\xi,\ \frac{\sigma^2}{2\lambda_{\mathbf{k}}^{1+\alpha}} \Big(1 - e^{-2\lambda_{\mathbf{k}} t} \Big) + e^{-2\lambda_{\mathbf{k}} t} \sigma_\xi^2 \bigg),$$

where $\mathbf{k} \in \mathbb{N}^d$. Assuming that the initial condition is deterministic, we can deduce that $x_{\mathbf{k}}$ is normally distributed with a variance of $\sigma^2(1 - e^{-2\lambda_{\mathbf{k}} t})/(2\lambda_{\mathbf{k}}^{1+\alpha})$. Notably, the variance of the Fourier modes $x_{\mathbf{k}}$ is influenced by the damping parameter α. A larger value of α implies a stronger damping and quicker convergence of the variance towards zero, when $\mathbf{k} \to \infty$. On the other hand, a smaller value of α indicates a weaker damping and slower convergence of the variance. To simulate the Fourier modes $x_{\mathbf{k}}$, we have for $t = 0, \ldots, (n-1)\Delta_n$ that

$$\begin{aligned} x_{\mathbf{k}}(t+\Delta_n) - x_{\mathbf{k}}(t)e^{-\lambda_{\mathbf{k}}\Delta_n} &= \sigma\lambda_{\mathbf{k}}^{-\alpha/2}\left(\int\limits_0^{t+\Delta_n} e^{-\lambda_{\mathbf{k}}(t+\Delta_n-s)}\,\mathrm{d}W_s^{\mathbf{k}} - e^{-\lambda_{\mathbf{k}}\Delta_n}\int\limits_0^{t} e^{-\lambda_{\mathbf{k}}(t-s)}\,\mathrm{d}W_s^{\mathbf{k}}\right) \\ &= \sigma\lambda_{\mathbf{k}}^{-\alpha/2}\int_t^{t+\Delta_n} e^{-\lambda_{\mathbf{k}}(t+\Delta_n-s)}\,\mathrm{d}W_s^{\mathbf{k}}, \end{aligned}$$

implying the following recursive representation:

$$x_{\mathbf{k}}(t+\Delta_n) = x_k(t)e^{-\lambda_{\mathbf{k}}\Delta_n} + \sigma\sqrt{\frac{1-\exp[-2\lambda_{\mathbf{k}}\Delta_n]}{2\lambda_{\mathbf{k}}^{1+\alpha}}}\mathcal{N}_t,$$

with i.i.d. standard normals $\mathcal{N}_t$ and $x_{\mathbf{k}}(0) = \langle \xi, e_{\mathbf{k}}\rangle_\vartheta$, where ξ is either deterministic or normally distributed. Hence, the truncation method involves approximating the Fourier series of $X_t(\mathbf{y})$ using a cut-off frequency $\mathcal{K} := \{1, \ldots, K\}^d$, where $K \in \mathbb{N}$, i.e.:

$$X_t(\mathbf{y} \approx \sum_{\mathbf{k}\in\mathcal{K}} e_{\mathbf{k}}(y)x_{\mathbf{k}}(t).$$

Note that we set $\mathbf{K} = (K, \ldots, K)$, since we want to approximate the SPDE model equally in each spatial dimension. To simulate a solution of a one-dimensional SPDE, it is recommended to use a cut-off frequency of at least $K = 10^5$. This choice helps to prevent a significant bias in the generated data, cf. Section 2.5.1. When simulating multi-dimensional SPDEs, it is reasonable to choose a cut-off frequency of at least $K = 10^5$ as well, leading to $(K+1)^d$ loop iterations. For example, in a two-dimensional case ($d = 2$), Tonaki et al. (2023) performed simulations at 200×200 equi-spaced coordinates with a temporal resolution of $N = 10^3$. With a cut-off rate of $K = 10^5$, the simulation of one sample path took approximately 100 hours while using three personal computers. This highlights the computational challenge of simulating multi-dimensional SPDEs with a large cut-off frequency K, as it requires a substantial amount of computing power and time. However, the use of a sufficiently high cut-off frequency is crucial to ensure accurate and unbiased simulations of the SPDEs.

This challenge motivates the development of alternative approaches, one of which is the replacement method. The replacement method describes a simulation technique used to address the computational burden caused by large cut-off frequencies. Instead of using the Fourier series with a large cut-off K, the replacement method replaces the higher Fourier modes with some suitable approximations, cf. Section 2.5.1 for the one-dimensional replacement method. Assume $\xi = 0$ and equidistant spatial points $\mathbf{y} \in \{0, 1/M, \ldots, (M-1)/M, 1\}^d$ along each space dimension, i.e., $\mathbf{y_j} = \mathbf{j}/M = (j_1/M, \ldots, j_d/M)$ and

$\mathbf{j} \in \{0, \ldots, M\}^d =: \mathcal{J}$. We define the inner product by

$$\langle f, g \rangle_{\vartheta,M} := \frac{1}{M^d} \sum_{\mathbf{j} \in \mathcal{J}} f(\mathbf{y_j}) g(\mathbf{y_j}) e^{\|\kappa \cdot \mathbf{y_j}\|_1},$$

where $f, g : [0,1]^d \to \mathbb{R}$. It holds that $(e_\mathbf{k})_{\mathbf{k} \in \mathcal{M}}$ from equation (52) form an orthonormal system with respect to the inner product $\langle \cdot, \cdot \rangle_{\vartheta,M}$, where $\mathcal{M} := \{1, \ldots, M-1\}^d$. The clarity of this statement is enhanced when considering the one-dimensional case, as demonstrated by Hildebrandt (2020), where it is known that

$$\frac{2}{M} \sum_{k=0}^{M} \sin(\pi\beta k/M) \sin(\pi\gamma k/M) = \mathbb{1}_{\{\beta=\gamma\}},$$

for $\beta, \gamma \in \mathbb{N}$ and $1 \leqslant \beta, \gamma < M$. Therefore, with $\beta, \gamma \in \{1, \ldots, M-1\}^d$ we obtain

$$\begin{aligned} \langle e_\beta, e_\gamma \rangle_{\vartheta,M} &= \frac{2}{M} \sum_{j_1=0}^{M} \sin(\pi\beta_1 k_1/M) \sin(\pi\gamma_1 k_1/M) \cdots \frac{2}{M} \sum_{j_d=0}^{M} \sin(\pi\beta_1 k_1/M) \sin(\pi\gamma_d k_d/M) \\ &= \mathbb{1}_{\{\beta_1=\gamma_1\}} \cdots \mathbb{1}_{\{\beta_d=\gamma_d\}} = \mathbb{1}_{\{\beta=\gamma\}}. \end{aligned}$$

Hence, we can express a solution X_t as

$$X_t(\mathbf{y_j}) = \sum_{\mathbf{m} \in \mathcal{M}} U_\mathbf{m}(t) e_\mathbf{m}(\mathbf{y_j}), \qquad \text{with} \qquad U_\mathbf{m}(t) = \langle X_t, e_\mathbf{m} \rangle_{\vartheta,M}.$$

Note that $e_\mathbf{m}(\mathbf{y_j}) = 0$, if $\mathbf{m} = (m_1, \ldots, m_d)$ contains at least one entry m_l, which is either zero or M, i.e., $m_l \in \{0, M\}$, for a $l \in \{1, \ldots, d\}$. Using the Fourier representation, as given in equation (58), we have

$$U_\mathbf{m}(t) = \sum_{\mathbf{k} \in \mathbb{N}^d} x_\mathbf{k}(t) \langle e_\mathbf{k}, e_\mathbf{m} \rangle_{\vartheta,M}.$$

Let $\mathbf{k} \in \mathbb{N}^d$, then we can decompose the inner product by

$$\langle e_\mathbf{k}, e_\mathbf{m} \rangle_{\vartheta,M} = \frac{2^d}{M^d} \sum_{\mathbf{j} \in \mathcal{J}} \prod_{l=1}^{d} \sin(\pi k_l \mathbf{y}_{\mathbf{j}_l}) \sin(\pi m_l \mathbf{y}_{\mathbf{j}_l}) = \prod_{l=1}^{d} \langle \tilde{e}_{k_l}, \tilde{e}_{m_l} \rangle_{\vartheta,M,1},$$

where $\tilde{e}_k$ and $\langle \cdot, \cdot \rangle_{\vartheta,M,1}$ denote the respective one-dimensional orthonormal basis and inner product from equations (2) and (39), respectively. As established in Section 2.5.1, we already know that

$$|\langle \tilde{e}_k, \tilde{e}_m \rangle_{\vartheta,M,1}| = 1,$$

if $k = m + 2lM$ or $k = 2M - m + 2lM$, for $l \in \mathbb{N}_0$, $k \in \mathbb{N}$ and $m \in \{1, \ldots, M-1\}$. Therefore, the index set $\mathcal{I}_\mathbf{m}$ is given by the following d-fold Cartesian product:

$$\mathcal{I}_\mathbf{m} := \bigtimes_{l=1}^{d} \mathcal{I}_{m_l,1},$$

where $\mathcal{I}_{m,1}$ denotes the one-dimensional index set from equation (40). Since $x_\mathbf{l} \overset{d}{=} -x_\mathbf{l}$, for all $\mathbf{l} \in \mathbb{N}^d$, we have

$$U_{\mathbf{m}}(t) = \sum_{\mathbf{k}\in\mathbb{N}^d} x_{\mathbf{k}}(t)\langle e_{\mathbf{k}}, e_{\mathbf{m}}\rangle_{\vartheta,M} = \sum_{\mathbf{l}\in\mathcal{I}_{\mathbf{m}}} x_{\mathbf{l}}(t),$$

where $x_{\mathbf{l}}$ denote the coordinate processes from equation (59). As calculated in equation (77), the covariances of the coordinate processes, given by

$$\mathbb{C}\mathrm{ov}\big(x_{\mathbf{k}}(t_i), x_{\mathbf{k}}(t_j)\big) = \frac{\sigma^2}{2\lambda_{\mathbf{k}}^{1+\alpha}}\Big(e^{-\lambda_{\mathbf{k}}|i-j|\Delta_n} - e^{-\lambda_{\mathbf{k}}(i+j)\Delta_n}\Big) = \frac{\sigma^2}{2\lambda_{\mathbf{k}}^{1+\alpha}}e^{-\lambda_{\mathbf{k}}|i-j|\Delta_n}\Big(1 - e^{-2\lambda_{\mathbf{k}}\min(i,j)\Delta_n}\Big),$$

are vanishing for $\lambda_{\mathbf{k}} \propto \|\mathbf{k}\|_2^2$ being significantly larger than $1/\Delta_N$, due to the presence of the exponential term. Therefore, the coordinate processes $(x_{\mathbf{k}}(t_i))_{1\leqslant i\leqslant N}$ effectively behave like i.i.d. centred normal random variables, with variances

$$\mathbb{V}\mathrm{ar}\big(x_{\mathbf{k}}(t_i)\big) \approx \frac{\sigma^2}{2\lambda_{\mathbf{k}}^{1+\alpha}}.$$

for a sufficiently large $\mathbf{k}\in\mathbb{N}^d$. Analogously to Hildebrandt (2020), we choose a bound $L\in\mathbb{N}$ and replace all coordinate processes $(x_{\mathbf{k}})_{\mathbf{k}\in\mathbb{N}^d}$, with $\mathbf{k}\notin(0,LM)^d$, by a vector of independent normal random variables $(z_{\mathbf{l}})_{\mathbf{l}\in\mathbb{N}^d}$ with variance $\sigma^2/(2\lambda_{\mathbf{l}}^{1+\alpha})$, i.e.:

$$U_{\mathbf{m}}(t) = \sum_{\substack{\mathbf{l}\in\mathcal{I}_{\mathbf{m}}\\ \mathbf{l}\in(0,LM)^d}} x_{\mathbf{l}}(t) + \sum_{\substack{\mathbf{l}\in\mathcal{I}_{\mathbf{m}}\\ \mathbf{l}\notin(0,LM)^d}} z_{\mathbf{l}}(t).$$

Since the normal distribution is stable with respect to summation, we can replace the sum of the normal random variables with centred normal random variables $R_{\mathbf{m}}\sim\mathcal{N}(0,s_{\mathbf{m}}^2)$, where

$$s_{\mathbf{m}}^2 = \sum_{\substack{\mathbf{l}\in\mathcal{I}_{\mathbf{m}}\\ \mathbf{l}\notin(0,LM)^d}} \frac{\sigma^2}{2\lambda_{\mathbf{l}}^{1+\alpha}}.$$

By performing analogous computations as in display (56), it is evident that the series in $s_{\mathbf{m}}^2$ converges. In the one-dimensional case, as recalled in Section 2.5.1, a formula exists to precisely compute the one-dimensional replacement variance, as shown in equation (41). One key advantage of this formula is its closed form, which enables fast computation with minimal computational time.

However, in the multivariate case, the series becomes more intricate due to the additional exponent $1+\alpha$ and the squaring of the summation indices. This complexity renders direct application of related series, such as the multiple zeta function or its extension, the multiple Lerch zeta function, impractical, cf. Arakawa and Kaneko (1999) or Gun and Saha (2018).

Nonetheless, the outlook Section 7.2 proposes an approach for the exact computation of the variance $s_{\mathbf{m}}^2$. Consequently, we currently resort to numerical approximation methods to estimate the variance $s_{\mathbf{m}}^2$, given by

$$s_{\mathbf{m}}^2 \approx \sum_{\substack{\mathbf{l}\in\mathcal{I}_{\mathbf{m}}\\ \mathbf{l}\in(0,KM)^d\setminus(0,LM)^d}} \frac{\sigma^2}{2\lambda_{\mathbf{l}}^{1+\alpha}} =: \tilde{s}_{\mathbf{m}},$$

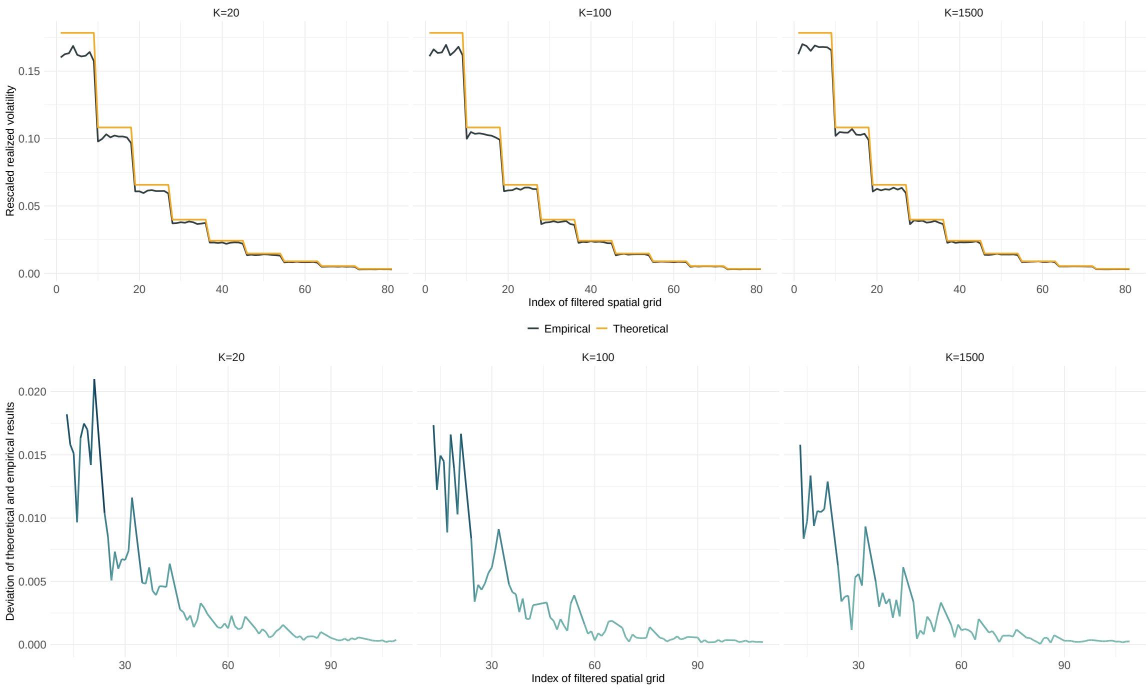

Figure 4.3.: The figure shows a comparison between the theoretical expected values of the rescaled realized volatilities, as described in Proposition 4.2.6, and their empirical counterparts (top row). The underlying two-dimensional SPDE model was simulated on an equidistant grid in both time and space, with $N = 10^4$ and $M = 10$. The SPDE model parameters are given by: $\vartheta_0 = 0$, $\nu = (5, 0)$, $\eta = 1$, $\sigma = 1$, and $\alpha' = 4/10$, while the replacement bound was fixed at $L = 10$. The results for different values of K are displayed in three columns: $K = 20$ (left), $K = 100$ (middle), and $K = 1500$ (right). The bottom row illustrates the deviation between the theoretical and empirical results.

where $K > L$, $K \in \mathbb{N}$ denotes the cut-off of the approximation. The multi-dimensional replacement method is then given by

$$X_{t_i}(\mathbf{y_j}) = \sum_{\mathbf{m}\in\mathcal{M}} U_{\mathbf{m}}(t_i) e_{\mathbf{m}}(\mathbf{y_j}), \quad \text{where} \quad U_{\mathbf{m}}(t_i) = \sum_{\substack{\mathbf{l}\in\mathcal{I}_{\mathbf{m}} \\ \mathbf{l}\in(0,LM)^d}} x_{\mathbf{l}}(t_i) + \tilde{R}_{\mathbf{m}}(i), \tag{79}$$

where $\tilde{R}_{\mathbf{m}}(i) \sim \mathcal{N}(0, \tilde{s}_{\mathbf{m}})$ denote the respective replacement random variables with the cut-off variance $\tilde{s}_{\mathbf{m}}$ and $t_{i+1} - t_i = 1/N$, where $i = 1, \ldots, N$. In this numerical approach, the quality of the simulation is highly dependent on the chosen variance cut-off K, as this cut-off effects the quality of the replacements $\tilde{R}_{\mathbf{m}}$. If K is selected to be too small, it will result in a negative bias in the simulations. Therefore, it is essential to carefully select an appropriate value for K to ensure accurate and reliable simulations without introducing any significant bias.

In Figure 4.3, we conducted a simulation of a two-dimensional SPDE model on a grid with $N = 10^4$ temporal points and $M = 10$ spatial points on each axis. The top row displays a comparison between the theoretical expected values, as per Proposition 4.2.6, and the sample mean of the rescaled realized volatility for three different cut-off values: $K = 20, 100, 1500$. The bottom row illustrates the corresponding deviations between the theoretical predictions and the empirical outcomes. Notably, for the case of $K = 20$, a significant negative bias is observed, while the bias diminishes as the cut-off frequency increases.

To address the deterministic nature of the variance $s_{\mathbf{m}}$ in equation (79), especially when calculating it for a large K, we have implemented an option within the function `simulateSPDEmodelMulti` from the R-package `SecondOrderSPDEMulti`[5]. This option allows for the utilization of the precomputed variance $s_{\mathbf{m}}$ using the function `variance_approx`. This enhancement dramatically reduces runtime, particularly in the context of Monte Carlo studies. Table 4.1 provides a summary of essential indicators, including the minimum and maximum deviations, as well as the mean deviation, for three distinct cut-off frequencies: $K = 20, 100, 1500$:

K	20	100	1500
min	0.0002015715	0.0001696648	0.0000496963
max	0.02098774	0.01734903	0.01579611
mean	0.003906285	0.003148307	0.002716894

Table 4.1.: We present three indicators for quantifying the disparity between the theoretical and empirical results in Figure 4.3. We illustrate the minimum deviation, maximum deviation, and mean deviation for each of the three cut-off frequencies: $K = 20, 100, 1500$.

While the bias decreases with larger values of K, there still exists a bias resulting from the approximation of $s_{\mathbf{m}}$.

4.4. Proofs

In this section, we present the proofs for the spectral framework as introduced in Section 4.1. Additionally, we include various other proofs from Section 4.2, one of which is the proof of the technical Riemann approximation from Lemma 4.2.1

Lemma 4.4.1

The eigenvalues and eigenvectors corresponding to the eigenvalue problem $A_\vartheta e_{\mathbf{k}} = -\lambda_{\mathbf{k}} e_{\mathbf{k}}$, for the operator A_ϑ from equation (50) are given by

$$e_{\mathbf{k}}(\mathbf{y}) = 2^{d/2} \prod_{l=1}^{d} \sin(\pi k_l y_l) e^{-\kappa_l y_l/2} \qquad \text{and} \qquad \lambda_{\mathbf{k}} := -\vartheta_0 + \sum_{l=1}^{d} \left(\frac{\nu_l^2}{4\eta} + \pi^2 k_l^2 \eta \right),$$

where $\mathbf{k} \in \mathbb{N}^d$. Additionally, the following properties hold:

(i) A_ϑ is self-adjoint on H_ϑ,

(ii) $e_{\mathbf{k}}$ form an orthonormal basis of the Hilbert space H_ϑ from display (51).

Proof. We establish the eigenfunction and eigenvalue property of $e_{\mathbf{k}}(\mathbf{y})$ and $\lambda_{\mathbf{k}}$, respectively, as defined in equations (52) and (53). We begin by evaluating the action of the operator A_ϑ on $e_{\mathbf{k}}(\mathbf{y})$:

$$A_\vartheta e_{\mathbf{k}}(\mathbf{y}) = \vartheta_0 e_{\mathbf{k}}(\mathbf{y}) + \sum_{l=1}^{d} \nu_l \frac{\partial}{\partial y_l} e_{\mathbf{k}}(y_1, \ldots, y_d) + \eta \sum_{l=1}^{d} \frac{\partial^2}{\partial y_l^2} e_{\mathbf{k}}(y_1, \ldots, y_d).$$

[5] see: https://github.com/pabolang/SecondOrderSPDEMulti.

Now, for a fixed $l_0 \in 1, \ldots, d$, we obtain the following:

$$
\begin{aligned}
\frac{\partial}{\partial y_{l_0}} e_{\mathbf{k}}(y_1, \ldots, y_d) &= 2^{d/2}\bigg(\cos(\pi k_{l_0} y_{l_0}) \pi k_{l_0} e^{-\kappa_{l_0} y_{l_0}/2} - \sin(\pi k_{l_0} y_{l_0}) e^{-\kappa_{l_0} y_{l_0}/2} \frac{\kappa_{l_0}}{2}\bigg) \prod_{\substack{l=1\\ l\neq l_0}}^{d} \sin(\pi k_l y_l) e^{-\kappa_l y_l/2} \\
&= e^{-\kappa_{l_0} y_{l_0}/2}\bigg(\cos(\pi k_{l_0} y_{l_0}) \pi k_{l_0} - \sin(\pi k_{l_0} y_{l_0}) \frac{\kappa_{l_0}}{2}\bigg) 2^{d/2} \prod_{\substack{l=1\\ l\neq l_0}}^{d} \sin(\pi k_l y_l) e^{-\kappa_l y_l/2},
\end{aligned}
$$

and

$$
\begin{aligned}
\frac{\partial^2}{\partial y_{l_0}^2} e_{\mathbf{k}}(y_1, \ldots, y_d) &= \bigg(\sin(\pi k_{l_0} y_{l_0}) \frac{\kappa_{l_0}^2}{4} - \cos(\pi k_{l_0} y_{l_0}) \frac{\kappa_{l_0} \pi k_{l_0}}{2} - \sin(\pi k_{l_0} y_{l_0}) \pi^2 k_{l_0}^2 - \cos(\pi k_{l_0} y_{l_0}) \frac{\kappa_{l_0} \pi k_{l_0}}{2} \bigg) \\
&\quad \times e^{-\kappa_{l_0} y_{l_0}/2} 2^{d/2} \prod_{\substack{l=1\\ l\neq l_0}}^{d} \sin(\pi k_l y_l) e^{-\kappa_l y_l/2} \\
&= e^{-\kappa_{l_0} y_{l_0}/2}\bigg(\sin(\pi k_{l_0} y_{l_0}) \Big(\frac{\kappa_{l_0}^2}{4} - \pi^2 k_{l_0}^2 \Big) - \cos(\pi k_{l_0} y_{l_0}) \kappa_{l_0} \pi k_{l_0} \bigg) \\
&\quad \times 2^{d/2} \prod_{\substack{l=1\\ l\neq l_0}}^{d} \sin(\pi k_l y_l) e^{-\kappa_l y_l/2}.
\end{aligned}
$$

Based on these calculations, we deduce the eigenvalue problem property as follows:

$$
\begin{aligned}
&\nu_{l_0} \frac{\partial}{\partial y_{l_0}} e_{\mathbf{k}}(y_1, \ldots, y_d) + \eta \frac{\partial^2}{\partial y_{l_0}^2} e_{\mathbf{k}}(y_1, \ldots, y_d) = e_{\mathbf{k}}(\mathbf{y}) \bigg(- \frac{\nu_{l_0}^2}{2\eta} + \frac{\nu_{l_0}^2 \eta}{4\eta^2} - \pi^2 k_{l_0}^2 \eta \bigg) \\
&\quad + e^{-\kappa_{l_0} y_{l_0}/2}\bigg(\cos(\pi k_{l_0} y_{l_0}) \pi k_{l_0} \nu_{l_0} - \cos(\pi k_{l_0} y_{l_0}) \pi k_{l_0} \kappa_{l_0} \eta \bigg) 2^{d/2} \prod_{\substack{l=1\\ l\neq l_0}}^{d} \sin(\pi k_l y_l) e^{-\kappa_l y_l/2} \\
&= e_{\mathbf{k}}(\mathbf{y}) \bigg(- \frac{\nu_{l_0}^2}{4\eta} - \pi^2 k_{l_0}^2 \eta \bigg),
\end{aligned}
$$

which implies the eigenvalue equation $A_\vartheta e_{\mathbf{k}}(\mathbf{y}) = -\lambda_{\mathbf{k}} e_{\mathbf{k}}(\mathbf{y})$. Thus, we have established the eigenvalue problem property as stated.

Furthermore, we will prove that the operator A_ϑ is self-adjoint on the Hilbert space H_ϑ. To demonstrate this, we consider arbitrary functions $f, g \in H_\vartheta$. Then, we have

$$
\begin{aligned}
\langle A_\vartheta f, g \rangle_\vartheta &= \int_0^1 \cdots \int_0^1 \bigg(\vartheta_0 f(y_1, \ldots, y_d) + \sum_{l=1}^{d} \nu_l \frac{\partial}{\partial y_l} f(y_1, \ldots, y_d) + \eta \sum_{l=1}^{d} \frac{\partial^2}{\partial y_l^2} f(y_1, \ldots, y_d) \bigg) \\
&\quad \times g(y_1, \ldots, y_d) \exp\bigg[\sum_{l=1}^{d} \kappa_l y_l \bigg] \mathrm{d}y_1 \cdots \mathrm{d}y_d \\
&= \langle f, \vartheta_0 g \rangle_\vartheta + \sum_{l=1}^{d} \nu_l \int_0^1 \cdots \int_0^1 \bigg(\frac{\partial}{\partial y_l} f(y_1, \ldots, y_d) \bigg) g(y_1, \ldots, y_d) \exp\bigg[\sum_{l=1}^{d} \kappa_l y_l \bigg] \mathrm{d}y_1 \cdots \mathrm{d}y_d \\
&\quad + \eta \sum_{l=1}^{d} \int_0^1 \cdots \int_0^1 \bigg(\frac{\partial^2}{\partial y_l^2} f(y_1, \ldots, y_d) \bigg) g(y_1, \ldots, y_d) \exp\bigg[\sum_{l=1}^{d} \kappa_l y_l \bigg] \mathrm{d}y_1 \cdots \mathrm{d}y_d.
\end{aligned}
$$

By employing Fubini's theorem for a fixed $l_0 \in 1, \ldots, d$, we obtain

$$\begin{aligned}
&\nu_{l_0} \int_0^1 \cdots \int_0^1 \Big(\frac{\partial}{\partial y_{l_0}} f(y_1, \ldots, y_d)\Big) g(y_1, \ldots, y_d) \exp\Big[\sum_{l=1}^d \kappa_l y_l\Big] \,\mathrm{d}y_1 \cdots \mathrm{d}y_d \\
&\quad + \eta \int_0^1 \cdots \int_0^1 \Big(\frac{\partial^2}{\partial y_{l_0}^2} f(y_1, \ldots, y_d)\Big) g(y_1, \ldots, y_d) \exp\Big[\sum_{l=1}^d \kappa_l y_l\Big] \,\mathrm{d}y_1 \cdots \mathrm{d}y_d \\
&= \nu_{l_0} \int_0^1 \cdots \int_0^1 \Big(\int_0^1 \Big(\frac{\partial}{\partial y_{l_0}} f(y_1, \ldots, y_d)\Big) g(y_1, \ldots, y_d) \exp\Big[\sum_{l=1}^d \kappa_l y_l\Big] \,\mathrm{d}y_{l_0} \Big) \,\mathrm{d}y_1 \cdots \mathrm{d}y_d \\
&\quad + \eta \int_0^1 \cdots \int_0^1 \Big(\int_0^1 \Big(\frac{\partial^2}{\partial y_{l_0}^2} f(y_1, \ldots, y_d)\Big) g(y_1, \ldots, y_d) \exp\Big[\sum_{l=1}^d \kappa_l y_l\Big] \,\mathrm{d}y_{l_0} \Big) \,\mathrm{d}y_1 \cdots \mathrm{d}y_d \\
&= \int_0^1 \cdots \int_0^1 \nu_{l_0} I_1 + \eta I_2 \,\mathrm{d}y_1 \cdots \mathrm{d}y_d.
\end{aligned}$$

Using integration by parts and taking the boundary property of f and g into account, we get that

$$\begin{aligned}
\nu_{l_0} I_1 &:= \nu_{l_0} \int_0^1 \Big(\frac{\partial}{\partial y_{l_0}} f(y_1, \ldots, y_d)\Big) g(y_1, \ldots, y_d) \exp\Big[\sum_{l=1}^d \kappa_l y_l\Big] \,\mathrm{d}y_{l_0} \\
&= \nu_{l_0} \Big[f(y_1, \ldots, y_d) g(y_1, \ldots, y_d) \exp\Big[\sum_{l=1}^d \kappa_l y_l\Big]\Big]_{y_{l_0}=0}^1 \\
&\quad - \nu_{l_0} \int_0^1 f(y_1, \ldots, y_d) \Big(\frac{\partial}{\partial y_{l_0}} g(y_1, \ldots, y_d)\Big) \exp\Big[\sum_{l=1}^d \kappa_l y_l\Big] \,\mathrm{d}y_{l_0} \\
&\quad - \nu_{l_0} \int_0^1 f(y_1, \ldots, y_d) g(y_1, \ldots, y_d) \exp\Big[\sum_{l=1}^d \kappa_l y_l\Big] \kappa_{l_0} \,\mathrm{d}y_{l_0} \\
&= -\nu_{l_0} \int_0^1 f(y_1, \ldots, y_d) \Big(\frac{\partial}{\partial y_{l_0}} g(y_1, \ldots, y_d)\Big) \exp\Big[\sum_{l=1}^d \kappa_l y_l\Big] \,\mathrm{d}y_{l_0} \\
&\quad - \frac{\nu_{l_0}^2}{\eta} \int_0^1 f(y_1, \ldots, y_d) g(y_1, \ldots, y_d) \exp\Big[\sum_{l=1}^d \kappa_l y_l\Big] \,\mathrm{d}y_{l_0},
\end{aligned}$$

and

$$\begin{aligned}
\eta I_2 &:= \eta \int_0^1 \Big(\frac{\partial^2}{\partial y_{l_0}^2} f(y_1, \ldots, y_d)\Big) g(y_1, \ldots, y_d) \exp\Big[\sum_{l=1}^d \kappa_l y_l\Big] \,\mathrm{d}y_{l_0} \\
&= \eta \Big[\Big(\frac{\partial}{\partial y_{l_0}} f(y_1, \ldots, y_d)\Big) g(y_1, \ldots, y_d) \exp\Big[\sum_{l=1}^d \kappa_l y_l\Big]\Big]_{y_{l_0}=0}^1 \\
&\quad - \eta \int_0^1 \Big(\frac{\partial}{\partial y_{l_0}} f(y_1, \ldots, y_d)\Big) \Big(\frac{\partial}{\partial y_{l_0}} g(y_1, \ldots, y_d)\Big) \exp\Big[\sum_{l=1}^d \kappa_l y_l\Big] \,\mathrm{d}y_{l_0} \\
&\quad - \eta \int_0^1 \Big(\frac{\partial}{\partial y_{l_0}} f(y_1, \ldots, y_d)\Big) g(y_1, \ldots, y_d) \exp\Big[\sum_{l=1}^d \kappa_l y_l\Big] \kappa_{l_0} \,\mathrm{d}y_{l_0} \\
&= -\eta \Big[f(y_1, \ldots, y_d) \Big(\frac{\partial}{\partial y_{l_0}} g(y_1, \ldots, y_d)\Big) \exp\Big[\sum_{l=1}^d \kappa_l y_l\Big]\Big]_{y_{l_0}=0}^1
\end{aligned}$$

$$
\begin{aligned}
&+\eta\int_0^1 f(y_1,\dots,y_d)\Big(\frac{\partial^2}{\partial y_{l_0}^2}g(y_1,\dots,y_d)\Big)\exp\Big[\sum_{l=1}^d \kappa_l y_l\Big]\,\mathrm{d}y_{l_0}\\
&+\eta\int_0^1 f(y_1,\dots,y_d)\Big(\frac{\partial}{\partial y_{l_0}}g(y_1,\dots,y_d)\Big)\exp\Big[\sum_{l=1}^d \kappa_l y_l\Big]\kappa_{l_0}\,\mathrm{d}y_{l_0}\\
&-\eta\Big[f(y_1,\dots,y_d)g(y_1,\dots,y_d)\exp\Big[\sum_{l=1}^d \kappa_l y_l\Big]\kappa_{l_0}\Big]_{y_{l_0}=0}^1\\
&+\eta\int_0^1 f(y_1,\dots,y_d)\Big(\frac{\partial}{\partial y_{l_0}}g(y_1,\dots,y_d)\Big)\exp\Big[\sum_{l=1}^d \kappa_l y_l\Big]\kappa_{l_0}\,\mathrm{d}y_{l_0}\\
&+\eta\int_0^1 f(y_1,\dots,y_d)g(y_1,\dots,y_d)\exp\Big[\sum_{l=1}^d \kappa_l y_l\Big]\kappa_{l_0}^2\,\mathrm{d}y_{l_0}\\
=\;&\eta\int_0^1 f(y_1,\dots,y_d)\Big(\frac{\partial^2}{\partial y_{l_0}^2}g(y_1,\dots,y_d)\Big)\exp\Big[\sum_{l=1}^d \kappa_l y_l\Big]\,\mathrm{d}y_{l_0}\\
&+2\nu_{l_0}\int_0^1 f(y_1,\dots,y_d)\Big(\frac{\partial}{\partial y_{l_0}}g(y_1,\dots,y_d)\Big)\exp\Big[\sum_{l=1}^d \kappa_l y_l\Big]\,\mathrm{d}y_{l_0}\\
&+\frac{\nu_{l_0}^2}{\eta}\int_0^1 f(y_1,\dots,y_d)g(y_1,\dots,y_d)\exp\Big[\sum_{l=1}^d \kappa_l y_l\Big]\,\mathrm{d}y_{l_0}.
\end{aligned}
$$

Combining both terms yields

$$
\begin{aligned}
\nu_{l_0}I_1+\eta I_2 &= \eta\int_0^1 f(y_1,\dots,y_d)\Big(\frac{\partial^2}{\partial y_{l_0}^2}g(y_1,\dots,y_d)\Big)\exp\Big[\sum_{l=1}^d \kappa_l y_l\Big]\,\mathrm{d}y_{l_0}\\
&\quad+\nu_{l_0}\int_0^1 f(y_1,\dots,y_d)\Big(\frac{\partial}{\partial y_{l_0}}g(y_1,\dots,y_d)\Big)\exp\Big[\sum_{l=1}^d \kappa_l y_l\Big]\,\mathrm{d}y_{l_0},
\end{aligned}
$$

and therefore, we conclude

$$
\begin{aligned}
\langle A_\vartheta f,g\rangle_\vartheta &= \langle f,\vartheta_0 g\rangle_\vartheta+\sum_{l=1}^d \nu_l\int_0^1\cdots\int_0^1\Big(\frac{\partial}{\partial y_l}f(y_1,\dots,y_d)\Big)g(y_1,\dots,y_d)\exp\Big[\sum_{l=1}^d \kappa_l y_l\Big]\,\mathrm{d}y_1\cdots\mathrm{d}y_d\\
&\quad+\eta\sum_{l=1}^d\int_0^1\cdots\int_0^1\Big(\frac{\partial^2}{\partial y_l^2}f(y_1,\dots,y_d)\Big)g(y_1,\dots,y_d)\exp\Big[\sum_{l=1}^d \kappa_l y_l\Big]\,\mathrm{d}y_1\cdots\mathrm{d}y_d\\
&= \langle f,\vartheta_0 g\rangle_\vartheta+\sum_{l=1}^d \nu_l\int_0^1\cdots\int_0^1 f(y_1,\dots,y_d)\Big(\frac{\partial}{\partial y_l}g(y_1,\dots,y_d)\Big)\exp\Big[\sum_{l=1}^d \kappa_l y_l\Big]\,\mathrm{d}y_1\cdots\mathrm{d}y_d\\
&\quad+\eta\sum_{l=1}^d\int_0^1\cdots\int_0^1 f(y_1,\dots,y_d)\Big(\frac{\partial^2}{\partial y_l^2}g(y_1,\dots,y_d)\Big)\exp\Big[\sum_{l=1}^d \kappa_l y_l\Big]\,\mathrm{d}y_1\cdots\mathrm{d}y_d\\
&= \langle f,A_\vartheta g\rangle_\vartheta,
\end{aligned}
$$

which demonstrates that A_ϑ is self-adjoint on H_ϑ.

According to the spectral theorem, the eigenfunctions $(e_{\mathbf{k}})_{\mathbf{k}\in\mathbb{N}^d}$ form an orthonormal system in the Hilbert space H_ϑ. Moreover, the orthonormal property of $(e_{\mathbf{k}})_{\mathbf{k}\in\mathbb{N}^d}$ can be verified through standard calculations. Let $\mathbf{k},\mathbf{j}\in\mathbb{N}^d$, with $\mathbf{k}\neq\mathbf{j}$. Then, there exists at least one index $l_0\in 1,\dots,d$, with $k_{l_0}\neq j_{l_0}$, and we have

$$\begin{aligned}\langle e_{\mathbf{k}}, e_{\mathbf{j}}\rangle_\vartheta &= 2^d \int_0^1 \cdots \int_0^1 \prod_{l=1}^d \sin(\pi k_l y_l)\sin(\pi j_l y_l)\,\mathrm{d}y_1\cdots\mathrm{d}y_d \\ &= 2^d \int_0^1 \cdots \int_0^1 \left(\int_0^1 \sin(\pi k_{l_0} y_{l_0})\sin(\pi j_{l_0} y_{l_0})\,\mathrm{d}y_{l_0}\right) \prod_{\substack{l=1\\ l\neq l_0}}^d \sin(\pi k_l y_l)\sin(\pi j_l y_l)\,\mathrm{d}y_1\cdots\mathrm{d}y_d.\end{aligned}$$

By evaluating the inner integral, we find

$$\int_0^1 \sin(\pi k_{l_0} y_{l_0})\sin(\pi j_{l_0} y_{l_0})\,\mathrm{d}y_{l_0} = \left[\frac{\sin\left(\pi(k_{l_0}-j_{l_0})y_{l_0}\right)}{2\pi(k_{l_0}-j_{l_0})} - \frac{\sin\left(\pi(k_{l_0}+j_{l_0})y_{l_0}\right)}{2\pi(k_{l_0}+j_{l_0})}\right]_{y_{l_0}=0}^1 = 0,$$

which implies that the eigenfunctions are orthogonal. Now, consider $\mathbf{k},\mathbf{j}\in\mathbb{N}^d$, with $\mathbf{k}=\mathbf{j}$. Then, we have

$$\begin{aligned}\langle e_{\mathbf{k}}, e_{\mathbf{k}}\rangle_\vartheta &= 2^d \int_0^1 \cdots \int_0^1 \prod_{l=1}^d \sin(\pi k_l y_l)^2\,\mathrm{d}y_1\cdots\mathrm{d}y_d \\ &= 2^d \left(\int_0^1 \sin(\pi k y)^2\,\mathrm{d}y\right)^d \\ &= 2^d \left(\left[\frac{y}{2} - \frac{\sin(2\pi k y)}{4\pi k}\right]_0^1\right)^d = 1,\end{aligned}$$

demonstrating the orthonormality of $(e_{\mathbf{k}})_{\mathbf{k}\in\mathbb{N}^d}$. □

Next, we proceed with the proof of Lemma 4.2.1.

Proof of Lemma 4.2.1. We begin this proof by making the substitution $z_l^2 = k_l^2\Delta_n$, such that

$$\lambda_{\mathbf{k}}\Delta_n = \pi^2\eta\sum_{l=1}^d z_l^2 + \Delta_n\left(\sum_{l=1}^d\left(\frac{\nu_l^2}{4\eta}\right) - \vartheta_0\right).$$

Subsequently, employing the Taylor expansion with the Lagrange remainder, we obtain that

$$f(\lambda_{\mathbf{k}}\Delta_n) = f\left(\pi^2\eta\sum_{l=1}^d z_l^2\right) + f'(\xi)\left(\lambda_{\mathbf{k}}\Delta_n - \pi^2\eta\sum_{l=1}^d z_l^2\right) = f\left(\pi^2\eta\sum_{l=1}^d z_l^2\right) + \mathcal{O}(\Delta_n).$$

For $\mathbf{k}\in\mathbb{N}^d$ we define

$$a_{\mathbf{k}} := (a_{k_1},\ldots,a_{k_d})\in\mathbb{R}_+^d, \qquad \text{with} \qquad a_{k_l} := \sqrt{\Delta}_n(k_l+1/2),$$

where $l=1,\ldots,d$ and

$$[a_{\mathbf{k-1}}, a_{\mathbf{k}}] := [a_{k_1-1}, a_{k_1}]\times\ldots\times[a_{k_d-1}, a_{k_d}]\subset(0,\infty)^d.$$

Note that $|a_{k_l} - a_{k_l-1}| = \sqrt{\Delta_n}$, for $l = 1, \ldots, d$ and $a_0 := \Delta_n^{1/2}/2$. Moreover, by defining $\tilde{f}(x) := f(\pi^2\eta x^2)$, we observe that

$$\begin{aligned}
&\Delta_n^{d/2} \sum_{\mathbf{k}\in\mathbb{N}^d} f(\lambda_{\mathbf{k}}\Delta_n) - \int_{[\sqrt{\Delta_n}/2,\infty)^d} f(\pi^2\eta \|\mathbf{z}\|_2^2)\,\mathrm{d}\mathbf{z} \\
&= \Delta_n^{d/2} \sum_{k_1=1}^{\infty} \cdots \sum_{k_d=1}^{\infty} f(\lambda_{(k_1,\ldots,k_d)}\Delta_n) - \int_{\frac{\sqrt{\Delta_n}}{2}}^{\infty} \cdots \int_{\frac{\sqrt{\Delta_n}}{2}}^{\infty} f\Big(\pi^2\eta \sum_{l=1}^{d} z_l^2\Big)\,\mathrm{d}z_1 \cdots \mathrm{d}z_d \\
&= \Delta_n^{d/2} \sum_{k_1=1}^{\infty} \cdots \sum_{k_d=1}^{\infty} f\Big(\pi^2\eta\Delta_n \sum_{l=1}^{d} k_l^2\Big) \\
&\quad - \sum_{k_1=1}^{\infty} \cdots \sum_{k_d=1}^{\infty} \int_{a_{k_1-1}}^{a_{k_1}} \cdots \int_{a_{k_d-1}}^{a_{k_d}} f\Big(\pi^2\eta \sum_{l=1}^{d} z_l^2\Big)\,\mathrm{d}z_1 \cdots \mathrm{d}z_d + \mathcal{O}(\Delta_n) \\
&= \sum_{k_1=1}^{\infty} \cdots \sum_{k_d=1}^{\infty} \int_{a_{k_1-1}}^{a_{k_1}} \cdots \int_{a_{k_d-1}}^{a_{k_d}} \Big(f\Big(\pi^2\eta\Delta_n \sum_{l=1}^{d} k_l^2\Big) - f\Big(\pi^2\eta \sum_{l=1}^{d} z_l^2\Big)\Big)\,\mathrm{d}z_1 \cdots \mathrm{d}z_d + \mathcal{O}(\Delta_n) \\
&= \sum_{\mathbf{k}\in\mathbb{N}^d} \int_{a_{\mathbf{k-1}}}^{a_{\mathbf{k}}} f(\pi^2\eta\Delta_n \|\mathbf{k}\|_2^2) - f(\pi^2\eta \|\mathbf{z}\|_2^2)\,\mathrm{d}\mathbf{z} + \mathcal{O}(\Delta_n) \\
&= \sum_{\mathbf{k}\in\mathbb{N}^d} \int_{a_{\mathbf{k-1}}}^{a_{\mathbf{k}}} \tilde{f}(\sqrt{\Delta_n}\, \|\mathbf{k}\|_2) - \tilde{f}(\|\mathbf{z}\|_2)\,\mathrm{d}\mathbf{z} + \mathcal{O}(\Delta_n) =: T_1 + \mathcal{O}(\Delta_n),
\end{aligned}$$

where $\|\cdot\|_2$ denotes the euclidean norm. Define the function $g : \mathbb{R}_+^d \to \mathbb{R}_+$, with $g(\mathbf{x}) = \tilde{f}(\|\mathbf{x}\|_2)$. Since $\sqrt{\Delta_n}\mathbf{k}$ represents the mid-point of the interval $[a_{\mathbf{k-1}}, a_{\mathbf{k}}]$, for a $\mathbf{k} \in \mathbb{N}^d$, we can apply a Taylor expansion at the point $\sqrt{\Delta_n}\mathbf{k}$, leading to the following expression:

$$\begin{aligned}
g(\sqrt{\Delta_n}\mathbf{k}) - g(\mathbf{z}) &= g(\sqrt{\Delta_n}\mathbf{k}) - \Big(g(\sqrt{\Delta_n}\mathbf{k}) + \nabla g(\sqrt{\Delta_n}\mathbf{k})^\top (\mathbf{z} - \sqrt{\Delta_n}\mathbf{k}) \\
&\quad + \frac{1}{2}(\mathbf{z} - \sqrt{\Delta_n}\mathbf{k})^\top H_g(\xi_{\mathbf{k}})(\mathbf{z} - \sqrt{\Delta_n}\mathbf{k})\Big),
\end{aligned} \tag{80}$$

where ∇g denotes the gradient of g, H_g the Hessian-matrix of g and $\xi_{\mathbf{k}} \in [a_{\mathbf{k-1}}, a_{\mathbf{k}}]$. We introduce the shorthand notation $g_l'(\mathbf{z}) := \partial g(\mathbf{z})/(\partial z_l)$, which represents the partial derivative of $g(\mathbf{z})$ with respect to z_l. Then, we have

$$\begin{aligned}
\int_{a_{\mathbf{k-1}}}^{a_{\mathbf{k}}} \nabla g(\sqrt{\Delta_n}\mathbf{k})^\top (\mathbf{z} - \sqrt{\Delta_n}\mathbf{k})\,\mathrm{d}\mathbf{z} &= \sum_{l=1}^{d} g_l'(\sqrt{\Delta_n}\mathbf{k}) \int_{a_{k_1-1}}^{a_{k_1}} \cdots \int_{a_{k_d-1}}^{a_{k_d}} (z_l - \sqrt{\Delta_n}k_l)\,\mathrm{d}z_1 \cdots \mathrm{d}z_d \\
&= \Delta_n^{(d-1)/2} \sum_{l=1}^{d} g_l'(\sqrt{\Delta_n}\mathbf{k}) \int_{a_{k_l-1}}^{a_{k_l}} (z_l - \sqrt{\Delta_n}k_l)\,\mathrm{d}z_l \\
&= \Delta_n^{(d-1)/2} \sum_{l=1}^{d} g_l'(\sqrt{\Delta_n}\mathbf{k}) \Big[\frac{z_l^2}{2} - \sqrt{\Delta_n}k_l z_l\Big]_{a_{k_l}-1}^{a_{k_l}} \\
&= \Delta_n^{(d-1)/2} \sum_{l=1}^{d} g_l'(\sqrt{\Delta_n}\mathbf{k}) \Big(\frac{a_{k_l}^2 - a_{k_l-1}^2}{2} - \sqrt{\Delta_n}k_l(a_{k_l} - a_{k_l-1})\Big) \\
&= 0.
\end{aligned}$$

Since every term in the Taylor expansion from equation (80) vanishes, we proceed by redefining the term

T_1 as follows:

$$T_1 := -\sum_{\mathbf{k}\in\mathbb{N}^d} \int_{a_{\mathbf{k-1}}}^{a_{\mathbf{k}}} \frac{1}{2}(\mathbf{z}-\sqrt{\Delta}_n\mathbf{k})^\top H_g(\xi_{\mathbf{k}})(\mathbf{z}-\sqrt{\Delta}_n\mathbf{k})\,\mathrm{d}\mathbf{z}. \tag{81}$$

Additionally, the order of the term T_1 is analysed in display (86). For now, our primary focus is on the main term, which we can express by

$$\begin{aligned}
\Delta_n^{d/2}\sum_{k_1=1}^\infty\cdots\sum_{k_d=1}^\infty f(\lambda_{(k_1,\dots,k_d)}\Delta_n) &= \int_{\frac{\sqrt{\Delta}_n}{2}}^\infty\cdots\int_{\frac{\sqrt{\Delta}_n}{2}}^\infty f\Big(\pi^2\eta\sum_{l=1}^d z_l^2\Big)\,\mathrm{d}z_1\cdots\mathrm{d}z_d + \mathcal{O}(T_1\vee\Delta_n)\\
&= \int_0^\infty\cdots\int_0^\infty f\Big(\pi^2\eta\sum_{l=1}^d z_l^2\Big)\,\mathrm{d}z_1\cdots\mathrm{d}z_d\\
&\quad - \int_{\mathbb{R}_+^d\setminus[\sqrt{\Delta}_n/2,\infty)^d} f(\pi^2\eta\,\|\mathbf{z}\|_2^2)\,\mathrm{d}\mathbf{z} + \mathcal{O}(T_1\vee\Delta_n).
\end{aligned}$$

Before delving into the analysis of the compensation integral, defined by

$$\mathcal{I} := \int_{\mathbb{R}_+^d\setminus[\sqrt{\Delta}_n/2,\infty)^d} f(\pi^2\eta\,\|\mathbf{z}\|_2^2)\,\mathrm{d}\mathbf{z},$$

and the error term T_1, we first examine a transformation of the main integral. To facilitate our analysis, we employ d-dimensional spherical coordinates, which are reviewed in equation (57). Here, we have

$$\begin{aligned}
&\int_0^\infty\cdots\int_0^\infty f\Big(\eta\pi^2\sum_{l=1}^d z_l^2\Big)\,\mathrm{d}z_1\cdots\mathrm{d}z_d = \int_0^\infty\int_0^{\pi/2}\cdots\int_0^{\pi/2} f(\pi^2\eta r^2)|J_d|\,\mathrm{d}\varphi_{d-1}\cdots\mathrm{d}\varphi_1\,\mathrm{d}r\\
&= \int_0^\infty r^{d-1}f(\pi^2\eta r^2)\,\mathrm{d}r\int_0^{\pi/2}\sin^{d-2}(\varphi_1)\,\mathrm{d}\varphi_1\cdots\int_0^{\pi/2}\sin(\varphi_{d-2})\,\mathrm{d}\varphi_{d-2}\int_0^{\pi/2}\mathrm{d}\varphi_{d-1}.
\end{aligned}$$

For $l\in\mathbb{N}$ it holds that

$$\int_0^{\pi/2}\sin^l(x)\,\mathrm{d}x = \frac{\sqrt{\pi}\Gamma\big(\frac{1+l}{2}\big)}{2\Gamma\big(1+\frac{l}{2}\big)},$$

where $\Gamma(x)$ denotes the Gamma function. Furthermore, we obtain that

$$\prod_{l=1}^{d-2}\int_0^{\pi/2}\sin^l(x)\,\mathrm{d}x = \frac{\pi^{d/2-1}}{2^{d-2}\Gamma(d/2)}.$$

Thus, we have

$$\int_0^\infty\cdots\int_0^\infty f\Big(\eta\pi^2\sum_{l=1}^d z_l^2\Big)\,\mathrm{d}z_1\cdots\mathrm{d}z_d = \frac{\pi^{d/2}}{2^{d-1}\Gamma(d/2)}\int_0^\infty r^{d-1}f(\pi^2\eta r^2)\,\mathrm{d}r.$$

A last transformation yields the following:

$$\int_0^\infty r^{d-1}f(\pi^2\eta r^2)\,\mathrm{d}r = \frac{1}{2\pi^2\eta}\int_0^\infty\Big(\frac{x}{\pi^2\eta}\Big)^{d/2-1}f(x)\,\mathrm{d}x = \frac{1}{2(\pi^2\eta)^{d/2}}\int_0^\infty x^{d/2-1}f(x)\,\mathrm{d}x.$$

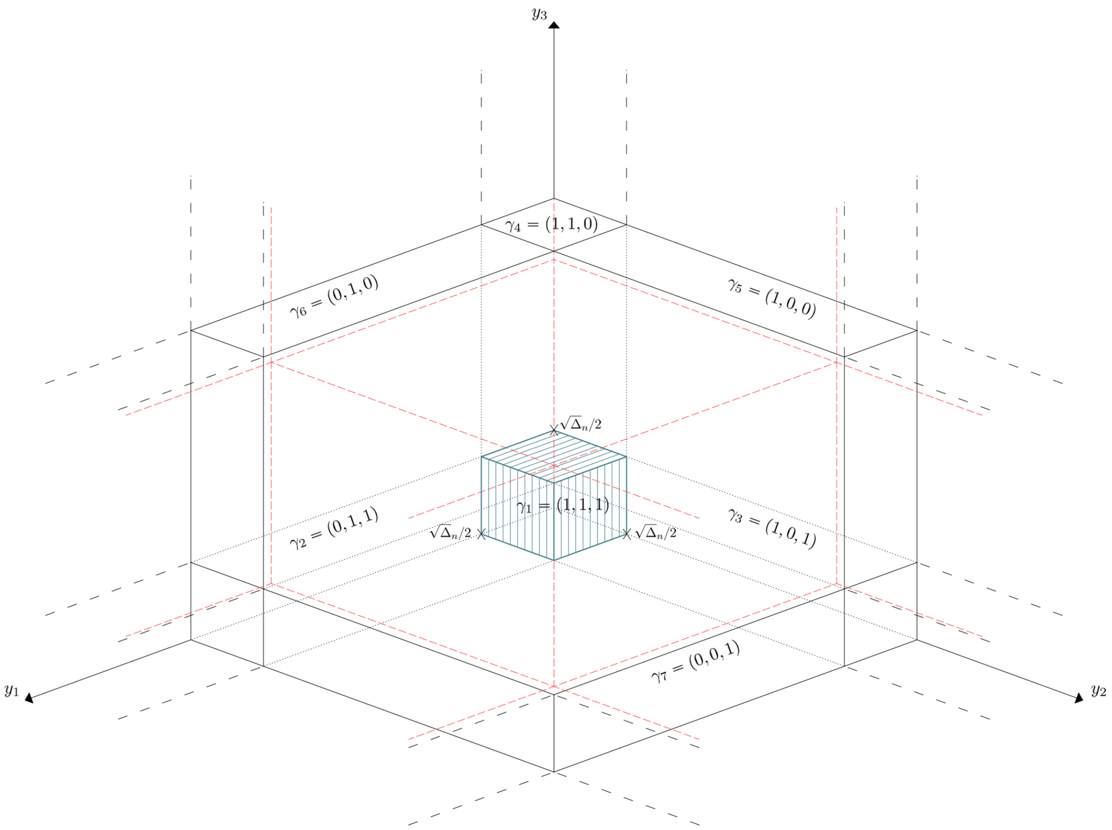

Figure 4.4.: Exemplary sketch of the different combinations for the sets B_γ in the three-dimensional space. The red dashed lines represent an excerpt of the set $[\sqrt{\Delta_n}/2,\infty)^d$. The remaining space $\mathbb{R}^d_+\backslash[\sqrt{\Delta_n}/2,\infty)^d$ is separated into the different disjoint sets B_{γ_i} given by the different combinations of γ_i as shown in the figure, where $i=1,\dots,7$.

Finally, we have

$$\begin{aligned}\Delta_n^{d/2}\sum_{\mathbf{k}\in\mathbb{N}^d} f(\lambda_{\mathbf{k}}\Delta_n) &= \frac{\pi^{d/2}}{2^{d-1}\Gamma(d/2)}\cdot\frac{1}{2\pi^d\eta^{d/2}}\int_0^\infty x^{d/2-1}f(x)\,\mathrm{d}x - \mathcal{I} + \mathcal{O}(T_1\vee\Delta_n)\\ &= \frac{1}{2^d(\pi\eta)^{d/2}\Gamma(d/2)}\int_0^\infty x^{d/2-1}f(x)\,\mathrm{d}x - \mathcal{I} + \mathcal{O}(T_1\vee\Delta_n).\end{aligned}$$

To analyse the compensation term $\mathcal{I}$, we initiate the process by decomposing the set $\mathbb{R}^d_+\backslash[\sqrt{\Delta_n}/2,\infty)^d$. Let $\gamma\in\{0,1\}^d\backslash\{0\}^d$, where $\gamma=(\gamma_1,\dots,\gamma_d)$ and let $\psi(x)=\mathbb{1}_{[0,\sqrt{\Delta_n}/2)}(x)$. With these definitions, we can introduce the following set:

$$B_\gamma := \{x\in[0,\infty)^d | x_1\in\psi^{-1}(\gamma_1),\dots,x_d\in\psi^{-1}(\gamma_d)\}\subset[0,\infty)^d. \tag{82}$$

An exemplary presentation for different combinations of B_γ in the three-dimensional space is provided in Figure 4.4. Hence, we can decompose the set $\mathbb{R}^d_+\backslash[\sqrt{\Delta_n}/2,\infty)^d$ using the following disjoint union:

$$\mathbb{R}^d_+\backslash[\sqrt{\Delta_n}/2,\infty)^d = \bigcup_{\substack{\|\gamma\|_1=1\\ \gamma\in\{0,1\}^d}}^{d} B_\gamma, \tag{83}$$

which enables the decomposition of the integral $\mathcal{I}$ as follows:

$$\mathcal{I} = \int_{\mathbb{R}_+^d \setminus [\sqrt{\Delta}_n/2, \infty)^d} f(\pi^2 \eta \|\mathbf{z}\|_2^2)\,\mathrm{d}\mathbf{z} = \sum_{\substack{\|\gamma\|_1 = 1 \\ \gamma \in \{0,1\}^d}}^{d} \int_{B_\gamma} f(\pi^2 \eta \|\mathbf{z}\|_2^2)\,\mathrm{d}\mathbf{z}.$$

We now focus on two cases. Firstly, the case where $\|\gamma\|_1 < d$, and secondly, the case where $\|\gamma\|_1 = d$. In the first case, we assume that $\|\gamma\|_1 = l$, where $l \in \{1, \ldots, d-1\}$. This implies that there exist indices $\{i_1, \ldots, i_l\} \subset \{1, \ldots, d\}$ and $\{1, \ldots, d\} \setminus \{i_1, \ldots, i_l\} = \{j_1, \ldots, j_{d-l}\}$, with $\gamma_{i_k} = 1$ for $k = 1, \ldots, l$, and $\gamma_{j_k} = 0$ for $k = 1, \ldots, d-l$. Moreover, we assume that $i_1 < \ldots < i_l$ and $j_1 < \ldots < j_{d-l}$.

Although we are integrating over an area corresponding to an infinite hyperrectangle, transforming into d-dimensional spherical coordinates provides a convenient representation, facilitating the analysis of the integral's order. During the transformation into d-dimensional spherical coordinates, we can always ensure that the angles $\varphi_1, \ldots, \varphi_{d-1}$ are bounded by $(0, \pi/2)$, and consequently, we have

$$\int_{B_\gamma} f(\pi^2 \eta \|\mathbf{z}\|_2^2)\,\mathrm{d}\mathbf{z} = \mathcal{O}\bigg(\int_{\sqrt{\Delta}_n/2}^{\infty} r^{d-1} f(r^2)\,\mathrm{d}r \bigg),$$

where we used that the radius r is always greater or equal than $\sqrt{\Delta}_n/2$. However, given that l dimensions vanish when integrating and as n tends to infinity, we can determine the order more precisely. Therefore, we can always consider the transformation

$$\begin{aligned}
&x_{i_1} = r\cos(\varphi_1), \quad x_{i_2} = r\sin(\varphi_1)\cos(\varphi_2), \quad \cdots, \quad x_{i_l} = r\sin(\varphi_1)\cdot \ldots \cdot \sin(\varphi_{l-1})\cos(\varphi_l), \quad \ldots, \\
&x_{j_1} = r\prod_{k=1}^{l}\sin(\varphi_k)\cos(\varphi_{l+1}), \quad \cdots, \quad x_{j_{d-l-1}} = r\prod_{k=1}^{d-2}\sin(\varphi_k)\cos(\varphi_{d-1}), \quad x_{j_{d-l}} = r\prod_{k=1}^{d-1}\sin(\varphi_k),
\end{aligned} \tag{84}$$

which allows without loss of generality to set $i_1 = 1, \ldots, i_l = l$ and $j_1 = l+1, \ldots j_{d-l} = d$, such that we use a spherical transformation as recalled in equation (57). As we aim to specify the order concerning the vanishing dimensions, we can bound the angles $\varphi_1, \ldots, \varphi_l$ as follows:

$$\begin{aligned}
0 \leqslant x_k = r\cos(\varphi_k)\prod_{l=1}^{k-1}\sin(\varphi_l) \leqslant \frac{\sqrt{\Delta}_n}{2} &\Leftrightarrow \arccos(0) \geqslant \varphi_k \geqslant \arccos\left(\frac{\sqrt{\Delta}_n}{2r\prod_{l=1}^{k-1}\sin(\varphi_l)}\right) \\
&\Leftrightarrow \arccos\left(\frac{\sqrt{\Delta}_n}{2r\prod_{l=1}^{k-1}\sin(\varphi_l)}\right) \leqslant \varphi_k \leqslant \frac{\pi}{2},
\end{aligned}$$

where $k = 1, \ldots, l$ and $1 \leqslant l \leqslant (d-1)$. Now, by rearranging the integration order using Fubini's theorem, we have

$$\begin{aligned}
\int_{B_\gamma} f(\pi^2\eta\|\mathbf{z}\|_2^2)\,\mathrm{d}\mathbf{z} &= \int_{\sqrt{\Delta}_n/2}^{\infty} \cdots \int_{\sqrt{\Delta}_n/2}^{\infty} \int_0^{\sqrt{\Delta}_n/2} \cdots \int_0^{\sqrt{\Delta}_n/2} f\bigg(\pi^2\eta\sum_{l=1}^{d} z_l^2\bigg)\,\mathrm{d}z_{i_l}\cdots\mathrm{d}z_{i_1}\,\mathrm{d}z_{j_1}\cdots\mathrm{d}z_{j_{d-l}} \\
&\leqslant \int_{\sqrt{\Delta}_n/2}^{\infty} f(\pi^2\eta r^2)\int_0^{\pi/2}\cdots\int_0^{\pi/2}\int_{\arccos(b_1)}^{\pi/2}\cdots\int_{\arccos(b_l)}^{\pi/2} |J_d|\,\mathrm{d}\varphi_l\cdots\mathrm{d}\varphi_1\,\mathrm{d}\varphi_{l+1}\cdots\mathrm{d}\varphi_{d-1}\,\mathrm{d}r,
\end{aligned}$$

where

$$b_1 := \frac{\sqrt{\Delta_n}}{2r}, \qquad \cdots \qquad , b_l := \frac{\sqrt{\Delta_n}}{2r \prod_{k=1}^{l-1} \sin(\varphi_k)}.$$

Note that we can use the following inequality for the determinant $|J_d|$:

$$|J_d| \leqslant r^{d-1} \sin(\varphi_1)^{l-1} \sin(\varphi_2)^{l-2} \cdots \sin(\varphi_{l-1}).$$

By utilizing the identity $\pi/2 - \arccos(x) = \arcsin(x)$ and the inequality $\arcsin(x) \leqslant x\pi/2$, for $x \in [0,1]$, we deduce that

$$\begin{aligned}
&\int_{\arccos(b_1)}^{\pi/2} \cdots \int_{\arccos(b_l)}^{\pi/2} |J_d| \,\mathrm{d}\varphi_l \cdots \mathrm{d}\varphi_1 \\
&\leqslant r^{d-1} \int_{\arccos(b_1)}^{\pi/2} \cdots \int_{\arccos(b_{l-1})}^{\pi/2} \int_{\arccos(b_l)}^{\pi/2} \mathrm{d}\varphi_l \sin(\varphi_1)^{l-1} \cdots \sin(\varphi_{l-1}) \,\mathrm{d}\varphi_{l-1} \cdots \mathrm{d}\varphi_1 \\
&\leqslant \frac{r^{d-1}\pi}{2} \int_{\arccos(b_1)}^{\pi/2} \cdots \int_{\arccos(b_{l-1})}^{\pi/2} \frac{\sin(\varphi_1)^{l-1} \cdots \sin(\varphi_{l-1}) \sqrt{\Delta_n}}{2r \sin(\varphi_1) \cdots \sin(\varphi_{l-1})} \,\mathrm{d}\varphi_{l-1} \cdots \mathrm{d}\varphi_1 \\
&= \sqrt{\Delta_n} \frac{r^{d-2}\pi}{4} \int_{\arccos(b_1)}^{\pi/2} \cdots \int_{\arccos(b_{l-2})}^{\pi/2} \int_{\arccos(b_{l-1})}^{\pi/2} \mathrm{d}\varphi_{l-1} \sin(\varphi_1)^{l-2} \cdots \sin(\varphi_{l-2}) \,\mathrm{d}\varphi_{l-2} \cdots \mathrm{d}\varphi_1 \\
&\leqslant C \Delta_n^{l/2} r^{d-1-l}.
\end{aligned}$$

Therefore, we have

$$\int_{B_\gamma} f(\pi^2 \eta \,\|\mathbf{z}\|_2^2) \,\mathrm{d}\mathbf{z} = \mathcal{O}\bigg(\Delta_n^{l/2} \int_{\sqrt{\Delta_n}/2}^{\infty} r^{d-1-l} f(r^2) \,\mathrm{d}r \bigg) = \mathcal{O}\bigg(\Delta_n^{l/2} \int_{\sqrt{\Delta_n}}^{1} r^{d-1-l} f(r^2) \,\mathrm{d}r \bigg).$$

Note that this order applies to the derivatives as well, i.e.:

$$\int_{B_\gamma} h(\pi^2 \eta \,\|\mathbf{z}\|_2^2) \,\mathrm{d}\mathbf{z} = \mathcal{O}\bigg(\Delta_n^{l/2} \int_{\sqrt{\Delta_n}}^{1} r^{d-1-l} h(r^2) \,\mathrm{d}r \bigg), \tag{85}$$

where $h = f, f', f''$. Now, we consider the last case, where $\|\gamma\|_1 = d$. Since the radius is bounded by $\|\{\sqrt{\Delta_n}/2\}^d\|_2 = \sqrt{d\Delta_n}/2$, we can perform a transformation into d-dimensional spherical coordinates and obtain the following order:

$$\begin{aligned}
\int_{B_\gamma} f(\pi^2 \eta \,\|\mathbf{z}\|_2^2) \,\mathrm{d}\mathbf{z} &= \int_0^{\sqrt{\Delta_n}/2} \cdots \int_0^{\sqrt{\Delta_n}/2} f\bigg(\pi^2 \eta \sum_{l=1}^{d} z_l^2 \bigg) \,\mathrm{d}z_1 \cdots \mathrm{d}z_d \\
&\leqslant \int_{\substack{\|\mathbf{z}\|_2 \leqslant \sqrt{d\Delta_n}/2 \\ \mathbf{z} \in [0,\infty)^d}} f(\pi^2 \eta \|\mathbf{z}\|_2^2) \,\mathrm{d}\mathbf{z} \\
&\leqslant \int_0^{\sqrt{d\Delta_n}/2} r^{d-1} f(\pi^2 \eta r^2) \int_0^{\pi/2} \cdots \int_0^{\pi/2} \mathrm{d}\varphi_1 \cdots \mathrm{d}\varphi_{d-1} \,\mathrm{d}r \\
&= \mathcal{O}\bigg(\int_0^{\sqrt{\Delta_n}} r^{d-1} f(r^2) \,\mathrm{d}r \bigg).
\end{aligned}$$

Consequently, the order of the compensation integral $\mathcal{I}$ is given by

$$\begin{aligned}\mathcal{I} &= \sum_{\substack{\|\gamma\|_1=1\\ \gamma\in\{0,1\}^d}}^{d-1} \int_{B_\gamma} f(\pi^2\eta\,\|\mathbf{z}\|_2^2)\,\mathrm{d}\mathbf{z} + \mathcal{O}\bigg(\int_0^{\sqrt{\Delta_n}} r^{d-1} f(r^2)\,\mathrm{d}r\bigg)\\ &= \mathcal{O}\bigg(\max_{l=1,\dots,d-1} \Delta_n^{l/2} \int_{\sqrt{\Delta_n}}^1 r^{d-1-l} f(r^2)\,\mathrm{d}r \vee \int_0^{\sqrt{\Delta_n}} r^{d-1} f(r^2)\,\mathrm{d}r\bigg).\end{aligned}$$

Regarding the error term T_1 from equation (81), we observe the following expression for $\mathbf{z} \in [a_{\mathbf{k-1}}, a_{\mathbf{k}}]$ and $\mathbf{k} \in \mathbb{N}^d$:

$$\begin{aligned}(\mathbf{z}-\sqrt{\Delta_n}\mathbf{k})^\top H_g(\mathbf{z})(\mathbf{z}-\sqrt{\Delta_n}\mathbf{k}) &= \sum_{l_1=1}^d \sum_{l_2=1}^d \big(z_{l_1}-\sqrt{\Delta_n}k_{l_1}\big)\big(z_{l_2}-\sqrt{\Delta_n}k_{l_2}\big)\frac{\partial^2}{\partial z_{l_1}\partial z_{l_2}} g(\mathbf{z})\\ &\leqslant \frac{\Delta_n}{4}\sum_{l_1=1}^d \sum_{l_2=1}^d \frac{\partial^2}{\partial z_{l_1}\partial z_{l_2}} f(\pi^2\eta\|\mathbf{z}\|_2^2)\\ &\leqslant C\bigg(\Delta_n \sum_{\substack{l_1,l_2=1\\ l_1\neq l_2}}^d z_{l_1}z_{l_2} f''(\pi^2\eta\|\mathbf{z}\|_2^2) + \frac{d\Delta_n}{2} f'(\pi^2\eta\|\mathbf{z}\|_2^2) + \Delta_n \sum_{l=1}^d z_l^2 f''(\pi^2\eta\|\mathbf{z}\|_2^2)\bigg)\\ &= C\bigg(\Delta_n \sum_{l_1=1}^d \sum_{l_2=1}^d z_{l_1}z_{l_2} f''(\pi^2\eta\|\mathbf{z}\|_2^2) + \frac{d\Delta_n}{2} f'(\pi^2\eta\|\mathbf{z}\|_2^2)\bigg)\\ &\leqslant C\bigg(\frac{\Delta_n}{2} f''(\pi^2\eta\|\mathbf{z}\|_2^2)\sum_{l_1=1}^d \sum_{l_2=1}^d (z_{l_1}^2+z_{l_2}^2) + \frac{d\Delta_n}{2} f'(\pi^2\eta\|\mathbf{z}\|_2^2)\bigg)\\ &\leqslant C' d\Delta_n\Big(\|\mathbf{z}\|_2^2 f''(\pi^2\eta\|\mathbf{z}\|_2^2) + f'(\pi^2\eta\|\mathbf{z}\|_2^2)\Big),\end{aligned}$$

where $C, C' > 0$ are suitable constants. Hence, we have

$$T_1 = \mathcal{O}\bigg(\Delta_n \int_{[\sqrt{\Delta_n}/2,\infty)^d} \|\mathbf{z}\|_2^2 f''(\|\mathbf{z}\|_2^2)\,\mathrm{d}\mathbf{z} \vee \Delta_n \int_{[\sqrt{\Delta_n}/2,\infty)^d} f'(\|\mathbf{z}\|_2^2)\,\mathrm{d}\mathbf{z}\bigg).$$

Once more, through the transformation into d-dimensional spherical coordinates, we can deduce the order of the Lagrange remainder T_1 as follows:

$$\begin{aligned}|T_1| &= \mathcal{O}\bigg(\Delta_n \int_{\sqrt{\Delta_n}}^\infty r^{d+1}|f''(r^2)|\,\mathrm{d}r \vee \Delta_n \int_{\sqrt{\Delta_n}}^\infty r^{d-1}|f'(r^2)|\,\mathrm{d}r\bigg)\\ &= \mathcal{O}\bigg(\Delta_n \int_{\sqrt{\Delta_n}}^1 r^{d+1}|f''(r^2)|\,\mathrm{d}r \vee \Delta_n \int_{\sqrt{\Delta_n}}^1 r^{d-1}|f'(r^2)|\,\mathrm{d}r\bigg),\end{aligned} \tag{86}$$

which completes the proof of the first assertion.

We begin the proof of (ii) by establishing the following identity:

$$\prod_{l=1}^n \cos(x_l) = \frac{1}{2^{n-1}} \sum_{\mathbf{u}\in C_n} \cos(\mathbf{u}^\top \mathbf{x}), \tag{87}$$

where $\mathbf{x} = (x_1, \dots, x_n)^\top$ and $C_n := \{1\} \times \{-1,1\}^{n-1}$, with $|C_n| = 2^{n-1}$ and $n \geqslant 1$. We demonstrate that this identity can be derived using induction. For $n \in \{1, 2\}$, the identity is readily observed by utilizing the elementary trigonometric identity $\cos(x \pm y) = \cos(x)\cos(y) \mp \sin(x)\sin(y)$. Now, we assume that the advanced identity holds for an arbitrary $n \in \mathbb{N}$. For $n+1$, we consider $\mathbf{x} = (\mathbf{y}, z) \in \mathbb{R}^{n+1}$, where $\mathbf{y} \in \mathbb{R}^n$ and $z \in \mathbb{R}$. Then, we have

$$\begin{aligned}\frac{1}{2^n}\sum_{\mathbf{u}\in C_{n+1}}\cos(\mathbf{u}^\top\mathbf{x}) &= \frac{1}{2^n}\sum_{\mathbf{u}\in C_n}\big(\cos(\mathbf{u}^\top\mathbf{y}+z)+\cos(\mathbf{u}^\top\mathbf{y}-z)\big)\\ &= \frac{1}{2^{n-1}}\sum_{\mathbf{u}\in C_n}\cos(\mathbf{u}^\top\mathbf{y})\cos(z)\\ &= \prod_{l=1}^{n+1}\cos(x_l).\end{aligned}$$

By utilizing equation (87), we arrive at the following structure:

$$\begin{aligned}&\Delta_n^{d/2}\sum_{\mathbf{k}\in\mathbb{N}^d} f(\lambda_{\mathbf{k}}\Delta_n)\cos(2\pi k_{j_1}y_{j_1})\cdot\ldots\cdot\cos(2\pi k_{j_l}y_{j_l}) = \frac{\Delta_n^{d/2}}{2^{l-1}}\sum_{\mathbf{k}\in\mathbb{N}^d} f(\lambda_{\mathbf{k}}\Delta_n)\sum_{\mathbf{u}\in C_l}\cos(2\pi\mathbf{u}^\top(\mathbf{y}\bullet\mathbf{k})_{j,l})\\ &= \mathrm{Re}\left(\frac{\Delta_n^{d/2}}{2^{l-1}}\sum_{\mathbf{k}\in\mathbb{N}^d} g(\sqrt{\Delta_n}\mathbf{k})\sum_{\mathbf{u}\in C_l} e^{\mathrm{i}2\pi\mathbf{u}^\top(\mathbf{y}\bullet\mathbf{k})_{j,l}}\right)+\mathcal{O}(\Delta_n),\end{aligned}$$

where $(\mathbf{y}\bullet\mathbf{k})_{j,l} := (k_{j_1}y_{j_1},\ldots,k_{j_l}y_{j_l})$ and $\{j_1,\ldots,j_l\}\subset\{1,\ldots,d\}$ and $l = 1,\ldots,(d-1)$. Furthermore, it holds with $u_i \in \{-1, 1\}$, $i \in \mathbb{N}$, that

$$\begin{aligned}\int_{a_{\mathbf{k-1}}}^{a_{\mathbf{k}}} e^{\mathrm{i}2\pi\sum_{i=1}^l u_i y_{j_i} z_{j_i}\Delta_n^{-1/2}}\,\mathrm{d}\mathbf{z} &= \Delta_n^{\frac{d-l}{2}}\int_{a_{k_{j_1}-1}}^{a_{k_{j_1}}} e^{\mathrm{i}2\pi u_1 y_{j_1} z_{j_1}\Delta_n^{-1/2}}\,\mathrm{d}z_{j_1}\cdots\int_{a_{k_{j_l}-1}}^{a_{k_{j_l}}} e^{\mathrm{i}2\pi u_l y_{j_l} z_{j_l}\Delta_n^{-1/2}}\,\mathrm{d}z_{j_l}\\ &= \frac{\Delta_n^{d/2}}{(\mathrm{i}2\pi)^l\prod_{i=1}^l u_i y_{j_i}}\prod_{i=1}^l\left(e^{\mathrm{i}2\pi a_{k_{j_i}} u_i y_{j_i}\Delta_n^{-1/2}} - e^{\mathrm{i}2\pi a_{k_{j_i}-1} u_i y_{j_i}\Delta_n^{-1/2}}\right)\\ &= \frac{\Delta_n^{d/2}}{(\mathrm{i}2\pi)^l\prod_{i=1}^l u_i y_{j_i}} e^{\mathrm{i}2\pi\sum_{i=1}^l u_i k_{j_i} y_{j_i}}\prod_{i=1}^l\left(e^{\mathrm{i}\pi u_i y_{j_i}} - e^{-\mathrm{i}\pi u_i y_{j_i}}\right)\\ &= \frac{\Delta_n^{d/2}}{(\mathrm{i}2\pi)^l\prod_{i=1}^l u_i y_{j_i}} e^{\mathrm{i}2\pi\sum_{i=1}^l u_i k_{j_i} y_{j_i}}\prod_{i=1}^l\big(\mathrm{i}2\sin(\pi u_i y_{j_i})\big)\\ &= \frac{\Delta_n^{d/2}\prod_{i=1}^l\sin(\pi y_{j_i})}{\pi^l\prod_{i=1}^l y_{j_i}} e^{\mathrm{i}2\pi\sum_{i=1}^l u_i k_{j_i} y_{j_i}}.\end{aligned}$$

Defining $\mathbf{y}_{j,l} := (y_{j_1},\ldots,y_{j_l})$ and $\chi := \chi_{j,l} : \mathbb{R}^l \to \mathbb{R}^d$, where the i-th component $(\chi_{j,l}(\mathbf{x}))_i$ of $\chi_{j,l}(\mathbf{x})$ is zero if $i \in \{1,\ldots,d\}\backslash\{j_1,\ldots,j_l\}$ or else the coordinate x_{j_i}, leads to

$$\begin{aligned}&\mathrm{Re}\left(\frac{\Delta_n^{d/2}}{2^{l-1}}\sum_{\mathbf{k}\in\mathbb{N}^d} g(\sqrt{\Delta_n}\mathbf{k})\sum_{\mathbf{u}\in C_l} e^{\mathrm{i}2\pi\mathbf{u}^\top(\mathbf{y}\bullet\mathbf{k})_{j,l}}\right)\\ &= \mathrm{Re}\left(\sum_{\mathbf{k}\in\mathbb{N}^d} g(\sqrt{\Delta_n}\mathbf{k})\int_{a_{\mathbf{k-1}}}^{a_{\mathbf{k}}}\sum_{\mathbf{u}\in C_l}\frac{\pi^l\prod_{i=1}^l y_{j_i}}{2^{l-1}\prod_{i=1}^l\sin(\pi y_{j_i})} e^{\mathrm{i}2\pi\sum_{i=1}^l u_i y_{j_i} z_{j_i}\Delta_n^{-1/2}}\,\mathrm{d}\mathbf{z}\right)\\ &= \sum_{\mathbf{u}\in C_l}\mathrm{Re}\left(\frac{\pi^l\prod_{i=1}^l y_{j_i}}{2^{l-1}\prod_{i=1}^l\sin(\pi y_{j_i})}\sum_{\mathbf{k}\in\mathbb{N}^d}\int_{a_{\mathbf{k-1}}}^{a_{\mathbf{k}}} g(\sqrt{\Delta_n}\mathbf{k}) e^{\mathrm{i}2\pi\chi(\mathbf{u}\bullet\mathbf{y}_{j,l})^\top\mathbf{z}\Delta_n^{-1/2}}\,\mathrm{d}\mathbf{z}\right)\end{aligned}$$

$$= \sum_{\mathbf{u}\in C_l} \operatorname{Re}\left(\frac{\pi^l \prod_{i=1}^l y_{j_i}}{2^{l-1}\prod_{i=1}^l \sin(\pi y_{j_i})}\mathcal{F}\Big[\sum_{\mathbf{k}\in\mathbb{N}^d} g(\sqrt{\Delta}_n\mathbf{k})\mathbb{1}_{(a_{\mathbf{k-1}},a_{\mathbf{k}}]}\Big]\big(-2\pi\chi(\mathbf{u}\bullet\mathbf{y}_{j,l})\Delta_n^{-1/2}\big)\right)$$
$$=: T_2 + T_3, \tag{88}$$

where $\mathcal{F}$ denotes the Fourier transformation which is given by

$$\mathcal{F}[f](\mathbf{x}) := \int_{\mathbb{R}^d} f(t)e^{-\mathrm{i}\mathbf{x}^\top\mathbf{t}}\,\mathrm{d}\mathbf{t},$$

for a $f \in \mathcal{L}^1(\mathbb{R}^d)$. Since we analyse functions $f : [0,\infty)^d \to \mathbb{R}$ the Fourier transformation is given by integrating over $[0,\infty)^d$. Hence, we define $T_2 := \sum_{\mathbf{u}\in C_l} T_{2,\mathbf{u}}$, $T_3 := \sum_{\mathbf{u}\in C_l} T_{3,\mathbf{u}}$, where the components are given by

$$T_{2,\mathbf{u}} := \operatorname{Re}\left(\frac{\pi^l \prod_{i=1}^l y_{j_i}}{2^{l-1}\prod_{i=1}^l \sin(\pi y_{j_i})}\mathcal{F}\Big[\sum_{\mathbf{k}\in\mathbb{N}^d} g(\sqrt{\Delta}_n\mathbf{k})\mathbb{1}_{(a_{\mathbf{k-1}},a_{\mathbf{k}}]} - (-1)^l g\mathbb{1}_{B_{\gamma_{j,l}}}\Big]\big(-2\pi\chi(\mathbf{u}\bullet\mathbf{y}_{j,l})\Delta_n^{-1/2}\big)\right),$$
$$T_{3,\mathbf{u}} := (-1)^l\operatorname{Re}\left(\frac{\pi^l \prod_{i=1}^l y_{j_i}}{2^{l-1}\prod_{i=1}^l \sin(\pi y_{j_i})}\mathcal{F}\big[g\mathbb{1}_{B_{\gamma_{j,l}}}\big]\big(-2\pi\chi(\mathbf{u}\bullet\mathbf{y}_{j,l})\Delta_n^{-1/2}\big)\right),$$

with B_γ defined in equation (82) and $\gamma_{j,l} \in \{0,1\}^d$, where $(\gamma_{j,l})_i = 1$ if $i \in \{j_1,\ldots,j_l\}$ or zero otherwise. Beginning with the analysis of the term T_3, we have for $1 \leqslant l \leqslant (d-1)$ that

$$\begin{aligned}
(-1)^l T_3 &= \sum_{\mathbf{u}\in C_l} \operatorname{Re}\left(\frac{\pi^l \prod_{i=1}^l y_{j_i}}{2^{l-1}\prod_{i=1}^l \sin(\pi y_{j_i})}\mathcal{F}\big[g\mathbb{1}_{B_{\gamma_{j,l}}}\big]\big(-2\pi\chi(\mathbf{u}\bullet\mathbf{y}_{j,l})\Delta_n^{-1/2}\big)\right)\\
&= \frac{\pi^l \prod_{i=1}^l y_{j_i}}{\prod_{i=1}^l \sin(\pi y_{j_i})}\int_{B_{\gamma_{j,l}}} g(\mathbf{z})\sum_{u\in C_l}\frac{1}{2^{l-1}}\cos(2\pi\chi(\mathbf{u}\bullet\mathbf{y}_{j,l})^\top\mathbf{z}\Delta_n^{-1/2})\,\mathrm{d}\mathbf{z}\\
&= \frac{\pi^l \prod_{i=1}^l y_{j_i}}{\prod_{i=1}^l \sin(\pi y_{j_i})}\int_{B_{\gamma_{j,l}}} g(\mathbf{z})\cos(2\pi y_{j_1}z_{j_1}\Delta_n^{-1/2})\cdot\ldots\cdot\cos(2\pi y_{j_l}z_{j_l}\Delta_n^{-1/2})\,\mathrm{d}\mathbf{z}\\
&= \frac{\pi^l \prod_{i=1}^l y_{j_i}}{\prod_{i=1}^l \sin(\pi y_{j_i})}\int_{\sqrt{\Delta}_n/2}^{\infty}\cdots\int_{\sqrt{\Delta}_n/2}^{\infty}\int_0^{\sqrt{\Delta}_n/2}\cos(2\pi y_{j_l}z_{j_l}\Delta_n^{-1/2})\cdots\\
&\qquad\times\int_0^{\sqrt{\Delta}_n/2} g(\mathbf{z})\cos(2\pi y_{j_1}z_{j_1}\Delta_n^{-1/2})\,\mathrm{d}z_{j_1}\cdots\mathrm{d}z_{j_l}\,\mathrm{d}z_{i_1}\cdots\mathrm{d}z_{i_{d-l}}.
\end{aligned}$$

To simplify the notation, we introduce $g(z_1,\ldots,z_d) = \tilde{g}(z_{j_1},\ldots,z_{j_l},z_{i_1},\ldots,z_{i_{d-l}})$. Moreover, we can apply integration by parts to obtain

$$\begin{aligned}
&\frac{\pi^l \prod_{i=1}^l y_{j_i}}{\prod_{i=1}^l \sin(\pi y_{j_i})}\int_{\sqrt{\Delta}_n/2}^{\infty}\cdots\int_{\sqrt{\Delta}_n/2}^{\infty}\int_0^{\sqrt{\Delta}_n/2}\cos(2\pi y_{j_l}z_{j_l}\Delta_n^{-1/2})\cdots\\
&\quad\times\int_0^{\sqrt{\Delta}_n/2} g(\mathbf{z})\cos(2\pi y_{j_1}z_{j_1}\Delta_n^{-1/2})\,\mathrm{d}z_{j_1}\cdots\mathrm{d}z_{j_l}\,\mathrm{d}z_{i_1}\cdots\mathrm{d}z_{i_{d-l}}\\
&= \frac{\Delta_n^{1/2}\pi^{l-1}\prod_{i=2}^l y_{j_i}}{2\prod_{i=2}^l \sin(\pi y_{j_i})}\int_{\sqrt{\Delta}_n/2}^{\infty}\cdots\int_{\sqrt{\Delta}_n/2}^{\infty}\int_0^{\sqrt{\Delta}_n/2}\cos(2\pi y_{j_l}z_{j_l}\Delta_n^{-1/2})\cdots\\
&\quad\times\int_0^{\sqrt{\Delta}_n/2}\tilde{g}(\sqrt{\Delta}_n/2, z_{j_2},\ldots,z_{j_l},z_{i_1},\ldots,z_{i_{d-l}})\cos(2\pi y_{j_2}z_{j_2}\Delta_n^{-1/2})\,\mathrm{d}z_{j_2}\cdots\mathrm{d}z_{j_l}\,\mathrm{d}z_{i_1}\cdots\mathrm{d}z_{i_{d-l}}
\end{aligned}$$

$$
\begin{aligned}
&- \frac{\pi^l \prod_{i=1}^l y_{j_i}}{\prod_{i=1}^l \sin(\pi y_{j_i})} \int_{\sqrt{\Delta}_n/2}^{\infty} \cdots \int_{\sqrt{\Delta}_n/2}^{\infty} \int_0^{\sqrt{\Delta}_n/2} \cos(2\pi y_{j_l} z_{j_l} \Delta_n^{-1/2}) \cdots \\
&\times \int_0^{\sqrt{\Delta}_n/2} g'_{z_{j_1}}(z) \frac{\sin(2\pi y_{j_1} z_{j_1} \Delta_n^{-1/2})}{2\pi y_{j_1} \Delta_n^{-1/2}} \,\mathrm{d}z_{j_1} \cdots \mathrm{d}z_{j_l} \,\mathrm{d}z_{i_1} \cdots \mathrm{d}z_{i_{d-l}}.
\end{aligned}
$$

By induction, we have

$$
\begin{aligned}
&\sum_{\mathbf{u} \in C_l} \operatorname{Re}\left(\frac{\pi^l \prod_{i=1}^l y_{j_i}}{2^{l-1} \prod_{i=1}^l \sin(\pi y_{j_i})} \mathcal{F}\big[g \mathbb{1}_{B_{\gamma_{j,l}}}\big]\big(-2\pi \chi(\mathbf{u} \cdot \mathbf{y}_{j,l}) \Delta_n^{-1/2}\big) \right) \\
&= \left(\frac{\Delta_n^{1/2}}{2} \right)^l \int_{\sqrt{\Delta}_n/2}^{\infty} \cdots \int_{\sqrt{\Delta}_n/2}^{\infty} \tilde{g}(\sqrt{\Delta}_n/2, \dots, \sqrt{\Delta}_n/2, z_{i_1}, \dots, z_{i_{d-l}}) \,\mathrm{d}z_{i_1} \cdots \mathrm{d}z_{i_{d-l}} - \sum_{k=1}^l I_k, \qquad (89)
\end{aligned}
$$

where we infer by a simple transformation, that

$$
\begin{aligned}
I_k :=& \frac{\Delta_n^{(k-1)/2} \pi^{l-k+1} \prod_{i=k}^l y_{j_i}}{2^{k-1} \prod_{i=k}^l \sin(\pi y_{j_i})} \int_{\sqrt{\Delta}_n/2}^{\infty} \cdots \int_{\sqrt{\Delta}_n/2}^{\infty} \int_0^{\sqrt{\Delta}_n/2} \cos(2\pi y_{j_l} z_{j_l} \Delta_n^{-1/2}) \cdots \\
&\times \int_0^{\sqrt{\Delta}_n/2} \Big(\tilde{g}'_{z_{j_k}}(\sqrt{\Delta}_n/2, \dots, \sqrt{\Delta}_n/2, z_{j_k}, \dots, z_{j_l}, z_{i_1}, \dots, z_{i_{d-l}}) \\
&\qquad \times \frac{\sin(2\pi y_{j_k} z_{j_k} \Delta_n^{-1/2})}{2\pi y_{j_k} \Delta_n^{-1/2}} \Big) \,\mathrm{d}z_{j_k} \cdots \mathrm{d}z_{j_l} \,\mathrm{d}z_{i_1} \cdots \mathrm{d}z_{i_{d-l}} \\
=& \frac{\Delta_n^{(l+1)/2} \pi^{l-k} \prod_{i=k+1}^l y_{j_i}}{2^k \prod_{i=k}^l \sin(\pi y_{j_i})} \int_{\sqrt{\Delta}_n/2}^{\infty} \cdots \int_{\sqrt{\Delta}_n/2}^{\infty} \int_0^{1/2} \cos(2\pi y_{j_l} z_{j_l}) \cdots \\
&\times \int_0^{1/2} \Big(\tilde{g}'_{z_{j_k}}(\sqrt{\Delta}_n/2, \dots, \sqrt{\Delta}_n/2, z_{j_k} \Delta_n^{1/2}, \dots, z_{j_l} \Delta_n^{1/2}, z_{i_1}, \dots, z_{i_{d-l}}) \\
&\qquad \times \sin(2\pi y_{j_k} z_{j_k}) \Big) \,\mathrm{d}z_{j_k} \cdots \mathrm{d}z_{j_l} \,\mathrm{d}z_{i_1} \cdots \mathrm{d}z_{i_{d-l}}. \qquad (90)
\end{aligned}
$$

In order to determine the order of the terms I_k we proceed by re-transforming the integral as follows:

$$
\begin{aligned}
I_k &= \mathcal{O}\Big(\frac{\Delta_n^{(l+1)/2}}{\delta^{l-k+1}} \int_{\sqrt{\Delta}_n/2}^{\infty} \cdots \int_{\sqrt{\Delta}_n/2}^{\infty} \int_0^{1/2} \cdots \\
&\quad \times \int_0^{1/2} \tilde{g}'_{z_{j_k}}(\sqrt{\Delta}_n/2, \dots, \sqrt{\Delta}_n/2, z_{j_k} \Delta_n^{1/2}, \dots, z_{j_l} \Delta_n^{1/2}, z_{i_1}, \dots, z_{i_{d-l}}) \,\mathrm{d}z_{j_k} \cdots \mathrm{d}z_{j_l} \,\mathrm{d}z_{i_1} \cdots \mathrm{d}z_{i_{d-l}} \Big) \\
&= \mathcal{O}\Big(\frac{\Delta_n^{k/2}}{\delta^{l-k+1}} \int_{\sqrt{\Delta}_n/2}^{\infty} \cdots \int_{\sqrt{\Delta}_n/2}^{\infty} \int_0^{\sqrt{\Delta}_n/2} \cdots \\
&\quad \times \int_0^{\sqrt{\Delta}_n/2} \tilde{g}'_{z_{j_k}}\big(\sqrt{\Delta}_n/2, \dots, \sqrt{\Delta}_n/2, z_{j_k}, \dots, z_{j_l}, z_{i_1}, \dots, z_{i_{d-l}}\big) \,\mathrm{d}z_{j_k} \cdots \mathrm{d}z_{j_l} \,\mathrm{d}z_{i_1} \cdots \mathrm{d}z_{i_{d-l}} \Big) \\
&= \mathcal{O}\Big(\frac{\Delta_n^{k/2}}{\delta^{l-k+1}} \int_{\sqrt{\Delta}_n/2}^{\infty} \cdots \int_{\sqrt{\Delta}_n/2}^{\infty} \int_0^{\sqrt{\Delta}_n/2} \cdots \\
&\quad \times \int_0^{\sqrt{\Delta}_n/2} z_{j_k} f'\Big((k-1)\Delta_n/4 + \sum_{i=k}^l z_{j_i}^2 + \sum_{j=1}^{d-l} z_{i_j}^2 \Big) \,\mathrm{d}z_{j_k} \cdots \mathrm{d}z_{j_l} \,\mathrm{d}z_{i_1} \cdots \mathrm{d}z_{i_{d-l}} \Big)
\end{aligned}
$$

$$= \mathcal{O}\bigg(\frac{\Delta_n^{k/2}}{\delta^{l-k+1}}\int_{\sqrt{\Delta}_n/2}^{\infty}\cdots\int_{\sqrt{\Delta}_n/2}^{\infty}\int_0^{\sqrt{\Delta}_n/2}\cdots\int_0^{\sqrt{\Delta}_n/2} z_{j_k} f'\bigg(\sum_{i=k}^{l} z_{j_i}^2 + \sum_{j=1}^{d-l} z_{i_j}^2\bigg)\,\mathrm{d}z_{j_k}\cdots\mathrm{d}z_{j_l}\,\mathrm{d}z_{i_1}\cdots\mathrm{d}z_{i_{d-l}}\bigg).$$

Analogously to the determination of the error term $\mathcal{I}$, we transform into $(d-k+1)$-dimensional spherical coordinates and obtain with $1 \leqslant k \leqslant l \leqslant (d-1)$ that

$$I_k = \mathcal{O}\bigg(\frac{\Delta_n^{(l+1)/2}}{\delta^{l-k+1}}\int_{\sqrt{\Delta}_n}^{1} r^{d-l} f'(r^2)\,\mathrm{d}r\bigg), \tag{91}$$

which implies

$$\sum_{k=1}^{l} I_k = \mathcal{O}\bigg(\frac{\Delta_n^{(l+1)/2}}{\delta^{l}}\int_{\sqrt{\Delta}_n}^{1} r^{d-l} f'(r^2)\,\mathrm{d}r\bigg).$$

Next, we have

$$\begin{aligned}
&\bigg(\frac{\Delta_n^{1/2}}{2}\bigg)^l\int_{\sqrt{\Delta}_n/2}^{\infty}\cdots\int_{\sqrt{\Delta}_n/2}^{\infty}\tilde{g}(\sqrt{\Delta}_n/2,\ldots,\sqrt{\Delta}_n/2,z_{i_1},\ldots,z_{i_{d-l}})\,\mathrm{d}z_{i_1}\cdots\mathrm{d}z_{i_{d-l}}\\
&=\int_{\sqrt{\Delta}_n/2}^{\infty}\cdots\int_{\sqrt{\Delta}_n/2}^{\infty}\int_0^{\sqrt{\Delta}_n/2}\cdots\int_0^{\sqrt{\Delta}_n/2}\tilde{g}(\sqrt{\Delta}_n/2,\ldots,\sqrt{\Delta}_n/2,z_{i_1},\ldots,z_{i_{d-l}})\,\mathrm{d}z_{j_1}\ldots\mathrm{d}z_{j_l}\,\mathrm{d}z_{i_1}\cdots\mathrm{d}z_{i_{d-l}}\\
&=: J_1.
\end{aligned}$$

Utilizing Taylor expansion, we can decompose g as follows:

$$\begin{aligned}
g(z_1,\ldots,z_d) &= \tilde{g}(z_{j_1},\ldots,z_{j_l},z_{i_1},\ldots,z_{i_{d-l}})\\
&= \tilde{g}(\sqrt{\Delta}_n/2,\ldots,\sqrt{\Delta}_n/2,z_{i_1},\ldots,z_{i_{d-l}}) + \nabla_l\tilde{g}(\xi_1,\ldots,\xi_l,z_{i_1},\ldots,z_{i_{d-l}})^\top(\tilde{z}-a)\\
&= \tilde{g}(\sqrt{\Delta}_n/2,\ldots,\sqrt{\Delta}_n/2,z_{i_1},\ldots,z_{i_{d-l}}) + \sum_{k=1}^{l}\tilde{g}'_{z_{j_k}}(\xi_1,\ldots,\xi_l,z_{i_1},\ldots,z_{i_{d-l}})\big(z_{j_k}-\sqrt{\Delta}_n/2\big),
\end{aligned}$$

where

$$\nabla_l := \begin{pmatrix}\frac{\partial}{\partial z_{j_1}}\\ \vdots\\ \frac{\partial}{\partial z_{j_l}}\\ \mathrm{id}\\ \vdots\\ \mathrm{id}\end{pmatrix},\qquad a := \begin{pmatrix}\sqrt{\Delta}_n/2\\ \vdots\\ \sqrt{\Delta}_n/2\\ z_{i_1}\\ \vdots\\ z_{i_{d-l}}\end{pmatrix},\qquad \tilde{z} := \begin{pmatrix}z_{j_1}\\ \vdots\\ z_{j_l}\\ z_{i_1}\\ \vdots\\ z_{i_{d-l}}\end{pmatrix},$$

and $\xi_1,\ldots,\xi_l \in [0,\sqrt{\Delta}_n/2]$. Thus, it holds that

$$\begin{aligned}
\bigg|J_1 - \int_{B_{\gamma_{j,l}}} g(\mathbf{z})\,\mathrm{d}\mathbf{z}\bigg| &\leqslant \int_{B_{\gamma_{j,l}}}|\tilde{g}(\sqrt{\Delta}_n/2,\ldots,\sqrt{\Delta}_n/2,z_{i_1},\ldots,z_{i_{d-l}}) - g(\mathbf{z})|\,\mathrm{d}\mathbf{z}\\
&= \mathcal{O}\bigg(\sum_{k=1}^{l}\int_{B_{\gamma_{j,l}}}|f'_{z_{j_k}}(\|\mathbf{z}\|_2^2)|\cdot|z_{j_k}-\sqrt{\Delta}_n/2|\,\mathrm{d}\mathbf{z}\bigg)
\end{aligned}$$

$$= \mathcal{O}\bigg(\sqrt{\Delta}_n \sum_{k=1}^{l} \int_{B_{\gamma_{j,l}}} z_{j_k} |f'(\|\mathbf{z}\|_2^2)| \,\mathrm{d}\mathbf{z}\bigg)$$
$$= \mathcal{O}\bigg(\Delta_n^{(l+1)/2} \int_{\sqrt{\Delta}_n}^{1} r^{d-l} |f'(r^2)| \,\mathrm{d}r\bigg).$$

Hence, we have

$$J_1 = \int_{B_{\gamma_{j,l}}} g(\mathbf{z}) \,\mathrm{d}\mathbf{z} + \mathcal{O}\bigg(\Delta_n^{(l+1)/2} \int_{\sqrt{\Delta}_n}^{1} r^{d-l} |f'(r^2)| \,\mathrm{d}r\bigg),$$

and therefore, we derive the following:

$$T_3 = (-1)^l \int_{B_{\gamma_{j,l}}} g(\mathbf{z}) \,\mathrm{d}\mathbf{z} + \mathcal{O}\bigg(\frac{\Delta_n^{(l+1)/2}}{\delta^l} \int_{\sqrt{\Delta}_n}^{1} r^{d-l} f'(r^2) \,\mathrm{d}r\bigg).$$

To analyse the order of the term T_2, we begin by distinguishing between two cases: l being an odd natural number and l being an even natural number. Considering that the term $T_{2,\mathbf{u}}$ corresponds to the Fourier transform of the function

$$\sum_{\mathbf{k}\in\mathbb{N}^d} g(\sqrt{\Delta}_n \mathbf{k}) \mathbb{1}_{(a_{\mathbf{k-1}}, a_{\mathbf{k}}]} - (-1)^l g \mathbb{1}_{B_{\gamma_{j,l}}},$$

we can analyse the order of this term by adding the following terms:

$$\begin{aligned}
&\sum_{\mathbf{k}\in\mathbb{N}^d} g(\sqrt{\Delta}_n \mathbf{k}) \mathbb{1}_{(a_{\mathbf{k-1}}, a_{\mathbf{k}}]} - (-1)^l g \mathbb{1}_{B_{\gamma_{j,l}}} \\
&\quad = \sum_{\mathbf{k}\in\mathbb{N}^d} g(\sqrt{\Delta}_n \mathbf{k}) \mathbb{1}_{(a_{\mathbf{k-1}}, a_{\mathbf{k}}]} - (-1)^l g \cdot \big(\mathbb{1}_{B_{\gamma_{j,l}}} + \mathbb{1}_{(\sqrt{\Delta}_n/2,\infty)^d} - \mathbb{1}_{(\sqrt{\Delta}_n/2,\infty)^d}\big).
\end{aligned}$$

If l is odd, we have

$$\sum_{\mathbf{k}\in\mathbb{N}^d} g(\sqrt{\Delta}_n \mathbf{k}) \mathbb{1}_{(a_{\mathbf{k-1}}, a_{\mathbf{k}}]} - (-1)^l g \mathbb{1}_{B_{\gamma_{j,l}}} = \sum_{\mathbf{k}\in\mathbb{N}^d} g(\sqrt{\Delta}_n \mathbf{k}) \mathbb{1}_{(a_{\mathbf{k-1}}, a_{\mathbf{k}}]} - g \mathbb{1}_{(\sqrt{\Delta}_n/2,\infty)^d} + g \mathbb{1}_{(\sqrt{\Delta}_n/2,\infty)^d \cup B_{\gamma_{j,l}}},$$

since we have disjoint sets. For the case where l is even, we find that

$$\begin{aligned}
\sum_{\mathbf{k}\in\mathbb{N}^d} g(\sqrt{\Delta}_n \mathbf{k}) \mathbb{1}_{(a_{\mathbf{k-1}}, a_{\mathbf{k}}]} - (-1)^l g \mathbb{1}_{B_{\gamma_{j,l}}} &= \sum_{\mathbf{k}\in\mathbb{N}^d} g(\sqrt{\Delta}_n \mathbf{k}) \mathbb{1}_{(a_{\mathbf{k-1}}, a_{\mathbf{k}}]} - g \mathbb{1}_{(\sqrt{\Delta}_n/2,\infty)^d} \\
&\quad + g \cdot \big(\mathbb{1}_{(\sqrt{\Delta}_n/2,\infty)^d} - \mathbb{1}_{B_{\gamma_{j,l}}}\big) \\
&\leqslant \sum_{\mathbf{k}\in\mathbb{N}^d} g(\sqrt{\Delta}_n \mathbf{k}) \mathbb{1}_{(a_{\mathbf{k-1}}, a_{\mathbf{k}}]} - g \mathbb{1}_{(\sqrt{\Delta}_n/2,\infty)^d} + g \mathbb{1}_{(\sqrt{\Delta}_n/2,\infty)^d \cup B_{\gamma_{j,l}}}.
\end{aligned}$$

Therefore, we decompose T_2 for general $l = 1, \dots, d-1$ into the following parts:

$$\begin{aligned}
T_{2,\mathbf{u}} \leqslant \mathrm{Re}\bigg(&\frac{\pi^l \prod_{i=1}^{l} y_{j_i}}{2^{l-1} \prod_{i=1}^{l} \sin(\pi y_{j_i})} \mathcal{F}\bigg[\sum_{\mathbf{k}\in\mathbb{N}^d} g(\sqrt{\Delta}_n \mathbf{k}) \mathbb{1}_{(a_{\mathbf{k-1}}, a_{\mathbf{k}}]} - g \mathbb{1}_{(\sqrt{\Delta}_n/2,\infty)^d}\bigg]\big(-2\pi\chi(\mathbf{u}\boldsymbol{\cdot}\mathbf{y}_{j,l})\Delta_n^{-1/2}\big)\bigg) \\
&+ \mathrm{Re}\bigg(\frac{\pi^l \prod_{i=1}^{l} y_{j_i}}{2^{l-1} \prod_{i=1}^{l} \sin(\pi y_{j_i})} \mathcal{F}\Big[g \mathbb{1}_{(\sqrt{\Delta}_n/2,\infty)^d \cup B_{\gamma_{j,l}}}\Big]\big(-2\pi\chi(\mathbf{u}\boldsymbol{\cdot}\mathbf{y}_{j,l})\Delta_n^{-1/2}\big)\bigg)
\end{aligned}$$

$$=: S_{1,\mathbf{u}} + S_{2,\mathbf{u}}.$$

Furthermore, we define $S_i := \sum_{\mathbf{u}\in C_l} S_{i,\mathbf{u}}$, for $i = 1, 2$. Starting with S_2, it holds for $q \in \{1, 2\}$ that

$$|x_j^q \mathcal{F}[g](\mathbf{x})| = \left|\mathcal{F}\left[\frac{\partial^q}{\partial x_j^q} g\right](\mathbf{x})\right| \leqslant \left\|\frac{\partial^q}{\partial x_j^q} g(\mathbf{x})\right\|_{\mathcal{L}_1} \quad \text{and} \quad |\mathcal{F}[g](\mathbf{x})| \leqslant |x_j^{-q}| \left\|\frac{\partial^q}{\partial x_j^q} g(\mathbf{x})\right\|_{\mathcal{L}_1}, \tag{92}$$

where we use $x_j \neq 0$ in the last inequality, for $j = 1, \dots, d$ and $\mathbf{x} \in \mathbb{R}^d$. Hence, we have

$$S_{2,\mathbf{u}} = \mathcal{O}\bigg(\frac{\Delta_n \pi^{l-2} \prod_{i=2}^l y_{j_i}}{2^{l+1} y_{j_1} \prod_{i=1}^l \sin(\pi y_{j_i})} \left\|\frac{\partial^2}{\partial z_{j_1}^2} g \mathbb{1}_{[\sqrt{\Delta_n}/2,\infty)^d \cup B_{\gamma_{j,l}}}\right\|_{\mathcal{L}_1}\bigg).$$

To compute the $\mathcal{L}_1$ norm, we first obtain the following:

$$\begin{aligned}\left\|\frac{\partial^2}{\partial z_{j_1}^2} g \mathbb{1}_{[\sqrt{\Delta_n}/2,\infty)^d \cup B_{\gamma_{j,l}}}\right\|_{\mathcal{L}_1} &= \int_{[\sqrt{\Delta_n}/2,\infty)^d \cup B_{\gamma_{j,l}}} \frac{\partial^2}{\partial z_{j_1}^2} g(\mathbf{z}) \,\mathrm{d}\mathbf{z} \\ &= \int_{([\sqrt{\Delta_n}/2,\infty)\dot\cup(0,\sqrt{\Delta_n}/2))^l \times [\sqrt{\Delta_n}/2,\infty)^{d-l}} \frac{\partial^2}{\partial z_{j_1}^2} g(\mathbf{z}) \,\mathrm{d}\tilde{\mathbf{z}},\end{aligned}$$

where $\tilde{\mathbf{z}} = (z_{j_1}, \dots, z_{j_l}, z_{i_1}, \dots, z_{i_{d-l}})$. At this point, it is possible that none of the integration variables $z_{j_1}, \dots, z_{j_l}$ fall within the range $(0, \sqrt{\Delta_n}/2)$, or one to all of them. Assume we have $0 \leqslant k \leqslant l$ of these integration variable within the range $(0, \sqrt{\Delta_n}/2)$, then there are $\binom{l}{k}$ possible combinations to choose k variables from $z_{j_1}, \dots, z_{j_l}$. As each choice results in the same order of the integral, which is evident by the argumentation followed by display (84), it is sufficient to analyse the order of the integral, where we set the first k integration variables $z_{j_1}, \dots, z_{j_k} \in (0, \sqrt{\Delta_n}/2)$. Hence, we have

$$\begin{aligned}\left\|\frac{\partial^2}{\partial z_{j_1}^2} g \mathbb{1}_{[\sqrt{\Delta_n}/2,\infty)^d \cup B_{\gamma_{j,l}}}\right\|_{\mathcal{L}_1} &= \int_{([\sqrt{\Delta_n}/2,\infty)\dot\cup(0,\sqrt{\Delta_n}/2))^l \times [\sqrt{\Delta_n}/2,\infty)^{d-l}} \frac{\partial^2}{\partial z_{j_1}^2} g(\mathbf{z}) \,\mathrm{d}\tilde{\mathbf{z}} \\ &= \mathcal{O}\bigg(\max_{k=0,\dots,l} \int_{(0,\sqrt{\Delta_n}/2)^k \times [\sqrt{\Delta_n}/2,\infty)^{d-k}} z_{j_1}^2 f''(\|\mathbf{z}\|_2^2) + f'(\|\mathbf{z}\|_2^2) \,\mathrm{d}\tilde{\mathbf{z}}\bigg) \\ &= \mathcal{O}\bigg(\max_{k=1,\dots,l} \Delta_n^{k/2} \int_{\sqrt{\Delta_n}}^1 r^{d-k+1} f''(r^2) \,\mathrm{d}r \vee \int_{\sqrt{\Delta_n}}^\infty r^{d+1} f''(r^2) \,\mathrm{d}r \\ &\qquad \vee \max_{k=1,\dots,l} \Delta_n^{k/2} \int_{\sqrt{\Delta_n}}^1 r^{d-k-1} f'(r^2) \,\mathrm{d}r \vee \int_{\sqrt{\Delta_n}}^\infty r^{d-1} f'(r^2) \,\mathrm{d}r\bigg).\end{aligned}$$

Thus, we infer the following:

$$S_2 = \sum_{\mathbf{u}\in C_l} S_{2,\mathbf{u}} = \mathcal{O}\bigg(\max_{k=0,\dots,l} \frac{\Delta_n^{k/2+1}}{\delta^{l+1}} \int_{\sqrt{\Delta_n}}^1 r^{d-k+1} f''(r^2) \,\mathrm{d}r \vee \max_{k=0,\dots,l} \frac{\Delta_n^{k/2+1}}{\delta^{l+1}} \int_{\sqrt{\Delta_n}}^1 r^{d-k-1} f'(r^2) \,\mathrm{d}r\bigg), \tag{93}$$

where we have used that $\mathbf{y} \in [\delta, 1-\delta]^d$. We commence the analysis of the term S_1. Here, we find that

$$|S_{1,\mathbf{u}}| = \frac{\pi^l \prod_{i=1}^l y_{j_i}}{2^{l-1} \prod_{i=1}^l \sin(\pi y_{j_i})} \bigg|\operatorname{Re}\bigg(\sum_{\mathbf{k}\in\mathbb{N}^d} \int_{a_{\mathbf{k-1}}}^{a_{\mathbf{k}}} \big(g(\sqrt{\Delta_n}\mathbf{k}) - g(\mathbf{z})\big) \exp\big[2\pi\mathrm{i}\chi(\mathbf{u}\cdot\mathbf{y}_{j,l})^\top \mathbf{z} \Delta_n^{-1/2}\big] \,\mathrm{d}\mathbf{z}\bigg)\bigg|.$$

By considering display (80), we deduce

$$\begin{aligned}|S_{1,\mathbf{u}}| &\leqslant \frac{\pi^l\prod_{i=1}^l y_{j_i}}{2^{l-1}\prod_{i=1}^l \sin(\pi y_{j_i})}\bigg|\mathrm{Re}\bigg(-\sum_{\mathbf{k}\in\mathbb{N}^d}\int_{a_{\mathbf{k-1}}}^{a_{\mathbf{k}}}\nabla g(\sqrt{\Delta_n}\mathbf{k})^\top(\mathbf{z}-\sqrt{\Delta_n}\mathbf{k})\exp\big[2\pi\mathrm{i}\chi(\mathbf{u}\cdot\mathbf{y}_{j,l})^\top\mathbf{z}\Delta_n^{-1/2}\big]\,\mathrm{d}\mathbf{z}\bigg)\bigg| \\ &\quad+\frac{\pi^l\prod_{i=1}^l y_{j_i}}{2^{l-1}\prod_{i=1}^l \sin(\pi y_{j_i})}\mathrm{Re}\bigg(\sum_{\mathbf{k}\in\mathbb{N}^d}\int_{a_{\mathbf{k-1}}}^{a_{\mathbf{k}}}\Big|\frac{1}{2}(\mathbf{z}-\sqrt{\Delta_n}\mathbf{k})^\top H_g(\xi) \\ &\qquad\times(\mathbf{z}-\sqrt{\Delta_n}\mathbf{k})\exp\big[2\pi\mathrm{i}\chi(\mathbf{u}\cdot\mathbf{y}_{j,l})^\top\mathbf{z}\Delta_n^{-1/2}\big]\Big|\,\mathrm{d}\mathbf{z}\bigg) \\ &\leqslant \frac{\pi^l\prod_{i=1}^l y_{j_i}}{2^{l-1}\prod_{i=1}^l \sin(\pi y_{j_i})}\bigg|\mathrm{Re}\bigg(-\sum_{\mathbf{k}\in\mathbb{N}^d}\int_{a_{\mathbf{k-1}}}^{a_{\mathbf{k}}}\nabla g(\sqrt{\Delta_n}\mathbf{k})^\top(\mathbf{z}-\sqrt{\Delta_n}\mathbf{k})\exp\big[2\pi\mathrm{i}\chi(\mathbf{u}\cdot\mathbf{y}_{j,l})^\top\mathbf{z}\Delta_n^{-1/2}\big]\,\mathrm{d}\mathbf{z}\bigg)\bigg| \\ &\quad+\frac{\pi^l\prod_{i=1}^l y_{j_i}}{2^{l-1}\prod_{i=1}^l \sin(\pi y_{j_i})}\sum_{\mathbf{k}\in\mathbb{N}^d}\int_{a_{\mathbf{k-1}}}^{a_{\mathbf{k}}}\Big|\frac{1}{2}(\mathbf{z}-\sqrt{\Delta_n}\mathbf{k})^\top H_g(\xi)(\mathbf{z}-\sqrt{\Delta_n}\mathbf{k})\Big|\,\mathrm{d}\mathbf{z}.\end{aligned}$$

We employ a similar approach as for the term T_1, given in the equations (81) and (86), for the second integral, leading to the term

$$\begin{aligned}|S_{1,\mathbf{u}}| &\leqslant \frac{\pi^l\prod_{i=1}^l y_{j_i}}{2^{l-1}\prod_{i=1}^l \sin(\pi y_{j_i})}\bigg|\sum_{\mathbf{k}\in\mathbb{N}^d}\int_{a_{\mathbf{k-1}}}^{a_{\mathbf{k}}}\nabla g(\sqrt{\Delta_n}\mathbf{k})^\top(\mathbf{z}-\sqrt{\Delta_n}\mathbf{k})\cos\big[2\pi\chi(\mathbf{u}\cdot\mathbf{y}_{j,l})^\top\mathbf{z}\Delta_n^{-1/2}\big]\,\mathrm{d}\mathbf{z}\bigg| \\ &\quad+\mathcal{O}\bigg(\frac{\Delta_n}{\delta^l}\int_{\sqrt{\Delta_n}}^1 r^{d+1}|f''(r^2)|\,\mathrm{d}r\vee\frac{\Delta_n}{\delta^l}\int_{\sqrt{\Delta_n}}^1 r^{d-1}|f'(r^2)|\,\mathrm{d}r\bigg).\end{aligned}$$

Employing equation (87), we obtain

$$\begin{aligned}|S_1| &\leqslant \frac{\pi^l\prod_{i=1}^l y_{j_i}}{\prod_{i=1}^l \sin(\pi y_{j_i})}\bigg|\sum_{\mathbf{k}\in\mathbb{N}^d}\int_{a_{\mathbf{k-1}}}^{a_{\mathbf{k}}}\nabla g(\sqrt{\Delta_n}\mathbf{k})^\top(\mathbf{z}-\sqrt{\Delta_n}\mathbf{k})\cos(2\pi y_{j_1}z_{j_1}\Delta_n^{-1/2})\cdots\cos(2\pi y_{j_l}z_{j_l}\Delta_n^{-1/2})\,\mathrm{d}\mathbf{z}\bigg| \\ &\quad+\mathcal{O}\bigg(\frac{\Delta_n}{\delta^l}\int_{\sqrt{\Delta_n}}^1 r^{d+1}|f''(r^2)|\,\mathrm{d}r\vee\frac{\Delta_n}{\delta^l}\int_{\sqrt{\Delta_n}}^1 r^{d-1}|f'(r^2)|\,\mathrm{d}r\bigg).\end{aligned}$$

Let $\mathbf{k}\in\mathbb{N}^d$, then it holds that

$$\begin{aligned}&\int_{a_{\mathbf{k-1}}}^{a_{\mathbf{k}}}\nabla g(\sqrt{\Delta_n}\mathbf{k})^\top(\mathbf{z}-\sqrt{\Delta_n}\mathbf{k})\cos(2\pi y_{j_1}z_{j_1}\Delta_n^{-1/2})\cdots\cos(2\pi y_{j_l}z_{j_l}\Delta_n^{-1/2})\,\mathrm{d}\mathbf{z} \\ &=\sum_{l=1}^d\int_{a_{\mathbf{k-1}}}^{a_{\mathbf{k}}}g'_{z_l}(\sqrt{\Delta_n}\mathbf{k})(z_l-\sqrt{\Delta_n}k_l)\cos(2\pi y_{j_1}z_{j_1}\Delta_n^{-1/2})\cdots\cos(2\pi y_{j_l}z_{j_l}\Delta_n^{-1/2})\,\mathrm{d}\mathbf{z}.\end{aligned}$$

Firstly, for $\tilde{l}\notin\{j_1,\ldots,j_l\}$, we have

$$\int_{a_{k_{j_1}-1}}^{a_{k_{j_1}}}\cos(2\pi y_{j_1}z_{j_1}\Delta_n^{-1/2})\,\mathrm{d}z_{j_1}\cdots\int_{a_{k_{j_l}-1}}^{a_{k_{j_l}}}\cos(2\pi y_{j_l}z_{j_l}\Delta_n^{-1/2})\,\mathrm{d}z_{j_l}\int_{a_{k_{j_{\tilde{l}}}-1}}^{a_{k_{j_{\tilde{l}}}}}(z_{j_{\tilde{l}}}-\sqrt{\Delta_n}k_{j_{\tilde{l}}})\,\mathrm{d}z_{j_{\tilde{l}}}=0,$$

since it holds that

$$\int_{\sqrt{\Delta_n}(\tilde{k}-1/2)}^{\sqrt{\Delta_n}(\tilde{k}+1/2)}(x-\sqrt{\Delta_n}\tilde{k})\,\mathrm{d}x=\int_{-\sqrt{\Delta_n}/2}^{\sqrt{\Delta_n}/2}x=0,$$

for a $\tilde{k} \in \mathbb{N}$. Suppose $\tilde{l} \in \{j_1, \dots, j_l\}$, then we obtain

$$\int_{a_{k_{j_1}-1}}^{a_{k_{j_1}}} \cos(2\pi y_{j_1} z_{j_1} \Delta_n^{-1/2})\,\mathrm{d}z_{j_1} \cdots \int_{a_{k_{j_{\tilde{l}}}-1}}^{a_{k_{j_{\tilde{l}}}}} (z_{j_{\tilde{l}}} - \sqrt{\Delta_n} k_{j_{\tilde{l}}}) \cos(2\pi y_{j_{\tilde{l}}} z_{j_{\tilde{l}}} \Delta_n^{-1/2})\,\mathrm{d}z_{j_{\tilde{l}}} \cdots \int_{a_{k_{j_l}-1}}^{a_{k_{j_l}}} \cos(2\pi y_{j_l} z_{j_l} \Delta_n^{-1/2})\,\mathrm{d}z_{j_l}.$$

For $\tilde{k} \in \mathbb{N}$ and $\tilde{y} \in [\delta, 1-\delta]$, we have

$$\int_{\sqrt{\Delta_n}(\tilde{k}-1/2)}^{\sqrt{\Delta_n}(\tilde{k}+1/2)} \cos(2\pi \tilde{y} x \Delta_n^{-1/2})\,\mathrm{d}x = \frac{\sqrt{\Delta_n}\cos(2\pi\tilde{y}\tilde{k})\sin(\pi\tilde{y})}{\pi\tilde{y}} = \mathcal{O}(\Delta_n^{1/2}/\delta),$$

and by a linear transformation we obtain that

$$\begin{aligned}\int_{\sqrt{\Delta_n}(\tilde{k}-1/2)}^{\sqrt{\Delta_n}(\tilde{k}+1/2)} (x - \sqrt{\Delta_n}\tilde{k}) \cos(2\pi \tilde{y} x \Delta_n^{-1/2})\,\mathrm{d}x &= \int_{-\sqrt{\Delta_n}/2}^{\sqrt{\Delta_n}/2} x \cos(2\pi\tilde{y}(x + \sqrt{\Delta_n}\tilde{k})\Delta_n^{-1/2})\,\mathrm{d}x \\ &= \frac{\Delta_n\big(\pi\tilde{y}\cos(\pi\tilde{y}) - \sin(\pi\tilde{y})\big)}{2\pi^2\tilde{y}^2}\sin(2\pi\tilde{k}\tilde{y}). \end{aligned} \tag{94}$$

Hence, we get for $1 \leqslant l \leqslant d-1$ that

$$\begin{aligned}|S_1| = \mathcal{O}\bigg(&\frac{\Delta_n^{(d+1)/2}}{\delta} \sum_{i=1}^{l} \sum_{\mathbf{k}\in\mathbb{N}^d} |g'_{z_{j_i}}(\sqrt{\Delta_n}\mathbf{k}) \cos(2\pi y_{j_1} k_{j_1}) \cdots \cos(2\pi y_{j_{i-1}} k_{j_{i-1}}) \sin(2\pi k_{j_i} y_{j_i}) \\ &\times \cos(2\pi y_{j_{i+1}} k_{j_{i+1}}) \cdots \cos(2\pi y_{j_l} k_{j_l})|\bigg) + \mathcal{O}\bigg(\frac{\Delta_n}{\delta^l}\int_{\sqrt{\Delta_n}}^1 r^{d+1}|f''(r^2)|\,\mathrm{d}r \vee \frac{\Delta_n}{\delta^l}\int_{\sqrt{\Delta_n}}^1 r^{d-1}|f'(r^2)|\,\mathrm{d}r\bigg),\end{aligned}$$

where we set $y_{j_0} = y_{j_{l+1}} = 0$. It remains to determine the order of the series. Therefore, we use the following identity:

$$\sin(x_1)\cos(x_2)\cdot\ldots\cdot\cos(x_n) = \frac{1}{2^{n-1}}\sum_{\mathbf{u}\in C_n}\sin(\mathbf{u}^\top\mathbf{x}),$$

where $\mathbf{x} = (x_1, \dots, x_n) \in \mathbb{R}^n$ and $C_n = \{1\} \times \{-1, 1\}^{n-1}$. This identity can be proven similarly to identity in display (87). Without loss of generality, we set the coordinates of the sine term to be j_1, leading to the expression

$$\begin{aligned}&\sum_{\mathbf{k}\in\mathbb{N}^d} g'_{z_{j_1}}(\sqrt{\Delta_n}\mathbf{k})\sin(2\pi k_{j_1} y_{j_1})\cos(2\pi y_{j_2} k_{j_2})\cdots\cos(2\pi y_{j_l} k_{j_l}) \\ &\quad= \frac{1}{2^{l-1}}\sum_{\mathbf{u}\in C_l}\sum_{\mathbf{k}\in\mathbb{N}^d} g'_{z_{j_1}}(\sqrt{\Delta_n}\mathbf{k})\sin\big(2\pi(\mathbf{u}^\top(\mathbf{y}\bullet\mathbf{k})_{j,l}\big),\end{aligned}$$

where $(\mathbf{y}\bullet\mathbf{k})_{j,l} := (k_{j_1} y_{j_1}, \dots, k_{j_l} y_{j_l})$. By following similar steps as in display (88), we find that

$$\begin{aligned}&\Delta_n^{(d+1)/2}\sum_{\mathbf{k}\in\mathbb{N}^d} g'_{z_{j_1}}(\sqrt{\Delta_n}\mathbf{k})\sin(2\pi k_{j_1} y_{j_1})\cos(2\pi y_{j_2} k_{j_2})\cdots\cos(2\pi y_{j_l} k_{j_l}) \\ &= \sum_{\mathbf{u}\in C_l}\mathrm{Im}\bigg(\frac{\Delta_n^{1/2}\pi^l\prod_{i=1}^l y_{j_i}}{2^{l-1}\prod_{i=1}^l\sin(\pi y_{j_i})}\mathcal{F}\Big[\sum_{\mathbf{k}\in\mathbb{N}^d} g'_{z_{j_1}}(\sqrt{\Delta_n}\mathbf{k})\mathbb{1}_{(a_{\mathbf{k-1}}, a_{\mathbf{k}}]}\Big]\big(-2\pi\chi(\mathbf{u}\bullet\mathbf{y}_{j,l})\Delta_n^{-1/2}\big)\bigg) =: U_1 + U_2 - U_3,\end{aligned}$$

where $U_i := \sum_{\mathbf{u}\in C_l} U_{i,\mathbf{u}}$ for $i=1,2,3$ and

$$U_{1,\mathbf{u}} := \operatorname{Im}\bigg(\frac{\Delta_n^{1/2}\pi^l\prod_{i=1}^l y_{j_i}}{2^{l-1}\prod_{i=1}^l\sin(\pi y_{j_i})}\mathcal{F}\bigg[\sum_{\mathbf{k}\in\mathbb{N}^d} g'_{z_{j_1}}(\sqrt{\Delta}_n\mathbf{k})\mathbb{1}_{(a_{\mathbf{k-1}},a_{\mathbf{k}}]} - g'_{z_{j_1}}\mathbb{1}_{(\sqrt{\Delta}_n/2,\infty)^d}\bigg]\big(-2\pi\chi(\mathbf{u}\cdot\mathbf{y}_{j,l})\Delta_n^{-1/2}\big)\bigg),$$

$$U_{2,\mathbf{u}} := \operatorname{Im}\bigg(\frac{\Delta_n^{1/2}\pi^l\prod_{i=1}^l y_{j_i}}{2^{l-1}\prod_{i=1}^l\sin(\pi y_{j_i})}\mathcal{F}\Big[g'_{z_{j_1}}\mathbb{1}_{(\sqrt{\Delta}_n/2,\infty)^d\cup B_{\gamma_{j,l}}}\Big]\big(-2\pi\chi(\mathbf{u}\cdot\mathbf{y}_{j,l})\Delta_n^{-1/2}\big)\bigg),$$

$$U_{3,\mathbf{u}} := \operatorname{Im}\bigg(\frac{\Delta_n^{1/2}\pi^l\prod_{i=1}^l y_{j_i}}{2^{l-1}\prod_{i=1}^l\sin(\pi y_{j_i})}\mathcal{F}\Big[g'_{z_{j_1}}\mathbb{1}_{B_{\gamma_{j,l}}}\Big]\big(-2\pi\chi(\mathbf{u}\cdot\mathbf{y}_{j,l})\Delta_n^{-1/2}\big)\bigg).$$

By employing the inequality $\|\mathcal{F}[f]\|_\infty \leqslant \|f\|_{\mathcal{L}_1}$, we obtain, for a $\mathbf{u}\in C_l$:

$$\begin{aligned}|U_{1,\mathbf{u}}| &\leqslant \frac{\Delta_n^{1/2}\pi^l\prod_{i=1}^l y_{j_i}}{2^{l-1}\prod_{i=1}^l\sin(\pi y_{j_i})}\bigg\|\sum_{\mathbf{k}\in\mathbb{N}^d} g'_{z_{j_1}}(\sqrt{\Delta}_n\mathbf{k})\mathbb{1}_{(a_{\mathbf{k-1}},a_{\mathbf{k}}]} - g'_{z_{j_1}}\mathbb{1}_{(\sqrt{\Delta}_n/2,\infty)^d}\bigg\|_{\mathcal{L}_1(\mathbb{R}^d)}\\ &\leqslant \frac{\Delta_n^{1/2}\pi^l\prod_{i=1}^l y_{j_i}}{2^{l-1}\prod_{i=1}^l\sin(\pi y_{j_i})}\sum_{\mathbf{k}\in\mathbb{N}^d}\int_{\mathbb{R}^d}\big|g'_{z_{j_1}}(\sqrt{\Delta}_n\mathbf{k}) - g'_{z_{j_1}}(\mathbf{z})\big|\mathbb{1}_{(a_{\mathbf{k-1}},a_{\mathbf{k}}]}(\mathbf{z})\,\mathrm{d}\mathbf{z}.\end{aligned}$$

Applying Taylor's expansion, we find that

$$|U_{1,\mathbf{u}}| \leqslant \frac{\Delta_n^{1/2}\pi^l\prod_{i=1}^l y_{j_i}}{2^{l-1}\prod_{i=1}^l\sin(\pi y_{j_i})}\sum_{\mathbf{k}\in\mathbb{N}^d}\int_{a_{\mathbf{k-1}}}^{a_{\mathbf{k}}}\big|\nabla g'_{z_{j_1}}(\xi_{\mathbf{k}})^\top(\mathbf{z}-\sqrt{\Delta}_n\mathbf{k})\big|\,\mathrm{d}\mathbf{z}.$$

Following analogous steps as for the term T_1, we have for $\mathbf{k}\in[a_{\mathbf{k-1}},a_{\mathbf{k}}]$ that

$$\begin{aligned}\nabla g'_{z_{j_1}}(\mathbf{z})^\top(\mathbf{z}-\sqrt{\Delta}_n\mathbf{k}) &= \sum_{l=1}^d\frac{\partial^2}{\partial z_{j_1}\partial z_l}g(\mathbf{z})(z_l-\sqrt{\Delta}_n k_l)\\ &\leqslant C\sqrt{\Delta}_n\Big(f''(\pi^2\eta\|\mathbf{z}\|_2^2)(dz_{j_1}^2+\|\mathbf{z}\|_2^2) + f'(\pi^2\eta\|\mathbf{z}\|_2^2)\Big),\end{aligned}$$

and therefore, it holds that

$$\begin{aligned}|U_{1,\mathbf{u}}| &= \mathcal{O}\bigg(\frac{\Delta_n}{\delta^l}\int_{[\sqrt{\Delta}_n/2,\infty)^d}\|\mathbf{z}\|_2^2 f''(\pi^2\eta\|\mathbf{z}\|_2^2)\,\mathrm{d}\mathbf{z} + \frac{\Delta_n}{\delta^l}\int_{[\sqrt{\Delta}_n/2,\infty)^d} f'(\pi^2\eta\|\mathbf{z}\|_2^2)\,\mathrm{d}\mathbf{z}\bigg)\\ &= \mathcal{O}\bigg(\frac{\Delta_n}{\delta^l}\Big(\int_{\sqrt{\Delta}_n/2}^\infty r^{d+1}f''(r^2)\,\mathrm{d}r + \int_{\sqrt{\Delta}_n/2}^\infty r^{d-1}f'(r^2)\,\mathrm{d}r\Big)\bigg)\\ &= \mathcal{O}\bigg(\frac{\Delta_n}{\delta^l}\int_{\sqrt{\Delta}_n}^1 r^{d+1}f''(r^2)\,\mathrm{d}r \vee \frac{\Delta_n}{\delta^l}\int_{\sqrt{\Delta}_n}^1 r^{d-1}f'(r^2)\,\mathrm{d}r\bigg).\end{aligned}$$

Note that U_1 is of the same order as $U_{1,\mathbf{u}}$. Using display (92) with $q=1$ we have for $U_{2,\mathbf{u}}$ that

$$|U_{2,\mathbf{u}}| = \mathcal{O}\bigg(\frac{\Delta_n\pi^{l-1}\prod_{i=2}^l y_{j_i}}{2^l\prod_{i=1}^l\sin(\pi y_{j_i})}\bigg\|\frac{\partial^2}{\partial z_{j_1}^2}g\mathbb{1}_{(\sqrt{\Delta}_n/2,\infty)^d\cup B_{\gamma_{j,l}}}\bigg\|_{\mathcal{L}_1}\bigg).$$

Utilizing the order of the term S_2 yields the following:

$$|U_2| = \mathcal{O}\bigg(\max_{k=0,\dots,l}\frac{\Delta_n^{k/2+1}}{\delta^l}\int_{\sqrt{\Delta}_n}^1 r^{d-k+1}|f''(r^2)|\,\mathrm{d}r \vee \max_{k=0,\dots,l}\frac{\Delta_n^{k/2+1}}{\delta^l}\int_{\sqrt{\Delta}_n}^1 r^{d-k-1}|f'(r^2)|\,\mathrm{d}r\bigg).$$

For the last term U_3 we have with the equations (92) and (85) that

$$\begin{aligned} U_{3,\mathbf{u}} &= \mathcal{O}\bigg(\frac{\Delta_n \pi^{l-1} \prod_{i=2}^l y_{j_i}}{2^l \prod_{i=1}^l \sin(\pi y_{j_i})} \bigg\| \frac{\partial^2}{\partial y_{j_1}^2} g \mathbb{1}_{B_{\gamma_{j,l}}} \bigg\|_{\mathcal{L}_1} \bigg) \\ &= \mathcal{O}\bigg(\frac{\Delta_n}{\delta^l} \Big(\Delta_n^{l/2} \int_{\sqrt{\Delta_n}}^1 r^{d-l+1} f''(r)\,\mathrm{d}r + \Delta_n^{l/2} \int_{\sqrt{\Delta_n}}^1 r^{d-l-1} f'(r)\,\mathrm{d}r \Big) \bigg) \\ &= \mathcal{O}\bigg(\frac{\Delta_n^{l/2+1}}{\delta^l} \int_{\sqrt{\Delta_n}}^1 r^{d-l+1} f''(r)\,\mathrm{d}r \vee \frac{\Delta_n^{l/2+1}}{\delta^l} \int_{\sqrt{\Delta_n}}^1 r^{d-l-1} f'(r)\,\mathrm{d}r \bigg). \end{aligned}$$

Hence, we find

$$|S_1| = \mathcal{O}\bigg(\max_{k=0,\dots,l} \frac{\Delta_n^{k/2+1}}{\delta^{l+1}} \int_{\sqrt{\Delta_n}}^1 r^{d-k+1} |f''(r^2)|\,\mathrm{d}r \vee \max_{k=0,\dots,l} \frac{\Delta_n^{k/2+1}}{\delta^{l+1}} \int_{\sqrt{\Delta_n}}^1 r^{d-k-1} |f'(r^2)|\,\mathrm{d}r \bigg) = |S_2|$$

and

$$\begin{aligned} &\Delta_n^{d/2} \sum_{\mathbf{k}\in\mathbb{N}^d} f(\lambda_{\mathbf{k}}\Delta_n) \cos(2\pi k_{j_1} y_{j_1}) \cdot \ldots \cdot \cos(2\pi k_{j_l} y_{j_l}) = T_2 + T_3 + \mathcal{O}(\Delta_n) \\ &= (-1)^l \int_{B_{\gamma_{j,l}}} g(\mathbf{z})\,\mathrm{d}\mathbf{z} + \mathcal{O}\bigg(\Delta_n^{(l+1)/2} \int_{\sqrt{\Delta_n}}^1 r^{d+1-l} |f'(r^2)|\,\mathrm{d}r \vee \frac{\Delta_n^{(l+1)/2}}{\delta^l} \int_{\sqrt{\Delta_n}}^1 r^{d-l} f'(r^2)\,\mathrm{d}r \bigg) \\ &\quad + \mathcal{O}\bigg(\max_{k=0,\dots,l} \frac{\Delta_n^{k/2+1}}{\delta^{l+1}} \int_{\sqrt{\Delta_n}}^1 r^{d-k+1} |f''(r^2)|\,\mathrm{d}r \vee \max_{k=0,\dots,l} \frac{\Delta_n^{k/2+1}}{\delta^{l+1}} \int_{\sqrt{\Delta_n}}^1 r^{d-k-1} |f'(r^2)|\,\mathrm{d}r \bigg), \end{aligned}$$

which completes the proof of (ii).
For the proof of (iii), we proceed in a manner similar to the proof of (ii). Firstly, for a $\gamma \in \{0,1\}^d$, with $\|\gamma\|_1 = d-1$, we find that

$$\Delta_n^{d/2} \sum_{\mathbf{k}\in\mathbb{N}^d} f(\lambda_{\mathbf{k}}\Delta_n) \cos(2\pi k_1 y_1) \cdot \ldots \cdot \cos(2\pi k_d y_d) =: T_2 + T_3 - T_4 + \mathcal{O}(\Delta_n),$$

where we redefine $T_i := \sum_{\mathbf{u}\in C_d} T_{i,\mathbf{u}}$, with $i = 2,3,4$, by the following:

$$\begin{aligned} T_{2,\mathbf{u}} &:= \mathrm{Re}\bigg(\frac{\pi^d \prod_{i=1}^d y_i}{2^{d-1} \prod_{i=1}^d \sin(\pi y_i)} \mathcal{F}\Big[\sum_{\mathbf{k}\in\mathbb{N}^d} g(\sqrt{\Delta_n}\mathbf{k}) \mathbb{1}_{(a_{\mathbf{k-1}}, a_{\mathbf{k}}]} - g \mathbb{1}_{[\sqrt{\Delta_n}/2,\infty)^d} \Big] \big(-2\pi (\mathbf{u}\cdot\mathbf{y}) \Delta_n^{-1/2} \big) \bigg), \\ T_{3,\mathbf{u}} &:= \mathrm{Re}\bigg(\frac{\pi^d \prod_{i=1}^d y_i}{2^{d-1} \prod_{i=1}^d \sin(\pi y_i)} \mathcal{F}\Big[g \mathbb{1}_{[\sqrt{\Delta_n}/2,\infty)^d \cup B_\gamma} \Big] \big(-2\pi (\mathbf{u}\cdot\mathbf{y}) \Delta_n^{-1/2} \big) \bigg), \\ T_{4,\mathbf{u}} &:= \mathrm{Re}\bigg(\frac{\pi^d \prod_{i=1}^d y_i}{2^{d-1} \prod_{i=1}^d \sin(\pi y_i)} \mathcal{F}\Big[g \mathbb{1}_{B_\gamma} \Big] \big(-2\pi (\mathbf{u}\cdot\mathbf{y}) \Delta_n^{-1/2} \big) \bigg), \end{aligned}$$

where $\mathbf{y} = (y_1,\dots,y_d) \in [\delta, 1-\delta]^d$. For T_2, we apply the same procedure as for S_1 in statement (ii) to obtain

$$\begin{aligned} |T_2| &= \mathcal{O}\bigg(\frac{\Delta_n^{(d+1)/2}}{\delta} \sum_{i=1}^d \sum_{\mathbf{k}\in\mathbb{N}^d} |g'_{z_i}(\sqrt{\Delta_n}\mathbf{k})| \cos(2\pi y_1 k_1) \cdots \cos(2\pi y_{i-1} k_{i-1}) \sin(2\pi k_i y_i) \\ &\quad \times \cos(2\pi y_{i+1} k_{i+1}) \cdots \cos(2\pi y_d k_d) \bigg) + \mathcal{O}\bigg(\frac{\Delta_n}{\delta^d} \int_{\sqrt{\Delta_n}}^1 r^{d+1} |f''(r^2)|\,\mathrm{d}r \vee \frac{\Delta_n}{\delta^d} \int_{\sqrt{\Delta_n}}^1 r^{d-1} |f'(r^2)|\,\mathrm{d}r \bigg) \end{aligned}$$

$$= \mathcal{O}\Big(\frac{\Delta_n^{(d+1)/2}}{\delta}\sum_{\mathbf{k}\in\mathbb{N}^d}|g'_{z_1}(\sqrt{\Delta_n}\mathbf{k})|\sin(2\pi y_1k_1)\cos(2\pi y_2k_2)\cdots\cos(2\pi y_dk_d)\Big)$$
$$+\mathcal{O}\Big(\frac{\Delta_n}{\delta^d}\int_{\sqrt{\Delta_n}}^1 r^{d+1}|f''(r^2)|\,\mathrm{d}r\vee\frac{\Delta_n}{\delta^d}\int_{\sqrt{\Delta_n}}^1 r^{d-1}|f'(r^2)|\,\mathrm{d}r\Big).$$

Furthermore, it holds that

$$\Delta_n^{(d+1)/2}\sum_{\mathbf{k}\in\mathbb{N}^d}g'_{z_1}(\sqrt{\Delta_n}\mathbf{k})\sin(2\pi k_1y_1)\cos(2\pi y_2k_2)\cdots\cos(2\pi y_dk_d)$$
$$=\sum_{\mathbf{u}\in C_l}\mathrm{Im}\left(\frac{\Delta_n^{1/2}\pi^d\prod_{i=1}^d y_i}{2^{d-1}\prod_{i=1}^d\sin(\pi y_i)}\mathcal{F}\Big[\sum_{\mathbf{k}\in\mathbb{N}^d}g'_{z_1}(\sqrt{\Delta_n}\mathbf{k})\mathbb{1}_{(a_{\mathbf{k-1}},a_{\mathbf{k}}]}\Big]\big(-2\pi(\mathbf{u}\cdot\mathbf{y})\Delta_n^{-1/2}\big)\right)=:U_1+U_2-U_3,$$

where we redefine $U_i:=\sum_{\mathbf{u}\in C_l}U_{i,\mathbf{u}}$, for $i=1,2,3$, by the following terms:

$$U_{1,\mathbf{u}}:=\mathrm{Im}\left(\frac{\Delta_n^{1/2}\pi^d\prod_{i=1}^d y_i}{2^{d-1}\prod_{i=1}^d\sin(\pi y_i)}\mathcal{F}\Big[\sum_{\mathbf{k}\in\mathbb{N}^d}g'_{z_{j_1}}(\sqrt{\Delta_n}\mathbf{k})\mathbb{1}_{(a_{\mathbf{k-1}},a_{\mathbf{k}}]}-g'_{z_{j_1}}\mathbb{1}_{(\sqrt{\Delta}_n/2,\infty)^d}\Big]\big(-2\pi(\mathbf{u}\cdot\mathbf{y})\Delta_n^{-1/2}\big)\right),$$
$$U_{2,\mathbf{u}}:=\mathrm{Im}\left(\frac{\Delta_n^{1/2}\pi^d\prod_{i=1}^d y_i}{2^{d-1}\prod_{i=1}^d\sin(\pi y_i)}\mathcal{F}\Big[g'_{z_{j_1}}\mathbb{1}_{(\sqrt{\Delta}_n/2,\infty)^d\cup B_\gamma}\Big]\big(-2\pi(\mathbf{u}\cdot\mathbf{y})\Delta_n^{-1/2}\big)\right),$$
$$U_{3,\mathbf{u}}:=-\mathrm{Im}\left(\frac{\Delta_n^{1/2}\pi^d\prod_{i=1}^d y_i}{2^{d-1}\prod_{i=1}^d\sin(\pi y_i)}\mathcal{F}\Big[g'_{z_{j_1}}\mathbb{1}_{B_\gamma}\Big]\big(-2\pi(\mathbf{u}\cdot\mathbf{y})\Delta_n^{-1/2}\big)\right).$$

For the term U_1, U_2 and U_3 we obtain the same order as in statement (ii), resulting in

$$|U_1|=\mathcal{O}\Big(\frac{\Delta_n}{\delta^d}\int_{\sqrt{\Delta_n}}^1 r^{d+1}|f''(r^2)|\,\mathrm{d}r\vee\frac{\Delta_n}{\delta^d}\int_{\sqrt{\Delta_n}}^1 r^{d-1}|f'(r^2)|\,\mathrm{d}r\Big),$$
$$|U_2|=\mathcal{O}\Big(\max_{k=0,\dots,d-1}\frac{\Delta_n^{k/2+1}}{\delta^d}\int_{\sqrt{\Delta_n}}^1 r^{d-k+1}|f''(r^2)|\,\mathrm{d}r\vee\max_{k=0,\dots,d-1}\frac{\Delta_n^{k/2+1}}{\delta^d}\int_{\sqrt{\Delta_n}}^1 r^{d-k-1}|f'(r^2)|\,\mathrm{d}r\Big),$$
$$|U_3|=\mathcal{O}\Big(\frac{\Delta_n^{(d+1)/2}}{\delta^d}\int_{\sqrt{\Delta_n}}^1 r^2|f''(r)|\,\mathrm{d}r\vee\frac{\Delta_n^{(d+1)/2}}{\delta^d}\int_{\sqrt{\Delta_n}}^1|f'(r)|\,\mathrm{d}r\Big).$$

Hence, we have

$$|T_2|=\mathcal{O}\Big(\max_{k=0,\dots,d-1}\frac{\Delta_n^{k/2+1}}{\delta^{d+1}}\int_{\sqrt{\Delta_n}}^1 r^{d-k+1}|f''(r^2)|\,\mathrm{d}r\vee\max_{k=0,\dots,d-1}\frac{\Delta_n^{k/2+1}}{\delta^{d+1}}\int_{\sqrt{\Delta_n}}^1 r^{d-k-1}|f'(r^2)|\,\mathrm{d}r\Big).$$

For T_3 we infer the same order as for S_2 in equation (93) and have $T_3=\mathcal{O}(T_2)$. For T_4 we set without loss of generality that $\gamma=\{1,\dots,1,0\}\in\{0,1\}^d$ and have

$$T_4=\frac{\pi^d\prod_{i=1}^d y_i}{\prod_{i=1}^d\sin(\pi y_i)}\int_{\sqrt{\Delta}_n/2}^\infty\cos(2\pi y_dz_d\Delta_n^{-1/2})\int_0^{\sqrt{\Delta}_n/2}\cos(2\pi y_{d-1}z_{d-1}\Delta_n^{-1/2})\cdots$$
$$\times\int_0^{\sqrt{\Delta}_n/2}g(\mathbf{z})\cos(2\pi y_1z_1\Delta_n^{-1/2})\,\mathrm{d}z_1\cdots\mathrm{d}z_{d-1}\,\mathrm{d}z_d.$$

Using analogous steps as in equations (89) and (91), we have

$$T_4 = \left(\frac{\Delta_n^{1/2}}{2}\right)^{d-1} \frac{\pi y_d}{\sin(\pi y_d)} \int_{\sqrt{\Delta}_n/2}^{\infty} \tilde{g}(\sqrt{\Delta}_n/2, \dots, \sqrt{\Delta}_n/2, z_d) \cos(2\pi y_d z_d \Delta_n^{-1/2}) \,\mathrm{d}z_d \\ + \mathcal{O}\Big(\frac{\Delta_n^{d/2}}{\delta^d} \int_{\sqrt{\Delta}_n}^{1} r f'(r^2) \,\mathrm{d}r\Big).$$

Integration by parts yields

$$\begin{aligned}
&\frac{\pi y_d}{\sin(\pi y_d)} \int_{\sqrt{\Delta}_n/2}^{\infty} \tilde{g}(\sqrt{\Delta}_n/2, \dots, \sqrt{\Delta}_n/2, z_d) \cos(2\pi y_d z_d \Delta_n^{-1/2}) \,\mathrm{d}z_d \\
&= \frac{\Delta_n^{1/2}}{2\sin(\pi y_d)} \Big[\tilde{g}(\sqrt{\Delta}_n/2, \dots, \sqrt{\Delta}_n/2, z_d) \sin(2\pi y_d z_d \Delta_n^{-1/2})\Big]_{\sqrt{\Delta}_n/2}^{\infty} \\
&\quad - \frac{\Delta_n^{1/2}}{2\sin(\pi y_d)} \int_{\sqrt{\Delta}_n/2}^{\infty} \frac{\partial}{\partial z_d} \tilde{g}(\sqrt{\Delta}_n/2, \dots, \sqrt{\Delta}_n/2, z_d) \sin(2\pi y_d z_d \Delta_n^{-1/2}) \,\mathrm{d}z_d \\
&= \mathcal{O}\Big(\Delta_n^{1/2} g(\sqrt{\Delta}_n/2, \dots, \sqrt{\Delta}_n/2)\Big) - I_d,
\end{aligned}$$

where

$$I_d := \frac{\Delta_n^{1/2}}{2\sin(\pi y_d)} \int_{\sqrt{\Delta}_n/2}^{\infty} \frac{\partial}{\partial z_d} \tilde{g}(\sqrt{\Delta}_n/2, \dots, \sqrt{\Delta}_n/2, z_d) \sin(2\pi y_d z_d \Delta_n^{-1/2}) \,\mathrm{d}z_d.$$

Furthermore, we have

$$I_d = \mathcal{O}\Big(\frac{\Delta_n^{1/2}}{\delta} \int_{\sqrt{\Delta}_n/2}^{\infty} z_d f'\big((d-1)\Delta_n/4 + z_d^2\big) \,\mathrm{d}z_d\Big) = \mathcal{O}\Big(\frac{\Delta_n^{1/2}}{\delta} \int_{\sqrt{\Delta}_n/2}^{1} r f'\big(r^2\big) \,\mathrm{d}r\Big)$$

and therefore, we find that

$$T_4 = \mathcal{O}\big(\Delta_n^{d/2} f(\Delta_n)\big) + \mathcal{O}\Big(\frac{\Delta_n^{d/2}}{\delta^d} \int_{\sqrt{\Delta}_n}^{1} r f'(r^2) \,\mathrm{d}r\Big).$$

Finally, we obtain that

$$\Delta_n^{d/2} \sum_{\mathbf{k} \in \mathbb{N}^d} f(\lambda_{\mathbf{k}} \Delta_n) \cos(2\pi k_1 y_1) \cdot \ldots \cdot \cos(2\pi k_d y_d) = \mathcal{O}\big(\Delta_n^{d/2} f(\Delta_n)\big) + \mathcal{O}\Big(\frac{\Delta_n^{d/2}}{\delta^d} \int_{\sqrt{\Delta}_n}^{1} r f'(r^2) \,\mathrm{d}r\Big) \\ + \mathcal{O}\Big(\max_{k=0,\dots,d-1} \frac{\Delta_n^{k/2+1}}{\delta^{d+1}} \int_{\sqrt{\Delta}_n}^{1} r^{d-k+1} |f''(r^2)| \,\mathrm{d}r \vee \max_{k=0,\dots,d-1} \frac{\Delta_n^{k/2+1}}{\delta^{d+1}} \int_{\sqrt{\Delta}_n}^{1} r^{d-k-1} |f'(r^2)| \,\mathrm{d}r\Big),$$

which completes the proof. □

Next, we present the proof of Corollary 4.2.2.

Proof of Corollary 4.2.2. Let $m \in \mathbb{N}$ and $\beta > 0$, with $\lim_{x\to 0} |h(x^2)/x^{-\beta}| = C < \infty$, for a function h. Then, it holds

$$\int_a^b x^m h(x^2) = \mathcal{O}\Big(\Big[\frac{x^{m-\beta+1}}{m-\beta+1}\Big]_a^b\Big) = \mathcal{O}\big(b^{m-\beta+1} + a^{m-\beta+1}\big),$$

for real numbers $a < b$ and $\beta \neq m+1$. Therefore, we have

$$\int_0^{\sqrt{\Delta_n}} r^{d-1} f(r^2)\,\mathrm{d}r = \mathcal{O}\big(\Delta_n^{(d-\beta_0)/2}\big), \qquad \Delta_n \int_{\sqrt{\Delta_n}}^1 r^{d-1} |f'(r^2)|\,\mathrm{d}r = \mathcal{O}\big(\Delta_n \vee \Delta_n^{(d+2-\beta_1)/2}\big)$$
$$\Delta_n \int_{\sqrt{\Delta_n}}^1 r^{d+1} |f''(r^2)|\,\mathrm{d}r = \mathcal{O}\big(\Delta_n \vee \Delta_n^{(d+4-\beta_2)/2}\big).$$

The first assertion is concluded by utilizing Lemma 4.2.1. Similarly, for $1 \leqslant l \leqslant d-1$ and $0 \leqslant k \leqslant l$, we get that

$$\frac{\Delta_n^{(l+1)/2}}{\delta^l} \int_{\sqrt{\Delta_n}}^1 r^{d-l} f'(r^2)\,\mathrm{d}r = \mathcal{O}\big(\delta^{-l}\Delta_n^{(l+1)/2} \vee \delta^{-l}\Delta_n^{(d+2-\beta_1)/2}\big),$$
$$\frac{\Delta_n^{k/2+1}}{\delta^{l+1}} \int_{\sqrt{\Delta_n}}^1 r^{d-k+1} |f''(r^2)|\,\mathrm{d}r = \mathcal{O}\big(\delta^{-(l+1)}\Delta_n^{k/2+1} \vee \delta^{-(l+1)}\Delta_n^{(d+4-\beta_2)/2}\big),$$
$$\frac{\Delta_n^{k/2+1}}{\delta^{l+1}} \int_{\sqrt{\Delta_n}}^1 r^{d-k-1} |f'(r^2)|\,\mathrm{d}r = \mathcal{O}\big(\delta^{-(l+1)}\Delta_n^{k/2+1} \vee \delta^{-(l+1)}\Delta_n^{(d+2-\beta_1)/2}\big).$$

The proof follows with the subsequent identity:

$$\Delta_n^{d/2} f(\Delta_n) = \mathcal{O}\big(\Delta_n^{(d-\beta_0)/2}\big). \qquad \square$$

Next, we proceed to prove that $f_\alpha, g_{\alpha,\tau} \in \mathcal{Q}_\beta$, where $\mathcal{Q}_\beta$ is defined in display (66).

Proof of Lemma 4.2.3. First, it holds that

$$\begin{aligned}\int_0^\infty \frac{e^{-cx}}{x^m}\,\mathrm{d}x &= \Big[\frac{1}{1-m} x^{1-m} e^{-cx}\Big]_0^\infty + \frac{c}{1-m}\int_0^\infty x^{1-m} e^{-cx}\,\mathrm{d}x \\ &= \frac{1}{1-m}\int_0^\infty \Big(\frac{u}{c}\Big)^{1-m} e^{-u}\,\mathrm{d}u = \frac{c^{m-1}}{1-m}\Gamma(2-m) = c^{m-1}\Gamma(1-m),\end{aligned} \tag{95}$$

for $m < 1$ and $c > 0$, where $\Gamma(z) = \int_0^\infty t^{z-1} e^{-t}\,\mathrm{d}t$ denotes the Gamma function for $z \in \mathbb{C}$ and $\mathrm{Re}(z) \notin \{0, -1, -2, \ldots\}$. Note that $\Gamma(1+z) = z\Gamma(z)$. By utilizing equation (95), we find

$$\int_0^\infty \frac{e^{-cx^2}}{x^m}\,\mathrm{d}x = \int_0^\infty \frac{e^{-cx}}{2x^{(m+1)/2}}\,\mathrm{d}x = \frac{c^{(m-1)/2}}{2}\Gamma\Big(\frac{1}{2} - \frac{m}{2}\Big), \tag{96}$$

where $m < 1$ and $c > 0$ and

$$\int_0^\infty \frac{1-e^{-cx^2}}{x^m}\,\mathrm{d}x = \Big[\frac{x^{1-m}}{1-m}\big(1-e^{-cx^2}\big)\Big]_0^\infty - \frac{2c}{1-m}\int_0^\infty x^{2-m} e^{-cx^2}\,\mathrm{d}x = -\frac{c^{(m-1)/2}}{2}\Gamma\Big(\frac{1}{2} - \frac{m}{2}\Big) < C, \tag{97}$$

for $1 < m < 3$, $c > 0$ and a constant $0 < C < \infty$. We begin by examining the conditions of the class $\mathcal{Q}_\beta$ for the functions f_α and $g_{\alpha,\tau}$. First and foremost, both functions f_α and $g_{\alpha,\tau}$ are evidently twice continuously differentiable. Here, we find

$$\begin{aligned}
f'_\alpha(x) &= \frac{e^{-x}}{x^{1+\alpha}} - (1+\alpha)\frac{1-e^{-x}}{x^{2+\alpha}},\\
f''_\alpha(x) &= -\frac{e^{-x}}{x^{1+\alpha}} - (1+\alpha)\frac{2e^{-x}}{x^{2+\alpha}} + (1+\alpha)(2+\alpha)\frac{1-e^{-x}}{x^{3+\alpha}},\\
g'_{\alpha,\tau}(x) &= e^{-x(\tau+1)}f_\alpha(x) - \frac{1+\alpha}{x}g_{\alpha,\tau}(x) - \tau g_{\alpha,\tau}(x),\\
g''_{\alpha,\tau}(x) &= -(\tau+1)e^{-x(\tau+1)}f_\alpha(x) + e^{-x(\tau+1)}f'_\alpha(x) + \frac{1+\alpha}{x^2}g_{\alpha,\tau}(x) - \frac{1+\alpha}{x}g'_{\alpha,\tau}(x) - \tau g'_{\alpha,\tau}(x).
\end{aligned}$$

Furthermore, we obtain

$$\int_1^\infty x^m e^{-x^2}\,\mathrm{d}x = \frac{1}{2}\int_1^\infty x^{(m-1)/2}e^{-x} = \frac{1}{2}\Gamma\big((m+1)/2, 1\big) \leqslant C, \tag{98}$$

and

$$\begin{aligned}
\int_1^\infty x^m(1-e^{-x^2})\,\mathrm{d}x &= \left[\frac{x^{m+1}}{m+1}(1-e^{-x^2})\right]_1^\infty - \frac{2}{m+1}\int_1^\infty x^{m+2}e^{-x^2}\,\mathrm{d}x\\
&= \left[\frac{x^{m+1}}{m+1}(1-e^{-x^2})\right]_1^\infty - \frac{1}{m+1}\Gamma\big((m+3)/2, 1\big) \leqslant C,
\end{aligned} \tag{99}$$

if $m < -1$. Here, $\Gamma(z,s) = \int_s^\infty t^{z-1}e^{-z}\,\mathrm{d}z$ denotes the upper incomplete Gamma function. For the left limit, we obtain in general

$$\lim_{x\to 0}\frac{1-e^{-x^2}}{x^{m-\beta}} = \lim_{x\to 0}\frac{2e^{-x^2}}{(m-\beta)x^{m-\beta-2}} < \infty \Leftrightarrow m-2 \leqslant \beta, \tag{100}$$

and

$$\lim_{x\to 0}\frac{e^{-x^2}}{x^{m-\beta}} < \infty \Leftrightarrow m \leqslant \beta. \tag{101}$$

Concerning the integration criteria for f_α, we have by equation (97) that $\|x^{d-1}f_\alpha(x^2)\|_{\mathcal{L}^1([0,\infty))}$ since $1 < 1+2\alpha' < 3$. The integration criteria for the first and second derivative, f' and f'', are established based on the equations (98) and (99), since it holds that $d-4-2\alpha = -2-\alpha' < -1$ and $(d+1)-6-2\alpha = -3-2\alpha' < -1$. Therefore, it remains to determine the parameters $\beta_0, \beta_1, \beta_2$, which are associated to f, f' and f'', respectively. Using the displays (100) and (101), we have $f \in \mathcal{Q}_\beta$, with

$$\beta_0 = 2\alpha, \qquad \beta_1 = 2(1+\alpha), \qquad \text{and} \qquad \beta_2 = 2(2+\alpha).$$

Starting with the analysis of the function $g_{\alpha,\tau}$, we find that

$$\begin{aligned}
x^m g_{\alpha,\tau}(x^2) &= \frac{1}{2}\left(\frac{e^{-\tau x^2}}{x^{2(1+\alpha)-m}} - 2\frac{e^{-x^2(\tau+1)}}{x^{2(1+\alpha)-m}} + \frac{e^{-x^2(\tau+2)}}{x^{2(1+\alpha)-m}}\right)\\
&= -\frac{1}{2}\left(\frac{1-e^{-\tau x^2}}{x^{2(1+\alpha)-m}} - 2\frac{1-e^{-x^2(\tau+1)}}{x^{2(1+\alpha)-m}} + \frac{1-e^{-x^2(\tau+2)}}{x^{2(1+\alpha)-m}}\right).
\end{aligned} \tag{102}$$

By using equation (97), we infer that $\|x^{d-1}g_{\alpha,\tau}(x^2)\|_{\mathcal{L}^1([0,\infty))}$, since $1<1+2\alpha'<3$. As for the integration criteria for the first and second derivatives of $g_{\alpha,\tau}$, we observe that the displays (98) and (99) apply to each term. Therefore, it remains to determine the parameter β. Here, for $x^{\beta_0}g_{\alpha,\tau}(x^2)$, we have $\beta_0=2\alpha$ due to the displays (102) and (100). For the first derivative, we find, using display (101), that

$$
\begin{aligned}
x^{\beta_1}e^{-x^2(\tau+1)}f_\alpha(x^2)&=e^{-x^2(\tau+1)}\frac{1-e^{-x^2}}{x^{2(1+\alpha)-\beta_1}}=\frac{e^{-x^2(\tau+1)}}{x^{2(1+\alpha)-\beta_1}}-\frac{e^{-x^2(\tau+2)}}{x^{2(1+\alpha)-\beta_1}}<\infty\Leftrightarrow\beta_1\geqslant 2\alpha,\\
x^{\beta_1}\frac{1+\alpha}{x^2}g_{\alpha,\tau}(x^2)&<\infty\Leftrightarrow\beta_1\geqslant 2(1+\alpha),\\
x^{\beta_1}\tau g_{\alpha,\tau}(x^2)&<\infty\Leftrightarrow\beta_1\geqslant 2\alpha,
\end{aligned}
$$

and therefore $\beta_1=2(1+\alpha)$. For the second derivative, we get, by using analogous argumentations, that $\beta_2=2(1+\alpha)$, which completes the proof. □

We conclude this section by presenting the proof of Lemma 4.2.4.

Proof of Lemma 4.2.4. Given that Lemma 4.2.3 establishes $f_\alpha\in\mathcal{Q}_{\beta_1}$ and $g_{\alpha,\tau}\in\mathcal{Q}_{\beta_2}$, with $\beta_1=\big(2\alpha,2(1+\alpha),2(2+\alpha)\big)$ and $\beta_2=\big(2\alpha,2(1+\alpha),2(1+\alpha)\big)$, we can employ Corollary 4.2.2 on these functions. In addition, by utilizing analogous steps as in equation (95), we find

$$
\int_0^\infty\frac{1-e^{-cx}}{x^m}=\frac{c^{m-1}}{m-1}\Gamma(2-m), \tag{103}
$$

for $1<m<2$ and $c>0$. Considering $\alpha=d/2-1+\alpha'$, where $\alpha'\in(0,1)$, and equation (103), we obtain the following:

$$
\begin{aligned}
\Delta_n^{d/2}\sum_{\mathbf{k}\in\mathbb{N}^d}f_\alpha(\lambda_{\mathbf{k}}\Delta_n)&=\frac{1}{2^d(\pi\eta)^{d/2}\Gamma(d/2)}\int_0^\infty x^{d/2-1}\frac{1-e^{-x}}{x^{1+\alpha}}\,\mathrm{d}x+R_{n,1}\\
&=\frac{1}{2^d(\pi\eta)^{d/2}\Gamma(d/2)}\int_0^\infty\frac{1-e^{-x}}{x^{1+\alpha'}}\,\mathrm{d}x+R_{n,1}\\
&=\frac{1}{2^d(\pi\eta)^{d/2}\Gamma(d/2)}\cdot\frac{\Gamma(1-\alpha')}{\alpha'}+R_{n,1},
\end{aligned}
$$

where

$$
\begin{aligned}
R_{n,1}&:=-\sum_{\substack{\|\gamma\|_1=1\\ \gamma\in\{0,1\}^d}}^{d-1}\int_{B_\gamma}f(\pi^2\eta\,\|\mathbf{z}\|_2^2)\,\mathrm{d}\mathbf{z}+\mathcal{O}\big(\Delta_n\vee\Delta_n^{(d-2\alpha)/2}\vee\Delta_n^{(d+2-2(1+\alpha))/2}\vee\Delta_n^{(d+4-2(2+\alpha))/2}\big)\\
&=-\sum_{\substack{\|\gamma\|_1=1\\ \gamma\in\{0,1\}^d}}^{d-1}\int_{B_\gamma}f(\pi^2\eta\,\|\mathbf{z}\|_2^2)\,\mathrm{d}\mathbf{z}+\mathcal{O}\big(\Delta_n^{1-\alpha'}\big).
\end{aligned}
$$

For statement (ii), we have

$$
\Delta_n^{d/2}\sum_{\mathbf{k}\in\mathbb{N}^d}g_{\alpha,\tau}(\lambda_{\mathbf{k}}\Delta_n)=\frac{1}{2^d(\pi\eta)^{d/2}\Gamma(d/2)}\int_0^\infty\frac{(1-e^{-x})^2}{2x^{1+\alpha'}}e^{-\tau x}\,\mathrm{d}x+R_{n,2}
$$

$$= \frac{1}{2^{d+1}(\pi\eta)^{d/2}\Gamma(d/2)}\left(\int_0^\infty \frac{e^{-\tau x}}{x^{1+\alpha'}} - 2\int_0^\infty \frac{e^{-x(1+\tau)}}{x^{1+\alpha'}} + \int_0^\infty \frac{e^{-x(2+\tau)}}{x^{1+\alpha}}\right) + R_{n,2}.$$

By using equation (95), we find that

$$\Delta_n^{d/2}\sum_{\mathbf{k}\in\mathbb{N}^d} g_{\alpha,\tau}(\lambda_{\mathbf{k}}\Delta_n) = \frac{\Gamma(1-\alpha')}{2^{d+1}(\pi\eta)^{d/2}\alpha'\Gamma(d/2)}\big(-\tau^{\alpha'} + 2(1+\tau)^{\alpha'} - (2+\tau)^{\alpha'}\big) + R_{n,2},$$

where

$$\begin{aligned} R_{n,2} &:= -\sum_{\substack{\|\gamma\|_1=1\\ \gamma\in\{0,1\}^d}}^{d-1}\int_{B_\gamma} f(\pi^2\eta\,\|\mathbf{z}\|_2^2)\,\mathrm{d}\mathbf{z} + \mathcal{O}\big(\Delta_n \vee \Delta_n^{(d-2\alpha)/2} \vee \Delta_n^{(d+2-2(1+\alpha))/2} \vee \Delta_n^{(d+4-2(1+\alpha))/2}\big) \\ &= -\sum_{\substack{\|\gamma\|_1=1\\ \gamma\in\{0,1\}^d}}^{d-1}\int_{B_\gamma} f(\pi^2\eta\,\|\mathbf{z}\|_2^2)\,\mathrm{d}\mathbf{z} + \mathcal{O}\big(\Delta_n^{1-\alpha'}\big). \end{aligned}$$

The proof follows by utilizing the following identity for half-integer arguments:

$$\Gamma(n/2) = \frac{(n-2)!!\sqrt{\pi}}{2^{(n-1)/2}}. \qquad \square$$

5. Asymptotic for the volatility estimators

In the beginning of Part II, we initiated an analysis of the temporal quadratic increments of the multi-dimensional SPDE model as defined in equation (49). By employing the method of moments, we derived two estimators for the volatility parameter σ^2. The first estimator is given by

$$\hat{\sigma}_n^2(\mathbf{y}) = \hat{\sigma}_{\mathbf{y}}^2 = \frac{2^d(\pi\eta)^{d/2}\alpha'\Gamma(d/2)}{n\Delta_n^{\alpha'}\Gamma(1-\alpha')}\sum_{i=1}^{n}(\Delta_i X)^2(\mathbf{y})e^{\|\kappa\bullet\mathbf{y}\|_1},$$

which can be directly inferred from Proposition 4.2.6. The second estimator is the robustified version of $\hat{\sigma}_{\mathbf{y}}^2$ and is given by

$$\hat{\sigma}^2 = \hat{\sigma}_{n,m}^2 = \frac{2^d(\pi\eta)^{d/2}\alpha'\Gamma(d/2)}{nm\Delta_n^{\alpha'}\Gamma(1-\alpha')}\sum_{j=1}^{m}\sum_{i=1}^{n}(\Delta_i X)^2(\mathbf{y}_j)e^{\|\kappa\bullet\mathbf{y}_j\|_1}.$$

The objective of this chapter is to establish asymptotic properties for the volatility estimators $\hat{\sigma}_{\mathbf{y}}^2$ and $\hat{\sigma}^2$, particularly proving central limit theorems. To accomplish this, we begin with a preparatory part in which we demonstrate that the initial condition can be substituted with a stationary initial condition to prove asymptotic properties. In the subsequent section, Section 5.2, we determine the variance-covariance structure of realized volatilities with an extra rescaling term. Proposition 4.2.7 has revealed dependencies between the increments $(\Delta_i X)(\mathbf{y})$ at two distinct temporal points, rendering standard methods for proving central limit theorems inapplicable. The authors Bibinger and Trabs (2020) demonstrated the applicability of a general central limit theorem based on ρ-mixing schemes in their one-dimensional SPDE model. More precisely, they used Proposition 1.2.4 for proving the CLT given in Proposition 1.2.3. In addition, we used Proposition 1.2.4 for proving CLTs for our novel estimators in Part I. For its application, it is essential to bound the temporal dependencies, which is formalized in Condition (IV) in Proposition 1.2.4. In the third section, we extend these results to multiple spatial dimensions and conclude by proving a central limit theorem for the robustified volatility estimator $\hat{\sigma}_{n,m}$, which implies a CLT for $\hat{\sigma}_n^2(\mathbf{y})$. Throughout this chapter, we assume that the parameters $\eta > 0$, $\alpha' \in (0,1)$, and $\kappa \in \mathbb{R}^d$ are known since both estimators rely on information about these parameters in the model.

5.1. Preparations

We begin this section by decomposing a temporal increment of a mild solution $\tilde{X}_t$ with a stationary initial condition $\langle \xi, e_{\mathbf{k}}\rangle_\vartheta \sim \mathcal{N}(0,\sigma^2/(2\lambda_{\mathbf{k}}^{1+\alpha}))$. For any initial condition, we can utilize the spectral decomposition similarly to Section 4.1, and thus we have $\Delta_i\tilde{X}(\mathbf{y}) = \sum_{\mathbf{k}\in\mathbb{N}^d}\Delta_i\tilde{x}_{\mathbf{k}}e_{\mathbf{k}}(\mathbf{y})$, where

$$\Delta_i\tilde{x}_{\mathbf{k}} = \Big(e^{-\lambda_{\mathbf{k}}i\Delta_n} - e^{-\lambda_{\mathbf{k}}(i-1)\Delta_n}\Big)\langle \xi, e_{\mathbf{k}}\rangle + B_{i,\mathbf{k}} + C_{i,\mathbf{k}}, \tag{104}$$

and $B_{i,\mathbf{k}}$ and $C_{i,\mathbf{k}}$ are defined as in equations (64) and (65), respectively. Having decomposed an arbitrary temporal increment of the coordinate processes $\Delta_i x_{\mathbf{k}}$ by separating the initial condition $A_{i,\mathbf{k}}$ from the evolution in time, i.e., $B_{i,\mathbf{k}}, C_{i,\mathbf{k}}$, it is intuitive that only the term $A_{i,\mathbf{k}}$ changes when $\Delta_i \tilde{x}_{\mathbf{k}}$ is decomposed. Furthermore, we proceed to analyse the term containing the stationary initial condition in equation (104). Therefore, consider the following Itô integral:

$$H(t) := \sigma\lambda_{\mathbf{k}}^{-\alpha/2}\int_{-\infty}^{0} e^{-\lambda_{\mathbf{k}}(t-s)}\big(e^{-\lambda_{\mathbf{k}}\Delta_n}-1\big)\,\mathrm{d}W_s^{\mathbf{k}},$$

where we extend the Brownian motions $(W^{\mathbf{k}})_{\mathbf{k}\in\mathbb{N}^d}$ to the whole real line for each $\mathbf{k}\in\mathbb{N}^d$. We can directly observe that $\mathbb{E}[H(t)]=0$. For two arbitrary time points $t,u>0$, we find the following covariance structure:

$$\begin{aligned}\mathbb{C}\mathrm{ov}\big(H(t),H(u)\big) &= \sigma^2\lambda_{\mathbf{k}}^{-\alpha}\big(e^{-\lambda_{\mathbf{k}}\Delta_n}-1\big)^2 e^{-\lambda_{\mathbf{k}}(t+u)}\mathbb{E}\Bigg[\bigg(\int_{-\infty}^{0} e^{\lambda_{\mathbf{k}}s}\,\mathrm{d}W_s^{\mathbf{k}}\bigg)^2\Bigg]\\ &= \sigma^2\lambda_{\mathbf{k}}^{-\alpha}\big(e^{-\lambda_{\mathbf{k}}\Delta_n}-1\big)^2 e^{-\lambda_{\mathbf{k}}(t+u)}\int_{-\infty}^{0} e^{2\lambda_{\mathbf{k}}s}\,\mathrm{d}s\\ &= \frac{\sigma^2}{2\lambda_{\mathbf{k}}^{1+\alpha}}\big(e^{-\lambda_{\mathbf{k}}\Delta_n}-1\big)^2 e^{-\lambda_{\mathbf{k}}(t+u)}.\end{aligned} \tag{105}$$

Setting $t=u=(i-1)\Delta_n$, we obtain

$$\mathbb{V}\mathrm{ar}\Big(H\big((i-1)\Delta_n\big)\Big) = \frac{\sigma^2}{2\lambda_{\mathbf{k}}^{1+\alpha}}\big(e^{-\lambda_{\mathbf{k}}\Delta_n-\lambda_{\mathbf{k}}(i-1)\Delta_n}-e^{-\lambda_{\mathbf{k}}(i-1)\Delta_n}\big)^2 = \frac{\sigma^2}{2\lambda_{\mathbf{k}}^{1+\alpha}}\big(e^{-\lambda_{\mathbf{k}}i\Delta_n}-e^{-\lambda_{\mathbf{k}}(i-1)\Delta_n}\big)^2.$$

Therefore, it holds that

$$\begin{aligned}\tilde{A}_{i,\mathbf{k}} := \langle\xi,e_{\mathbf{k}}\rangle_\vartheta\big(e^{-\lambda_{\mathbf{k}}i\Delta_n}-e^{-\lambda_{\mathbf{k}}(i-1)\Delta_n}\big) &= H\big((i-1)\Delta_n\big)\\ &= \sigma\lambda_{\mathbf{k}}^{-\alpha/2}\int_{-\infty}^{0} e^{-\lambda_{\mathbf{k}}((i-1)\Delta_n-s)}\big(e^{-\lambda_{\mathbf{k}}\Delta_n}-1\big)\,\mathrm{d}W_s^{\mathbf{k}}.\end{aligned}$$

By comparing the term $B_{i,\mathbf{k}}$ from equation (64) with the integral representation for $\tilde{A}_{i,\mathbf{k}}$, we deduce that

$$\begin{aligned}\Delta_i\tilde{x}_{\mathbf{k}} &= \tilde{A}_{i,\mathbf{k}} + B_{i,\mathbf{k}} + C_{i,\mathbf{k}} \qquad (106)\\ &= \sigma\lambda_{\mathbf{k}}^{-\alpha/2}\int_{-\infty}^{0} e^{-\lambda_{\mathbf{k}}((i-1)\Delta_n-s)}\big(e^{-\lambda_{\mathbf{k}}\Delta_n}-1\big)\,\mathrm{d}W_s^{\mathbf{k}}\\ &\quad + \sigma\lambda_{\mathbf{k}}^{-\alpha/2}\int_{0}^{(i-1)\Delta_n} e^{-\lambda_{\mathbf{k}}((i-1)\Delta_n-s)}\big(e^{-\lambda_{\mathbf{k}}\Delta_n}-1\big)\,\mathrm{d}W_s^{\mathbf{k}} + C_{i,\mathbf{k}}\\ &= \sigma\lambda_{\mathbf{k}}^{-\alpha/2}\int_{-\infty}^{(i-1)\Delta_n} e^{-\lambda_{\mathbf{k}}((i-1)\Delta_n-s)}\big(e^{-\lambda_{\mathbf{k}}\Delta_n}-1\big)\,\mathrm{d}W_s^{\mathbf{k}} + C_{i,\mathbf{k}}\\ &= \tilde{B}_{i,\mathbf{k}} + C_{i,\mathbf{k}},\end{aligned}$$

where

$$\tilde{B}_{i,\mathbf{k}} := \sigma\lambda_{\mathbf{k}}^{-\alpha/2} \int_{-\infty}^{(i-1)\Delta_n} e^{-\lambda_{\mathbf{k}}\big((i-1)\Delta_n - s\big)} \big(e^{-\lambda_{\mathbf{k}}\Delta_n} - 1\big)\,\mathrm{d}W_s^{\mathbf{k}}, \tag{107}$$

$$C_{i,\mathbf{k}} = \sigma\lambda_{\mathbf{k}}^{-\alpha/2} \int_{(i-1)\Delta_n}^{i\Delta_n} e^{-\lambda_{\mathbf{k}}(i\Delta_n - s)}\,\mathrm{d}W_s^{\mathbf{k}}. \tag{108}$$

Thus, $(\Delta_i \tilde{X})(\mathbf{y})$ is centred, Gaussian and stationary. To prove a central limit theorem based on Proposition 1.2.4 for the volatility estimator $\hat{\sigma}^2_{n,m}$, we define the associated weakly dependent preliminary triangular arrays as follows:

$$\xi_{n,i} := \frac{2^d(\pi\eta)^{d/2}\alpha'\Gamma(d/2)}{\sqrt{nm}\Delta_n^{\alpha'}\Gamma(1-\alpha')} \sum_{j=1}^m (\Delta_i X)^2(\mathbf{y}_j) e^{\|\kappa\cdot\mathbf{y}_j\|_1}.$$

In the following lemma, we prove that working with triangular arrays based on a mild solution with a stationary initial condition, i.e.:

$$\tilde{\xi}_{n,i} := \frac{2^d(\pi\eta)^{d/2}\alpha'\Gamma(d/2)}{\sqrt{nm}\Delta_n^{\alpha'}\Gamma(1-\alpha')} \sum_{j=1}^m (\Delta_i \tilde{X})^2(\mathbf{y}_j) e^{\|\kappa\cdot\mathbf{y}_j\|_1}, \tag{109}$$

is sufficient.

Lemma 5.1.1

On Assumptions 4.1.1 and 4.1.2, it holds that

$$\sqrt{m}_n \sum_{i=1}^n \Big((\Delta_i \tilde{X})^2(\mathbf{y}) - (\Delta_i X)^2(\mathbf{y}) \Big) \overset{\mathbb{P}}{\to} 0,$$

as $n \to \infty$.

Proof. We initiate the proof with the following:

$$(\Delta_i \tilde{X})^2(\mathbf{y}) - (\Delta_i X)^2(\mathbf{y}) = \sum_{\mathbf{k}_1,\mathbf{k}_2 \in \mathbb{N}} \Big(\Delta_i \tilde{x}_{\mathbf{k}_1} \Delta_i \tilde{x}_{\mathbf{k}_2} - \Delta_i x_{\mathbf{k}_1} \Delta_i x_{\mathbf{k}_2} \Big) e_{\mathbf{k}_1}(\mathbf{y}) e_{\mathbf{k}_2}(\mathbf{y}) = \tilde{T}_i - T_i,$$

where we define

$$\tilde{T}_i := \sum_{\mathbf{k}_1,\mathbf{k}_2 \in \mathbb{N}^d} \Big(\tilde{A}_{i,\mathbf{k}_1}\tilde{A}_{i,\mathbf{k}_2} + \tilde{A}_{i,\mathbf{k}_1}\big(B_{i,\mathbf{k}_2} + C_{i,\mathbf{k}_2}\big) + \tilde{A}_{i,\mathbf{k}_2}\big(B_{i,\mathbf{k}_1} + C_{i,\mathbf{k}_1}\big) \Big) e_{\mathbf{k}_1}(\mathbf{y}) e_{\mathbf{k}_2}(\mathbf{y}),$$

$$T_i := \sum_{\mathbf{k}_1,\mathbf{k}_2 \in \mathbb{N}^d} \Big(A_{i,\mathbf{k}_1}A_{i,\mathbf{k}_2} + A_{i,\mathbf{k}_1}\big(B_{i,\mathbf{k}_2} + C_{i,\mathbf{k}_2}\big) + A_{i,\mathbf{k}_2}\big(B_{i,\mathbf{k}_1} + C_{i,\mathbf{k}_1}\big) \Big) e_{\mathbf{k}_1}(\mathbf{y}) e_{\mathbf{k}_2}(\mathbf{y}).$$

It remains to show that $\sqrt{m}_n \sum_{i=1}^n T_i \overset{\mathbb{P}}{\to} 0$, since this implies $\sqrt{m}_n \sum_{i=1}^n \tilde{T}_i \overset{\mathbb{P}}{\to} 0$. Here, we have the following:

$$\sum_{i=1}^{n} T_i = \sum_{i=1}^{n}\Big(\sum_{\mathbf{k}\in\mathbb{N}^d} A_{i,\mathbf{k}} e_{\mathbf{k}}(\mathbf{y})\Big)^2 + 2\sum_{i=1}^{n}\Big(\sum_{\mathbf{k}\in\mathbb{N}^d} A_{i,\mathbf{k}} e_{\mathbf{k}}(\mathbf{y})\Big)\Big(\sum_{\mathbf{k}\in\mathbb{N}^d}\Big(B_{i,\mathbf{k}}+C_{i,\mathbf{k}}\Big)e_{\mathbf{k}}(\mathbf{y})\Big). \tag{110}$$

Using Hölder's inequality, we obtain

$$\begin{aligned}
\mathbb{E}\Bigg[\sum_{i=1}^{n}\Big(\sum_{\mathbf{k}\in\mathbb{N}^d} A_{i,\mathbf{k}} e_{\mathbf{k}}(\mathbf{y})\Big)^2\Bigg] &= \mathbb{E}\Bigg[\sum_{i=1}^{n}\sum_{\mathbf{k}\in\mathbb{N}^d} A_{i,\mathbf{k}}^2 e_{\mathbf{k}}^2(\mathbf{y})\Bigg] + \mathbb{E}\Bigg[\sum_{i=1}^{n}\sum_{\substack{\mathbf{k}_1,\mathbf{k}_2\in\mathbb{N}^d\\ \mathbf{k}_1\neq\mathbf{k}_2}} A_{i,\mathbf{k}_1}A_{i,\mathbf{k}_2}e_{\mathbf{k}_1}(\mathbf{y})e_{\mathbf{k}_2}(\mathbf{y})\Bigg]\\
&\leqslant C\mathbb{E}\Bigg[\sum_{i=1}^{n}\sum_{\mathbf{k}\in\mathbb{N}^d} A_{i,\mathbf{k}}^2\Bigg] + \mathbb{E}\Bigg[\Bigg|\sum_{i=1}^{n}\sum_{\substack{\mathbf{k}_1,\mathbf{k}_2\in\mathbb{N}^d\\ \mathbf{k}_1\neq\mathbf{k}_2}} A_{i,\mathbf{k}_1}A_{i,\mathbf{k}_2}e_{\mathbf{k}_1}(\mathbf{y})e_{\mathbf{k}_2}(\mathbf{y})\Bigg|\Bigg]\\
&\leqslant C\mathbb{E}\Bigg[\sum_{i=1}^{n}\sum_{\mathbf{k}\in\mathbb{N}^d} A_{i,\mathbf{k}}^2\Bigg] + \mathbb{E}\Bigg[\Bigg|\sum_{i=1}^{n}\sum_{\substack{\mathbf{k}_1,\mathbf{k}_2\in\mathbb{N}^d\\ \mathbf{k}_1\neq\mathbf{k}_2}} A_{i,\mathbf{k}_1}A_{i,\mathbf{k}_2}e_{\mathbf{k}_1}(\mathbf{y})e_{\mathbf{k}_2}(\mathbf{y})\Bigg|^2\Bigg]^{1/2},
\end{aligned}$$

where $C>0$ is a suitable constant. Let $C_\xi := \sup_{\mathbf{k}\in\mathbb{N}^d}\lambda_{\mathbf{k}}^{1+\alpha}\mathbb{E}[\langle\xi,e_{\mathbf{k}}\rangle_\vartheta^2]$. With analogous steps as in Lemma 4.2.5, we find

$$\begin{aligned}
\sum_{i=1}^{n}\sum_{\mathbf{k}\in\mathbb{N}^d}\mathbb{E}\big[A_{i,\mathbf{k}}^2\big] &= \sum_{i=1}^{n}\sum_{\mathbf{k}\in\mathbb{N}^d}\big(e^{-\lambda_{\mathbf{k}} i\Delta_n}-e^{-\lambda_{\mathbf{k}}(i-1)\Delta_n}\big)^2\mathbb{E}\Big[\langle\xi,e_{\mathbf{k}}\rangle_\vartheta^2\Big]\\
&= \sum_{i=1}^{n}\sum_{\mathbf{k}\in\mathbb{N}^d}\big(e^{-\lambda_{\mathbf{k}}\Delta_n}-1\big)^2 e^{-2\lambda_{\mathbf{k}}(i-1)\Delta_n}\mathbb{E}\Big[\langle\xi,e_{\mathbf{k}}\rangle_\vartheta^2\Big]\\
&\leqslant C_\xi\sum_{\mathbf{k}\in\mathbb{N}^d}\frac{\big(1-e^{-\lambda_{\mathbf{k}}\Delta_n}\big)^2}{\lambda_{\mathbf{k}}^{1+\alpha}}\sum_{i=1}^{n}e^{-2\lambda_{\mathbf{k}}(i-1)\Delta_n}\\
&\leqslant C_\xi\sum_{\mathbf{k}\in\mathbb{N}^d}\frac{\big(1-e^{-\lambda_{\mathbf{k}}\Delta_n}\big)^2}{\lambda_{\mathbf{k}}^{1+\alpha}(1-e^{-2\lambda_{\mathbf{k}}\Delta_n})}\\
&\leqslant C_\xi\sum_{\mathbf{k}\in\mathbb{N}^d}\frac{1-e^{-\lambda_{\mathbf{k}}\Delta_n}}{\lambda_{\mathbf{k}}^{1+\alpha}} = \mathcal{O}\big(\Delta_n^{\alpha'}\big).
\end{aligned} \tag{111}$$

Furthermore, we have

$$\begin{aligned}
&\mathbb{E}\Bigg[\Bigg|\sum_{i=1}^{n}\sum_{\substack{\mathbf{k}_1,\mathbf{k}_2\in\mathbb{N}^d\\ \mathbf{k}_1\neq\mathbf{k}_2}} A_{i,\mathbf{k}_1}A_{i,\mathbf{k}_2}e_{\mathbf{k}_1}(\mathbf{y})e_{\mathbf{k}_2}(\mathbf{y})\Bigg|^2\Bigg]\\
&= \sum_{i,j=1}^{n}\sum_{\substack{\mathbf{k}_1,\mathbf{k}_2\in\mathbb{N}^d\\ \mathbf{k}_1\neq\mathbf{k}_2}}\sum_{\substack{\mathbf{k}_3,\mathbf{k}_4\in\mathbb{N}^d\\ \mathbf{k}_3\neq\mathbf{k}_4}} e_{\mathbf{k}_1}(\mathbf{y})e_{\mathbf{k}_2}(\mathbf{y})e_{\mathbf{k}_3}(\mathbf{y})e_{\mathbf{k}_4}(\mathbf{y})\mathbb{E}\Big[A_{i,\mathbf{k}_1}A_{i,\mathbf{k}_2}A_{j,\mathbf{k}_3}A_{j,\mathbf{k}_4}\Big].
\end{aligned}$$

We assume that $\mathbb{E}[\langle\xi,e_{\mathbf{k}}\rangle_\vartheta]=0$ from Assumption 4.1.2. Then, for $\mathbf{k}_1=\mathbf{k}_3$ and $\mathbf{k}_2=\mathbf{k}_4$, we have

$$\sum_{i,j=1}^{n}\sum_{\substack{\mathbf{k}_1,\mathbf{k}_2\in\mathbb{N}^d\\ \mathbf{k}_1\neq\mathbf{k}_2}}\mathbb{E}\big[A_{i,\mathbf{k}_1}A_{i,\mathbf{k}_2}A_{j,\mathbf{k}_1}A_{j,\mathbf{k}_2}\big] = \sum_{i,j=1}^{n}\sum_{\substack{\mathbf{k}_1,\mathbf{k}_2\in\mathbb{N}^d\\ \mathbf{k}_1\neq\mathbf{k}_2}}\big(1-e^{-\lambda_{\mathbf{k}_1}\Delta_n}\big)^2\big(1-e^{-\lambda_{\mathbf{k}_2}\Delta_n}\big)^2$$

$$\times\, e^{-\lambda_{\mathbf{k}_1}(i+j-2)\Delta_n-\lambda_{\mathbf{k}_2}(i+j-2)\Delta_n}\mathbb{E}\Big[\langle\xi,e_{\mathbf{k}_1}\rangle_\vartheta^2\Big]\mathbb{E}\Big[\langle\xi,e_{\mathbf{k}_2}\rangle_\vartheta^2\Big]$$
$$\leqslant C_\xi^2\sum_{\substack{\mathbf{k}_1,\mathbf{k}_2\in\mathbb{N}^d\\ \mathbf{k}_1\neq\mathbf{k}_2}}\frac{\big(1-e^{-\lambda_{\mathbf{k}_1}\Delta_n}\big)^2\big(1-e^{-\lambda_{\mathbf{k}_2}\Delta_n}\big)^2}{\lambda_{\mathbf{k}_1}^{1+\alpha}\lambda_{\mathbf{k}_2}^{1+\alpha}}\sum_{i,j=1}^n e^{-(\lambda_{\mathbf{k}_1}+\lambda_{\mathbf{k}_2})(i+j-2)\Delta_n},$$

where an analogous result holds for the case $\mathbf{k}_1=\mathbf{k}_4$ and $\mathbf{k}_2=\mathbf{k}_3$. By using the geometric series, we obtain

$$\sum_{i,j=1}^n e^{-(\lambda_{\mathbf{k}_1}+\lambda_{\mathbf{k}_2})(i+j-2)\Delta_n}\leqslant\frac{1}{(1-e^{-(\lambda_{\mathbf{k}_1}+\lambda_{\mathbf{k}_2})\Delta_n})^2},$$

and therefore, we have

$$\sum_{i,j=1}^n\sum_{\substack{\mathbf{k}_1,\mathbf{k}_2\in\mathbb{N}^d\\ \mathbf{k}_1\neq\mathbf{k}_2}}\mathbb{E}\big[A_{i,\mathbf{k}_1}A_{i,\mathbf{k}_2}A_{j,\mathbf{k}_1}A_{j,\mathbf{k}_2}\big]\leqslant C_\xi^2\sum_{\mathbf{k}_1,\mathbf{k}_2\in\mathbb{N}^d}\frac{\big(1-e^{-\lambda_{\mathbf{k}_1}\Delta_n}\big)^2\big(1-e^{-\lambda_{\mathbf{k}_2}\Delta_n}\big)^2}{\lambda_{\mathbf{k}_1}^{1+\alpha}\lambda_{\mathbf{k}_2}^{1+\alpha}\big(1-e^{-(\lambda_{\mathbf{k}_1}+\lambda_{\mathbf{k}_2})\Delta_n}\big)^2}$$
$$\leqslant C_\xi^2\sum_{\mathbf{k}_1,\mathbf{k}_2\in\mathbb{N}^d}\frac{\big(1-e^{-\lambda_{\mathbf{k}_1}\Delta_n}\big)\big(1-e^{-\lambda_{\mathbf{k}_2}\Delta_n}\big)}{\lambda_{\mathbf{k}_1}^{1+\alpha}\lambda_{\mathbf{k}_2}^{1+\alpha}}=\mathcal{O}(\Delta_n^{2\alpha'}),$$

where we have used $(1-p)(1-q)/(1-pq)\leqslant 1-p$, for $0\leqslant p,q<1$. For the second option in Assumption 4.1.2, we use an analogous procedure as in Lemma 4.2.5. Here, we have with $C_\xi':=\sum_{\mathbf{k}\in\mathbb{N}}\lambda_{\mathbf{k}}^{1+\alpha}\mathbb{E}[\langle\xi,e_{\mathbf{k}}\rangle_\vartheta^2]<\infty$ and Parseval's identity that

$$\sum_{i,j=1}^n\sum_{\substack{\mathbf{k}_1,\mathbf{k}_2\in\mathbb{N}^d\\ \mathbf{k}_1\neq\mathbf{k}_2}}\sum_{\substack{\mathbf{k}_3,\mathbf{k}_4\in\mathbb{N}^d\\ \mathbf{k}_3\neq\mathbf{k}_4}}\mathbb{E}\big[A_{i,\mathbf{k}_1}A_{i,\mathbf{k}_2}A_{j,\mathbf{k}_3}A_{j,\mathbf{k}_4}\big]\leqslant\left(\sum_{i=1}^n\bigg(\sum_{\mathbf{k}\in\mathbb{N}^d}\mathbb{E}[A_{i,\mathbf{k}}]\bigg)^2\right)^2$$
$$\leqslant\left(\sum_{i=1}^n\bigg(\sum_{\mathbf{k}\in\mathbb{N}^d}\big(e^{-\lambda_{\mathbf{k}}\Delta_n}-1\big)e^{-\lambda_{\mathbf{k}}(i-1)\Delta_n}\mathbb{E}\Big[\big|\langle\xi,e_{\mathbf{k}}\rangle_\vartheta\big|\Big]\bigg)^2\right)^2$$
$$\leqslant\left(\sum_{i=1}^n\bigg(\sum_{\mathbf{k}\in\mathbb{N}^d}\frac{\big(e^{-\lambda_{\mathbf{k}}\Delta_n}-1\big)e^{-\lambda_{\mathbf{k}}(i-1)\Delta_n}}{\lambda_{\mathbf{k}}^{(1+\alpha)/2}}\lambda_{\mathbf{k}}^{(1+\alpha)/2}\mathbb{E}\Big[\langle\xi,e_{\mathbf{k}}\rangle_\vartheta^2\Big]^{1/2}\bigg)^2\right)^2$$
$$\leqslant\left(\sum_{i=1}^n\bigg(\sum_{\mathbf{k}\in\mathbb{N}^d}\frac{\big(1-e^{-\lambda_{\mathbf{k}}\Delta_n}\big)^2e^{-2\lambda_{\mathbf{k}}(i-1)\Delta_n}}{\lambda_{\mathbf{k}}^{1+\alpha}}\bigg)\bigg(\sum_{\mathbf{k}\in\mathbb{N}^d}\lambda_{\mathbf{k}}^{1+\alpha}\mathbb{E}\Big[\langle\xi,e_{\mathbf{k}}\rangle_\vartheta^2\Big]\bigg)\right)^2$$
$$\leqslant C_\xi'^2\left(\sum_{\mathbf{k}\in\mathbb{N}^d}\frac{(1-e^{-\lambda_{\mathbf{k}}\Delta_n})^2}{\lambda_{\mathbf{k}}^{1+\alpha}(1-e^{-2\lambda_{\mathbf{k}}\Delta_n})}\right)^2=\mathcal{O}(\Delta_n^{2\alpha'}).$$

By using Markov's inequality, we conclude with

$$\sum_{i=1}^n\bigg(\sum_{\mathbf{k}\in\mathbb{N}^d}A_{i,\mathbf{k}}e_{\mathbf{k}}(\mathbf{y})\bigg)^2=\mathcal{O}_{\mathbb{P}}(\Delta_n^{\alpha'}).$$

We proceed to bound the following term:

$$2\sum_{i=1}^n\bigg(\sum_{\mathbf{k}\in\mathbb{N}^d}A_{i,\mathbf{k}}e_{\mathbf{k}}(\mathbf{y})\bigg)\bigg(\sum_{\mathbf{k}\in\mathbb{N}^d}\Big(B_{i,\mathbf{k}}+C_{i,\mathbf{k}}\Big)e_{\mathbf{k}}(\mathbf{y})\bigg).$$

Utilizing the independence of $A_{i,\mathbf{k}}, B_{i,\mathbf{k}}$ and $C_{i,\mathbf{k}}$, we find that

$$\begin{aligned}
&\mathbb{E}\Bigg[\Big|\sum_{i=1}^{n}\Big(\sum_{\mathbf{k}\in\mathbb{N}^d} A_{i,\mathbf{k}}e_{\mathbf{k}}(\mathbf{y})\Big)\Big(\sum_{\mathbf{k}\in\mathbb{N}^d}\Big(B_{i,\mathbf{k}}+C_{i,\mathbf{k}}\Big)e_{\mathbf{k}}(\mathbf{y})\Big)\Big|^2\Bigg]\\
&=\sum_{i,j=1}^{n}\mathbb{E}\Bigg[\Big(\sum_{\mathbf{k}\in\mathbb{N}^d} A_{i,\mathbf{k}}e_{\mathbf{k}}(\mathbf{y})\Big)\Big(\sum_{\mathbf{k}\in\mathbb{N}^d} A_{j,\mathbf{k}}e_{\mathbf{k}}(\mathbf{y})\Big)\Bigg]\mathbb{E}\Bigg[\Big(\sum_{\mathbf{k}\in\mathbb{N}^d}\Big(B_{i,\mathbf{k}}+C_{i,\mathbf{k}}\Big)e_{\mathbf{k}}(\mathbf{y})\Big)\Big(\sum_{\mathbf{k}\in\mathbb{N}^d}\Big(B_{j,\mathbf{k}}+C_{j,\mathbf{k}}\Big)e_{\mathbf{k}}(\mathbf{y})\Big)\Bigg]\\
&=\sum_{i,j=1}^{n}\Bigg(\sum_{\mathbf{k}_1,\mathbf{k}_2\in\mathbb{N}^d}\mathbb{E}\big[A_{i,\mathbf{k}_1}A_{j,\mathbf{k}_2}\big]e_{\mathbf{k}_1}(\mathbf{y})e_{\mathbf{k}_2}(\mathbf{y})\Bigg)\Bigg(\sum_{\mathbf{k}_1,\mathbf{k}_2\in\mathbb{N}^d}\mathbb{E}\Big[\big(B_{i,\mathbf{k}_1}+C_{i,\mathbf{k}_1}\big)\big(B_{j,\mathbf{k}_2}+C_{j,\mathbf{k}_2}\big)\Big]e_{\mathbf{k}_1}(\mathbf{y})e_{\mathbf{k}_2}(\mathbf{y})\Bigg)\\
&=\sum_{i,j=1}^{n}\Bigg(\sum_{\mathbf{k}_1,\mathbf{k}_2\in\mathbb{N}^d}\mathbb{E}\big[A_{i,\mathbf{k}_1}A_{j,\mathbf{k}_2}\big]e_{\mathbf{k}_1}(\mathbf{y})e_{\mathbf{k}_2}(\mathbf{y})\Bigg)\Bigg(\sum_{\mathbf{k}\in\mathbb{N}^d}\mathbb{E}\Big[\big(B_{i,\mathbf{k}}+C_{i,\mathbf{k}}\big)\big(B_{j,\mathbf{k}}+C_{j,\mathbf{k}}\big)\Big]e_{\mathbf{k}}^2(\mathbf{y})\Bigg)=:\sum_{i,j=1}^{n}R_{i,j}S_{i,j},
\end{aligned}$$

where

$$\begin{aligned}
R_{i,j}&:=\sum_{\mathbf{k}_1,\mathbf{k}_2\in\mathbb{N}^d}\mathbb{E}\big[A_{i,\mathbf{k}_1}A_{j,\mathbf{k}_2}\big]e_{\mathbf{k}_1}(\mathbf{y})e_{\mathbf{k}_2}(\mathbf{y}),\\
S_{i,j}&:=\sum_{\mathbf{k}\in\mathbb{N}^d}\mathbb{E}\Big[\big(B_{i,\mathbf{k}}+C_{i,\mathbf{k}}\big)\big(B_{j,\mathbf{k}}+C_{j,\mathbf{k}}\big)\Big]e_{\mathbf{k}}^2(\mathbf{y}).
\end{aligned}$$

Assume the first option in Assumption 4.1.2 holds. Analogously to equation (111), we obtain that

$$R_{i,j}=\sum_{\mathbf{k}\in\mathbb{N}^d}\mathbb{E}\big[A_{i,\mathbf{k}}A_{j,\mathbf{k}}\big]e_{\mathbf{k}}^2(\mathbf{y})\leqslant CC_\xi\sum_{\mathbf{k}\in\mathbb{N}^d}\frac{(1-e^{-\lambda_{\mathbf{k}}\Delta_n})^2}{\lambda_{\mathbf{k}}^{1+\alpha}}e^{-\lambda_{\mathbf{k}}(i+j-2)\Delta_n}=\mathcal{O}\big(\Delta_n^{\alpha'}\big),$$

and therefore it holds that $\sum_{i,j=1}^{n}R_{i,j}=\mathcal{O}(\Delta_n^{\alpha'})$ and $\sup_{i,j=1,\dots,n}|R_{i,j}|=\mathcal{O}(\Delta_n^{\alpha'})$ as well as $\sup_{j=1,\dots,n}\sum_{i=1}^{n}|R_{i,j}|=\mathcal{O}(\Delta_n^{\alpha'})$. For the second option in Assumption 4.1.2, we find

$$\begin{aligned}
R_{i,j}&\leqslant C\sum_{\mathbf{k}_1,\mathbf{k}_2\in\mathbb{N}^d}\frac{\big(1-e^{-\lambda_{\mathbf{k}_1}\Delta_n}\big)\big(1-e^{-\lambda_{\mathbf{k}_2}\Delta_n}\big)}{\lambda_{\mathbf{k}_1}^{(1+\alpha)/2}\lambda_{\mathbf{k}_2}^{(1+\alpha)/2}}e^{-\big(\lambda_{\mathbf{k}_1}(i-1)+\lambda_{\mathbf{k}_2}(j-1)\big)\Delta_n}\\
&\quad\times\lambda_{\mathbf{k}_1}^{(1+\alpha)/2}\mathbb{E}\Big[\,|\langle\xi,e_{\mathbf{k}_1}\rangle_\vartheta|\,\Big]\lambda_{\mathbf{k}_2}^{(1+\alpha)/2}\mathbb{E}\Big[\,|\langle\xi,e_{\mathbf{k}_2}\rangle_\vartheta|\,\Big]\\
&\leqslant C\sum_{\mathbf{k}_1,\mathbf{k}_2\in\mathbb{N}^d}\frac{\big(1-e^{-\lambda_{\mathbf{k}_1}\Delta_n}\big)\big(1-e^{-\lambda_{\mathbf{k}_2}\Delta_n}\big)}{\lambda_{\mathbf{k}_1}^{(1+\alpha)/2}\lambda_{\mathbf{k}_2}^{(1+\alpha)/2}}e^{-\big(\lambda_{\mathbf{k}_1}(i-1)+\lambda_{\mathbf{k}_2}(j-1)\big)\Delta_n}\\
&\quad\times\lambda_{\mathbf{k}_1}^{(1+\alpha)/2}\mathbb{E}\Big[\,|\langle\xi,e_{\mathbf{k}_1}\rangle_\vartheta|^2\,\Big]^{1/2}\lambda_{\mathbf{k}_2}^{(1+\alpha)/2}\mathbb{E}\Big[\,|\langle\xi,e_{\mathbf{k}_2}\rangle_\vartheta|^2\,\Big]^{1/2}\\
&=C\sum_{\mathbf{k}_1\in\mathbb{N}^d}\frac{\big(1-e^{-\lambda_{\mathbf{k}_1}\Delta_n}\big)}{\lambda_{\mathbf{k}_1}^{(1+\alpha)/2}}e^{-\lambda_{\mathbf{k}_1}(i-1)\Delta_n}\lambda_{\mathbf{k}_1}^{(1+\alpha)/2}\mathbb{E}\Big[\,|\langle\xi,e_{\mathbf{k}_1}\rangle_\vartheta|^2\,\Big]^{1/2}\sum_{\mathbf{k}_2\in\mathbb{N}^d}\frac{\big(1-e^{-\lambda_{\mathbf{k}_2}\Delta_n}\big)}{\lambda_{\mathbf{k}_2}^{(1+\alpha)/2}}\\
&\quad\times e^{-\lambda_{\mathbf{k}_2}(j-1)\Delta_n}\lambda_{\mathbf{k}_2}^{(1+\alpha)/2}\mathbb{E}\Big[\,|\langle\xi,e_{\mathbf{k}_2}\rangle_\vartheta|^2\,\Big]^{1/2}\\
&\leqslant CC'_\xi\Bigg(\sum_{\mathbf{k}_1\in\mathbb{N}^d}\frac{\big(1-e^{-\lambda_{\mathbf{k}_1}\Delta_n}\big)^2}{\lambda_{\mathbf{k}_1}^{1+\alpha}}e^{-2\lambda_{\mathbf{k}_1}(i-1)\Delta_n}\sum_{\mathbf{k}_2\in\mathbb{N}^d}\frac{\big(1-e^{-\lambda_{\mathbf{k}_2}\Delta_n}\big)^2}{\lambda_{\mathbf{k}_2}^{1+\alpha}}e^{-2\lambda_{\mathbf{k}_2}(j-1)\Delta_n}\Bigg)^{1/2},
\end{aligned}$$

and therefore, we have

$$\sum_{i,j=1}^{n} R_{i,j} \leqslant CC'_\xi \sum_{\mathbf{k}\in\mathbb{N}^d} \frac{1-e^{-\lambda_\mathbf{k}\Delta_n}}{\lambda_\mathbf{k}^{1+\alpha}} = \mathcal{O}(\Delta_n^{\alpha'}).$$

Thus, we infer for both options in Assumption 4.1.2, that $\sup_{i,j}|R_{i,j}| = \mathcal{O}(\Delta_n^{\alpha'})$ and $\sup_j \sum_{i=1}^n |R_{i,j}| = \mathcal{O}(\Delta_n^{\alpha'})$. For the term $S_{i,j}$, we obtain

$$\begin{aligned} S_{i,j} &= \sum_{\mathbf{k}\in\mathbb{N}^d} \mathbb{E}\Big[\big(B_{i,\mathbf{k}}+C_{i,\mathbf{k}}\big)\big(B_{j,\mathbf{k}}+C_{j,\mathbf{k}}\big)\Big] e_\mathbf{k}^2(\mathbf{y}) \\ &= \sum_{\mathbf{k}\in\mathbb{N}^d} \Big(\Sigma_{i,j}^{B,\mathbf{k}} + \Sigma_{i,j}^{BC,\mathbf{k}} + \Sigma_{j,i}^{BC,\mathbf{k}} + \Sigma_{i,j}^{C,\mathbf{k}}\Big) e_\mathbf{k}^2(\mathbf{y}), \end{aligned}$$

where we used the notation of the proof of Proposition 4.2.7, where

$$\Sigma_{i,j}^{B,\mathbf{k}} := \mathbb{C}\mathrm{ov}(B_{i,\mathbf{k}}, B_{j,\mathbf{k}}), \qquad \Sigma_{i,j}^{BC,\mathbf{k}} := \mathbb{C}\mathrm{ov}(B_{i,\mathbf{k}}, C_{j,\mathbf{k}}), \qquad \Sigma_{i,j}^{C,\mathbf{k}} := \mathbb{C}\mathrm{ov}(C_{i,\mathbf{k}}, C_{j,\mathbf{k}}).$$

Upon inserting the calculations of Proposition 4.2.7, we infer for $i<j$ that

$$\begin{aligned} S_{i,j} &= \sum_{\mathbf{k}\in\mathbb{N}^d} \Big(\Sigma_{i,j}^{B,\mathbf{k}} + \Sigma_{j,i}^{BC,\mathbf{k}}\Big) e_\mathbf{k}^2(\mathbf{y}) \\ &\leqslant -\sigma^2 e^{-\|\kappa\bullet\mathbf{y}\|_1} \Delta_n^{\alpha'} \frac{\Gamma(1-\alpha')}{2^d(\pi\eta)^{d/2}\alpha'\Gamma(d/2)} \Big(-\frac{1}{2}\big(j-i-1\big)^{\alpha'} + \big(j-i\big)^{\alpha'} - \frac{1}{2}\big(j-i+1\big)^{\alpha'}\Big) \\ &\quad + C\sigma^2 \sum_{\mathbf{k}\in\mathbb{N}^d} e^{-\lambda_\mathbf{k}(i+j-2)\Delta_n} \frac{\big(1-e^{-\lambda_\mathbf{k}\Delta_n}\big)^2}{\lambda_\mathbf{k}^{1+\alpha}} + \mathcal{O}(\Delta_n). \end{aligned}$$

For $i=j$ we obtain

$$S_{i,i} = \sum_{\mathbf{k}\in\mathbb{N}^d} \Big(\Sigma_{ii}^{B,\mathbf{k}} + \Sigma_{ii}^{C,\mathbf{k}}\Big) e_\mathbf{k}^2(\mathbf{y}) \leqslant C\sigma^2 \sum_{\mathbf{k}\in\mathbb{N}^d} \left(\frac{\big(1-e^{-\lambda_\mathbf{k}\Delta_n}\big)^2}{2\lambda_\mathbf{k}^{1+\alpha}} + \frac{1-e^{-2\lambda_\mathbf{k}\Delta_n}}{2\lambda_\mathbf{k}^{1+\alpha}}\right) = C\sigma^2 \sum_{\mathbf{k}\in\mathbb{N}^d} \frac{1-e^{-\lambda_\mathbf{k}\Delta_n}}{\lambda_\mathbf{k}^{1+\alpha}}.$$

Utilizing equation (70), we find that

$$\begin{aligned} \sum_{i,j=1}^{n} R_{i,j} S_{i,j} &\leqslant C \sum_{i,j=1}^{n} \Bigg(\sum_{\mathbf{k}\in\mathbb{N}^d} \frac{(1-e^{-\lambda_\mathbf{k}\Delta_n})^2}{\lambda_\mathbf{k}^{1+\alpha}} e^{-\lambda_\mathbf{k}(i+j-2)\Delta_n}\Bigg)\Bigg(\mathbb{1}_{\{i\neq j\}}\Delta_n^{\alpha'}\,|i-j|^{\alpha'-2} \\ &\qquad + \sum_{\mathbf{k}\in\mathbb{N}^d} \Big(\frac{\big(1-e^{-\lambda_\mathbf{k}\Delta_n}\big)^2}{\lambda_\mathbf{k}^{1+\alpha}} e^{-\lambda_\mathbf{k}(i+j-2)\Delta_n} + \mathbb{1}_{\{i=j\}} \frac{1-e^{-\lambda_\mathbf{k}\Delta_n}}{\lambda_\mathbf{k}^{1+\alpha}}\Big) + \mathcal{O}(\Delta_n)\Bigg) \\ &= \mathcal{O}\Bigg(\Delta_n^{2\alpha'} \sum_{j=1}^{\infty} j^{\alpha'-2} + \Delta_n^{2\alpha'}\Bigg) = \mathcal{O}(\Delta_n^{2\alpha'}), \end{aligned}$$

where $C>0$ is a suitable constant. From the analysis above, we find that both terms in display (110) are of order $\mathcal{O}_\mathbb{P}(\Delta_n^{\alpha'})$. Therefore, we conclude that $\sqrt{m_n}\sum_{i=1}^n T_i \xrightarrow{\mathbb{P}} 0$, which completes the proof. □

The preceding lemma demonstrated that

$$\sqrt{m}_n \sum_{i=1}^{n} \Big((\Delta_i \tilde{X})^2(\mathbf{y}) - (\Delta_i X)^2(\mathbf{y}) \Big) \xrightarrow{\mathbb{P}} 0,$$

uniformly in $\mathbf{y} \in [0,1]^d$. Consequently, we deduce that

$$\sum_{i=1}^{n} \big(\tilde{\xi}_{n,i} - \xi_{n,i} \big) \xrightarrow{\mathbb{P}} 0,$$

as $n \to \infty$, which allows us to investigate a mild solution under a stationary condition from now on.

5.2. Variance-covariance structure

The purpose of this section is to explore the variance-covariance structure of the exponentially rescaled realized volatilities, which are defined as follows:

$$V_{p,\Delta_n}(\mathbf{y}) := \frac{1}{p\Delta_n^{\alpha'}} \sum_{i=1}^{p} (\Delta_i \tilde{X})^2(\mathbf{y}) e^{\|\kappa \bullet \mathbf{y}\|_1}, \tag{112}$$

for $\mathbf{y} \in [\delta, 1-\delta]^d$. Note that rescaling in $V_{p,\Delta_n}(\mathbf{y})$ involves two terms. The term $p\Delta_n^{\alpha'}$ rescales the temporal intensity, while the exponential term $e^{\|\kappa \bullet \mathbf{y}\|_1}$ compensates the exponential term resulting from the inner product $\langle \cdot, \cdot \rangle_\vartheta$.

Proposition 5.2.1
On the Assumptions 4.1.1 and 4.1.2, we have for the exponentially rescaled realized volatility in two spacial coordinates $\mathbf{y}_1, \mathbf{y}_2 \in [\delta, 1-\delta]^d$ that

$$\begin{aligned} \mathbb{C}\mathrm{ov}\big(V_{p,\Delta_n}(\mathbf{y}_1), V_{p,\Delta_n}(\mathbf{y}_2)\big) &= \mathbb{1}_{\{\mathbf{y}_1 = \mathbf{y}_2\}} \frac{\Upsilon_{\alpha'}}{p} \left(\frac{\Gamma(1-\alpha')\sigma^2}{2^d (\pi\eta)^{d/2} \alpha' \Gamma(d/2)} \right)^2 \left(1 + \mathcal{O}\left(\Delta_n^{1/2} \vee \frac{\Delta_n^{1-\alpha'}}{\delta^{d+1}} \vee \frac{\Delta_n^{-\alpha'}}{p} \right) \right) \\ &\quad + \mathcal{O}\left(\frac{\Delta_n^{1-\alpha'}}{p} \Big(\mathbb{1}_{\{\mathbf{y}_1 \neq \mathbf{y}_2\}} \|\mathbf{y}_1 - \mathbf{y}_2\|_0^{-(d+1)} + \delta^{-(d+1)} \Big) \vee \frac{\Delta_n^{-\alpha'}}{p^2} \right), \end{aligned}$$

where $\Upsilon_{\alpha'}$ is a numerical constant depending on $\alpha' \in (0,1)$, given in equation (121). In particular we have

$$\mathbb{V}\mathrm{ar}\big(V_{n,\Delta_n}(\mathbf{y})\big) = \frac{\Upsilon_{\alpha'}}{n} \left(\frac{\Gamma(1-\alpha')\sigma^2}{2^d (\pi\eta)^{d/2} \alpha' \Gamma(d/2)} \right)^2 \Big(1 + \mathcal{O}\big(\Delta_n^{1/2} \vee \Delta_n^{1-\alpha'} \big) \Big).$$

Proof. It holds that

$$\begin{aligned} &\mathbb{C}\mathrm{ov}\big(V_{p,\Delta_n}(\mathbf{y}_1), V_{p,\Delta_n}(\mathbf{y}_2)\big) \\ &= \frac{2e^{\|\kappa \bullet (\mathbf{y}_1 + \mathbf{y}_2)\|_1}}{p^2 \Delta_n^{2\alpha'}} \sum_{i,j=1}^{p} \left(\sum_{\mathbf{k}_1, \mathbf{k}_2 \in \mathbb{N}^d} e_{\mathbf{k}_1}(\mathbf{y}_1) e_{\mathbf{k}_1}(\mathbf{y}_2) e_{\mathbf{k}_2}(\mathbf{y}_1) e_{\mathbf{k}_2}(\mathbf{y}_2) \mathbb{C}\mathrm{ov}\Big(\Delta_i \tilde{x}_{\mathbf{k}_1} \Delta_i \tilde{x}_{\mathbf{k}_2},\ \Delta_j \tilde{x}_{\mathbf{k}_1} \Delta_j \tilde{x}_{\mathbf{k}_2} \Big) \right) \end{aligned}$$

$$= \frac{2e^{\|\kappa\boldsymbol{\cdot}(\mathbf{y}_1+\mathbf{y}_2)\|_1}}{p\Delta_n^{2\alpha'}} \sum_{\mathbf{k}_1,\mathbf{k}_2\in\mathbb{N}^d} e_{\mathbf{k}_1}(\mathbf{y}_1)e_{\mathbf{k}_1}(\mathbf{y}_2)e_{\mathbf{k}_2}(\mathbf{y}_1)e_{\mathbf{k}_2}(\mathbf{y}_2)D_{\mathbf{k}_1,\mathbf{k}_2},$$

where

$$D_{\mathbf{k}_1,\mathbf{k}_2} := \frac{1}{p}\sum_{i,j=1}^{p} \mathbb{C}\mathrm{ov}\Big(\big(\tilde{B}_{i,\mathbf{k}_1}+C_{i,\mathbf{k}_1}\big)\big(\tilde{B}_{i,\mathbf{k}_2}+C_{i,\mathbf{k}_2}\big),\ \big(\tilde{B}_{j,\mathbf{k}_1}+C_{j,\mathbf{k}_1}\big)\big(\tilde{B}_{j,\mathbf{k}_2}+C_{j,\mathbf{k}_2}\big)\Big).$$

Consider $(Z_{\mathbf{k}})_{\mathbf{k}\in\mathbb{N}^d}$ as independent standard normally distributed random variables, which are independent of $B_{i,\mathbf{k}}$. Utilizing equation (105), we can express $\tilde{B}_{i,\mathbf{k}}$ as

$$\tilde{B}_{i,\mathbf{k}} = B_{i,\mathbf{k}} + \frac{\sigma}{(2\lambda_{\mathbf{k}}^{1+\alpha})^{1/2}}\big(e^{-\lambda_{\mathbf{k}}\Delta_n}-1\big)e^{-\lambda_{\mathbf{k}}(i-1)\Delta_n}Z_{\mathbf{k}}.$$

Hence, we derive the following covariance structures:

$$\begin{aligned}
\mathbb{C}\mathrm{ov}\Big(\tilde{B}_{i,\mathbf{k}},C_{j,\mathbf{k}}\Big) &= \mathbb{C}\mathrm{ov}(B_{i,\mathbf{k}},C_{j,\mathbf{k}}) = \Sigma_{i,j}^{BC,\mathbf{k}},\\
\mathbb{C}\mathrm{ov}\Big(\tilde{B}_{i,\mathbf{k}},\tilde{B}_{j,\mathbf{k}}\Big) &= \mathbb{C}\mathrm{ov}(B_{i,\mathbf{k}},B_{j,\mathbf{k}}) + \frac{\sigma^2}{2\lambda_{\mathbf{k}}^{1+\alpha}}\big(e^{-\lambda_{\mathbf{k}}\Delta_n}-1\big)^2 e^{-\lambda_{\mathbf{k}}(i+j-2)\Delta_n}\mathbb{V}\mathrm{ar}(Z_{\mathbf{k}})\\
&= \sigma^2\big(e^{-\lambda_{\mathbf{k}}\Delta_n|i-j|}-e^{-\lambda_{\mathbf{k}}(i+j-2)\Delta_n}\big)\frac{\big(e^{-\lambda_{\mathbf{k}}\Delta_n}-1\big)^2}{2\lambda_{\mathbf{k}}^{1+\alpha}} + \frac{\sigma^2}{2\lambda_{\mathbf{k}}^{1+\alpha}}\big(e^{-\lambda_{\mathbf{k}}\Delta_n}-1\big)^2 e^{-\lambda_{\mathbf{k}}(i+j-2)\Delta_n}\\
&= \frac{\sigma^2}{2\lambda_{\mathbf{k}}^{1+\alpha}}\big(e^{-\lambda_{\mathbf{k}}\Delta_n}-1\big)^2 e^{-\lambda_{\mathbf{k}}\Delta_n|i-j|} =: \tilde{\Sigma}_{i,j}^{B,\mathbf{k}}, \qquad (113)
\end{aligned}$$

where we applied equation (73). As $\tilde{B}_{i,\mathbf{k}}+C_{i,\mathbf{k}}$ is centred normally distributed, we can use Isserlis' theorem to deduce that

$$\begin{aligned}
D_{\mathbf{k}_1,\mathbf{k}_2} = \frac{1}{p}\sum_{i,j=1}^{p}\Big(&\mathbb{E}\Big[\big(\tilde{B}_{i,\mathbf{k}_1}+C_{i,\mathbf{k}_1}\big)\big(\tilde{B}_{j,\mathbf{k}_1}+C_{j,\mathbf{k}_1}\big)\Big]\mathbb{E}\Big[\big(\tilde{B}_{i,\mathbf{k}_2}+C_{i,\mathbf{k}_2}\big)\big(\tilde{B}_{j,\mathbf{k}_2}+C_{j,\mathbf{k}_2}\big)\Big]\\
&+\mathbb{E}\Big[\big(\tilde{B}_{i,\mathbf{k}_1}+C_{i,\mathbf{k}_1}\big)\big(\tilde{B}_{j,\mathbf{k}_2}+C_{j,\mathbf{k}_2}\big)\Big]\mathbb{E}\Big[\big(\tilde{B}_{i,\mathbf{k}_2}+C_{i,\mathbf{k}_2}\big)\big(\tilde{B}_{j,\mathbf{k}_1}+C_{j,\mathbf{k}_1}\big)\Big]\Big).
\end{aligned}$$

For further reading on the Isserlis theorem, we recommend referring to Isserlis (1918). Assume $\mathbf{k}_1 \neq \mathbf{k}_2$, then we have

$$\begin{aligned}
D_{\mathbf{k}_1,\mathbf{k}_2} &= \frac{1}{p}\sum_{i,j=1}^{p}\mathbb{E}\Big[\big(\tilde{B}_{i,\mathbf{k}_1}+C_{i,\mathbf{k}_1}\big)\big(\tilde{B}_{j,\mathbf{k}_1}+C_{j,\mathbf{k}_1}\big)\Big]\mathbb{E}\Big[\big(\tilde{B}_{i,\mathbf{k}_2}+C_{i,\mathbf{k}_2}\big)\big(\tilde{B}_{j,\mathbf{k}_2}+C_{j,\mathbf{k}_2}\big)\Big]\\
&= \frac{1}{p}\sum_{i,j=1}^{p}\Big(\tilde{\Sigma}_{i,j}^{B,\mathbf{k}_1}+\Sigma_{i,j}^{BC,\mathbf{k}_1}+\Sigma_{j,i}^{BC,\mathbf{k}_1}+\Sigma_{i,j}^{C,\mathbf{k}_1}\Big)\Big(\tilde{\Sigma}_{i,j}^{B,\mathbf{k}_2}+\Sigma_{i,j}^{BC,\mathbf{k}_2}+\Sigma_{j,i}^{BC,\mathbf{k}_2}+\Sigma_{i,j}^{C,\mathbf{k}_2}\Big). \qquad (114)
\end{aligned}$$

We proceed by calculating each combination separately. First, we use the following identity:

$$\sum_{i,j=1}^{p} q^{|i-j|} = 2\frac{q^{p+1}-q}{(1-q)^2} + p\frac{1+q}{1-q}, \qquad (115)$$

for $q \neq 1$. Then, we have

$$\begin{aligned}\frac{1}{p}\sum_{i,j=1}^{p}\tilde{\Sigma}_{i,j}^{B,\mathbf{k}_1}\tilde{\Sigma}_{i,j}^{B,\mathbf{k}_2} &= \sigma^4\frac{\big(e^{-\lambda_{\mathbf{k}_1}\Delta_n}-1\big)^2\big(e^{-\lambda_{\mathbf{k}_2}\Delta_n}-1\big)^2}{4p\lambda_{\mathbf{k}_1}^{1+\alpha}\lambda_{\mathbf{k}_2}^{1+\alpha}}\sum_{i,j=1}^{p}e^{-(\lambda_{\mathbf{k}_1}+\lambda_{\mathbf{k}_2})\Delta_n|i-j|}\\ &= \sigma^4\frac{\big(e^{-\lambda_{\mathbf{k}_1}\Delta_n}-1\big)^2\big(e^{-\lambda_{\mathbf{k}_2}\Delta_n}-1\big)^2}{4\lambda_{\mathbf{k}_1}^{1+\alpha}\lambda_{\mathbf{k}_2}^{1+\alpha}}\cdot\frac{1+e^{-(\lambda_{\mathbf{k}_1}+\lambda_{\mathbf{k}_2})\Delta_n}}{1-e^{-(\lambda_{\mathbf{k}_1}+\lambda_{\mathbf{k}_2})\Delta_n}}\\ &\quad\times\Big(1+\mathcal{O}\Big(1\wedge\frac{p^{-1}}{1-e^{-(\lambda_{\mathbf{k}_1}+\lambda_{\mathbf{k}_2})\Delta_n}}\Big)\Big).\end{aligned}$$

By utilizing equation (74), we obtain

$$\begin{aligned}\frac{1}{p}\sum_{i,j=1}^{p}\Sigma_{i,j}^{C,\mathbf{k}_1}\Sigma_{i,j}^{C,\mathbf{k}_2} &= \frac{1}{p}\sum_{i,j=1}^{p}\mathbb{1}_{\{j=i\}}\sigma^4\frac{\big(1-e^{-2\lambda_{\mathbf{k}_1}\Delta_n}\big)\big(1-e^{-2\lambda_{\mathbf{k}_2}\Delta_n}\big)}{4\lambda_{\mathbf{k}_1}^{1+\alpha}\lambda_{\mathbf{k}_2}^{1+\alpha}}\\ &= \sigma^4\frac{\big(1-e^{-2\lambda_{\mathbf{k}_1}\Delta_n}\big)\big(1-e^{-2\lambda_{\mathbf{k}_2}\Delta_n}\big)}{4\lambda_{\mathbf{k}_1}^{1+\alpha}\lambda_{\mathbf{k}_2}^{1+\alpha}}.\end{aligned}$$

Using equation (75) and the identity

$$\sum_{i,j=1}^{p}\mathbb{1}_{\{i>j\}}q^{i-j} = \frac{pq}{1-q}+\frac{q-q^{p+1}}{(1-q)^2},$$

yields that

$$\begin{aligned}\frac{1}{p}\sum_{i,j=1}^{p}\Sigma_{i,j}^{BC,\mathbf{k}_1}\Sigma_{i,j}^{BC,\mathbf{k}_2} &= \frac{1}{p}\sum_{i,j=1}^{p}\mathbb{1}_{\{i>j\}}\sigma^4\frac{\big(e^{-\lambda_{\mathbf{k}_1}\Delta_n}-1\big)\big(e^{-\lambda_{\mathbf{k}_2}\Delta_n}-1\big)}{4\lambda_{\mathbf{k}_1}^{1+\alpha}\lambda_{\mathbf{k}_2}^{1+\alpha}}\\ &\quad\times e^{-(\lambda_{\mathbf{k}_1}+\lambda_{\mathbf{k}_2})\Delta_n(i-j)}\big(e^{\lambda_{\mathbf{k}_1}\Delta_n}-e^{-\lambda_{\mathbf{k}_1}\Delta_n}\big)\big(e^{\lambda_{\mathbf{k}_2}\Delta_n}-e^{-\lambda_{\mathbf{k}_2}\Delta_n}\big)\\ &= \sigma^4\frac{\big(e^{-\lambda_{\mathbf{k}_1}\Delta_n}-1\big)\big(e^{-\lambda_{\mathbf{k}_2}\Delta_n}-1\big)}{4\lambda_{\mathbf{k}_1}^{1+\alpha}\lambda_{\mathbf{k}_2}^{1+\alpha}}\big(e^{\lambda_{\mathbf{k}_1}\Delta_n}-e^{-\lambda_{\mathbf{k}_1}\Delta_n}\big)\big(e^{\lambda_{\mathbf{k}_2}\Delta_n}-e^{-\lambda_{\mathbf{k}_2}\Delta_n}\big)\\ &\quad\times\frac{e^{-(\lambda_{\mathbf{k}_1}+\lambda_{\mathbf{k}_2})\Delta_n}}{1-e^{-(\lambda_{\mathbf{k}_1}+\lambda_{\mathbf{k}_2})\Delta_n}}\Big(1+\mathcal{O}\Big(1\wedge\frac{p^{-1}}{1-e^{-(\lambda_{\mathbf{k}_1}+\lambda_{\mathbf{k}_2})\Delta_n}}\Big)\Big)\\ &= \sigma^4\frac{\big(e^{-\lambda_{\mathbf{k}_1}\Delta_n}-1\big)\big(e^{-\lambda_{\mathbf{k}_2}\Delta_n}-1\big)}{4\lambda_{\mathbf{k}_1}^{1+\alpha}\lambda_{\mathbf{k}_2}^{1+\alpha}}\cdot\frac{(1-e^{-2\lambda_{\mathbf{k}_1}\Delta_n})(1-e^{-2\lambda_{\mathbf{k}_2}\Delta_n})}{1-e^{-(\lambda_{\mathbf{k}_1}+\lambda_{\mathbf{k}_2})\Delta_n}}\\ &\quad\times\Big(1+\mathcal{O}\Big(1\wedge\frac{p^{-1}}{1-e^{-(\lambda_{\mathbf{k}_1}+\lambda_{\mathbf{k}_2})\Delta_n}}\Big)\Big).\end{aligned}$$

The same calculations apply to $\Sigma_{j,i}^{BC,\mathbf{k}_1}\Sigma_{j,i}^{BC,\mathbf{k}_2}$. As for the cross-terms, we obtain

$$\begin{aligned}&\frac{1}{p}\sum_{i,j=1}^{p}\tilde{\Sigma}_{i,j}^{B,\mathbf{k}_1}\big(\Sigma_{i,j}^{BC,\mathbf{k}_2}+\Sigma_{j,i}^{BC,\mathbf{k}_2}\big)\\ &= \frac{1}{p}\sum_{i,j=1}^{p}\frac{\sigma^2}{2\lambda_{\mathbf{k}_1}^{1+\alpha}}\big(e^{-\lambda_{\mathbf{k}_1}\Delta_n}-1\big)^2e^{-\lambda_{\mathbf{k}_1}\Delta_n|i-j|}\Big(\mathbb{1}_{\{i>j\}}\sigma^2e^{-\lambda_{\mathbf{k}_2}\Delta_n(i-j)}\big(e^{\lambda_{\mathbf{k}_2}\Delta_n}-e^{-\lambda_{\mathbf{k}_2}\Delta_n}\big)\frac{e^{-\lambda_{\mathbf{k}_2}\Delta_n}-1}{2\lambda_{\mathbf{k}_2}^{1+\alpha}}\\ &\quad+\mathbb{1}_{\{j>i\}}\sigma^2e^{-\lambda_{\mathbf{k}_2}\Delta_n(j-i)}\big(e^{\lambda_{\mathbf{k}_2}\Delta_n}-e^{-\lambda_{\mathbf{k}_2}\Delta_n}\big)\frac{e^{-\lambda_{\mathbf{k}_2}\Delta_n}-1}{2\lambda_{\mathbf{k}_2}^{1+\alpha}}\Big)\end{aligned}$$

$$= \sigma^4 \frac{\big(e^{-\lambda_{\mathbf{k}_1}\Delta_n}-1\big)^2\big(e^{-\lambda_{\mathbf{k}_2}\Delta_n}-1\big)}{4\lambda_{\mathbf{k}_1}^{1+\alpha}\lambda_{\mathbf{k}_2}^{1+\alpha}}\big(e^{\lambda_{\mathbf{k}_2}\Delta_n}-e^{-\lambda_{\mathbf{k}_2}\Delta_n}\big)\frac{1}{p}\sum_{i,j=1}^{p}\mathbb{1}_{\{i>j\}}e^{-(\lambda_{\mathbf{k}_1}+\lambda_{\mathbf{k}_2})\Delta_n(i-j)}$$
$$+ \sigma^4 \frac{\big(e^{-\lambda_{\mathbf{k}_1}\Delta_n}-1\big)^2\big(e^{-\lambda_{\mathbf{k}_2}\Delta_n}-1\big)}{4\lambda_{\mathbf{k}_1}^{1+\alpha}\lambda_{\mathbf{k}_2}^{1+\alpha}}\big(e^{\lambda_{\mathbf{k}_2}\Delta_n}-e^{-\lambda_{\mathbf{k}_2}\Delta_n}\big)\frac{1}{p}\sum_{i,j=1}^{p}\mathbb{1}_{\{j>i\}}e^{-(\lambda_{\mathbf{k}_1}+\lambda_{\mathbf{k}_2})\Delta_n(j-i)}$$
$$= \sigma^4 \frac{\big(e^{-\lambda_{\mathbf{k}_1}\Delta_n}-1\big)^2\big(e^{-\lambda_{\mathbf{k}_2}\Delta_n}-1\big)}{4\lambda_{\mathbf{k}_1}\lambda_{\mathbf{k}_2}}\big(e^{\lambda_{\mathbf{k}_2}\Delta_n}-e^{-\lambda_{\mathbf{k}_2}\Delta_n}\big)\frac{e^{-(\lambda_{\mathbf{k}_1}+\lambda_{\mathbf{k}_2})\Delta_n}}{1-e^{-(\lambda_{\mathbf{k}_1}+\lambda_{\mathbf{k}_2})\Delta_n}}$$
$$\times\Big(1+\mathcal{O}\Big(1\wedge\frac{p^{-1}}{1-e^{-(\lambda_{\mathbf{k}_1}+\lambda_{\mathbf{k}_2})\Delta_n}}\Big)\Big)$$
$$+ \sigma^4 \frac{\big(e^{-\lambda_{\mathbf{k}_1}\Delta_n}-1\big)^2\big(e^{-\lambda_{\mathbf{k}_2}\Delta_n}-1\big)}{4\lambda_{\mathbf{k}_1}^{1+\alpha}\lambda_{\mathbf{k}_2}^{1+\alpha}}\big(e^{\lambda_{\mathbf{k}_2}\Delta_n}-e^{-\lambda_{\mathbf{k}_2}\Delta_n}\big)\frac{e^{-(\lambda_{\mathbf{k}_1}+\lambda_{\mathbf{k}_2})\Delta_n}}{1-e^{-(\lambda_{\mathbf{k}_1}+\lambda_{\mathbf{k}_2})\Delta_n}}$$
$$\times\Big(1+\mathcal{O}\Big(1\wedge\frac{p^{-1}}{1-e^{-(\lambda_{\mathbf{k}_1}+\lambda_{\mathbf{k}_2})\Delta_n}}\Big)\Big)$$
$$= \sigma^4 \frac{\big(e^{-\lambda_{\mathbf{k}_1}\Delta_n}-1\big)^2\big(e^{-\lambda_{\mathbf{k}_2}\Delta_n}-1\big)}{2\lambda_{\mathbf{k}_1}^{1+\alpha}\lambda_{\mathbf{k}_2}}\big(e^{\lambda_{\mathbf{k}_2}\Delta_n}-e^{-\lambda_{\mathbf{k}_2}\Delta_n}\big)\frac{e^{-(\lambda_{\mathbf{k}_1}+\lambda_{\mathbf{k}_2})\Delta_n}}{1-e^{-(\lambda_{\mathbf{k}_1}+\lambda_{\mathbf{k}_2})\Delta_n}}$$
$$\times\Big(1+\mathcal{O}\Big(1\wedge\frac{p^{-1}}{1-e^{-(\lambda_{\mathbf{k}_1}+\lambda_{\mathbf{k}_2})\Delta_n}}\Big)\Big)$$
$$= \sigma^4 \frac{\big(e^{-\lambda_{\mathbf{k}_1}\Delta_n}-1\big)^2\big(e^{-\lambda_{\mathbf{k}_2}\Delta_n}-1\big)}{2\lambda_{\mathbf{k}_1}^{1+\alpha}\lambda_{\mathbf{k}_2}^{1+\alpha}}e^{-\lambda_{\mathbf{k}_1}\Delta_n}\frac{1-e^{-2\lambda_{\mathbf{k}_2}\Delta_n}}{1-e^{-(\lambda_{\mathbf{k}_1}+\lambda_{\mathbf{k}_2})\Delta_n}}\Big(1+\mathcal{O}\Big(1\wedge\frac{p^{-1}}{1-e^{-(\lambda_{\mathbf{k}_1}+\lambda_{\mathbf{k}_2})\Delta_n}}\Big)\Big),$$

and

$$\frac{1}{p}\sum_{i,j=1}^{p}\tilde{\Sigma}_{i,j}^{B,\mathbf{k}_1}\Sigma_{i,j}^{C,\mathbf{k}_2} = \frac{1}{p}\sum_{i,j=1}^{p}\frac{\sigma^2}{2\lambda_{\mathbf{k}_1}^{1+\alpha}}\big(e^{-\lambda_{\mathbf{k}_1}\Delta_n}-1\big)^2 e^{-\lambda_{\mathbf{k}_1}\Delta_n|i-j|}\mathbb{1}_{\{i=j\}}\sigma^2\frac{1-e^{-2\lambda_{\mathbf{k}_2}\Delta_n}}{2\lambda_{\mathbf{k}_2}^{1+\alpha}}$$
$$= \sigma^4\frac{\big(e^{-\lambda_{\mathbf{k}_1}\Delta_n}-1\big)^2\big(1-e^{-2\lambda_{\mathbf{k}_2}\Delta_n}\big)}{4\lambda_{\mathbf{k}_1}^{1+\alpha}\lambda_{\mathbf{k}_2}^{1+\alpha}}.$$

Furthermore, the following cross-terms vanish:

$$\frac{1}{p}\sum_{i,j=1}^{p}\Sigma_{i,j}^{BC,\mathbf{k}_1}\Sigma_{i,j}^{C,\mathbf{k}_2} = \frac{1}{p}\sum_{i,j=1}^{p}\Sigma_{j,i}^{BC,\mathbf{k}_1}\Sigma_{i,j}^{C,\mathbf{k}_2} = \frac{1}{p}\sum_{i,j=1}^{p}\Sigma_{i,j}^{BC,\mathbf{k}_1}\Sigma_{j,i}^{BC,\mathbf{k}_2} = 0.$$

Inserting the auxiliary calculations into equation (114) results in

$$D_{\mathbf{k}_1,\mathbf{k}_2} = \frac{1}{p}\sum_{i,j=1}^{p}\Big(\tilde{\Sigma}_{i,j}^{B,\mathbf{k}_1}+\Sigma_{i,j}^{BC,\mathbf{k}_1}+\Sigma_{j,i}^{BC,\mathbf{k}_1}+\Sigma_{i,j}^{C,\mathbf{k}_1}\Big)\Big(\tilde{\Sigma}_{i,j}^{B,\mathbf{k}_2}+\Sigma_{i,j}^{BC,\mathbf{k}_2}+\Sigma_{j,i}^{BC,\mathbf{k}_2}+\Sigma_{i,j}^{C,\mathbf{k}_2}\Big)$$
$$= \frac{1}{p}\sum_{i,j=1}^{p}\Big(\tilde{\Sigma}_{i,j}^{B,\mathbf{k}_1}\tilde{\Sigma}_{i,j}^{B,\mathbf{k}_2}+\tilde{\Sigma}_{i,j}^{B,\mathbf{k}_1}\big(\Sigma_{i,j}^{BC,\mathbf{k}_2}+\Sigma_{j,i}^{BC,\mathbf{k}_2}\big)+\tilde{\Sigma}_{i,j}^{B,\mathbf{k}_1}\Sigma_{i,j}^{C,\mathbf{k}_2}+\big(\Sigma_{i,j}^{BC,\mathbf{k}_1}+\Sigma_{j,i}^{BC,\mathbf{k}_1}\big)\tilde{\Sigma}_{i,j}^{B,\mathbf{k}_2}$$
$$+\Sigma_{i,j}^{BC,\mathbf{k}_1}\Sigma_{i,j}^{BC,\mathbf{k}_2}+\Sigma_{j,i}^{BC,\mathbf{k}_1}\Sigma_{j,i}^{BC,\mathbf{k}_2}+\Sigma_{i,j}^{C,\mathbf{k}_1}\tilde{\Sigma}_{i,j}^{B,\mathbf{k}_2}+\Sigma_{i,j}^{C,\mathbf{k}_1}\Sigma_{i,j}^{C,\mathbf{k}_2}\Big)$$
$$= \sigma^4\Bigg(\frac{\big(e^{-\lambda_{\mathbf{k}_1}\Delta_n}-1\big)^2\big(e^{-\lambda_{\mathbf{k}_2}\Delta_n}-1\big)^2}{4\lambda_{\mathbf{k}_1}^{1+\alpha}\lambda_{\mathbf{k}_2}^{1+\alpha}}\cdot\frac{1+e^{-(\lambda_{\mathbf{k}_1}+\lambda_{\mathbf{k}_2})\Delta_n}}{1-e^{-(\lambda_{\mathbf{k}_1}+\lambda_{\mathbf{k}_2})\Delta_n}}\Big(1+\mathcal{O}\Big(1\wedge\frac{p^{-1}}{1-e^{-(\lambda_{\mathbf{k}_1}+\lambda_{\mathbf{k}_2})\Delta_n}}\Big)\Big)$$
$$+\frac{\big(e^{-\lambda_{\mathbf{k}_1}\Delta_n}-1\big)^2\big(e^{-\lambda_{\mathbf{k}_2}\Delta_n}-1\big)}{2\lambda_{\mathbf{k}_1}^{1+\alpha}\lambda_{\mathbf{k}_2}^{1+\alpha}}e^{-\lambda_{\mathbf{k}_1}\Delta_n}\frac{1-e^{-2\lambda_{\mathbf{k}_2}\Delta_n}}{1-e^{-(\lambda_{\mathbf{k}_1}+\lambda_{\mathbf{k}_2})\Delta_n}}$$

$$
\begin{aligned}
&\quad \times \Big(1+\mathcal{O}\Big(1 \wedge \frac{p^{-1}}{1-e^{-(\lambda_{\mathbf{k}_1}+\lambda_{\mathbf{k}_2})\Delta_n}}\Big)\Big) \\
&+ \frac{\big(e^{-\lambda_{\mathbf{k}_1}\Delta_n}-1\big)^2\big(1-e^{-2\lambda_{\mathbf{k}_2}\Delta_n}\big)}{4\lambda_{\mathbf{k}_1}^{1+\alpha}\lambda_{\mathbf{k}_2}^{1+\alpha}} \\
&+ \frac{\big(e^{-\lambda_{\mathbf{k}_2}\Delta_n}-1\big)^2\big(e^{-\lambda_{\mathbf{k}_1}\Delta_n}-1\big)}{2\lambda_{\mathbf{k}_1}^{1+\alpha}\lambda_{\mathbf{k}_2}^{1+\alpha}} e^{-\lambda_{\mathbf{k}_2}\Delta_n}\frac{1-e^{-2\lambda_{\mathbf{k}_1}\Delta_n}}{1-e^{-(\lambda_{\mathbf{k}_1}+\lambda_{\mathbf{k}_2})\Delta_n}}\Big(1+\mathcal{O}\Big(1 \wedge \frac{p^{-1}}{1-e^{-(\lambda_{\mathbf{k}_1}+\lambda_{\mathbf{k}_2})\Delta_n}}\Big)\Big) \\
&+ 2\frac{\big(e^{-\lambda_{\mathbf{k}_1}\Delta_n}-1\big)\big(e^{-\lambda_{\mathbf{k}_2}\Delta_n}-1\big)}{4\lambda_{\mathbf{k}_1}^{1+\alpha}\lambda_{\mathbf{k}_2}^{1+\alpha}} \cdot \frac{(1-e^{-2\lambda_{\mathbf{k}_1}\Delta_n})(1-e^{-2\lambda_{\mathbf{k}_2}\Delta_n})}{1-e^{-(\lambda_{\mathbf{k}_1}+\lambda_{\mathbf{k}_2})\Delta_n}} \\
&\quad \times \Big(1+\mathcal{O}\Big(1 \wedge \frac{p^{-1}}{1-e^{-(\lambda_{\mathbf{k}_1}+\lambda_{\mathbf{k}_2})\Delta_n}}\Big)\Big) \\
&+ \frac{\big(e^{-\lambda_{\mathbf{k}_2}\Delta_n}-1\big)^2\big(1-e^{-2\lambda_{\mathbf{k}_1}\Delta_n}\big)}{4\lambda_{\mathbf{k}_1}^{1+\alpha}\lambda_{\mathbf{k}_2}^{1+\alpha}} \\
&+ \frac{\big(1-e^{-2\lambda_{\mathbf{k}_1}\Delta_n}\big)\big(1-e^{-2\lambda_{\mathbf{k}_2}\Delta_n}\big)}{4\lambda_{\mathbf{k}_1}^{1+\alpha}\lambda_{\mathbf{k}_2}^{1+\alpha}}\Big) \\
&= \sigma^4\Big(\frac{\big(e^{-\lambda_{\mathbf{k}_1}\Delta_n}-1\big)^2\big(e^{-\lambda_{\mathbf{k}_2}\Delta_n}-1\big)^2}{4\lambda_{\mathbf{k}_1}^{1+\alpha}\lambda_{\mathbf{k}_2}^{1+\alpha}}\Big(\frac{1+e^{-(\lambda_{\mathbf{k}_1}+\lambda_{\mathbf{k}_2})\Delta_n}}{1-e^{-(\lambda_{\mathbf{k}_1}+\lambda_{\mathbf{k}_2})\Delta_n}} \\
&+ \frac{e^{-\lambda_{\mathbf{k}_1}\Delta_n}(1-e^{-2\lambda_{\mathbf{k}_2}\Delta_n})}{1-e^{-(\lambda_{\mathbf{k}_1}+\lambda_{\mathbf{k}_2})\Delta_n}}\cdot\frac{2}{e^{-\lambda_{\mathbf{k}_2}\Delta_n}-1} + \frac{e^{-\lambda_{\mathbf{k}_2}\Delta_n}(1-e^{-2\lambda_{\mathbf{k}_1}\Delta_n})}{1-e^{-(\lambda_{\mathbf{k}_1}+\lambda_{\mathbf{k}_2})\Delta_n}}\cdot\frac{2}{e^{-\lambda_{\mathbf{k}_1}\Delta_n}-1} \\
&+ \frac{(1-e^{-2\lambda_{\mathbf{k}_1}\Delta_n})(1-e^{-2\lambda_{\mathbf{k}_2}\Delta_n})}{1-e^{-(\lambda_{\mathbf{k}_1}+\lambda_{\mathbf{k}_2})\Delta_n}}\cdot\frac{2}{\big(e^{-\lambda_{\mathbf{k}_1}\Delta_n}-1\big)\big(e^{-\lambda_{\mathbf{k}_2}\Delta_n}-1\big)}\Big) \\
&+ \frac{\big(e^{-\lambda_{\mathbf{k}_1}\Delta_n}-1\big)^2\big(1-e^{-2\lambda_{\mathbf{k}_2}\Delta_n}\big)}{4\lambda_{\mathbf{k}_1}^{1+\alpha}\lambda_{\mathbf{k}_2}^{1+\alpha}} + \frac{\big(e^{-\lambda_{\mathbf{k}_2}\Delta_n}-1\big)^2\big(1-e^{-2\lambda_{\mathbf{k}_1}\Delta_n}\big)}{4\lambda_{\mathbf{k}_1}^{1+\alpha}\lambda_{\mathbf{k}_2}^{1+\alpha}} \\
&+ \frac{\big(1-e^{-2\lambda_{\mathbf{k}_1}\Delta_n}\big)\big(1-e^{-2\lambda_{\mathbf{k}_2}\Delta_n}\big)}{4\lambda_{\mathbf{k}_1}^{1+\alpha}\lambda_{\mathbf{k}_2}^{1+\alpha}}\Big)\Big(1+\mathcal{O}\Big(1 \wedge \frac{p^{-1}}{1-e^{-(\lambda_{\mathbf{k}_1}+\lambda_{\mathbf{k}_2})\Delta_n}}\Big)\Big).
\end{aligned}
$$

Using the identity $(e^{2x}-1)/(e^x-1)=e^x+1$, we have

$$
\begin{aligned}
D_{\mathbf{k}_1,\mathbf{k}_2} &= \sigma^4\Big(\frac{\big(e^{-\lambda_{\mathbf{k}_1}\Delta_n}-1\big)^2\big(e^{-\lambda_{\mathbf{k}_2}\Delta_n}-1\big)^2}{4\lambda_{\mathbf{k}_1}^{1+\alpha}\lambda_{\mathbf{k}_2}^{1+\alpha}}\Big(\frac{1+e^{-(\lambda_{\mathbf{k}_1}+\lambda_{\mathbf{k}_2})\Delta_n}+2(e^{-\lambda_{\mathbf{k}_1}\Delta_n}+1)(e^{-\lambda_{\mathbf{k}_2}\Delta_n}+1)}{1-e^{-(\lambda_{\mathbf{k}_1}+\lambda_{\mathbf{k}_2})\Delta_n}} \\
&\quad + \frac{-2e^{-\lambda_{\mathbf{k}_1}\Delta_n}(e^{-\lambda_{\mathbf{k}_2}\Delta_n}+1)-2e^{-\lambda_{\mathbf{k}_2}\Delta_n}(e^{-\lambda_{\mathbf{k}_1}\Delta_n}+1)}{1-e^{-(\lambda_{\mathbf{k}_1}+\lambda_{\mathbf{k}_2})\Delta_n}}\Big) \\
&\quad + \frac{\big(e^{-\lambda_{\mathbf{k}_1}\Delta_n}-1\big)^2\big(1-e^{-2\lambda_{\mathbf{k}_2}\Delta_n}\big)}{4\lambda_{\mathbf{k}_1}^{1+\alpha}\lambda_{\mathbf{k}_2}^{1+\alpha}} + \frac{\big(e^{-\lambda_{\mathbf{k}_2}\Delta_n}-1\big)^2\big(1-e^{-2\lambda_{\mathbf{k}_1}\Delta_n}\big)}{4\lambda_{\mathbf{k}_1}^{1+\alpha}\lambda_{\mathbf{k}_2}^{1+\alpha}} \\
&\quad + \frac{\big(1-e^{-2\lambda_{\mathbf{k}_1}\Delta_n}\big)\big(1-e^{-2\lambda_{\mathbf{k}_2}\Delta_n}\big)}{4\lambda_{\mathbf{k}_1}^{1+\alpha}\lambda_{\mathbf{k}_2}^{1+\alpha}}\Big) \times \Big(1+\mathcal{O}\Big(1 \wedge \frac{p^{-1}}{1-e^{-(\lambda_{\mathbf{k}_1}+\lambda_{\mathbf{k}_2})\Delta_n}}\Big)\Big) \\
&= \sigma^4\Big(\frac{\big(e^{-\lambda_{\mathbf{k}_1}\Delta_n}-1\big)^2\big(e^{-\lambda_{\mathbf{k}_2}\Delta_n}-1\big)^2}{4\lambda_{\mathbf{k}_1}^{1+\alpha}\lambda_{\mathbf{k}_2}^{1+\alpha}}\cdot\frac{3-e^{-(\lambda_{\mathbf{k}_1}+\lambda_{\mathbf{k}_2})\Delta_n}}{1-e^{-(\lambda_{\mathbf{k}_1}+\lambda_{\mathbf{k}_2})\Delta_n}} \\
&\quad + \frac{\big(e^{-\lambda_{\mathbf{k}_1}\Delta_n}-1\big)^2\big(1-e^{-2\lambda_{\mathbf{k}_2}\Delta_n}\big)}{4\lambda_{\mathbf{k}_1}^{1+\alpha}\lambda_{\mathbf{k}_2}^{1+\alpha}} + \frac{\big(e^{-\lambda_{\mathbf{k}_2}\Delta_n}-1\big)^2\big(1-e^{-2\lambda_{\mathbf{k}_1}\Delta_n}\big)}{4\lambda_{\mathbf{k}_1}^{1+\alpha}\lambda_{\mathbf{k}_2}^{1+\alpha}} \\
&\quad + \frac{\big(1-e^{-2\lambda_{\mathbf{k}_1}\Delta_n}\big)\big(1-e^{-2\lambda_{\mathbf{k}_2}\Delta_n}\big)}{4\lambda_{\mathbf{k}_1}^{1+\alpha}\lambda_{\mathbf{k}_2}^{1+\alpha}}\Big) \times \Big(1+\mathcal{O}\Big(1 \wedge \frac{p^{-1}}{1-e^{-(\lambda_{\mathbf{k}_1}+\lambda_{\mathbf{k}_2})\Delta_n}}\Big)\Big)
\end{aligned}
$$

$$
\begin{aligned}
&= \sigma^4 \Bigg(\frac{\big(e^{-\lambda_{\mathbf{k}_1}\Delta_n}-1\big)^2\big(e^{-\lambda_{\mathbf{k}_2}\Delta_n}-1\big)^2}{4\lambda_{\mathbf{k}_1}^{1+\alpha}\lambda_{\mathbf{k}_2}^{1+\alpha}} \cdot \frac{3-e^{-(\lambda_{\mathbf{k}_1}+\lambda_{\mathbf{k}_2})\Delta_n}}{1-e^{-(\lambda_{\mathbf{k}_1}+\lambda_{\mathbf{k}_2})\Delta_n}} \\
&\quad + \frac{\big(1-e^{-\lambda_{\mathbf{k}_1}\Delta_n}\big)\big(1-e^{-\lambda_{\mathbf{k}_2}\Delta_n}\big)}{4\lambda_{\mathbf{k}_1}^{1+\alpha}\lambda_{\mathbf{k}_2}^{1+\alpha}} \Big(\big(1-e^{-\lambda_{\mathbf{k}_1}\Delta_n}\big)\big(1+e^{-\lambda_{\mathbf{k}_2}\Delta_n}\big) \\
&\quad + \big(1-e^{-\lambda_{\mathbf{k}_2}\Delta_n}\big)\big(1+e^{-\lambda_{\mathbf{k}_1}\Delta_n}\big) + \big(1+e^{-\lambda_{\mathbf{k}_1}\Delta_n}\big)\big(1+e^{-\lambda_{\mathbf{k}_2}\Delta_n}\big)\Big)\Bigg) \\
&\quad \times \bigg(1+\mathcal{O}\Big(1\wedge \frac{p^{-1}}{1-e^{-(\lambda_{\mathbf{k}_1}+\lambda_{\mathbf{k}_2})\Delta_n}}\Big)\bigg) \\
&= \sigma^4 \Bigg(\frac{\big(e^{-\lambda_{\mathbf{k}_1}\Delta_n}-1\big)^2\big(e^{-\lambda_{\mathbf{k}_2}\Delta_n}-1\big)^2}{4\lambda_{\mathbf{k}_1}^{1+\alpha}\lambda_{\mathbf{k}_2}^{1+\alpha}} \cdot \frac{4-2e^{-(\lambda_{\mathbf{k}_1}+\lambda_{\mathbf{k}_2})\Delta_n}}{1-e^{-(\lambda_{\mathbf{k}_1}+\lambda_{\mathbf{k}_2})\Delta_n}} \\
&\quad + \frac{\big(1-e^{-\lambda_{\mathbf{k}_1}\Delta_n}\big)\big(1-e^{-\lambda_{\mathbf{k}_2}\Delta_n}\big)}{4\lambda_{\mathbf{k}_1}^{1+\alpha}\lambda_{\mathbf{k}_2}^{1+\alpha}} \Big(\big(1-e^{-\lambda_{\mathbf{k}_1}\Delta_n}\big)\big(1+e^{-\lambda_{\mathbf{k}_2}\Delta_n}\big) \\
&\quad + \big(1-e^{-\lambda_{\mathbf{k}_2}\Delta_n}\big)\big(1+e^{-\lambda_{\mathbf{k}_1}\Delta_n}\big) + \big(1+e^{-\lambda_{\mathbf{k}_1}\Delta_n}\big)\big(1+e^{-\lambda_{\mathbf{k}_2}\Delta_n}\big) \\
&\quad - \big(1-e^{-\lambda_{\mathbf{k}_1}\Delta_n}\big)\big(1-e^{-\lambda_{\mathbf{k}_2}\Delta_n}\big)\Big)\Bigg) \times \bigg(1+\mathcal{O}\Big(1\wedge \frac{p^{-1}}{1-e^{-(\lambda_{\mathbf{k}_1}+\lambda_{\mathbf{k}_2})\Delta_n}}\Big)\bigg) \\
&= \sigma^4 \Bigg(\frac{\big(e^{-\lambda_{\mathbf{k}_1}\Delta_n}-1\big)^2\big(e^{-\lambda_{\mathbf{k}_2}\Delta_n}-1\big)^2}{4\lambda_{\mathbf{k}_1}^{1+\alpha}\lambda_{\mathbf{k}_2}^{1+\alpha}} \cdot \frac{4-2e^{-(\lambda_{\mathbf{k}_1}+\lambda_{\mathbf{k}_2})\Delta_n}}{1-e^{-(\lambda_{\mathbf{k}_1}+\lambda_{\mathbf{k}_2})\Delta_n}} + \frac{\big(1-e^{-\lambda_{\mathbf{k}_1}\Delta_n}\big)\big(1-e^{-\lambda_{\mathbf{k}_2}\Delta_n}\big)}{4\lambda_{\mathbf{k}_1}^{1+\alpha}\lambda_{\mathbf{k}_2}^{1+\alpha}} \\
&\quad \times 2\Big(2-\big(1-e^{-\lambda_{\mathbf{k}_1}\Delta_n}\big)\big(1-e^{-\lambda_{\mathbf{k}_2}\Delta_n}\big)\Big)\Bigg)\bigg(1+\mathcal{O}\Big(1\wedge \frac{p^{-1}}{1-e^{-(\lambda_{\mathbf{k}_1}+\lambda_{\mathbf{k}_2})\Delta_n}}\Big)\bigg) \\
&= \sigma^4 \Bigg(\frac{\big(1-e^{-\lambda_{\mathbf{k}_1}\Delta_n}\big)^2\big(1-e^{-\lambda_{\mathbf{k}_2}\Delta_n}\big)^2}{2\lambda_{\mathbf{k}_1}^{1+\alpha}\lambda_{\mathbf{k}_2}^{1+\alpha}} \cdot \frac{1}{1-e^{-(\lambda_{\mathbf{k}_1}+\lambda_{\mathbf{k}_2})\Delta_n}} + \frac{\big(1-e^{-\lambda_{\mathbf{k}_1}\Delta_n}\big)\big(1-e^{-\lambda_{\mathbf{k}_2}\Delta_n}\big)}{\lambda_{\mathbf{k}_1}^{1+\alpha}\lambda_{\mathbf{k}_2}^{1+\alpha}} \Bigg) \\
&\quad \times \bigg(1+\mathcal{O}\Big(1\wedge \frac{p^{-1}}{1-e^{-(\lambda_{\mathbf{k}_1}+\lambda_{\mathbf{k}_2})\Delta_n}}\Big)\bigg).
\end{aligned}
$$

Recalling the calculations of the covariance yields

$$
\begin{aligned}
&\mathbb{C}\mathrm{ov}\big(V_{p,\Delta_n}(\mathbf{y}_1), V_{p,\Delta_n}(\mathbf{y}_2)\big) \\
&= \frac{2e^{\|\kappa\cdot(\mathbf{y}_1+\mathbf{y}_2)\|_1}\sigma^4}{p\Delta_n^{2\alpha'}} \sum_{\substack{\mathbf{k}_1,\mathbf{k}_2\in\mathbb{N}^d \\ \mathbf{k}_1\neq\mathbf{k}_2}} e_{\mathbf{k}_1}(\mathbf{y}_1)e_{\mathbf{k}_1}(\mathbf{y}_2)e_{\mathbf{k}_2}(\mathbf{y}_1)e_{\mathbf{k}_2}(\mathbf{y}_2)\bar{D}_{\mathbf{k}_1,\mathbf{k}_2}\bigg(1+\mathcal{O}\Big(1\wedge \frac{p^{-1}}{1-e^{-(\lambda_{\mathbf{k}_1}+\lambda_{\mathbf{k}_2})\Delta_n}}\Big)\bigg) \\
&\quad + \frac{2e^{\|\kappa\cdot(\mathbf{y}_1+\mathbf{y}_2)\|_1}}{p\Delta_n^{2\alpha'}} \sum_{\mathbf{k}\in\mathbb{N}^d} e_{\mathbf{k}}^2(\mathbf{y}_1)e_{\mathbf{k}}^2(\mathbf{y}_2)D_{\mathbf{k},\mathbf{k}},
\end{aligned}
$$

where we define

$$
\bar{D}_{\mathbf{k}_1,\mathbf{k}_2} := \frac{\big(1-e^{-\lambda_{\mathbf{k}_1}\Delta_n}\big)^2\big(1-e^{-\lambda_{\mathbf{k}_2}\Delta_n}\big)^2}{2\lambda_{\mathbf{k}_1}^{1+\alpha}\lambda_{\mathbf{k}_2}^{1+\alpha}} \cdot \frac{1}{1-e^{-(\lambda_{\mathbf{k}_1}+\lambda_{\mathbf{k}_2})\Delta_n}} + \frac{\big(1-e^{-\lambda_{\mathbf{k}_1}\Delta_n}\big)\big(1-e^{-\lambda_{\mathbf{k}_2}\Delta_n}\big)}{\lambda_{\mathbf{k}_1}^{1+\alpha}\lambda_{\mathbf{k}_2}^{1+\alpha}}. \tag{116}
$$

Regarding the remainder, we utilize the inequality $(1-e^{-(x+y)})^{-1} \leqslant (1-e^{-x})^{-1/2}(1-e^{-y})^{-1/2}$. For a sufficiently large p, we deduce that

$$
\frac{1}{p^2\Delta_n^{2\alpha'}} \sum_{\substack{\mathbf{k}_1,\mathbf{k}_2\in\mathbb{N}^d \\ \mathbf{k}_1\neq\mathbf{k}_2}} \frac{\overline{D}_{\mathbf{k}_1,\mathbf{k}_2}}{1-e^{-(\lambda_{\mathbf{k}_1}+\lambda_{\mathbf{k}_2})\Delta_n}}
$$

$$\leqslant \frac{1}{p^2\Delta_n^{2\alpha'}} \sum_{\substack{\mathbf{k}_1,\mathbf{k}_2\in\mathbb{N}^d\\ \mathbf{k}_1\neq\mathbf{k}_2}} \frac{\big(1-e^{-\lambda_{\mathbf{k}_1}\Delta_n}\big)\big(1-e^{-\lambda_{\mathbf{k}_2}\Delta_n}\big)}{2\lambda_{\mathbf{k}_1}^{1+\alpha}\lambda_{\mathbf{k}_2}^{1+\alpha}} + 2\frac{\big(1-e^{-\lambda_{\mathbf{k}_1}\Delta_n}\big)^{1/2}\big(1-e^{-\lambda_{\mathbf{k}_2}\Delta_n}\big)^{1/2}}{2\lambda_{\mathbf{k}_1}^{1+\alpha}\lambda_{\mathbf{k}_2}^{1+\alpha}}$$

$$\leqslant \frac{3}{p^2\Delta_n^{2\alpha'}}\bigg(\sum_{\mathbf{k}\in\mathbb{N}^d}\frac{\big(1-e^{-\lambda_{\mathbf{k}}\Delta_n}\big)^{1/2}}{2\lambda_{\mathbf{k}}^{1+\alpha}}\bigg)^2.$$

Thanks to Lemma 4.2.1 and $\lambda_{\mathbf{k}}\propto\|\mathbf{k}\|_2^2$, we obtain the convergence of the series, such that

$$\begin{aligned}
\frac{1}{p^2\Delta_n^{2\alpha'}} \sum_{\substack{\mathbf{k}_1,\mathbf{k}_2\in\mathbb{N}^d\\ \mathbf{k}_1\neq\mathbf{k}_2}} \frac{\overline{D}_{\mathbf{k}_1,\mathbf{k}_2}}{1-e^{-(\lambda_{\mathbf{k}_1}+\lambda_{\mathbf{k}_2})\Delta_n}} &= \mathcal{O}\bigg(\frac{1}{p^2\Delta_n^{2\alpha'}}\bigg(\Delta_n^{1+d/2-1+\alpha'/2}\sum_{\mathbf{k}\in\mathbb{N}^d}\frac{\sqrt{1-e^{-\lambda_{\mathbf{k}}\Delta_n}}}{\lambda_{\mathbf{k}}^{1+\alpha}\Delta_n^{1+d/2-1+\alpha'/2}}\bigg)^2\bigg)\\
&= \mathcal{O}\bigg(\frac{\Delta_n^{-\alpha'}}{p^2}\bigg(\Delta_n^{d/2}\sum_{\mathbf{k}\in\mathbb{N}^d}\frac{\sqrt{1-e^{-\lambda_{\mathbf{k}}\Delta_n}}}{(\lambda_{\mathbf{k}}\Delta_n)^{1+d/2-1+\alpha'/2}}\cdot\frac{1}{\|\mathbf{k}\|_2^{\alpha'}}\bigg)^2\bigg)\\
&= \mathcal{O}\bigg(\frac{\Delta_n^{-\alpha'}}{p^2}\bigg(\Delta_n^{d/2}\sum_{\mathbf{k}\in\mathbb{N}^d}\frac{\sqrt{1-e^{-\lambda_{\mathbf{k}}\Delta_n}}}{(\lambda_{\mathbf{k}}\Delta_n)^{1+d/2-1+\alpha'/2}}\bigg)^2\bigg)\\
&= \mathcal{O}\bigg(\frac{\Delta_n^{-\alpha'}}{p^2}\bigg(\int_0^\infty\frac{\sqrt{1-e^{-x}}}{x^{1+\alpha'/2}}\,\mathrm{d}x\bigg)^2\bigg) = \mathcal{O}\big(\Delta_n^{-\alpha'}p^{-2}\big),
\end{aligned}$$

where we used $\alpha = d/2-1+\alpha'$, for $\alpha'\in(0,1)$. For small p we always obtain a bound of order $\mathcal{O}(p^{-1})$, such that

$$\frac{1}{p\Delta_n^{2\alpha'}}\sum_{\substack{\mathbf{k}_1,\mathbf{k}_2\in\mathbb{N}^d\\ \mathbf{k}_1\neq\mathbf{k}_2}} e_{\mathbf{k}_1}(\mathbf{y}_1)e_{\mathbf{k}_1}(\mathbf{y}_2)e_{\mathbf{k}_2}(\mathbf{y}_1)e_{\mathbf{k}_2}(\mathbf{y}_2)\bar{D}_{\mathbf{k}_1,\mathbf{k}_2}\cdot\mathcal{O}\bigg(1\wedge\frac{p^{-1}}{1-e^{-(\lambda_{\mathbf{k}_1}+\lambda_{\mathbf{k}_2})\Delta_n}}\bigg) = \mathcal{O}\bigg(\frac{1}{p}\Big(1\wedge\frac{\Delta_n^{-\alpha'}}{p}\Big)\bigg).$$

Thus, we find

$$\begin{aligned}
\mathbb{C}\mathrm{ov}\big(V_{p,\Delta_n}(\mathbf{y}_1),V_{p,\Delta_n}(\mathbf{y}_2)\big) &= \frac{2e^{\|\kappa\cdot(\mathbf{y}_1+\mathbf{y}_2)\|_1}\sigma^4}{p\Delta_n^{2\alpha'}}\sum_{\substack{\mathbf{k}_1,\mathbf{k}_2\in\mathbb{N}^d\\ \mathbf{k}_1\neq\mathbf{k}_2}} e_{\mathbf{k}_1}(\mathbf{y}_1)e_{\mathbf{k}_1}(\mathbf{y}_2)e_{\mathbf{k}_2}(\mathbf{y}_1)e_{\mathbf{k}_2}(\mathbf{y}_2)\bar{D}_{\mathbf{k}_1,\mathbf{k}_2}\\
&\quad+\frac{2e^{\|\kappa\cdot(\mathbf{y}_1+\mathbf{y}_2)\|_1}}{p\Delta_n^{2\alpha'}}\sum_{\mathbf{k}\in\mathbb{N}^d} e_{\mathbf{k}}^2(\mathbf{y}_1)e_{\mathbf{k}}^2(\mathbf{y}_2)D_{\mathbf{k},\mathbf{k}} + \mathcal{O}\bigg(\frac{1}{p}\Big(1\wedge\frac{\Delta_n^{-\alpha'}}{p}\Big)\bigg).
\end{aligned}$$

For $\mathbf{k}_1=\mathbf{k}_2=\mathbf{k}$, we have

$$\begin{aligned}
D_{\mathbf{k},\mathbf{k}} &= \frac{1}{p}\sum_{i,j=1}^{p}\bigg(\mathbb{E}\Big[\big(\tilde{B}_{i,\mathbf{k}}+C_{i,\mathbf{k}}\big)\big(\tilde{B}_{j,\mathbf{k}}+C_{j,\mathbf{k}}\big)\Big]\mathbb{E}\Big[\big(\tilde{B}_{i,\mathbf{k}}+C_{i,\mathbf{k}}\big)\big(\tilde{B}_{j,\mathbf{k}}+C_{j,\mathbf{k}}\big)\Big]\\
&\qquad+\mathbb{E}\Big[\big(\tilde{B}_{i,\mathbf{k}}+C_{i,\mathbf{k}}\big)\big(\tilde{B}_{j,\mathbf{k}}+C_{j,\mathbf{k}}\big)\Big]\mathbb{E}\Big[\big(\tilde{B}_{i,\mathbf{k}}+C_{i,\mathbf{k}}\big)\big(\tilde{B}_{j,\mathbf{k}}+C_{j,\mathbf{k}}\big)\Big]\bigg)\\
&= \frac{2}{p}\sum_{i,j=1}^{p}\mathbb{E}\Big[\big(\tilde{B}_{i,\mathbf{k}}+C_{i,\mathbf{k}}\big)\big(\tilde{B}_{j,\mathbf{k}}+C_{j,\mathbf{k}}\big)\Big]^2\\
&= \frac{2}{p}\sum_{i,j=1}^{p}\Big(\tilde{\Sigma}_{i,j}^{B,\mathbf{k}}+\Sigma_{i,j}^{BC,\mathbf{k}}+\Sigma_{j,i}^{BC,\mathbf{k}}+\Sigma_{i,j}^{C,\mathbf{k}}\Big)^2\\
&= \frac{2}{p}\sum_{i,j=1}^{p}\Big(\tilde{\Sigma}_{i,j}^{B,\mathbf{k}}\Big)^2+\Big(\Sigma_{i,j}^{BC,\mathbf{k}}\Big)^2+\Big(\Sigma_{j,i}^{BC,\mathbf{k}}\Big)^2+\Big(\Sigma_{i,j}^{C,\mathbf{k}}\Big)^2+2\tilde{\Sigma}_{i,j}^{B,\mathbf{k}}\Big(\Sigma_{i,j}^{BC,\mathbf{k}}+\Sigma_{j,i}^{BC,\mathbf{k}}\Big)+2\tilde{\Sigma}_{i,j}^{B,\mathbf{k}}\Sigma_{i,j}^{C,\mathbf{k}}
\end{aligned}$$

$$
\begin{aligned}
&\leqslant \frac{4}{p}\sum_{i,j=1}^{p}\Big(\tilde{\Sigma}_{i,j}^{B,\mathbf{k}}\Big)^2+\Big(\Sigma_{i,j}^{BC,\mathbf{k}}\Big)^2+\Big(\Sigma_{j,i}^{BC,\mathbf{k}}\Big)^2+\Big(\Sigma_{i,j}^{C,\mathbf{k}}\Big)^2\\
&= \frac{4}{p}\sum_{i,j=1}^{p}\Big(\tilde{\Sigma}_{i,j}^{B,\mathbf{k}}\Big)^2+2\Big(\Sigma_{i,j}^{BC,\mathbf{k}}\Big)^2+\Big(\Sigma_{i,j}^{C,\mathbf{k}}\Big)^2.
\end{aligned}
$$

Calculating the covariance terms results in

$$
\begin{aligned}
\frac{1}{p}\sum_{i,j=1}^{p}\tilde{\Sigma}_{i,j}^{B,\mathbf{k}}\tilde{\Sigma}_{i,j}^{B,\mathbf{k}} &= \sigma^4\frac{\big(1-e^{-\lambda_{\mathbf{k}}\Delta_n}\big)^4}{4\lambda_{\mathbf{k}}^{2(1+\alpha)}}\frac{1+e^{-2\lambda_{\mathbf{k}}\Delta_n}}{1-e^{-2\lambda_{\mathbf{k}}\Delta_n}}\bigg(1+\mathcal{O}\Big(1\wedge\frac{p^{-1}}{1-e^{-2\lambda_{\mathbf{k}}\Delta_n}}\Big)\bigg),\\
\frac{1}{p}\sum_{i,j=1}^{p}\Sigma_{i,j}^{BC,\mathbf{k}}\Sigma_{i,j}^{BC,\mathbf{k}} &= \sigma^4\frac{\big(1-e^{-\lambda_{\mathbf{k}}\Delta_n}\big)^2}{4\lambda_{\mathbf{k}}^{2(1+\alpha)}}\cdot\frac{(1-e^{-2\lambda_{\mathbf{k}}\Delta_n})^2}{1-e^{-2\lambda_{\mathbf{k}}\Delta_n}}\bigg(1+\mathcal{O}\Big(1\wedge\frac{p^{-1}}{1-e^{-2\lambda_{\mathbf{k}}\Delta_n}}\Big)\bigg),\\
\frac{1}{p}\sum_{i,j=1}^{p}\Sigma_{i,j}^{C,\mathbf{k}}\Sigma_{i,j}^{C,\mathbf{k}} &= \sigma^4\frac{\big(1-e^{-2\lambda_{\mathbf{k}}\Delta_n}\big)^2}{4\lambda_{\mathbf{k}}^{2(1+\alpha)}},
\end{aligned}
$$

where we used analogous steps as for $\mathbf{k}_1\neq\mathbf{k}_2$. For $\mathbf{k}_1=\mathbf{k}_2=\mathbf{k}$ we derive that

$$
\begin{aligned}
D_{\mathbf{k},\mathbf{k}} \leqslant \sigma^4\Bigg(&\frac{\big(1-e^{-\lambda_{\mathbf{k}}\Delta_n}\big)^4}{\lambda_{\mathbf{k}}^{2(1+\alpha)}}\frac{1+e^{-2\lambda_{\mathbf{k}}\Delta_n}}{1-e^{-2\lambda_{\mathbf{k}}\Delta_n}}\\
&+2\frac{\big(1-e^{-\lambda_{\mathbf{k}}\Delta_n}\big)^2}{\lambda_{\mathbf{k}}^{2(1+\alpha)}}\big(1-e^{-2\lambda_{\mathbf{k}}\Delta_n}\big)+\frac{\big(1-e^{-2\lambda_{\mathbf{k}}\Delta_n}\big)^2}{\lambda_{\mathbf{k}}^{2(1+\alpha)}}\Bigg)\bigg(1+\mathcal{O}\Big(1\wedge\frac{p^{-1}}{1-e^{-2\lambda_{\mathbf{k}}\Delta_n}}\Big)\bigg),
\end{aligned}
$$

where we define

$$
\overline{D}_{\mathbf{k},\mathbf{k}} := \frac{\big(1-e^{-\lambda_{\mathbf{k}}\Delta_n}\big)^4}{\lambda_{\mathbf{k}}^{2(1+\alpha)}}\frac{1+e^{-2\lambda_{\mathbf{k}}\Delta_n}}{1-e^{-2\lambda_{\mathbf{k}}\Delta_n}}+2\frac{\big(1-e^{-\lambda_{\mathbf{k}}\Delta_n}\big)^2}{\lambda_{\mathbf{k}}^{2(1+\alpha)}}\big(1-e^{-2\lambda_{\mathbf{k}}\Delta_n}\big)+\frac{\big(1-e^{-2\lambda_{\mathbf{k}}\Delta_n}\big)^2}{\lambda_{\mathbf{k}}^{2(1+\alpha)}}.
$$

We demonstrate that $D_{\mathbf{k},\mathbf{k}}$ is negligible, which is evident by the following calculation:

$$
\begin{aligned}
\frac{1}{p\Delta_n^{2\alpha'}}\sum_{\mathbf{k}\in\mathbb{N}^d}\overline{D}_{\mathbf{k},\mathbf{k}} &= \frac{1}{p\Delta_n^{2\alpha'}}\sum_{\mathbf{k}\in\mathbb{N}^d}\frac{\big(1-e^{-2\lambda_{\mathbf{k}}\Delta_n}\big)^2}{\lambda_{\mathbf{k}}^{2(1+\alpha)}}\Bigg(\frac{\big(1-e^{-\lambda_{\mathbf{k}}\Delta_n}\big)^4\big(1+e^{-2\lambda_{\mathbf{k}}\Delta_n}\big)}{\big(1-e^{-2\lambda_{\mathbf{k}}\Delta_n}\big)^3}+2\frac{\big(1-e^{-\lambda_{\mathbf{k}}\Delta_n}\big)^2}{1-e^{-2\lambda_{\mathbf{k}}\Delta_n}}+1\Bigg)\\
&\leqslant \frac{4}{p\Delta_n^{2\alpha'}}\sum_{\mathbf{k}\in\mathbb{N}^d}\frac{\big(1-e^{-2\lambda_{\mathbf{k}}\Delta_n}\big)^2}{\lambda_{\mathbf{k}}^{2(1+\alpha)}}\\
&= \frac{4}{p\Delta_n^{2\alpha'}}\sum_{\mathbf{k}\in\mathbb{N}^d}\bigg(\Delta_n^{1+\alpha}\frac{1-e^{-2\lambda_{\mathbf{k}}\Delta_n}}{(\lambda_{\mathbf{k}}\Delta_n)^{1+\alpha}}\bigg)^2\\
&= \frac{4\Delta_n^{d/2}}{p}\Delta_n^{d/2}\sum_{\mathbf{k}\in\mathbb{N}^d}\bigg(\frac{1-e^{-2\lambda_{\mathbf{k}}\Delta_n}}{(\lambda_{\mathbf{k}}\Delta_n)^{1+\alpha}}\bigg)^2=\mathcal{O}(p^{-1}\Delta_n^{2(1-\alpha')}),
\end{aligned}
\tag{117}
$$

where we can use analogous steps as in Lemma 4.2.3 to show that

$$
\bigg(\frac{1-e^{-2x}}{x^{1+\alpha}}\bigg)^2 = f_\alpha^2(x)\in\mathcal{Q}_\beta,\qquad\text{with}\qquad \beta=\big(4\alpha,1+4\alpha,2+4\alpha\big).
$$

Hence, we have

$$\mathbb{C}\mathrm{ov}\big(V_{p,\Delta_n}(\mathbf{y}_1),V_{p,\Delta_n}(\mathbf{y}_2)\big)=\frac{2\sigma^4 e^{\|\kappa\bullet(\mathbf{y}_1+\mathbf{y}_2)\|_1}}{p\Delta_n^{2\alpha'}}\sum_{\substack{\mathbf{k}_1,\mathbf{k}_2\in\mathbb{N}^d\\ \mathbf{k}_1\neq\mathbf{k}_2}}e_{\mathbf{k}_1}(\mathbf{y}_1)e_{\mathbf{k}_1}(\mathbf{y}_2)e_{\mathbf{k}_2}(\mathbf{y}_1)e_{\mathbf{k}_2}(\mathbf{y}_2)\bar{D}_{\mathbf{k}_1,\mathbf{k}_2}$$
$$+\mathcal{O}\bigg(\frac{1}{p}\Big(\Delta_n^{2(1-\alpha')}+\frac{\Delta_n^{-\alpha'}}{p}\wedge 1\Big)\bigg).$$

We can represent the term $\bar{D}_{\mathbf{k}_1,\mathbf{k}_2}$ from equation (116) as

$$\bar{D}_{\mathbf{k}_1,\mathbf{k}_2}=\frac{\big(1-e^{-\lambda_{\mathbf{k}_1}\Delta_n}\big)^2\big(1-e^{-\lambda_{\mathbf{k}_2}\Delta_n}\big)^2}{2\lambda_{\mathbf{k}_1}^{1+\alpha}\lambda_{\mathbf{k}_2}^{1+\alpha}}\sum_{r=0}^{\infty}e^{-r(\lambda_{\mathbf{k}_1}+\lambda_{\mathbf{k}_2})\Delta_n}+\frac{\big(1-e^{-\lambda_{\mathbf{k}_1}\Delta_n}\big)\big(1-e^{-\lambda_{\mathbf{k}_2}\Delta_n}\big)}{\lambda_{\mathbf{k}_1}^{1+\alpha}\lambda_{\mathbf{k}_2}^{1+\alpha}},$$

and decompose as follows:

$$\bar{D}^1_{\mathbf{k}_1,\mathbf{k}_2}:=\sum_{r=0}^{\infty}\frac{\big(1-e^{-\lambda_{\mathbf{k}_1}\Delta_n}\big)^2\big(1-e^{-\lambda_{\mathbf{k}_2}\Delta_n}\big)^2}{2\lambda_{\mathbf{k}_1}^{1+\alpha}\lambda_{\mathbf{k}_2}^{1+\alpha}}e^{-r(\lambda_{\mathbf{k}_1}+\lambda_{\mathbf{k}_2})\Delta_n},$$
$$\bar{D}^2_{\mathbf{k}_1,\mathbf{k}_2}:=\frac{\big(1-e^{-\lambda_{\mathbf{k}_1}\Delta_n}\big)\big(1-e^{-\lambda_{\mathbf{k}_2}\Delta_n}\big)}{\lambda_{\mathbf{k}_1}^{1+\alpha}\lambda_{\mathbf{k}_2}^{1+\alpha}}.$$

Assume $\mathbf{y}_1\neq\mathbf{y}_2$, then we have

$$e_{\mathbf{k}}(\mathbf{y}_1)e_{\mathbf{k}}(\mathbf{y}_2)=e^{-\|\kappa\bullet(\mathbf{y}_1+\mathbf{y}_2)\|_1}2^d\prod_{l=1}^d\sin(\pi k_l y_l^{(1)})\sin(\pi k_l y_l^{(2)})$$
$$=e^{-\|\kappa\bullet(\mathbf{y}_1+\mathbf{y}_2)\|_1}\prod_{l=1}^d\Big(\cos\big(\pi k_l(y_l^{(1)}-y_l^{(2)})\big)-\cos\big(\pi k_l(y_l^{(1)}+y_l^{(2)})\big)\Big). \tag{118}$$

Let $x_l^{(1)},x_l^{(2)}\in\{(y_l^{(1)}-y_l^{(2)})/2,(y_l^{(1)}+y_l^{(2)})/2\}$, then we find

$$\frac{1}{p\Delta_n^{2\alpha'}}\sum_{\mathbf{k}_1,\mathbf{k}_2\in\mathbb{N}^d}\bar{D}^1_{\mathbf{k}_1,\mathbf{k}_2}\prod_{l=1}^d\cos(2\pi k_l^{(1)}x_l^{(1)})\cos(2\pi k_l^{(2)}x_l^{(2)})$$
$$=\frac{2}{p\Delta_n^{2\alpha'}}\sum_{r=0}^{\infty}\bigg(\Delta_n^{1+\alpha}\sum_{\mathbf{k}_1\in\mathbb{N}^d}g_{\alpha,r}(\lambda_{\mathbf{k}_1}\Delta_n)\prod_{l=1}^d\cos(2\pi k_l^{(1)}x_l^{(1)})\bigg)\bigg(\Delta_n^{1+\alpha}\sum_{\mathbf{k}_2\in\mathbb{N}^d}g_{\alpha,r}(\lambda_{\mathbf{k}_2}\Delta_n)\prod_{l=1}^d\cos(2\pi k_l^{(2)}x_l^{(2)})\bigg)$$
$$=\frac{2}{p}\sum_{r=0}^{\infty}\bigg(\Delta_n^{d/2}\sum_{\mathbf{k}_1\in\mathbb{N}^d}g_{\alpha,r}(\lambda_{\mathbf{k}_1}\Delta_n)\prod_{l=1}^d\cos(2\pi k_l^{(1)}x_l^{(1)})\bigg)\bigg(\Delta_n^{d/2}\sum_{\mathbf{k}_2\in\mathbb{N}^d}g_{\alpha,r}(\lambda_{\mathbf{k}_2}\Delta_n)\prod_{l=1}^d\cos(2\pi k_l^{(2)}x_l^{(2)})\bigg).$$

Note that $\mathbf{y}_1\neq\mathbf{y}_2$ only implies that one coordinate $y_l^{(1)}\neq y_l^{(2)}$ differs. To analyse the order of the latter display, we utilize Corollary 4.2.2 (ii) and (iii) on the function $g_{\alpha,\tau}\in\mathcal{Q}_{(2\alpha,2(1+\alpha),2(1+\alpha))}$ from display (67), which gives the following:

$$\Delta_n^{d/2}\sum_{\mathbf{k}_2\in\mathbb{N}^d}g_{\alpha,r}(\lambda_{\mathbf{k}_2}\Delta_n)\prod_{l=1}^d\cos(2\pi k_l^{(2)}x_l^{(2)})=\mathcal{O}\bigg(\frac{\Delta_n^{1-\alpha'}}{\|\mathbf{y}_1-\mathbf{y}_2\|_0^{d+1}}+\frac{\Delta_n^{1-\alpha'}}{\delta^{d+1}}\bigg).$$

Here, we considered the case when $\mathbf{y}_1\neq\mathbf{y}_2$ differing in every component, i.e., we used the order from

Lemma 4.2.2 (iii) and took into account that x_l can exceed or fall below the limit of $1-\delta$ and δ, respectively, by inserting the bounds $\|\mathbf{y}_1-\mathbf{y}_2\|_0$ and δ. Hence, we have

$$\begin{aligned}
&\frac{2}{p}\sum_{r=0}^{\infty}\Big(\Delta_n^{d/2}\sum_{\mathbf{k}_1\in\mathbb{N}^d}g_{\alpha,r}(\lambda_{\mathbf{k}_1}\Delta_n)\prod_{l=1}^{d}\cos(2\pi k_l^{(1)}x_l^{(1)})\Big)\Big(\Delta_n^{d/2}\sum_{\mathbf{k}_2\in\mathbb{N}^d}g_{\alpha,r}(\lambda_{\mathbf{k}_2}\Delta_n)\prod_{l=1}^{d}\cos(2\pi k_l^{(2)}x_l^{(2)})\Big)\\
&=\mathcal{O}\bigg(\frac{\Delta_n^{1-\alpha'}}{p}\big(\|\mathbf{y}_1-\mathbf{y}_2\|_0^{-(d+1)}+\delta^{-(d+1)}\big)\sum_{r=0}^{\infty}\Delta_n^{d/2}\sum_{\mathbf{k}\in\mathbb{N}^d}|g_{\alpha,r}(\lambda_{\mathbf{k}}\Delta_n)|\bigg)\\
&=\mathcal{O}\bigg(\frac{\Delta_n^{1-\alpha'}}{p}\big(\|\mathbf{y}_1-\mathbf{y}_2\|_0^{-(d+1)}+\delta^{-(d+1)}\big)\Big(\Delta_n^{d/2}\sum_{\mathbf{k}\in\mathbb{N}^d}\frac{1-e^{-\lambda_{\mathbf{k}}\Delta_n}}{(\lambda_{\mathbf{k}}\Delta_n)^{1+\alpha}}\Big)\bigg)\\
&=\mathcal{O}\bigg(\frac{\Delta_n^{1-\alpha'}}{p}\big(\|\mathbf{y}_1-\mathbf{y}_2\|_0^{-(d+1)}+\delta^{-(d+1)}\big)\bigg). \qquad (119)
\end{aligned}$$

Analogous considerations hold for the second term $\bar{D}^2$, where we can employ the function f_α from equation (67), yielding the following:

$$\begin{aligned}
\mathbb{C}\mathrm{ov}\big(V_{p,\Delta_n}(\mathbf{y}_1),V_{p,\Delta_n}(\mathbf{y}_2)\big)&=\mathcal{O}\bigg(\frac{\Delta_n^{1-\alpha'}}{p}\big(\|\mathbf{y}_1-\mathbf{y}_2\|_0^{-(d+1)}+\delta^{-(d+1)}\big)\bigg)+\mathcal{O}\bigg(\frac{1}{p}\Big(\Delta_n^{2(1-\alpha')}+\frac{\Delta_n^{-\alpha'}}{p}\wedge 1\Big)\bigg)\\
&=\mathcal{O}\bigg(\frac{\Delta_n^{1-\alpha'}}{p}\big(\|\mathbf{y}_1-\mathbf{y}_2\|_0^{-(d+1)}+\delta^{-(d+1)}\big)\vee\frac{\Delta_n^{-\alpha'}}{p^2}\bigg),
\end{aligned}$$

for $\mathbf{y}_1\neq\mathbf{y}_2$. Thus, it remains to compute the variance, where $\mathbf{y}_1=\mathbf{y}_2=\mathbf{y}\in[\delta,1-\delta]^d$. Again, utilizing

$$e_{\mathbf{k}}(\mathbf{y})e_{\mathbf{k}}(\mathbf{y})=e^{-2\|\kappa\cdot\mathbf{y}\|_1}\prod_{l=1}^{d}\Big(\cos(0)-\cos(2\pi k_l y_l)\Big),$$

and having $x_l^{(1)},x_l^{(2)}\in\{0,y_l\}$, we infer analogously to display (119) that

$$\begin{aligned}
&\frac{1}{p\Delta_n^{2\alpha'}}\sum_{\mathbf{k}_1,\mathbf{k}_2\in\mathbb{N}^d}\bar{D}^1_{\mathbf{k}_1,\mathbf{k}_2}\prod_{l=1}^{d}\cos(2\pi k_l^{(1)}x_l^{(1)})\cos(2\pi k_l^{(2)}x_l^{(2)})\\
&=\frac{2}{p}\sum_{r=0}^{\infty}\Big(\Delta_n^{d/2}\sum_{\mathbf{k}_1\in\mathbb{N}^d}g_{\alpha,r}(\lambda_{\mathbf{k}_1}\Delta_n)\prod_{l=1}^{d}\cos(2\pi k_l^{(1)}x_l^{(1)})\Big)\Big(\Delta_n^{d/2}\sum_{\mathbf{k}_2\in\mathbb{N}^d}g_{\alpha,r}(\lambda_{\mathbf{k}_2}\Delta_n)\prod_{l=1}^{d}\cos(2\pi k_l^{(2)}x_l^{(2)})\Big).
\end{aligned}$$

Now assume, without loss of generality, that $\sum_{j=1}^d \mathbb{1}_{\{x_j^{(1)}\neq 0\}}=l$, for $1\leqslant l\leqslant d$. Then, by Corollary 4.2.2 (ii) and (iii), we have

$$\Delta_n^{d/2}\sum_{\mathbf{k}_2\in\mathbb{N}^d}g_{\alpha,r}(\lambda_{\mathbf{k}_2}\Delta_n)\prod_{l=1}^{d}\cos(2\pi k_l^{(2)}x_l^{(2)})=\mathcal{O}\Big(\Delta_n^{l/2}\vee\frac{\Delta_n^{1-\alpha'}}{\delta^{d+1}}\Big).$$

Hence, we conclude that

$$\frac{1}{p\Delta_n^{2\alpha'}}\sum_{\mathbf{k}_1,\mathbf{k}_2\in\mathbb{N}^d}\bar{D}^1_{\mathbf{k}_1,\mathbf{k}_2}\prod_{l=1}^{d}\cos(2\pi k_l^{(1)}x_l^{(1)})\cos(2\pi k_l^{(2)}x_l^{(2)})=\mathcal{O}\Big(\frac{1}{p}\Big(\Delta_n^{1/2}\vee\frac{\Delta_n^{1-\alpha'}}{\delta^{d+1}}\Big)\Big),$$

and it follows that

$$\mathbb{V}\mathrm{ar}\big(V_{p,\Delta_n}(\mathbf{y})\big) = \frac{2\sigma^4 e^{2\|\kappa\bullet\mathbf{y}\|_1}}{p\Delta_n^{2\alpha'}} \sum_{\substack{\mathbf{k}_1,\mathbf{k}_2\in\mathbb{N}^d\\ \mathbf{k}_1\neq\mathbf{k}_2}} e_{\mathbf{k}_1}^2(\mathbf{y})e_{\mathbf{k}_2}^2(\mathbf{y})\bar{D}_{\mathbf{k}_1,\mathbf{k}_2} + \mathcal{O}\Big(\frac{1}{p}\Big(\Delta_n^{2(1-\alpha')} + \frac{\Delta_n^{-\alpha'}}{p}\wedge 1\Big)\Big)$$

$$= \frac{2\sigma^4}{p\Delta_n^{2\alpha'}} \sum_{\substack{\mathbf{k}_1,\mathbf{k}_2\in\mathbb{N}^d\\ \mathbf{k}_1\neq\mathbf{k}_2}} \bar{D}_{\mathbf{k}_1,\mathbf{k}_2} + \mathcal{O}\Big(\frac{1}{p}\Big(\Delta_n^{1/2}\vee\frac{\Delta_n^{1-\alpha'}}{\delta^{d+1}} + \frac{\Delta_n^{-\alpha'}}{p}\wedge 1\Big)\Big). \tag{120}$$

For the leading term we obtain

$$\frac{2\sigma^4}{p\Delta_n^{2\alpha'}} \sum_{\substack{\mathbf{k}_1,\mathbf{k}_2\in\mathbb{N}^d\\ \mathbf{k}_1\neq\mathbf{k}_2}} \bar{D}_{\mathbf{k}_1,\mathbf{k}_2} = \frac{\sigma^4}{p}\Bigg(\sum_{r=0}^{\infty}\Big(2\Delta_n^{d/2}\sum_{\mathbf{k}\in\mathbb{N}^d}\frac{(1-e^{-\lambda_{\mathbf{k}}\Delta_n})^2}{2(\lambda_{\mathbf{k}}\Delta_n)^{1+\alpha}}e^{-r\lambda_{\mathbf{k}}\Delta_n}\Big)^2 + 2\Big(\Delta_n^{d/2}\sum_{\mathbf{k}\in\mathbb{N}^d}\frac{1-e^{-\lambda_{\mathbf{k}}\Delta_n}}{(\lambda_{\mathbf{k}}\Delta_n)^{1+\alpha}}\Big)^2\Bigg)$$

$$= \frac{\sigma^4}{p}\Bigg(\sum_{r=0}^{\infty}\Big(2\Delta_n^{d/2}\sum_{\mathbf{k}\in\mathbb{N}^d} g_{\alpha,r}(\lambda_{\mathbf{k}}\Delta_n)\Big)^2 + 2\Big(\Delta_n^{d/2}\sum_{\mathbf{k}\in\mathbb{N}^d} f_\alpha(\lambda_{\mathbf{k}}\Delta_n)\Big)^2\Bigg),$$

and by Lemma 4.2.4 we have

$$\mathbb{V}\mathrm{ar}\big(V_{p,\Delta_n}(\mathbf{y})\big) = \frac{1}{p}\bigg(\frac{\Gamma(1-\alpha')\sigma^2}{2^d(\pi\eta)^{d/2}\alpha'\Gamma(d/2)}\bigg)^2\bigg(\sum_{r=0}^{\infty}\big(-r^{\alpha'}+2(r+1)^{\alpha'}-(r+2)^{\alpha'}\big)^2+2\bigg)$$
$$+\mathcal{O}\Big(\frac{1}{p}\Big(\Delta_n^{1/2}\vee\frac{\Delta_n^{1-\alpha'}}{\delta^{d+1}} + \frac{\Delta_n^{-\alpha'}}{p}\wedge 1\Big)\Big).$$

Defining the constant

$$\Upsilon_{\alpha'} := \bigg(\sum_{r=0}^{\infty}\big(-r^{\alpha'}+2(r+1)^{\alpha'}-(r+2)^{\alpha'}\big)^2+2\bigg) \tag{121}$$

completes the proof. □

Comparing the volatility estimators from the equations (71) and (72), with the exponentially rescaled realized volatility from display (112), we gain valuable insights into the asymptotic behaviour of both estimators, as revealed in the preceding proposition. In Chapter 4, we explored the impact of the damping parameter on the model, particularly on the temporal covariance structure. In Section 4.2, we discussed how the pure damping parameter α' governs the roughness of the temporal marginal processes. The previous proposition confirmed the conjecture that, due to this roughness property, α' is a crucial factor contributing to the asymptotic variance, denoted by $\Upsilon_{\alpha'}$. Note that we assume the pure damping parameter α' to be known within this section. The behaviour of the covariances is also of significant interest. We observe that the covariance structures vanish when we apply an appropriate relationship between spatial observations and temporal resolution. This relationship is already incorporated in Assumption 4.1.1 as a sufficient condition. However, a similar restriction is already evident in the one-dimension case, as discussed in Bibinger and Trabs (2020, Assumption 1). Nonetheless, we have tightened the intuitive extension of the one-dimensional case for the proportion ρ, which would be given by $0<\rho<(1-\alpha')/(d+1)$. The adjustment $0<\rho<(1-\alpha')/(d+2)$ is necessary due to the differing orders in the Riemann approximation from Lemma 4.2.1 when compared to the one-dimensional case. As the number of spatial dimensions increases, the restrictive nature of Assumption 4.1.1 becomes more pronounced.

5.3. Controlling temporal dependencies of the quadratic increments

Our aim in the upcoming section is to demonstrate central limit theorems for the estimator $\hat{\sigma}_n^2(\mathbf{y})$ from equation (71) and its robustification $\hat{\sigma}_{n,m}^2$ from equation (72). Hence, the objective of this section is to establish the proof that the dependencies of temporal quadratic increments can be appropriately bounded following the Condition (III) outlined in Proposition 1.2.4 by Peligrad et al. (1997). To achieve this, we control the temporal dependencies in two steps. In a first step, we bound the covariance of empirical characteristic functions in a single spatial coordinate. In a second step, we extend this result to encompass multiple spatial coordinates. In the case of multiple spatial coordinates, we observe that the dependencies are manageable only when the relationship between spatial and temporal observations is suitably chosen, as specified in Assumption 4.1.1.

Proposition 5.3.1

Grant the Assumptions 4.1.1 and 4.1.2. Let $\mathbf{y} \in [\delta, 1-\delta]^d$ for a $\delta > 0$, $1 \leqslant r < r+u \leqslant v \leqslant n$ natural numbers and

$$Q_1^r = \sum_{i=1}^{r} (\Delta_i \tilde{X})^2(\mathbf{y}), \qquad Q_{r+u}^v = \sum_{i=r+u}^{v} (\Delta_i \tilde{X})^2(\mathbf{y}),$$

then there exists a constant C, where $0 < C < \infty$, such that it holds for all $t \in \mathbb{R}$ that

$$\left| \mathbb{C}\mathrm{ov}\left(e^{\mathrm{i}t(Q_1^r - \mathbb{E}[Q_1^r])},\ e^{\mathrm{i}t(Q_{r+u}^v - \mathbb{E}[Q_{r+u}^v])} \right) \right| \leqslant \frac{Ct^2}{u^{1-\alpha'/2}} \sqrt{\mathbb{V}\mathrm{ar}(Q_1^r)\mathbb{V}\mathrm{ar}(Q_{r+u}^v)}.$$

Proof. Assume $Q_{r+u}^v = A_1 + A_2$, with some A_2 which is independent of Q_1^r. Then, we know by Bibinger and Trabs (2020, Prop. 6.6.) that

$$\mathbb{C}\mathrm{ov}\left(e^{\mathrm{i}t\bar{Q}_1^r}, e^{\mathrm{i}t\bar{Q}_{r+u}^v} \right) \leqslant 2t^2 \mathbb{E}\left[\left(\bar{Q}_1^r \right)^2 \right]^{1/2} \mathbb{E}\left[\left(\bar{A}_1 \right)^2 \right]^{1/2},$$

where $\bar{X} = X - \mathbb{E}[X]$. For $r \leqslant i-1$ we obtain

$$\begin{aligned}
\Delta_i \tilde{X}(\mathbf{y}) &= \sum_{\mathbf{k} \in \mathbb{N}^d} \left(\sigma \lambda_{\mathbf{k}}^{-\alpha/2} \int_{-\infty}^{r\Delta_n} e^{-\lambda_{\mathbf{k}}\left((i-1)\Delta_n - s\right)} \left(e^{-\lambda_{\mathbf{k}}\Delta_n} - 1 \right) \mathrm{d}W_s^{\mathbf{k}} \right) e_{\mathbf{k}}(\mathbf{y}) \\
&\quad + \sum_{\mathbf{k} \in \mathbb{N}^d} \left(\sigma \lambda_{\mathbf{k}}^{-\alpha/2} \int_{r\Delta_n}^{(i-1)\Delta_n} e^{-\lambda_{\mathbf{k}}\left((i-1)\Delta_n - s\right)} \left(e^{-\lambda_{\mathbf{k}}\Delta_n} - 1 \right) \mathrm{d}W_s^{\mathbf{k}} \right. \\
&\quad \left. + \sigma \lambda_{\mathbf{k}}^{-\alpha/2} \int_{(i-1)\Delta_n}^{i\Delta_n} e^{-\lambda_{\mathbf{k}}(i\Delta_n - s)} \, \mathrm{d}W_s^{\mathbf{k}} \right) e_{\mathbf{k}}(\mathbf{y}) \\
&= \sum_{\mathbf{k} \in \mathbb{N}^d} D_1^{\mathbf{k},i} e_{\mathbf{k}}(\mathbf{y}) + \sum_{\mathbf{k} \in \mathbb{N}^d} D_2^{\mathbf{k},i} e_{\mathbf{k}}(\mathbf{y}),
\end{aligned}$$

where

$$D_1^{\mathbf{k},i} := \sigma\lambda_{\mathbf{k}}^{-\alpha/2} \int_{-\infty}^{r\Delta_n} e^{-\lambda_{\mathbf{k}}\left((i-1)\Delta_n - s\right)} \left(e^{-\lambda_{\mathbf{k}}\Delta_n} - 1\right) \mathrm{d}W_s^{\mathbf{k}}, \tag{122}$$

$$D_2^{\mathbf{k},i} := \sigma\lambda_{\mathbf{k}}^{-\alpha/2} \int_{r\Delta_n}^{(i-1)\Delta_n} e^{-\lambda_{\mathbf{k}}\left((i-1)\Delta_n - s\right)} \left(e^{-\lambda_{\mathbf{k}}\Delta_n} - 1\right) \mathrm{d}W_s^{\mathbf{k}} + \sigma\lambda_{\mathbf{k}}^{-\alpha/2} \int_{(i-1)\Delta_n}^{i\Delta_n} e^{-\lambda_{\mathbf{k}}(i\Delta_n - s)} \,\mathrm{d}W_s^{\mathbf{k}}. \tag{123}$$

Note that $D_1^{\mathbf{k},i}$ and $D_2^{\mathbf{k},i}$ are independent, thus we have

$$Q_{r+u}^v = \sum_{i=r+u}^{v} \Big(\sum_{\mathbf{k}\in\mathbb{N}^d} D_1^{\mathbf{k},i} e_{\mathbf{k}}(\mathbf{y})\Big)^2 + 2\sum_{i=r+u}^{v} \Big(\sum_{\mathbf{k}\in\mathbb{N}^d} D_1^{\mathbf{k},i} e_{\mathbf{k}}(\mathbf{y})\Big)\Big(\sum_{\mathbf{k}\in\mathbb{N}^d} D_2^{\mathbf{k},i} e_{\mathbf{k}}(\mathbf{y})\Big) + \sum_{i=r+u}^{v} \Big(\sum_{\mathbf{k}\in\mathbb{N}^d} D_2^{\mathbf{k},i} e_{\mathbf{k}}(\mathbf{y})\Big)^2,$$

which implies the following decomposition:

$$\begin{aligned}
A_1 &:= \sum_{i=r+u}^{v} \Big(\sum_{\mathbf{k}\in\mathbb{N}^d} D_1^{\mathbf{k},i} e_{\mathbf{k}}(\mathbf{y})\Big)^2 + 2\sum_{i=r+u}^{v} \Big(\sum_{\mathbf{k}\in\mathbb{N}^d} D_1^{\mathbf{k},i} e_{\mathbf{k}}(\mathbf{y})\Big)\Big(\sum_{\mathbf{k}\in\mathbb{N}^d} D_2^{\mathbf{k},i} e_{\mathbf{k}}(\mathbf{y})\Big),\\
A_2 &:= \sum_{i=r+u}^{v} \Big(\sum_{\mathbf{k}\in\mathbb{N}^d} D_2^{\mathbf{k},i} e_{\mathbf{k}}(\mathbf{y})\Big)^2,
\end{aligned}$$

where A_2 is independent of Q_1^r. Hence, our focus shifts to bounding the term $\mathbb{E}[\bar{A}_1^2]$, which is equivalent to computing $\mathbb{V}\mathrm{ar}(A_1)$. We begin with the following considerations:

$$\begin{aligned}
\mathbb{E}[\bar{A}_1^2] &\leqslant \mathbb{E}[A_1^2]\\
&= \mathbb{E}\left[\left(\sum_{i=r+u}^{v} \Big(\sum_{\mathbf{k}\in\mathbb{N}^d} D_1^{\mathbf{k},i} e_{\mathbf{k}}(\mathbf{y})\Big)^2 + 2\sum_{i=r+u}^{v} \Big(\sum_{\mathbf{k}\in\mathbb{N}^d} D_1^{\mathbf{k},i} e_{\mathbf{k}}(\mathbf{y})\Big)\Big(\sum_{\mathbf{k}\in\mathbb{N}^d} D_2^{\mathbf{k},i} e_{\mathbf{k}}(\mathbf{y})\Big)\right)^2\right]\\
&= \sum_{i,j=r+u}^{v} \mathbb{E}\Big[\Big(\sum_{\mathbf{k}\in\mathbb{N}^d} D_1^{\mathbf{k},i} e_{\mathbf{k}}(\mathbf{y})\Big)^2\Big(\sum_{\mathbf{k}\in\mathbb{N}^d} D_1^{\mathbf{k},j} e_{\mathbf{k}}(\mathbf{y})\Big)^2\Big]\\
&\quad + 4\sum_{i,j=r+u}^{v} \mathbb{E}\Big[\Big(\sum_{\mathbf{k}\in\mathbb{N}^d} D_1^{\mathbf{k},i} e_{\mathbf{k}}(\mathbf{y})\Big)^2\Big(\sum_{\mathbf{k}\in\mathbb{N}^d} D_1^{\mathbf{k},j} e_{\mathbf{k}}(\mathbf{y})\Big)\Big(\sum_{\mathbf{k}\in\mathbb{N}^d} D_2^{\mathbf{k},j} e_{\mathbf{k}}(\mathbf{y})\Big)\Big]\\
&\quad + 4\sum_{i,j=r+u}^{v} \mathbb{E}\Big[\Big(\sum_{\mathbf{k}\in\mathbb{N}^d} D_1^{\mathbf{k},i} e_{\mathbf{k}}(\mathbf{y})\Big)\Big(\sum_{\mathbf{k}\in\mathbb{N}^d} D_2^{\mathbf{k},i} e_{\mathbf{k}}(\mathbf{y})\Big)\Big(\sum_{\mathbf{k}\in\mathbb{N}^d} D_1^{\mathbf{k},j} e_{\mathbf{k}}(\mathbf{y})\Big)\Big(\sum_{\mathbf{k}\in\mathbb{N}^d} D_2^{\mathbf{k},j} e_{\mathbf{k}}(\mathbf{y})\Big)\Big],
\end{aligned}$$

where the cross-term between $D_1^{\mathbf{k},i}, D_2^{\mathbf{k},i}$ vanishes as both terms are centred normally distributed. Therefore, we use $\mathbb{E}[\bar{A}_1^2] \leqslant T_1 + 4T_2$, where we define

$$T_1 := \sum_{i,j=r+u}^{v} \mathbb{E}\Big[\Big(\sum_{\mathbf{k}\in\mathbb{N}^d} D_1^{\mathbf{k},i} e_{\mathbf{k}}(\mathbf{y})\Big)^2\Big(\sum_{\mathbf{k}\in\mathbb{N}^d} D_1^{\mathbf{k},j} e_{\mathbf{k}}(\mathbf{y})\Big)^2\Big], \tag{124}$$

$$T_2 := \sum_{i,j=r+u}^{v} \mathbb{E}\Big[\Big(\sum_{\mathbf{k}\in\mathbb{N}^d} D_1^{\mathbf{k},i} e_{\mathbf{k}}(\mathbf{y})\Big)\Big(\sum_{\mathbf{k}\in\mathbb{N}^d} D_2^{\mathbf{k},i} e_{\mathbf{k}}(\mathbf{y})\Big)\Big(\sum_{\mathbf{k}\in\mathbb{N}^d} D_1^{\mathbf{k},j} e_{\mathbf{k}}(\mathbf{y})\Big)\Big(\sum_{\mathbf{k}\in\mathbb{N}^d} D_2^{\mathbf{k},j} e_{\mathbf{k}}(\mathbf{y})\Big)\Big]. \tag{125}$$

To bound the term T_1, we can utilize the expression $D_1^{\mathbf{k},i} = e^{-\lambda_{\mathbf{k}}(i-r-1)\Delta_n}\tilde{B}_{r+1,\mathbf{k}}$, where $\tilde{B}_{i,\mathbf{k}}$ is defined in equation (107), leading to the following calculation:

$$T_1 = \sum_{i,j=r+u}^{v} \sum_{\mathbf{k}_1,\mathbf{k}_2,\mathbf{k}_3,\mathbf{k}_4 \in \mathbb{N}^d} \mathbb{E}\Big[e^{-\lambda_{\mathbf{k}_1}(i-r-1)\Delta_n} \tilde{B}_{r+1,\mathbf{k}_1} e_{\mathbf{k}_1}(\mathbf{y}) e^{-\lambda_{\mathbf{k}_2}(i-r-1)\Delta_n} \tilde{B}_{r+1,\mathbf{k}_2} e_{\mathbf{k}_2}(\mathbf{y}) \times e^{-\lambda_{\mathbf{k}_3}(j-r-1)\Delta_n} \tilde{B}_{r+1,\mathbf{k}_3} e_{\mathbf{k}_3}(\mathbf{y}) e^{-\lambda_{\mathbf{k}_4}(j-r-1)\Delta_n} \tilde{B}_{r+1,\mathbf{k}_4} e_{\mathbf{k}_4}(\mathbf{y})\Big].$$

Note that any combination of indices results in a value of zero, unless, exactly two indices are equal, or all four indices are equal. Thus, we obtain for $\mathbf{k}_1 = \ldots = \mathbf{k}_4 = \mathbf{k}$ that

$$\sum_{i,j=r+u}^{v} \sum_{\mathbf{k} \in \mathbb{N}^d} e^{-2\lambda_{\mathbf{k}}(i+j-2r-2)\Delta_n} \mathbb{E}\Big[\tilde{B}_{r+1,\mathbf{k}}^4\Big] e_{\mathbf{k}}^4(\mathbf{y}).$$

For $\mathbf{k}_1 = \mathbf{k}_2$ and $\mathbf{k}_3 = \mathbf{k}_4$, with $\mathbf{k}_1 \neq \mathbf{k}_3$ we find that

$$\begin{aligned}
&\sum_{i,j=r+u}^{v} \sum_{\substack{\mathbf{k}_1,\mathbf{k}_2 \in \mathbb{N}^d \\ \mathbf{k}_1 \neq \mathbf{k}_2}} e^{-2\lambda_{\mathbf{k}_1}(i-r-1)\Delta_n} e^{-2\lambda_{\mathbf{k}_2}(j-r-1)\Delta_n} \mathbb{E}\Big[\tilde{B}_{r+1,\mathbf{k}_1}^2 \tilde{B}_{r+1,\mathbf{k}_2}^2\Big] e_{\mathbf{k}_1}^2(\mathbf{y}) e_{\mathbf{k}_2}^2(\mathbf{y}) \\
&= \sum_{i,j=r+u}^{v} \sum_{\substack{\mathbf{k}_1,\mathbf{k}_2 \in \mathbb{N}^d \\ \mathbf{k}_1 \neq \mathbf{k}_2}} e^{-2\lambda_{\mathbf{k}_1}(i-r-1)\Delta_n - 2\lambda_{\mathbf{k}_2}(j-r-1)\Delta_n} \mathbb{E}\Big[\tilde{B}_{r+1,\mathbf{k}_1}^2\Big] \mathbb{E}\Big[\tilde{B}_{r+1,\mathbf{k}_2}^2\Big] e_{\mathbf{k}_1}^2(\mathbf{y}) e_{\mathbf{k}_2}^2(\mathbf{y}).
\end{aligned}$$

The remaining combinations yield the following:

$$\begin{aligned}
&\sum_{i,j=r+u}^{v} \sum_{\substack{\mathbf{k}_1,\mathbf{k}_2 \in \mathbb{N}^d \\ \mathbf{k}_1 \neq \mathbf{k}_2}} e^{-\lambda_{\mathbf{k}_1}(i+j-2r-2)\Delta_n} e^{-\lambda_{\mathbf{k}_2}(i+j-2r-2)\Delta_n} \mathbb{E}\Big[\tilde{B}_{r+1,\mathbf{k}_1}^2 \tilde{B}_{r+1,\mathbf{k}_2}^2\Big] e_{\mathbf{k}_1}^2(\mathbf{y}) e_{\mathbf{k}_2}^2(\mathbf{y}) \\
&= \sum_{i,j=r+u}^{v} \sum_{\substack{\mathbf{k}_1,\mathbf{k}_2 \in \mathbb{N}^d \\ \mathbf{k}_1 \neq \mathbf{k}_2}} e^{-(\lambda_{\mathbf{k}_1}+\lambda_{\mathbf{k}_2})(i+j-2r-2)\Delta_n} \mathbb{E}\Big[\tilde{B}_{r+1,\mathbf{k}_1}^2\Big] \mathbb{E}\Big[\tilde{B}_{r+1,\mathbf{k}_2}^2\Big] e_{\mathbf{k}_1}^2(\mathbf{y}) e_{\mathbf{k}_2}^2(\mathbf{y}),
\end{aligned}$$

and we observe

$$\begin{aligned}
T_1 &= \sum_{i,j=r+u}^{v} \sum_{\substack{\mathbf{k}_1,\mathbf{k}_2 \in \mathbb{N}^d \\ \mathbf{k}_1 \neq \mathbf{k}_2}} e^{-2\lambda_{\mathbf{k}_1}(i-r-1)\Delta_n - 2\lambda_{\mathbf{k}_2}(j-r-1)\Delta_n} \mathbb{E}\Big[\tilde{B}_{r+1,\mathbf{k}_1}^2\Big] \mathbb{E}\Big[\tilde{B}_{r+1,\mathbf{k}_2}^2\Big] e_{\mathbf{k}_1}^2(\mathbf{y}) e_{\mathbf{k}_2}^2(\mathbf{y}) \\
&\quad + 2 \sum_{i,j=r+u}^{v} \sum_{\substack{\mathbf{k}_1,\mathbf{k}_2 \in \mathbb{N}^d \\ \mathbf{k}_1 \neq \mathbf{k}_2}} e^{-(\lambda_{\mathbf{k}_1}+\lambda_{\mathbf{k}_2})(i+j-2r-2)\Delta_n} \mathbb{E}\Big[\tilde{B}_{r+1,\mathbf{k}_1}^2\Big] \mathbb{E}\Big[\tilde{B}_{r+1,\mathbf{k}_2}^2\Big] e_{\mathbf{k}_1}^2(\mathbf{y}) e_{\mathbf{k}_2}^2(\mathbf{y}) \\
&\quad + \sum_{i,j=r+u}^{v} \sum_{\mathbf{k} \in \mathbb{N}^d} e^{-2\lambda_{\mathbf{k}}(i+j-2r-2)\Delta_n} \mathbb{E}\Big[\tilde{B}_{r+1,\mathbf{k}}^4\Big] e_{\mathbf{k}}^4(\mathbf{y}) \\
&= \sum_{\substack{\mathbf{k}_1,\mathbf{k}_2 \in \mathbb{N}^d \\ \mathbf{k}_1 \neq \mathbf{k}_2}} \sum_{i,j=r+u}^{v} \Big(e^{-2\lambda_{\mathbf{k}_1}(i-r-1)\Delta_n - 2\lambda_{\mathbf{k}_2}(j-r-1)\Delta_n} + 2e^{-(\lambda_{\mathbf{k}_1}+\lambda_{\mathbf{k}_2})(i+j-2r-2)\Delta_n}\Big) \\
&\quad \times \mathbb{E}\Big[\tilde{B}_{r+1,\mathbf{k}_1}^2\Big] \mathbb{E}\Big[\tilde{B}_{r+1,\mathbf{k}_2}^2\Big] e_{\mathbf{k}_1}^2(\mathbf{y}) e_{\mathbf{k}_2}^2(\mathbf{y}) + \sum_{\mathbf{k} \in \mathbb{N}^d} \sum_{i,j=r+u}^{v} e^{-2\lambda_{\mathbf{k}}(i+j-2r-2)\Delta_n} \mathbb{E}\Big[\tilde{B}_{r+1,\mathbf{k}}^4\Big] e_{\mathbf{k}}^4(\mathbf{y})
\end{aligned}$$

$$= \sigma^4 \sum_{\substack{\mathbf{k}_1,\mathbf{k}_2\in\mathbb{N}^d \\ \mathbf{k}_1\neq\mathbf{k}_2}} \frac{\big(1-e^{-\lambda_{\mathbf{k}_1}\Delta_n}\big)^2\big(1-e^{-\lambda_{\mathbf{k}_2}\Delta_n}\big)^2}{4\lambda_{\mathbf{k}_1}^{1+\alpha}\lambda_{\mathbf{k}_2}^{1+\alpha}} \left(\sum_{i=r+u}^{v} e^{-2\lambda_{\mathbf{k}_1}(i-r-1)\Delta_n}\right)\left(\sum_{j=r+u}^{v} e^{-2\lambda_{\mathbf{k}_2}(j-r-1)\Delta_n}\right)$$
$$\times e_{\mathbf{k}_1}^2(\mathbf{y})e_{\mathbf{k}_2}^2(\mathbf{y})$$
$$+ \sigma^4 \sum_{\substack{\mathbf{k}_1,\mathbf{k}_2\in\mathbb{N}^d \\ \mathbf{k}_1\neq\mathbf{k}_2}} \frac{\big(1-e^{-\lambda_{\mathbf{k}_1}\Delta_n}\big)^2\big(1-e^{-\lambda_{\mathbf{k}_2}\Delta_n}\big)^2}{4\lambda_{\mathbf{k}_1}^{1+\alpha}\lambda_{\mathbf{k}_2}^{1+\alpha}} 2\left(\sum_{i=r+u}^{v} e^{-(\lambda_{\mathbf{k}_1}+\lambda_{\mathbf{k}_2})(i-r-1)\Delta_n}\right)^2 e_{\mathbf{k}_1}^2(\mathbf{y})e_{\mathbf{k}_2}^2(\mathbf{y})$$
$$+ 3\sigma^4 \sum_{\mathbf{k}\in\mathbb{N}^d} \frac{\big(1-e^{-\lambda_{\mathbf{k}}\Delta_n}\big)^4}{4\lambda_{\mathbf{k}}^{2(1+\alpha)}} \left(\sum_{i=r+u}^{v} e^{-2\lambda_{\mathbf{k}}(i-r-1)\Delta_n}\right)^2 e_{\mathbf{k}}^4(\mathbf{y}).$$

Here, we used equation (113), which implies

$$\mathbb{E}\Big[\tilde{B}_{r+1,\mathbf{k}}^2\Big] = \frac{\sigma^2}{2\lambda_{\mathbf{k}}^{1+\alpha}}\big(1-e^{-\lambda_{\mathbf{k}}\Delta_n}\big)^2.$$

Let $\bar{p} = v-r-u+1$ and $u \geqslant 2$. First, we can bound the eigenfunctions $(e_{\mathbf{k}})_{\mathbf{k}\in\mathbb{N}^d}$ with a suitable constant $C>0$. Furthermore, we have

$$\begin{aligned}
\sum_{i=r+u}^{v} e^{-2\lambda_{\mathbf{k}}(i-r-1)\Delta_n} &= \sum_{i=0}^{v-r-u} e^{-2\lambda_{\mathbf{k}}(i+u-1)\Delta_n} \\
&= e^{-2\lambda_{\mathbf{k}}(u-1)\Delta_n}\frac{1-e^{-2\lambda_{\mathbf{k}}\Delta_n(v-r-u+1)}}{1-e^{-2\lambda_{\mathbf{k}}\Delta_n}} \\
&= e^{-2\lambda_{\mathbf{k}}(u-1)\Delta_n}\frac{1-e^{-2\lambda_{\mathbf{k}}\Delta_n\bar{p}}}{1-e^{-2\lambda_{\mathbf{k}}\Delta_n}}, \\
\sum_{i=r+u}^{v} e^{-(\lambda_{\mathbf{k}_1}+\lambda_{\mathbf{k}_2})(i-r-1)\Delta_n} &= e^{-(\lambda_{\mathbf{k}_1}+\lambda_{\mathbf{k}_2})(u-1)\Delta_n}\frac{1-e^{-(\lambda_{\mathbf{k}_1}+\lambda_{\mathbf{k}_2})\Delta_n\bar{p}}}{1-e^{-(\lambda_{\mathbf{k}_1}+\lambda_{\mathbf{k}_2})\Delta_n}}.
\end{aligned}$$

Thus, we obtain

$$\begin{aligned}
&\left(\sum_{i=r+u}^{v} e^{-2\lambda_{\mathbf{k}_1}(i-r-1)\Delta_n}\right)\left(\sum_{j=r+u}^{v} e^{-2\lambda_{\mathbf{k}_2}(j-r-1)\Delta_n}\right) \\
&= e^{-2(\lambda_{\mathbf{k}_1}+\lambda_{\mathbf{k}_2})(u-1)\Delta_n}\frac{\big(1-e^{-2\lambda_{\mathbf{k}_1}\Delta_n\bar{p}}\big)\big(1-e^{-2\lambda_{\mathbf{k}_2}\Delta_n\bar{p}}\big)}{\big(1-e^{-2\lambda_{\mathbf{k}_1}\Delta_n}\big)\big(1-e^{-2\lambda_{\mathbf{k}_2}\Delta_n}\big)} \\
&\leqslant e^{-2(\lambda_{\mathbf{k}_1}+\lambda_{\mathbf{k}_2})(u-1)\Delta_n}\frac{1-e^{-2\lambda_{\mathbf{k}_2}\Delta_n\bar{p}}}{\big(1-e^{-2\lambda_{\mathbf{k}_1}\Delta_n}\big)\big(1-e^{-2\lambda_{\mathbf{k}_2}\Delta_n}\big)} \\
&\leqslant e^{-2(\lambda_{\mathbf{k}_1}+\lambda_{\mathbf{k}_2})(u-1)\Delta_n}\frac{\bar{p}}{\big(1-e^{-2\lambda_{\mathbf{k}_1}\Delta_n}\big)},
\end{aligned}$$

as well as

$$\begin{aligned}
\left(\sum_{i=r+u}^{v} e^{-(\lambda_{\mathbf{k}_1}+\lambda_{\mathbf{k}_2})(i-r-1)\Delta_n}\right)^2 &= e^{-2(\lambda_{\mathbf{k}_1}+\lambda_{\mathbf{k}_2})(u-1)\Delta_n}\left(\frac{1-e^{-(\lambda_{\mathbf{k}_1}+\lambda_{\mathbf{k}_2})\Delta_n\bar{p}}}{1-e^{-(\lambda_{\mathbf{k}_1}+\lambda_{\mathbf{k}_2})\Delta_n}}\right)^2 \\
&\leqslant e^{-2(\lambda_{\mathbf{k}_1}+\lambda_{\mathbf{k}_2})(u-1)\Delta_n}\frac{1-e^{-(\lambda_{\mathbf{k}_1}+\lambda_{\mathbf{k}_2})\Delta_n\bar{p}}}{\big(1-e^{-(\lambda_{\mathbf{k}_1}+\lambda_{\mathbf{k}_2})\Delta_n}\big)^2}
\end{aligned}$$

$$\leqslant e^{-2(\lambda_{\mathbf{k}_1}+\lambda_{\mathbf{k}_2})(u-1)\Delta_n}\frac{\bar{p}}{1-e^{-(\lambda_{\mathbf{k}_1}+\lambda_{\mathbf{k}_2})\Delta_n}},$$

$$\begin{aligned}\bigg(\sum_{i=r+u}^{v}e^{-2\lambda_{\mathbf{k}}(i-r-1)\Delta_n}\bigg)^2 &= \bigg(e^{-2\lambda_{\mathbf{k}}(u-1)\Delta_n}\frac{1-e^{-2\lambda_{\mathbf{k}}\Delta_n\bar{p}}}{1-e^{-2\lambda_{\mathbf{k}}\Delta_n}}\bigg)^2\\ &\leqslant e^{-4\lambda_{\mathbf{k}}(u-1)\Delta_n}\frac{1-e^{-2\lambda_{\mathbf{k}}\Delta_n\bar{p}}}{\big(1-e^{-2\lambda_{\mathbf{k}}\Delta_n}\big)^2}\\ &\leqslant e^{-4\lambda_{\mathbf{k}}(u-1)\Delta_n}\frac{\bar{p}}{1-e^{-2\lambda_{\mathbf{k}}\Delta_n}}.\end{aligned}$$

Finally, we conclude with the following calculations:

$$\begin{aligned}T_1 \leqslant C^4\sigma^4\bigg(&\sum_{\substack{\mathbf{k}_1,\mathbf{k}_2\in\mathbb{N}^d\\ \mathbf{k}_1\neq\mathbf{k}_2}}\frac{\big(1-e^{-\lambda_{\mathbf{k}_1}\Delta_n}\big)^2\big(1-e^{-\lambda_{\mathbf{k}_2}\Delta_n}\big)^2}{4\lambda_{\mathbf{k}_1}^{1+\alpha}\lambda_{\mathbf{k}_2}^{1+\alpha}}e^{-2(\lambda_{\mathbf{k}_1}+\lambda_{\mathbf{k}_2})(u-1)\Delta_n}\frac{\bar{p}}{\big(1-e^{-2\lambda_{\mathbf{k}_1}\Delta_n}\big)}\\ &+\sum_{\substack{\mathbf{k}_1,\mathbf{k}_2\in\mathbb{N}^d\\ \mathbf{k}_1\neq\mathbf{k}_2}}\frac{\big(1-e^{-\lambda_{\mathbf{k}_1}\Delta_n}\big)^2\big(1-e^{-\lambda_{\mathbf{k}_2}\Delta_n}\big)^2}{4\lambda_{\mathbf{k}_1}^{1+\alpha}\lambda_{\mathbf{k}_2}^{1+\alpha}}e^{-2(\lambda_{\mathbf{k}_1}+\lambda_{\mathbf{k}_2})(u-1)\Delta_n}\frac{2\bar{p}}{1-e^{-(\lambda_{\mathbf{k}_1}+\lambda_{\mathbf{k}_2})\Delta_n}}\\ &+3\sum_{\mathbf{k}\in\mathbb{N}^d}\frac{\big(1-e^{-\lambda_{\mathbf{k}}\Delta_n}\big)^4}{4\lambda_{\mathbf{k}}^{2(1+\alpha)}}e^{-4\lambda_{\mathbf{k}}(u-1)\Delta_n}\frac{\bar{p}}{1-e^{-2\lambda_{\mathbf{k}}\Delta_n}}\bigg)\\ \leqslant C^4\sigma^4\bigg(&\bar{p}\sum_{\substack{\mathbf{k}_1,\mathbf{k}_2\in\mathbb{N}^d\\ \mathbf{k}_1\neq\mathbf{k}_2}}\frac{\big(1-e^{-\lambda_{\mathbf{k}_1}\Delta_n}\big)\big(1-e^{-\lambda_{\mathbf{k}_2}\Delta_n}\big)^2}{4\lambda_{\mathbf{k}_1}^{1+\alpha}\lambda_{\mathbf{k}_2}^{1+\alpha}}e^{-2(\lambda_{\mathbf{k}_1}+\lambda_{\mathbf{k}_2})(u-1)\Delta_n}\\ &+2\bar{p}\sum_{\substack{\mathbf{k}_1,\mathbf{k}_2\in\mathbb{N}^d\\ \mathbf{k}_1\neq\mathbf{k}_2}}\frac{\big(1-e^{-\lambda_{\mathbf{k}_1}\Delta_n}\big)\big(1-e^{-\lambda_{\mathbf{k}_2}\Delta_n}\big)^2}{4\lambda_{\mathbf{k}_1}^{1+\alpha}\lambda_{\mathbf{k}_2}^{1+\alpha}}e^{-2(\lambda_{\mathbf{k}_1}+\lambda_{\mathbf{k}_2})(u-1)\Delta_n}\\ &+3\bar{p}\sum_{\mathbf{k}\in\mathbb{N}^d}^{\infty}\frac{\big(1-e^{-\lambda_{\mathbf{k}}\Delta_n}\big)^3}{4\lambda_{\mathbf{k}}^{2(1+\alpha)}}e^{-4\lambda_{\mathbf{k}}(u-1)\Delta_n}\bigg)\\ \leqslant C^4\sigma^4 3\bar{p}&\bigg(\sum_{\mathbf{k}_1\in\mathbb{N}^d}\frac{\big(1-e^{-\lambda_{\mathbf{k}_1}\Delta_n}\big)}{2\lambda_{\mathbf{k}_1}^{1+\alpha}}e^{-2\lambda_{\mathbf{k}_1}(u-1)\Delta_n}\bigg)\bigg(\sum_{\mathbf{k}_2\in\mathbb{N}^d}\frac{\big(1-e^{-\lambda_{\mathbf{k}_2}\Delta_n}\big)^2}{2\lambda_{\mathbf{k}_2}^{1+\alpha}}e^{-2\lambda_{\mathbf{k}_2}(u-1)\Delta_n}\bigg)\\ = C^4\sigma^4 3\bar{p}\Delta_n^{2\alpha'}&\bigg(\Delta_n^{d/2}\sum_{\mathbf{k}_1\in\mathbb{N}^d}\frac{\big(1-e^{-\lambda_{\mathbf{k}_1}\Delta_n}\big)}{2(\lambda_{\mathbf{k}_1}\Delta_n)^{1+\alpha}}e^{-2\lambda_{\mathbf{k}_1}(u-1)\Delta_n}\bigg)\bigg(\Delta_n^{d/2}\sum_{\mathbf{k}_2\in\mathbb{N}^d}\frac{\big(1-e^{-\lambda_{\mathbf{k}_2}\Delta_n}\big)^2}{2(\lambda_{\mathbf{k}_2}\Delta_n)^{1+\alpha}}e^{-2\lambda_{\mathbf{k}_2}(u-1)\Delta_n}\bigg)\\ \leqslant C'\sigma^4\bar{p}\Delta_n^{2\alpha'}&\bigg(\int_0^\infty x^{d/2-1}\frac{(1-e^{-x})}{2x^{1+\alpha}}e^{-2x(u-1)}\,\mathrm{d}x\bigg)\bigg(\int_0^\infty x^{d/2-1}\frac{(1-e^{-x})^2}{2x^{1+\alpha}}e^{-2x(u-1)}\,\mathrm{d}x\bigg).\end{aligned}$$

Utilizing analogous steps as for Lemma 4.2.4, we obtain for both integrals that

$$\begin{aligned}\int_0^\infty x^{d/2-1}\frac{(1-e^{-x})}{2x^{1+\alpha}}e^{-2x\tau}\,\mathrm{d}x &= \int_0^\infty\frac{(1-e^{-x})}{2x^{1+\alpha'}}e^{-2x\tau}\,\mathrm{d}x = \frac{1}{2\alpha'}\big(-(2\tau)^{\alpha'}+(1+2\tau)^{\alpha'}\big)\Gamma(1-\alpha'),\\ \int_0^\infty x^{d/2-1}\frac{(1-e^{-x})^2}{2x^{1+\alpha}}e^{-2x\tau}\,\mathrm{d}x &= \int_0^\infty\frac{(1-e^{-x})^2}{2x^{1+\alpha'}}e^{-2x\tau}\,\mathrm{d}x\\ &= \frac{1}{2\alpha'}\big(-(2\tau)^{\alpha'}+2(1+2\tau)^{\alpha'}-(2+2\tau)^{\alpha'}\big)\Gamma(1-\alpha').\end{aligned}$$

Hence, by equation (69) it holds for $l=1,2$:

$$\int_0^\infty x^{d/2-1}\frac{(1-e^{-x})^l}{2x^{1+\alpha}}e^{-2x\tau}\,\mathrm{d}x=\mathcal{O}\Big(\frac{1}{\tau^{l-\alpha'}}\Big),$$

and we conclude

$$T_1\leqslant C\sigma^4\frac{\bar{p}\Delta_n^{2\alpha'}}{(u-1)^{3-2\alpha'}},$$

for a suitable $C>0$. For the term T_2, according to equation (125), we obtain the following:

$$\begin{aligned}T_2&=\sum_{i,j=r+u}^{v}\mathbb{E}\Big[\Big(\sum_{\mathbf{k}\in\mathbb{N}^d}D_1^{\mathbf{k},i}e_{\mathbf{k}}(\mathbf{y})\Big)\Big(\sum_{\mathbf{k}\in\mathbb{N}^d}D_2^{\mathbf{k},i}e_{\mathbf{k}}(\mathbf{y})\Big)\Big(\sum_{\mathbf{k}\in\mathbb{N}^d}D_1^{\mathbf{k},j}e_{\mathbf{k}}(\mathbf{y})\Big)\Big(\sum_{\mathbf{k}\in\mathbb{N}^d}D_2^{\mathbf{k},j}e_{\mathbf{k}}(\mathbf{y})\Big)\Big]\\&=\sum_{i,j=r+u}^{v}\mathbb{E}\Big[\Big(\sum_{\mathbf{k}\in\mathbb{N}^d}D_1^{\mathbf{k},i}e_{\mathbf{k}}(\mathbf{y})\Big)\Big(\sum_{\mathbf{k}\in\mathbb{N}^d}D_1^{\mathbf{k},j}e_{\mathbf{k}}(\mathbf{y})\Big)\Big]\mathbb{E}\Big[\Big(\sum_{\mathbf{k}\in\mathbb{N}^d}D_2^{\mathbf{k},i}e_{\mathbf{k}}(\mathbf{y})\Big)\Big(\sum_{\mathbf{k}\in\mathbb{N}^d}D_2^{\mathbf{k},j}e_{\mathbf{k}}(\mathbf{y})\Big)\Big]\\&=\sum_{i,j=r+u}^{v}\Big(\sum_{\mathbf{k}\in\mathbb{N}^d}\mathbb{E}\big[D_1^{\mathbf{k},i}D_1^{\mathbf{k},j}\big]e_{\mathbf{k}}^2(\mathbf{y})\Big)\Big(\sum_{\mathbf{k}\in\mathbb{N}^d}\mathbb{E}\big[D_2^{\mathbf{k},i}D_2^{\mathbf{k},j}\big]e_{\mathbf{k}}^2(\mathbf{y})\Big).\end{aligned}$$

For the first expected value, we find that

$$\begin{aligned}\mathbb{E}\big[D_1^{\mathbf{k},i}D_1^{\mathbf{k},j}\big]&=\sigma^2\lambda_{\mathbf{k}}^{-\alpha}(1-e^{-\lambda_{\mathbf{k}}\Delta_n})^2e^{-\lambda_{\mathbf{k}}(i+j-2)\Delta_n}\int_{-\infty}^{r\Delta_n}e^{2\lambda_{\mathbf{k}}s}\,\mathrm{d}s\\&=\sigma^2\lambda_{\mathbf{k}}^{-\alpha}(1-e^{-\lambda_{\mathbf{k}}\Delta_n})^2e^{-\lambda_{\mathbf{k}}(i+j-2)\Delta_n}\frac{e^{2\lambda_{\mathbf{k}}r\Delta_n}}{2\lambda_{\mathbf{k}}}\\&=\sigma^2\frac{(1-e^{-\lambda_{\mathbf{k}}\Delta_n})^2}{2\lambda_{\mathbf{k}}^{1+\alpha}}e^{-\lambda_{\mathbf{k}}(i+j-2r-2)\Delta_n}.\end{aligned}$$

The second expected value calculates for $i\leqslant j$ as follows:

$$\begin{aligned}\mathbb{E}\big[D_2^{\mathbf{k},i}D_2^{\mathbf{k},j}\big]&=\mathbb{E}\Big[\Big(\sigma\lambda_{\mathbf{k}}^{-\alpha/2}\int_{r\Delta_n}^{(i-1)\Delta_n}e^{-\lambda_{\mathbf{k}}\big((i-1)\Delta_n-s\big)}\big(e^{-\lambda_{\mathbf{k}}\Delta_n}-1\big)\,\mathrm{d}W_s^{\mathbf{k}}+C_{i,\mathbf{k}}\Big)\\&\qquad\times\Big(\sigma\lambda_{\mathbf{k}}^{-\alpha/2}\int_{r\Delta_n}^{(j-1)\Delta_n}e^{-\lambda_{\mathbf{k}}\big((j-1)\Delta_n-s\big)}\big(e^{-\lambda_{\mathbf{k}}\Delta_n}-1\big)\,\mathrm{d}W_s^{\mathbf{k}}+C_{j,\mathbf{k}}\Big)\Big]\\&=\sigma^2\lambda_{\mathbf{k}}^{-\alpha}(1-e^{-\lambda_{\mathbf{k}}\Delta_n})^2e^{-\lambda_{\mathbf{k}}(i+j-2)\Delta_n}\int_{r\Delta_n}^{(i-1)\Delta_n}e^{2\lambda_{\mathbf{k}}s}\,\mathrm{d}s+\Sigma_{j,i}^{BC,\mathbf{k}}+\Sigma_{i,j}^{C,\mathbf{k}}\\&=\sigma^2\frac{(1-e^{-\lambda_{\mathbf{k}}\Delta_n})^2}{2\lambda_{\mathbf{k}}^{1+\alpha}}\big(e^{-\lambda_{\mathbf{k}}(j-i)\Delta_n}-e^{-\lambda_{\mathbf{k}}(i+j-2r-2)\Delta_n}\big)+\Sigma_{j,i}^{BC,\mathbf{k}}+\Sigma_{i,j}^{C,\mathbf{k}}.\end{aligned}$$

As discussed in Proposition 4.2.7, we find that $\Sigma_{j,i}^{BC,\mathbf{k}}=0$, when $i=j$, and $\Sigma_{i,j}^{C,\mathbf{k}}=0$, when $i\neq j$. In particular, for the case when $i<j$, we find that

$$\mathbb{E}\big[D_2^{\mathbf{k},i}D_2^{\mathbf{k},j}\big]=\sigma^2\frac{(1-e^{-\lambda_{\mathbf{k}}\Delta_n})^2}{2\lambda_{\mathbf{k}}^{1+\alpha}}\big(e^{-\lambda_{\mathbf{k}}(j-i)\Delta_n}-e^{-\lambda_{\mathbf{k}}(i+j-2r-2)\Delta_n}\big)$$

$$
\begin{aligned}
&+ \sigma^2 e^{-\lambda_{\mathbf{k}}\Delta_n(j-i)}\Big(e^{\lambda_{\mathbf{k}}\Delta_n} - e^{-\lambda_{\mathbf{k}}\Delta_n}\Big)\frac{e^{-\lambda_{\mathbf{k}}\Delta_n}-1}{2\lambda_{\mathbf{k}}^{1+\alpha}} \\
&= \sigma^2 e^{-\lambda_{\mathbf{k}}(j-i)\Delta_n}\frac{1-e^{-\lambda_{\mathbf{k}}\Delta_n}}{2\lambda_{\mathbf{k}}^{1+\alpha}}\big((1-e^{-\lambda_{\mathbf{k}}\Delta_n})(1-e^{-2\lambda_{\mathbf{k}}(i-r-1)\Delta_n}) - (e^{\lambda_{\mathbf{k}}\Delta_n} - e^{-\lambda_{\mathbf{k}}\Delta_n})\big) \\
&\leqslant \sigma^2 e^{-\lambda_{\mathbf{k}}(j-i)\Delta_n}\frac{1-e^{-\lambda_{\mathbf{k}}\Delta_n}}{2\lambda_{\mathbf{k}}^{1+\alpha}}\big(1-e^{\lambda_{\mathbf{k}}\Delta_n}\big) \leqslant 0.
\end{aligned}
$$

Using this calculations along with equation (74), we derive the following:

$$
\begin{aligned}
T_2 &\leqslant C^4\sigma^4 \sum_{i=r+u}^{v}\Bigg(\sum_{\mathbf{k}\in\mathbb{N}^d}\frac{(1-e^{-\lambda_{\mathbf{k}}\Delta_n})^2}{2\lambda_{\mathbf{k}}^{1+\alpha}}e^{-2\lambda_{\mathbf{k}}(i-r-1)\Delta_n}\Bigg) \\
&\quad\times\Bigg(\sum_{\mathbf{k}\in\mathbb{N}^d}\frac{(1-e^{-\lambda_{\mathbf{k}}\Delta_n})^2}{2\lambda_{\mathbf{k}}^{1+\alpha}}\big(1-e^{-2\lambda_{\mathbf{k}}(i-r-1)\Delta_n}\big) + \sigma^{-2}\Sigma_{i,i}^{C,\mathbf{k}}\Bigg) \\
&\quad + 2\sum_{\substack{i,j=r+u\\ i<j}}^{v}\Bigg(\sum_{\mathbf{k}\in\mathbb{N}^d}\frac{(1-e^{-\lambda_{\mathbf{k}}\Delta_n})^2}{2\lambda_{\mathbf{k}}^{1+\alpha}}e^{-\lambda_{\mathbf{k}}(i+j-2r-2)\Delta_n}e_{\mathbf{k}}^2(\mathbf{y})\Bigg)\Bigg(\sum_{\mathbf{k}\in\mathbb{N}^d}\mathbb{E}\big[D_2^{\mathbf{k},i}D_2^{\mathbf{k},j}\big]e_{\mathbf{k}}^2(\mathbf{y})\Bigg) \\
&\leqslant C^4\sigma^4 \sum_{i=r+u}^{v}\Bigg(\sum_{\mathbf{k}\in\mathbb{N}^d}\frac{(1-e^{-\lambda_{\mathbf{k}}\Delta_n})^2}{2\lambda_{\mathbf{k}}^{1+\alpha}}e^{-2\lambda_{\mathbf{k}}(i-r-1)\Delta_n}\Bigg) \\
&\quad\times\Bigg(\sum_{\mathbf{k}\in\mathbb{N}^d}\frac{(1-e^{-\lambda_{\mathbf{k}}\Delta_n})^2}{2\lambda_{\mathbf{k}}^{1+\alpha}}\big(1-e^{-2\lambda_{\mathbf{k}}(i-r-1)\Delta_n}\big) + \frac{1-e^{-2\lambda_{\mathbf{k}}\Delta_n}}{2\lambda_{\mathbf{k}}^{1+\alpha}}\Bigg) \\
&\leqslant C^4\sigma^4 \sum_{i=r+u}^{v}\Bigg(\sum_{\mathbf{k}\in\mathbb{N}^d}\frac{(1-e^{-\lambda_{\mathbf{k}}\Delta_n})^2}{2\lambda_{\mathbf{k}}^{1+\alpha}}e^{-2\lambda_{\mathbf{k}}(i-r-1)\Delta_n}\Bigg)\Bigg(\sum_{\mathbf{k}\in\mathbb{N}^d}\frac{(1-e^{-\lambda_{\mathbf{k}}\Delta_n})^2+1-e^{-2\lambda_{\mathbf{k}}\Delta_n}}{2\lambda_{\mathbf{k}}^{1+\alpha}}\Bigg) \\
&= C^4\sigma^4\Delta_n^{2\alpha'} \sum_{i=r+u}^{v}\Bigg(\Delta_n^{d/2}\sum_{\mathbf{k}\in\mathbb{N}^d}\frac{(1-e^{-\lambda_{\mathbf{k}}\Delta_n})^2}{2(\lambda_{\mathbf{k}}\Delta_n)^{1+\alpha}}e^{-2\lambda_{\mathbf{k}}(i-r-1)\Delta_n}\Bigg)\Bigg(\Delta_n^{d/2}\sum_{\mathbf{k}\in\mathbb{N}^d}\frac{1-e^{-\lambda_{\mathbf{k}}\Delta_n}}{(\lambda_{\mathbf{k}}\Delta_n)^{1+\alpha}}\Bigg) \\
&\leqslant C^4\sigma^4\Delta_n^{2\alpha'}\bar{p}\Bigg(\Delta_n^{d/2}\sum_{\mathbf{k}\in\mathbb{N}^d}\frac{(1-e^{-\lambda_{\mathbf{k}}\Delta_n})^2}{2(\lambda_{\mathbf{k}}\Delta_n)^{1+\alpha}}e^{-2\lambda_{\mathbf{k}}(u-1)\Delta_n}\Bigg)\Bigg(\Delta_n^{d/2}\sum_{\mathbf{k}\in\mathbb{N}^d}\frac{1-e^{-\lambda_{\mathbf{k}}\Delta_n}}{(\lambda_{\mathbf{k}}\Delta_n)^{1+\alpha}}\Bigg).
\end{aligned}
$$

By utilizing analogous steps as for the term T_1, we obtain for the term T_2 that

$$
T_2 \leqslant C\sigma^4\frac{\bar{p}\Delta_n^{2\alpha'}}{(u-1)^{2-\alpha'}},
$$

where $C>0$ denotes a suitable constant. Thereby, we conclude for $u\geqslant 2$ that

$$
\mathbb{E}[\bar{A}_1^2] \leqslant C\sigma^4\frac{\bar{p}\Delta_n^{2\alpha'}}{(u-1)^{2-\alpha'}}. \tag{126}
$$

Finally, using Proposition 4.2.6, we find that

$$
\mathbb{V}\mathrm{ar}\big(Q_{r+u}^v\big) \geqslant C\mathbb{E}\Big[\big(Q_{r+u}^v\big)^2\Big] = C\mathbb{E}\Bigg[\Bigg(\sum_{i=r+u}^{v}(\Delta_i\tilde{X})^2(y)\Bigg)^2\Bigg] \geqslant C\sum_{i=r+u}^{v}\mathbb{E}\Big[(\Delta_i\tilde{X})^4(y)\Big] \geqslant C''\sigma^4\bar{p}\Delta_n^{2\alpha'},
$$

which completes the proof for $u\geqslant 2$. The case $u=1$ can be demonstrated similarly to the univariate case in Proposition 2.4.1. □

We directly build upon Proposition 5.3.1 and present the following corollary, which extends Proposition 5.3.1 to multiple space coordinates.

Corollary 5.3.2
On the assumptions of Proposition 5.3.1, it holds for $1 \leqslant r < r+u \leqslant v \leqslant n$ and

$$\tilde{Q}_1^r = \sum_{i=1}^{r} \tilde{\xi}_{n,i}, \qquad \tilde{Q}_{r+u}^v = \sum_{i=r+u}^{v} \tilde{\xi}_{n,i},$$

that there is a constant C, with $0 < C < \infty$ and $\tilde{\xi}_{n,i}$ from equation (109), such that for all $t \in \mathbb{R}$ it holds

$$\left|\mathbb{C}\mathrm{ov}\left(e^{\mathrm{i}t(\tilde{Q}_1^r - \mathbb{E}[\tilde{Q}_1^r])},\; e^{\mathrm{i}t(\tilde{Q}_{r+u}^v - \mathbb{E}[\tilde{Q}_{r+u}^v])}\right)\right| \leqslant \frac{Ct^2}{u^{1-\alpha'/2}} \sqrt{\mathbb{V}\mathrm{ar}(\tilde{Q}_1^r)\mathbb{V}\mathrm{ar}(\tilde{Q}_{r+u}^v)}.$$

Proof. We present the proof analogously to Proposition 5.3.1 and begin by decomposing the term $\tilde{Q}_{r+u}^v$ as follows:

$$\tilde{Q}_{r+u}^v = \sum_{i=r+u}^{v} \tilde{\xi}_{n,i} = \frac{2^d(\pi\eta)^{d/2}\alpha'\Gamma(d/2)}{\sqrt{nm}\Delta_n^{\alpha'}\Gamma(1-\alpha')} \sum_{j=1}^{m} \big(A_1(\mathbf{y}_j) + A_2(\mathbf{y}_j)\big) e^{\|\kappa \cdot \mathbf{y}_j\|_1},$$

where

$$\begin{aligned} A_1(\mathbf{y}) &:= \sum_{i=r+u}^{v} \Big(\sum_{\mathbf{k}\in\mathbb{N}^d} D_1^{\mathbf{k},i} e_{\mathbf{k}}(\mathbf{y})\Big)^2 + 2 \sum_{i=r+u}^{v} \Big(\sum_{\mathbf{k}\in\mathbb{N}^d} D_1^{\mathbf{k},i} e_{\mathbf{k}}(\mathbf{y})\Big)\Big(\sum_{\mathbf{k}\in\mathbb{N}^d} D_2^{\mathbf{k},i} e_{\mathbf{k}}(\mathbf{y})\Big), \\ A_2(\mathbf{y}) &:= \sum_{i=r+u}^{v} \Big(\sum_{\mathbf{k}\in\mathbb{N}^d} D_2^{\mathbf{k},i} e_{\mathbf{k}}(\mathbf{y})\Big)^2, \end{aligned}$$

and an analogous definition of $D_1^{\mathbf{k},i}$ and $D_2^{\mathbf{k},i}$ as in the equations (122) and (123). Thereby, we need to bound the following expression:

$$\begin{aligned} \mathbb{V}\mathrm{ar}\left(\frac{K}{\sqrt{nm}\Delta_n^{\alpha'}} \sum_{j=1}^{m} A_1(\mathbf{y}_j) e^{\|\kappa\cdot\mathbf{y}_j\|_1}\right) &= \frac{K^2}{nm\Delta_n^{2\alpha'}} \sum_{j=1}^{m} \mathbb{V}\mathrm{ar}\big(A_1(\mathbf{y}_j)\big) e^{2\|\kappa\cdot\mathbf{y}_j\|_1} \\ &\quad + \frac{K^2}{nm\Delta_n^{2\alpha'}} \sum_{\substack{j_1,j_2=1 \\ j_1\neq j_2}}^{m} \mathbb{C}\mathrm{ov}\big(A_1(\mathbf{y}_{j_1}), A_1(\mathbf{y}_{j_2})\big) e^{\|\kappa\cdot(\mathbf{y}_{j_1}+\mathbf{y}_{j_2})\|_1}, \end{aligned}$$

where

$$K := \frac{2^d(\pi\eta)^{d/2}\alpha'\Gamma(d/2)}{\Gamma(1-\alpha')}.$$

Let $\bar{p} = v - r - u + 1$ and $u \geqslant 2$. Thanks to Proposition 5.3.1, we obtain that

$$\frac{K^2}{nm\Delta_n^{2\alpha'}} \sum_{j=1}^{m} \mathbb{V}\mathrm{ar}\big(A_1(\mathbf{y}_j)\big) e^{2\|\kappa\cdot\mathbf{y}_j\|_1} \leqslant C\sigma^4 \frac{\bar{p}K^2\Delta_n}{(u-1)^{2-\alpha'}},$$

where we used the bound for $\mathbb{E}[\bar{A}_1^2]$ from display (126). For the covariance, we exploit the independence of $D_1^{\mathbf{k},i}$ and $D_2^{\mathbf{k},i}$, along with both terms being centred normals. This allows us to derive the following:

$$\begin{aligned}\mathbb{C}\mathrm{ov}\big(A_1(\mathbf{y}_1), A_1(\mathbf{y}_2)\big) = &\sum_{i,j=r+u}^{v} \mathbb{E}\Big[\Big(\sum_{\mathbf{k}\in\mathbb{N}^d} D_1^{\mathbf{k},i} e_{\mathbf{k}}(\mathbf{y}_1)\Big)^2 \Big(\sum_{\mathbf{k}\in\mathbb{N}^d} D_1^{\mathbf{k},j} e_{\mathbf{k}}(\mathbf{y}_2)\Big)^2\Big] \\ &+ 4 \sum_{i,j=r+u}^{v} \mathbb{E}\Big[\Big(\sum_{\mathbf{k}\in\mathbb{N}^d} D_1^{\mathbf{k},i} e_{\mathbf{k}}(\mathbf{y}_1)\Big)\Big(\sum_{\mathbf{k}\in\mathbb{N}^d} D_2^{\mathbf{k},i} e_{\mathbf{k}}(\mathbf{y}_1)\Big) \\ &\times \Big(\sum_{\mathbf{k}\in\mathbb{N}^d} D_1^{\mathbf{k},j} e_{\mathbf{k}}(\mathbf{y}_2)\Big)\Big(\sum_{\mathbf{k}\in\mathbb{N}^d} D_2^{\mathbf{k},j} e_{\mathbf{k}}(\mathbf{y}_2)\Big)\Big] \\ &- \sum_{i,j=r+u}^{v} \mathbb{E}\Big[\Big(\sum_{\mathbf{k}\in\mathbb{N}^d} D_1^{\mathbf{k},i} e_{\mathbf{k}}(\mathbf{y}_1)\Big)^2\Big] \mathbb{E}\Big[\Big(\sum_{\mathbf{k}\in\mathbb{N}^d} D_1^{\mathbf{k},j} e_{\mathbf{k}}(\mathbf{y}_2)\Big)^2\Big].\end{aligned}$$

Since we can bound the eigenfunctions $(e_{\mathbf{k}})_{\mathbf{k}\in\mathbb{N}^d}$ by a suitable constant $C > 0$, for all $\mathbf{k} \in \mathbb{N}^d$, we observe that the covariance includes the terms T_1 and T_2 from the displays (124) and (125), respectively. Therefore, we can repeat the calculations from Proposition 5.3.1 concerning the eigenfunctions, leading to the following:

$$\begin{aligned}\tilde{T}_1 = &\sum_{i,j=r+u}^{v} \sum_{\mathbf{k}_1,\mathbf{k}_2,\mathbf{k}_3,\mathbf{k}_4\in\mathbb{N}^d} \mathbb{E}\Big[e^{-\lambda_{\mathbf{k}_1}(i-r-1)\Delta_n} \tilde{B}_{r+1,\mathbf{k}_1} e_{\mathbf{k}_1}(\mathbf{y}_1) e^{-\lambda_{\mathbf{k}_2}(i-r-1)\Delta_n} \tilde{B}_{r+1,\mathbf{k}_2} e_{\mathbf{k}_2}(\mathbf{y}_1) \\ &\times e^{-\lambda_{\mathbf{k}_3}(j-r-1)\Delta_n} \tilde{B}_{r+1,\mathbf{k}_3} e_{\mathbf{k}_3}(\mathbf{y}_2) e^{-\lambda_{\mathbf{k}_4}(j-r-1)\Delta_n} \tilde{B}_{r+1,\mathbf{k}_4} e_{\mathbf{k}_4}(\mathbf{y}_2)\Big],\end{aligned}$$

for $\mathbf{y}_1 \neq \mathbf{y}_2$ and

$$\tilde{T}_1 := \sum_{i,j=r+u}^{v} \mathbb{E}\Big[\Big(\sum_{\mathbf{k}\in\mathbb{N}^d} D_1^{\mathbf{k},i} e_{\mathbf{k}}(\mathbf{y}_1)\Big)^2 \Big(\sum_{\mathbf{k}\in\mathbb{N}^d} D_1^{\mathbf{k},j} e_{\mathbf{k}}(\mathbf{y}_2)\Big)^2\Big].$$

Assume $\mathbf{k}_1 = \ldots = \mathbf{k}_4 = \mathbf{k}$, then we have

$$\sum_{i,j=r+u}^{v} \sum_{\mathbf{k}\in\mathbb{N}^d} e^{-2\lambda_{\mathbf{k}}(i+j-2r-2)\Delta_n} \mathbb{E}\Big[\tilde{B}^4_{r+1,\mathbf{k}}\Big] e^2_{\mathbf{k}}(\mathbf{y}_1) e^2_{\mathbf{k}}(\mathbf{y}_2).$$

For $\mathbf{k}_1 = \mathbf{k}_2$, $\mathbf{k}_3 = \mathbf{k}_4$, with $\mathbf{k}_1 \neq \mathbf{k}_3$, we obtain

$$\sum_{i,j=r+u}^{v} \sum_{\substack{\mathbf{k}_1,\mathbf{k}_2\in\mathbb{N}^d \\ \mathbf{k}_1\neq\mathbf{k}_2}} e^{-2\lambda_{\mathbf{k}_1}(i-r-1)\Delta_n - 2\lambda_{\mathbf{k}_2}(j-r-1)\Delta_n} \mathbb{E}\Big[\tilde{B}^2_{r+1,\mathbf{k}_1}\Big] \mathbb{E}\Big[\tilde{B}^2_{r+1,\mathbf{k}_2}\Big] e^2_{\mathbf{k}_1}(\mathbf{y}_1) e^2_{\mathbf{k}_2}(\mathbf{y}_2),$$

as well as the following expression for the remaining combinations:

$$\sum_{i,j=r+u}^{v} \sum_{\substack{\mathbf{k}_1,\mathbf{k}_2\in\mathbb{N}^d \\ \mathbf{k}_1\neq\mathbf{k}_2}} e^{-(\lambda_{\mathbf{k}_1}+\lambda_{\mathbf{k}_2})(i+j-2r-2)\Delta_n} \mathbb{E}\Big[\tilde{B}^2_{r+1,\mathbf{k}_1}\Big] \mathbb{E}\Big[\tilde{B}^2_{r+1,\mathbf{k}_2}\Big] e_{\mathbf{k}_1}(\mathbf{y}_1) e_{\mathbf{k}_1}(\mathbf{y}_2) e_{\mathbf{k}_2}(\mathbf{y}_1) e_{\mathbf{k}_2}(\mathbf{y}_2).$$

Thus, we derive

$$
\begin{aligned}
\tilde{T}_1 &= \sigma^4 \sum_{\substack{\mathbf{k}_1,\mathbf{k}_2\in\mathbb{N}^d\\ \mathbf{k}_1\neq\mathbf{k}_2}} \frac{\big(1-e^{-\lambda_{\mathbf{k}_1}\Delta_n}\big)^2\big(1-e^{-\lambda_{\mathbf{k}_2}\Delta_n}\big)^2}{4\lambda_{\mathbf{k}_1}^{1+\alpha}\lambda_{\mathbf{k}_2}^{1+\alpha}} \Bigg(\sum_{i=r+u}^{v} e^{-2\lambda_{\mathbf{k}_1}(i-r-1)\Delta_n}\Bigg)\Bigg(\sum_{j=r+u}^{v} e^{-2\lambda_{\mathbf{k}_2}(j-r-1)\Delta_n}\Bigg)\\
&\qquad \times e_{\mathbf{k}_1}^2(\mathbf{y}_1)e_{\mathbf{k}_2}^2(\mathbf{y}_2)\\
&\quad + \sigma^4 \sum_{\substack{\mathbf{k}_1,\mathbf{k}_2\in\mathbb{N}^d\\ \mathbf{k}_1\neq\mathbf{k}_2}} \frac{\big(1-e^{-\lambda_{\mathbf{k}_1}\Delta_n}\big)^2\big(1-e^{-\lambda_{\mathbf{k}_2}\Delta_n}\big)^2}{4\lambda_{\mathbf{k}_1}^{1+\alpha}\lambda_{\mathbf{k}_2}^{1+\alpha}} 2\Bigg(\sum_{i=r+u}^{v} e^{-(\lambda_{\mathbf{k}_1}+\lambda_{\mathbf{k}_2})(i-r-1)\Delta_n}\Bigg)^2\\
&\qquad \times e_{\mathbf{k}_1}(\mathbf{y}_1)e_{\mathbf{k}_1}(\mathbf{y}_2)e_{\mathbf{k}_2}(\mathbf{y}_1)e_{\mathbf{k}_2}(\mathbf{y}_2)\\
&\quad + 3\sigma^4 \sum_{\mathbf{k}\in\mathbb{N}^d}^{\infty} \frac{\big(1-e^{-\lambda_{\mathbf{k}}\Delta_n}\big)^4}{4\lambda_{\mathbf{k}}^{2(1+\alpha)}} \Bigg(\sum_{i=r+u}^{v} e^{-2\lambda_{\mathbf{k}}(i-r-1)\Delta_n}\Bigg)^2 e_{\mathbf{k}}^2(\mathbf{y}_1)e_{\mathbf{k}}^2(\mathbf{y}_2)\\
&\leqslant \sigma^4\Bigg(\bar{p} \sum_{\substack{\mathbf{k}_1,\mathbf{k}_2\in\mathbb{N}^d\\ \mathbf{k}_1\neq\mathbf{k}_2}} \frac{\big(1-e^{-\lambda_{\mathbf{k}_1}\Delta_n}\big)\big(1-e^{-\lambda_{\mathbf{k}_2}\Delta_n}\big)^2}{4\lambda_{\mathbf{k}_1}^{1+\alpha}\lambda_{\mathbf{k}_2}^{1+\alpha}} e^{-2(\lambda_{\mathbf{k}_1}+\lambda_{\mathbf{k}_2})(u-1)\Delta_n} e_{\mathbf{k}_1}^2(\mathbf{y}_1)e_{\mathbf{k}_2}^2(\mathbf{y}_2)\\
&\quad + 2\bar{p} \sum_{\substack{\mathbf{k}_1,\mathbf{k}_2\in\mathbb{N}^d\\ \mathbf{k}_1\neq\mathbf{k}_2}} \frac{\big(1-e^{-\lambda_{\mathbf{k}_1}\Delta_n}\big)\big(1-e^{-\lambda_{\mathbf{k}_2}\Delta_n}\big)^2}{4\lambda_{\mathbf{k}_1}^{1+\alpha}\lambda_{\mathbf{k}_2}^{1+\alpha}} e^{-2(\lambda_{\mathbf{k}_1}+\lambda_{\mathbf{k}_2})(u-1)\Delta_n} e_{\mathbf{k}_1}(\mathbf{y}_1)e_{\mathbf{k}_1}(\mathbf{y}_2)e_{\mathbf{k}_2}(\mathbf{y}_1)e_{\mathbf{k}_2}(\mathbf{y}_2)\\
&\quad + 3\bar{p} \sum_{\mathbf{k}\in\mathbb{N}^d}^{\infty} \frac{\big(1-e^{-\lambda_{\mathbf{k}}\Delta_n}\big)^3}{4\lambda_{\mathbf{k}}^{2(1+\alpha)}} e^{-4\lambda_{\mathbf{k}}(u-1)\Delta_n} e_{\mathbf{k}}^2(\mathbf{y}_1)e_{\mathbf{k}}^2(\mathbf{y}_2)\Bigg)\\
&= \sigma^4\Bigg(\bar{p} \sum_{\mathbf{k}_1,\mathbf{k}_2\in\mathbb{N}^d} \frac{\big(1-e^{-\lambda_{\mathbf{k}_1}\Delta_n}\big)\big(1-e^{-\lambda_{\mathbf{k}_2}\Delta_n}\big)^2}{4\lambda_{\mathbf{k}_1}^{1+\alpha}\lambda_{\mathbf{k}_2}^{1+\alpha}} e^{-2(\lambda_{\mathbf{k}_1}+\lambda_{\mathbf{k}_2})(u-1)\Delta_n} e_{\mathbf{k}_1}^2(\mathbf{y}_1)e_{\mathbf{k}_2}^2(\mathbf{y}_2)\\
&\quad + 2\bar{p} \sum_{\mathbf{k}_1,\mathbf{k}_2\in\mathbb{N}^d} \frac{\big(1-e^{-\lambda_{\mathbf{k}_1}\Delta_n}\big)\big(1-e^{-\lambda_{\mathbf{k}_2}\Delta_n}\big)^2}{4\lambda_{\mathbf{k}_1}^{1+\alpha}\lambda_{\mathbf{k}_2}^{1+\alpha}} e^{-2(\lambda_{\mathbf{k}_1}+\lambda_{\mathbf{k}_2})(u-1)\Delta_n} e_{\mathbf{k}_1}(\mathbf{y}_1)e_{\mathbf{k}_1}(\mathbf{y}_2)e_{\mathbf{k}_2}(\mathbf{y}_1)e_{\mathbf{k}_2}(\mathbf{y}_2)\Bigg)\\
&= \sigma^4\bar{p}\Bigg(\sum_{\mathbf{k}\in\mathbb{N}^d} \frac{\big(1-e^{-\lambda_{\mathbf{k}}\Delta_n}\big)}{2\lambda_{\mathbf{k}}^{1+\alpha}} e^{-2\lambda_{\mathbf{k}}(u-1)\Delta_n} e_{\mathbf{k}}^2(\mathbf{y}_1)\Bigg)\Bigg(\sum_{\mathbf{k}\in\mathbb{N}^d} \frac{\big(1-e^{-\lambda_{\mathbf{k}}\Delta_n}\big)^2}{2\lambda_{\mathbf{k}}^{1+\alpha}} e^{-2\lambda_{\mathbf{k}}(u-1)\Delta_n} e_{\mathbf{k}}^2(\mathbf{y}_2)\Bigg)\\
&\quad + \sigma^4 2\bar{p}\Bigg(\sum_{\mathbf{k}\in\mathbb{N}^d} \frac{\big(1-e^{-\lambda_{\mathbf{k}}\Delta_n}\big)}{2\lambda_{\mathbf{k}}^{1+\alpha}} e^{-2\lambda_{\mathbf{k}}(u-1)\Delta_n} e_{\mathbf{k}}(\mathbf{y}_1)e_{\mathbf{k}}(\mathbf{y}_2)\Bigg)\\
&\qquad \times \Bigg(\sum_{\mathbf{k}\in\mathbb{N}^d} \frac{\big(1-e^{-\lambda_{\mathbf{k}}\Delta_n}\big)^2}{2\lambda_{\mathbf{k}}^{1+\alpha}} e^{-2\lambda_{\mathbf{k}}(u-1)\Delta_n} e_{\mathbf{k}}(\mathbf{y}_1)e_{\mathbf{k}}(\mathbf{y}_2)\Bigg).
\end{aligned}
$$

Furthermore, we have

$$
\begin{aligned}
&\tilde{T}_1 - \sum_{i,j=r+u}^{v} \mathbb{E}\Bigg[\Bigg(\sum_{\mathbf{k}\in\mathbb{N}^d} D_1^{\mathbf{k},i} e_{\mathbf{k}}(\mathbf{y}_1)\Bigg)^2\Bigg]\mathbb{E}\Bigg[\Bigg(\sum_{\mathbf{k}\in\mathbb{N}^d} D_1^{\mathbf{k},j} e_{\mathbf{k}}(\mathbf{y}_2)\Bigg)^2\Bigg]\\
&\leqslant \sigma^4 2\bar{p}\Bigg(\sum_{\mathbf{k}\in\mathbb{N}^d} \frac{\big(1-e^{-\lambda_{\mathbf{k}}\Delta_n}\big)}{2\lambda_{\mathbf{k}}^{1+\alpha}} e^{-2\lambda_{\mathbf{k}}(u-1)\Delta_n} e_{\mathbf{k}}(\mathbf{y}_1)e_{\mathbf{k}}(\mathbf{y}_2)\Bigg)\Bigg(\sum_{\mathbf{k}\in\mathbb{N}^d} \frac{\big(1-e^{-\lambda_{\mathbf{k}}\Delta_n}\big)^2}{2\lambda_{\mathbf{k}}^{1+\alpha}} e^{-2\lambda_{\mathbf{k}}(u-1)\Delta_n} e_{\mathbf{k}}(\mathbf{y}_1)e_{\mathbf{k}}(\mathbf{y}_2)\Bigg).
\end{aligned}
$$

Hence, we can bound the latter term by using display (118) and Lemma 4.2.1. Similar to Proposition

5.2.1, we find that

$$
\begin{aligned}
&\tilde{T}_1 - \sum_{i,j=r+u}^{v} \mathbb{E}\Big[\Big(\sum_{\mathbf{k}\in\mathbb{N}^d} D_1^{\mathbf{k},i} e_{\mathbf{k}}(\mathbf{y}_1)\Big)^2\Big]\mathbb{E}\Big[\Big(\sum_{\mathbf{k}\in\mathbb{N}^d} D_1^{\mathbf{k},j} e_{\mathbf{k}}(\mathbf{y}_2)\Big)^2\Big] \\
&= \mathcal{O}\Big(\sigma^4 \bar{p}\Delta_n^{2\alpha'}\Delta_n^{1-\alpha'}\|\mathbf{y}_1-\mathbf{y}_2\|_0^{-(d+1)}\Big(\Delta_n^{d/2}\sum_{\mathbf{k}\in\mathbb{N}^d}\frac{(1-e^{-\lambda_{\mathbf{k}}\Delta_n})^2}{(\lambda_{\mathbf{k}}\Delta_n)^{1+\alpha}} e^{-2\lambda_{\mathbf{k}}(u-1)\Delta_n}\Big)\Big) \\
&= \mathcal{O}\Big(\sigma^4 \frac{\bar{p}\Delta_n^{2\alpha'}}{(u-1)^{2-\alpha'}}\Delta_n^{1-\alpha'}\|\mathbf{y}_1-\mathbf{y}_2\|_0^{-(d+1)}\Big), \qquad (127)
\end{aligned}
$$

where we used analogous steps as in display (119). For the last term in the covariance, we redefine

$$
\begin{aligned}
\tilde{T}_2 &:= \sum_{i,j=r+u}^{v} \mathbb{E}\Big[\Big(\sum_{\mathbf{k}\in\mathbb{N}^d} D_1^{\mathbf{k},i} e_{\mathbf{k}}(\mathbf{y}_1)\Big)\Big(\sum_{\mathbf{k}\in\mathbb{N}^d} D_2^{\mathbf{k},i} e_{\mathbf{k}}(\mathbf{y}_1)\Big) \\
&\quad \times \Big(\sum_{\mathbf{k}\in\mathbb{N}^d} D_1^{\mathbf{k},j} e_{\mathbf{k}}(\mathbf{y}_2)\Big)\Big(\sum_{\mathbf{k}\in\mathbb{N}^d} D_2^{\mathbf{k},j} e_{\mathbf{k}}(\mathbf{y}_2)\Big)\Big] \\
&= \sum_{i,j=r+u}^{v} \Big(\sum_{\mathbf{k}\in\mathbb{N}^d} \mathbb{E}\big[D_1^{\mathbf{k},i} D_1^{\mathbf{k},j}\big] e_{\mathbf{k}}(\mathbf{y}_1)e_{\mathbf{k}}(\mathbf{y}_2)\Big)\Big(\sum_{\mathbf{k}\in\mathbb{N}^d} \mathbb{E}\big[D_2^{\mathbf{k},i} D_2^{\mathbf{k},j}\big] e_{\mathbf{k}}(\mathbf{y}_1)e_{\mathbf{k}}(\mathbf{y}_2)\Big).
\end{aligned}
$$

With similar steps as in Proposition 5.2.1, we obtain

$$
\begin{aligned}
\tilde{T}_2 &\leqslant \sum_{i=r+u}^{v} \Big(\sum_{\mathbf{k}\in\mathbb{N}^d} \mathbb{E}\big[D_1^{\mathbf{k},i} D_1^{\mathbf{k},i}\big] e_{\mathbf{k}}(\mathbf{y}_1)e_{\mathbf{k}}(\mathbf{y}_2)\Big)\Big(\sum_{\mathbf{k}\in\mathbb{N}^d} \mathbb{E}\big[D_2^{\mathbf{k},i} D_2^{\mathbf{k},i}\big] e_{\mathbf{k}}(\mathbf{y}_1)e_{\mathbf{k}}(\mathbf{y}_2)\Big) \\
&= \sigma^4 \sum_{i=r+u}^{v} \Big(\sum_{\mathbf{k}\in\mathbb{N}^d} \frac{(1-e^{-\lambda_{\mathbf{k}}\Delta_n})^2}{2\lambda_{\mathbf{k}}^{1+\alpha}} e^{-2\lambda_{\mathbf{k}}(i-r-1)\Delta_n} e_{\mathbf{k}}(\mathbf{y}_1)e_{\mathbf{k}}(\mathbf{y}_2)\Big) \\
&\quad \times \Big(\sum_{\mathbf{k}\in\mathbb{N}^d} \Big(\frac{(1-e^{-\lambda_{\mathbf{k}}\Delta_n})^2}{2\lambda_{\mathbf{k}}^{1+\alpha}}\big(e^{-\lambda_{\mathbf{k}}(i-1)\Delta_n} - e^{-2\lambda_{\mathbf{k}}(i-r-1)\Delta_n}\big) + \frac{1-e^{-2\lambda_{\mathbf{k}}\Delta_n}}{2\lambda_{\mathbf{k}}^{1+\alpha}}\Big) e_{\mathbf{k}}(\mathbf{y}_1)e_{\mathbf{k}}(\mathbf{y}_2)\Big) \\
&\leqslant \sigma^4\Delta_n^{2\alpha'} \sum_{i=r+u}^{v} \Big(\Delta_n^{d/2}\sum_{\mathbf{k}\in\mathbb{N}^d} \frac{(1-e^{-\lambda_{\mathbf{k}}\Delta_n})^2}{2(\lambda_{\mathbf{k}}\Delta_n)^{1+\alpha}} e^{-2\lambda_{\mathbf{k}}(i-r-1)\Delta_n} e_{\mathbf{k}}(\mathbf{y}_1)e_{\mathbf{k}}(\mathbf{y}_2)\Big) \\
&\quad \times \Big(\Delta_n^{d/2}\sum_{\mathbf{k}\in\mathbb{N}^d} \frac{1-e^{-\lambda_{\mathbf{k}}\Delta_n}}{(\lambda_{\mathbf{k}}\Delta_n)^{1+\alpha}} e_{\mathbf{k}}(\mathbf{y}_1)e_{\mathbf{k}}(\mathbf{y}_2)\Big) \\
&\leqslant \sigma^4\Delta_n^{2\alpha'}\bar{p}\Big(\Delta_n^{d/2}\sum_{\mathbf{k}\in\mathbb{N}^d} \frac{(1-e^{-\lambda_{\mathbf{k}}\Delta_n})^2}{2(\lambda_{\mathbf{k}}\Delta_n)^{1+\alpha}} e^{-2\lambda_{\mathbf{k}}(u-1)\Delta_n} e_{\mathbf{k}}(\mathbf{y}_1)e_{\mathbf{k}}(\mathbf{y}_2)\Big)\Big(\Delta_n^{d/2}\sum_{\mathbf{k}\in\mathbb{N}^d} \frac{1-e^{-\lambda_{\mathbf{k}}\Delta_n}}{(\lambda_{\mathbf{k}}\Delta_n)^{1+\alpha}} e_{\mathbf{k}}(\mathbf{y}_1)e_{\mathbf{k}}(\mathbf{y}_2)\Big) \\
&= \mathcal{O}\Big(\sigma^4\bar{p}\Delta_n^{2\alpha'}\Delta_n^{1-\alpha'}\|\mathbf{y}_1-\mathbf{y}_2\|_0^{-(d+1)}\Big(\Delta_n^{d/2}\sum_{\mathbf{k}\in\mathbb{N}^d} \frac{(1-e^{-\lambda_{\mathbf{k}}\Delta_n})^2}{(\lambda_{\mathbf{k}}\Delta_n)^{1+\alpha}} e^{-2\lambda_{\mathbf{k}}(u-1)\Delta_n}\Big)\Big) = \mathcal{O}(\tilde{T}_1).
\end{aligned}
$$

Hence, we have

$$
\frac{K^2}{nm\Delta_n^{2\alpha'}} \sum_{\substack{j_1,j_2=1\\ j_1\neq j_2}}^{m} \mathbb{C}\mathrm{ov}\big(A_1(\mathbf{y}_{j_1}), A_1(\mathbf{y}_{j_2})\big) = \mathcal{O}\Big(\sigma^4\frac{\bar{p}\Delta_n}{(u-1)^{2-\alpha'}}\cdot\frac{\Delta_n^{1-\alpha'}}{m}\sum_{\substack{j_1,j_2=1\\ j_1\neq j_2}}^{m}\frac{1}{\|\mathbf{y}_{j_1}-\mathbf{y}_{j_2}\|_0^{d+1}}\Big).
$$

According to Assumption 4.1.1, the distance between any two arbitrary spatial coordinates is bounded from below, leading to the following order:

$$\sum_{\substack{j_1,j_2=1\\ j_1\neq j_2}}^{m}\left(\frac{1}{\|\mathbf{y}_{j_1}-\mathbf{y}_{j_2}\|_0}\right)^{d+1}=\mathcal{O}\bigg(m^{d+1}\sum_{\substack{j_1,j_2=1\\ j_1\neq j_2}}^{m}\left(\frac{1}{m\|\mathbf{y}_{j_1}-\mathbf{y}_{j_2}\|_0}\right)^{d+1}\bigg)=\mathcal{O}\big(m^{d+3}\big). \tag{128}$$

Thus, we conclude that

$$\frac{K^2}{nm\Delta_n^{2\alpha'}}\sum_{\substack{j_1,j_2=1\\ j_1\neq j_2}}^{m}\mathbb{C}\mathrm{ov}\big(A_1(\mathbf{y}_{j_1}),A_1(\mathbf{y}_{j_2})\big)=\mathcal{O}\bigg(\sigma^4\frac{\bar{p}\Delta_n}{(u-1)^{2-\alpha'}}\Delta_n^{1-\alpha'}m^{d+2}\bigg).$$

Using the following display:

$$\mathbb{E}[(Q_{r+u}^v)^2]\geqslant\sum_{i=r+u}^{v}\mathbb{E}[\xi_{n,i}^2]\geqslant C\frac{K^2\bar{p}}{nm\Delta_n^{2\alpha'}}\sum_{j=1}^{m}\mathbb{E}\big[(\Delta_i\tilde{X})^4(\mathbf{y}_j)\big]\geqslant C'\sigma^4\Delta_n\bar{p},$$

completes the proof. □

The previous proof demonstrated that the temporal dependencies can be controlled, if $\Delta_n^{1-\alpha'}m_n^{d+2}$ tends to zero. In the one-dimensional case, the authors Bibinger and Trabs (2020) fixed $\alpha'=1/2$, which led to the restriction $m_n^2\Delta_n^{1/2}\overset{n\to\infty}{\longrightarrow}0$. However, in higher dimensions, we cannot directly transfer the relationship between spatial and temporal observations, i.e., $\Delta_n m_n^{d+1}\overset{n\to\infty}{\longrightarrow}0$ is not sufficient. As discussed at the end of Section 5.2, the discrepancy arises from the different rates of the Riemann approximation. For a comparison between the Riemann approximations in one and multiple spatial dimensions, see Bibinger and Trabs (2020, Lemma 6.2.) and Lemma 4.2.1, respectively.

5.4. Central limit theorem and simulation results

The objective of this section is to establish a central limit theorem for the volatility estimator $\hat{\sigma}^2_{n,m}$ from equation (72), which, in turn, implies a central limit theorem for $\hat{\sigma}^2_n(\mathbf{y})$, given in equation (71). To achieve this, we will employ the general central limit theorem given in Proposition 1.2.4.

With the assistance of Proposition 5.2.1 in Section 5.2, we will determine the asymptotic variance of the volatility estimator $\hat{\sigma}^2_{n,m}$. This proposition furthermore reveals an optimal rate of convergence of $\sqrt{nm}$. Subsequently, we will present simulation results for the volatility estimator $\hat{\sigma}^2_{n,m}$, thereby concluding this chapter.

Proposition 5.4.1
On Assumptions 4.1.1 and 4.1.2, we have

$$\sqrt{nm_n}(\hat{\sigma}^2_{n,m_n}-\sigma^2)\overset{d}{\longrightarrow}\mathcal{N}(0,\Upsilon_{\alpha'}\sigma^4),$$

as $n\to\infty$, $\Upsilon_{\alpha'}$ defined in equation (121) and $m_n=\mathcal{O}(n^\rho)$, with $\rho\in\big(0,(1-\alpha')/(d+2)\big)$.

Proof. To prove this central limit theorem, we employ Proposition 1.2.4. Therefore, we define

$$\Xi_{n,i} := \tilde{\xi}_{n,i} - \mathbb{E}[\tilde{\xi}_{n,i}],$$

where $\tilde{\xi}_{n,i}$ is defined in equation (109), and we set

$$\tilde{K} = \frac{2^d(\pi\eta)^{d/2}\alpha'\Gamma(d/2)}{\Gamma(1-\alpha')}.$$

The asymptotic variance is given by

$$\begin{aligned}
\mathbb{V}\mathrm{ar}\Big(\sum_{i=1}^{n}\Xi_{n,i}\Big) &= \mathbb{V}\mathrm{ar}\Big(\sum_{i=1}^{n}\tilde{\xi}_{n,i}\Big) = \frac{\tilde{K}^2}{nm_n\Delta_n^{2\alpha'}}\mathbb{V}\mathrm{ar}\Big(\sum_{j=1}^{m_n}\sum_{i=1}^{n}(\Delta_i\tilde{X})^2(\mathbf{y}_j)e^{\|\kappa\cdot\mathbf{y}_j\|_1}\Big)\\
&= \frac{\tilde{K}^2n^2\Delta_n^{2\alpha'}}{nm_n\Delta_n^{2\alpha'}}\Big(\sum_{j=1}^{m_n}\mathbb{V}\mathrm{ar}\big(V_{n,\Delta_n}(\mathbf{y}_j)\big) + \sum_{\substack{j_1,j_2=1\\ j_1\neq j_2}}^{m_n}\mathbb{C}\mathrm{ov}\big(V_{n,\Delta_n}(\mathbf{y}_{j_1}),V_{n,\Delta_n}(\mathbf{y}_{j_2})\big)\Big)\\
&= \frac{\tilde{K}^2n}{m_n}\cdot\frac{m_n\Upsilon_{\alpha'}\sigma^4}{n}\Big(\frac{\Gamma(1-\alpha')}{2^d(\pi\eta)^{d/2}\alpha'\Gamma(d/2)}\Big)^2\big(1+\mathcal{O}(\Delta_n^{1/2}\vee\Delta_n^{1-\alpha'})\big)\\
&\quad + \mathcal{O}\Big(\frac{\tilde{K}^2n}{m_n}\cdot\frac{\Delta_n^{1-\alpha'}}{n}\sum_{\substack{j_1,j_2=1\\ j_1\neq j_2}}^{m_n}\Big(\|\mathbf{y}_1-\mathbf{y}_2\|_0^{-(d+1)}+\delta^{-(d+1)}\Big)\Big)\\
&= \Upsilon_{\alpha'}\sigma^4\big(1+\mathcal{O}(\Delta_n^{1/2}\vee\Delta_n^{1-\alpha'})\big)+\mathcal{O}(m_n^{d+2}\Delta_n^{1-\alpha'}) \overset{n\to\infty}{\longrightarrow} \Upsilon_{\alpha'}\sigma^4,
\end{aligned}$$

where we used Proposition 5.2.1 and equation (128). It remains to verify the Conditions (I)-(IV) from Proposition 1.2.4.

(I) By Proposition 5.2.1 we have

$$\begin{aligned}
\sum_{i=a}^{b}\mathbb{V}\mathrm{ar}(\Xi_{n,i}) &= \sum_{i=a}^{b}\mathbb{V}\mathrm{ar}(\tilde{\xi}_{n,i}) = \frac{\tilde{K}^2\Delta_n^{2\alpha'}}{nm_n\Delta_n^{2\alpha'}}\sum_{i=a}^{b}\mathbb{V}\mathrm{ar}\Big(\sum_{j=1}^{m_n}\frac{1}{\Delta_n^{\alpha'}}(\Delta_i\tilde{X})^2(\mathbf{y}_j)e^{\|\kappa\cdot\mathbf{y}_j\|_1}\Big)\\
&= \frac{\tilde{K}^2}{nm_n}\sum_{i=a}^{b}\Big(\sum_{j=1}^{m_n}\mathbb{V}\mathrm{ar}\big(V_{1,\Delta_n}(\mathbf{y}_j)\big) + \sum_{\substack{j_1,j_2=1\\ j_1\neq j_2}}^{m_n}\mathbb{C}\mathrm{ov}\big(V_{1,\Delta_n}(\mathbf{y}_{j_1}),V_{1,\Delta_n}(\mathbf{y}_{j_2})\big)\Big)\\
&= \mathcal{O}\Big(\Delta_n(b-a+1)+\Delta_n(b-a+1)\Delta_n^{1-\alpha'}m_n^{d+2}\Big) = \mathcal{O}\big(\Delta_n(b-a+1)\big).
\end{aligned}$$

We utilize the calculations for the asymptotic variance as shown in this proof and thus conclude

$$\begin{aligned}
\mathbb{V}\mathrm{ar}\Big(\sum_{i=a}^{b}\Xi_{n,i}\Big) &= \mathbb{V}\mathrm{ar}\Big(\sum_{i=a}^{b}\tilde{\xi}_{n,i}\Big)\\
&= \mathcal{O}\Big(\frac{\tilde{K}^2(b-a+1)^2}{nm_n}\cdot\frac{m_n}{(b-a+1)\tilde{K}^2}+\frac{(b-a+1)^2}{nm_n}\cdot\frac{\Delta_n^{1-\alpha'}m_n^{d+3}}{(b-a+1)}\Big)\\
&= \mathcal{O}\big(\Delta_n(b-a+1)\big),
\end{aligned}$$

which shows the first condition.

(II) Since $\Xi_{n,i}$ is a centred random variable, it is sufficient to consider the variance in order to prove the second condition. According to Condition (I), we obtain

$$\sum_{i=1}^{n} \mathbb{V}\mathrm{ar}(\Xi_{n,i}) = \mathcal{O}(n\Delta_n) < \infty,$$

which verifies Condition (II).

(III) We prove that a Lyapunov condition is satisfied. By utilizing the Cauchy-Schwarz inequality, we have

$$\begin{aligned}\mathbb{E}[\tilde{\xi}_{n,i}^4] &= \frac{\tilde{K}^4}{n^2 m_n^2 \Delta_n^{4\alpha'}} \sum_{j_1,\ldots,j_4=1}^{m_n} e^{\|\kappa\cdot(\mathbf{y}_{j_1}+\ldots+\mathbf{y}_{j_4})\|_1} \mathbb{E}[(\Delta_i \tilde{X})^2(\mathbf{y}_{j_1}) \cdots (\Delta_i \tilde{X})^2(\mathbf{y}_{j_4})] \\ &\leqslant \frac{\tilde{K}^4}{n^2 m_n^2 \Delta_n^{4\alpha'}} \sum_{j_1,\ldots,j_4=1}^{m_n} e^{\|\kappa\cdot(\mathbf{y}_{j_1}+\ldots+\mathbf{y}_{j_4})\|_1} \mathbb{E}[(\Delta_i \tilde{X})^8(\mathbf{y}_{j_1})]^{1/4} \cdots \mathbb{E}[(\Delta_i \tilde{X})^8(\mathbf{y}_{j_4})]^{1/4} \\ &\leqslant \frac{\tilde{K}^4}{n^2 \Delta_n^{4\alpha'}} m_n^2 e^{4\|\kappa\|_1} \max_{\mathbf{y}\in\{\mathbf{y}_1,\ldots\mathbf{y}_{m_n}\}} \mathbb{E}[(\Delta_i \tilde{X})^8(\mathbf{y})].\end{aligned}$$

Since $(\Delta_n \tilde{X})(\mathbf{y})$ is a centred Gaussian random variable, we can infer that $\mathbb{E}[(\Delta_i \tilde{X})^8(\mathbf{y})] = \mathcal{O}(\Delta_n^{4\alpha'})$ by using Proposition 4.2.6. Thus, we have

$$\sum_{i=1}^{n} \mathbb{E}[\tilde{\xi}_{n,i}^4] = \mathcal{O}(\Delta_n m^2) = o(1),$$

which shows the third condition.

(IV) The last condition is verified by Corollary 5.3.2, which completes the proof. □

The preceding proposition establishes that a central limit theorem holds for both volatility estimators, $\hat{\sigma}_n^2(\mathbf{y})$ from equation (71) and $\hat{\sigma}_{n,m}^2$ from equation (72), under both regimes from Assumption 4.1.1, with an asymptotic variance of $\Upsilon_{\alpha'}\sigma^4$. Comparing this result to a SPDE model in one space dimension, as presented in Bibinger and Trabs (2020), where $\alpha' = 1/2$, reveals that the same asymptotic behaviour is achieved. Hence, this asymptotic behaviour extends to multiple space dimensions. Thanks to the condition $\Delta_n^{1-\alpha'} m^{d+2} \overset{n\to\infty}{\longrightarrow} 0$ in Assumption 4.1.1, the covariances $\mathbb{C}\mathrm{ov}(\hat{\sigma}_{\mathbf{y}_1}^2, \hat{\sigma}_{\mathbf{y}_2}^2)$ vanish asymptotically, where $\mathbf{y}_1, \mathbf{y}_2 \in [\delta, 1-\delta]^d$ represents two distinct spatial points.

In the standard model with i.i.d. random variables $X_1, \ldots, X_n \sim \mathcal{N}(\mu, \sigma^2)$, where μ is known, the Cramér-Rao lower bound for estimating the variance is $2\sigma^4$. The difference $(\Upsilon_{\alpha'} - 2)$ of the asymptotic variances in this model compared to the standard model is given by the following term:

$$\sum_{r=0}^{\infty} \big(- r^{\alpha'} + 2(r+1)^{\alpha'} - (r+2)^{\alpha'} \big)^2, \tag{129}$$

which arises due to the non-negligible temporal covariances of the squared increments in this model. Table 5.1 shows numerical values of this deviation for different values of α'.

As observed, the deviation shrinks as the parameter α' increases. Consequently, the underlying process behaves more like i.i.d. normals from the standard model. On the other hand, if α' approaches 1, the error terms become more pronounced, necessitating the use of fewer spatial coordinates or significantly

α'	0.1	0.2	0.3	0.4	0.5	0.6	0.7	0.8	0.9
$(\Upsilon_{\alpha'}-2)$	0.8626	0.7283	0.5984	0.4742	0.3575	0.2504	0.1558	0.0776	0.0222

Table 5.1.: The table shows the deviation between the variance resulting from the standard model with i.i.d. normals and the asymptotic variance in the SPDE model from equation (49) for various values of the pure damping parameter α'. The results are rounded to four decimal places, and the series in equation (129) was calculated with a cut-off $K = 10^5$.

increasing the number of temporal observations to reliably estimate the volatility. This behaviour aligns intuitively with the fact that α' controls the roughness of the temporal marginal processes. Moreover, the simulation results also confirm that the error term becomes more significant as α' approaches 1.

Since the asymptotic variance in Proposition 5.4.1 relies on the unknown parameter σ^4, we are unable to directly observe asymptotic confidence intervals. To address this, we introduce the following quarticity estimator:

$$\hat{\sigma}^4 := \hat{\sigma}^4_{n,m} := \left(\frac{2^d(\pi\eta)^{d/2}\alpha'\Gamma(d/2)}{\Gamma(1-\alpha')}\right)^2 \frac{1}{3mn\Delta_n^{2\alpha'}} \sum_{j=1}^{m}\sum_{i=1}^{n}(\Delta_i X)^4(\mathbf{y}_j)e^{2\|\kappa\boldsymbol{\cdot}\mathbf{y}_j\|_1},$$

for estimating the quarticity parameter σ^4. Assume we can establish consistency for this estimator $\hat{\sigma}^4$, then asymptotic confidence intervals can be constructed using Slutsky's theorem. With this, we conclude the theoretical part of this chapter with the following proposition.

Proposition 5.4.2
Suppose that $\sup_{\mathbf{k}\in\mathbb{N}^d}\lambda_{\mathbf{k}}^{1+\alpha}\mathbb{E}[\langle\xi,e_{\mathbf{k}}\rangle_\vartheta^l]<\infty$, for $l=4,8$. On Assumptions 4.1.1 and 4.1.2 it holds for the quarticity estimator that

$$\hat{\sigma}^4_{n,m_n} \xrightarrow{\mathbb{P}} \sigma^4,$$

as $n\to\infty$. In addition, we obtain for $n\to\infty$ that

$$\sqrt{nm_n}\big(\Upsilon_{\alpha'}\hat{\sigma}^4_{n,m_n}\big)^{-1/2}(\hat{\sigma}^2_{n,m_n}-\sigma^2) \xrightarrow{d} \mathcal{N}(0,1).$$

Proof. It remains to show the consistency of the estimator $\hat{\sigma}^4$. Therefore, we prove that

$$\mathbb{E}\big[(\hat{\sigma}^4_{n,m}-\sigma^4)^2\big] = \mathbb{V}\mathrm{ar}(\hat{\sigma}^4_{n,m}) + \big(\mathbb{E}[\hat{\sigma}^4_{n,m_n}-\sigma^4]\big)^2 \xrightarrow{n\to\infty} 0,$$

implying consistency. As we assume that $\sup_{\mathbf{k}\in\mathbb{N}^d}\lambda_{\mathbf{k}}^{1+\alpha}\mathbb{E}[\langle\xi,e_{\mathbf{k}}\rangle_\vartheta^l]<\infty$, for $l=4,8$, we can replace the initial condition by a stationary initial condition, which is evident by analogous considerations as in Proposition 5.1.1. For the bias term, we have

$$\begin{aligned}\frac{\tilde{K}^2e^{2\|\kappa\boldsymbol{\cdot}\mathbf{y}\|_1}}{3n\Delta_n^{2\alpha'}}\sum_{i=1}^{n}\mathbb{E}\big[(\Delta_i X)^4(\mathbf{y}_j)\big] &= \frac{\tilde{K}^2e^{2\|\kappa\boldsymbol{\cdot}\mathbf{y}\|_1}}{n\Delta_n^{2\alpha'}}\sum_{i=1}^{n}\mathbb{E}\big[(\Delta_i\tilde{X})^2(\mathbf{y}_j)\big]^2\big(1+\mathcal{O}(1)\big)\\ &= \sigma^4\big(1+\mathcal{O}(1)\big),\end{aligned}$$

for an arbitrary $\mathbf{y} \in [\delta, 1-\delta]^d$ and

$$\tilde{K} := \frac{2^d(\pi\eta)^{d/2}\alpha'\Gamma(d/2)}{\Gamma(1-\alpha')}.$$

Hence, we obtain $\mathbb{E}[\hat{\sigma}^4_{n,m}] = \sigma^4 + \mathcal{o}(1)$. For the variance term we use that $\xi^2_{n,i} = \tilde{\xi}^2_{n,i}\big(1+\mathcal{o}(1)\big)$ from equation (109) and observe for $i_2 < i_1$:

$$\begin{aligned}
\mathbb{C}\mathrm{ov}(\tilde{\xi}^2_{n,i_1}, \tilde{\xi}^2_{n,i_2}) &= \sum_{j_1,\ldots,j_4} \frac{\tilde{K}^4 e^{\|\kappa\cdot(\mathbf{y}_{j_1}+\ldots+\mathbf{y}_{j_4})\|_1}}{n^2m^2\Delta_n^{4\alpha'}} \mathbb{C}\mathrm{ov}\big((\Delta_{i_1}\tilde{X})^2(\mathbf{y}_{j_1})(\Delta_{i_1}\tilde{X})^2(\mathbf{y}_{j_2}), (\Delta_{i_2}\tilde{X})^2(\mathbf{y}_{j_3})(\Delta_{i_2}\tilde{X})^2(\mathbf{y}_{j_4})\big) \\
&\leqslant \frac{\tilde{K}^4m^2e^{\|\kappa\|_1}}{n^2\Delta_n^{4\alpha'}} \max_{j_1,\ldots,j_4} \Big|\mathbb{C}\mathrm{ov}\big((\Delta_{i_1}\tilde{X})^2(\mathbf{y}_{j_1})(\Delta_{i_1}\tilde{X})^2(\mathbf{y}_{j_2}), (\Delta_{i_2}\tilde{X})^2(\mathbf{y}_{j_3})(\Delta_{i_2}\tilde{X})^2(\mathbf{y}_{j_4})\big)\Big| \\
&\leqslant \frac{Cm^2}{n^2\Delta_n^{4\alpha'}}\Bigg(\sum_{\mathbf{k}\in\mathbb{N}^d}(\tilde{\Sigma}^{B,\mathbf{k}}_{i_1,i_2} + \Sigma^{BC,\mathbf{k}}_{i_1,i_2})\Bigg)^4 \\
&= \mathcal{O}\Bigg(\frac{m^2\Delta_n^{4\alpha'}}{n^2\Delta_n^{4\alpha'}}\Bigg(\Delta_n^{d/2}\sum_{\mathbf{k}\in\mathbb{N}^d}\frac{(1-e^{-\lambda_\mathbf{k}\Delta_n})^2}{(\lambda_\mathbf{k}\Delta_n)^{1+\alpha}}e^{-\lambda_\mathbf{k}(i_1-i_2-1)\Delta_n}\Bigg)^4\Bigg) \\
&= \mathcal{O}\Bigg(\Delta_n^2m^2(i-j-1)^{4\alpha'-8}\Bigg),
\end{aligned}$$

where $\tilde{\Sigma}^{B,\mathbf{k}}_{i,j}$ and $\Sigma^{BC,\mathbf{k}}_{i,j}$ are defined in the equations (113) and (75), respectively. We additionally used Lemma 4.2.4 in the latter display. Using these calculations and $\mathbb{E}[\xi^4_{n,i}] = \mathcal{O}(\Delta_n^2m^2)$, we obtain that

$$\begin{aligned}
\mathbb{V}\mathrm{ar}\Bigg(\sum_{i=1}^n \xi^2_{n,i}\Bigg) &\leqslant \sum_{i=1}^n \mathbb{E}\big[\xi^4_{n,i}\big] + \sum_{i\neq j}\mathbb{C}\mathrm{ov}\big(\xi^2_{n,i},\xi^2_{n,j}\big) \\
&= \mathcal{O}\Bigg(\Delta_n^2m^2 + \Delta_n^2m^2\sum_{i\neq j}|i-j-1|^{4\alpha'-8}\Bigg) = \mathcal{O}\big(\Delta_n^2m^2\big) = \mathcal{o}(1),
\end{aligned}$$

which completes the proof. □

To illustrate the central limit theorem described in Proposition 5.4.1, we conduct a Monte Carlo study. In this study, we simulated a two-dimensional SPDE model given in equation (49). Each simulation was performed on an equidistant grid in both time and space, where $N = 10^4$ and $M = 10$, resulting in a total of 121 spatial points. The simulation employed the following parameter values: $\vartheta_0 = 0$, $\nu = (6,0)$, $\eta = 1$, $\sigma = 1$, and α' taking on values from the set $\{4/10, 1/2, 6/10\}$, corresponding to three distinct damping scenarios. In each scenario, we performed 1000 Monte Carlo iterations. We utilized the replacement method, as described in Section 4.3, with $L = 10^3$, and for $\alpha' = 4/10$ and $\alpha' = 1/2$, we set a cut-off frequency of $K = 10^3$, while for $\alpha' = 6/10$, we used $K = 1500$.

Figure 5.1 presents a comparison between the empirical distribution of each scenario and the asymptotic normal distribution as stipulated in Proposition 5.4.1. To estimate the kernel density, we employed a Gaussian kernel with Silverman's 'rule of thumb'. As discussed in Section 4.3, the replacement method introduced a notable negative bias due to the cut-off frequency K. To address this bias, we centred the data by utilizing the sample mean of the volatility estimations. This approach provides a clear visual comparison of the empirical and theoretical distributions. All three scenarios exhibit a substantial fit,

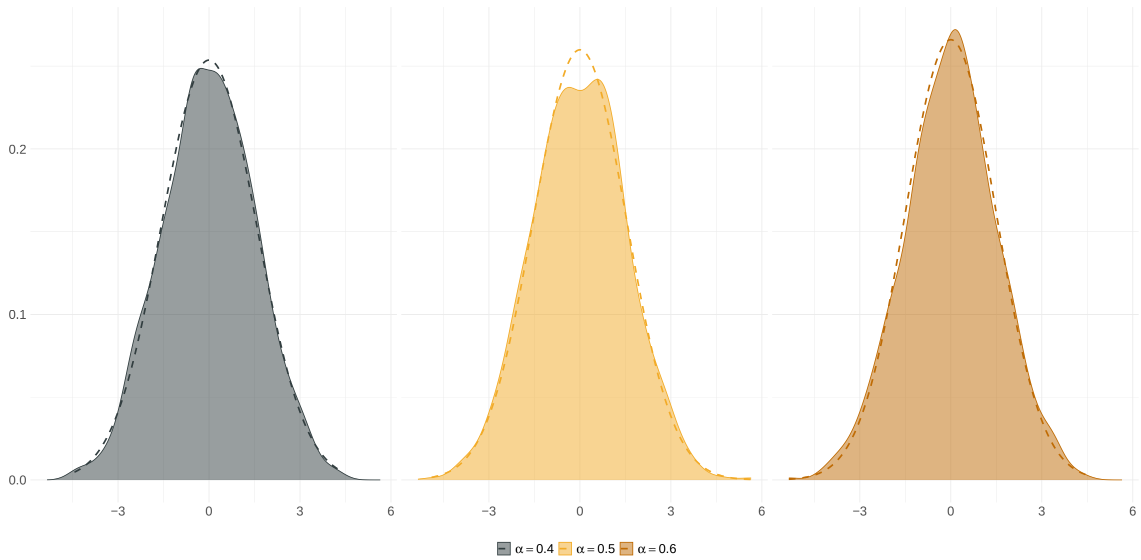

Figure 5.1.: Comparison of the empirical distributions of normalized estimation errors for σ^2 obtained through simulation with $N = 10^4$, $M = 10$, and $\delta = 0.05$ is presented. The kernel-density estimation utilized a Gaussian kernel with Silverman's 'rule of thumb' and was performed over 1000 Monte Carlo iterations. The specific parameter values for simulation are given as follows: $d = 2$, $\vartheta_0 = 0$, $\nu = (6, 0)$, $\eta = 1$, $\sigma = 1$, $L = 10$. Three scenarios were considered, with different values of α': $\alpha' = 4/10, K = 10^3$ (left), $\alpha' = 1/2, K = 10^3$ (middle), and $\alpha' = 6/10, K = 1300$ (right). The corresponding asymptotic distributions are represented by the dotted lines.

with the volatility estimator employing a spatial boundary of $\delta = 0.05$, resulting in 81 spatial points for estimation. The sample mean of the volatility estimations were found to be 0.986 for $\alpha' = 4/10$, 0.975 for $\alpha' = 1/2$, and 0.988 for $\alpha' = 6/10$.

Furthermore, following the same methodology as described in Part I, we illustrate the corresponding QQ-plots in Figure B.2, which can be found in Appendix B.

6. Parametric estimation based on a log-linear model

The objective of this chapter is to extend the concepts presented in Chapters 2 and 3 to encompass multiple spatial dimensions. In one spatial dimension, we have already demonstrated the construction of efficient estimators for the parameters κ and σ_0^2 based on ordinary least squares, when considering statistics involving realized volatilities. By asymptotically linking log-realized volatilities to a log-linear model featuring a spatial explanatory variable, we obtained estimators with optimal rates of convergence and minimal variances. Importantly, the construction of the estimators for κ and σ_0^2 does not necessitate any knowledge regarding the parameters within the differential operator A_ϑ.

However, in higher spatial dimensions, particularly starting from two dimensions, an additional parameter α needs to be incorporated into the random field. As a result, we divide this chapter into two distinct sections. The initial section will introduce the log-linear model for multiple spatial dimensions, assuming the damping parameter α to be known. Subsequently, the second section will concentrate on the estimation of the damping parameter α without any prior information on the model parameters.

6.1. Asymptotic for the normalized volatility and the curvature estimators

Within this section, our primary objective is to formulate estimators for both the multi-dimensional curvature parameter $\kappa = (\kappa_1, \ldots, \kappa_d)$ and the normalized volatility σ_0^2, utilizing a log-linear model. To achieve this, we draw upon the concepts elucidated in Chapters 2 and 3, and extend them to multiple spatial dimensions. Commencing this section, a preliminary segment provides a motivation part, focusing on the development of estimators for the aforementioned curvature parameter and normalized volatility. Therefore, we will introduce another assumption into our observation scheme, essential to ensure the well-defined nature of these estimators.

In the subsequent part of this section we delve into the methodology part, particularly examining the corresponding triangular array related to the constructed estimators. This will be followed by preparatory steps aimed to prove a central limit theorem. For proving a central limit theorem for the constructed estimators, we utilize the general multi-dimensional central limit theorem, as presented in Corollary 3.1.2. We close this section by providing simulation results for our new estimators.

Throughout this entire section we assume the damping parameter $\alpha \in (d/2 - 1, d/2)$ to be a known constant.

6.1.1. Motivation and methodology

In Chapter 4, Proposition 4.2.7 analyses the autocovariance structure of temporal increments. This proposition effectively demonstrated that we can consistently estimate the parameters $\sigma_0^2 = \sigma^2/\eta^{d/2}$ and $\kappa = (\kappa_1, \ldots, \kappa_d)$, where $\kappa_l = \nu_l/\eta$ for $l = 1, \ldots, d$, by utilizing realized volatilities. Consequently, these

parameters are labelled as the natural parameters within the SPDE model described by equation (49). Hence, our current aim is to construct consistent estimators for these parameters. This endeavour begins with the employment of a log-linear model, much akin to the framework outlined in equation (9).
Building upon the foundation laid by Proposition 5.4.1, it becomes apparent that rescaled realized volatilities exhibit qualitative resemblance to normal random variables when the number of temporal observations is sufficiently large. Thus, we observe, for n sufficiently large, that

$$\sqrt{n}\big(\hat{\sigma}^2_{\mathbf{y}}-\sigma^2\big)\approx\mathcal{N}(0,\Upsilon_{\alpha'}\sigma^4),$$

where the estimator for the volatility parameter σ^2 is given by

$$\hat{\sigma}^2_{\mathbf{y}}=\frac{2^d(\pi\eta)^{d/2}\alpha'\Gamma(d/2)}{n\Delta_n^{\alpha'}\Gamma(1-\alpha')}\sum_{i=1}^n(\Delta_iX)^2(\mathbf{y})e^{\|\kappa\bullet\mathbf{y}\|_1}.$$

Rearranging this approximation results in

$$\sqrt{n}\cdot\frac{2^d(\pi\eta)^{d/2}\alpha'\Gamma(d/2)}{n\Delta_n^{\alpha'}\Gamma(1-\alpha')}e^{\|\kappa\bullet\mathbf{y}\|_1}\mathrm{RV}_n(\mathbf{y})\approx\sigma^2\big(\sqrt{n}+\sqrt{\Upsilon_{\alpha'}}Z\big),$$

where $Z\sim\mathcal{N}(0,1)$. The latter display also implies

$$\begin{aligned}\frac{\mathrm{RV}_n(\mathbf{y})}{n\Delta_n^{\alpha'}}&\approx e^{-\|\kappa\bullet\mathbf{y}\|_1}\frac{\Gamma(1-\alpha')\sigma^2}{\eta^{d/2}\alpha'}\cdot\frac{1}{\pi^{d/2}\Gamma(d/2)2^d\sqrt{n}}\big(\sqrt{n}+\sqrt{\Upsilon_{\alpha'}}Z\big)\\&=e^{-\|\kappa\bullet\mathbf{y}\|_1}\frac{\Gamma(1-\alpha')\sigma_0^2}{\alpha'}\cdot\frac{1}{\pi^{d/2}\Gamma(d/2)2^d}\left(1+\sqrt{\frac{\Upsilon_{\alpha'}}{n}}Z\right).\end{aligned}\tag{130}$$

As our focus lies in estimating the natural parameters σ_0^2 and κ, we apply the strategy of converting this approximation into a log-linear model, namely:

$$\log\left(\frac{\mathrm{RV}_n(\mathbf{y})}{n\Delta_n^{\alpha'}}\right)\approx-\|\kappa\bullet\mathbf{y}\|_1+\log\left(\sigma_0^2\frac{\Gamma(1-\alpha')}{\alpha'}\cdot\frac{1}{\pi^{d/2}\Gamma(d/2)2^d}\right)+\log\left(1+\sqrt{\frac{\Upsilon_{\alpha'}}{n}}Z\right).$$

As the number of temporal observations n increases, the variance of the normal random variable in the preceding expression decreases. Utilizing the approximation $\log(1+x)\approx x$ for small $x\approx0$, the resemblance to a linear model becomes clear through

$$\log\left(\frac{\mathrm{RV}_n(\mathbf{y})}{n\Delta_n^{\alpha'}}\right)\approx-\|\kappa\bullet\mathbf{y}\|_1+\log\big(\sigma_0^2K\big)+\sqrt{\frac{\Upsilon_{\alpha'}}{n}}Z,\tag{131}$$

where

$$K:=\frac{\Gamma(1-\alpha')}{\alpha'}\cdot\frac{1}{2^d\pi^{d/2}\Gamma(d/2)}.\tag{132}$$

To be more precise, display (131) suggests the link to a multiple linear regression model. Considering that the covariance of the realized volatilities in two distinct spatial points asymptotically vanishes, we can establish a linear model with homoscedastic normal errors by examining $\log(\mathrm{RV}_n(\mathbf{y}_j)/(n\Delta_n^{\alpha'}))$, for $j=1,\ldots,m$.

To illustrate parameter estimation within a multiple linear regression model, we present the following example.

Example 6.1.1
An ordinary multiple linear regression model is given by

$$Y = X\beta + \varepsilon,$$

where

$$Y = \begin{pmatrix} Y_1 \\ \vdots \\ Y_m \end{pmatrix}, \qquad X = \begin{pmatrix} 1 & y_1^{(1)} & \dots & y_d^{(1)} \\ \vdots & \vdots & \ddots & \vdots \\ 1 & y_1^{(m)} & \dots & y_d^{(m)} \end{pmatrix}, \qquad \beta = \begin{pmatrix} \beta_0 \\ \beta_1 \\ \vdots \\ \beta_d \end{pmatrix},$$

and homoscedastic errors $\varepsilon = (\varepsilon_1, \dots, \varepsilon_m)^\top$, with $\mathbb{E}[\varepsilon_i] = 0$, $\mathbb{V}\mathrm{ar}(\varepsilon_i) = \sigma^2 > 0$, for $i = 1, \dots, m$ and $\mathbb{C}\mathrm{ov}(\varepsilon_i, \varepsilon_j) = 0$, for all $i, j = 1, \dots, m$, with $i \neq j$. In addition, the variance-covariance matrix of ε is given by $\Sigma := \mathbb{C}\mathrm{ov}(\varepsilon) = \sigma^2 E_m$. We call the parameter β_0 intercept and the parameters β_i as slope, where $i = 1, \dots, d$. Suppose that $m \geqslant (d+1)$, and the matrix X possesses a full rank of $(d+1)$. Under these assumptions, the least squares estimator for the unobservable parameter β within this model is given by

$$\hat{\beta} = (X^\top X)^{-1} X^\top Y.$$

Substituting the representation of Y into the estimator $\hat{\beta}$ results in the following identity:

$$\hat{\beta} = (X^\top X)^{-1} X^\top Y = \beta + (X^\top X)^{-1} X^\top \varepsilon, \tag{133}$$

which shows that the estimator $\hat{\beta}$ is unbiased. In particular, the inverse of $(X^\top X)^{-1}$ exists due to the full rank condition on the design matrix X.

The component-wise estimators highlighted in Example 6.1.1 are commonly referred to as Gauss-Markov estimators, exhibiting favourable characteristics. The Gauss-Markov theorem states that the corresponding estimators qualify as BLUE (best linear unbiased estimators), implying that they possess minimum variance among all linear and unbiased estimators. However, we acknowledge that the number of observations $(Y_j)_{1 \leqslant j \leqslant m}$ is intrinsically linked to the dimensionality, specifically requiring $m \geqslant (d+1)$, as stated in the preceding example. Consequently, we introduce the ensuing Assumption to formalize this connection.

Assumption 6.1.2
Let $\mathbf{y}_1, \dots, \mathbf{y}_m \in [\delta, 1-\delta]^d$, where $m \geqslant d$ such that the linear span

$$\mathrm{span}(\mathbf{Y}_m) = \mathbb{R}^{d+1}, \qquad \text{where} \qquad \mathbf{Y}_m := \big\{(1, \mathbf{y}_1), \dots, (1, \mathbf{y}_m)\big\},$$

is a spanning set of $\mathbb{R}^{d+1}$.

The stipulation outlined in the preceding Assumption is equivalent with requiring that the matrix X possesses full rank. This equivalence thus establishes the presence of the estimator $\hat{\beta}$ as well-defined. Assumption 6.1.2 also holds intuitive significance. Consider a scenario, where we observe the vector $Y = \big(Y_1(\mathbf{y}_1), \dots, Y_m(\mathbf{y}_m)\big)^\top$ within the spatial points $\mathbf{y}_1$ and $\mathbf{y}_2, \dots, \mathbf{y}_m$, following the framework described in Example 6.1.1. Here, we set the spatial coordinates $\mathbf{y}_j$ as

$$\mathbf{y}_j = \mathbf{y}_1 + \epsilon_j e_l,$$

where $\epsilon_j > 0$, for $j = 1, \dots, m$, and e_l representing the l-th unit vector, for $l = 1, \dots, d$. While, by definition, these spatial points are distinct from one another, from a statistical perspective, it is likely that we obtain multiple pieces of information for estimating the parameter β_l, while the information content for estimating the remaining parameters is limited.

In accordance with Assumption 4.1.1, it is established that the discretization of the random field is more refined in time than in space, denoted by $m = \mathcal{O}(n^\rho)$, where $\rho \in \big(0, (1-\alpha')/(d+2)\big)$. Additionally, Assumption 6.1.2 imposes the requirement that a minimum of $(d+1)$ observations is necessary to construct an estimator for the natural parameters. Collectively, these assumptions enforce a minimal number of temporal points, indicated by

$$n > (d+1)^{\frac{d+2}{1-\alpha'}}. \tag{134}$$

Asymptotically, this restriction is evidently satisfied since the spatial dimensions d is assumed to be fixed. However, the restrictive nature becomes significant in a simulation scenario. The latter display implies that n grows exponentially with the spatial dimensions. Moreover, if α' is close to one, the growth of n becomes particularly pronounced. Therefore, estimating the natural parameters using this least squares approach based on realized volatilities might only be accurate for lower dimensions, such as $d = 2, 3$, or when a large number of temporal observations is available. To demonstrate this effect, we provide numerical values for the dimension $d = 2, 3$. For the case of $d = 2$, the relationship in display (134) yields

α'	0.1	0.2	0.3	0.4	0.5	0.6	0.7	0.8	0.9
$n \gtrsim$	132	243	533	1517	6561	59049	2.3×10^6	3.49×10^9	1.22×10^{19}

Table 6.1.: The table demonstrates the minimal number of temporal observations in two space dimensions depending on the pure damping parameter α' according to Assumptions 4.1.1 and 6.1.2.

and for $d = 3$ we find

α'	0.1	0.2	0.3	0.4	0.5	0.6	0.7	0.8	0.9
$n \gtrsim$	2212	5793	19973	104032	1.1×10^6	3.4×10^7	1.1×10^{10}	1.13×10^{15}	1.3×10^{30}

Table 6.2.: The table demonstrates the minimal number of temporal observations in three space dimensions depending on the pure damping parameter α' according to Assumptions 4.1.1 and 6.1.2.

As the temporal marginal processes become progressively rougher with decreasing values of $\alpha' \in (0,1)$, it becomes apparent that we require a reduced amount of data for estimating the natural model parameters. Conversely, if $\alpha \approx 1$, a substantial number of temporal observations will be required.

With the groundwork laid, we can now establish the estimators for the natural parameters $\sigma_0^2, \kappa_1, \ldots, \kappa_d$ within the context of the SPDE model from equation (49). Leveraging the approximation (131) and referencing Example 6.1.1, we proceed by defining the following multi-dimensional parameter and its corresponding estimator:

$$\Psi := \begin{pmatrix} \log(\sigma_0^2 K) \\ -\kappa_1 \\ \vdots \\ -\kappa_d \end{pmatrix} \in \mathbb{R}^{d+1} \quad \text{and} \quad \hat{\Psi} := \hat{\Psi}_{n,m} := (X^\top X)^{-1} X^\top Y \in \mathbb{R}^{d+1}, \tag{135}$$

where

$$X := \begin{pmatrix} 1 & y_1^{(1)} & \ldots & y_d^{(1)} \\ \vdots & \vdots & \ddots & \vdots \\ 1 & y_1^{(m)} & \ldots & y_d^{(m)} \end{pmatrix} \in \mathbb{R}^{m \times (d+1)} \quad \text{and} \quad Y := \begin{pmatrix} \log\left(\frac{\mathrm{RV}_n(\mathbf{y}_1)}{n\Delta_n^{\alpha'}}\right) \\ \vdots \\ \log\left(\frac{\mathrm{RV}_n(\mathbf{y}_m)}{n\Delta_n^{\alpha'}}\right) \end{pmatrix} \in \mathbb{R}^m.$$

To effectively estimate the natural parameters $\sigma_0^2, \kappa_1, \ldots, \kappa_d$, we introduce the parameter $\upsilon \in (0,\infty) \times \mathbb{R}^d$ along with its associated estimator $\hat{\upsilon}$, defined as follows:

$$\upsilon := \begin{pmatrix} \sigma_0^2 \\ \kappa_1 \\ \vdots \\ \kappa_d \end{pmatrix} \quad \text{and} \quad \hat{\upsilon} := \hat{\upsilon}_{n,m} := h^{-1}(\hat{\Psi}) := \begin{pmatrix} h_1^{-1}(\hat{\Psi}_1) \\ \vdots \\ h_{d+1}^{-1}(\hat{\Psi}_{d+1}) \end{pmatrix}, \tag{136}$$

where $\hat{\Psi} = (\hat{\Psi}_1, \ldots, \hat{\Psi}_{d+1})^\top$ and $h : (0,\infty) \times \mathbb{R}^d \to \mathbb{R}^{d+1}$, $h^{-1} : \mathbb{R}^{d+1} \to (0,\infty) \times \mathbb{R}^d$, with

$$h(\mathbf{x}) = \begin{pmatrix} \log(x_1 K) \\ -x_2 \\ \vdots \\ -x_{d+1} \end{pmatrix} \quad \text{and} \quad h^{-1}(\mathbf{x}) = \begin{pmatrix} e^{x_1}/K \\ -x_2 \\ \vdots \\ -x_{d+1} \end{pmatrix}. \tag{137}$$

Since Ψ represents a strictly monotonic transformation of the parameter υ, i.e., $h(\upsilon) = \Psi$, we restrict our analysis to the determination of asymptotic properties for the estimator $\hat{\Psi}$. Subsequently, by utilizing the multivariate delta method, we can infer these asymptotic properties for the estimator $\hat{\upsilon}$.

Concluding the motivation segment, we now shift our focus towards the variance-covariance matrix of the estimator $\hat{\beta}$ introduced in Example 6.1.1, which can be derived through standard calculus, resulting in

$$\begin{aligned}\mathbb{V}\mathrm{ar}(\hat{\beta}) &= (X^\top X)^{-1}X^\top \mathbb{V}\mathrm{ar}(Y)\big((X^\top X)^{-1}X^\top\big)^\top = (X^\top X)^{-1}X^\top \mathbb{V}\mathrm{ar}(\varepsilon)X(X^\top X)^{-1}\\ &= \sigma^2(X^\top X)^{-1}X^\top X(X^\top X)^{-1} = \sigma^2(X^\top X)^{-1},\end{aligned}$$

where we employed the fact that the matrix $X^\top X$ is a symmetric matrix. Assuming that we are observing spatial coordinates $\mathbf{y}_1, \ldots, \mathbf{y}_m \in [a,b]^d$, where $c := |a-b|$. When considering a central limit theorem, one concern is on determining the asymptotic variance of:

$$\mathbb{V}\mathrm{ar}\big(\sqrt{m}(\hat{\beta}-\beta)\big) = \mathbb{V}\mathrm{ar}\big(\sqrt{m}\hat{\beta}\big) = \sigma^2 c\left(\frac{c}{m}X^\top X\right)^{-1} \overset{n\to\infty}{\longrightarrow} \sigma^2 c\Sigma^{-1},$$

where we assume that $c/m(X^\top X)$ converges to a symmetric positive-definite variance-covariance matrix $\Sigma \in \mathbb{R}^{(d+1)\times(d+1)}$. This assumption consequently entails that Σ^{-1} is also symmetric and positive-definite. In our model, we observe spatial coordinates $\mathbf{y}_1, \ldots, \mathbf{y}_m \in [\delta, 1-\delta]^d$, signifying that these spatial observations are situated at least $\delta > 0$ distance away from the boundaries of the unit hypercube. We can examine the structure of the matrix $X^\top X$ by utilizing the explicitly provided expression of X from Example 6.1.1. With $c = 1-2\delta$, we have the following:

$$\frac{1-2\delta}{m}X^\top X = \frac{1-2\delta}{m}\begin{pmatrix} m & \sum_{j=1}^m y_1^{(j)} & \sum_{j=1}^m y_2^{(j)} & \cdots & \sum_{j=1}^m y_d^{(j)} \\ \sum_{j=1}^m y_1^{(j)} & \sum_{j=1}^m (y_1^{(j)})^2 & \sum_{j=1}^m y_1^{(j)}y_2^{(j)} & \cdots & \sum_{j=1}^m y_1^{(j)}y_d^{(j)} \\ \sum_{j=1}^m y_2^{(j)} & \sum_{j=1}^m y_2^{(j)}y_1^{(j)} & \sum_{j=1}^m (y_2^{(j)})^2 & \cdots & \sum_{j=1}^m y_2^{(j)}y_d^{(j)} \\ \vdots & \vdots & \vdots & \ddots & \vdots \\ \sum_{j=1}^m y_d^{(j)} & \sum_{j=1}^m y_d^{(j)}y_1^{(j)} & \sum_{j=1}^m y_d^{(j)}y_2^{(j)} & \cdots & \sum_{j=1}^m (y_d^{(j)})^2 \end{pmatrix} \overset{m\to\infty}{\longrightarrow} \Sigma,$$

where $\Sigma = (\Sigma_{i,l})_{1\leqslant i,l\leqslant d+1}$, with

$$\Sigma_{i,l} := \begin{cases} 1-2\delta & \text{, if } i=l=1, \\ \lim_{m\to\infty} \frac{1-2\delta}{m}\sum_{j=1}^m y_{l-1}^{(j)} & \text{, if } i=1, 2\leqslant l\leqslant d+1, \\ \lim_{m\to\infty} \frac{1-2\delta}{m}\sum_{j=1}^m y_{i-1}^{(j)} & \text{, if } 2\leqslant i\leqslant d+1, l=1, \\ \lim_{m\to\infty} \frac{1-2\delta}{m}\sum_{j=1}^m \big(y_{i-1}^{(j)}\big)^2 & \text{, if } 2\leqslant i=l\leqslant d+1, \\ \lim_{m\to\infty} \frac{1-2\delta}{m}\sum_{j=1}^m y_{i-1}^{(j)}y_{l-1}^{(j)} & \text{, if } 2\leqslant i,l\leqslant d+1, \text{ with } i\neq l \end{cases}. \tag{138}$$

The convergence of the Riemann sums is guaranteed by the straightforward bounds

$$0 \leqslant \frac{1-2\delta}{m}\sum_{j=1}^m a_j \leqslant 1,$$

for all $m \in \mathbb{N}$, where the sequence (a_j) corresponds to the respective sequence within the Riemann sums in equation (138).

Contrasting this assumption regarding the asymptotic variance with the analogous one-dimensional log-linear model. In Chapter 3, we employed a simple linear regression model to estimate the natural parameters of the one-dimensional SPDE model from equation (1). Within this simple linear regression model, the design matrix X was given by

$$X = \begin{pmatrix} 1 & y_1 \\ \vdots & \vdots \\ 1 & y_m \end{pmatrix},$$

where $\delta = y_1 < \ldots < y_m = 1-\delta$. The estimator provided in matrix notation for the unknown parameters within Example 6.1.1 readily translates into the estimators outlined in Example 3.1.1. Proposition 3.2.2 presented an asymptotic variance of

$$\Sigma = \begin{pmatrix} \frac{4\Gamma\pi(1-\delta+\delta^2)}{(1-2\delta)^2} & \frac{6\Gamma\pi}{(1-2\delta)^2} \\ \frac{6\Gamma\pi}{(1-2\delta)^2} & \frac{12\Gamma\pi}{(1-2\delta)^2} \end{pmatrix}, \tag{139}$$

which is also implied by

$$\Gamma\pi(1-2\delta)\Sigma^{-1} = \Gamma\pi(1-2\delta) \begin{pmatrix} 1-2\delta & \int_\delta^{1-\delta} y \,\mathrm{d}y \\ \int_\delta^{1-\delta} y \,\mathrm{d}y & \int_\delta^{1-\delta} y^2 \,\mathrm{d}y \end{pmatrix}^{-1} = \Gamma\pi \begin{pmatrix} \frac{4(1-\delta+\delta^2)}{(1-2\delta)^2} & -\frac{6}{(1-2\delta)^2} \\ -\frac{6}{(1-2\delta)^2} & \frac{12}{(1-2\delta)^2} \end{pmatrix}.$$

Note that the signs in the covariance entries within Proposition 3.2.2 are reversed due to the corresponding estimator in the simple linear regression model being directed towards estimating the parameter $-\kappa$. However, when transitioning to a multiple linear regression model, involving spatial coordinates in multiple dimensions, establishing a feasible ordering for the spatial vectors $\mathbf{y}_1, \ldots, \mathbf{y}_m$ becomes challenging. Furthermore, there is no guarantee that coordinates won't be duplicated along a particular axis. Consequently, representing the multi-dimensional case similarly to display (139) becomes impractical. Therefore, the derivation of the asymptotic variance matrix must be tailored to the specific observation scheme in use. Given our focus on the asymptotic properties of the estimator $\hat{\Psi}$, it is reasonable to anticipate this estimator to be asymptotically unbiased, with an asymptotic variance of $\Upsilon_{\alpha'}(1-2\delta)\Sigma^{-1}$, where Σ is defined in equation (138).

We proceed to tackle the methodology section for the estimator $\hat{\Psi}$ by deriving the corresponding multi-dimensional triangular array. To construct the multi-dimensional triangular array, we leverage the Taylor expansion for $\log(a+x)$, which is given in equation (27). With the incorporation of Proposition 4.2.6, we observe that

$$\log\left(\frac{\mathrm{RV}_n(\mathbf{y})}{n\Delta_n^{\alpha'}}\right) = \log(\sigma_0^2 K) - \|\kappa \bullet \mathbf{y}\|_1 + \frac{\sum_{i=1}^n \overline{(\Delta_i \tilde{X})^2(\mathbf{y})}}{n\Delta_n^{\alpha'}\sigma_0^2 K} e^{\|\kappa\bullet\mathbf{y}\|_1} + \mathcal{O}\big(\Delta_n^{1-\alpha'}\big) + \mathcal{O}_{\mathbb{P}}\left(\left(\overline{\frac{\mathrm{RV}_n(\mathbf{y})}{n\Delta_n^{\alpha'}}}\right)^2\right),$$

where the constant K is defined in equation (132). Utilizing Proposition 5.2.1, we conclude that

$$\log\left(\frac{\mathrm{RV}_n(\mathbf{y})}{n\Delta_n^{\alpha'}}\right) = \log(\sigma_0^2 K) - \|\kappa \bullet \mathbf{y}\|_1 + \frac{\sum_{i=1}^n \overline{(\Delta_i \tilde{X})^2(\mathbf{y})}}{n\Delta_n^{\alpha'}\sigma_0^2 K} e^{\|\kappa\bullet\mathbf{y}\|_1} + \mathcal{O}\big(\Delta_n^{1-\alpha'}\big) + \mathcal{O}_{\mathbb{P}}(\Delta_n). \tag{140}$$

The previous expression simplifies the analysis by allowing us to focus on the term

$$\log(\sigma_0^2 K) - \|\kappa \bullet \mathbf{y}\|_1 + \frac{\sum_{i=1}^n \overline{(\Delta_i \tilde{X})^2(\mathbf{y})}}{n\Delta_n^{\alpha'}\sigma_0^2 K} e^{\|\kappa \bullet \mathbf{y}\|_1},$$

since the last components in equation (140) represent the negligible model errors. Our goal is to establish a central limit theorem in the form of $\sqrt{nm}(\hat{\Psi} - \Psi)$. To achieve this, we develop the triangular array associated with the estimator $\hat{\Psi}$ by employing the equations (133) and (140). The triangular array is thus defined as $\Xi_{n,i} := \xi_{n,i} - \mathbb{E}[\xi_{n,i}]$, where

$$\xi_{n,i} := \sqrt{nm} \cdot \frac{1-2\delta}{m} \left(\frac{1-2\delta}{m} X^\top X \right)^{-1} X^\top \begin{pmatrix} \frac{(\Delta_i \tilde{X})^2(\mathbf{y}_1)}{n\Delta_n^{\alpha'}\sigma_0^2 K} e^{\|\kappa \bullet \mathbf{y}_1\|_1} \\ \vdots \\ \frac{(\Delta_i \tilde{X})^2(\mathbf{y}_m)}{n\Delta_n^{\alpha'}\sigma_0^2 K} e^{\|\kappa \bullet \mathbf{y}_m\|_1} \end{pmatrix}$$

$$= \frac{\sqrt{n}(1-2\delta)}{\sqrt{m} K \sigma_0^2} \left(\frac{1-2\delta}{m} X^\top X \right)^{-1} X^\top \begin{pmatrix} \frac{(\Delta_i \tilde{X})^2(\mathbf{y}_1)}{n\Delta_n^{\alpha'}} e^{\|\kappa \bullet \mathbf{y}_1\|_1} \\ \vdots \\ \frac{(\Delta_i \tilde{X})^2(\mathbf{y}_m)}{n\Delta_n^{\alpha'}} e^{\|\kappa \bullet \mathbf{y}_m\|_1} \end{pmatrix}. \tag{141}$$

With the triangular array $\Xi_{n,i}$ in place, we can now proceed to the preparations for a CLT.

6.1.2. Preparations for the central limit theorem

In the preceding section, we established a triangular array $\Xi_{n,i} = \xi_{n,i} - \mathbb{E}[\xi_{n,i}]$ corresponding to the estimator $\hat{\Psi}$ presented in equation (135). The objective of this section is to provide the technical details required to prove a central limit theorem for the estimator $\hat{\Psi}$.

In Chapter 3, we utilized Corollary 3.2.1 to establish a central limit theorem for multi-dimensional triangular arrays, a simplified version of the central limit theorem from Proposition 1.2.4. This corollary exploited a special structure of triangular arrays, based on temporal quadratic increments, which enabled us to leverage pre-existing results. While the triangular array $\Xi_{n,i}$ from equation (141) similarly employs quadratic increments, the extension to higher dimensions prevents the direct applicability of Corollary 3.2.1. Nonetheless, we can adapt the essential ideas of Corollary 3.2.1 combined with results from Chapter 5 to establish a central limit theorem for $\Xi_{n,i}$. This involves employing the Crámer-Wold device and Corollary 3.1.2. For the application of Corollary 3.1.2, we will analyse the following one-dimensional triangular array:

$$\gamma^\top \Xi_{n,i} = \gamma^\top \big(\xi_{n,i} - \mathbb{E}[\xi_{n,i}]\big) = \gamma^\top \xi_{n,i} - \gamma^\top \mathbb{E}[\xi_{n,i}],$$

where $\gamma \in \mathbb{R}^{d+1}$ is arbitrary but fixed. The upcoming discussion will derive the asymptotic variance of the triangular array $\gamma^\top \Xi_{n,i}$ and verify the conditions stated in Corollary 3.1.2.

Lemma 6.1.3
On the Assumptions 4.1.1, 4.1.2 and 6.1.2, we have

$$\lim_{n\to\infty} \mathbb{V}\mathrm{ar}\bigg(\sum_{i=1}^{n} \gamma^\top \Xi_{n,i}\bigg) = (1-2\delta)\Upsilon_{\alpha'}\gamma^\top\Sigma^{-1}\gamma,$$

where $\Xi_{n,i}$ is defined in equation (141), $\Upsilon_{\alpha'}$ defined in equation (121), Σ^{-1} from equation (138), $\delta \in (0,1/2)$ and $\gamma \in \mathbb{R}^{d+1}$ arbitrary but fixed.

Proof. Consider an arbitrary but fixed vector $\gamma \in \mathbb{R}^{d+1}$. We initiate this proof by performing the following calculations:

$$\begin{aligned}\mathbb{V}\mathrm{ar}\bigg(\sum_{i=1}^{n} \gamma^\top \Xi_{n,i}\bigg) &= \gamma^\top \mathbb{V}\mathrm{ar}\bigg(\sum_{i=1}^{n} \xi_{n,i}\bigg)\gamma \\ &= \gamma^\top \frac{n(1-2\delta)^2}{mK^2\sigma_0^4}\bigg(\frac{1-2\delta}{m}X^\top X\bigg)^{-1} X^\top \mathbb{V}\mathrm{ar}(\tilde{Y}_n) X \bigg(\frac{1-2\delta}{m}X^\top X\bigg)^{-1}\gamma,\end{aligned}$$

where

$$\tilde{Y}_n := \begin{pmatrix} \sum_{i=1}^{n} \frac{(\Delta_i \tilde{X})^2(\mathbf{y}_1)}{n\Delta_n^{\alpha'}} e^{\|\kappa\cdot\mathbf{y}_1\|_1} \\ \vdots \\ \sum_{i=1}^{n} \frac{(\Delta_i \tilde{X})^2(\mathbf{y}_m)}{n\Delta_n^{\alpha'}} e^{\|\kappa\cdot\mathbf{y}_m\|_1}\end{pmatrix} = \begin{pmatrix} V_{n,\Delta_n}(\mathbf{y}_1) \\ \vdots \\ V_{n,\Delta_n}(\mathbf{y}_m)\end{pmatrix} \in \mathbb{R}^m.$$

We determine the entries of the variance-covariance matrix $V_{n,m} := \mathbb{V}\mathrm{ar}(\tilde{Y}_n)$ of $\tilde{Y}_{n,i}$ with Proposition 5.2.1 and have

$$(V_{n,m})_{j_1,j_2} = \begin{cases} \frac{\Upsilon_{\alpha'}}{n} K^2\sigma_0^4\big(1+\Delta_n^{1/2} \vee \Delta_n^{1-\alpha'}\big) & \text{, if } 1 \leqslant j_1 = j_2 \leqslant m \\ \mathcal{O}\big(\Delta_n^{2-\alpha'}(\|\mathbf{y}_{j_1}-\mathbf{y}_{j_2}\|_0^{-(d+1)} + \delta^{-(d+1)})\big) & \text{, if } 1 \leqslant j_1, j_2 \leqslant m, \text{ for } j_1 \neq j_2 \end{cases},$$

for $1 \leqslant j_1, j_2 \leqslant m$. Hence, we have

$$\mathbb{V}\mathrm{ar}\bigg(\sum_{i=1}^{n} \gamma^\top \Xi_{n,i}\bigg) = \gamma^\top \frac{(1-2\delta)^2}{m}\bigg(\frac{1-2\delta}{m}X^\top X\bigg)^{-1} X^\top\bigg(\frac{n}{K^2\sigma_0^4}V_{n,m}\bigg) X \bigg(\frac{1-2\delta}{m}X^\top X\bigg)^{-1}\gamma,$$

where we define

$$\frac{n}{K^2\sigma_0^4}V_{n,m} =: V_{n,m,1} + V_{n,m,2},$$

with

$$V_{n,m,1} := \Upsilon_{\alpha'}\big(1+\Delta_n^{1/2} \vee \Delta_n^{1-\alpha'}\big)E_m,$$

where E_m denotes the $m \times m$ dimensional identity matrix and

$$V_{n,m,2} := \begin{cases} 0 & \text{, if } 1 \leqslant j_1 = j_2 \leqslant m \\ \mathcal{O}\big(\Delta_n^{1-\alpha'}(\|\mathbf{y}_{j_1} - \mathbf{y}_{j_2}\|_0^{-(d+1)} + \delta^{-(d+1)})\big) & \text{, if } 1 \leqslant j_1, j_2 \leqslant m, \text{ for } j_1 \neq j_2 \end{cases}.$$

We conclude that

$$\begin{aligned} \mathbb{V}\text{ar}\bigg(\sum_{i=1}^n \gamma^\top \Xi_{n,i}\bigg) &= \gamma^\top \bigg(\frac{(1-2\delta)^2}{m}\bigg(\frac{1-2\delta}{m} X^\top X\bigg)^{-1} X^\top V_{n,m,1} X \bigg(\frac{1-2\delta}{m} X^\top X\bigg)^{-1} \\ &\quad + \frac{(1-2\delta)^2}{m}\bigg(\frac{1-2\delta}{m} X^\top X\bigg)^{-1} X^\top V_{n,m,2} X \bigg(\frac{1-2\delta}{m} X^\top X\bigg)^{-1}\bigg)\gamma \\ &= \gamma^\top \bigg((1-2\delta)\Upsilon_{\alpha'}\big(1 + \Delta_n^{1/2} \vee \Delta_n^{1-\alpha'}\big)\bigg(\frac{1-2\delta}{m} X^\top X\bigg)^{-1} \\ &\quad \times \bigg(\frac{1-2\delta}{m} X^\top X\bigg)\bigg(\frac{1-2\delta}{m} X^\top X\bigg)^{-1} \\ &\quad + (1-2\delta)\bigg(\frac{1-2\delta}{m} X^\top X\bigg)^{-1}\bigg(\frac{1-2\delta}{m} X^\top V_{n,m,2} X\bigg)\bigg(\frac{1-2\delta}{m} X^\top X\bigg)^{-1}\bigg)\gamma \\ &= \gamma^\top \bigg((1-2\delta)\Upsilon_{\alpha'}\big(1 + \Delta_n^{1/2} \vee \Delta_n^{1-\alpha'}\big)\bigg(\frac{1-2\delta}{m} X^\top X\bigg)^{-1} \\ &\quad + (1-2\delta)\bigg(\frac{1-2\delta}{m} X^\top X\bigg)^{-1}\bigg(\frac{1-2\delta}{m} X^\top V_{n,m,2} X\bigg)\bigg(\frac{1-2\delta}{m} X^\top X\bigg)^{-1}\bigg)\gamma. \end{aligned}$$

Let $m = m_n$ be in accordance with Assumption 4.1.1. As the convergence of $(1-2\delta)/m_n \cdot X^\top X$ is established for $n \to \infty$, the focus shifts on demonstrating the convergence of $m_n^{-1}(X^\top V_{n,m_n,2} X)$ towards the zero matrix, denoted by $\mathbf{0}$. Consider matrices $A \in \mathbb{R}^{a \times b}$, $B \in \mathbb{R}^{b \times b}$ and $C \in \mathbb{R}^{b \times a}$, where $(B)_{i_1,i_2} \geqslant 0$ and $(A)_{l,i}, (C)_{i,l} \in [0,1]$ for all $1 \leqslant i, i_1, i_2 \leqslant b, 1 \leqslant l \leqslant a$. Here, we obtain

$$(ABC)_{i,l} \leqslant (\mathbf{1}_{a,b} B \mathbf{1}_{b,a})_{i,l},$$

for each $1 \leqslant i, l \leqslant a$, where $\mathbf{1}_{a,b} = \{1\}^{a \times b}$ denotes the matrix with each entry being one. Thus, we find

$$\bigg(\frac{1}{m} X^\top V_{n,m,2} X\bigg)_{i,l} \leqslant \bigg(\frac{1}{m} \mathbf{1}_{(d+1),m} V_{n,m,2} \mathbf{1}_{m,(d+1)}\bigg)_{i,l},$$

for each $1 \leqslant i, l \leqslant (d+1)$. It holds for $1 \leqslant i \leqslant (d+1)$ and $1 \leqslant l \leqslant m$ that

$$\bigg(\frac{1}{m} \mathbf{1}_{(d+1),m} V_{n,m,2}\bigg)_{i,l} = \mathcal{O}\bigg(\frac{\Delta_m^{1-\alpha'}}{m}\bigg(\sum_{\substack{j_1=1 \\ j_1 \neq l}}^m \|\mathbf{y}_{j_1} - \mathbf{y}_l\|_0^{-(d+1)} + (m-1)\delta^{-(d+1)}\bigg)\bigg),$$

and therefore, we have for $1 \leqslant i, l \leqslant (d+1)$ that

$$\begin{aligned} \bigg(\frac{1}{m} \mathbf{1}_{(d+1),m} V_{n,m,2} \mathbf{1}_{m,(d+1)}\bigg)_{i,l} &= \mathcal{O}\bigg(\frac{\Delta_m^{1-\alpha'}}{m}\bigg(\sum_{j_2=1}^m \sum_{\substack{j_1=1 \\ j_1 \neq j_2}}^m \|\mathbf{y}_{j_1} - \mathbf{y}_{j_2}\|_0^{-(d+1)} + m(m-1)\delta^{-(d+1)}\bigg)\bigg) \\ &= \mathcal{O}\bigg(\frac{\Delta_n^{1-\alpha'}}{m}(m^{d+3} + m^2)\bigg) \end{aligned}$$

$$= \mathcal{O}\big(\Delta_n^{1-\alpha'} m^{d+2}\big).$$

Utilizing Assumption 4.1.1, we can establish that

$$\left(\frac{1}{m_n} X^\top V_{n,m_n,2} X\right)_{i,l} = \mathcal{O}\big(\Delta_n^{1-\alpha'} m_n^{d+2}\big) \stackrel{n\to\infty}{\longrightarrow} 0,$$

for all $1 \leqslant i, l \leqslant (d+1)$. This, in turn, implies

$$\frac{1}{m_n} X^\top V_{n,m_n,2} X \stackrel{n\to\infty}{\longrightarrow} \mathbf{0}.$$

The conclusion follows accordingly. □

The preceding lemma confirms that the estimator $\hat{\Psi}$ for the parameter Ψ possesses an asymptotic variance of $(1-2\delta)\Upsilon_{\alpha'}\Sigma^{-1}$. The following lemma verifies the Conditions (I) and (II) in Corollary 3.1.2.

Lemma 6.1.4

On the Assumptions 4.1.1, 4.1.2 and 6.1.2, we have

$$\mathbb{V}\mathrm{ar}\left(\sum_{i=a}^{b} \gamma^\top \Xi_{n,i}\right) \leqslant C \sum_{i=a}^{b} \mathbb{V}\mathrm{ar}(\gamma^\top \Xi_{n,i}),$$

for all $1 \leqslant a \leqslant b \leqslant n$, $\Xi_{n,i}$ defined in equation (141), an universal constant $C > 0$ and $\gamma \in \mathbb{R}^{d+1}$ arbitrary but fixed.

Proof. For an arbitrary but fixed vector $\gamma \in \mathbb{R}^{d+1}$, we can establish, analogously to Lemma 6.1.3, that

$$\begin{aligned}
\mathbb{V}\mathrm{ar}\left(\sum_{i=a}^{b} \gamma^\top \Xi_{n,i}\right) &= \gamma^\top \mathbb{V}\mathrm{ar}\left(\sum_{i=a}^{b} \xi_{n,i}\right)\gamma \\
&= \gamma^\top \frac{(b-a+1)^2(1-2\delta)^2}{nmK^2\sigma_0^4}\left(\frac{1-2\delta}{m} X^\top X\right)^{-1} X^\top \mathbb{V}\mathrm{ar}\big(\tilde{Y}_{a,b}\big) X \left(\frac{1-2\delta}{m} X^\top X\right)^{-1}\gamma,
\end{aligned}$$

where

$$\tilde{Y}_{a,b} := \begin{pmatrix} \sum_{i=a}^{b} \frac{(\Delta_i \tilde{X})^2(\mathbf{y}_1)}{(b-a+1)\Delta_n^{\alpha'}} e^{\|\kappa \bullet \mathbf{y}_1\|_1} \\ \vdots \\ \sum_{i=a}^{b} \frac{(\Delta_i \tilde{X})^2(\mathbf{y}_m)}{(b-a+1)\Delta_n^{\alpha'}} e^{\|\kappa \bullet \mathbf{y}_m\|_1} \end{pmatrix} \in \mathbb{R}^m.$$

For the variance $\mathbb{V}\mathrm{ar}(\tilde{Y}_{a,b}) := V_{a,b,n,m} := V_{a,b,n,m,1} + V_{a,b,n,m,2}$ we find

$$(V_{a,b,n,m,1})_{j_1,j_2} := \begin{cases} \frac{\Upsilon_{\alpha'}}{(b-a+1)} K^2 \sigma_0^4 \big(1 + \Delta_n^{1/2} \vee \Delta_n^{1-\alpha'}\big) & , \text{ if } 1 \leqslant j_1 = j_2 \leqslant m \\ 0 & , \text{ if } 1 \leqslant j_1, j_2 \leqslant m \text{ for } j_1 \neq j_2 \end{cases},$$

$$(V_{a,b,n,m,2})_{j_1,j_2} := \begin{cases} 0 & \text{, if } 1 \leqslant j_1 = j_2 \leqslant m \\ \mathcal{O}\big(\frac{1}{b-a+1}\Delta_n^{1-\alpha'}(\|\mathbf{y}_{j_1} - \mathbf{y}_{j_2}\|_0^{-(d+1)} + \delta^{-(d+1)})\big) & \text{, if } 1 \leqslant j_1, j_2 \leqslant m, \text{ for } j_1 \neq j_2 \end{cases},$$

and thus, we have

$$\begin{aligned} &\mathbb{V}\mathrm{ar}\Big(\sum_{i=a}^{b} \gamma^\top \Xi_{n,i}\Big) \\ &= \mathcal{O}\bigg(\frac{(b-a+1)^2(1-2\delta)}{nK^2\sigma_0^4} \cdot \frac{K^2\sigma_0^4 \Upsilon_{\alpha'}}{b-a+1}\gamma^\top \Big(\frac{1-2\delta}{m}X^\top X\Big)^{-1}\Big(\frac{1-2\delta}{m}X^\top X\Big)\Big(\frac{1-2\delta}{m}X^\top X\Big)^{-1}\gamma\bigg) \\ &\quad + \frac{(b-a+1)(1-2\delta)^2}{nK^2\sigma_0^4}\gamma^\top \Big(\frac{1-2\delta}{m}X^\top X\Big)^{-1}\Big(\frac{b-a+1}{m}X^\top V_{a,b,n,m,2}X\Big)\Big(\frac{1-2\delta}{m}X^\top X\Big)^{-1}\gamma. \end{aligned}$$

Similar to the proof of Lemma 6.1.3, we observe that

$$\Big(\frac{b-a+1}{m}X^\top V_{a,b,n,m,2}X\Big)_{i,l} = \mathcal{O}(\Delta_n^{1-\alpha'} m^{d+2}),$$

where we used that $((1-2\delta)/m_n \cdot X^\top X)^{-1} \to \Sigma^{-1}$, as $n \to \infty$, and $\gamma^\top \Sigma^{-1}\gamma = \mathcal{O}(\|\gamma\|_\infty)$. Hence, it holds

$$\mathbb{V}\mathrm{ar}\Big(\sum_{i=a}^{b} \gamma^\top \Xi_{n,i}\Big) = \mathcal{O}\big(\|\gamma\|_\infty \Delta_n(b-a+1) + \|\gamma\|_\infty \Delta_n (b-a+1)\Delta_n^{1-\alpha'} m^{d+2}\big) = \mathcal{O}\big(\|\gamma\|_\infty \Delta_n (b-a+1)\big).$$

Applying a similar approach to $\mathbb{V}\mathrm{ar}(\gamma^\top \Xi_{n,i})$ yields

$$\mathbb{V}\mathrm{ar}(\gamma^\top \Xi_{n,i}) = \gamma^\top \frac{(1-2\delta)^2}{nmK^2\sigma_0^4}\Big(\frac{1-2\delta}{m}X^\top X\Big)^{-1} X^\top \mathbb{V}\mathrm{ar}\big(\tilde{Y}_i\big) X \Big(\frac{1-2\delta}{m}X^\top X\Big)^{-1}\gamma,$$

where

$$\tilde{Y}_i := \begin{pmatrix} \frac{(\Delta_i \tilde{X})^2(\mathbf{y}_1)}{\Delta_n^{\alpha'}} e^{\|\kappa \cdot \mathbf{y}_1\|_1} \\ \vdots \\ \frac{(\Delta_i \tilde{X})^2(\mathbf{y}_m)}{\Delta_n^{\alpha'}} e^{\|\kappa \cdot \mathbf{y}_m\|_1} \end{pmatrix} \in \mathbb{R}^m.$$

Defining $\mathbb{V}\mathrm{ar}(\tilde{Y}_i) := V_{i,n,m} := V_{i,n,m,1} + V_{i,n,m,2}$, where

$$(V_{i,n,m,1})_{j_1,j_2} := \begin{cases} \Upsilon_{\alpha'} K^2 \sigma_0^4 \big(1 + \Delta_n^{1/2} \vee \Delta_n^{1-\alpha'}\big) & \text{, if } 1 \leqslant j_1 = j_2 \leqslant m \\ 0 & \text{, if } 1 \leqslant j_1, j_2 \leqslant m, \text{ for } j_1 \neq j_2 \end{cases},$$

$$(V_{i,n,m,2})_{j_1,j_2} := \begin{cases} 0 & \text{, if } 1 \leqslant j_1 = j_2 \leqslant m \\ \mathcal{O}\big(\Delta_n^{1-\alpha'}(\|\mathbf{y}_{j_1} - \mathbf{y}_{j_2})\|_0^{-(d+1)} + \delta^{-(d+1)}\big) & \text{, if } 1 \leqslant j_1, j_2 \leqslant m, \text{ for } j_1 \neq j_2 \end{cases},$$

yields

$$\mathbb{V}\mathrm{ar}(\gamma^\top \Xi_{n,i}) = \mathcal{O}(\|\gamma\|_\infty \Delta_n + \|\gamma\|_\infty \Delta_n \Delta_n^{1-\alpha'} m^{d+2}) = \mathcal{O}(\|\gamma\|_\infty \Delta_n).$$

Consequently, we obtain $\sum_{i=a}^{b} \mathbb{V}\mathrm{ar}(\gamma^\top \Xi_{n,i}) = \mathcal{O}\big(\|\gamma\|_\infty \Delta_n (b-a+1)\big)$, which concludes the proof. □

The subsequent lemma establishes the proof for the third condition of Corollary 3.1.2. The proof of this lemma employs the approach of relating the triangular array from equation (109) to the triangular array presented in equation (141), since we have already proved a CLT for the triangular array from equation (109).

Lemma 6.1.5
On the Assumptions 4.1.1, 4.1.2 and 6.1.2, it holds that

$$\sum_{i=1}^{n} \mathbb{E}[(\gamma^\top \Xi_{n,i})^4] = \mathcal{O}\big(\|\gamma\|_\infty^4 \Delta_n m^2\big),$$

where $\Xi_{n,i}$ defined in equation (141) and $\gamma \in \mathbb{R}^{d+1}$ is arbitrary but fixed.

Proof. We initiate the proof by examining

$$\mathbb{E}[(\gamma^\top \Xi_{n,i})^4] = \mathcal{O}\Big(\mathbb{E}\big[(\gamma^\top \xi_{n,i})^4\big]\Big).$$

Thus, we proceed by analysing the term $\mathbb{E}[(\gamma^\top \xi_{n,i})^4]$. Utilizing the Cauchy-Schwarz inequality, we obtain

$$\begin{aligned}
\mathbb{E}[(\gamma^\top \xi_{n,i})^4] &= \mathbb{E}\Big[\sum_{l_1,\ldots,l_4=1}^{d+1} \gamma_{l_1}(\xi_{n,i})_{l_1}\cdots\gamma_{l_4}(\xi_{n,i})_{l_4}\Big] \\
&= \sum_{l_1,\ldots,l_4=1}^{d+1} \gamma_{l_1}\cdots\gamma_{l_4}\mathbb{E}\big[(\xi_{n,i})_{l_1}\cdots(\xi_{n,i})_{l_4}\big] \\
&\leqslant \sum_{l_1,\ldots,l_4=1}^{d+1} \gamma_{l_1}\cdots\gamma_{l_4}\mathbb{E}\big[(\xi_{n,i})_{l_1}^4\big]^{1/4}\cdots\mathbb{E}\big[(\xi_{n,i})_{l_4}^4\big]^{1/4} \\
&\leqslant \|\gamma\|_\infty^4 (d+1)^4 \max_{l=1,\ldots,d+1} \mathbb{E}\big[(\xi_{n,i})_l^4\big].
\end{aligned}$$

We exploit the fact that $X \leqslant \mathbf{1}_{m,d+1}$, where $\mathbf{1}_{a,b} \in \mathbb{R}^{a\times b}$ represents the matrix of ones, which leads to

$$\begin{aligned}
\xi_{n,i} &= \frac{(1-2\delta)}{\sqrt{nm}\Delta_n^{\alpha'} K\sigma_0^2}\left(\frac{1-2\delta}{m}X^\top X\right)^{-1} X^\top \begin{pmatrix} (\Delta_i\tilde{X})^2(\mathbf{y}_1)e^{\|\kappa\bullet\mathbf{y}_1\|_1} \\ \vdots \\ (\Delta_i\tilde{X})^2(\mathbf{y}_m)e^{\|\kappa\bullet\mathbf{y}_m\|_1}\end{pmatrix} \\
&\leqslant \frac{(1-2\delta)e^{\|\kappa\|_1}}{\sqrt{nm}\Delta_n^{\alpha'} K\sigma_0^2}\left(\frac{1-2\delta}{m}X^\top X\right)^{-1} \mathbf{1}_{(d+1),m} \begin{pmatrix} (\Delta_i\tilde{X})^2(\mathbf{y}_1) \\ \vdots \\ (\Delta_i\tilde{X})^2(\mathbf{y}_m)\end{pmatrix} \\
&= \frac{(1-2\delta)e^{\|\kappa\|_1}}{\sqrt{nm}\Delta_n^{\alpha'} K\sigma_0^2}\left(\frac{1-2\delta}{m}X^\top X\right)^{-1} \begin{pmatrix} \sum_{j=1}^m (\Delta_i\tilde{X})^2(\mathbf{y}_j) \\ \vdots \\ \sum_{j=1}^m (\Delta_i\tilde{X})^2(\mathbf{y}_j))\end{pmatrix}.
\end{aligned} \tag{142}$$

Thus, we find that

$$\begin{aligned}\mathbb{E}[(\gamma^\top\xi_{n,i})^4] &\leqslant \|\gamma\|_\infty^4\frac{(1-2\delta)^4e^{4\|\kappa\|_1}(d+1)^4}{n^2m^2\Delta_n^{4\alpha'}K^4\sigma_0^8}\max_{l=1,\dots,d+1}\mathbb{E}\Big[\Big(\sum_{j=1}^m(\Delta_i\tilde{X})^2(\mathbf{y}_j)\Big)^4\Big(\Big(\frac{1-2\delta}{m}X^\top X\Big)^{-1}\mathbf{1}_{d+1,1}\Big)_l^4\Big]\\ &= \|\gamma\|_\infty^4\frac{(1-2\delta)^4e^{4\|\kappa\|_1}(d+1)^4}{n^2m^2\Delta_n^{4\alpha'}K^4\sigma_0^8}\mathbb{E}\Big[\Big(\sum_{j=1}^m(\Delta_i\tilde{X})^2(\mathbf{y}_j)\Big)^4\Big]\max_{l=1,\dots,d+1}\Big(\Big(\frac{1-2\delta}{m}X^\top X\Big)^{-1}\mathbf{1}_{d+1,1}\Big)_l^4.\end{aligned}$$

Given that the matrix $\big((1-2\delta)m_n^{-1}(X^\top X)\big)^{-1}$ is converging to Σ^{-1}, as $n\to\infty$, we can constrain

$$\max_{l=1,\dots,d+1}\Big(\Big(\frac{1-2\delta}{m}X^\top X\Big)^{-1}\mathbf{1}_{d+1,1}\Big)_l^4\leqslant\Big((d+1)\Big\|\Big(\frac{1-2\delta}{m_n}X^\top X\Big)^{-1}\Big\|_\infty\Big)^4<\infty,$$

for all $n\in\mathbb{N}$ and especially for $n\to\infty$. As a result, employing the Cauchy-Schwarz inequality yields

$$\begin{aligned}\mathbb{E}[(\gamma^\top\xi_{n,i})^4] &\leqslant C\|\gamma\|_\infty^4\frac{(1-2\delta)^4e^{4\|\kappa\|_1}(d+1)^4}{n^2m^2\Delta_n^{4\alpha'}K^4\sigma_0^8}\mathbb{E}\Big[\Big(\sum_{j=1}^m(\Delta_i\tilde{X})^2(\mathbf{y}_j)\Big)^4\Big]\\ &= C\|\gamma\|_\infty^4\frac{(1-2\delta)^4e^{4\|\kappa\|_1}(d+1)^4}{n^2m^2\Delta_n^{4\alpha'}K^4\sigma_0^8}\sum_{j_1,\dots,j_4}\mathbb{E}\big[(\Delta_i\tilde{X})^2(\mathbf{y}_{j_1})\cdots(\Delta_i\tilde{X})^2(\mathbf{y}_{j_4})\big]\\ &\leqslant C\|\gamma\|_\infty^4\frac{m^2(1-2\delta)^4e^{4\|\kappa\|_1}(d+1)^4}{n^2\Delta_n^{4\alpha'}K^4\sigma_0^8}\max_{j=1,\dots,m}\mathbb{E}\big[(\Delta_i\tilde{X})^8(\mathbf{y}_j)\big].\end{aligned}$$

Similarly to the demonstration of Condition (III) in Proposition 5.4.1, we have $\mathbb{E}[(\Delta_i\tilde{X})^8(\mathbf{y})]=\mathcal{O}(\Delta_n^{4\alpha'})$. Thus, we obtain

$$\sum_{i=1}^n\mathbb{E}[(\gamma^\top\xi_{n,i})^4]=\mathcal{O}\big(\|\gamma\|_\infty^4\Delta_n m^2\big),$$

which completes the proof. □

We conclude this section by establishing that the temporal dependencies within the triangular array, as outlined in Condition (IV) of Corollary 3.1.2, can be bounded suitably.

Corollary 6.1.6

On the Assumptions 4.1.1, 4.1.2 and 6.1.2, it holds for $1\leqslant r<r+u\leqslant v\leqslant n$ and

$$\tilde{Q}_1^r=\sum_{i=1}^r\gamma^\top\xi_{n,i},\qquad \tilde{Q}_{r+u}^v=\sum_{i=r+u}^v\gamma^\top\xi_{n,i},$$

where $\xi_{n,i}$ is defined in equation (141), that there is a constant C, with $0<C<\infty$, such that for all $t\in\mathbb{R}$ it holds

$$\Big|\mathbb{C}\mathrm{ov}\Big(e^{\mathrm{i}t(\tilde{Q}_1^r-\mathbb{E}[\tilde{Q}_1^r])},\ e^{\mathrm{i}t(\tilde{Q}_{r+u}^v-\mathbb{E}[\tilde{Q}_{r+u}^v])}\Big)\Big|\leqslant\frac{Ct^2}{u^{3/4}}\sqrt{\mathbb{V}\mathrm{ar}(\tilde{Q}_1^r)\mathbb{V}\mathrm{ar}(\tilde{Q}_{r+u}^v)}.$$

Proof. We follow a similar approach as in display (142), resulting in

$$\begin{aligned}\gamma^\top \xi_{n,i} &\leqslant \frac{\sqrt{n}(1-2\delta)}{\sqrt{m}K\sigma_0^2}\gamma^\top \left(\frac{1-2\delta}{m}X^\top X\right)^{-1} \mathbf{1}_{(d+1),m} \begin{pmatrix} \frac{(\Delta_i \tilde{X})^2(\mathbf{y}_1)}{n\Delta_n^{\alpha'}} e^{\|\kappa \bullet \mathbf{y}_1\|_1} \\ \vdots \\ \frac{(\Delta_i \tilde{X})^2(\mathbf{y}_m)}{n\Delta_n^{\alpha'}} e^{\|\kappa \bullet \mathbf{y}_m\|_1} \end{pmatrix} \\ &= \frac{1-2\delta}{\sqrt{nm}\Delta_n^{\alpha'}K\sigma_0^2}\sum_{j=1}^m (\Delta_i\tilde{X})^2(\mathbf{y}_j)e^{\|\kappa \bullet \mathbf{y}_j\|_1}\gamma^\top \left(\frac{1-2\delta}{m}X^\top X\right)^{-1} \mathbf{1}_{(d+1),1} \\ &\leqslant C\|\gamma\|_\infty \frac{1}{\sqrt{nm}\Delta_n^{\alpha'}K\sigma_0^2}\sum_{j=1}^m (\Delta_i\tilde{X})^2(\mathbf{y}_j)e^{\|\kappa \bullet \mathbf{y}_j\|_1} \\ &= C\|\gamma\|_\infty \sigma^2 \frac{\eta^{d/2}}{\sqrt{nm}\Delta_n^{\alpha'}K}\sum_{j=1}^m (\Delta_i\tilde{X})^2(\mathbf{y}_j)e^{\|\kappa \bullet \mathbf{y}_j\|_1}.\end{aligned}$$

With reference to Corollary 5.3.2, it is evident that the statement holds for

$$\frac{\eta^{d/2}}{\sqrt{nm}\Delta_n^{\alpha'}K}\sum_{j=1}^m (\Delta_i\tilde{X})^2(\mathbf{y}_j)e^{\|\kappa \bullet \mathbf{y}_j\|_1},$$

since we can establish a connection between the triangular array $\xi_{n,i}$ from equation (141) and $\tilde{\xi}_{n,i}$ from equation (109). Thus, the conclusion follows. □

6.1.3. Central limit theorems and simulation results

In this section, our objective is to present a central limit theorem for both estimators, $\hat{\Psi}$ and $\hat{\upsilon}$. Similar to the one-dimensional case, the asymptotic variance within the central limit theorem for the estimator $\hat{\Psi}$ will solely rely on the known pure damping parameter α'. By applying the multivariate delta method, we will also present a central limit theorem for the estimator $\hat{\upsilon}$, which serves to estimate the natural parameters of the SPDE model from equation (49). To conclude this section, we will present simulation results for the estimator $\hat{\upsilon}$.

Thanks to the developments in Section 6.1.2, we are now equipped to establish the initial central limit theorem for the estimator $\hat{\Psi}$ as outlined in equation (135).

Proposition 6.1.7
On Assumptions 4.1.1, 4.1.2 and 6.1.2, we have

$$\sqrt{nm_n}(\hat{\Psi}_{n,m_n}-\Psi) \xrightarrow{d} \mathcal{N}\big(\mathbf{0}, \Upsilon_{\alpha'}(1-2\delta)\Sigma^{-1}\big),$$

as $n\to\infty$, $\delta \in (0,1/2)$, $\mathbf{0}=(0,\dots,0)^\top \in \mathbb{R}^{d+1}$, $\Upsilon_{\alpha'}$ defined in equation (121) and Σ defined in equation (138).

Proof. To prove this proposition, we leverage Corollary 3.1.2. The asymptotic variance is provided by Lemma 6.1.3. Condition (I) is verified by Lemma 6.1.4. In order to establish Condition (II), it suffices to consider the $\mathbb{V}\mathrm{ar}(\Xi_{n,i})$, as Ξ is centred. Revisiting Lemma 6.1.4 confirms Condition (II). The Conditions (III) and (IV) are validated by Lemma 6.1.5 and Corollary 6.1.6, respectively, which concludes the proof. □

The previous central limit theorem demonstrates the capability to extend the outcomes from Chapter 3 directly into the multi-dimensional context. Additionally, we observe the variance-stabilizing nature of utilizing log-realized volatilities, wherein the asymptotic variances are constant and only relying on δ, α', and the provided spatial observation scheme, as indicated by Σ^{-1}. As we assume the damping parameter to be known, we can leverage Proposition 6.1.7 to derive asymptotic confidence intervals, with a confidence level of $1-\alpha$, for the components of the multi-dimensional parameter υ from equation (136). For the parameter $\upsilon_1 = \sigma_0^2$, we have

$$I_{n,m} := \left[\exp\left[\hat{\Psi}_{n,m} - q_{1-\alpha/2}\gamma_1/\sqrt{nm}\right]K^{-1},\ \exp\left[\hat{\Psi}_{n,m} + q_{1-\alpha/2}\gamma_1/\sqrt{nm}\right]K^{-1}\right],$$

where q_α represents the α-quantile of the standard normal distribution, K is defined in equation (132), and

$$\gamma_1 := \big(\Upsilon_{\alpha'}(1-2\delta)\Sigma_{1,1}^{-1}\big)^{1/2}.$$

For the parameter $\upsilon_{l+1} = \kappa_l$, where $l = 1, \ldots, d$, we obtain the following asymptotic confidence intervals:

$$I_{n,m} := \left[-\hat{\Psi}_{n,m} - q_{1-\alpha/2}\gamma_{l+1}/\sqrt{nm},\ -\hat{\Psi}_{n,m} + q_{1-\alpha/2}\gamma_{l+1}/\sqrt{nm}\right],$$

where

$$\gamma_{l+1} := \big(\Upsilon_{\alpha'}(1-2\delta)\Sigma_{l+1,l+1}^{-1}\big)^{1/2}.$$

The following corollary introduces a central limit theorem for estimating the natural parameters of the multi-dimensional SPDE model, given in equation (49).

Corollary 6.1.8
On Assumptions 4.1.1, 4.1.2 and 6.1.2, we have

$$\sqrt{nm_n}(\hat{\upsilon}_{n,m_n} - \upsilon) \xrightarrow{d} \mathcal{N}\big(\mathbf{0}, \Upsilon_{\alpha'}(1-2\delta)J_{\sigma_0^2}\Sigma^{-1}J_{\sigma_0^2}\big),$$

as $n \to \infty$, $\delta \in (0, 1/2)$, $\mathbf{0} = (0, \ldots, 0)^\top \in \mathbb{R}^{d+1}$, $\Upsilon_{\alpha'}$ defined in equation (121), Σ^{-1} defined in equation (138) and $J_{\sigma_0^2}$ defined in equation (143).

Proof. Utilizing the multivariate delta method on the central limit theorem presented in Proposition 6.1.7 and employing the function $h^{-1}(\mathbf{x}) = (e^{x_1}/K, -x_2, \ldots, -x_{d+1})$, as defined in equation (137), yields

$$\sqrt{nm_n}(\hat{\upsilon} - \upsilon) = \sqrt{nm_n}\big(h^{-1}(\hat{\Psi}) - h^{-1}(\Psi)\big) \xrightarrow{d} \mathcal{N}\big(\mathbf{0}, \Upsilon_{\alpha'}(1-2\delta)J_{h^{-1}}(\Psi)\Sigma^{-1}J_{h^{-1}}(\Psi)^\top\big),$$

where $J_{h^{-1}}$ denotes the Jacobian matrix of h^{-1}, given by

$$J_{h^{-1}}(\mathbf{x}) = \begin{pmatrix} e^{x_1}/K & 0 & 0 & \dots & 0 \\ 0 & -1 & 0 & \dots & 0 \\ 0 & 0 & -1 & \dots & 0 \\ \vdots & \vdots & \vdots & \ddots & \vdots \\ 0 & 0 & 0 & \dots & -1 \end{pmatrix}.$$

We complete the proof by defining the following matrix:

$$J_{\sigma_0^2} := J_{h^{-1}}(\Psi) = \begin{pmatrix} \sigma_0^2 & 0 & 0 & \dots & 0 \\ 0 & -1 & 0 & \dots & 0 \\ 0 & 0 & -1 & \dots & 0 \\ \vdots & \vdots & \vdots & \ddots & \vdots \\ 0 & 0 & 0 & \dots & -1 \end{pmatrix}. \tag{143}$$

□

We illustrate the preceding corollary by presenting simulation results for the estimator $\hat{\upsilon}_{n,m}$ from equation (136), derived from the Monte Carlo study as discussed in Section 5.4. This study involved simulating three scenarios of a two-dimensional SPDE model based on equation (49), with 1000 Monte Carlo iterations each. In all three cases, simulations were conducted on an equidistant grid in both time and space, with $N = 10^4$ and $M = 10$, using the parameters $\vartheta_0 = 0$, $\nu = (6, 0)$, $\eta = 1$, and $\sigma = 1$. The simulations employed the replacement method outlined in Section 4.3, with $L = 10$. For the first case we used a pure damping rate of $\alpha' = 4/10$, the second case used $\alpha' = 1/2$, and the third case used $\alpha' = 6/10$.

Figure 6.1 depicts a comparison between the empirical distribution of each case and the asymptotic normal distribution as described in Corollary 6.1.8. The top row shows the simulation results for $\alpha' = 4/10$, the middle row displays the results for $\alpha' = 1/2$, and the bottom row presents the results for $\alpha' = 6/10$. Each row consists of three plots, which assess the goodness of fit between the kernel density estimation and the centred normal distribution, as outlined in Corollary 6.1.8. In these plots, grey represents the results for estimating the normalized volatility parameter σ_0^2, while the other panels in each row (yellow and brown) represent the results for the curvature parameters κ_1 and κ_2, respectively. To estimate the kernel density, we employed a Gaussian kernel with Silverman's 'rule of thumb'. As discussed in Section 5.4, we observe a negative bias in the simulated data due to the cut-off solution applied in the replacement method. To address this bias, we centred the data by utilizing the sample mean of the respective estimations. This adjustment enables a visual comparison between the empirical and theoretical distributions.

In this simulation study, where $N = 10^4$, we must adhere to the following restriction, as outlined in Assumption 4.1.1:

$$M < N^{(1-\alpha')/(d+2)} = \begin{cases} 3.98 & \text{, if } \alpha' = 4/10 \\ 3.16 & \text{, if } \alpha' = 1/2 \\ 2.51 & \text{, if } \alpha' = 6/10 \end{cases}.$$

As Assumption 6.1.2 necessitates a minimum of three observations for the application of the estimator

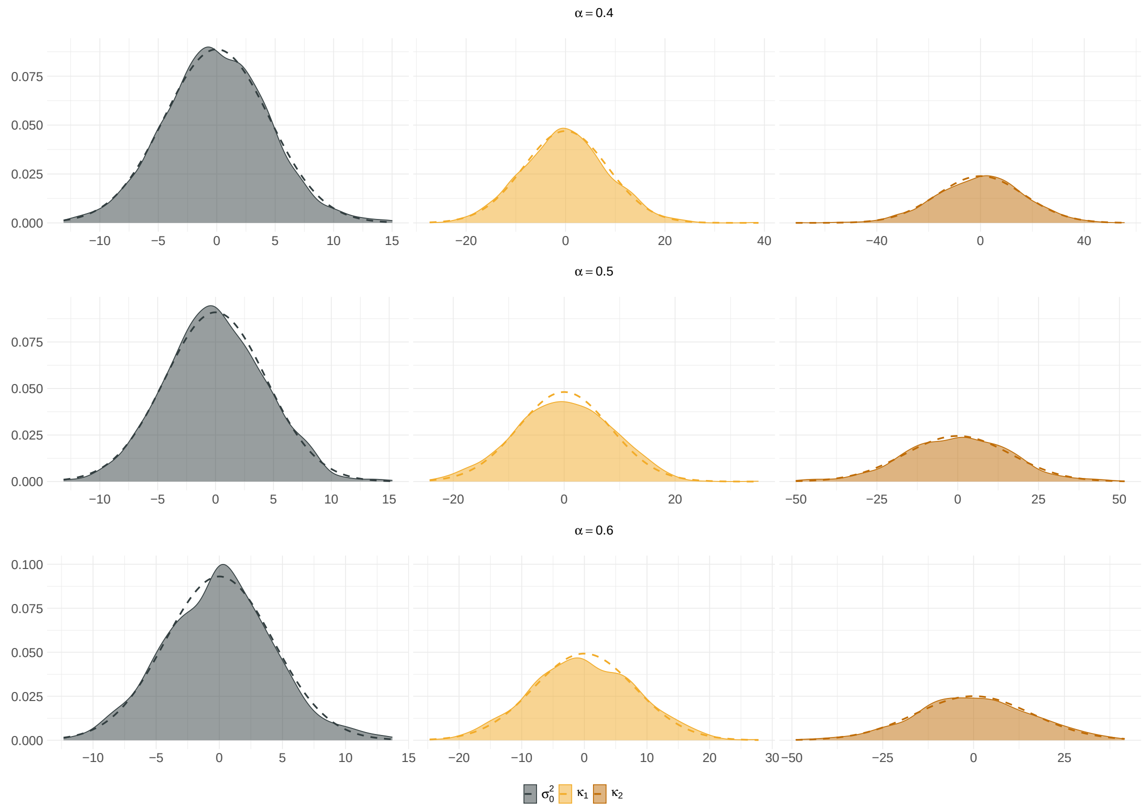

Figure 6.1.: The figure provides a comparison of empirical distributions for centred estimation errors of the parameter vector $\upsilon = (\sigma_0^2, \kappa_1, \kappa_2)$, which are obtained through simulations on an equidistant grid in both, time and space, where $N = 10^4$ and $M = 10$, and their empirical counterparts. The kernel-density estimation employed a Gaussian kernel with Silverman's 'rule of thumb' and was conducted over 1000 Monte Carlo iterations. The specific parameter values used for the simulations are as follows: $d = 2$, $\vartheta_0 = 0$, $\nu = (6, 0)$, $\eta = 1$, $\sigma = 1$, and $L = 10$. Three different scenarios were considered, each with a distinct value of the pure damping parameter α': $\alpha' = 4/10, K = 10^3$ (top row), $\alpha' = 1/2, K = 10^3$ (middle row), and $\alpha' = 6/10, K = 1300$ (bottom row). The corresponding asymptotic distributions are represented by dotted lines. The results for the normalized volatility parameter σ_0^2 are depicted in grey lines, while the estimates for κ_1 are shown in yellow lines, and those for κ_2 are represented by brown lines. For estimation of $\upsilon = (\sigma_0^2, \kappa_1, \kappa_2)$, we utilized the set of spatial points $\mathcal{S}_3$, as defined in equation (144).

$\hat{\upsilon}$, we have chosen the following observation scheme:

$$\mathcal{S}_3 := \big\{(1/10, 3/10), (4/10, 2/10), (7/10, 5/10)\big\}. \tag{144}$$

Indeed, this observation scheme satisfies the Assumption 6.1.2, as evident by the following calculation:

$$\begin{vmatrix} 1 & 1/10 & 3/10 \\ 1 & 4/10 & 2/10 \\ 1 & 7/10 & 5/10 \end{vmatrix} = 0.12 \neq 0,$$

where $|A|$ denotes the determinant of a matrix $A \in \mathbb{R}^{p \times p}$, $p \in \mathbb{N}$. For the cases $\alpha' \in \{4/10, 1/2\}$, we obtain that $|\mathcal{S}_3| < N^{(1-\alpha')/(d+2)}$, whereas the Assumption 4.1.1 is (slightly) violated for $\alpha = 6/10$, since $|\mathcal{S}_3| > N^{(1-\alpha')/(d+2)}$. Nevertheless, we present the simulation results in Figure 6.1 for all three cases of the pure damping parameter α' and observe that all three scenarios exhibit a substantial fit. The sample means of the respective estimations are summarized in the following table:

α'	mean $\hat{\sigma}_0^2$	mean $\hat{\kappa}_1$	mean $\hat{\kappa}_2$
4/10	0.985	5.986	0.011
5/10	0.972	5.979	0.028
6/10	0.987	5.941	0.038

Table 6.3.: The table presents the sample means of the estimations for the natural parameters σ_0^2 and $\kappa = (\kappa_1, \kappa_2)$ in a two-dimensional SPDE model. The estimations are derived from a dataset with parameters set at $\vartheta_0 = 0$, $\nu = (6, 0)$, $\eta = 1$, and $\sigma = 1$, based on 1000 Monte Carlo iterations. Each row in the table corresponds to the outcomes for three selections of the pure damping parameter, where $\alpha' \in \{4/10, 1/2, 6/10\}$.

Additionally, we provide corresponding QQ-plots in Figure B.3, which can be found in Appendix B.

6.2. Asymptotic for the damping parameter

When transferring SPDE models from one to multiple dimensions, the appearance of a damping parameter is inevitable. In this section, we discuss how to consistently estimate the pure damping parameter $\alpha' = \alpha + 1 - d/2 \in (0, 1)$ in the SPDE model from equation (49) and we will prove a central limit theorem for such an estimator $\hat{\alpha}'$.

6.2.1. Motivation and methodology

We start this section by recalling Proposition 4.2.7. This proposition analysed the autocovariance structure of temporal increments and stated

$$\mathbb{C}\text{ov}(\Delta_i X(\mathbf{y}), \Delta_j X(\mathbf{y})) = -\sigma^2 e^{-\|\kappa \boldsymbol{\cdot} \mathbf{y}\|_1} \Delta_n^{\alpha'} \frac{\Gamma(1-\alpha')}{2^{d+1}(\pi\eta)^{d/2}\alpha'\Gamma(d/2)} f(i, j, \alpha') + r_{i,j} + \mathcal{O}(\Delta_n),$$

where $r_{i,j}$ is a remainder defined in Proposition 4.2.7 and f a function, representing covariance behaviour for the temporal lags. As mentioned before, it is not clear how to extract information on α' through a transformation of the temporal increments, since the damping parameter nearly affects all constants. Therefore, we follow an approach, often used for estimating the Hurst parameter $H < 3/4$ in fractional Brownian motions, which focuses on the roughness property. In this context we also refer to the work of Chong (2020a), who also investigated potential estimators for estimating the parameter α' in one space dimension, which the paper refers to as "spatial correlation parameter". Here, we obtain that α' also appears in the term $\Delta_n^{\alpha'}$, which suggests the idea of comparing two different temporal resolution. As the estimators from the previous chapters are dependent on information on α', we do not assume any knowledge on the other parameters in the SPDE model from equation (49), i.e., on the differential operator A_ϑ.

We start the motivation part by considering equation (130) from Section 6.1. Here, we have

$$\frac{\mathrm{RV}_n(\mathbf{y})}{n} \approx \Delta_n^{\alpha'} e^{-\|\kappa \boldsymbol{\cdot} \mathbf{y}\|_1} \frac{\Gamma(1-\alpha')\sigma_0^2}{\alpha'} \cdot \frac{1}{\pi^{d/2}\Gamma(d/2)2^d}\left(1 + \sqrt{\frac{\Upsilon_{\alpha'}}{n}} Z\right),$$

and obtain by the transition to a log-linear model that

$$\log\left(\frac{\mathrm{RV}_n(\mathbf{y})}{n}\right) \approx \alpha' \log(\Delta_n) - ||\kappa \bullet \mathbf{y}||_1 + \log\left(\sigma_0^2 K_{\alpha'}\right) + \sqrt{\frac{\Upsilon_{\alpha'}}{n}} Z,$$

where we used analogous steps as in equation (131) and $K_{\alpha'} := K$ defined in equation (132). We consider a mild solution $X_t(\mathbf{y})$ of the SPDE model from equation (49). Assume we obtain X on a grid with $2n$ temporal and m spatial points according to Assumption 4.1.1. As we follow the approach of constructing an estimator for α' using realized volatilities on two distinct temporal resolutions, we need to specify how we understand this new grid with a lower temporal resolution. First, we want the new grid to be equidistant in time with $\tilde{n} = \mathcal{O}(2n)$, $\tilde{n} < 2n$ temporal points, such that it satisfies the observation scheme as outlined in Assumption 4.1.1. Furthermore, Proposition 5.2.1 suggests to filter the original grid such that the new grid contains the maximum amount of temporal points. Intuitively, having the most possible temporal points, while respecting an equidistant order of these, should shrink the variance of the estimator. Hence, we set $\tilde{n} = n$. As we need to distinguish between both temporal resolutions we introduce the following notations. The temporal increments for both grids are denoted by

$$(\Delta_{2n,i_1} X)(\mathbf{y}) := X_{i_1 \Delta_{2n}} - X_{(i_1-1)\Delta_{2n}} \qquad \text{and} \qquad (\Delta_{n,i_2} X)(\mathbf{y}) := X_{i_2 \Delta_n} - X_{(i_2-1)\Delta_n},$$

where $1 \leqslant i_1 \leqslant 2n$ and $1 \leqslant i_2 \leqslant n$. The increments of the filtered temporal grid can be rewritten by

$$\begin{aligned}(\Delta_{n,i} X)(\mathbf{y}) = X_{2i\Delta_{2n}} - X_{2(i-1)\Delta_{2n}} &= \Big(X_{2i\Delta_{2n}} - X_{(2i-1)\Delta_{2n}}\Big) + \Big(X_{(2i-1)\Delta_{2n}} - X_{2(i-1)\Delta_{2n}}\Big) \\ &= (\Delta_{2n,2i} X)(\mathbf{y}) + (\Delta_{2n,2i-1} X)(\mathbf{y}),\end{aligned}$$

where $i = 1, \ldots, n$. Furthermore, by using an index transformation, we can write

$$(\Delta_{n,i} X)(\mathbf{y}) = \mathbb{1}_{2\mathbb{N}}(i)\big((\Delta_{2n,i} X)(\mathbf{y}) + (\Delta_{2n,i-1} X)(\mathbf{y})\big), \tag{145}$$

for $i = 1, \ldots, 2n$, where $2\mathbb{N}$ denotes the set of all even and non-negative integers, i.e.: $2\mathbb{N} = \{0, 2, 4, \ldots\}$. Note that we incorporate zero into the set $2\mathbb{N}$. Moreover, the realized volatilities are redefined as

$$\mathrm{RV}_{2n}(\mathbf{y}) := \sum_{i=1}^{2n} (\Delta_{2n,i} X)^2(\mathbf{y}) \qquad \text{and} \qquad \mathrm{RV}_n(\mathbf{y}) := \sum_{i=1}^{n} (\Delta_{n,i} X)^2(\mathbf{y}).$$

By using equation (145), we can link the filtered realized volatilities with the original grid and obtain

$$\begin{aligned}\mathrm{RV}_n(\mathbf{y}) &= \sum_{i=2}^{2n} \mathbb{1}_{2\mathbb{N}}(i)\big((\Delta_{2n,i} X)(\mathbf{y}) + (\Delta_{2n,i-1} X)(\mathbf{y})\big)^2 \\ &= \sum_{i=2}^{2n} \mathbb{1}_{2\mathbb{N}}(i)(\Delta_{2n,i} X)^2(\mathbf{y}) + \sum_{i=2}^{2n} \mathbb{1}_{2\mathbb{N}}(i)(\Delta_{2n,i-1} X)^2(\mathbf{y}) + 2\sum_{i=2}^{2n} \mathbb{1}_{2\mathbb{N}}(i)(\Delta_{2n,i} X)(\mathbf{y})(\Delta_{2n,i-1} X)(\mathbf{y}) \\ &= \sum_{i=2}^{2n} \mathbb{1}_{2\mathbb{N}}(i)(\Delta_{2n,i} X)^2(\mathbf{y}) + \sum_{i=1}^{2n-1} \mathbb{1}_{(2\mathbb{N})^{\complement}}(i)(\Delta_{2n,i} X)^2(\mathbf{y}) + 2\sum_{i=2}^{2n} \mathbb{1}_{2\mathbb{N}}(i)(\Delta_{2n,i} X)(\mathbf{y})(\Delta_{2n,i-1} X)(\mathbf{y}) \\ &= \mathrm{RV}_{2n}(\mathbf{y}) + 2\sum_{i=2}^{2n} \mathbb{1}_{2\mathbb{N}}(i)(\Delta_{2n,i} X)(\mathbf{y})(\Delta_{2n,i-1} X)(\mathbf{y}).\end{aligned} \tag{146}$$

Note that the approximation as used in the Chapters 4 and 5 for the log-realized volatilities, i.e.:

$$\log\left(\frac{\mathrm{RV}_n(\mathbf{y})}{n}\right) \approx \alpha' \log(\Delta_n) - ||\kappa \bullet \mathbf{y}||_1 + \log\left(\sigma_0^2 K_{\alpha'}\right) + \sqrt{\frac{\Upsilon_{\alpha'}}{n}} Z,$$

where $Z \sim \mathcal{N}(0,1)$, still holds, since the grid with a low temporal resolution still satisfies Assumption 4.1.1. Therefore, we follow up with considering the following statistic:

$$\begin{aligned}\log\left(\frac{\mathrm{RV}_n(\mathbf{y})}{n}\right) - \log\left(\frac{\mathrm{RV}_{2n}(\mathbf{y})}{2n}\right) &\approx \alpha'\big(\log(\Delta_n) - \log(\Delta_{2n})\big) + \sqrt{\frac{\Upsilon_{\alpha'}}{n}} Z_1 - \sqrt{\frac{\Upsilon_{\alpha'}}{2n}} Z_2 \\ &= \alpha' \log(2) + \sqrt{\frac{\Upsilon_{\alpha'}}{n}} Z_1 - \sqrt{\frac{\Upsilon_{\alpha'}}{2n}} Z_2, \end{aligned} \tag{147}$$

where $Z_1, Z_2 \sim \mathcal{N}(0,1)$ and $\mathbf{y} \in [\delta, 1-\delta]^d$. Hence, by equation (147) we obtain a simple linear model $X_j = \alpha y_j + \beta + \varepsilon_j$, with centred errors and a known slope of zero. Hence, the intercept estimator estimates the parameter $\alpha' \log(2)$, which yields the following estimator:

$$\hat{\alpha}' := \hat{\alpha}'_{2n,m} := \frac{1}{\log(2)m} \sum_{j=1}^{m} \log\left(\frac{2\mathrm{RV}_n(\mathbf{y}_j)}{\mathrm{RV}_{2n}(\mathbf{y}_j)}\right). \tag{148}$$

For recalling details on the ordinary simple linear model, cf. Example 3.1.1.

We start the methodology part by linking to equation (140), where we rescale the realized volatility by the term Δ_n. Thus, we obtain the following decompositions:

$$\log\left(\frac{\mathrm{RV}_n(\mathbf{y})}{n}\right) = \log(\sigma_0^2 K) - \|\kappa \bullet \mathbf{y}\|_1 + \alpha' \log(\Delta_n) + \frac{\sum_{i=1}^{n} \overline{(\Delta_{n,i}\tilde{X})^2(\mathbf{y})}}{n\Delta_n^{\alpha'} \sigma_0^2 K} e^{\|\kappa \bullet \mathbf{y}\|_1} + \mathcal{O}(\Delta_n) + \mathcal{O}_{\mathbb{P}}(\Delta_n), \tag{149}$$

as well as

$$\log\left(\frac{\mathrm{RV}_{2n}(\mathbf{y})}{2n}\right) = \log(\sigma_0^2 K) - \|\kappa \bullet \mathbf{y}\|_1 + \alpha' \log(\Delta_{2n}) + \frac{\sum_{i=1}^{2n} \overline{(\Delta_{2n,i}\tilde{X})^2(\mathbf{y})}}{2n\Delta_{2n}^{\alpha'} \sigma_0^2 K} e^{\|\kappa \bullet \mathbf{y}\|_1} + \mathcal{O}(\Delta_{2n}) + \mathcal{O}_{\mathbb{P}}(\Delta_{2n}). \tag{150}$$

For the latter decomposition we used the Propositions 4.2.6 and 5.2.1, since both grids satisfy the Assumption 4.1.1. By utilizing the equations (149) and (150) we can decompose the estimator as follows:

$$\begin{aligned}\hat{\alpha}'_{2n,m} &= \frac{1}{\log(2)m} \sum_{j=1}^{m} \left(\log\left(\frac{\mathrm{RV}_n(\mathbf{y}_j)}{n}\right) - \log\left(\frac{\mathrm{RV}_{2n}(\mathbf{y}_j)}{2n}\right)\right) \\ &= \frac{1}{\log(2)m} \sum_{j=1}^{m} \left(\alpha'\big(\log(\Delta_n) - \log(\Delta_{2n})\big) + \frac{e^{\|\kappa \bullet \mathbf{y}_j\|_1}}{\sigma_0^2 K} \left(\sum_{i=1}^{n} \frac{\overline{(\Delta_{n,i}\tilde{X})^2(\mathbf{y}_j)}}{n\Delta_n^{\alpha'}} - \sum_{i=1}^{2n} \frac{\overline{(\Delta_{2n,i}\tilde{X})^2(\mathbf{y}_j)}}{2n\Delta_{2n}^{\alpha'}} \right)\right) \\ &\quad + \mathcal{O}(\Delta_n) + \mathcal{O}_{\mathbb{P}}(\Delta_n) \\ &= \alpha' + \frac{1}{\log(2)m\sigma_0^2 K} \sum_{j=1}^{m} \left(\overline{V_{n,\Delta_n}(\mathbf{y}_j) - V_{2n,\Delta_{2n}}(\mathbf{y}_j)}\right) + \mathcal{O}(\Delta_n) + \mathcal{O}_{\mathbb{P}}(\Delta_n), \end{aligned}$$

where

$$V_{p_1,\Delta_n}(\mathbf{y}) := \frac{1}{p_1 \Delta_n^{\alpha'}} \sum_{i=1}^{p_1} (\Delta_{n,i}\tilde{X})^2(\mathbf{y}) e^{||\kappa \bullet \mathbf{y}||_1} \qquad \text{and} \qquad V_{p_2,\Delta_{2n}}(\mathbf{y}) := \frac{1}{p_2 \Delta_{2n}^{\alpha'}} \sum_{i=1}^{p_2} (\Delta_{2n,i}\tilde{X})^2(\mathbf{y}) e^{||\kappa \bullet \mathbf{y}||_1},$$

with $1 \leqslant p_1 \leqslant n$ and $1 \leqslant p_2 \leqslant 2n$. Furthermore, utilizing equation (146) yields that

$$\begin{aligned} V_{n,\Delta_n}(\mathbf{y}) &= \frac{e^{||\kappa \bullet \mathbf{y}||_1}}{n \Delta_n^{\alpha'}} \mathrm{RV}_n(\mathbf{y}) = \frac{2n\Delta_{2n}^{\alpha'}}{n\Delta_n^{\alpha'}} V_{2n,\Delta_{2n}}(\mathbf{y}) + \frac{2e^{||\kappa \bullet \mathbf{y}||_1}}{n\Delta_n^{\alpha'}} \sum_{i=2}^{2n} \mathbb{1}_{2\mathbb{N}}(i)(\Delta_{2n,i}\tilde{X})(\mathbf{y})(\Delta_{2n,i-1}\tilde{X})(\mathbf{y}) \\ &= 2^{1-\alpha'} V_{2n,\Delta_{2n}}(\mathbf{y}) + \frac{4n\Delta_{2n}^{\alpha'}}{n\Delta_n^{\alpha'}} W_{2n,\Delta_{2n}}, \end{aligned}$$

where we define for $1 \leqslant p \leqslant 2n$:

$$W_{p,\Delta_{2n}}(\mathbf{y}) := \frac{1}{p\Delta_{2n}^{\alpha'}} \sum_{i=1}^{p} \mathbb{1}_{2\mathbb{N}}(i)(\Delta_{2n,i}\tilde{X})(\mathbf{y})(\Delta_{2n,i-1}\tilde{X})(\mathbf{y}) e^{||\kappa \bullet \mathbf{y}||_1}. \tag{151}$$

Note that we have

$$V_{p,\Delta_n}(\mathbf{y}) = 2^{1-\alpha'} V_{2p,\Delta_{2n}}(\mathbf{y}) + 2^{2-\alpha'} W_{2p,\Delta_{2n}}(\mathbf{y}), \tag{152}$$

for a $1 \leqslant p \leqslant n$. Hence, we obtain the following representation:

$$\hat{\alpha}'_{2n,m} = \alpha' + \frac{1}{\log(2) m \sigma_0^2 K} \sum_{j=1}^{m} \Big((2^{1-\alpha'} - 1)\overline{V_{2n,\Delta_{2n}}(\mathbf{y}_j)} + 2^{2-\alpha'} \overline{(W_{2n,\Delta_{2n}}(\mathbf{y}_j)} \Big) + \mathcal{O}(\Delta_n) + \mathcal{O}_{\mathbb{P}}(\Delta_n).$$

The corresponding triangular array is then given by $\Xi_{2n,i} := \xi_{2n,i} - \mathbb{E}[\xi_{2n,i}]$, where

$$\begin{aligned} \xi_{2n,i} &:= \sum_{j=1}^{m} \frac{e^{\|\kappa \bullet \mathbf{y}_j\|_1}}{\log(2)\sqrt{2nm}\Delta_{2n}^{\alpha'}\sigma_0^2 K} \Big((2^{1-\alpha'} - 1)(\Delta_{2n,i}\tilde{X})^2(\mathbf{y}_j) + 2^{2-\alpha'} \mathbb{1}_{2\mathbb{N}}(i)(\Delta_{2n,i}\tilde{X})(\mathbf{y}_j)(\Delta_{2n,i-1}\tilde{X})(\mathbf{y}_j) \Big) \qquad (153) \\ &= \xi_{2n,i}^1 + \xi_{2n,i}^2, \end{aligned}$$

with

$$\begin{aligned} \xi_{2n,i}^1 &:= \frac{2^{1-\alpha'} - 1}{\log(2)\sqrt{2nm}\Delta_{2n}^{\alpha'}\sigma_0^2 K} \sum_{j=1}^{m} (\Delta_{2n,i}\tilde{X})^2(\mathbf{y}_j) e^{\|\kappa \bullet \mathbf{y}_j\|_1}, \\ \xi_{2n,i}^2 &:= \mathbb{1}_{2\mathbb{N}}(i) \frac{2^{2-\alpha'}}{\log(2)\sqrt{2nm}\Delta_{2n}^{\alpha'}\sigma_0^2 K} \sum_{j=1}^{m} (\Delta_{2n,i}\tilde{X})(\mathbf{y}_j)(\Delta_{2n,i-1}\tilde{X})(\mathbf{y}_j) e^{\|\kappa \bullet \mathbf{y}_j\|_1}. \end{aligned}$$

For the asymptotic variance of the estimator $\hat{\alpha}'$, it remains to analyse the covariance of $V_{2n,\Delta_{2n}}$ and $W_{2n,\Delta_{2n}}$.

6.2.2. Covariance structure and dependencies of temporal increments on distinct temporal grids

The aim of this section is to present necessary results to establish a central limit theorem for the estimator $\hat{\alpha}'$ defined in equation (148). As discussed in the previous section, our focus now shifts to analysing the term $W_{2n,\Delta_{2n}}$ as defined in equation (151). Specifically, we will commence by investigating the covariance relationship between the rescaled realized volatilities $V_{2n,\Delta_{2n}}$ of the original grid and the mixed term $W_{2n,\Delta_{2n}}$. This mixed term arises when utilizing realized volatilities on two temporal grids with differing resolutions. Subsequently, we will demonstrate that the mixing-type condition, as outlined in Proposition 1.2.4, is applicable to the structure of our damping estimator.

Proposition 6.2.1
On Assumptions 4.1.1 and 4.1.2, we have for the covariance structure of the two temporal resolutions Δ_n and Δ_{2n} that

$$\mathbb{C}\mathrm{ov}\big(V_{p,\Delta_{2n}}(\mathbf{y}_1), W_{p,\Delta_{2n}}(\mathbf{y}_2)\big) = \mathbb{1}_{\{\mathbf{y}_1=\mathbf{y}_2\}}\frac{\Lambda_{\alpha'}}{2p}\left(\frac{\Gamma(1-\alpha')\sigma^2}{2^d(\pi\eta)^{d/2}\alpha'\Gamma(d/2)}\right)^2\left(1+\mathcal{O}\left(\Delta_{2n}^{1/2}\vee\frac{\Delta_{2n}^{1-\alpha'}}{\delta^{d+1}}\vee\frac{\Delta_{2n}^{-\alpha'}}{p}\right)\right)$$
$$+\mathcal{O}\left(\frac{\Delta_{2n}^{1-\alpha'}}{p}\left(\mathbb{1}_{\{\mathbf{y}_1\neq\mathbf{y}_2\}}\|\mathbf{y}_1-\mathbf{y}_2\|_0^{-(d+1)}+\delta^{-(d+1)}\right)\vee\frac{\Delta_{2n}^{-\alpha'}}{p^2}\right),$$

where $\mathbf{y}_1,\mathbf{y}_2\in[\delta,1-\delta]^d$, $\Lambda_{\alpha'}$ is a numerical constant depending on $\alpha'\in(0,1)$, defined in equation (166) and $2\leqslant p\leqslant 2n$.

Proof. Analogously to Proposition 5.2.1, we first obtain that

$$\mathbb{C}\mathrm{ov}\big(V_{p,\Delta_{2n}}(\mathbf{y}_1), W_{p,\Delta_{2n}}(\mathbf{y}_2)\big) = \frac{2e^{\|\kappa\cdot(\mathbf{y}_1+\mathbf{y}_2)\|_1}}{p\Delta_{2n}^{2\alpha'}}\sum_{\mathbf{k}_1,\mathbf{k}_2\in\mathbb{N}^d} e_{\mathbf{k}_1}(\mathbf{y}_1)e_{\mathbf{k}_1}(\mathbf{y}_2)e_{\mathbf{k}_2}(\mathbf{y}_1)e_{\mathbf{k}_2}(\mathbf{y}_2)D_{\mathbf{k}_1,\mathbf{k}_2},$$

where we redefine

$$D_{\mathbf{k}_1,\mathbf{k}_2} := \frac{1}{p}\sum_{i,j=1}^{p}\mathbb{1}_{2\mathbb{N}}(j)\mathbb{C}\mathrm{ov}\Big(\big(\tilde{B}_{i,\mathbf{k}_1}+C_{i,\mathbf{k}_1}\big)\big(\tilde{B}_{i,\mathbf{k}_2}+C_{i,\mathbf{k}_2}\big),\ \big(\tilde{B}_{j,\mathbf{k}_1}+C_{j,\mathbf{k}_1}\big)\big(\tilde{B}_{j-1,\mathbf{k}_2}+C_{j-1,\mathbf{k}_2}\big)\Big)$$
$$=\frac{1}{p}\sum_{i,j=1}^{p}\mathbb{1}_{2\mathbb{N}}(j)\Big(\mathbb{E}\Big[\big(\tilde{B}_{i,\mathbf{k}_1}+C_{i,\mathbf{k}_1}\big)\big(\tilde{B}_{j,\mathbf{k}_1}+C_{j,\mathbf{k}_1}\big)\Big]\mathbb{E}\Big[\big(\tilde{B}_{i,\mathbf{k}_2}+C_{i,\mathbf{k}_2}\big)\big(\tilde{B}_{j-1,\mathbf{k}_2}+C_{j-1,\mathbf{k}_2}\big)\Big]$$
$$+\mathbb{E}\Big[\big(\tilde{B}_{i,\mathbf{k}_1}+C_{i,\mathbf{k}_1}\big)\big(\tilde{B}_{j-1,\mathbf{k}_2}+C_{j-1,\mathbf{k}_2}\big)\Big]\mathbb{E}\Big[\big(\tilde{B}_{i,\mathbf{k}_2}+C_{i,\mathbf{k}_2}\big)\big(\tilde{B}_{j,\mathbf{k}_1}+C_{j,\mathbf{k}_1}\big)\Big]\Big).$$

Assume $\mathbf{k}_1\neq\mathbf{k}_2$, then we have

$$D_{\mathbf{k}_1,\mathbf{k}_2} = \frac{1}{p}\sum_{i,j=1}^{p}\mathbb{1}_{2\mathbb{N}}(j)\mathbb{E}\Big[\big(\tilde{B}_{i,\mathbf{k}_1}+C_{i,\mathbf{k}_1}\big)\big(\tilde{B}_{j,\mathbf{k}_1}+C_{j,\mathbf{k}_1}\big)\Big]\mathbb{E}\Big[\big(\tilde{B}_{i,\mathbf{k}_2}+C_{i,\mathbf{k}_2}\big)\big(\tilde{B}_{j-1,\mathbf{k}_2}+C_{j-1,\mathbf{k}_2}\big)\Big]$$
$$=\frac{1}{p}\sum_{i,j=1}^{p}\mathbb{1}_{2\mathbb{N}}(j)\Big(\tilde{\Sigma}_{i,j}^{B,\mathbf{k}_1}+\Sigma_{i,j}^{BC,\mathbf{k}_1}+\Sigma_{j,i}^{BC,\mathbf{k}_1}+\Sigma_{i,j}^{C,\mathbf{k}_1}\Big)\Big(\tilde{\Sigma}_{i,j-1}^{B,\mathbf{k}_2}+\Sigma_{i,j-1}^{BC,\mathbf{k}_2}+\Sigma_{j-1,i}^{BC,\mathbf{k}_2}+\Sigma_{i,j-1}^{C,\mathbf{k}_2}\Big).$$

For the covariance terms we have by Proposition 5.2.1, that

$$\frac{1}{p}\sum_{i,j=1}^{p}\mathbb{1}_{2\mathbb{N}}(j)\tilde{\Sigma}_{i,j}^{B,\mathbf{k}_1}\tilde{\Sigma}_{i,j-1}^{B,\mathbf{k}_2}=\sigma^4\frac{\big(1-e^{-\lambda_{\mathbf{k}_1}\Delta_{2n}}\big)^2\big(1-e^{-\lambda_{\mathbf{k}_2}\Delta_{2n}}\big)^2}{4\lambda_{\mathbf{k}_1}^{1+\alpha}\lambda_{\mathbf{k}_2}^{1+\alpha}}\frac{1}{p}\sum_{i,j=1}^{p}\mathbb{1}_{2\mathbb{N}}(j)e^{-\lambda_{\mathbf{k}_1}\Delta_{2n}|i-j|}e^{-\lambda_{\mathbf{k}_2}\Delta_{2n}|i-j+1|}.$$

For the geometric sum in the latter display, we obtain

$$\begin{aligned}\sum_{i,j=1}^{p}q_1^{|i-j|}q_2^{|i-j+1|}\mathbb{1}_{2\mathbb{N}}(j)&=\sum_{i,j=1}^{p}q_1^{|i-j|}q_2^{|i-j+1|}\mathbb{1}_{2\mathbb{N}}(j)\big(\mathbb{1}_{\{j\leqslant i\}}+\mathbb{1}_{\{i<j\}}\big)\\&=q_2\sum_{i=2}^{p}\sum_{j=2}^{i}(q_1q_2)^{i-j}\mathbb{1}_{2\mathbb{N}}(j)+q_2^{-1}\sum_{j=2}^{p}\sum_{i=1}^{j-1}(q_1q_2)^{j-i}\mathbb{1}_{2\mathbb{N}}(j)\\&=q_2\sum_{i=2}^{p}(q_1q_2)^{i}\sum_{j=2}^{i}(q_1q_2)^{-j}\mathbb{1}_{2\mathbb{N}}(j)+q_2^{-1}\sum_{j=2}^{p}(q_1q_2)^{j}\mathbb{1}_{2\mathbb{N}}(j)\sum_{i=1}^{j-1}(q_1q_2)^{-i},\end{aligned}$$

where $q_1,q_2\neq 0$. Furthermore, for a $q\neq 1$ it holds by analogous computations as for the partial sum of the geometric series, that

$$\sum_{i=0}^{n}q^i\mathbb{1}_{2\mathbb{N}}(i)=\begin{cases}\frac{1-q^{n+2}}{1-q^2}&,\text{ if } n \text{ is even}\\\frac{1-q^{n+1}}{1-q^2}&,\text{ if } n \text{ is odd}\end{cases},$$

where we consider zero as an even integer. Hence, we get

$$\begin{aligned}\sum_{i,j=1}^{p}q_1^{|i-j|}q_2^{|i-j+1|}\mathbb{1}_{2\mathbb{N}}(j)=&\frac{q_2}{(q_1q_2)^2(1-(q_1q_2)^{-2})}\Bigg(\sum_{i=2}^{p}(q_1q_2)^i\big(1-(q_1q_2)^{-i}\big)\mathbb{1}_{2\mathbb{N}}(i)\\&+\sum_{i=2}^{p}(q_1q_2)^i\big(1-(q_1q_2)^{-(i-1)}\big)\mathbb{1}_{(2\mathbb{N})^{\complement}}(i)\Bigg)\\&+\frac{q_2^{-1}}{q_1q_2(1-(q_1q_2)^{-1})}\sum_{j=2}^{p}(q_1q_2)^j\big(1-(q_1q_2)^{-(j-1)}\big)\mathbb{1}_{2\mathbb{N}}(j).\end{aligned}$$

Now, using that $|q_1|,|q_2|<1$ and that it holds for the floor function by the Fourier representation that

$$\frac{1}{p}\lfloor cp\rfloor=\begin{cases}c&,\text{ if } cp\in\mathbb{Z}\\c-\frac{1}{2p}+\frac{1}{p\pi}\sum_{k=1}^{\infty}\frac{\sin(2\pi kcp)}{k}&,\text{ if } cp\notin\mathbb{Z},\end{cases},$$

for $c\neq 0$ and $p\in\mathbb{N}$, we observe the following:

$$\begin{aligned}\sum_{i,j=1}^{p}q_1^{|i-j|}q_2^{|i-j+1|}\mathbb{1}_{2\mathbb{N}}(j)&=\left(\frac{q_2}{1-(q_1q_2)^2}\Big(\frac{p}{2}+\frac{p}{2}q_1q_2\Big)+\frac{q_2^{-1}}{1-q_1q_2}\cdot\frac{p}{2}q_1q_2\right)\left(1+\mathcal{O}\Big(\frac{p^{-1}}{1-q_1q_2}\Big)\right)\\&=\frac{q_1+q_2}{2(1-q_1q_2)}\left(1+\mathcal{O}\Big(\frac{p^{-1}}{1-q_1q_2}\Big)\right).\end{aligned}\tag{154}$$

Therefore, we have

$$\frac{1}{p}\sum_{i,j=1}^{p}\mathbb{1}_{2\mathbb{N}}(j)\tilde{\Sigma}_{i,j}^{B,\mathbf{k}_1}\tilde{\Sigma}_{i,j-1}^{B,\mathbf{k}_2} = \sigma^4\frac{\big(1-e^{-\lambda_{\mathbf{k}_1}\Delta_{2n}}\big)^2\big(1-e^{-\lambda_{\mathbf{k}_2}\Delta_{2n}}\big)^2}{4\lambda_{\mathbf{k}_1}^{1+\alpha}\lambda_{\mathbf{k}_2}^{1+\alpha}} \times\frac{e^{-\lambda_{\mathbf{k}_1}\Delta_{2n}}+e^{-\lambda_{\mathbf{k}_2}\Delta_{2n}}}{2(1-e^{-(\lambda_{\mathbf{k}_1}+\lambda_{\mathbf{k}_1})\Delta_{2n}})}\Big(1+\mathcal{O}\Big(1\wedge\frac{p^{-1}}{1-e^{-(\lambda_{\mathbf{k}_1}+\lambda_{\mathbf{k}_2})}}\Big)\Big). \tag{155}$$

Furthermore, we have

$$\frac{1}{p}\sum_{i,j=1}^{p}\mathbb{1}_{2\mathbb{N}}(j)\Sigma_{i,j}^{C,\mathbf{k}_1}\Sigma_{i,j-1}^{C,\mathbf{k}_2} = \frac{\sigma^4}{p}\sum_{i,j=1}^{p}\frac{(1-e^{-2\lambda_{\mathbf{k}_1}\Delta_{2n}})(1-e^{-2\lambda_{\mathbf{k}_2}\Delta_{2n}})}{4\lambda_{\mathbf{k}_1}^{1+\alpha}\lambda_{\mathbf{k}_2}^{1+\alpha}}\mathbb{1}_{\{j=i\}}\mathbb{1}_{\{j-1=i\}}\mathbb{1}_{2\mathbb{N}}(j)=0,$$

as well as

$$\frac{1}{p}\sum_{i,j=1}^{p}\mathbb{1}_{2\mathbb{N}}(j)\Sigma_{i,j}^{BC,\mathbf{k}_1}\Sigma_{i,j-1}^{BC,\mathbf{k}_2} = \sigma^4\frac{(1-e^{-\lambda_{\mathbf{k}_1}\Delta_{2n}})(1-e^{-\lambda_{\mathbf{k}_2}\Delta_{2n}})}{4\lambda_{\mathbf{k}_1}^{1+\alpha}\lambda_{\mathbf{k}_2}^{1+\alpha}}\big(e^{\lambda_{\mathbf{k}_1}\Delta_{2n}}-e^{-\lambda_{\mathbf{k}_1}\Delta_{2n}}\big)\big(e^{\lambda_{\mathbf{k}_2}\Delta_{2n}}-e^{-\lambda_{\mathbf{k}_2}\Delta_{2n}}\big) \times\frac{1}{p}\sum_{i,j=1}^{p}\mathbb{1}_{\{i>j\}}\mathbb{1}_{2\mathbb{N}}(j)e^{-\lambda_{\mathbf{k}_1}\Delta_{2n}(i-j)}e^{-\lambda_{\mathbf{k}_2}\Delta_{2n}(i-j+1)}.$$

For the sum structure in the latter display we obtain

$$\frac{1}{p}\sum_{i,j=1}^{p}\mathbb{1}_{\{i>j\}}\mathbb{1}_{2\mathbb{N}}(j)e^{-\lambda_{\mathbf{k}_1}\Delta_{2n}(i-j)}e^{-\lambda_{\mathbf{k}_2}\Delta_{2n}(i-j+1)} = \frac{e^{-\lambda_{\mathbf{k}_2}\Delta_{2n}}}{p}\sum_{i,j=1}^{p}\mathbb{1}_{\{i>j\}}\mathbb{1}_{2\mathbb{N}}(j)e^{-(\lambda_{\mathbf{k}_1}+\lambda_{\mathbf{k}_2})\Delta_{2n}(i-j)}.$$

Assume $|q|<1$, then we have

$$\begin{aligned}\frac{1}{p}\sum_{i,j=1}^{p}\mathbb{1}_{\{i>j\}}\mathbb{1}_{2\mathbb{N}}(j)q^{i-j} &= \frac{1}{p}\sum_{i=3}^{p}q^i\sum_{j=2}^{i-1}\mathbb{1}_{2\mathbb{N}}(j)q^{-j}\\ &= \frac{1}{pq^2}\sum_{i=3}^{p}\mathbb{1}_{2\mathbb{N}}(i)q^i\frac{1-q^{-(i-1)}}{1-q^{-2}}+\frac{1}{pq^2}\sum_{i=3}^{p}\mathbb{1}_{(2\mathbb{N})^{\complement}}(i)q^i\frac{1-q^{-(i-2)}}{1-q^{-2}}\\ &= -\frac{1}{pq^2(1-q^{-2})}\cdot\frac{p}{2}q(1+q)\Big(1+\mathcal{O}\Big(\frac{p^{-1}}{1-q}\Big)\Big)\\ &= \frac{q}{2(1-q)}\Big(1+\mathcal{O}\Big(\frac{p^{-1}}{1-q}\Big)\Big),\end{aligned} \tag{156}$$

where we used analogous steps as for equation (154). Hence, we get

$$\begin{aligned}\frac{1}{p}\sum_{i,j=1}^{p}\mathbb{1}_{2\mathbb{N}}(j)\Sigma_{i,j}^{BC,\mathbf{k}_1}\Sigma_{i,j-1}^{BC,\mathbf{k}_2} &= \sigma^4\frac{(1-e^{-\lambda_{\mathbf{k}_1}\Delta_{2n}})(1-e^{-\lambda_{\mathbf{k}_2}\Delta_{2n}})}{4\lambda_{\mathbf{k}_1}^{1+\alpha}\lambda_{\mathbf{k}_2}^{1+\alpha}}\big(e^{\lambda_{\mathbf{k}_1}\Delta_{2n}}-e^{-\lambda_{\mathbf{k}_1}\Delta_{2n}}\big)\big(e^{\lambda_{\mathbf{k}_2}\Delta_{2n}}-e^{-\lambda_{\mathbf{k}_2}\Delta_{2n}}\big)\\ &\quad\times e^{-\lambda_{\mathbf{k}_2}\Delta_{2n}}\frac{e^{-(\lambda_{\mathbf{k}_1}+\lambda_{\mathbf{k}_2})\Delta_{2n}}}{2(1-e^{-(\lambda_{\mathbf{k}_1}+\lambda_{\mathbf{k}_2})\Delta_{2n}})}\Big(1+\mathcal{O}\Big(1\wedge\frac{p^{-1}}{1-e^{-(\lambda_{\mathbf{k}_1}+\lambda_{\mathbf{k}_2})\Delta_{2n}}}\Big)\Big)\\ &= \sigma^4\frac{(1-e^{-\lambda_{\mathbf{k}_1}\Delta_{2n}})(1-e^{-\lambda_{\mathbf{k}_2}\Delta_{2n}})}{4\lambda_{\mathbf{k}_1}^{1+\alpha}\lambda_{\mathbf{k}_2}^{1+\alpha}}\big(1-e^{-2\lambda_{\mathbf{k}_1}\Delta_{2n}}\big)\big(1-e^{-2\lambda_{\mathbf{k}_2}\Delta_{2n}}\big)\\ &\quad\times\frac{e^{-\lambda_{\mathbf{k}_2}\Delta_{2n}}}{2(1-e^{-(\lambda_{\mathbf{k}_1}+\lambda_{\mathbf{k}_2})\Delta_{2n}})}\Big(1+\mathcal{O}\Big(1\wedge\frac{p^{-1}}{1-e^{-(\lambda_{\mathbf{k}_1}+\lambda_{\mathbf{k}_2})\Delta_{2n}}}\Big)\Big).\end{aligned} \tag{157}$$

Moreover, we have

$$\frac{1}{p}\sum_{i,j=1}^{p}\mathbb{1}_{2\mathbb{N}}(j)\Sigma_{j,i}^{BC,\mathbf{k}_1}\Sigma_{j-1,i}^{BC,\mathbf{k}_2}=\sigma^4\frac{(1-e^{-\lambda_{\mathbf{k}_1}\Delta_{2n}})(1-e^{-\lambda_{\mathbf{k}_2}\Delta_{2n}})}{4\lambda_{\mathbf{k}_1}^{1+\alpha}\lambda_{\mathbf{k}_2}^{1+\alpha}}\big(e^{\lambda_{\mathbf{k}_1}\Delta_{2n}}-e^{-\lambda_{\mathbf{k}_1}\Delta_{2n}}\big)\big(e^{\lambda_{\mathbf{k}_2}\Delta_{2n}}-e^{-\lambda_{\mathbf{k}_2}\Delta_{2n}}\big)$$
$$\times\frac{1}{p}\sum_{i,j=1}^{p}\mathbb{1}_{\{i<j-1\}}\mathbb{1}_{2\mathbb{N}}(j)e^{-\lambda_{\mathbf{k}_1}\Delta_{2n}(j-i)}e^{-\lambda_{\mathbf{k}_2}\Delta_{2n}(j-1-i)}.$$

Using the results for the following geometric series:

$$\begin{aligned}\frac{1}{p}\sum_{i,j=1}^{p}\mathbb{1}_{\{i<j-1\}}\mathbb{1}_{2\mathbb{N}}(j)q^{j-i}&=\frac{1}{p}\sum_{j=4}^{p}\mathbb{1}_{2\mathbb{N}}(j)q^{j}\sum_{i=1}^{j-2}q^{-i}\\&=\frac{1}{pq}\sum_{j=4}^{p}\mathbb{1}_{2\mathbb{N}}(j)q^{j}\cdot\frac{1-q^{-(j-2)}}{1-q^{-1}}\\&=\frac{1}{p(1-q)}\sum_{j=4}^{p}\mathbb{1}_{2\mathbb{N}}(j)\big(q^2-q^j\big)\\&=\frac{q^2}{2(1-q)}\Big(1+\mathcal{O}\Big(\frac{p^{-1}}{1-q}\Big)\Big),\end{aligned}\tag{158}$$

yields that

$$\begin{aligned}\frac{1}{p}\sum_{i,j=1}^{p}\mathbb{1}_{2\mathbb{N}}(j)\Sigma_{j,i}^{BC,\mathbf{k}_1}\Sigma_{j-1,i}^{BC,\mathbf{k}_2}&=\sigma^4\frac{(1-e^{-\lambda_{\mathbf{k}_1}\Delta_{2n}})(1-e^{-\lambda_{\mathbf{k}_2}\Delta_{2n}})}{4\lambda_{\mathbf{k}_1}^{1+\alpha}\lambda_{\mathbf{k}_2}^{1+\alpha}}\big(e^{\lambda_{\mathbf{k}_1}\Delta_{2n}}-e^{-\lambda_{\mathbf{k}_1}\Delta_{2n}}\big)\big(e^{\lambda_{\mathbf{k}_2}\Delta_{2n}}-e^{-\lambda_{\mathbf{k}_2}\Delta_{2n}}\big)\\&\quad\times e^{\lambda_{\mathbf{k}_2}\Delta_{2n}}\frac{e^{-2(\lambda_{\mathbf{k}_1}+\lambda_{\mathbf{k}_2})\Delta_{2n}}}{2(1-e^{-(\lambda_{\mathbf{k}_1}+\lambda_{\mathbf{k}_2})\Delta_{2n}})}\Big(1+\mathcal{O}\Big(1\wedge\frac{p^{-1}}{1-e^{-(\lambda_{\mathbf{k}_1}+\lambda_{\mathbf{k}_2})\Delta_{2n}}}\Big)\Big)\\&=\sigma^4\frac{(1-e^{-\lambda_{\mathbf{k}_1}\Delta_{2n}})(1-e^{-\lambda_{\mathbf{k}_2}\Delta_{2n}})}{4\lambda_{\mathbf{k}_1}^{1+\alpha}\lambda_{\mathbf{k}_2}^{1+\alpha}}\big(1-e^{-2\lambda_{\mathbf{k}_1}\Delta_{2n}}\big)\big(1-e^{-2\lambda_{\mathbf{k}_2}\Delta_{2n}}\big)\\&\quad\times\frac{e^{-\lambda_{\mathbf{k}_1}\Delta_{2n}}}{2(1-e^{-(\lambda_{\mathbf{k}_1}+\lambda_{\mathbf{k}_2})\Delta_{2n}})}\Big(1+\mathcal{O}\Big(1\wedge\frac{p^{-1}}{1-e^{-(\lambda_{\mathbf{k}_1}+\lambda_{\mathbf{k}_2})\Delta_{2n}}}\Big)\Big).\end{aligned}\tag{159}$$

For the cross-terms, we obtain that

$$\frac{1}{p}\sum_{i,j=1}^{p}\mathbb{1}_{2\mathbb{N}}(j)\tilde{\Sigma}_{i,j}^{B,\mathbf{k}_1}\big(\Sigma_{i,j-1}^{BC,\mathbf{k}_2}+\Sigma_{j-1,i}^{BC,\mathbf{k}_2}\big)=\sigma^4\frac{(1-e^{-\lambda_{\mathbf{k}_1}\Delta_{2n}})^2(e^{-\lambda_{\mathbf{k}_2}\Delta_{2n}}-1)}{4\lambda_{\mathbf{k}_1}^{1+\alpha}\lambda_{\mathbf{k}_2}^{1+\alpha}}\big(e^{\lambda_{\mathbf{k}_2}\Delta_{2n}}-e^{-\lambda_{\mathbf{k}_2}\Delta_{2n}}\big)$$
$$\times\frac{1}{p}\sum_{i,j=1}^{p}\mathbb{1}_{2\mathbb{N}}(j)e^{-\lambda_{\mathbf{k}_1}\Delta_{2n}|i-j|}\big(\mathbb{1}_{\{i>j-1\}}e^{-\lambda_{\mathbf{k}_2}\Delta_{2n}(i-j+1)}+\mathbb{1}_{\{i<j-1\}}e^{-\lambda_{\mathbf{k}_2}\Delta_{2n}(j-1-i)}\big)$$
$$=\sigma^4\frac{(1-e^{-\lambda_{\mathbf{k}_1}\Delta_{2n}})^2(e^{-\lambda_{\mathbf{k}_2}\Delta_{2n}}-1)}{4\lambda_{\mathbf{k}_1}^{1+\alpha}\lambda_{\mathbf{k}_2}^{1+\alpha}}\big(e^{\lambda_{\mathbf{k}_2}\Delta_{2n}}-e^{-\lambda_{\mathbf{k}_2}\Delta_{2n}}\big)$$
$$\times\Big(\frac{e^{-\lambda_{\mathbf{k}_2}\Delta_{2n}}}{p}\sum_{i,j=1}^{p}\mathbb{1}_{2\mathbb{N}}(j)\mathbb{1}_{\{i>j-1\}}e^{-(\lambda_{\mathbf{k}_1}+\lambda_{\mathbf{k}_2})\Delta_{2n}(i-j)}+\frac{e^{\lambda_{\mathbf{k}_2}\Delta_{2n}}}{p}\sum_{i,j=1}^{p}\mathbb{1}_{2\mathbb{N}}(j)\mathbb{1}_{\{i<j-1\}}e^{-(\lambda_{\mathbf{k}_1}+\lambda_{\mathbf{k}_2})\Delta_{2n}(j-i)}\Big).$$

Analogous to equation (156), we have

$$\frac{1}{p}\sum_{i,j=1}^{p}\mathbb{1}_{\{i>j-1\}}\mathbb{1}_{2\mathbb{N}}(j)q^{i-j}=\frac{1}{2(1-q)}\Big(1+\mathcal{O}\Big(\frac{p^{-1}}{1-q}\Big)\Big),$$

which yields in combination with equation (158) that

$$\begin{aligned}\frac{1}{p}\sum_{i,j=1}^{p}\mathbb{1}_{2\mathbb{N}}(j)\tilde{\Sigma}^{B,\mathbf{k}_1}_{i,j}\big(\Sigma^{BC,\mathbf{k}_2}_{i,j-1}+\Sigma^{BC,\mathbf{k}_2}_{j-1,i}\big)&=\sigma^4\frac{(1-e^{-\lambda_{\mathbf{k}_1}\Delta_{2n}})^2(e^{-\lambda_{\mathbf{k}_2}\Delta_{2n}}-1)}{4\lambda_{\mathbf{k}_1}^{1+\alpha}\lambda_{\mathbf{k}_2}^{1+\alpha}}\big(e^{\lambda_{\mathbf{k}_2}\Delta_{2n}}-e^{-\lambda_{\mathbf{k}_2}\Delta_{2n}}\big)\\&\quad\times\big(1+e^{-2\lambda_{\mathbf{k}_1}\Delta_{2n}}\big)\frac{e^{-\lambda_{\mathbf{k}_2}\Delta_{2n}}}{2(1-e^{-(\lambda_{\mathbf{k}_1}+\lambda_{\mathbf{k}_2})\Delta_{2n}})}\Big(1+\mathcal{O}\Big(1\wedge\frac{p^{-1}}{1-e^{-(\lambda_{\mathbf{k}_1}+\lambda_{\mathbf{k}_2})\Delta_{2n}}}\Big)\Big)\\&=\sigma^4\frac{(1-e^{-\lambda_{\mathbf{k}_1}\Delta_{2n}})^2(e^{-\lambda_{\mathbf{k}_2}\Delta_{2n}}-1)}{4\lambda_{\mathbf{k}_1}^{1+\alpha}\lambda_{\mathbf{k}_2}^{1+\alpha}}\big(1-e^{-2\lambda_{\mathbf{k}_2}\Delta_{2n}}\big)\\&\quad\times\frac{1+e^{-2\lambda_{\mathbf{k}_1}\Delta_{2n}}}{2(1-e^{-(\lambda_{\mathbf{k}_1}+\lambda_{\mathbf{k}_2})\Delta_{2n}})}\Big(1+\mathcal{O}\Big(1\wedge\frac{p^{-1}}{1-e^{-(\lambda_{\mathbf{k}_1}+\lambda_{\mathbf{k}_2})\Delta_{2n}}}\Big)\Big).\end{aligned}\tag{160}$$

Moreover, it holds that

$$\begin{aligned}&\frac{1}{p}\sum_{i,j=1}^{p}\mathbb{1}_{2\mathbb{N}}(j)\tilde{\Sigma}^{B,\mathbf{k}_2}_{i,j-1}\big(\Sigma^{BC,\mathbf{k}_1}_{i,j}+\Sigma^{BC,\mathbf{k}_1}_{j,i}\big)=\sigma^4\frac{(1-e^{-\lambda_{\mathbf{k}_2}\Delta_{2n}})^2(e^{-\lambda_{\mathbf{k}_1}\Delta_{2n}}-1)}{4\lambda_{\mathbf{k}_1}^{1+\alpha}\lambda_{\mathbf{k}_2}^{1+\alpha}}\big(e^{\lambda_{\mathbf{k}_1}\Delta_{2n}}-e^{-\lambda_{\mathbf{k}_1}\Delta_{2n}}\big)\\&\quad\times\frac{1}{p}\sum_{i,j=1}^{p}\mathbb{1}_{2\mathbb{N}}(j)e^{-\lambda_{\mathbf{k}_2}\Delta_{2n}|i-(j-1)|}\big(\mathbb{1}_{\{i>j\}}e^{-\lambda_{\mathbf{k}_1}\Delta_{2n}(i-j)}+\mathbb{1}_{\{j>i\}}e^{-\lambda_{\mathbf{k}_1}\Delta_{2n}(j-i)}\big)\\&=\sigma^4\frac{(1-e^{-\lambda_{\mathbf{k}_2}\Delta_{2n}})^2(e^{-\lambda_{\mathbf{k}_1}\Delta_{2n}}-1)}{4\lambda_{\mathbf{k}_1}^{1+\alpha}\lambda_{\mathbf{k}_2}^{1+\alpha}}\big(e^{\lambda_{\mathbf{k}_1}\Delta_{2n}}-e^{-\lambda_{\mathbf{k}_1}\Delta_{2n}}\big)\\&\quad\times\bigg(\frac{e^{-\lambda_{\mathbf{k}_2}\Delta_{2n}}}{p}\sum_{i,j=1}^{p}\mathbb{1}_{2\mathbb{N}}(j)\mathbb{1}_{\{i>j\}}e^{-(\lambda_{\mathbf{k}_1}+\lambda_{\mathbf{k}_2})\Delta_{2n}(i-j)}+\frac{e^{\lambda_{\mathbf{k}_2}\Delta_{2n}}}{p}\sum_{i,j=1}^{p}\mathbb{1}_{2\mathbb{N}}(j)\mathbb{1}_{\{j>i\}}e^{-(\lambda_{\mathbf{k}_1}+\lambda_{\mathbf{k}_2})\Delta_{2n}(j-i)}\bigg)\\&=\sigma^4\frac{(1-e^{-\lambda_{\mathbf{k}_2}\Delta_{2n}})^2(e^{-\lambda_{\mathbf{k}_1}\Delta_{2n}}-1)}{4\lambda_{\mathbf{k}_1}^{1+\alpha}\lambda_{\mathbf{k}_2}^{1+\alpha}}\big(e^{\lambda_{\mathbf{k}_1}\Delta_{2n}}-e^{-\lambda_{\mathbf{k}_1}\Delta_{2n}}\big)\\&\quad\times\big(e^{-\lambda_{\mathbf{k}_2}\Delta_{2n}}+e^{\lambda_{\mathbf{k}_2}\Delta_{2n}}\big)\frac{e^{-(\lambda_{\mathbf{k}_1}+\lambda_{\mathbf{k}_2})\Delta_{2n}}}{2(1-e^{-(\lambda_{\mathbf{k}_1}+\lambda_{\mathbf{k}_2})\Delta_{2n}})}\Big(1+\mathcal{O}\Big(1\wedge\frac{p^{-1}}{1-e^{-(\lambda_{\mathbf{k}_1}+\lambda_{\mathbf{k}_2})\Delta_{2n}}}\Big)\Big)\\&=\sigma^4\frac{(1-e^{-\lambda_{\mathbf{k}_2}\Delta_{2n}})^2(e^{-\lambda_{\mathbf{k}_1}\Delta_{2n}}-1)}{4\lambda_{\mathbf{k}_1}^{1+\alpha}\lambda_{\mathbf{k}_2}^{1+\alpha}}\big(1-e^{-2\lambda_{\mathbf{k}_1}\Delta_{2n}}\big)\\&\quad\times\big(1+e^{-2\lambda_{\mathbf{k}_2}\Delta_{2n}}\big)\frac{1}{2(1-e^{-(\lambda_{\mathbf{k}_1}+\lambda_{\mathbf{k}_2})\Delta_{2n}})}\Big(1+\mathcal{O}\Big(1\wedge\frac{p^{-1}}{1-e^{-(\lambda_{\mathbf{k}_1}+\lambda_{\mathbf{k}_2})\Delta_{2n}}}\Big)\Big),\end{aligned}\tag{161}$$

where we used equation (156) and

$$\frac{1}{p}\sum_{i,j=1}^{p}\mathbb{1}_{\{i<j\}}\mathbb{1}_{2\mathbb{N}}(j)q^{j-i}=\frac{q}{2(1-q)}\Big(1+\mathcal{O}\Big(\frac{p^{-1}}{1-q}\Big)\Big).$$

We also observe that

$$\begin{aligned}\frac{1}{p}\sum_{i,j=1}^{p}\mathbb{1}_{2\mathbb{N}}(j)\tilde{\Sigma}^{B,\mathbf{k}_1}_{i,j}\Sigma^{C,\mathbf{k}_2}_{i,j-1}&=\sigma^4\frac{(1-e^{-\lambda_{\mathbf{k}_1}\Delta_{2n}})^2(1-e^{-2\lambda_{\mathbf{k}_2}\Delta_{2n}})}{4\lambda_{\mathbf{k}_1}^{1+\alpha}\lambda_{\mathbf{k}_2}^{1+\alpha}}\frac{1}{p}\sum_{i,j=1}^{p}\mathbb{1}_{2\mathbb{N}}(j)e^{-\lambda_{\mathbf{k}_1}\Delta_{2n}|i-j|}\mathbb{1}_{\{j-1=i\}}\\&=\sigma^4e^{-\lambda_{\mathbf{k}_1}\Delta_{2n}}\frac{(1-e^{-\lambda_{\mathbf{k}_1}\Delta_{2n}})^2(1-e^{-2\lambda_{\mathbf{k}_2}\Delta_{2n}})}{8\lambda_{\mathbf{k}_1}^{1+\alpha}\lambda_{\mathbf{k}_2}^{1+\alpha}}\big(1+\mathcal{O}(p^{-1})\big),\end{aligned}\tag{162}$$

as well as

$$\frac{1}{p}\sum_{i,j=1}^{p}\mathbb{1}_{2\mathbb{N}}(j)\tilde{\Sigma}^{B,\mathbf{k}_2}_{i,j-1}\Sigma^{C,\mathbf{k}_1}_{i,j} = \sigma^4\frac{(1-e^{-2\lambda_{\mathbf{k}_1}\Delta_{2n}})(1-e^{-\lambda_{\mathbf{k}_2}\Delta_{2n}})^2}{4\lambda_{\mathbf{k}_1}^{1+\alpha}\lambda_{\mathbf{k}_2}^{1+\alpha}}\frac{1}{p}\sum_{i,j=1}^{p}\mathbb{1}_{2\mathbb{N}}(j)\mathbb{1}_{\{j=i\}}e^{-\lambda_{\mathbf{k}_2}\Delta_{2n}|i-j+1|}$$
$$= \sigma^4 e^{-\lambda_{\mathbf{k}_2}\Delta_{2n}}\frac{(1-e^{-2\lambda_{\mathbf{k}_1}\Delta_{2n}})(1-e^{-\lambda_{\mathbf{k}_2}\Delta_{2n}})^2}{8\lambda_{\mathbf{k}_1}^{1+\alpha}\lambda_{\mathbf{k}_2}^{1+\alpha}}\Big(1+\mathcal{O}(p^{-1})\Big). \tag{163}$$

In comparison to Proposition 5.2.1, the following structures do not vanish and we get

$$\frac{1}{p}\sum_{i,j=1}^{p}\mathbb{1}_{2\mathbb{N}}(j)\Sigma^{BC,\mathbf{k}_1}_{j,i}\Sigma^{C,\mathbf{k}_2}_{i,j-1} = \sigma^4\frac{(1-e^{-2\lambda_{\mathbf{k}_2}\Delta_{2n}})(e^{-\lambda_{\mathbf{k}_1}\Delta_{2n}}-1)}{4\lambda_{\mathbf{k}_1}^{1+\alpha}\lambda_{\mathbf{k}_2}^{1+\alpha}}\Big(e^{\lambda_{\mathbf{k}_1}\Delta_{2n}}-e^{-\lambda_{\mathbf{k}_1}\Delta_{2n}}\Big)$$
$$\times\frac{1}{p}\sum_{i,j=1}^{p}\mathbb{1}_{2\mathbb{N}}(j)\mathbb{1}_{\{j-1=i\}}e^{-\lambda_{\mathbf{k}_1}\Delta_{2n}(j-i)}$$
$$= \sigma^4\frac{(1-e^{-2\lambda_{\mathbf{k}_2}\Delta_{2n}})(e^{-\lambda_{\mathbf{k}_1}\Delta_{2n}}-1)}{4\lambda_{\mathbf{k}_1}^{1+\alpha}\lambda_{\mathbf{k}_2}^{1+\alpha}}\Big(e^{\lambda_{\mathbf{k}_1}\Delta_{2n}}-e^{-\lambda_{\mathbf{k}_1}\Delta_{2n}}\Big)$$
$$\times\frac{e^{-\lambda_{\mathbf{k}_1}\Delta_{2n}}}{2}\Big(1+\mathcal{O}(p^{-1})\Big)$$
$$= \sigma^4\frac{(1-e^{-2\lambda_{\mathbf{k}_2}\Delta_{2n}})(e^{-\lambda_{\mathbf{k}_1}\Delta_{2n}}-1)}{8\lambda_{\mathbf{k}_1}^{1+\alpha}\lambda_{\mathbf{k}_2}^{1+\alpha}}\Big(1-e^{-2\lambda_{\mathbf{k}_1}\Delta_{2n}}\Big)\Big(1+\mathcal{O}(p^{-1})\Big), \tag{164}$$

as well as

$$\frac{1}{p}\sum_{i,j=1}^{p}\mathbb{1}_{2\mathbb{N}}(j)\Sigma^{C,\mathbf{k}_1}_{i,j}\Sigma^{BC,\mathbf{k}_2}_{i,j-1} = \sigma^4\frac{(1-e^{-2\lambda_{\mathbf{k}_1}\Delta_{2n}})(e^{-\lambda_{\mathbf{k}_2}\Delta_{2n}}-1)}{4\lambda_{\mathbf{k}_1}^{1+\alpha}\lambda_{\mathbf{k}_2}^{1+\alpha}}\Big(e^{\lambda_{\mathbf{k}_2}\Delta_{2n}}-e^{-\lambda_{\mathbf{k}_2}\Delta_{2n}}\Big)$$
$$\times\frac{1}{p}\sum_{i,j=1}^{p}\mathbb{1}_{2\mathbb{N}}(j)\mathbb{1}_{\{j=i\}}e^{-\lambda_{\mathbf{k}_2}\Delta_{2n}(i-j+1)}$$
$$= \sigma^4\frac{(1-e^{-2\lambda_{\mathbf{k}_1}\Delta_{2n}})(e^{-\lambda_{\mathbf{k}_2}\Delta_{2n}}-1)}{4\lambda_{\mathbf{k}_1}^{1+\alpha}\lambda_{\mathbf{k}_2}^{1+\alpha}}\Big(e^{\lambda_{\mathbf{k}_2}\Delta_{2n}}-e^{-\lambda_{\mathbf{k}_2}\Delta_{2n}}\Big)$$
$$\times\frac{e^{-\lambda_{\mathbf{k}_2}\Delta_{2n}}}{2}\Big(1+\mathcal{O}(p^{-1})\Big)$$
$$= \sigma^4\frac{(1-e^{-2\lambda_{\mathbf{k}_1}\Delta_{2n}})(e^{-\lambda_{\mathbf{k}_2}\Delta_{2n}}-1)}{8\lambda_{\mathbf{k}_1}^{1+\alpha}\lambda_{\mathbf{k}_2}^{1+\alpha}}\Big(1-e^{-2\lambda_{\mathbf{k}_2}\Delta_{2n}}\Big)\Big(1+\mathcal{O}(p^{-1})\Big), \tag{165}$$

whereas the following terms still vanish:

$$\frac{1}{p}\sum_{i,j=1}^{p}\mathbb{1}_{2\mathbb{N}}(j)\Sigma^{BC,\mathbf{k}_1}_{i,j}\Sigma^{BC,\mathbf{k}_2}_{j-1,i} = 0, \qquad \frac{1}{p}\sum_{i,j=1}^{p}\mathbb{1}_{2\mathbb{N}}(j)\Sigma^{BC,\mathbf{k}_1}_{i,j}\Sigma^{C,\mathbf{k}_2}_{i,j-1} = 0,$$
$$\frac{1}{p}\sum_{i,j=1}^{p}\mathbb{1}_{2\mathbb{N}}(j)\Sigma^{BC,\mathbf{k}_1}_{j,i}\Sigma^{BC,\mathbf{k}_2}_{i,j-1} = 0, \qquad \frac{1}{p}\sum_{i,j=1}^{p}\mathbb{1}_{2\mathbb{N}}(j)\Sigma^{C,\mathbf{k}_1}_{i,j}\Sigma^{BC,\mathbf{k}_2}_{j-1,i} = 0.$$

Combining the calculations form the displays (155),(157),(159),(160),(161),(162),(163),(164) and (165), yields for $\mathbf{k}_1\neq\mathbf{k}_2$ that

$$D_{\mathbf{k}_1,\mathbf{k}_2} = \frac{1}{p}\sum_{i,j=1}^{p}\mathbb{1}_{2\mathbb{N}}(j)\Big(\tilde{\Sigma}^{B,\mathbf{k}_1}_{i,j}+\Sigma^{BC,\mathbf{k}_1}_{i,j}+\Sigma^{BC,\mathbf{k}_1}_{j,i}+\Sigma^{C,\mathbf{k}_1}_{i,j}\Big)\Big(\tilde{\Sigma}^{B,\mathbf{k}_2}_{i,j-1}+\Sigma^{BC,\mathbf{k}_2}_{i,j-1}+\Sigma^{BC,\mathbf{k}_2}_{j-1,i}+\Sigma^{C,\mathbf{k}_2}_{i,j-1}\Big)$$

$$
\begin{aligned}
&= \frac{1}{p}\sum_{i,j=1}^{p} \mathbb{1}_{2\mathbb{N}}(j)\Big(\tilde\Sigma^{B,\mathbf{k}_1}_{i,j}\tilde\Sigma^{B,\mathbf{k}_2}_{i,j-1} + \tilde\Sigma^{B,\mathbf{k}_1}_{i,j}(\tilde\Sigma^{BC,\mathbf{k}_2}_{i,j-1} + \tilde\Sigma^{B,\mathbf{k}_2}_{j-1,i}) + \tilde\Sigma^{B,\mathbf{k}_1}_{i,j}\tilde\Sigma^{C,\mathbf{k}_2}_{i,j-1} + \tilde\Sigma^{B,\mathbf{k}_2}_{i,j-1}(\Sigma^{BC,\mathbf{k}_1}_{i,j} + \Sigma^{BC,\mathbf{k}_1}_{j,i})\\
&\quad + \Sigma^{BC,\mathbf{k}_1}_{i,j}\Sigma^{BC,\mathbf{k}_2}_{i,j-1} + \Sigma^{BC,\mathbf{k}_1}_{j,i}\Sigma^{BC,\mathbf{k}_2}_{j-1,i} + \Sigma^{BC,\mathbf{k}_1}_{j,i}\Sigma^{C,\mathbf{k}_2}_{i,j-1} + \Sigma^{C,\mathbf{k}_1}_{i,j}\tilde\Sigma^{B,\mathbf{k}_2}_{i,j-1} + \Sigma^{C,\mathbf{k}_1}_{i,j}\Sigma^{BC,\mathbf{k}_2}_{i,j-1}\Big)\\
&= \sigma^4\Bigg(\frac{\big(1-e^{-\lambda_{\mathbf{k}_1}\Delta_{2n}}\big)^2\big(1-e^{-\lambda_{\mathbf{k}_2}\Delta_{2n}}\big)^2}{4\lambda_{\mathbf{k}_1}^{1+\alpha}\lambda_{\mathbf{k}_2}^{1+\alpha}}\cdot\frac{e^{-\lambda_{\mathbf{k}_1}\Delta_{2n}}+e^{-\lambda_{\mathbf{k}_2}\Delta_{2n}}}{2(1-e^{-(\lambda_{\mathbf{k}_1}+\lambda_{\mathbf{k}_1})\Delta_{2n}})}\\
&\quad + \frac{(1-e^{-\lambda_{\mathbf{k}_1}\Delta_{2n}})^2(e^{-\lambda_{\mathbf{k}_2}\Delta_{2n}}-1)}{4\lambda_{\mathbf{k}_1}^{1+\alpha}\lambda_{\mathbf{k}_2}^{1+\alpha}}\big(1-e^{-2\lambda_{\mathbf{k}_2}\Delta_{2n}}\big)\big(1+e^{-2\lambda_{\mathbf{k}_1}\Delta_{2n}}\big)\frac{1}{2(1-e^{-(\lambda_{\mathbf{k}_1}+\lambda_{\mathbf{k}_2})\Delta_{2n}})}\\
&\quad + e^{-\lambda_{\mathbf{k}_1}\Delta_{2n}}\frac{(1-e^{-\lambda_{\mathbf{k}_1}\Delta_{2n}})^2(1-e^{-2\lambda_{\mathbf{k}_2}\Delta_{2n}})}{8\lambda_{\mathbf{k}_1}^{1+\alpha}\lambda_{\mathbf{k}_2}^{1+\alpha}}\\
&\quad + \frac{(1-e^{-\lambda_{\mathbf{k}_2}\Delta_{2n}})^2(e^{-\lambda_{\mathbf{k}_1}\Delta_{2n}}-1)}{4\lambda_{\mathbf{k}_1}^{1+\alpha}\lambda_{\mathbf{k}_2}^{1+\alpha}}\big(1-e^{-2\lambda_{\mathbf{k}_1}\Delta_{2n}}\big)\big(1+e^{-2\lambda_{\mathbf{k}_2}\Delta_{2n}}\big)\frac{1}{2(1-e^{-(\lambda_{\mathbf{k}_1}+\lambda_{\mathbf{k}_2})\Delta_{2n}})}\\
&\quad + \frac{(1-e^{-\lambda_{\mathbf{k}_1}\Delta_{2n}})(1-e^{-\lambda_{\mathbf{k}_2}\Delta_{2n}})}{4\lambda_{\mathbf{k}_1}^{1+\alpha}\lambda_{\mathbf{k}_2}^{1+\alpha}}\big(1-e^{-2\lambda_{\mathbf{k}_1}\Delta_{2n}}\big)\big(1-e^{-2\lambda_{\mathbf{k}_2}\Delta_{2n}}\big)\frac{e^{-\lambda_{\mathbf{k}_2}\Delta_{2n}}}{2(1-e^{-(\lambda_{\mathbf{k}_1}+\lambda_{\mathbf{k}_2})\Delta_{2n}})}\\
&\quad + \frac{(1-e^{-\lambda_{\mathbf{k}_1}\Delta_{2n}})(1-e^{-\lambda_{\mathbf{k}_2}\Delta_{2n}})}{4\lambda_{\mathbf{k}_1}^{1+\alpha}\lambda_{\mathbf{k}_2}^{1+\alpha}}\big(1-e^{-2\lambda_{\mathbf{k}_1}\Delta_{2n}}\big)\big(1-e^{-2\lambda_{\mathbf{k}_2}\Delta_{2n}}\big)\frac{e^{-\lambda_{\mathbf{k}_1}\Delta_{2n}}}{2(1-e^{-(\lambda_{\mathbf{k}_1}+\lambda_{\mathbf{k}_2})\Delta_{2n}})}\\
&\quad + \frac{(1-e^{-2\lambda_{\mathbf{k}_2}\Delta_{2n}})(e^{-\lambda_{\mathbf{k}_1}\Delta_{2n}}-1)}{8\lambda_{\mathbf{k}_1}^{1+\alpha}\lambda_{\mathbf{k}_2}^{1+\alpha}}\Big(1-e^{-2\lambda_{\mathbf{k}_1}\Delta_{2n}}\Big)\\
&\quad + e^{-\lambda_{\mathbf{k}_2}\Delta_{2n}}\frac{(1-e^{-2\lambda_{\mathbf{k}_1}\Delta_{2n}})(1-e^{-\lambda_{\mathbf{k}_2}\Delta_{2n}})^2}{8\lambda_{\mathbf{k}_1}^{1+\alpha}\lambda_{\mathbf{k}_2}^{1+\alpha}}\\
&\quad + \frac{(1-e^{-2\lambda_{\mathbf{k}_1}\Delta_{2n}})(e^{-\lambda_{\mathbf{k}_2}\Delta_{2n}}-1)}{8\lambda_{\mathbf{k}_1}^{1+\alpha}\lambda_{\mathbf{k}_2}^{1+\alpha}}\Big(1-e^{-2\lambda_{\mathbf{k}_2}\Delta_{2n}}\Big)\Bigg)\Bigg(1+\mathcal{O}\Big(1\wedge\frac{p^{-1}}{1-e^{-(\lambda_{\mathbf{k}_1}+\lambda_{\mathbf{k}_2})\Delta_{2n}}}\Big)\Bigg)\\
&= \sigma^4\Bigg(\frac{(1-e^{-\lambda_{\mathbf{k}_1}\Delta_{2n}})^2(1-e^{-\lambda_{\mathbf{k}_2}\Delta_{2n}})^2}{8\lambda_{\mathbf{k}_1}^{1+\alpha}\lambda_{\mathbf{k}_2}^{1+\alpha}}\Big(\frac{e^{-\lambda_{\mathbf{k}_1}\Delta_{2n}}+e^{-\lambda_{\mathbf{k}_2}\Delta_{2n}}}{1-e^{-(\lambda_{\mathbf{k}_1}+\lambda_{\mathbf{k}_1})\Delta_{2n}}} - \frac{(1-e^{-2\lambda_{\mathbf{k}_2}\Delta_{2n}})(1+e^{-2\lambda_{\mathbf{k}_1}\Delta_{2n}})}{(1-e^{-(\lambda_{\mathbf{k}_1}+\lambda_{\mathbf{k}_2})\Delta_{2n}})(1-e^{-\lambda_{\mathbf{k}_2}\Delta_{2n}})}\\
&\quad - \frac{(1-e^{-2\lambda_{\mathbf{k}_1}\Delta_{2n}})(1+e^{-2\lambda_{\mathbf{k}_2}\Delta_{2n}})}{(1-e^{-\lambda_{\mathbf{k}_1}\Delta_{2n}})(1-e^{-(\lambda_{\mathbf{k}_1}+\lambda_{\mathbf{k}_2})\Delta_{2n}})} + \frac{(e^{-\lambda_{\mathbf{k}_1}\Delta_{2n}}+e^{-\lambda_{\mathbf{k}_2}\Delta_{2n}})(1-e^{-2\lambda_{\mathbf{k}_1}\Delta_{2n}})(1-e^{-2\lambda_{\mathbf{k}_2}\Delta_{2n}})}{(1-e^{-\lambda_{\mathbf{k}_1}\Delta_{2n}})(1-e^{-\lambda_{\mathbf{k}_2}\Delta_{2n}})(1-e^{-(\lambda_{\mathbf{k}_1}+\lambda_{\mathbf{k}_2})\Delta_{2n}})}\Big)\\
&\quad + \frac{(1-e^{-\lambda_{\mathbf{k}_1}\Delta_{2n}})(1-e^{-\lambda_{\mathbf{k}_2}\Delta_{2n}})}{8\lambda_{\mathbf{k}_1}^{1+\alpha}\lambda_{\mathbf{k}_2}^{1+\alpha}}\Big(\frac{e^{-\lambda_{\mathbf{k}_1}\Delta_{2n}}(1-e^{-\lambda_{\mathbf{k}_1}\Delta_{2n}})(1-e^{-2\lambda_{\mathbf{k}_2}\Delta_{2n}})}{(1-e^{-\lambda_{\mathbf{k}_2}\Delta_{2n}})}\\
&\quad + \frac{e^{-\lambda_{\mathbf{k}_2}\Delta_{2n}}(1-e^{-\lambda_{\mathbf{k}_2}\Delta_{2n}})(1-e^{-2\lambda_{\mathbf{k}_1}\Delta_{2n}})}{(1-e^{-\lambda_{\mathbf{k}_1}\Delta_{2n}})} - \frac{(1-e^{-2\lambda_{\mathbf{k}_1}\Delta_{2n}})(1-e^{-2\lambda_{\mathbf{k}_2}\Delta_{2n}})}{(1-e^{-\lambda_{\mathbf{k}_2}\Delta_{2n}})}\\
&\quad - \frac{(1-e^{-2\lambda_{\mathbf{k}_1}\Delta_{2n}})(1-e^{-2\lambda_{\mathbf{k}_2}\Delta_{2n}})}{(1-e^{-\lambda_{\mathbf{k}_1}\Delta_{2n}})}\Big)\Bigg)\Bigg(1+\mathcal{O}\Big(1\wedge\frac{p^{-1}}{1-e^{-(\lambda_{\mathbf{k}_1}+\lambda_{\mathbf{k}_2})\Delta_{2n}}}\Big)\Bigg)\\
&= \sigma^4\Bigg(\frac{(1-e^{-\lambda_{\mathbf{k}_1}\Delta_{2n}})^2(1-e^{-\lambda_{\mathbf{k}_2}\Delta_{2n}})^2}{8\lambda_{\mathbf{k}_1}^{1+\alpha}\lambda_{\mathbf{k}_2}^{1+\alpha}}\Big(\frac{e^{-\lambda_{\mathbf{k}_1}\Delta_{2n}}+e^{-\lambda_{\mathbf{k}_2}\Delta_{2n}}}{1-e^{-(\lambda_{\mathbf{k}_1}+\lambda_{\mathbf{k}_1})\Delta_{2n}}} - \frac{(1+e^{-\lambda_{\mathbf{k}_2}\Delta_{2n}})(1+e^{-2\lambda_{\mathbf{k}_1}\Delta_{2n}})}{(1-e^{-(\lambda_{\mathbf{k}_1}+\lambda_{\mathbf{k}_2})\Delta_{2n}})}\\
&\quad - \frac{(1+e^{-\lambda_{\mathbf{k}_1}\Delta_{2n}})(1+e^{-2\lambda_{\mathbf{k}_2}\Delta_{2n}})}{(1-e^{-(\lambda_{\mathbf{k}_1}+\lambda_{\mathbf{k}_2})\Delta_{2n}})} + \frac{(e^{-\lambda_{\mathbf{k}_1}\Delta_{2n}}+e^{-\lambda_{\mathbf{k}_2}\Delta_{2n}})(1+e^{-\lambda_{\mathbf{k}_1}\Delta_{2n}})(1+e^{-\lambda_{\mathbf{k}_2}\Delta_{2n}})}{(1-e^{-(\lambda_{\mathbf{k}_1}+\lambda_{\mathbf{k}_2})\Delta_{2n}})}\Big)\\
&\quad + \frac{(1-e^{-\lambda_{\mathbf{k}_1}\Delta_{2n}})(1-e^{-\lambda_{\mathbf{k}_2}\Delta_{2n}})}{8\lambda_{\mathbf{k}_1}^{1+\alpha}\lambda_{\mathbf{k}_2}^{1+\alpha}}\Big(e^{-\lambda_{\mathbf{k}_1}\Delta_{2n}}(1-e^{-\lambda_{\mathbf{k}_1}\Delta_{2n}})(1+e^{-\lambda_{\mathbf{k}_2}\Delta_{2n}})\\
&\quad + e^{-\lambda_{\mathbf{k}_2}\Delta_{2n}}(1-e^{-\lambda_{\mathbf{k}_2}\Delta_{2n}})(1+e^{-\lambda_{\mathbf{k}_1}\Delta_{2n}}) - (1-e^{-2\lambda_{\mathbf{k}_1}\Delta_{2n}})(1+e^{-\lambda_{\mathbf{k}_2}\Delta_{2n}})\\
&\quad - (1-e^{-2\lambda_{\mathbf{k}_2}\Delta_{2n}})(1+e^{-\lambda_{\mathbf{k}_1}\Delta_{2n}})\Big)\Bigg)\Bigg(1+\mathcal{O}\Big(1\wedge\frac{p^{-1}}{1-e^{-(\lambda_{\mathbf{k}_1}+\lambda_{\mathbf{k}_2})\Delta_{2n}}}\Big)\Bigg)
\end{aligned}
$$

$$= \sigma^4\Big(\frac{(1-e^{-\lambda_{\mathbf{k}_1}\Delta_{2n}})^2(1-e^{-\lambda_{\mathbf{k}_2}\Delta_{2n}})^2}{8\lambda_{\mathbf{k}_1}^{1+\alpha}\lambda_{\mathbf{k}_2}^{1+\alpha}}\Big(-2+\frac{e^{-\lambda_{\mathbf{k}_1}\Delta_{2n}}+e^{-\lambda_{\mathbf{k}_2}\Delta_{2n}}}{1-e^{-(\lambda_{\mathbf{k}_1}+\lambda_{\mathbf{k}_2})\Delta_{2n}}}\Big)$$
$$-2\frac{(1-e^{-\lambda_{\mathbf{k}_1}\Delta_{2n}})(1-e^{-\lambda_{\mathbf{k}_2}\Delta_{2n}})}{8\lambda_{\mathbf{k}_1}^{1+\alpha}\lambda_{\mathbf{k}_2}^{1+\alpha}}(1-e^{-(\lambda_{\mathbf{k}_1}+\lambda_{\mathbf{k}_2})\Delta_{2n}})\Big)\Big(1+\mathcal{O}\Big(1\wedge\frac{p^{-1}}{1-e^{-(\lambda_{\mathbf{k}_1}+\lambda_{\mathbf{k}_2})\Delta_{2n}}}\Big)\Big).$$

Recalling the calculations of the covariance yields

$$\mathbb{C}\mathrm{ov}\big(V_{p,\Delta_{2n}}(\mathbf{y}_1),W_{p,\Delta_{2n}}(\mathbf{y}_2)\big)=\frac{2e^{\|\kappa\bullet(\mathbf{y}_1+\mathbf{y}_2)\|_1}\sigma^4}{p\Delta_{2n}^{2\alpha'}}\sum_{\substack{\mathbf{k}_1,\mathbf{k}_2\in\mathbb{N}^d\\ \mathbf{k}_1\neq\mathbf{k}_2}}e_{\mathbf{k}_1}(\mathbf{y}_1)e_{\mathbf{k}_1}(\mathbf{y}_2)e_{\mathbf{k}_2}(\mathbf{y}_1)e_{\mathbf{k}_2}(\mathbf{y}_2)\bar{D}_{\mathbf{k}_1,\mathbf{k}_2}$$
$$+\mathcal{O}\Big(\frac{1}{p^2\Delta_{2n}^{2\alpha'}}\sum_{\substack{\mathbf{k}_1,\mathbf{k}_2\in\mathbb{N}^d\\ \mathbf{k}_1\neq\mathbf{k}_2}}\frac{\bar{D}_{\mathbf{k}_1,\mathbf{k}_2}}{1-e^{-(\lambda_{\mathbf{k}_1}+\lambda_{\mathbf{k}_2})\Delta_{2n}}}\Big)$$
$$+\frac{2e^{\|\kappa\bullet(\mathbf{y}_1+\mathbf{y}_2)\|_1}}{p\Delta_{2n}^{2\alpha'}}\sum_{\mathbf{k}\in\mathbb{N}^d}e_{\mathbf{k}}^2(\mathbf{y}_1)e_{\mathbf{k}}^2(\mathbf{y}_2)D_{\mathbf{k},\mathbf{k}},$$

where

$$\bar{D}_{\mathbf{k}_1,\mathbf{k}_2}=\frac{(1-e^{-\lambda_{\mathbf{k}_1}\Delta_{2n}})^2(1-e^{-\lambda_{\mathbf{k}_2}\Delta_{2n}})^2}{8\lambda_{\mathbf{k}_1}^{1+\alpha}\lambda_{\mathbf{k}_2}^{1+\alpha}}\Big(-2+\frac{e^{-\lambda_{\mathbf{k}_1}\Delta_{2n}}+e^{-\lambda_{\mathbf{k}_2}\Delta_{2n}}}{1-e^{-(\lambda_{\mathbf{k}_1}+\lambda_{\mathbf{k}_2})\Delta_{2n}}}\Big)$$
$$-2\frac{(1-e^{-\lambda_{\mathbf{k}_1}\Delta_{2n}})(1-e^{-\lambda_{\mathbf{k}_2}\Delta_{2n}})}{8\lambda_{\mathbf{k}_1}^{1+\alpha}\lambda_{\mathbf{k}_2}^{1+\alpha}}(1-e^{-(\lambda_{\mathbf{k}_1}+\lambda_{\mathbf{k}_2})\Delta_{2n}}).$$

First, we obtain for sufficiently large p that

$$\mathcal{O}\Big(\frac{1}{p^2\Delta_{2n}^{2\alpha'}}\sum_{\substack{\mathbf{k}_1,\mathbf{k}_2\in\mathbb{N}^d\\ \mathbf{k}_1\neq\mathbf{k}_2}}\frac{\bar{D}_{\mathbf{k}_1,\mathbf{k}_2}}{1-e^{-(\lambda_{\mathbf{k}_1}+\lambda_{\mathbf{k}_2})\Delta_{2n}}}\Big)=\mathcal{O}(p^{-2}\Delta_{2n}^{-\alpha'}),$$

where we used Lemma 4.2.4 and analogous steps as in Proposition 5.2.1. Hence, we obtain

$$\mathcal{O}\Big(\frac{1}{p^2\Delta_{2n}^{2\alpha'}}\sum_{\substack{\mathbf{k}_1,\mathbf{k}_2\in\mathbb{N}^d\\ \mathbf{k}_1\neq\mathbf{k}_2}}\frac{\bar{D}_{\mathbf{k}_1,\mathbf{k}_2}}{1-e^{-(\lambda_{\mathbf{k}_1}+\lambda_{\mathbf{k}_2})\Delta_{2n}}}\Big)=\mathcal{O}\Big(\frac{1}{p}\Big(1\wedge\frac{\Delta_{2n}^{-\alpha'}}{p}\Big)\Big).$$

Furthermore, we have for $\mathbf{k}_1=\mathbf{k}_2=\mathbf{k}$ that

$$D_{\mathbf{k},\mathbf{k}}=\frac{2}{p}\sum_{i,j=1}^{p}\mathbb{1}_{2\mathbb{N}}(j)\mathbb{E}\Big[\big(\tilde{B}_{i,\mathbf{k}}+C_{i,\mathbf{k}}\big)\big(\tilde{B}_{j,\mathbf{k}}+C_{j,\mathbf{k}}\big)\Big]\mathbb{E}\Big[\big(\tilde{B}_{i,\mathbf{k}}+C_{i,\mathbf{k}}\big)\big(\tilde{B}_{j-1,\mathbf{k}}+C_{j-1,\mathbf{k}}\big)\Big]$$
$$=\sigma^4\Big(\frac{(1-e^{-\lambda_{\mathbf{k}}\Delta_{2n}})^4}{8\lambda_{\mathbf{k}}^{2(1+\alpha)}}\Big(-2+2\frac{e^{-\lambda_{\mathbf{k}}\Delta_{2n}}}{1-e^{-2\lambda_{\mathbf{k}}\Delta_{2n}}}\Big)-2\frac{(1-e^{-\lambda_{\mathbf{k}}\Delta_{2n}})^2}{8\lambda_{\mathbf{k}}^{2(1+\alpha)}}(1-e^{-2\lambda_{\mathbf{k}}\Delta_{2n}})\Big)$$
$$\times\Big(1+\mathcal{O}\Big(1\wedge\frac{p^{-1}}{1-e^{-2\lambda_{\mathbf{k}}\Delta_{2n}}}\Big)\Big)$$
$$=-\frac{(1-e^{-\lambda_{\mathbf{k}}\Delta_{2n}})^2}{4\lambda_{\mathbf{k}}^{2(1+\alpha)}}\Big((1-e^{-\lambda_{\mathbf{k}}\Delta_{2n}})^2-\frac{e^{-\lambda_{\mathbf{k}}\Delta_{2n}}(1-e^{-\lambda_{\mathbf{k}}\Delta_{2n}})^2}{1-e^{-2\lambda_{\mathbf{k}}\Delta_{2n}}}+1-e^{-2\lambda_{\mathbf{k}}\Delta_{2n}}\Big)$$
$$\times\Big(1+\mathcal{O}\Big(1\wedge\frac{p^{-1}}{1-e^{-2\lambda_{\mathbf{k}}\Delta_{2n}}}\Big)\Big).$$

Defining the following term:

$$\bar{D}_{\mathbf{k},\mathbf{k}} := \frac{(1-e^{-\lambda_{\mathbf{k}}\Delta_{2n}})^4}{8\lambda_{\mathbf{k}}^{2(1+\alpha)}}\Big(-2+2\frac{e^{-\lambda_{\mathbf{k}}\Delta_{2n}}}{1-e^{-2\lambda_{\mathbf{k}}\Delta_{2n}}}\Big)-2\frac{(1-e^{-\lambda_{\mathbf{k}}\Delta_{2n}})^2}{8\lambda_{\mathbf{k}}^{2(1+\alpha)}}(1-e^{-2\lambda_{\mathbf{k}}\Delta_{2n}}),$$

yields

$$\frac{1}{\Delta_{2n}^{2\alpha'}p}\sum_{\mathbf{k}\in\mathbb{N}^d}\bar{D}_{\mathbf{k},\mathbf{k}} = \mathcal{O}\Big(\frac{\Delta_{2n}^{d/2}}{p}\Delta_{2n}^{d/2}\sum_{\mathbf{k}\in\mathbb{N}^d}\Big(\frac{(1-e^{-\lambda_{\mathbf{k}}\Delta_{2n}})}{2(\lambda_{\mathbf{k}}\Delta_{2n})^{1+\alpha}}\Big)^2\Big) = \mathcal{O}\big(p^{-1}\Delta_{2n}^{2(1-\alpha')}\big),$$

where we used analogous steps as in display (117). We decompose the leading term $\bar{D}_{\mathbf{k}_1,\mathbf{k}_2}$ as follows:

$$\bar{D}_{\mathbf{k}_1,\mathbf{k}_2} = \bar{D}^1_{\mathbf{k}_1,\mathbf{k}_2}+\bar{D}^2_{\mathbf{k}_1,\mathbf{k}_2}+\bar{D}^3_{\mathbf{k}_1,\mathbf{k}_2}+\bar{D}^4_{\mathbf{k}_1,\mathbf{k}_2},$$

where

$$\begin{aligned}
\bar{D}^1_{\mathbf{k}_1,\mathbf{k}_2} &= -\frac{(1-e^{-\lambda_{\mathbf{k}_1}\Delta_{2n}})^2(1-e^{-\lambda_{\mathbf{k}_2}\Delta_{2n}})^2}{4\lambda_{\mathbf{k}_1}^{1+\alpha}\lambda_{\mathbf{k}_2}^{1+\alpha}} = -\frac{\Delta_{2n}^{2(1+\alpha)}}{4}f_{2,\alpha}(\lambda_{\mathbf{k}_1}\Delta_{2n})f_{2,\alpha}(\lambda_{\mathbf{k}_2}\Delta_{2n}),\\
\bar{D}^2_{\mathbf{k}_1,\mathbf{k}_2} &= \frac{(1-e^{-\lambda_{\mathbf{k}_1}\Delta_{2n}})^2(1-e^{-\lambda_{\mathbf{k}_2}\Delta_{2n}})^2}{8\lambda_{\mathbf{k}_1}^{1+\alpha}\lambda_{\mathbf{k}_2}^{1+\alpha}}\cdot\frac{e^{-\lambda_{\mathbf{k}_1}\Delta_{2n}}+e^{-\lambda_{\mathbf{k}_2}\Delta_{2n}}}{1-e^{-(\lambda_{\mathbf{k}_1}+\lambda_{\mathbf{k}_2})\Delta_{2n}}}\\
&= \frac{\Delta_{2n}^{2(1+\alpha)}}{2}\sum_{r=0}^{\infty}\big(g_{1,\alpha,r+1}(\lambda_{\mathbf{k}_1}\Delta_{2n})g_{1,\alpha,r}(\lambda_{\mathbf{k}_2}\Delta_{2n})+g_{1,\alpha,r+1}(\lambda_{\mathbf{k}_2}\Delta_{2n})g_{1,\alpha,r}(\lambda_{\mathbf{k}_1}\Delta_{2n})\big),\\
\bar{D}^3_{\mathbf{k}_1,\mathbf{k}_2} &= -\frac{(1-e^{-\lambda_{\mathbf{k}_1}\Delta_{2n}})(1-e^{-\lambda_{\mathbf{k}_2}\Delta_{2n}})}{4\lambda_{\mathbf{k}_1}^{1+\alpha}\lambda_{\mathbf{k}_2}^{1+\alpha}} = -\frac{\Delta_{2n}^{2(1+\alpha)}}{4}f_{1,\alpha}(\lambda_{\mathbf{k}_1}\Delta_{2n})f_{1,\alpha}(\lambda_{\mathbf{k}_2}\Delta_{2n}),\\
\bar{D}^4_{\mathbf{k}_1,\mathbf{k}_2} &= \frac{(1-e^{-\lambda_{\mathbf{k}_1}\Delta_{2n}})(1-e^{-\lambda_{\mathbf{k}_2}\Delta_{2n}})}{4\lambda_{\mathbf{k}_1}^{1+\alpha}\lambda_{\mathbf{k}_2}^{1+\alpha}}e^{-(\lambda_{\mathbf{k}_1}+\lambda_{\mathbf{k}_2})\Delta_{2n}} = \Delta_{2n}^{2(1+\alpha)}g_{2,\alpha,1}(\lambda_{\mathbf{k}_1}\Delta_{2n})g_{2,\alpha,1}(\lambda_{\mathbf{k}_2}\Delta_{2n}).
\end{aligned}$$

Here, we use the following functions defined by

$$\begin{aligned}
f_{1,\alpha}(x) := f_\alpha(x) &= \frac{1-e^{-x}}{x^{1+\alpha}}, & f_{2,\alpha}(x) &:= \frac{(1-e^{-x})^2}{x^{1+\alpha}},\\
g_{1,\alpha,\tau}(x) := g_{\alpha,\tau}(x) &= \frac{(1-e^{-x})^2}{2x^{1+\alpha}}e^{-\tau x}, & g_{2,\alpha,\tau}(x) &:= \frac{1-e^{-x}}{2x^{1+\alpha}}e^{-\tau x}.
\end{aligned}$$

By Lemma 4.2.3, we know that $f_{1,\alpha}\in\mathcal{Q}_{\beta_1}$ and $g_{1,\alpha,\tau}\in\mathcal{Q}_{\beta_2}$, where $\beta_1=\big(2\alpha,2(1+\alpha),2(2+2\alpha)\big)$ and $\beta_2=\big(2\alpha,2(1+\alpha),2(1+2\alpha)\big)$. By analogous computations as used in Lemma 4.2.3, we obtain that $f_{2,\alpha}\in\mathcal{Q}_{\beta_1}$ and $g_{2,\alpha,\tau}\in\mathcal{Q}_{\beta_1}$. Assume $\mathbf{y}_1\neq\mathbf{y}_2$. We can repeat the calculations leading to equation (119) and have

$$\begin{aligned}
\mathbb{C}\mathrm{ov}\big(V_{p,\Delta_{2n}}(\mathbf{y}_1),W_{p,\Delta_{2n}}(\mathbf{y}_2)\big) &= \mathcal{O}\Big(\frac{\Delta_{2n}^{1-\alpha'}}{p}\big(\|\mathbf{y}_1-\mathbf{y}_2\|_0^{-(d+1)}+\delta^{-(d+1)}\big)\Big)+\mathcal{O}\Big(\frac{1}{p}\Big(\Delta_{2n}^{2(1-\alpha')}+\frac{\Delta_{2n}^{-\alpha'}}{p}\wedge 1\Big)\Big)\\
&= \mathcal{O}\Big(\frac{\Delta_{2n}^{1-\alpha'}}{p}\big(\|\mathbf{y}_1-\mathbf{y}_2\|_0^{-(d+1)}+\delta^{-(d+1)}\big)\vee\frac{\Delta_{2n}^{-\alpha'}}{p^2}\Big).
\end{aligned}$$

Therefore, it remains to analyse the case where $\mathbf{y}_1=\mathbf{y}_2$. Again, by utilizing the fact that the functions $f_{1,\alpha}$, $f_{2,\alpha}$, and $g_{2,\alpha,\tau}$ belong to the same class $\mathcal{Q}_{\beta_1}$ as the function f_α defined in equation (67), and additionally that $g_{1,\alpha,\tau}=g_{\alpha,\tau}$, we can conclude, analogous to equation (120) from Proposition 5.2.1, that

$$\mathbb{C}\mathrm{ov}\big(V_{p,\Delta_{2n}}(\mathbf{y}_1), W_{p,\Delta_{2n}}(\mathbf{y}_2)\big) = \frac{2\sigma^4}{p\Delta_{2n}^{2\alpha'}} \sum_{\mathbf{k}_1,\mathbf{k}_2\in\mathbb{N}^d} \bar{D}_{\mathbf{k}_1,\mathbf{k}_2} + \mathcal{O}\bigg(\frac{1}{p}\Big(\Delta_{2n}^{1/2} \vee \frac{\Delta_{2n}^{1-\alpha'}}{\delta^{d+1}} + \frac{\Delta_{2n}^{-\alpha'}}{p} \wedge 1\Big)\bigg).$$

First, we obtain that

$$\begin{aligned}
\frac{1}{\Delta_{2n}^{2\alpha'}} \sum_{\mathbf{k}_1,\mathbf{k}_2\in\mathbb{N}^d} \bar{D}^1_{\mathbf{k}_1,\mathbf{k}_2} &= -\frac{1}{4}\bigg(\Delta_{2n}^{d/2}\sum_{\mathbf{k}\in\mathbb{N}^d} f_{2,\alpha}(\lambda_{\mathbf{k}}\Delta_{2n})\bigg)^2 =: I_1,\\
\frac{1}{\Delta_{2n}^{2\alpha'}} \sum_{\mathbf{k}_1,\mathbf{k}_2\in\mathbb{N}^d} \bar{D}^2_{\mathbf{k}_1,\mathbf{k}_2} &= \sum_{r=0}^{\infty}\bigg(\Delta_{2n}^{d/2}\sum_{\mathbf{k}\in\mathbb{N}^d} g_{1,\alpha,r+1}(\lambda_{\mathbf{k}}\Delta_{2n})\bigg)\bigg(\Delta_{2n}^{d/2}\sum_{\mathbf{k}\in\mathbb{N}^d} g_{1,\alpha,r}(\lambda_{\mathbf{k}}\Delta_{2n})\bigg) =: I_2,\\
\frac{1}{\Delta_{2n}^{2\alpha'}} \sum_{\mathbf{k}_1,\mathbf{k}_2\in\mathbb{N}^d} \bar{D}^3_{\mathbf{k}_1,\mathbf{k}_2} &= -\frac{1}{4}\bigg(\Delta_{2n}^{d/2}\sum_{\mathbf{k}\in\mathbb{N}^d} f_{1,\alpha}(\lambda_{\mathbf{k}}\Delta_{2n})\bigg)^2 =: I_3,\\
\frac{1}{\Delta_{2n}^{2\alpha'}} \sum_{\mathbf{k}_1,\mathbf{k}_2\in\mathbb{N}^d} \bar{D}^3_{\mathbf{k}_1,\mathbf{k}_2} &= \bigg(\Delta_{2n}^{d/2}\sum_{\mathbf{k}\in\mathbb{N}^d} g_{2,\alpha,1}(\lambda_{\mathbf{k}}\Delta_{2n})\bigg)^2 =: I_4.
\end{aligned}$$

Using Corollary 4.2.2 and analogous steps as in Lemma 4.2.4 yields

$$\begin{aligned}
I_1 &= -\frac{1}{4}\bigg(\frac{1}{2^d(\pi\eta)^{d/2}\Gamma(d/2)}\bigg)^2\bigg(\frac{(2-2^{\alpha'})\pi}{\Gamma(1+\alpha')\sin(\pi\alpha')}\bigg)^2 = -\frac{1}{4}\bigg(\frac{\Gamma(1-\alpha')}{2^d(\pi\eta)^{d/2}\alpha'\Gamma(d/2)}\bigg)^2(2^{\alpha'}-2)^2,\\
I_2 &= \frac{1}{4}\bigg(\frac{\Gamma(1-\alpha')}{2^d(\pi\eta)^{d/2}\alpha'\Gamma(d/2)}\bigg)^2\sum_{r=0}^{\infty}\Big(-(r+1)^{\alpha'}+2(r+2)^{\alpha'}-(r+3)^{\alpha'}\Big)\Big(-r^{\alpha'}+2(r+1)^{\alpha'}-(r+2)^{\alpha'}\Big),\\
I_3 &= -\frac{1}{4}\bigg(\frac{\Gamma(1-\alpha')}{2^d(\pi\eta)^{d/2}\alpha'\Gamma(d/2)}\bigg)^2,\\
I_4 &= \frac{1}{4}\bigg(\frac{\Gamma(1-\alpha')}{2^d(\pi\eta)^{d/2}\alpha'\Gamma(d/2)}\bigg)^2(2^{\alpha'}-1)^2.
\end{aligned}$$

Hence, we obtain for $\mathbf{y}_1 = \mathbf{y}_2$ that

$$\begin{aligned}
\mathbb{C}\mathrm{ov}\big(V_{p,\Delta_{2n}}(\mathbf{y}_1), W_{p,\Delta_{2n}}(\mathbf{y}_2)\big) &= \frac{1}{2p}\bigg(\frac{\Gamma(1-\alpha')\sigma^2}{2^d(\pi\eta)^{d/2}\alpha'\Gamma(d/2)}\bigg)^2\bigg((2^{\alpha'}-1)^2-(2^{\alpha'}-2)^2-1\\
&\quad+\sum_{r=0}^{\infty}\Big(-(r+1)^{\alpha'}+2(r+2)^{\alpha'}-(r+3)^{\alpha'}\Big)\Big(-r^{\alpha'}+2(r+1)^{\alpha'}-(r+2)^{\alpha'}\Big)\bigg)\\
&\quad+\mathcal{O}\bigg(\frac{1}{p}\Big(\Delta_{2n}^{1/2} \vee \frac{\Delta_{2n}^{1-\alpha'}}{\delta^{d+1}} + \frac{\Delta_{2n}^{-\alpha'}}{p} \wedge 1\Big)\bigg).
\end{aligned}$$

Defining the following constant:

$$\Lambda_{\alpha'} := 2(2^{\alpha'}-2) + \sum_{r=0}^{\infty}\bigg(\Big(-(r+1)^{\alpha'}+2(r+2)^{\alpha'}-(r+3)^{\alpha'}\Big)\Big(-r^{\alpha'}+2(r+1)^{\alpha'}-(r+2)^{\alpha'}\Big)\bigg), \tag{166}$$

completes the proof. □

The prior proposition demonstrates that the covariance structure of the rescaled realized volatility $V_{2n\Delta_{2n}}$ and the mix-term $W_{2n\Delta_{2n}}$ exhibits an analogous asymptotic behaviour as the variance-covariance structure of the rescaled realized volatilities outlined in Proposition 5.2.1. This observation simplifies the proof of the central limit theorem presented in Proposition 6.2.3. Note that we consider the case where $p \geqslant 2$ since the covariances mentioned in Proposition 6.2.1 become zero when $p = 1$.

Upon comparing the constant $\Lambda_{\alpha'}$, defined in equation (166), with the constant $\Upsilon_{\alpha'}$ from equation (121), we observe that $\Lambda_{\alpha'}$ contains non-negligible covariances. Notably, when comparing the structures of the series in $\Lambda_{\alpha'}$ and $\Upsilon_{\alpha'}$, it becomes apparent that the structure of non-negligible quadratic increments is transmitted to the product of consecutive temporal increments. The factor of $1/2$ arises due to the thinned temporal grid, which retains half the number of temporal data points from the original grid.

We conclude this section by proving the general mixing-type condition from Proposition 1.2.4.

Corollary 6.2.2

Grant the Assumptions 4.1.1 and 4.1.2. For $1 \leqslant r < r+u \leqslant v \leqslant 2n$ and

$$\tilde{Q}_1^r = \sum_{i=1}^{r} \tilde{\xi}_{2n,i}, \qquad \tilde{Q}_{r+u}^v = \sum_{i=r+u}^{v} \tilde{\xi}_{2n,i},$$

it holds that there is a constant C, with $0 < C < \infty$ and $\tilde{\xi}_{2n,i}$ from equation (153), such that for all $t \in \mathbb{R}$ we have

$$\left|\mathbb{C}\mathrm{ov}\left(e^{\mathrm{i}t(\tilde{Q}_1^r - \mathbb{E}[\tilde{Q}_1^r])},\ e^{\mathrm{i}t(\tilde{Q}_{r+u}^v - \mathbb{E}[\tilde{Q}_{r+u}^v])}\right)\right| \leqslant \frac{Ct^2}{u^{1-\alpha'/2}} \sqrt{\mathbb{V}\mathrm{ar}(\tilde{Q}_1^r)\mathbb{V}\mathrm{ar}(\tilde{Q}_{r+u}^v)}.$$

Proof. Recalling the triangular array $\xi_{2n,i}$ from equation (153) shows, that we can bound $\xi_{2n,i}$ as follows:

$$\begin{aligned}
\xi_{2n,i} &= \xi_{2n,i}^1 + \mathbb{1}_{2\mathbb{N}}(i) \frac{2^{1-\alpha'}}{\log(2)\sqrt{2nm}\Delta_{2n}^{\alpha'}\sigma_0^2 K} \sum_{j=1}^{m} 2(\Delta_{2n,i}\tilde{X})(\mathbf{y}_j)(\Delta_{2n,i-1}\tilde{X})(\mathbf{y}_j) e^{\|\kappa\cdot\mathbf{y}_j\|_1} \\
&\leqslant \xi_{2n,i}^1 + \mathbb{1}_{2\mathbb{N}}(i) \frac{2^{1-\alpha'}}{\log(2)\sqrt{2nm}\Delta_{2n}^{\alpha'}\sigma_0^2 K} \sum_{j=1}^{m} \big((\Delta_{2n,i}\tilde{X})^2(\mathbf{y}_j) + (\Delta_{2n,i-1}\tilde{X})^2(\mathbf{y}_j)\big) e^{\|\kappa\cdot\mathbf{y}_j\|_1} \\
&\leqslant \frac{2^{2-\alpha'}-1}{\log(2)\sqrt{2nm}\Delta_{2n}^{\alpha'}\sigma_0^2 K} \sum_{j=1}^{m} (\Delta_{2n,i}\tilde{X})^2(\mathbf{y}_j) e^{\|\kappa\cdot\mathbf{y}_j\|_1} \\
&\quad + \frac{2^{1-\alpha'}\mathbb{1}_{\{i\geqslant 2\}}}{\log(2)\sqrt{2nm}\Delta_{2n}^{\alpha'}\sigma_0^2 K} \sum_{j=1}^{m} (\Delta_{2n,i-1}\tilde{X})^2(\mathbf{y}_j) e^{\|\kappa\cdot\mathbf{y}_j\|_1}.
\end{aligned}$$

Applying Corollary 5.3.2 completes the proof. □

6.2.3. Central limit theorem and simulation results

To end this chapter, we prove that a central limit theorem holds for the damping estimator $\hat{\alpha}'$ from equation (148). Subsequently, we will discuss the case, where every parameter from the multi-dimensional SPDE model, outlined in equation (49), is unknown and close the research part of this thesis by providing a Monte Carlo simulation study for our novel estimator $\hat{\alpha}'$.

Proposition 6.2.3
On Assumptions 4.1.1 and 4.1.2 we have

$$\sqrt{2nm_n}(\hat{\alpha}'_{2n,m_n} - \alpha') \xrightarrow{d} \mathcal{N}\Big(0, \log(2)^{-2}\big(3\Upsilon_{\alpha'} - 2^{2-\alpha'}(\Upsilon_{\alpha'} + \Lambda_{\alpha'})\big)\Big),$$

as $n \to \infty$, where $m_n = \mathcal{O}\big((2n)^\rho\big)$ with $\rho \in \big(0, (1-\alpha')/(d+2)\big)$, $\Upsilon_{\alpha'}$ defined in equation (121) and $\Lambda_{\alpha'}$ defined in equation (166).

Proof. We determine the asymptotic variance:

$$\begin{aligned}\mathbb{V}\mathrm{ar}\Big(\sum_{i=1}^{2n} \Xi_{2n,i}\Big) &= \mathbb{V}\mathrm{ar}\Big(\sum_{i=1}^{n} \xi_{2n,i}\Big) = \mathbb{V}\mathrm{ar}\Big(\frac{\sqrt{2n}}{\log(2)\sqrt{m}\sigma_0^2 K} \sum_{j=1}^{m} \big(V_{n,\Delta_n})(\mathbf{y}_j) - V_{2n,\Delta_{2n}}(\mathbf{y}_j)\big)\Big) \\ &= \frac{2n}{\log(2)^2 m \sigma_0^4 K^2}\Big(\sum_{j=1}^{m} \mathbb{V}\mathrm{ar}\big(V_{n,\Delta_n}(\mathbf{y}_j)\big) + \sum_{j=1}^{m} \mathbb{V}\mathrm{ar}\big(V_{2n,\Delta_{2n}}(\mathbf{y}_j)\big) \\ &\quad - 2\sum_{j_1,j_2=1}^{m} \mathbb{C}\mathrm{ov}\big(V_{n,\Delta_{2n}}(\mathbf{y}_{j_1}), V_{2n,\Delta_{2n}}(\mathbf{y}_{j_2})\big)\Big) + o(1),\end{aligned}$$

where $\xi_{2n,i}$ is defined in equation (153). For the covariance structure of both temporal resolutions we have by using equation (152) that

$$\begin{aligned}\mathbb{C}\mathrm{ov}\big(V_{n,\Delta_{2n}}(\mathbf{y}_{j_1}), V_{2n,\Delta_{2n}}(\mathbf{y}_{j_2})\big) &= 2^{1-\alpha'}\mathbb{C}\mathrm{ov}\big(V_{2n,\Delta_{2n}}(\mathbf{y}_{j_1}), V_{2n,\Delta_{2n}}(\mathbf{y}_{j_2})\big) \\ &\quad + 2^{2-\alpha'}\mathbb{C}\mathrm{ov}\big(V_{2n,\Delta_{2n}}(\mathbf{y}_{j_1}), W_{2n,\Delta_{2n}}(\mathbf{y}_{j_2})\big).\end{aligned}$$

Note that the covariances vanish for $\mathbf{y}_1 \neq \mathbf{y}_2$. Hence, by utilizing the Propositions 5.2.1 and 6.2.1 we conclude that

$$\begin{aligned}\mathbb{V}\mathrm{ar}\Big(\sum_{i=1}^{2n} \Xi_{2n,i}\Big) &= \frac{2n}{\log(2)^2 m_n \sigma_0^4 K^2}\Big(m_n \frac{\Upsilon_{\alpha'}}{n}\sigma_0^4 K^2 + m_n \frac{\Upsilon_{\alpha'}}{2n}\sigma_0^4 K^2 - 2^{2-\alpha'} m_n \frac{\Upsilon_{\alpha'}}{2n}\sigma_0^4 K^2 \\ &\quad - 2^{3-\alpha'} m_n \frac{\Lambda_{\alpha'}}{4n}\sigma_0^4 K^2\Big) + o(1) \\ &= \frac{1}{\log(2)^2}\big(3\Upsilon_{\alpha'} - 2^{2-\alpha'}(\Upsilon_{\alpha'} + \Lambda_{\alpha'})\big) + o(1) \xrightarrow{n\to\infty} \frac{1}{\log(2)^2}\big(3\Upsilon_{\alpha'} - 2^{2-\alpha'}(\Upsilon_{\alpha'} + \Lambda_{\alpha'})\big).\end{aligned}$$

It remains to verify the Conditions (I)-(IV) from Proposition 1.2.4.

(I) Let $1 \leqslant a \leqslant b \leqslant 2n$, then we obtain for the first condition that

$$\sum_{i=a}^{b} \mathbb{V}\mathrm{ar}(\Xi_{2n,i}) = \sum_{i=a}^{b} \mathbb{V}\mathrm{ar}(\xi_{2n,i}) = \sum_{i=a}^{b} \mathbb{V}\mathrm{ar}(\xi_{2n,i}^1) + \sum_{i=a}^{b} \mathbb{V}\mathrm{ar}(\xi_{2n,i}^2) + \sum_{i=a}^{b} \mathbb{1}_{\{i\geqslant 2\}}\mathbb{C}\mathrm{ov}(\xi_{2n,i}^1, \xi_{2n,i}^2).$$

For the variance structure of $\xi_{2n,i}^1$ we have analogously to Proposition 5.4.1 that

$$\sum_{i=a}^{b} \mathbb{V}\mathrm{ar}(\xi_{2n,i}) = \sum_{i=a}^{b} \mathbb{V}\mathrm{ar}(\xi_{2n,i}^1) = \mathcal{O}\big((b-a+1)\Delta_{2n}\big).$$

For the variance structure of $\xi^2_{2n,i}$, we obtain the same order through analogous considerations as in the proof of Corollary 6.2.2. Hence, it remains to analyse the covariance term. Upon comparing Proposition 6.2.1 with Proposition 5.2.1, we observe that both statements differ only in the constants, whereas the asymptotic behaviour is identical. Therefore, we conclude that

$$\sum_{i=a}^{b} \mathbb{V}\mathrm{ar}(\Xi_{2n,i}) = \mathcal{O}\big((b-a+1)\Delta_{2n}\big).$$

The same argumentation holds for the following term:

$$\mathbb{V}\mathrm{ar}\bigg(\sum_{i=a}^{b} \Xi_{2n,i}\bigg) = \mathcal{O}\big((b-a+1)\Delta_{2n}\big),$$

which proves the first condition as well as Condition (II).

(III) For the third condition we have

$$\mathbb{E}[\xi^4_{2n,i}] \leqslant 8\Big(\mathbb{E}\big[(\xi^1_{2n,i})^4\big] + \mathbb{E}\big[(\xi^2_{2n,i})^4\big]\Big).$$

For $\xi^1_{2n,i}$ we use analogous steps as in Proposition 5.4.1 and have

$$\sum_{i=1}^{2n} \mathbb{E}[(\xi^1_{2n,i})^4] = \mathcal{O}(\Delta_{2n} m^2).$$

For $\xi^2_{2n,i}$ we obtain by using the Cauchy-Schwarz inequality that

$$\begin{aligned}\mathbb{E}[(\xi^2_{2n,i})^4] &\leqslant \mathbb{1}_{2\mathbb{N}}(i)\bigg(\frac{2^{2-\alpha'}}{\log(2)\sigma_0^2 K}\bigg)^4 \frac{1}{\Delta_{2n}^{4\alpha'}(2n)^2 m^2} \sum_{j_1,\dots,j_4} \Big(e^{\|\kappa\boldsymbol{\cdot}(\mathbf{y}_{j_1}+\dots+\mathbf{y}_{j_4})\|}\mathbb{E}\big[(\Delta_{2n,i}\tilde{X})^8(\mathbf{y}_{j_1})\big]^{1/8} \\ &\qquad \times \mathbb{E}\big[(\Delta_{2n,i-1}\tilde{X})^8(\mathbf{y}_{j_1})\big]^{1/8} \cdot \ldots \cdot \mathbb{E}\big[(\Delta_{2n,i}\tilde{X})^8(\mathbf{y}_{j_4})\big]^{1/8}\mathbb{E}\big[(\Delta_{2n,i-1}\tilde{X})^8(\mathbf{y}_{j_4})\big]^{1/8}\Big) \\ &= \mathcal{O}\bigg(\frac{m^4}{\Delta_{2n}^{4\alpha'}(2n)^2 m^2}\Delta_{2n}^{4\alpha'}\bigg).\end{aligned}$$

Hence, we conclude

$$\sum_{i=1}^{2n} \mathbb{E}[(\xi^2_{2n,i})^4] = \mathcal{O}(\Delta_{2n} m^2) = \mathcal{o}(1),$$

and the proof of the third condition follows.

(IV) The last condition is given by Corollary 6.2.2, which completes the proof. □

The preceding central limit theorem reveals, that the asymptotic variance of the damping estimator $\hat{\alpha}'$ contains the non-negligible covariances of the rescaled realized volatilities, as well as additional non-negligible covariance structures resulting from using temporal grids with distinct resolutions, given by $-2^{2-\alpha'}(\Upsilon_{\alpha'} + \Lambda_{\alpha'})\big)$. We also witness, that the asymptotic variance hinges on the unknown pure damping parameter α'. To classify the magnitude of the asymptotic variance, we provide Table 6.4. This table

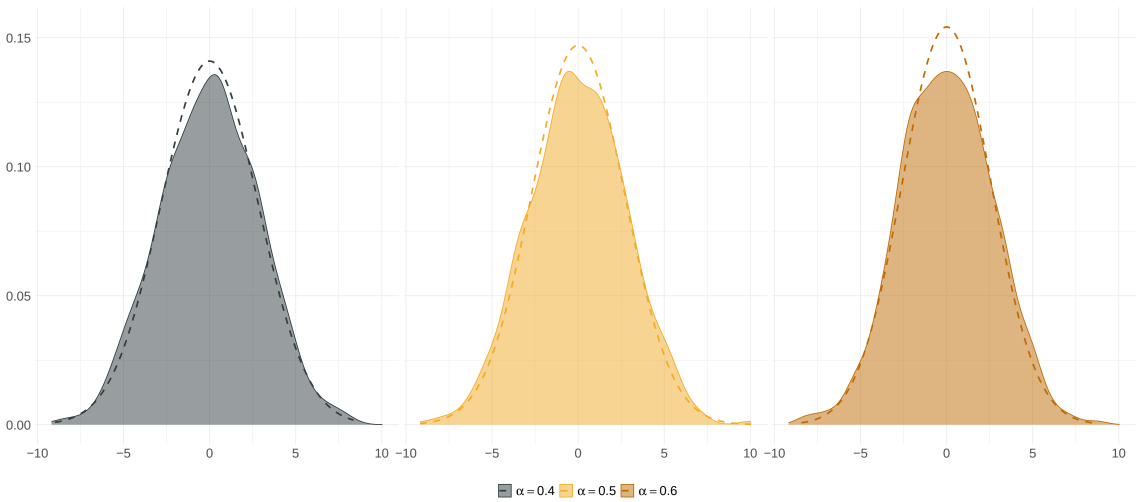

Figure 6.2.: The figure provides a comparison of empirical distributions for centred estimation errors of α', which are obtained through simulations on an equidistant grid in both, time and space, where $N = 10^4$ and $M = 10$ and $\delta = 0.05$. The kernel-density estimation employed a Gaussian kernel with Silverman's 'rule of thumb' and was conducted over 1000 Monte Carlo iterations. The specific parameter values used for the simulations are given as follows: $d = 2$, $\vartheta_0 = 0$, $\nu = (6, 0)$, $\eta = 1$, $\sigma = 1$, and $L = 10$. Three different scenarios were considered, each with a distinct value of the pure damping parameter α': $\alpha' = 4/10 K = 10^3$ (left), $\alpha' = 1/2, K = 10^3$ (middle), and $\alpha' = 6/10, K = 1300$ (right). The corresponding asymptotic distributions are represented by dotted lines.

presents numerical values of the asymptotic variance for different values of the pure damping parameter α'.

α'	0.1	0.2	0.3	0.4	0.5	0.6	0.7	0.8	0.9
AVAR($\hat{\alpha}'$)	4.74	4.45	4.16	3.85	3.53	3.22	2.9	2.59	2.29

Table 6.4.: The table shows the asymptotic variance as given in Proposition 6.2.3 for distinct values of the parameter α'. The values of the asymptotic variance are rounded to 2 decimal places.

Before turning to the simulation study for estimating the damping parameter, we discuss the case of estimating the natural parameters from the multi-dimensional SPDE model from equation (49). Here, we assume that the damping parameter and the parameters from the differential operator A_ϑ are unknown. As we have shown central limit theorems for the estimators $\hat{\sigma}^2$, $\hat{\Psi}$ and $\hat{\upsilon}$ in the Propositions 5.4.1, 6.1.7 and Corollary 6.1.8, respectively, we especially proved consistency for those estimators. Since Proposition 6.2.3 also establishes the consistency of the estimator $\hat{\alpha}'$, we can deduce that the estimators $\hat{\sigma}^2_{\mathbf{y}}$ and $\hat{\sigma}^2$ from Section 4, along with $\hat{\Psi}$ and $\hat{\upsilon}$ from Section 6, remain consistent when replacing the parameter α' by the estimator $\hat{\alpha}'$. We can also preserve the original CLTs for the estimators $\hat{\sigma}^2, \hat{\Psi}$ and $\hat{\upsilon}$ from the Propositions 5.4.1, 6.1.7 and Corollary 6.1.8, by accepting a slightly slower rate than $n^{1/2}$.

We close this chapter by providing density plots for estimating the parameter α'. Figure 6.2 shows a comparison between the empirical distribution of each case and the asymptotic normal distribution as described in Proposition 6.2.3. The left panel shows the simulation results for a true pure damping parameter of $\alpha' = 4/10$, the middle panel displays the results for $\alpha' = 1/2$, and the right panel presents the results for $\alpha' = 6/10$. To account for structural bias in the data, we centred the data by employing the sample mean of the corresponding estimates. To estimate the damping parameter, we adopted a spatial threshold of $\delta = 0.05$, resulting in the usage of 81 spatial coordinates for estimation. The parameter choices employed for the two-dimensional SPDE model are consistent with the simulation study presented earlier for the previous estimators, cf. Sections 5.4 and 6.1.3. All three scenarios exhibit a significant fit, where we observe a qualitative difference between lower and higher values for $\alpha' \in (0,1)$. This distinction can be attributed to the fact that α governs the Hölder regularity of the temporal marginal processes. Lower values of α result in rougher paths, thereby yielding a more accurate fit. The sample means of the estimates are given by 0.393 for $\alpha' = 4/10$, 0.484 for $\alpha' = 1/2$ and 0.554 for $\alpha' = 6/10$. Additionally, we provide the corresponding QQ-plots in Figure B.4, which can be found in Appendix B.

7. Conclusion and outlook

We conclude this thesis by providing a summary of the research conducted in both parts of the thesis. We will integrate the outcomes into the pre-existing body of knowledge concerning SPDEs, and identify potential areas for further exploration in both sections.

7.1. One-Dimensional Stochastic Partial Differential Equation

The research undertaken in the first part of the thesis centres on SPDEs within a one-dimensional space, with a primary focus on refining established estimation techniques for the natural parameters of the model from equation (1), namely the curvature parameter κ and the normalized volatility parameter σ_0^2.

Addressing the lack of comprehensive exploration into efficient estimators for the curvature parameter, we devised an oracle estimator denoted as $\hat{\kappa}$ using the maximum likelihood method. To address estimation of both natural parameters, we established a bridge between realized volatility as the foundation for our estimation challenges and the framework of the linear model. This connection allowed us to successfully apply statistical methodologies rooted in the linear model to SPDE models by incorporating log-realized volatilities. Consequently, central limit theorems were established for our novel estimators: $\hat{\kappa}$, $\hat{\varkappa}$, and $\hat{\sigma_0^2}$, all of which displayed optimal rates of convergence.

Although existing M-estimators, as introduced by Bibinger and Trabs (2020), were employed by many researchers to estimate the parameter $\eta = (\sigma_0^2, \kappa)$, our findings revealed the substantial advancements offered by our novel estimators. These estimators notably exhibit smaller asymptotic variances and the added benefit of explicit functional representation. Additionally, we demonstrated the feasibility of deriving asymptotic confidence intervals for the parameter κ as the asymptotic variances are given by known constants. The use of a variance-stabilizing transformation of the realized volatilities also allowed us to construct asymptotic confidence intervals for the parameter σ_0^2.

Furthermore, the extensively studied and well-understood linear model framework offers a wide range of statistical methods, such as χ^2-tests and F-tests. These methods provide an avenue to establish deeper connections between SPDE models and linear models. Future research has the potential to strengthen these linkages, where the foundations for proving such connections are laid out in this thesis.

In conclusion, this research advances the understanding and application of estimation techniques for SPDEs within a one-dimensional space and contributes to the existing literature by not only offering enhanced estimation techniques but also by establishing connections between disparate statistical fields.

7.2. Multi-Dimensional Stochastic Partial Differential Equation

While extensive research has been conducted on one-dimensional SPDE models over the past decades, the exploration of SPDEs in multiple spatial dimensions remains considerably limited. Our contribution to this emerging field involves establishing a theoretical framework for a general d-dimensional space and pioneering initial estimators for the natural parameters: σ_0^2, $\kappa_1, \ldots, \kappa_d$, and α'.

Our approach is based on the notion of linking multi-dimensional SPDE models to multiple linear regression models. We demonstrated the practicality of this idea by central limit theorems for the respective estimators and constructed asymptotic confidence intervals for the natural parameters of the multi-dimensional model. Furthermore, we embarked on investigating the identifiability of the damping parameter α, a concept that arises in multi-dimensional contexts, and successfully derived a corresponding central limit theorem. Hence, we have successfully demonstrated that key concepts from the one-dimensional space can be transferred to multiple space dimensions, thereby providing the basis for extending these linkages in future research.

Although we have laid the foundational groundwork, the field of multi-dimensional SPDEs offers ample avenues for further exploration and investigation. One intriguing technical question that remains unresolved surfaced during our analysis of the replacement method for multi-dimensional SPDEs in Section 4.3. In this context, we proposed a numerical approximation for the variance $s_{\mathbf{m}}$ of replacement centred normal random variables. While this approach introduced a bias into the simulations, we outlined a method to derive an exact determination of the variance $s_{\mathbf{m}}$ in this outlook section.

We continue with the notations and the equidistant observation scheme in time and space, as introduced in Section 4.3. Let X_t^{st} denote a solution of the random field from equation (49) with a stationary initial condition, i.e., $\langle \xi, e_{\mathbf{k}} \rangle_\vartheta \sim \mathcal{N}(0, \sigma^2/(2\lambda_{\mathbf{k}}^{1+\alpha}))$. Furthermore, let $x_{\mathbf{k}}^{\text{st}}$ be the corresponding coordinate processes for $\mathbf{k} \in \mathbb{N}^d$. According to equation (78), it holds that

$$\mathbb{V}\text{ar}\big(x_{\mathbf{k}}^{\text{st}}(t)\big) = \frac{\sigma^2}{2\lambda_{\mathbf{k}}^{1+\alpha}}.$$

Thus, we have

$$\begin{aligned}\sum_{\mathbf{l} \in \mathcal{I}_{\mathbf{m}}} \frac{\sigma^2}{2\lambda_{\mathbf{l}}^{1+\alpha}} &= \mathbb{V}\text{ar}(\langle X_t^{\text{st}}, e_{\mathbf{m}} \rangle_{\vartheta, M}) = \mathbb{V}\text{ar}\bigg(\frac{1}{M^d} \sum_{\mathbf{j} \in \mathcal{J}} X_t^{\text{st}}(\mathbf{y_j}) e_{\mathbf{m}}(\mathbf{y_j}) e^{||\kappa \boldsymbol{\cdot} \mathbf{y_j}||_1}\bigg) \\ &= \frac{1}{M^{2d}} \sum_{\mathbf{j}_1, \mathbf{j}_2 \in \mathcal{J}} e_{\mathbf{m}}(\mathbf{y}_{\mathbf{j}_1}) e_{\mathbf{m}}(\mathbf{y}_{\mathbf{j}_2}) e^{||\kappa \boldsymbol{\cdot} \mathbf{y}_{\mathbf{j}_1}||_1} e^{||\kappa \boldsymbol{\cdot} \mathbf{y}_{\mathbf{j}_2}||_1} \mathbb{C}\text{ov}\big(X_t^{\text{st}}(\mathbf{y}_{\mathbf{j}_1}), X_t^{\text{st}}(\mathbf{y}_{\mathbf{j}_2})\big),\end{aligned}$$

where $\mathbf{y_j} = \mathbf{j}/M$. The covariance of X_t^{st} in two different spatial points can be represented as follows:

$$\begin{aligned}\mathbb{C}\text{ov}\big(X_t^{\text{st}}(\mathbf{y}_1),\ X_t^{\text{st}}(\mathbf{y}_2)\big) &= \sum_{\mathbf{k} \in \mathbb{N}^d} e_{\mathbf{k}}(\mathbf{y}_1) e_{\mathbf{k}}(\mathbf{y}_2) \mathbb{V}\text{ar}\big(x_{\mathbf{k}}^{\text{st}}(t)\big) \\ &= \sigma^2 \sum_{\mathbf{k} \in \mathbb{N}^d} e_{\mathbf{k}}(\mathbf{y}_1) e_{\mathbf{k}}(\mathbf{y}_2) \frac{1}{2\lambda_{\mathbf{k}}^{1+\alpha}} \\ &= 2^{d-1} \sigma^2 e^{-||\kappa \boldsymbol{\cdot} (\mathbf{y}_1 + \mathbf{y}_2)||_1/2} \sum_{\mathbf{k} \in \mathbb{N}^d} \frac{1}{\lambda_{\mathbf{k}}^{1+\alpha}} \prod_{l=1}^d \sin(\pi k_l j_l^{(1)}/M) \sin(\pi k_l j_l^{(2)}/M).\end{aligned}$$

Defining the constant

$$\Lambda := (\pi^2\eta)^{-1}\left(\frac{||\nu||_2^2}{4\eta} - \vartheta_0\right) \qquad \text{and} \qquad a_l := (j_l^{(1)} + j_l^{(2)})/M,$$

results in analysing the following term:

$$\mathrm{Im}\left(\sum_{\mathbf{k}\in\mathbb{N}^d} \frac{\prod_{l=1}^d e^{\mathrm{i}\pi k_l a_l}}{(k_1^2 + \ldots + k_d^2 + \Lambda)^{1+\alpha}}\right).$$

Exploring a "closed" expression for this latter series could become the focus of forthcoming inquiries. Achieving such a closed form, as demonstrated by Hildebrandt (2020) for one-dimensional space, would not only significantly accelerate simulation runtimes and potentially yield nearly unbiased results, but opens up a novel avenue for investigating SPDEs in multiple spatial dimensions.

In Part II, we developed statistical methods under the assumption of observing the solution of the SPDE model from equation (49) through a high-frequency observation scheme. The understanding of the covariance structure of a mild solution X_t at two distinct spatial points introduces opportunities for exploring statistical inferences with deviating statistical assumptions. In the work by Hildebrandt and Trabs (2021), the investigation of SPDEs in one spatial dimension utilized space-time increments

$$(\delta_k X)(t_i) := X_{t_i}(y_k) - X_{t_i}(y_{k-1}),$$

offering novel statistical methodologies for estimating parameters of the one-dimensional SPDE model. The transferability of these ideas to higher spatial dimensions is conceivable, requiring the exploration of appropriate spatial coordinate selections.

As observed, the linkage between the linear model and multiple spatial dimensions establishes an opportunity to extend well-established techniques from linear models to SPDE models in this multi-dimensional context. One avenue involves the estimation of the damping parameter in combination with the log-linear model, akin to the approach highlighted in Section 6.2.1. Here, we can explore a statistic, represented by the equation

$$\begin{aligned}\log\left(\frac{\mathrm{RV}_n(\mathbf{y}_1)}{n}\right) - \log\left(\frac{\mathrm{RV}_{2n}(\mathbf{y}_2)}{2n}\right) &\approx \alpha'\big(\log(\Delta_n) - \log(\Delta_{2n})\big) - ||\kappa \bullet (\mathbf{y}_1 - \mathbf{y}_2)||_1 + \sqrt{\frac{\Upsilon_{\alpha'}}{n}}Z_1 - \sqrt{\frac{\Upsilon_{\alpha'}}{2n}}Z_2 \\ &= \alpha' \log(1/2) - ||\kappa \bullet (\mathbf{y}_1 - \mathbf{y}_2)||_1 + \sqrt{\frac{\Upsilon_{\alpha'}}{n}}Z_1 - \sqrt{\frac{\Upsilon_{\alpha'}}{2n}}Z_2,\end{aligned}$$

where $\mathbf{y}_1$ and $\mathbf{y}_2$ represent distinct spatial points, and Z_1 and Z_2 denote normal random variables. This approach not only enables the estimation of the pure damping parameter α' but also enables simultaneous estimation of the curvature parameter $\kappa = (\kappa_1, \ldots, \kappa_d)$. Conversely, employing this approach necessitates a full-rank assumption akin to Assumption 6.1.2.

Nevertheless, numerous other intriguing research areas await exploration in this nascent field. While constructing an oracle estimator for the volatility parameter σ^2, our findings showcased a connection to the one-dimensional case. Thus, it is plausible that estimation methods like those presented by Bibinger and Trabs (2020) could be applicable to estimate the integrated volatility $\int_0^1 \sigma_s^2\,\mathrm{d}s$ for a time-dependent volatility σ_s within a semi-parametric framework.

In conclusion, Part II of this thesis accomplishes the objective to extend the exploration of SPDEs to multiple spatial dimensions. As the field advances and more complex models are needed to capture real-world phenomena, our work provides a bridge between theory and application in this area. By developing a comprehensive statistical framework within the context of linear, second-order SPDEs with additive noise, we addressed the challenges and complexities that emerge in multiple dimensions. We proved that the statistical theory for one-dimensional SPDEs can be successfully extended to multiple space dimensions and provided a link to the linear model, enabling a wide range of statistical methods to multi-dimensional SPDEs. We anticipate that the groundwork established in this second part of the thesis will make a valuable contribution to future research extending beyond linear parabolic SPDE models with additive noise.

Part III.

Appendices

Appendix A. Notations

A.1. General Notations

In this thesis, we adopt the standard symbols for the sets of natural and real numbers, represented as $\mathbb{N} = \{1, 2, \ldots\}$ and $\mathbb{R}$, respectively. The set of all positive real numbers is denoted by $\mathbb{R}^+ = (0, \infty)$, where the set of non-negative real numbers is denoted as $\mathbb{R}_0^+ = [0, \infty)$. Similarly, we refer to the non-negative integers as $\mathbb{N}_0 = \mathbb{N} \cup \{0\}$. The set of all even natural numbers is given by $2\mathbb{N} = \{0, 2, 4, \ldots\}$, while the set of all odd natural numbers is represented as $(2\mathbb{N})^\complement$. Moreover, we employ $\mathbb{R}^d$ to represent the set of real numbers in d-dimensions, and $\mathbb{R}^{n \times m}$ to denote the set of all real-valued matrices with dimension $n \times m$, where $d, n, m \in \mathbb{N}$. Additionally, we define $A \times B = \{(a, b) | a \in A, b \in B\}$ for any sets A and B. For $\mathbf{x} \in \mathbb{R}^d$, we use the notation $\mathbf{x}^\top$ to denote the transpose of the vector $\mathbf{x}$.

For real numbers $a, b \in \mathbb{R}$ we denote the minimum and maximum operator as $a \wedge b := \min(a, b)$ and $a \vee b := \max(a, b)$, respectively. The expression $(a_n) \equiv a$ signifies that a sequence $(a_n)_{n \in \mathbb{N}}$ is identical to a certain real number $a \in \mathbb{R}$, for all $n \in \mathbb{N}$. We employ the notation $\mathbb{1}_A$ to denote the indicator function associated with a set A. Furthermore, when dealing with sums and products where the lower limit is greater than the upper limit, we employ the empty sum and empty product convention, i.e., $\sum_{k=a}^{b} c_k = 0$ and $\prod_{k=a}^{b} c_k = 1$, where $a, b \in \mathbb{N}$, with $a > b$ and a sequence $(c_k)_{k \in \mathbb{N}}$. Improper integrals are indicated as $\int_a^\infty f(x)\,\mathrm{d}x$ or alternatively as $[f]_0^\infty$ if the function f is integrable on the interval (a, ∞). Furthermore, we state that $f \in \mathcal{L}^p(A)$, if the expression $(\int_A |f(x)|^p \,\mathrm{d}x)^{1/p} < \infty$ is finite, where $p \in \mathbb{R}^+$. Consider a function $f : D \to \mathbb{R}$, with $D \subset \mathbb{R}$. In this context, the first and second derivatives are represented as f' and f'', respectively. Moreover, we employ the notation $f^{(n)}$ to indicate the n-th derivative. We consider a set $D \subset \mathbb{R}^d$ and a function $f : D \to \mathbb{R}$. In this context, ∇f represents the gradient of function f and H_f the Hessian matrix.
For two sequences a_n and b_n, the notation $a_n \propto b_n$ is employed, when $|a_n/b_n| \overset{n\to\infty}{\longrightarrow} C$, for a constant $0 < C < \infty$. Moreover, we utilize the notation $A_n = \mathcal{O}(B_n)$, when a constant $C > 0$ and a natural number $n_0 \in \mathbb{N}$ exist, such that $|A_n| \leqslant CB_n$ holds for all $n \geqslant n_0$. The constant C in this definition remains unaffected by the spatial and temporal resolutions m and n, cf. Assumptions 1.1.1 and 4.1.1, and is in particular independent of potential indices $1 \leqslant i \leqslant n$ and $1 \leqslant j \leqslant m$.

The abbreviation i.i.d., used in conjunction with random variables $X_1, \ldots, X_n \sim X$, signifies that the random variables $(X_i)_{i \in I}$, for a index set I, are independent and identically distributed with a distribution corresponding to the distribution of the random variable X. The normal distribution is represented as $\mathcal{N}(\mu, \Sigma)$, where $\mu \in \mathbb{R}^d$ is referred to as the expected value, and $\Sigma \in \mathbb{R}^{d \times d}$ is a symmetric positive definite covariance matrix, for $d \in \mathbb{N}$. In the case where $d = 1$, we consider a univariate normal distribution, with $\Sigma = \sigma^2 > 0$ representing the variance. Moreover, we state that $X \in \mathcal{L}^p$ if the random variable X is measurable and it holds that $\left(\int_\Omega |X|^p \,\mathrm{d}\mathbb{P}\right)^{1/p} < \infty$ remains finite. For a random variable $X \in \mathcal{L}$ that is integrable, we define the compensated random variable as $\bar{X} := X - \mathbb{E}[X]$.

We use the symbols $\xrightarrow{\mathbb{P}}$ and $\xrightarrow{d}$ to represent convergence in probability and convergence in distribution, respectively. Consider two random variables X and Y defined on the same probability space $(\Omega, \mathcal{A}, \mathbb{P})$. We express $X = Y$ almost surely ($X = Y$ a.s.) when the probability $\mathbb{P}(X = Y) = 1$. The symbol $\mathcal{O}_{\mathbb{P}}$ denotes the stochastic equivalent of the Landau notation. Let $(X_n)_{n\in\mathbb{N}}$ be a sequence of random variables defined on a probability space $(\Omega, \mathcal{A}, \mathbb{P})$. The notation $X_n = \mathcal{O}_{\mathbb{P}}(a_n)$ holds, when considering a positive sequence $(a_n)_{n\in\mathbb{N}}$ and for all $\varepsilon > 0$, there exists a $C > 0$ and a $n_0 \in \mathbb{N}$ such that $\mathbb{P}(|X_n/a_n| \geqslant C) \leqslant \varepsilon$ for all $n \geqslant n_0$. Similarly, we use the notation $X_n = o_{\mathbb{P}}(a_n)$ to convey that the ratio $X_n/a_n \xrightarrow{\mathbb{P}} 0$, as $n \to \infty$.

Consistently, we will use the notation $\hat{\vartheta}$ to refer to an estimator for an unknown parameter ϑ. While constructing estimators based on discrete spatiotemporal data, we employ both notations $\hat{\vartheta}_{n,m}$ and $\hat{\vartheta}$ for the same estimator. Assume an estimator $\hat{\vartheta}$, for which a central limit theorem applies, i.e., $a_n(\hat{\vartheta}_n - \vartheta) \xrightarrow{d} \mathcal{N}(0, \sigma^2)$, as $n \to \infty$ and a sequence $(a_n)_{n\in\mathbb{N}}$. In this context, we represent the asymptotic variance as $\mathrm{AVAR}(\hat{\vartheta}_n) = \lim_{n\to\infty} \mathbb{V}\mathrm{ar}(a_n \hat{\vartheta}_n) = \sigma^2$.

The subsequent sections address more detailed notations, distinguishing between those utilized in Part I and Part II of this thesis, as well as notations that are specifically employed within a particular chapter of this thesis.

A.2. Notational conventions in Part I

ϑ	$(\vartheta_0, \vartheta_1, \vartheta_2)^\top \in \mathbb{R}^2 \times (0, \infty)$
σ	Volatility parameter, $\sigma \in (0, \infty)$
A_ϑ	Differential operator, $\vartheta_0 + \vartheta_1 \frac{\partial}{\partial y} + \vartheta_2 \frac{\partial^2}{\partial y^2}$
H_ϑ	Hilbert space, $\{f : [0,1] \to \mathbb{R} : \|\|f\|\|_\vartheta < \infty, f(0) = f(1) = 0\}$
$\langle f, g\rangle_\vartheta$	Inner product, $\int_0^1 \exp\big[\frac{\vartheta_1}{\vartheta_2} y\big] f(y) g(y)\,\mathrm{d}y$, for $f, g \in H_\vartheta$
$\|f\|_\vartheta$	Norm, $\langle f, f\rangle_\vartheta$, for $f \in H_\vartheta$
$e_k(y)$	Eigenfunctions, $\sqrt{2}\sin(\pi k y)\exp\big[-\frac{\vartheta_1}{2\vartheta_2} y\big]$
λ_k	Eigenvalues, $-\vartheta_0 + \frac{\vartheta_1^2}{4\vartheta_2} + \vartheta_2 \pi^2 k^2$, for $k \in \mathbb{N}$
$x_k(t)$	Coordinate processes, $e^{-t\lambda_k}\langle \xi, e_k\rangle_\vartheta + \int_0^t e^{-\lambda_k(t-s)} \sigma_s \,\mathrm{d}B_s^k$, for $k \in \mathbb{N}$
$X_t(y)$	Mild solution of equation (1), $\sum_{k=1}^\infty x_k(t) e_k(y)$
$\tilde{X}_t(y)$	Mild solution with stationary initial condition, $\langle \xi, e_k\rangle_\vartheta \sim \mathcal{N}(0, \sigma^2/(2\lambda_k))$, $k \in \mathbb{N}$
B_t	Cylindrical Brownian motion, $\langle B_t, f\rangle_\vartheta = \sum_{k=1}^\infty \langle f, e_k\rangle_\vartheta W_t^k$
W_t^k	Independent Brownian motions for each $k \in \mathbb{N}$

ξ	Initial condition of equation (1), $\xi \in H_\vartheta$
δ	Spatial boundary, $\delta \in (0,1/2)$
Δ_n	Temporal resolution, $\Delta_n = 1/n$, $n \in \mathbb{N}$
ρ	Relationship of temporal and spatial observations, $\rho \in (0,1/2)$
κ	Curvature parameter of equation (1), $\kappa = \vartheta_1/\vartheta_2$
σ_0^2	Normalized volatility parameter of equation (1), $\sigma_0^2 = \sigma^2/\sqrt{\vartheta_2}$
$(\Delta_i X)(y)$	Temporal increment, $X_{i\Delta_n}(y) - X_{(i-1)\Delta_n}(y)$
$\mathrm{RV}_n(y)$	Realized volatility, $\sum_{i=1}^n (\Delta_i X)^2(y)$
Γ	Constant of covariances, $\Gamma \approx 0.75$
Ξ	Triangular array of a respective estimator, $\Xi_{n,i} = \xi_{n,i} - \mathbb{E}[\xi_{n,i}]$
$V_{p,\Delta_n}(y)$	Exponentially rescaled realized volatility, $\frac{1}{p\sqrt{\Delta_n}} \sum_{i=1}^p (\Delta_i \tilde{X})^2(y) e^{y\kappa}$

Chapter 2

$\hat{\kappa}_{n,m}$	Oracle curvature estimator, $\frac{-\sum_{j=1}^m \ln\left(\frac{\mathrm{RV}_n(y_j)}{\sqrt{n}}\right) y_j + \sum_{j=1}^m \ln\left(\frac{\sigma_0^2}{\sqrt{\pi}}\right) y_j}{\sum_{j=1}^m y_j^2}$
$\hat{\varkappa}_{n,m}$	Non-oracle curvature estimator, $\frac{\sum_{j\neq l} \ln\left(\frac{\mathrm{RV}_n(y_j)}{\mathrm{RV}_n(y_l)}\right)(y_l - y_j)}{\sum_{j\neq l}(y_j - y_l)^2}$
$\xi_{n,i}^{\sigma_0^2}$	$-\frac{\sqrt{m_n \pi}}{\sigma_0^2 \sum_{i=1}^{m_n} y_i^2} \sum_{j=1}^{m_n} (\Delta_i \tilde{X})^2(y_j) e^{y_j \kappa} y_j$
$\xi_{n,i}$	$\frac{\sqrt{m_n \pi}}{\sigma_0^2 \sum_{j\neq l}(y_j - y_l)^2} \sum_{j\neq l} \left((\Delta_i \tilde{X})^2(y_j) e^{\kappa y_j} - (\Delta_i \tilde{X})^2(y_l) e^{\kappa y_l}\right)(y_l - y_j)$
$\mathcal{F}_\alpha$	$\{f_\vartheta : \mathbb{N} \to \mathbb{R} \mid \exists C_\vartheta > 0 : f_\vartheta^2(m) \leqslant C_\vartheta m^{-(\alpha+1)}\}$
$\mathcal{G}_\alpha$	$\{g_\vartheta : \mathbb{N} \to \mathbb{R} \mid \exists C_\vartheta > 0 : \lvert g_\vartheta(m)\rvert \leqslant C_\vartheta m^{\alpha/2}$ uniformly in $m \in \mathbb{N}\}$
$\mathcal{H}_\alpha$	$\big\{(Z_{n,i}) : Z_{n,i} = \zeta_{n,i} - \mathbb{E}[\zeta_{n,i}], \zeta_{n,i} = f_\vartheta(m) \sum_{j=1}^m (\Delta_i \tilde{X})^2(y_j) g_\vartheta(j),$ with $f_\vartheta \in \mathcal{F}_\alpha, g_\vartheta \in \mathcal{G}_\alpha\big\}$
η	Parameter, $(\sigma_0^2, \kappa)^\top$
$\hat{\eta}_{n,m}$	M-Estimator for η, $\arg\min_{s,k} \sum_{j=1}^m \left(Z_j - f_{s,k}(y_j)\right)^2$

Chapter 3

ϱ	$\ln(\sigma_0^2/\pi)$
ν	Parameter, $(\varrho,\kappa)^\top$
$\mathcal{G}_\alpha^d$	$\{g_\vartheta:\mathbb{N}\to\mathbb{R}^d \mid \lvert\beta^\top g_\vartheta(m)\rvert\leqslant C_\vartheta\lVert\beta\rVert_\infty m^{\alpha/2}$ uniformly in $m\in\mathbb{N}, C_\vartheta>0\}$
$\mathcal{H}_\alpha^d$	$\big\{(Z_{n,i})_{1\leqslant i\leqslant n,n\in\mathbb{N}}: Z_{n,i}=\zeta_{n,i}-\mathbb{E}[\zeta_{n,i}]$ and $\zeta_{n,i}=f_\vartheta(m)\sum_{j=1}^m(\Delta_i\tilde{X})^2(y_j)g_\vartheta(j)$, where $f_\vartheta\in\mathcal{F}_\alpha, g_\vartheta\in\mathcal{G}_\alpha^d\big\}$
$\hat{\varrho}$	$\frac{\left(\sum_{j=1}^m y_j\right)\left(\sum_{j=1}^m \ln\left(\frac{\mathrm{RV}_n(y_j)}{\sqrt{n}}\right)y_j\right)-\left(\sum_{j=1}^m \ln\left(\frac{\mathrm{RV}_n(y_j)}{\sqrt{n}}\right)\right)\left(\sum_{j=1}^m y_j^2\right)}{\left(\sum_{j=1}^m y_j\right)^2-m\sum_{j=1}^m y_j^2}$
$\hat{\sigma}_0^2$	$e^{\hat{\varrho}}/\sqrt{\pi}$
$\hat{\nu}$	$(\hat{\varrho},\hat{\varkappa})^\top$
$\xi_{n,i}$	$\frac{\sqrt{m_n\pi}}{\sigma_0^2((\sum_{j=1}^{m_n}y_j)^2-m_n\sum_{j=1}^{m_n}y_j^2)}\sum_{j=1}^{m_n}(\Delta_i\tilde{X})^2(y_j)e^{\kappa y_j}\begin{pmatrix}\left(\sum_{l=1}^{m_n}y_l\right)y_j-\sum_{l=1}^{m_n}y_l^2\\ m_ny_j-\sum_{l=1}^{m_n}y_l\end{pmatrix}$
G_j^β	$G_j^{\beta_1}+G_j^{\beta_2}:=\beta_1\big((\sum_{l=1}^{m_n}y_l)y_j-\sum_{l=1}^{m_n}y_l^2\big)+\beta_2\big(m_ny_j-\sum_{l=1}^{m_n}y_l\big)$

A.3. Notational conventions in Part II

d	Spatial dimension, $d\in\mathbb{N}$, with $d\geqslant 2$
ϑ	$(\vartheta_0,\nu_1,\dots,\nu_d,\eta)^\top\in\mathbb{R}^{d+1}\times(0,\infty)$
σ	Volatility parameter, $\sigma\in(0,\infty)$
α,α'	Damping and pure damping parameter, $\alpha=d/2-1+\alpha'$ and $\alpha'\in(0,1)$
A_ϑ	Differential operator, $\eta\sum_{l=1}^d\frac{\partial}{\partial y_l^2}+\sum_{l=1}^d\nu_l\frac{\partial}{\partial y_l}+\vartheta_0$
H_ϑ	Hilbert space, $\{f:[0,1]^d\to\mathbb{R}, \lVert f\rVert_\vartheta<\infty$ and $f(\mathbf{y})=0,$ for $\mathbf{y}\in\partial[0,1]^d\}$
$\langle f,g\rangle_\vartheta$	Inner product, $\int_0^1\cdots\int_0^1 f(y_1,\dots,y_d)g(y_1,\dots,y_d)\exp\left[\sum_{l=1}^d\kappa_ly_l\right]\mathrm{d}y_1\cdots\mathrm{d}y_d$, for $f,g\in H_\vartheta$
$\lVert f\rVert_\vartheta$	Norm, $\langle f,f\rangle_\vartheta$, for $f\in H_\vartheta$
$e_{\mathbf{k}}(\mathbf{y})$	Eigenfunctions, $2^{d/2}\prod_{l=1}^d\sin(\pi k_ly_l)e^{-\kappa_ly_l/2}$, for $\mathbf{k}\in\mathbb{N}^d$
λ_k	Eigenvalues, $-\vartheta_0+\sum_{l=1}^d\left(\frac{\nu_l^2}{4\eta}+\pi^2k_l^2\eta\right)$, for $\mathbf{k}\in\mathbb{N}^d$

$x_{\mathbf{k}}(t)$	Coordinate processes, $e^{-\lambda_{\mathbf{k}}t}\langle \xi, e_{\mathbf{k}}\rangle_\vartheta + \sigma\lambda_{\mathbf{k}}^{-\alpha/2}\int_0^t e^{-\lambda_{\mathbf{k}}(t-s)}\,\mathrm{d}W_s^{\mathbf{k}}$, for $\mathbf{k} \in \mathbb{N}^d$
$X_t(y)$	Mild solution of equation equation (49), $\sum_{\mathbf{k}\in\mathbb{N}^d} x_{\mathbf{k}}(t)e_{\mathbf{k}}(y)$
$\tilde{X}_t(y)$	As X_t with stationary initial condition, $\langle \xi, e_{\mathbf{k}}\rangle_\vartheta \sim \mathcal{N}(0, \sigma^2/(2\lambda_{\mathbf{k}}^{1+\alpha}))$
B_t	Cylindrical Brownian motion, $\langle B_t, f\rangle_\vartheta := \sum_{\mathbf{k}\in\mathbb{N}^d} \lambda_{\mathbf{k}}^{-\alpha/2}\langle f, e_{\mathbf{k}}\rangle_\vartheta W_t^{\mathbf{k}}$
W_t^k	Independent Brownian motions for each $\mathbf{k} \in \mathbb{N}^d$
ξ	Initial condition of from equation (49), $\xi \in H_\vartheta$
δ	Spatial boundary, $\delta \in (0, 1/2)$
Δ_n	Temporal resolution, $\Delta_n = 1/n$, $n \in \mathbb{N}$
ρ	Relationship of temporal and spatial observations, $\rho \in \big(0, (1-\alpha')/(d+2)\big)$
κ	Curvature parameter, $\kappa = (\kappa_1, \ldots, \kappa_d)$, where $\kappa_l = \nu_l/\eta$, $l = 1, \ldots, d$
σ_0^2	Normalized volatility parameter, $\sigma_0^2 = \sigma^2/\sqrt{\vartheta_2}$
∂A	Boundary of the set $A \subset \mathbb{R}^d$
$\int_A f(\mathbf{x})\,\mathrm{d}\mathbf{x}$	d-dimensional Integral, $A \subset \mathbb{R}^d$
$\sum_{\mathbf{k}\in\mathbb{N}^d} a_{\mathbf{k}}$	d-dimensional series, $a_{\mathbf{k}} : \mathbb{N}^d \to \mathbb{R}$
$\lVert\mathbf{x}\rVert_0$	Function, $\min_{\substack{i=1,\ldots,d\\ x_i\neq 0}}\{\lvert x_1\rvert, \ldots, \lvert x_d\rvert\}$, $\mathbf{x} \in \mathbb{R}^d$
$\lVert\mathbf{x}\rVert_1$	Function $\sum_{l=1}^d x_l$, $\mathbf{x} \in \mathbb{R}^d$
$\lVert\mathbf{x}\rVert_2$	Norm, $\big(\sum_{l=1}^d x_l^2\big)^{1/2}$, $\mathbf{x} \in \mathbb{R}^d$
$\lVert\mathbf{x}\rVert_\infty$	Norm, $\max_{l=1,\ldots,d} \lvert x_l\rvert$, $\mathbf{x} \in \mathbb{R}^d$
$\lVert f\rVert_{\mathcal{L}^p(D)}$	Norm, $\big(\int_D \lvert f(x)\rvert^p\,\mathrm{d}x\big)^{1/p}$, $D \subset \mathbb{R}$
$\mathbf{x} \bullet \mathbf{y}$	Component-wise product, $\mathbf{x} \bullet \mathbf{y} = (x_1y_1, \ldots, x_dy_d)$, $\mathbf{x}, \mathbf{y} \in \mathbb{R}^d$
$y_l^{(j)}$	l-th component of the j-th observation
$\lvert J_d\rvert$	Determinant, $\prod_{l=1}^{d-2} r^{d-1}\sin^{d-1-l}(\varphi_l)$
$\Gamma(z)$	Gamma function, $\int_0^\infty t^{z-1}e^{-t}\,\mathrm{d}t$, $\mathrm{Re}(z) \notin \{0, -1, -2, \ldots\}$
$\Upsilon_{\alpha'}$	Constant of covariances, $\big(\sum_{r=0}^\infty \big(-r^{\alpha'} + 2(r+1)^{\alpha'} - (r+2)^{\alpha'}\big)^2 + 2\big)$, $\alpha' \in (0,1)$
K	Constant, $\frac{2^d(\pi\eta)^{d/2}\alpha'\Gamma(d/2)}{\Gamma(1-\alpha')}$

$A_{i,\mathbf{k}}$	Increment decomposition, $\langle \xi, e_{\mathbf{k}}\rangle_\vartheta \big(e^{-\lambda_{\mathbf{k}} i\Delta_n} - e^{-\lambda_{\mathbf{k}}(i-1)\Delta_n}\big)$
$\tilde{A}_{i,\mathbf{k}}$	Increment decomposition, $\sigma\lambda_{\mathbf{k}}^{-\alpha/2}\int_{-\infty}^{0} e^{-\lambda_{\mathbf{k}}((i-1)\Delta_n - s)}\big(e^{-\lambda_{\mathbf{k}}\Delta_n} - 1\big)\,\mathrm{d}W_s^{\mathbf{k}}$
$B_{i,\mathbf{k}}$	Increment decomposition, $\sigma\lambda_{\mathbf{k}}^{-\alpha/2}\int_{0}^{(i-1)\Delta_n} e^{-\lambda_{\mathbf{k}}((i-1)\Delta_n - s)}\big(e^{-\lambda_{\mathbf{k}}\Delta_n} - 1\big)\,\mathrm{d}W_s^{\mathbf{k}}$
$\tilde{B}_{i,\mathbf{k}}$	Increment decomposition, $\sigma\lambda_{\mathbf{k}}^{-\alpha/2}\int_{-\infty}^{(i-1)\Delta_n} e^{-\lambda_{\mathbf{k}}((i-1)\Delta_n - s)}\big(e^{-\lambda_{\mathbf{k}}\Delta_n} - 1\big)\,\mathrm{d}W_s^{\mathbf{k}}$
$C_{i,\mathbf{k}}$	Increment decomposition, $\sigma\lambda_{\mathbf{k}}^{-\alpha/2}\int_{(i-1)\Delta_n}^{i\Delta_n} e^{-\lambda_{\mathbf{k}}(i\Delta_n - s)}\,\mathrm{d}W_s^{\mathbf{k}}$
$\Sigma_{i,j}^{B,\mathbf{k}}$	Covariance, $\sigma^2\big(e^{-\lambda_{\mathbf{k}}\Delta_n\lvert i-j\rvert} - e^{-\lambda_{\mathbf{k}}(i+j-2)\Delta_n}\big)\frac{(1-e^{-\lambda_{\mathbf{k}}\Delta_n})^2}{2\lambda_{\mathbf{k}}^{1+\alpha}}$
$\tilde{\Sigma}_{i,j}^{B,\mathbf{k}}$	Covariance, $\frac{\sigma^2}{2\lambda_{\mathbf{k}}^{1+\alpha}}\big(e^{-\lambda_{\mathbf{k}}\Delta_n} - 1\big)^2 e^{-\lambda_{\mathbf{k}}\Delta_n\lvert i-j\rvert}$
$\Sigma_{i,j}^{C,\mathbf{k}}$	Covariance, $\mathbb{1}_{\{j=i\}}\sigma^2\frac{1-e^{-2\lambda_{\mathbf{k}}\Delta_n}}{2\lambda_{\mathbf{k}}^{1+\alpha}}$
$\Sigma_{i,j}^{BC,\mathbf{k}}$	Covariance, $\mathbb{1}_{\{i<j\}}\sigma^2 e^{-\lambda_{\mathbf{k}}\Delta_n(j-i)}\big(e^{\lambda_{\mathbf{k}}\Delta_n} - e^{-\lambda_{\mathbf{k}}\Delta_n}\big)\frac{e^{-\lambda_{\mathbf{k}}\Delta_n}-1}{2\lambda_{\mathbf{k}}^{1+\alpha}}$

Chapter 4

B_γ	$\{x \in [0,\infty)^d \mid x_1 \in \psi^{-1}(\gamma_1),\dots,x_d \in \psi^{-1}(\gamma_d)\} \subset [0,\infty)^d$
$f_\alpha(x)$	$\frac{1-e^{-x}}{x^{1+\alpha}}$
$g_{\alpha,\tau}(x)$	$\frac{(1-e^{-x})^2}{2x^{1+\alpha}}e^{-\tau x}$
$\mathcal{Q}_\beta$	$\big\{f:[0,\infty)\to\mathbb{R} \mid f$ twice differentiable, $\lVert x^{d-1}f(x^2)\rVert_{\mathcal{L}^1([0,\infty))}$, $\lVert x^d f^{(1)}(x^2)\rVert_{\mathcal{L}^1([1,\infty))}$, $\lVert x^{d+1}f^{(2)}(x^2)\rVert_{\mathcal{L}^1([1,\infty))}$ and $\limsup_{x\to 0}\lvert f^{(j)}(x^2)/s^{-\beta_j}\rvert \leqslant C < \infty, j=0,1,2\big\}$, where $\beta=(\beta_0,\beta_1,\beta_2)\in(0,2\alpha]\times(0,2(\alpha+1)]\times(0,2(\alpha+2)]$
$\mathcal{D}_{i,\mathbf{k}}$	$\Delta_n^{d/2+\alpha'}\big(\frac{1-e^{-\lambda_{\mathbf{k}}\Delta_n}}{(\lambda_{\mathbf{k}}\Delta_n)^{1+\alpha}} - \frac{(1-e^{-\lambda_{\mathbf{k}}\Delta_n})^2}{2(\lambda_{\mathbf{k}}\Delta_n)^{1+\alpha}}e^{-2\lambda_{\mathbf{k}}(i-1)\Delta_n}\big)$

Chapter 5

$\hat{\sigma}_{\mathbf{y}}^2$	$\frac{2^d(\pi\eta)^{d/2}\alpha'\Gamma(d/2)}{n\Delta_n^{\alpha'}\Gamma(1-\alpha')}\sum_{i=1}^n(\Delta_i X)^2(\mathbf{y})e^{\lVert\kappa\cdot\mathbf{y}\rVert_1}$
$\hat{\sigma}_{n,m}^2$	$\frac{2^d(\pi\eta)^{d/2}\alpha'\Gamma(d/2)}{nm\Delta_n^{\alpha'}\Gamma(1-\alpha')}\sum_{j=1}^m\sum_{i=1}^n(\Delta_i X)^2(\mathbf{y}_j)e^{\lVert\kappa\cdot\mathbf{y}_j\rVert_1}$
$\xi_{n,i}$	$\frac{2^d(\pi\eta)^{d/2}\alpha'\Gamma(d/2)}{\sqrt{nm}\Delta_n^{\alpha'}\Gamma(1-\alpha')}\sum_{j=1}^m(\Delta_i X)^2(\mathbf{y}_j)e^{\lVert\kappa\cdot\mathbf{y}_j\rVert_1}$
$\tilde{\xi}_{n,i}$	$\frac{2^d(\pi\eta)^{d/2}\alpha'\Gamma(d/2)}{\sqrt{nm}\Delta_n^{\alpha'}\Gamma(1-\alpha')}\sum_{j=1}^m(\Delta_i \tilde{X})^2(\mathbf{y}_j)e^{\lVert\kappa\cdot\mathbf{y}_j\rVert_1}$

Chapter 6

Ψ	Parameter, $(\log(\sigma_0^2 K), -\kappa_1, \ldots, -\kappa_d)^\top \in \mathbb{R}^{d+1}$
υ	Natural Parameter, $\upsilon := (\sigma_0^2, \kappa_1, \ldots, \kappa_d)^\top \in (0,\infty) \times \mathbb{R}^d$
$h(\mathbf{x})$	Transformation $h : (0,\infty) \times \mathbb{R}^d \to \mathbb{R}^{d+1}$, $h(\mathbf{x}) = (\log(Kx_1), -x_2, \ldots, -x_{d+1})$
X	$\begin{pmatrix} 1 & y_1^{(1)} & \ldots & y_d^{(1)} \\ \vdots & \vdots & \ddots & \vdots \\ 1 & y_1^{(m)} & \ldots & y_d^{(m)} \end{pmatrix} \in \mathbb{R}^{m\times(d+1)}$
Y	$\big(\log\big(\frac{\mathrm{RV}_n(\mathbf{y}_1)}{n\Delta_n^{\alpha'}}\big), \ldots, \log\big(\frac{\mathrm{RV}_n(\mathbf{y}_m)}{n\Delta_n^{\alpha'}}\big)\big)^\top \in \mathbb{R}^m$
$\hat{\Psi}$	$(X^\top X)^{-1} X^\top Y \in \mathbb{R}^m$
$\hat{\upsilon}$	$h(\hat{\Psi})$
$\xi_{n,i}$	$\frac{\sqrt{n}(1-2\delta)}{\sqrt{m}K\sigma_0^2}\big(\frac{1-2\delta}{m}X^\top X\big)^{-1} X^\top \begin{pmatrix} \frac{(\Delta_i\tilde{X})^2(\mathbf{y}_1)}{n\Delta_n^{\alpha'}} e^{\lVert\kappa\bullet\mathbf{y}_1\rVert_1} \\ \vdots \\ \frac{(\Delta_i\tilde{X})^2(\mathbf{y}_m)}{n\Delta_n^{\alpha'}} e^{\lVert\kappa\bullet\mathbf{y}_m\rVert_1} \end{pmatrix}$
E_m	$m \times m$ identity matrix
$\mathbf{1}_{a,b}$	Matrix of ones, $\mathbf{1}_{a,b} = \{1\}^{a\times b}$
$(\Delta_{2n,i}X)(\mathbf{y})$	Temporal increments, $X_{i\Delta_{2n}} - X_{(i-1)\Delta_{2n}}$, $1 \leqslant i \leqslant 2n$
$(\Delta_{n,i}X)(\mathbf{y})$	Temporal increments on thinned grid, $X_{i\Delta_n} - X_{(i-1)\Delta_n}$, $1 \leqslant i \leqslant n$
$\mathrm{RV}_{2n}(\mathbf{y})$	Realized volatility, $\sum_{i=1}^{2n}(\Delta_{2n,i}X)^2(\mathbf{y})$
$\mathrm{RV}_n(\mathbf{y})$	Realized volatility on thinned grid, $\sum_{i=1}^{n}(\Delta_{n,i}X)^2(\mathbf{y})$
$\hat{\alpha}'_{2n,m}$	Estimator for the pure damping parameter α', $\frac{1}{\log(2)m}\sum_{j=1}^m \log\Big(\frac{2\mathrm{RV}_n(\mathbf{y}_j)}{\mathrm{RV}_{2n}(\mathbf{y}_j)}\Big)$
$V_{p,\Delta_{2n}}(\mathbf{y})$	Rescaled realized volatility, $\frac{1}{p\Delta_{2n}^{\alpha'}}\sum_{i=1}^p(\Delta_{2n,i}\tilde{X})^2(\mathbf{y})e^{\lVert\kappa\bullet\mathbf{y}\rVert_1}$, $1 \leqslant p \leqslant 2n$
$V_{p,\Delta_n}(\mathbf{y})$	Rescaled realized volatility on thinned grid, $\frac{1}{p\Delta_n^{\alpha'}}\sum_{i=1}^p(\Delta_{n,i}\tilde{X})^2(\mathbf{y})e^{\lVert\kappa\bullet\mathbf{y}\rVert_1}$, $1 \leqslant p \leqslant n$
$W_{p,\Delta_{2n}}(\mathbf{y})$	$\frac{1}{p\Delta_{2n}^{\alpha'}}\sum_{i=1}^p \mathbb{1}_{2\mathbb{N}}(i)(\Delta_{2n,i}\tilde{X})(\mathbf{y})(\Delta_{2n,i-1}\tilde{X})(\mathbf{y})e^{\lVert\kappa\bullet\mathbf{y}\rVert}$, $1 \leqslant p \leqslant 2n$
$\xi_{2n,i}$	$\xi_{2n,i}^1 + \xi_{2n,i}^2$
$\xi_{2n,i}^1$	$\frac{2^{1-\alpha'}-1}{\log(2)\sqrt{2nm}\Delta_{2n}^{\alpha'}\sigma_0^2 K}\sum_{j=1}^m(\Delta_{2n,i}\tilde{X})^2(\mathbf{y}_j)e^{\lVert\kappa\bullet\mathbf{y}_j\rVert_1}$

$\xi^2_{2n,i}$	$\mathbb{1}_{2\mathbb{N}}(i)\frac{2^{2-\alpha'}}{\log(2)\sqrt{2nm}\Delta_{2n}^{\alpha'}\sigma_0^2 K}\sum_{j=1}^m(\Delta_{2n,i}\tilde{X})(\mathbf{y}_j)(\Delta_{2n,i-1}\tilde{X})(\mathbf{y}_j)e^{\\|\kappa\cdot\mathbf{y}_j\\|_1}$
$\Lambda_{\alpha'}$	$2(2^{\alpha'}-2)+\sum_{r=0}^{\infty}\Big(\big(-(r+1)^{\alpha'}+2(r+2)^{\alpha'}-(r+3)^{\alpha'}\big)$ $\times\big(-r^{\alpha'}+2(r+1)^{\alpha'}-(r+2)^{\alpha'}\big)\Big)$

Appendix B. Additional Plots

This appendix provides additional plots for Part II of this thesis. We start by providing a plot for a three-dimensional SPDE model from equation (49) with parameters $\vartheta_0 = 0$, $\nu = (-10, 10, 0)$, $\eta = 1$, $\sigma = 1$ and $\alpha' = 1/2$ on an equidistant grid in time and space, where $N = 10^4$ and $M = 10$.

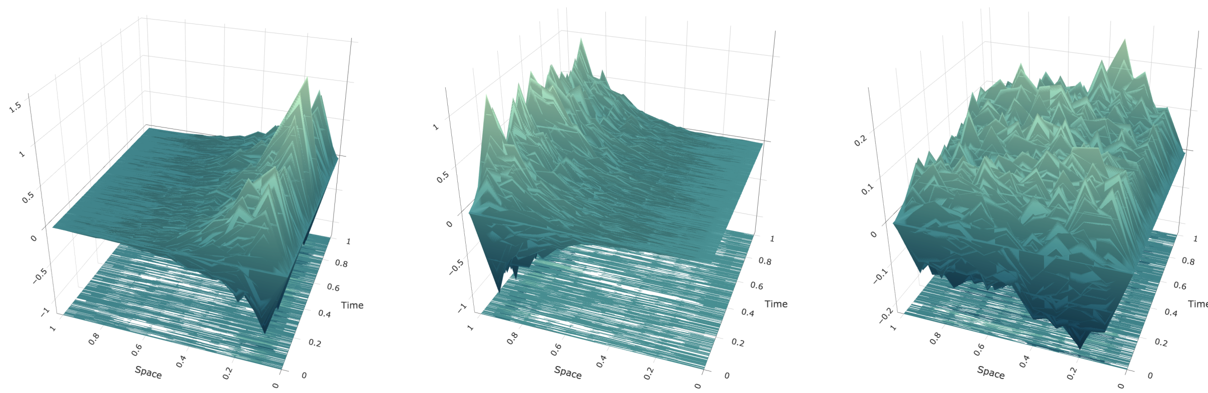

Figure B.1.: The figure depicts a three-dimensional SPDE on an equidistant grid in both time and space, where $N = 10^4$ and $M = 10$. The simulation utilizes the following parameter values: $\vartheta_0 = 0$, $\nu = (-10, 10, 0)$, $\eta = 1$, $\sigma = 1$, and $\alpha' = 1/2$. The visual representation consists of three panels: the left panel displays the random field for the first spatial axis, the middle panel showcases the second spatial axis, and the right panel presents the third spatial axis. For each spatial axis displayed, the coordinates of the remaining axes are held fixed at $(1/2, 1/2)$.

The QQ-plots for the volatility estimations are given by the following figure.

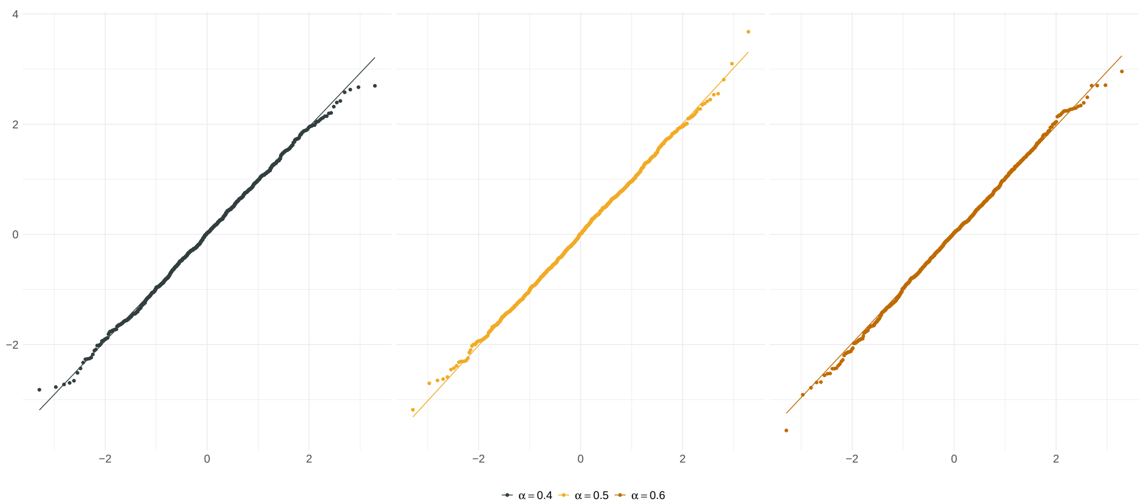

Figure B.2.: QQ-normal plots for normalized estimation errors for the parameter σ from simulations with $N = 10^4, M = 10, \vartheta_0 = 0, \nu = (6, 0), \eta = 1, \sigma = 1, \alpha' = 4/10$ in the left panel (grey), $\alpha' = 1/2$ in the middle panel (yellow) and $\alpha' = 6/10$ in the right panel (brown).

The QQ-plots for estimating the natural parameters σ_0^2 and $\kappa = (\kappa_1, \kappa_2)$ as well as the damping parameter α' are given by the following two figures.

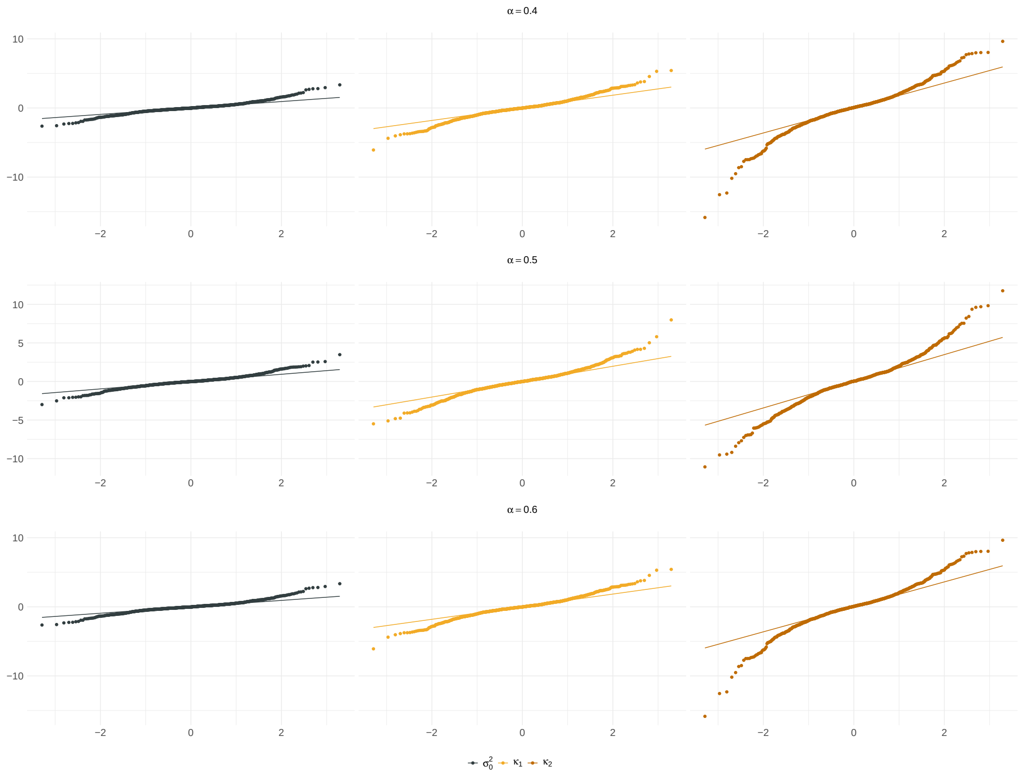

Figure B.3.: QQ-normal plots for normalized estimation errors for the parameter υ from simulations with $N = 10^4, M = 10, \vartheta_0 = 0, \nu = (6, 0), \eta = 1, \sigma = 1, \alpha' = 4/10$ in the top panel, $\alpha' = 1/2$ in the middle panel and $\alpha' = 6/10$ in the bottom panel. The results for the estimator $\hat{\sigma}_0^2$ is given by the grey color, the results for $\hat{\kappa}_1$ is given by the yellow color and for $\hat{\kappa}_2$ by the brown color.

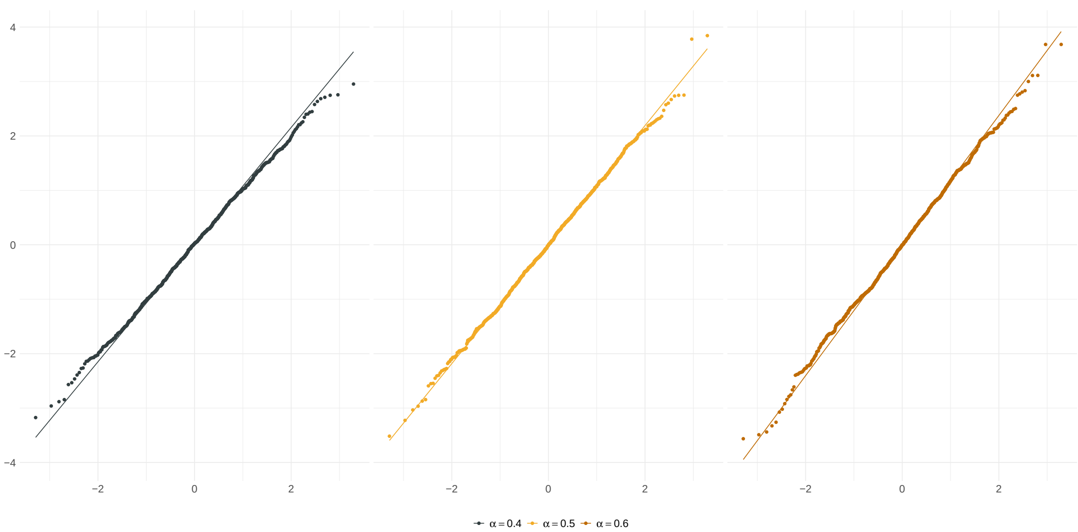

Figure B.4.: QQ-normal plots for normalized estimation errors for the parameter α' from simulations with $N = 10^4, M = 10, \vartheta_0 = 0, \nu = (6, 0), \eta = 1, \sigma = 1, \alpha' = 4/10$ in the left panel (grey), $\alpha' = 1/2$ in the middle panel (yellow) and $\alpha' = 6/10$ in the right panel (brown).

Bibliography

Randolf Altmeyer and Markus Reiß. Nonparametric estimation for linear SPDEs from local measurements. *The Annals of Applied Probability*, 31(1):1 – 38. 2021.

Randolf Altmeyer, Till Bretschneider, Josef Janák, and Markus Reiß. Parameter estimation in an spde model for cell repolarization. *SIAM/ASA Journal on Uncertainty Quantification*, 10(1):179–199. 2022.

Randolf Altmeyer, Igor Cialenco, and Gregor Pasemann. Parameter estimation for semilinear spdes from local measurements. *Bernoulli*, 29(3):2035–2061, 2023.

Tsuneo Arakawa and Masanobu Kaneko. Multiple zeta values, poly-bernoulli numbers, and related zeta functions. *Nagoya Mathematical Journal*, 153:189–209, 1999.

Fred Espen Benth, Dennis Schroers, and Almut ED Veraart. A feasible central limit theorem for realised covariation of spdes in the context of functional data. *arXiv preprint arXiv:2205.03927*, 2022a.

Fred Espen Benth, Dennis Schroers, and Almut ED Veraart. A weak law of large numbers for realised covariation in a hilbert space setting. *Stochastic Processes and their Applications*, 145:241–268, 2022b.

Markus Bibinger and Patrick Bossert. Efficient parameter estimation for parabolic spdes based on a log-linear model for realized volatilities. *Japanese Journal of Statistics and Data Science*, 6(1):407–429, 2023. doi: 10.1007/s42081-023-00192-4. URL https://doi.org/10.1007/s42081-023-00192-4.

Markus Bibinger and Mathias Trabs. On central limit theorems for power variations of the solution to the stochastic heat equation. In *Stochastic Models, Statistics and Their Applications. SMSA 2019. Springer Proceedings in Mathematics & Statistics, vol 294*, pages 69–84. Springer, Cham, 2019.

Markus Bibinger and Mathias Trabs. Volatility estimation for stochastic pdes using high-frequency observations. *Stochastic Processes and their Applications*, 130(5):3005–3052, 2020.

Nicholas H Bingham, Charles M Goldie, Jozef L Teugels, and JL Teugels. *Regular variation*. Number 27. Cambridge university press, 1989.

Patrick Bossert. Parameterschätzung für stochastische partielle Differentialgleichungen. Master's thesis, Philipps-Universität Marburg, 2020. Available at https://www.mathematik.uni-marburg.de/~stochastik/betreute_abschlussarbeiten/masterarbeiten/Masterarbeit%20Patrick%20Bossert.pdf.

Patrick Bossert. Parameter estimation for second-order spdes in multiple space dimensions. *arXiv preprint arXiv:2310.17828*, 2023.

Carsten Chong. High-frequency analysis of parabolic stochastic pdes. *The Annals of Statistics*, 48(2): 1143–1167, 2020a.

Carsten Chong. High-frequency analysis of parabolic stochastic pdes with multiplicative noise. *arXiv preprint arXiv:1908.04145*, 2020b.

Igor Cialenco. Statistical inference for spdes: an overview. *Statistical Inference for Stochastic Processes*, 21(2):309–329, 2018.

Igor Cialenco and Nathan Glatt-Holtz. Parameter estimation for the stochastically perturbed navier–stokes equations. *Stochastic Processes and their applications*, 121(4):701–724, 2011.

Igor Cialenco and Yicong Huang. A note on parameter estimation for discretely sampled spdes. *Stochastics and Dynamics*, 20(03):2050016, 2020.

Igor Cialenco and Hyun-Jung Kim. Parameter estimation for discretely sampled stochastic heat equation driven by space-only noise. *Stochastic Processes and their Applications*, 143:1–30, 2022.

Igor Cialenco, Francisco Delgado-Vences, and Hyun-Jung Kim. Drift estimation for discretely sampled spdes. *Stochastics and Partial Differential Equations: Analysis and Computations*, 8(4):895–920, 2020.

Giuseppe Da Prato and Jerzy Zabczyk. *Stochastic equations in infinite dimensions*. Cambridge university press, 2014.

A Davie and J Gaines. Convergence of numerical schemes for the solution of parabolic stochastic partial differential equations. *Mathematics of Computation*, 70(233):121–134, 2001.

Persi Diaconis and Susan Holmes. Stein's method: expository lectures and applications. IMS, 2004.

Guido Fioravanti, Sara Martino, Michela Cameletti, and Andrea Toreti. Interpolating climate variables by using inla and the spde approach. *International Journal of Climatology*, 2023. doi: https://doi.org/10.1002/joc.8240.

Harley Flanders. *Differential forms with applications to the physical sciences*, volume 11. Courier Corporation, 1963.

Geir-Arne Fuglstad and Stefano Castruccio. Compression of climate simulations with a nonstationary global SpatioTemporal SPDE model. *The Annals of Applied Statistics*, 14(2):542 – 559. 2020.

Leszek Gawarecki and Vidyadhar Mandrekar. *Stochastic differential equations in infinite dimensions: with applications to stochastic partial differential equations*. Springer Science & Business Media, 2010.

Sanoli Gun and Biswajyoti Saha. Multiple lerch zeta functions and an idea of ramanujan. *Michigan Mathematical Journal*, 67(2):267–287, 2018.

Ben Hambly and Andreas Søjmark. An spde model for systemic risk with endogenous contagion. *Finance and Stochastics*, 23(3):535–594. 2019.

Philip Hartman. Ordinary differential equations, classics in applied mathematics, vol. 38, society for industrial and applied mathematics (siam), philadelphia, pa, 2002, corrected reprint of the second (1982) edition. *Corrected reprint of the second*, 1982.

Florian Hildebrandt. On generating fully discrete samples of the stochastic heat equation on an interval. *Statistics & Probability Letters*, 162:108750, 2020.

Florian Hildebrandt. *Parameter estimation for SPDEs based on discrete observations in time and space.* PhD thesis, Universität Hamburg, 2021.

Florian Hildebrandt and Mathias Trabs. Parameter estimation for SPDEs based on discrete observations in time and space. *Electronic Journal of Statistics*, 15(1):2716 – 2776, 2021.

Florian Hildebrandt and Mathias Trabs. Nonparametric calibration for stochastic reaction–diffusion equations based on discrete observations. *Stochastic Processes and their Applications*, 162:171–217, 2023.

M. Huebner and B. Rozovskii. On asymptotic properties of maximum likelihood estimators for parabolic stochastic pde's. *Probability Theory and Related Fields*, 103(2):143–163, 1995.

M. Huebner, R. Khasminskii, and B. Rozovskii. Two examples of parameter estimation for stochastic partial differential equations. In *Stochastic Processes: A Festschrift in Honour of Gopinath Kallianpur*, pages 149–160. Springer, 1993.

Ildar Abdulovich Ibragimov and Yurii Antol'evich Rozanov. *Gaussian random processes*, volume 9. Springer Science & Business Media, 2012.

Leon Isserlis. On a formula for the product-moment coefficient of any order of a normal frequency distribution in any number of variables. *Biometrika*, 12(1/2):134–139, 1918.

Jean Jacod and Philip Protter. *Discretization of processes*, volume 67. Springer Science & Business Media, 2011.

Yusuke Kaino and Masayuki Uchida. Adaptive estimator for a parabolic linear spde with a small noise. *Japanese Journal of Statistics and Data Science*, 4(1):513–541, 2021a.

Yusuke Kaino and Masayuki Uchida. Parametric estimation for a parabolic linear spde model based on discrete observations. *Journal of Statistical Planning and Inference*, 211:190–220, 2021b.

Davar Khoshnevisan. An introduction to parabolic spdes. 2016.

Finn Lindgren, David Bolin, and Håvard Rue. The spde approach for gaussian and non-gaussian fields: 10 years and still running. *Spatial Statistics*, 50:100599, 2022.

Gabriel J Lord, Catherine E Powell, and Tony Shardlow. *An introduction to computational stochastic PDEs*, volume 50. Cambridge University Press, 2014.

Sergey V Lototsky, Boris L Rozovsky, et al. *Stochastic partial differential equations.* Springer, 2017.

Hermann Mena and Lena Pfurtscheller. An efficient spde approach for el niño. *Applied Mathematics and Computation*, 352:146–156, 2019.

Douglas C Montgomery, Elizabeth A Peck, and G Geoffrey Vining. *Introduction to linear regression analysis.* John Wiley & Sons, 2021.

Magda Peligrad, Sergey Utev, et al. Central limit theorem for linear processes. *The Annals of Probability*, 25(1):443–456, 1997.

Mike Pereira, Nicolas Desassis, Cédric Magneron, and Nathan Palmer. A matrix-free approach to geostatistical filtering. *arXiv preprint arXiv:2004.02799*, 2020.

Jan Pospíšil and Roger Tribe. Parameter estimates and exact variations for stochastic heat equations driven by space-time white noise. *Stochastic analysis and applications*, 25(3):593–611, 2007.

Walter Rudin. *Functional Analysis.* McGraw-Hill Science/Engineering/Math, 1987. ISBN 978-0070542365.

Elias M Stein and Rami Shakarchi. *Fourier analysis: an introduction*, volume 1. Princeton University Press, 2011.

Daniel W Stroock and SR Srinivasa Varadhan. *Multidimensional diffusion processes*, volume 233. Springer Science & Business Media, 1997.

Yozo Tonaki, Yusuke Kaino, and Masayuki Uchida. Parameter estimation for linear parabolic spdes in two space dimensions based on high frequency data. *Scandinavian Journal of Statistics*, 50(4):1568–1589, 2023. doi: https://doi.org/10.1111/sjos.12663. URL https://onlinelibrary.wiley.com/doi/abs/10.1111/sjos.12663.

Frederi Viens, Jin Feng, Yaozhong Hu, and Eulalia Nualart. *Malliavin calculus and stochastic analysis: a Festschrift in honor of David Nualart*, volume 34. Springer Science & Business Media, 2013.

Dale L Zimmerman. *Linear Model Theory: Exercises and Solutions.* Springer Nature, 2020.

List of Figures

List of Tables